ACTA CHIMICA

ACADEMIAE SCIENTIARUM HUNGARICAE

TOMUS 70 FASCICULI 1—2

AKADÉMIAI KIADÓ, BUDAPEST

1971

ACTA CHIM. (BUDAPEST) ACASA 2 70 (1—2) 1—174 (1971)

ACTA CHIMICA

A MAGYAR TUDOMÁNYOS AKADÉMIA KÉMIAI TUDOMÁNYOK OSZTÁLYÁNAK IDEGEN NYELVŰ KÖZLEMÉNYEI

Az Acta Chimica német, angol, francia és orosz nyelven közöl értekezéseket a kémiai tudományok köréből.

Az Acta Chimica változó terjedelmű füzetekben jelenik meg, egy-egy kötet négy füzetből áll. Évente átlag négy kötet jelenik meg.

A közlésre szánt kéziratok a szerkesztőség címére (Budapest 112/91 Műegyetem) küldendők.

Ugyanerre a címre küldendő minden szerkesztőségi levelezés. A szerkesztőség kéziratokat nem ad vissza.

Megrendelhető a belföld számára az „Akadémiai Kiadó"-nál (Budapest V., Alkotmány utca 21. Bankszámla 05-915-111-46), a külföld számára pedig a „Kultúra" Könyv- és Hírlap Külkereskedelmi Vállalatnál (Budapest I., Fő utca 32. Bankszámla: 43-790-057-181) vagy annak külföldi képviseleteinél és bizományosainál.

Die Acta Chimica veröffentlichen Abhandlungen aus dem Bereiche der chemischen Wissenschaften in deutscher, englischer, französischer und russischer Sprache.

Die Acta Chimica erscheinen in Heften wechselnden Umfanges. Vier Hefte bilden einen Band. Jährlich erscheinen 4 Bände.

Die zur Veröffentlichung bestimmten Manuskripte sind an folgende Adresse zu senden:

Acta Chimica
Budapest 112/91 Műegyetem

An die gleiche Anschrift ist auch jede für die Redaktion bestimmte Korrespondenz zu richten. Abonnementspreis pro Band: $ 16.00.

Bestellbar bei dem Buch- und Zeitungs-Außenhandels-Unternehmen »*Kultúra*« (Budapest I., Fő utca 32. Bankkonto No. 43-790-057-181) oder bei seinen Auslandsvertretungen und Kommissionären.

ACTA CHIMICA

ACADEMIAE SCIENTIARUM HUNGARICAE

TOMUS 70

AKADÉMIAI KIADÓ, BUDAPEST

1971

ACTA CHIMICA

TOMUS 70

Fasciculus 1: 1971
Fasciculus 2: 1971
Fasciculus 3: 1971
Fasciculus 4: 1971

INDEX

Acta Chimica Academiae Scientiarum Hungaricae, Tomus 70 (1–2), pp. 1–8 (1971)

PREPARATION AND PROPERTIES OF TRIPYRROLYLBORANE

P. SZARVAS, B. GYŐRI and J. EMRI

(Department of Inorganic and Analytical Chemistry, Kossuth University, Debrecen)

Received May 20, 1970

Some reactions leading to the formation of tripyrrolylborane have been investigated. It has been found that the reaction of BF_3, BCl_3 and B_2H_6 with $K(NC_4H_4)$, as well as the reaction of $K[BH(NC_4H_4)_3]$ with BF_3 and HCl result in the formation of tripyrrolylborane, in the case of appropriate mole ratios.

Satisfactory methods have been developed for its preparation in a pure state.

The chemical behaviour of tripyrrolylborane is characterized by the following reactions. Its reactions with water, methanol and acetic acid are fast, leading to the formation of $B(OH)_3$, $B(OCH_3)_3$ and $B_2O(OOCCH_3)_4$, respectively. Upon reaction with ammonia and pyridine, the corresponding complexes are formed, and with LiH, NaH, LiC_6H_5 and $K(NC_4H_4)$ stable anion complexes are obtained. Contrary to the above, the reaction with $KOCH_3$ and KOC_6H_5 affords the corresponding boric acid esters and $K[B(NC_4H_4)_4]$.

The following new compounds have been prepared: $B(NC_4H_4)_3$, $B(NC_4H_4)_3NH_3$, $B(NC_4H_4)_3NC_5H_5$, $Cs[BH(NC_4H_4)_3]$, $K[B(C_6H_5)(NC_4H_4)_3]$. $K[B(NC_4H_4)_4]$ has been prepared by a new method. On the basis of chemical and spectroscopic investigations it has been established that $B(NC_4H_4)_3$ is a relatively strong Lewis-acid.

In our earlier papers [1, 2] dealing with the reactions of pyrrole potassium with boron compounds, we referred to some reactions leading to the formation of tripyrrolylborane and briefly touched on the donor–acceptor properties of this compound. In this paper we wish to report in detail on the preparation of tripyrrolylborane and the reactions which characterize its chemical properties. In the course of the study of these reactions the following new compounds were prepared: ammine-tripyrrolylborane, pyridine-tripyrrolylborane, potassium phenyltripyrrolylborate and cesium hydrotripyrrolylborate, while potassium tetrapyrrolylborate and tetraacetatodiboronoxide were prepared by new methods. Our studies have shown that the formation of tripyrrolylboron takes place in the following reactions.

1. The compound of composition $K[B(NC_4H_4)_4]$ formed by reaction of $K(NC_4H_4)$ and BF_3 etherate in a 1 : 1 mole ratio [1, 2] reacts further with BF_3 etherate with the formation of $B(NC_4H_4)_3$:

$$3\ K[B(NC_4H_4)_4] + 4\ BF_3 = 4\ B(NC_4H_4)_3 + 3\ K[BF_4] \qquad (1)$$

2. Tripyrrolylborane is also formed when an ethereal solution of BCl_3 etherate is added to an ethereal suspension of $K(NC_4H_4)$:

$$3\ K(NC_4H_4) + BCl_3 = B(NC_4H_4)_3 + 3\ KCl \qquad (2)$$

3. A further formation of $B(NC_4H_4)_3$ is by the reaction of $K(NC_4H_4)$ and B_2H_6 at a 3 : 2 mole ratio, since the latter is able to extract the hydrine anion from the $K[BH(NC_4H_4)_3]$ [2] which is formed in a 2 : 1 mole ratio reaction.

However, this reaction occurs more slowly than the reaction leading to the formation of $K[BH(NC_4H_4)_3]$:

$$6K(NC_4H_4) + 3\ B_2H_6 = 2\ K[BH(NC_4H_4)_3] + 4\ K[BH_4]$$

$$2\ K[BH(NC_4H_4)_3] + B_2H_6 = 2\ B(NC_4H_4)_3 + 2\ K[BH_4] \qquad (3)$$

4. $B(NC_4H_4)_3$ may be prepared too by the reaction of BF_3 etherate with $K[BH(NC_4H_4)_3]$ in ether:

$$K[BH(NC_4H_4)_3] + BF_3 = B(NC_4H_4)_3 + K[BHF_3] \qquad (4)$$

The $K[BHF_3]$ reacts in part with BF_3 and some B_2H_6 is also formed in the reaction.

5. Similarly it may be prepared from $K[BH(NC_4H_4)_3]$ by reaction with HCl in an ethereal medium:

$$K[BH(NC_4H_4)_3] + HCl = B(NC_4H_4)_3 + H_2 + KCl \qquad (5)$$

Of the above reactions, (3) and (4) are the most suitable for the preparation of pure $B(NC_4H_4)_3$. The product thus obtained is completely white and does not become coloured even after long standing. Using the apparently most simple reactions (1) and (2), however, only a faintly red-coloured product is obtainable and the colour of this deepens on standing. But if a little $Na[BH_4]$ or B_2H_6 is added to the reaction mixture, the colour of the product can be reduced to a considerable extent.

The pure $B(NC_4H_4)_3$ crystallizes as white needles. It can be sublimed in vacuum between 160 and 200 °C. The melting point of the purified material is 211—212 °C It is readily soluble in THF, moderately in benzene, and only slightly in ether.

In CCl_4 solution the B—N stretching vibration appears at 1360 cm^{-1} in agreement with the data of KÖSTER [3], while in $CHCl_3$ it is shifted to 1334 cm^{-1}. The band at 1378 cm^{-1} can be assigned to the skeletal vibration of pyrrol [4] (Fig. 1).

Tripyrrolylborane, similarly to the alkyl esters of boric acid, is sensitive to water. In aqueous medium at room temperature it is hydrolyzed to boric acid and pyrrole. It is of interest that the aqueous solutions of four-coordinated anionic derivatives of $B(NC_4H_4)_3$ (*e.g.* $K[B(NC_4H_4)_4]$, $K[BH(NC_4H_4)]_3$) are much more stable than the corresponding anionic derivatives of $B(OR)_3$ (*e.g* $Na[B(OR)_4]$ [5] and $Na[BH(OR)_3]$ [6]).

Rapid methanolysis occurs on treatment with methanol at room temperature and the tripyrrolylborane is quantitatively converted to $B(OCH_3)_3$.

In ethereal solution tripyrrolylborane reacts with acetic acid (in a mole ratio of 1 : 3) to form $B_2O(OAc)_4$:

$$2\ B(NC_4H_4)_3 + 6\ HOAc = B_2O(OAc)_4 + 6\ NC_4H_5 + Ac_2O \qquad (6)$$

$B(NC_4H_4)_3$ dissolves in liquid ammonia; after evaporation of the ammonia, a compound of composition $H_3N \cdot B(NC_4H_4)_3$ is obtained, which is surprisingly insensitive to moisture. Similarly, $B(NC_4H_4)_3$ reacts with pyridine at room

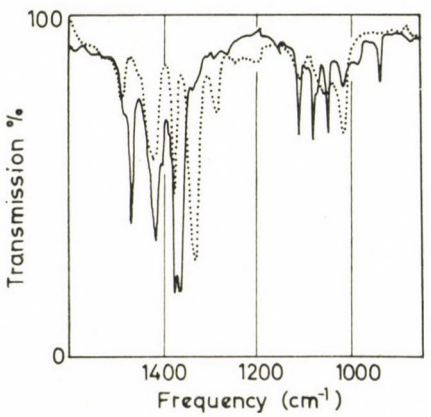

Fig. 1. Infrared spectrum of tripyrrolylboron between 850—1600 cm^{-1} in CCl_4 (—) and in $CHCl_3$ (. . . .), solution $C = 0.01\ M$

temperature. The product formed dissolves in pyridine on heating; on cooling, white crystals of a substance of composition $C_5H_5N \cdot B(NC_4H_4)_3$ separate out.

However, in contrast to strong Lewis-acids such as triarylboranes (*e.g.* BPh_3), tripyrrolylborane does not react under the normal conditions with PPh_3 [7], sodium and potassium [8], sodium and potassium amalgams [9], or KCN [10].

In a THF medium it reacts smoothly with $K(NC_4H_4)$ and potassium tetrapyrrolylborate is formed:

$$B(NC_4H_4)_3 + K(NC_4H_4) = K[B(NC_4H_4)_4] \qquad (7)$$

It reacts immediately with phenyl lithium in ether, and after evaporation of the ether a compound of composition $K[B(C_6H_5)\ (NC_4H_4)_3]$ separates out from aqueous solution on treatment with KCl:

$$B(NC_4H_4)_3 + LiC_6H_5 \xrightarrow{\text{ether}} Li[B(C_6H_5)\ (NC_4H_4)_3] \qquad (8)$$

$$Li[B(C_6H_5)(NC_4H_4)_3] + KCl \xrightarrow{water} K[B(C_6H_5)(NC_4H_4)_3] + LiCl \quad (9)$$

LiH and NaH react likewise in boiling ether and, after the removal of the ether, treatment of the aqueous solution with CsCl leads to the separation of a white compound of composition $Cs[BH(NC_4H_4)_3]$:

$$B(NC_4H_4)_3 \xrightarrow[ether]{LiH \text{ or } NaH} Li[BH(NC_4H_4)_3] \text{ (or Na salt)} \xrightarrow[ether]{CsCl} Cs[BH(NC_4H_4)_3] \quad (10)$$

It is known that NaH does not react with diborane in ether [11]. With $B(NC_4H_4)_3$ in ether, however, NaH reacts readily with the formation of $Na[BH(NC_4H_4)_3]$ and this latter compound reacts with diborane to yield $Na[BH_4]$ while the $B(NC_4H_4)_3$ used in the reaction is recovered. Thus $B(NC_4H_4)_3$ acts as a catalyst for the reaction between NaH and B_2H_6:

$$2\ NaH + 2\ B(NC_4H_4)_3 \xrightarrow{ether} 2\ Na[BH(NC_4H_4)_3] \quad (11)$$

$$2\ Na[BH(NC_4H_4)_3] + B_2H_6 \xrightarrow{ether} 2\ Na[BH_4] + 2\ B(NC_4H_4)_3 \quad (12)$$

i.e. the overall reaction is

$$2\ NaH + B_2H_6 \xrightarrow[ether]{B(NC_4H_4)_3} 2\ Na[BH_4] \quad (13)$$

$B(OCH_3)_3$ has a similar role in the preparation of $Na[BH_4]$ but in this case the reaction cannot be accomplished in ether [12, 13].

In contrast to the preceding reactions, a compound of composition $K[B(OR)(NC_4H_4)_3]$ cannot be prepared from K(OR) (R = CH_3, C_6H_5). In THF the following reaction takes place:

$$4\ B(NC_4H_4)_3 + 3K(OR) = 3\ K[B(NC_4H_4)_4] + B(OR)_3 \quad (14)$$

Discussion

The chemical properties of a three-coordinated boron compound are determined basically by the Lewis-acid strength of the compound in question. In the ammine complexes of boron compounds (*e.g.* $H_3N \cdot B(CH_3)_3$) the stretching frequency of the B–N bond is to be found in the region of 1100 cm^{-1} [14]. In those three-coordinated boron compounds where p_π–p_π bonding is possible between the B and N atoms, the stretching frequency for the B–N bond appears at higher frequency values [15]. For the case of the triamineboranes in general the greater the value of the B–N stretching frequency the

greater the electron density on the boron atom, and accordingly the weaker the Lewis-acid character of the compound concerned. The B–N frequency for $B(NC_4H_4)_3$ is found at 1360 cm^{-1} (in CCl_4). In the case of $B(NR_2)_3$ type compounds (where R = H, alkyl or aryl) the B–N absorption occurs in the range 1400—1500 cm^{-1} [16]. This means that the p_π–p_π character of the B–N bond in $B(NC_4H_4)_3$, although significant, is less pronounced than in the case of the simple amines of the above type, and hence $B(NC_4H_4)_3$ must be a stronger Lewis-acid than these compounds. This finding is unambiguously supported by the chemical reactions of $B(NC_4H_4)_3$:

a) Well-defined complexes are obtained with amines (NH_3, pyridine).

b) It readily reacts with LiH or NaH and $K(NC_4H_4)$, LiC_6H_5 with the formation of stable salts ($Li[BH(NC_4H_4)_3]$, $Na[BH(NC_4H_4)_3]$, $K[B(NC_4H_4)_4]$, $Li[B(C_6H_5)(NC_4H_4)_3]$) (reactions (7), (8), and (10)).

Such derivatives of the $B(NR_2)_3$ type compounds are not known. From the infrared spectroscopic data and the above reactions, it can be concluded that $B(NC_4H_4)_3$ is a stronger Lewis-acid than the triaminoboranes.

Since the B–N bonds in tripyrrolylborane have a significant p_π–p_π character, it is not expected to be a Lewis-acid of strength similar to that of B_2H_6, BF_3 or BPh_3. Direct chemical proof of this is that $K[B(NC_4H_4)_4]$ gives $B(NC_4H_4)_3$ with BF_3, as does $K[BH(NC_4H_4)_3]$ with BF_3 or B_2H_6 (reactions (1), (3) and (4)). The fact that $B(NC_4H_4)_3$ does not react with Na, K, Na/Hg, K/Hg, PPh_3 or with KCN points to the weaker Lewis-acid character of $B(NC_4H_4)_3$ compared with BPh_3. This latter is also proved by the reaction between $B(NC_4H_4)_3$ and phenyl lithium where $Li[B(C_6H_5)(NC_4H_4)_3]$ is formed and not $Li[BPh_4]$ and $Li[B(NC_4H_4)_4]$ (reaction (8)).

From thermodynamic [17] and spectroscopic [16] data it has been proved that in boron compounds the N atoms are capable of more significant back-coordination compared with O atoms. From our studies, however, $B(NC_4H_4)_3$ is a definitely stronger Lewis-acid than the alkyl esters of boric acid. $B(NC_4H_4)_3$ gives well-defined complexes with both NH_3 and pyridine, whereas $B(OCH_3)_3$ forms complexes only with very strong Lewis-bases (RNH_2, piperidine, etc.). Similar complexes of higher alkyl esters are unknown [18]. The course of the reaction between $B(NC_4H_4)_3$ and $K(OCH_3)$ (reaction (14)) is also in agreement with the stronger Lewis-acid character of tripyrrolylborane compared to the methyl ester of boric acid.

The phenyl ester of boric acid gives stable complexes with NH_3 and pyridine similar to $B(NC_4H_4)_3$, but $K(OC_6H_5)$ reacts with $B(NC_4H_4)_3$ similarly to $K(OCH_3)$. On the basis of this, it is probable that tripyrrolylborane is also a stronger Lewis-acid than the phenyl ester of boric acid.

The relatively strong Lewis-acid character of $B(NC_4H_4)_3$ is clearly a consequence of the aromatic character of the pyrrole ring which reduces back-coordination considerably.

Experimental

In all cases experiments were carried out in absolute solvents in a dry, oxygen-free atmosphere. Our methods were in the broad details identical with the anaerobic methods of HERZOG and DEHNERT [19]. BF_3, BCl_3 and B_2H_6 were prepared by the methods of BOOTH and WILSON [20], GAMBLE [21] and BROWN and TIERNEY [22], respectively, and $K(NC_4H_4)$ by a method similar to that of ISSLEIB and BRACK (see [2]). $K[BH(NC_4H_4)_3]$ was prepared by our own method [2]. The NaH used was obtained from Fluka, and the LiH from BDH. Infrared spectra were recorded on a Unicam Model SP 200 G spectrometer in about 0,01 *M* CCl_4 and $CHCl_3$ solution at an optical path length of 0.253 mm.

Preparation of tripyrrolylborane, $B(NC_4H_4)_3$

a) 11.9 ml (94 mmoles) of BF_3 etherate in 20 ml of ether is slowly added to a continuously stirred suspension of 7.15 g (68 mmoles) of $K(NC_4H_4)$ in 60 ml of ether. The reaction mixture is stirred for an hour and then filtered; the solid residue is extracted several times with the filtrate, then the $B(NC_4H_4)_3$ separated by extraction with 80—100 ml of benzene. The benzene solution is cooled and the separated tripyrrolylborane filtered. The benzene and ether solutions are combined and evaporated; thus a further significant amount of $B(NC_4H_4)_3$ can be obtained.

Yield: 2.8—3.1 g (59—65%).

The product thus obtained has a faint red colour. Even repeated extraction with benzene did not lead to a completely white product. If a little $Na[BH_4]$ is added to the reaction mixture (0.2—0.3 g to 7.15 g of $K(NC_4H_4)$), after recrystallization from benzene the product is much purer and completely white. An even purer product is obtained if the reaction is carried out in THF in the presence of a little $Na[BH_4]$ and B_2H_6. The $B(NC_4H_4)_3$ can be prepared in the form of white crystals by addition of ether to a concentrated solution in THF.

$C_{12}H_{12}N_3B$ (209.06). Calcd. B 5.17, N 20.10;
Found B 5.20, N 19.98%.

b) 6.45 g (55 mmoles) of BCl_3 is dissolved in 40 ml of ether and the solution obtained is added with slow stirring to a suspension of 16.2 g (154 mmoles) of pyrrole potassium in ether. After the addition, stirring is continued for half an hour and the mixture then filtered. The residue is extracted 2—3 times with the ethereal filtrate. $B(NC_4H_4)_3$ is obtained from the material remaining on the filter by extraction with benzene. By evaporation of the filtrate from this extraction, a slightly impure product is obtained.

Yield: 7.5—8.0 g (70—75%), strongly coloured.

c) 6.0 g (56 mmoles) of pyrrole potassium is suspended in 120 ml of ether. During 2—2.5 hours at room temperature a B_2H_6–N_2 mixture containing 1.09 g (39.2 mmoles) of B_2H_6 is introduced into the suspension with vigorous stirring. At the beginning (up to 0.78 g) the B_2H_6 reacts quickly; following this the reaction slows down and accordingly the rate of introduction of B_2H_6 must be substantially decreased. After the addition of the B_2H_6, stirring is continued for 3—4 hours and the solution then filtered. $B(NC_4H_4)_3$ is extracted from the solid residue with benzene. The product is pure white and is not coloured over a long period of time.

Yield: 2.5—2.7 g (63—68%).

d) 1.76 ml (14 mmoles) of BF_3 etherate in 10 ml of ether is added in 0.5—1 hour with stirring to a suspension of 2.49 g (10 mmoles) of well-powdered $K[BH(NC_4H_4)_3]$ in 30—40 ml of ether. A gas scrubber filled with acetone is connected to the reaction vessel to absorb the small amount (10—20% of the stoichiometric quantity) of B_2H_6 formed during the reaction: after a further hour's stirring the reaction mixture is filtered and the $B(NC_4H_4)_3$ separated from the residue as above. The quality of the product is the same as that of the product by the previous method.

Yield: 1.75—1.9 g (84—90%).

Preparation of ammine-tripyrrolylborane, $H_3N \cdot B(NC_4H_4)_3$

Na-dried NH_3 is condensed onto 2.09 g (10 mmoles) of purified $B(NC_4H_4)_3$ until the latter has completely dissolved. The NH_3 is then evaporated off. During the concentration of the solution, well-formed crystals separate out, but after the complete evaporation of the NH_3 these disintegrate into a powdered product. The last traces of NH_3 are removed in vacuum. The yield is almost quantitative.

$C_{12}H_{15}N_4B$ (226.09). Calcd. B 4.78, N 24.78, C 63.75, H 6.69;
Found B 4.81, N 24.21, C 63.44, H 6.62%.

Preparation of pyridine-tripyrrolylborane, $C_5H_5N \cdot B(NC_4H_4)_3$

6 ml of absolute pyridine is added to 1.05 g (5 mmoles) of $B(NC_4H_4)_3$. A powdered substance separates out with evolution of heat. If the temperature is raised to 100—110 °C, a clear solution is obtained from which the product separates out as crystals on slow cooling to 0 °C. The solution is filtered, washed with ether and dried. A further small amount of material may be obtained from the solution by precipitation with ether.

Yield: 1.25 g (86.5%), white crystalline material.

$C_{17}H_{17}N_4B$ (288.16). Calcd. B 3.75, N 19.44;
Found B 3.76, N 19.18%.

Preparation of potassium tetrapyrrolylborate, $K[B(NC_4H_4)_4]$

2.09 g (10 mmoles) of $B(NC_4H_4)_3$ in THF is added with stirring to a suspension of 1.2 g of pyrrole potassium in THF. A large part of the pyrrole potassium reacts during this time. The solution is refluxed for half an hour, cooled, treated with charcoal and filtered. The filtrate is evaporated and the product separated out by the addition of ether.

Yield: 2.5—2.7 g (80—86%).

$C_{16}H_{16}N_4BK$ (314.27). Calcd. K 12.44, B 3.44, N 17.83;
Found K 12.65, B 3.46, N 17.70%.

Preparation of potassium phenyltripyrrolylborate, $K[B(C_6H_5)(NC_4H_4)_3]$

20 ml of ether is added to 2.09 g (10 mmoles) of $B(NC_4H_4)_3$. An equivalent amount (10 mmoles) of phenyl lithium in ether solution is added to the suspension with stirring. The $B(NC_4H_4)_3$ dissolves completely and two phases appear. The solution is stirred for an hour, then evaporated to dryness. 10 ml of water is added, then a little charcoal, and after stirring for 1/2 hr. the mixture is filtered. A concentrated aqueous solution of 7—8 g of KCl is added dropwise to the filtrate and the product separates out in the form of white microcrystals. These are filtered off and washed alkali free with 10% KCl solution; the KCl is washed out with a little cold water, and the product dried in vacuum at 60—70 °C. The compound may be purified by a further KCl precipitation from aqueous solution.

Yield: 2.5—2.7 g (77—83%).

$C_{18}H_{17}N_3BK$ (325.27). Calcd. K 12.02, B 3.32, N 12.92;
Found K 11.83, B 3.30, N 12.36%.

Preparation of cesium hydrotripyrrolylborate, $Cs[BH(NC_4H_4)_3]$

20 ml of ether is added to 1.05 g (5 mmoles) of $B(NC_4H_4)_3$; this is followed by 0.045 g (5.65 mmoles) of LiH with stirring. The reaction mixture is refluxed for 2.5—3 hours during which time the $B(NC_4H_4)_3$ and the LiH react and only a small amount of solid residue can be seen in the solution. The ether solution is evaporated to dryness, 10 ml of water is added, and

the solution stirred for half an hour and then filtered (with the addition of a little charcoal the solution may be filtered pure). 10 ml of an aqueous solution of 1.05 g (6.0 mmoles) of CsCl is added dropwise with stirring to the clear filtrate and the product separates out in the form of white microcrystals. After standing for a short time the substance is filtered off, washed alkali-free with small amounts of cold water (total 30 ml) and dried in vacuum at 60—70 °C.

Yield: 1.55—1.6 g (90—93.5%).

The substance can be purified by recrystallization from methanol.

$Cs[BH(NC_4H_4)_3]$ can be prepared similarly also with sodium hydride. In this case the reaction proceeds more slowly, and therefore it is necessary to reflux the reaction mixture for 4—5 hours.

$C_{12}H_{13}N_3BCs$ (342.97). Calcd. Cs 38.75, B 3.15;
Found Cs 39.09, B 3.14%.

REFERENCES

1. Szarvas, P., Emri, J., Győri, B.: Magy. Kém. Foly., **74,** 142 (1968)
2. Szarvas, P., Emri, J., Győri, B.: Acta Chim. Acad. Sci. Hung. **64,** 203 (1970)
3. Köster, R., Bellut, H., Hattori, S.: Liebigs Ann. **720,** 1 (1968)
4. Lord, R. C., Miller, F. A.: J. Chem. Phys. **10,** 328 (1942)
5. Meerwein, H., Bersin, T.: Liebigs Ann. **476,** 113 (1929)
6. Wittig, G., Hornberger, P.: Liebigs Ann. **577,** 11 (1952)
7. Wittig, G., Haag, W.: Ber. **88,** 1654 (1955)
8. Krause, E.: Ber. **57B**, 216 (1924)
9. Krause, E., Polack, H.: Ber. **59B,** 777 (1926)
10. Wittig, G., Raff, P.: Liebigs Ann. **573,** 195 (1951)
11. Schlesinger, H. I., Brown, H. C.: J. Amer. Chem. Soc. **75,** 186 (1953)
12. Schlesinger, H. I., Brown, H. C.: U. S. Pat. 2 461 661 (1949); Chem. Abstr. **43,** 4684e (1949)
13. Schlesinger, H. I., Brown, H. C., Finholt, A. E.: J. Amer. Chem. Soc. **75,** 205 (1953)
14. Becher, H. J.: Z. anorg. allg. Chem. **271,** 243 (1953)
15. Becher, H. J.: Z. anorg. allg. Chem. **289,** 262 (1957)
16. Aubrey, D. W., Lappert, M. F., Pyszora, H.: J. Chem. Soc. **1960,** 5239
17. Skinner, H. A., Smith, N. B.: J. Chem. Soc. **1954,** 3930
18. Urs, S. V., Gould, E. S.: J. Amer. Chem. Soc. **74,** 2948 (1952)
19. Herzog, S., Dehnert, J.: Z. Chem. **4,** 1 (1964)
20. Booth H. S., Wilson, K. S.: J. Amer. Chem. Soc. **57,** 2273 (1935)
21. Gamble, E. L.: Inorg. Syntheses, Vol. III. 27 (1950)
22. Brown, H. C., Tierney, P. A.: J. Amer. Chem. Soc. **80,** 1552 (1958)

Pál Szarvas
Béla Győri
József Emri
Debrecen 10, Hungary.

Acta Chimica Academiae Scientiarum Hungaricae, Tomus 70 (1–2), pp. 9–21 (1971)

DESCRIPTION OF FIRST ORDER PHASE TRANSFORMATIONS BY POTENTIAL THEORY

L. MEZEY

(Department of Physics, University of Agricultural Sciences, Gödöllő)

Received April 18, 1970

A survey and generalization was made of some fundamental results in connection with the statistical thermodynamics of phase transformations. An assumption was made, in agreement with the literature data, for the distribution of the zero sites of the phase integrals, and then the consequences appearing in the formalism of the inverse Laplace transformation were discussed. Next the relation between the characteristic functions of the 'two-dimensional' electrostatic field and the field described by the 'complex potentials of statistical thermodynamics' was defined. In the course of the analysis of the relation, the physical meaning of the formalism recommended first by LEE and YANG is pointed out. The inversion of the applied considerations shows how the treatment of phase transformations follows from the differences between the structures of the individual phases.

1. Introduction

The complete description of phase transformations cannot be considered a solved question in either phenomenological or statistical thermodynamics. The greatest progress was produced by the work of TISZA [1], SEMENCHENKO [2] and FÉNYES [3] concerning phenomenological thermodynamic theory. According to TISZA, the nature of the matrix characterizing the stability of the equilibrium state of a studied system determines in how many phases the system exists; the phase changes occur in order that the system avoid an unstable state.

For a long time statistical thermodynamics were regarded as unsuitable for the treatment of the problem, for example as found by TEMPERLEY [4], since phase integrals (partition functions) playing a central role in statistical thermodynamics are continuous functions, differentiable any number of times with respect to their arguments. In their theory reported in 1952, LEE and YANG [5] gave the first, and so far the only, generally accepted description of phase transformations from the viewpoint of statistical thermodynamics. They have shown that phase changes can occur only in 'infinitely large' systems and that for their description (which they performed in the grandcanonical assembly) the grandcanonical partition function must be examined as the function of *complex* fugacity. They related the sites of the phase transformations with the zero sites of the complex grandcanonical partition function.

Phase change descriptions which were more or less analogous with the theory of LEE and YANG were given by LEWIS and SIEGERT [6, 7] and by JONES [8] in pressure and canonical assembly, respectively, in 1956 and 1966. GROSSMANN [9] dealt with second order phase transformations in canonical assembly.

As concerns the LEE—YANG description, it is still an open question whether this is the only possible method of treatment [10]. At all events, the usefulness of the LEE—YANG theory was already demonstrated in 1952 in the two-dimensional ISING model [11], and since then such a description of phase transformations in various models has been successful in numerous cases. In the present work, therefore, we set out from this formalism.

We try to give an answer to the question of why different authors could arrive at analogous results for the various assemblies, and of what this formalism reflects. Naturally, since the calculation of phase integrals and their analytical sequels for models which reflect a variety of actual interactions is an extremely difficult task, for the time being there can be no question of the 'confirmation' of the formalism. Rather we shall attempt to point out the physical background of the LEE—YANG description with generalizations and with new relations. We shall deal with some questions touched upon here, such as the existence of complex phase integrals as Laplace transforms, the description of phase changes in microcanonical assembly will be given in a subsequent paper [12].

2. Complex phase integrals and phase transformations

In the following, we briefly summarize the literature data on which the present considerations are based.

According to KUBO [13], the canonical phase integral is the Laplace transform of the microcanonical 'structure function' (the name was given by HINCSIN [14]), whilst the grandcanonical partition function is an infinite series of complex variables. LEWIS and SIEGERT [6, 7] refer to the phase integral of the pressure assembly as the Laplace transform. Nobody has yet dealt with the conditions sufficient for the existence of the Laplace transform; this will be the subject of a forthcoming paper [12].

In any case, the question arises in what regions the phase integrals, as functions of complex variables, will be analytical. This question has been dealt with independently of the Laplace transformation theory.

Under real conditions made to the potential of the interaction between the molecules, JONES [8] confirmed that the phase integral of the *canonical* assembly (Z) is an analytical function of the complex β values on the $Re\ \beta > 0$ half-plane. LEE and YANG [5] confirmed the analytical nature of the phase integral of the *grandcanonical* assembly (Θ) on the $Re\ z > 0$ half-plane (z

is the fugacity). In the paper of LEWIS and SIEGERT [6] on the phase integral of the pressure assembly (Y), it was noted that this, as a Laplace transform, is necessarily analytical too on the $Re\ \beta P > 0$ half-plane.

The phase integrals themselves are less important characteristics of physical systems than the thermodynamic functions obtainable from them. As is well-known, for infinitely large systems statistical thermodynamics gives results equivalent to the thermodynamics. Extrapolation from the properties of large but finite systems to those of 'infinitely large' systems is referred to as finding the 'thermodynamic limit'. In the following this will be denoted in short by th. lim. The results obtained in th. lim. are characteristic of any system of 'thermodynamic dimension' and so the specific quantities are usually calculated.

Let us consider the following limits:

$$-\beta f(\beta, v) = N, V \xrightarrow{\lim} \infty \quad \frac{\ln Z(\beta, V, N)}{N} \quad \left(\frac{N}{V} \to v = \text{const}\right) \tag{1}$$

$$-\beta g(\beta, P, \beta) = N \xrightarrow{\lim} \infty \quad \frac{\ln \Upsilon(\beta, \beta P, N)}{N} \tag{2}$$

$$-\beta P(z, \beta) = V \xrightarrow{\lim} \infty \quad \frac{\ln \Theta(\beta, z, V)}{V} \tag{3}$$

where f is the specific free energy, g the specific free enthalpy and P the pressure, taking into account the definitions of these functions.

In connection with each limit two analogous theorems have been confirmed. We now quote from the LEE—YANG theorems proved in connection with Eq. (3). *Theorem I*: for all positive values of z, $\lim_{V\to\infty} \frac{\ln \Theta(\beta, z, V)}{V}$ exists and is a monotonously decrasing function of z. *Theorem II*: Let R be a region of the complex plane z that contains a portion of the positive real axis; and let the roots of the equations

$$\Theta(z, V, \beta) = 0 \tag{4}$$

not fall in R for any value of V. Then the expression $\ln \Theta/V$ converges uniformly in R to the limit and the limit is an analytical function in R. The 'operations' $z\frac{\partial}{\partial z}$ and $\lim_{V\to\infty}$ in R are interchangeable.

ROUELLE [15] confirmed a theorem analogous to I for a *canonical* assembly, and JONES [8] proved the validity of theorem II for such an assembly. (In these proofs Z, β and N appear in place of Θ, z and V, respectively.) LEWIS and SIEGERT [6, 7] confirmed the correctness of the theo-

rems for *pressure* assemblies. (Here Y, βP and N appear in place of Θ, z and V, respectively.)

The description of phase transformations is based on the supposition that during determination of the limit described in Eqs. (1)—(3), the roots of Eq. (4) or the equations corresponding to this, each converge to a point of the real positive axis. Then, again taking as an example the work of LEE and YANG [5], the following obtains: in each such point z_0 two regions, R_1 and R_2, are in contact which satisfy the conditions of theorem II. Then, in these points of contact of the regions the density

$$\frac{1}{V(z)} = Z \frac{\partial}{\partial z} \beta P(z, \beta) \tag{5}$$

suffers a jump, but within the regions it changes continuously (for real values of z).

These regions may be identified with the phases of the system. It is easy to see that the density increases when we pass through the critical points z_0 towards higher z values:

$$z \frac{\partial}{\partial z} \frac{1}{v(z)} = \left\langle \left(\frac{N}{V} \right)^2 \right\rangle - \left\langle \left(\frac{N}{V} \right)^2 \right\rangle \geqslant 0 \tag{6}$$

The other two papers [6, 8] describe the phase transformations in the other two assemblies similarly.

From a consideration of the concrete example of the two-dimensional ISING model [11], LEE and YANG confirmed that the roots of Θ lie on a circle of unit radius about the origin in th. lim. with a distribution function $g(\vartheta)$, and thus only one phase transformation is possible. They also referred to the fact that the field strength behaves similarly to $1/z$ times $1/v(z)$ in an electrostatic field generated by charges lying on a cylinder of infinite length crossing the z plane perpendicularly in a circle of unit radius. (The distribution of charge on the cylinder is constant at right angles to the plane. The distribution in a given plane is described also by $g(\vartheta)$.) The potential of such a field is βP. LEWIS and SIEGERT [6] use an electrostatic analogy too, and compare the treated problem with the description of the field of an infinite dipole chain.

In connection with the correctness of the LEE—YANG theory, a decisive question is whether the roots of Θ in the case of th. lim. really do behave in the manner described above. If for example they converge not to a point but to a finite section, the usefulness of the entire description becomes questionable. Because of the well-known difficulties connected with the exact calculation of the phase integrals, this question can still not be considered as closed [10].

3. Generalizations

On the basis of the above we now make a few generalizations and unify the treatment. In the following the structure function is also included among the phase integrals in treatments where the formalism of the Laplace transformation is used.

The macro-state of a thermodynamic system is described by the values of variables characteristic of the relations existing with the environment of the system and the system itself. Thus, if the system is closed from the point of view of a connection, it is described by the extensive quantity characterizing the connection in question, if open, by the intensive quantity [3], and this will be the characteristic variable. (In the following these will be denoted by W and w.) A thermodynamic characteristic function (K) [3] belongs to each such connecting possibility, and the characteristic variables of this are its independent variables. From a statistical point of view the connection is also characterized by a phase integral Q and this belongs to that statistical (Gibbs) assembly which describes the systems in the connection. The relation between the two is given by the definition:

$$-\beta K \underset{=}{\text{def}} \ln Q \tag{7}$$

The phase integral Q is related to the phase integral q (which describes a connection where exchange of an extensive variable W is not allowed) by:

$$Q(w) = \int_{W=W_0}^{\infty} e^{-wW} q(W)\, dW \tag{8}$$

where the identical characteristic variables are not shown. Since changes of all extensives occur in 'quantized' portions, more correctly the Stielties integral should have been written in place of the Riemann integral (8), but in the case of th. lim. it is clear that the difference between the two disappears. W_0 is the minimum of the extensive W in the system studied (zero-point energy, minimum volume, minimum particle number: 0). With coordinate transformation $W' = W - W_0$, Eq. (8) assumes a shape similar to the Laplace transformation.

The preliminaries outlined in the previous section can be generalized as follows. First, with $Re\ w > 0$, phase integrals $Q(w)$ are analytical functions. It should be noted that, as characteristic intensives w, entropic intensive parameters [3] must be taken; these are β, βP and $\beta\nu$ for canonical, pressure and grandcanonical assemblies, respectively, where ν is the chemical potential which is related to the fugacity z by the known expression

$$\beta v = \ln z \tag{9}$$

Thus we may write: $$z \frac{\partial}{\partial z} \rightarrow \frac{\partial}{\partial(\beta v)}$$

The limits (1)—(3), however, can be generalized in the following way. Let J be a characteristic extensive variable or characteristic intensive variable depending on the concrete relation; let X be an extensive the value of which is established in the given relation; w is the intensive quantity 'controlling' the distribution of the variable extensive W in the given relation; and b is a specific extensive (the ratio of two extensives) or an intensive. Then the limit

$$-\beta l(w, b) = \lim_{X \to \infty} \frac{\ln Q(X, w, \tau)}{X} \tag{10}$$

does exist for $w > 0$ (theorem I), and it is analytical function of w in all regions R which do not contain the roots of any of the equations

$$Q(X, w, J) = 0 \tag{11}$$

for any value of X, and each contains a part of the real positive w axis (theorem II). The proof follows directly from the interpretation of the th. lim. operation, and so it has been omitted.

Thus Eq. (5) can be generalized: if the roots of Eq. (11) converge to separate points of the real positive w axis in the case of th. lim., then in these points the specific expectation values suffer a jump.

$$\frac{\partial}{\partial w} \lim_{X \to \infty} \frac{\ln Q(X, w, \tau)}{X} = \lim_{X \to \infty} \frac{1}{X} \frac{\partial \ln Q(X, w, \tau,)}{\partial w} \overset{\text{def}}{=\!=} -\frac{\langle W \rangle}{X} = -\left\langle \frac{W}{X} \right\rangle \tag{12}$$

($\langle\ \rangle$ signifies the expectation values.)

As regards the sign of the jump, since

$$\sigma^2\left(\frac{W}{X}\right) = \lim_{X \to \infty} \left| \frac{1}{X} \frac{\partial^2 \ln Q(X, w, \tau)}{\partial w^2} \right| = \frac{\partial}{\partial w} \left\langle -\frac{W}{X} \right\rangle \geqslant 0 \tag{13}$$

on the increase of $Re\ w$, $-W/X$ increases; *i.e.* W/X decreases. (For the grand-canonical assembly, with the previously described choice of w, $-W/X = +N/V = +\varrho$ increases.)

From the distribution of the zero sites we know that this must be symmetrical with respect to the $x = Re\ w$ axis. That is, for the $Q(w)$ Laplace transforms

$$Q(w) = Q(\overline{w}) \tag{14}$$

(The bar denotes the complex conjugate.)

Thus, while $X \to \infty$ the regions symmetrical to the x axis will be completely free from the roots of Eq. (14). These regions R_1, $R_2 \ldots R_n$ corresponding to phases $i = 1, 2, \ldots n$ will touch in points $x_1, x_2 \ldots x_{n-1}$ on the x axis.

Let us assume that curves $C_1, C_2 \ldots C_n$ confining the regions cut the x axis so that in the right-hand side limiting point x_i of R_i, the normal n to C_i point in the direction of the x axis. This condition imposes a meaning on the curvature of the C_i's *viz.* because of Eq. (14) the C_i's in any case cross the x axis in the point of intersection at right angles. The condition does not contradict the result found for the two-dimensional Ising model (there, $R_i = R_1$ was the interior of the circle of unit radius around the origin).

Because of this condition, the operations $\dfrac{\partial}{\partial x}$ and $\dfrac{\partial}{\partial n}$ at the points of intersection give equivalent results.

Because of Eq. (14), the regions between the R_i's are also symmetrical about the x axis, and so between R_i and R_{i-1} lies a region T_i which contains the roots of Eq. (11) for all values of X satisfying the condition $X_0 \leq X$; X_0 is the minimum of the extensive X in the system in question.

In a thermodynamic limit presumably the roots lie on closed curves $D_1, D_2 \ldots D_n$. This assumption would be extremely difficult to confirm (see the remarks of JONES in connection with the zero sites of the canonical assembly phase integral [8]). Clearly, for any i $D_i \in T_i$.

4. Phase changes and the inverse Laplace transformation

If the inverse operation of Laplace transformation (8) is carried out, knowing Q we obtain the phase integral q:

$$q(W) = \frac{1}{2\pi i} \int_{X-i\infty}^{X+i\infty} Q(w)\, e^{wW}\, dw = \frac{1}{2\pi} \int_{-\infty}^{+\infty} Q(w)\, e^{wW}\, dy \qquad (y = im\, w) \tag{15}$$

For a given value of $x = c$, the integration path passes through m regions of $R_i (m \geq n)$, and among these, through $m - 1$ the regions of T_i. In the case of th. lim., according to the previous section, we obtain altogether $2(m - 1)$ points of intersection with the curves D_i lying symmetrically in pairs about the x axis; the intervals (y_{i-1}, y_i) forming part of the region R_i correspond to the individual phases on the straight line $x = c$ above the x axis, or the intervals $(-y_{i-1}, -y_i)$ similarly forming part of R_i below the x axis.

Eq. (15) then reduces to the sum of m integrals:

$$q(W) = \frac{1}{2\pi} \sum_{i=1}^{m} \int_{Ri} Q(w)\, e^{wW} dy \tag{16}$$

We have obtained the interesting result that the phase integral $q(W)$ in theory consists of contributions from m phases.

5. Description of phase transformations by potential theory

In a singly interdependent region R, an analytical complex function can be regarded as the complex potential of an electrostatic field the *charges* of which lie outside R [16, 18]. The field-strength vector belonging to the complex potential

$$f(z) = U(x, y) + iV(x, y) \tag{17}$$

is given in R by the formula

$$e(z) = -\overline{if'(z)} = -iU_x - V_x = -iV_y + U_y \tag{18}$$

where the Cauchy—Riemann equations, too, have been taken into account.

Upon crossing the boundary C of region R in the direction of the positive normal the potential function V changes continuously if there are charges here, but the normal component of the field-strength E_n suffers a jump. E_n also suffers a jump if there are in fact no charges on C, but C separates two media, 1 and 2, of different dielectric constants. In such a case the cause of the jump is attributed to apparent charges which are created by *real* charges generating the field and lying outside R. The magnitude of the jump is:

$$\frac{E_{2n} - E_{1n}}{E_{1n}} = \frac{\varepsilon_1 - \varepsilon_2}{\varepsilon_2} \tag{19}$$

Let us consider a field which is due to charges distributed uniformly along the z axis. Then the course of the field-strength in the x, y plane is described by the function

$$E(r) = \frac{2t}{\varepsilon r} \tag{20}$$

where $r = \pm\sqrt{x^2 + y^2}$ and t is the constant linear charge density along the z axis.

On this basis the following analogies may be established. The limits appearing in Eq. (10) can be considered as the complex potential of an electrostatic field which is generated by a charge distribution of density t crossing

the origin of the complex w plane perpendicularly to the plane. These charges lie outside the half-plane $Re\, w > 0$ for all values of z (the phase integrals Q on the half-plane $Re\, w > 0$ and the limits mentioned are also analytical). More exactly the limits (10) within this half-plane will only be analytical where the dielectric constant ε changes continuously (in regions R_i); however, in the point of contact of two regions R_i the normal components of the field-strength belonging to them suffer a jump.

On the basis of this analogy limits (10) will be termed statistical thermodynamical complex potentials. According to Eq. (12), the specific expectation values

$$E_x = -\frac{\partial V}{\partial X} = \left\langle \frac{W}{X} \right\rangle \tag{21}$$

correspond to the normal components of the field-strength (in the points of intersection of the curves C with the x axis), where according to section 3 the normal points in the direction of the x axis.

The question may be asked of what corresponds in this formalism to the charge density q and the dielectric constant ε. Clearly, the expected value of any specific quantity may also be written in this way as a function of the intensive w:

$$\left\langle \frac{W}{X} \right\rangle = \frac{2t}{w\, Q(w)} \tag{22}$$

where only w may change, the values of X and J (or if J is extensive, J/X) are fixed numbers, and t is an arbitrarily chosen constant. With this the problem is only formally solved; the physical background is discussed in the following section.

6. Physical meaning of the analogy in terms of potential theory

Let us consider what has been said so far on a concrete example of a canonical assembly. The following quantities then appear in the general formalization of sections 3—5.

a) The given connection: exchange from the viewpoint of variation of E, and insulation with respect to that of N and V.

b) The characteristic variables of the phase integral: β, N and V.

c) The role of q is filled by the structure function $w(E, N, V)$ and the role of Q by the canonical phase integral $Z(\beta, N, V)$ in Eq. (8); in Eq. (7) K is the free energy.

d) Upon limit formation by Eq. (10), in the case of $X = N$ we obtain the specific free energy relating to the particle number, whereas in the case

of $X = V$ that relating to volume; in the former case $b = V/N$ and $J = V$, and in the latter case $J = N$ and $b = N/V$.

e) $-\left\langle \frac{W}{X} \right\rangle = \left\langle \frac{E}{N} \right\rangle$ or $-\left\langle \frac{E}{V} \right\rangle$, depending on the choice of X. In the following let us take the former case when $\left\langle \frac{E}{N} \right\rangle$ corresponds to the normal component of the field-strength. The dependence of this on β (for $b = N/V = = \text{const.}$) on the basis of (22) is:

$$\left\langle \frac{E}{N} \right\rangle = \frac{2t}{\beta \varphi(\beta)} \tag{23}$$

Because of (19), on crossing from a medium of higher dielectric constant to one of lower dielectric constant, this quantity is increased.

We know that according to the theory of equipartition, for a degree of freedom i (for one particle) the average thermal energy at temperature T is:

$$U_i = \left\langle \frac{E_i}{N} \right\rangle = \frac{kT}{2} = \frac{1}{2\beta} \tag{24}$$

However, this is only valid at high temperatures when

$$kT \gg A \tag{25}$$

where A is some number characterizing the distance between the energy levels for the degree of freedom in question. (Various energy level data can be found for example in the book of HERZBERG [19].) Otherwise, the average energy of the degree of freedom concerned $\langle E_i/N \rangle$ is smaller than this (in part it is 'frozen'). The difference is easily established for the usual models of statistical mechanics and this difference can be formally taken into consideration with a function $\varphi_i(\beta)$. Including the zero point energy U_{0i} too:

$$U_i(\beta) = \frac{1}{2\beta \varphi_i(\beta)} + U_{0i} \tag{26}$$

Thus, if a particle has f degrees of freedom, the total energy is:

$$U(\beta) = \sum_{i=1}^{f} \left[\frac{1}{2\beta \varphi_i(\beta)} \right] + U_{0i} \tag{27}$$

Now let us define a function

$$U(\beta) = \frac{f}{2\beta \varphi(\beta)} \tag{28}$$

On the basis of (27) and (28), $\varphi(\beta)$ can be obtained as follows:

$$\varphi(\beta) \overset{\text{def}}{=} \frac{1}{\sum_{i=1}^{f}\left[2U_{0i}\beta + \frac{1}{\varphi_i(\beta)}\right]} \tag{29}$$

If all this is used in Eq. (23), we obtain the following interpretation: $\varphi(\beta)$ corresponds to the dielectric constant, and $f/4$ to the charge density t.

Thus, in the canonical assembly we have obtained *via* the physical interpretation of the mathematical formalism that behind the LEE—YANG result derived with reasoning of a purely mathematical nature stands the physical meaning (at least in this case) that the character, number and position of the energy levels for the degrees of freedom are different in the individual phases. We shall deal briefly with this question too.

The heats of melting of simple substances are in most cases about kT [20—22]. Since the zero-point energies scarcely change in such cases, the heat of melting is turned in a decisive part to 'melting' of new degrees of freedom. Depending on the actual material, these are of a rotational or a translational character (the latter connected with the presence of 'common entropy') or appear in connection with the change of state of the electron shell [21].

All these changes cause the sudden decrease of the 'dielectric constant' defined in Eq. (29), that is the increase of the specific energy because of Eq. (23).

On boiling, however, the increase of the zero-point energy plays a decisive role. In this case $\varphi(\beta)$ decreases, *i.e.* the specific energy increases. We shall not deal in detail here with the changes occurring on boiling; we refer the reader instead to the book of FOWLER [22] for example.

As regards the other assemblies and changes of the expectation values of other specific extensives, considerations analogous to the above, combined with the analysis of the definition according to (22), lead to establishment of the actual meaning of the 'dielectric constant' and the charge. We shall not discuss this in detail now, but merely point to the fact that if we are concerned with something other than the expectation value of the energy, we can assume unit charge density along the z axis. For the pressure assembly, the function derivable from the virial series plays the role of the dielectric constant, which can be defined by the relation

$$\left\langle \frac{V}{N} \right\rangle = \frac{1}{(\beta P)\cdot\varphi(\beta P)} \tag{30}$$

whilst for the grandcanonical assembly, the function which can be derived from the fugacity series, and which can be defined by the relation

$$\left\langle \frac{N}{V} \right\rangle = \frac{1}{(\beta v) \cdot q(\beta v)} \tag{31}$$

On phase change, clearly these too suffer a discontinuous change.

7. Multicomponent systems and several interactions

Because of the considerable generality of the formalism used above, it is suitable for the statistical thermodynamical treatment of mixtures too. The generalization is fairly obvious. It is clear that the behaviour of a mixture of L components may be described by the introduction of a further $L-1$ chemical potentials v. It is expected that under such conditions the fact can be proved that the phase changes proceed in the entire sections of the positive axes of the corresponding intensives (*e.g.* the section between dew-point and bubble-point). In the one-component cases a study of the behaviour shown in complete polydimensional fields composed of sub-fields corresponding to the intensives would be necessary for several different interactions too (electric, magnetic, etc.), and for this likewise the formalism generalized in section 3 is suitable. After this the completely general treatment would follow for the case of physical interactions of arbitrary number and mixtures of an arbitrary number of components. With the application of suitable models and with the use of relations similar to (29), all these would make possible the use of modern statistical theory in the calculation of the phase-variable properties of more complex thermodynamic systems.

*

The author wishes to thank Prof. I. GYARMATI for his valuable advice, and J. GACS, Head of Department (Oil Design Bureau), for his help.

REFERENCES

1. TISZA, L.: Generalized Thermodynamics, MIT Press, Cambridge, Mass. 1966
2. SEMENCHENKO, V. K.: Izv. A. N. SSSR, Otdel. Khim. Nauk, **11**, 2047 (1959)
3. FÉNYES, I.: Thermostatics and Thermodynamics (In Hungarian), Műszaki Kiadó, Budapest, 1968
4. TEMPERLEY, H. N. V.: Changes of State, Pergamon, London, 1956
5. LEE, C. N., YANG, T. D.: Phys. Rev. **87**, 404 (1952)
6. LEWIS, M. B., SIEGERT, J. F.: Phys. Rev. **101**, 1227 (1956)
7. LEWIS, M. B.: Phys. Rev. **105**, 348, (1957)
8. JONES, P.: J. Math. Phys. **7**, 1800 (1966)
9. GROSSMANN, S.: Z. Physik **207**, 138 (1967)
10. HUANG, K.: Statistical Mechanics, Wiley and Sons, New York, 1963
11. LEE, C. N., YANG, T. D.: Phys. Rev. **87**, 410 (1952)
12. MEZEY, L.: On phase integrals of statistical thermodynamics (to be published)

13. KUBO, R.: Statistical Mechanics, North Holland, Amsterdam, 1965
14. HINCSIN, J.: Analytical Methods of Statistical Mechanics (In Hungarian), Akadémiai Kiadó, Budapest, 1951
15. ROUELLE, D.: Rigorous results in equilibrium statistical mechanics. Vol. I, p. l. In "Equilibrium theory of classical fluids", H. L. Frisch and J. L. Labowitz, Eds. Benjamin, New York, 1964
16. FENYŐ, I., FREY, T.: Mathematics for Electrical Engineers, II (In Hungarian), Műszaki Kiadó, Budapest, 1965
17. FRANK, P. H., MISES, R.: The Differential and Integral Equations of Mechanics and Physics, I—II, Műszaki Kiadó, Budapest, 1966—7
18. KORN, T., KORN, G.: Mathematical Handbook for Scientists and Engineers, McGraw-Hill, New York, 1961
19. HERZBERG, G.: Molecular Spectra and Molecular Structure (In Hungarian), Műszaki Kiadó, Budapest, 1957
20. ERDEY-GRŰZ, T., SCHAY, G.: Theoretical Physical Chemistry, I. Műszaki Kiadó, Budapest, 1962
21. UBBELOHDE, R.: Melting and Crystal Structure, Pergamon, Oxford, 1965
22. FOWLER, R., GUGGENHEIM, E. A.: Statistical Thermodynamics, Cambridge University Press, London, 1960

Lőrinc MEZEY; Budapest XI., Somlói ut 22.

Acta Chimica Academiae Scientiarum Hungaricae, Tomus 70 (1—2), pp. 23—39 (1971)

RADIATION CHEMISTRY OF SATURATED–UNSATURATED HYDROCARBON SYSTEMS, IV*

THE EFFECT OF CYCLIC STRUCTURE ON THE RADIATION-CHEMICAL HYDROGEN EVOLUTION FROM HYDROCARBONS WITH 5 TO 8 CARBON ATOMS

G. FÖLDIÁK and L. WOJNÁROVITS

(Institute of Isotopes of the Hungarian Academy of Sciences, Budapest)

Received May 8, 1970

The G_{H_2} values of mixtures of the C_5—C_8 alkanes (*n*-pentane, *n*-hexane, *n*-heptane, *n*-octane; cyclopentane, cyclohexane, cycloheptane, cyclooctane) with alkenes of the same carbon atom number (1-*n*-pentene, 1-*n*-hexene, 1-*n*-heptene, 1-*n*-octene; cyclopentene, cyclohexene, cycloheptene, cyclooctene), and also the G_{H_2} values of the pure components were determined.

The hydrogen evolution yields are strongly affected by the strain due to the ring structure in the cyclic hydrocarbons, and by the individual properties following from the structure of the molecules. When the G_{H_2} values were plotted as a function of the concentration of the unsaturated hydrocarbon, G_{H_2} values of mixtures containing an open-chain saturated hydrocarbon were smaller than the hydrogen evolution yields of saturated–unsaturated hydrocarbon mixtures containing a cyclic alkane. From kinetic calculations the explanation of the observed phenomenon is that, because of the ring strain, the monomolecular processes proceed more rapidly for the cycloalkanes than for the aliphatic alkanes, and so relatively less time is available for the participation of bimolecular processes of 'protection'.

The 'proctecting effect' towards a given saturated hydrocarbon depends on whether the other constituent is an aliphatic or a cyclic unsaturated hydrocarbon.

If the G_{H_2} values measured for the mixtures are plotted as a function of the 'double bond concentration' a reasonably common zone is given only in the case when the unsaturated hydrocarbon is an aliphatic one, while a well defined common curve is displayed only for *n*-alkane–1-*n*-alkene mixtures.

Conclusions were reached relating to the analogy of intermolecular and intramolecular protecting processes too.

1. Introduction

In many papers it is reported that the strain arising in cyclic hydrocarbons as a result of cyclization, and thus the structural properties which may be considered as individual for the molecules, strongly affect the chemical reactions and so the cyclic hydrocarbons of various carbon atom number differ in behaviour to a larger extent from one another than do the aliphatic hydrocarbons [1—6]. In this work we report on those studies in which we strived to compare the radiation-chemical hydrogen evolution processes of cycloalkanes and cyclomonoalkenes of carbon atom numbers 5—8 and the saturated–unsaturated hydrocarbon mixtures formed from them and containing hydrocarbons of the same carbon atom number; comparison was also made with the similar reactions of open-chain alkanes and terminal monoalkenes.

* Part III: Acta Chim. Acad. Sci. Hung. **69**, 177 (1971)

It is well known that the amount of hydrogen gas formed upon irradiation of saturated–unsaturated hydrocarbon mixtures (*e.g.* cyclohexane–cyclohexene [7—10], cyclohexane–benzene [7, 8, 11—13], methylcyclohexane–benzene [13]) is smaller than the amount expected by the assumption of simple additivity from the radiation-chemical yields of the pure components. The difference from the linear mixing rule is explained by the 'protecting effect' of the unsaturated component. This is assumed to consist of two main parts: the transfer of energy from the saturated to the unsaturated hydrocarbons, and secondly the radical capture reactions between the double bonds and the H· atoms formed as intermediates in hydrogen formation.

Table I

G_{H_2} values of the pure hydrocarbons

Alkane	G_{H_2}*	Alkene	G_{H_2}**
cyclopentane	5.1	cyclopentene	1.27
cyclohexane	5.3	cyclohexene	1.26
cycloheptane	5.7	cycloheptene	1.03
cyclooctane	5.9	cyclooctene	0.91
n-pentane	5.0	1-*n*-pentene	0.87
n-hexane	5.2	1-*n*-hexene	0.91
n-heptane	5.1	1-*n*-heptene	0.94
n-octane	5.3	1-*n*-octene	1.01

* $\pm$ 0.1
** $\pm$ 0.03

2. Experimental

For the purposes of our studies hydrocarbons produced by Merck and Fluka were used. According to the data of the respective catalogues, apart from cyclooctane which was of about 98% purity, the purity of the saturated hydrocarbons was better than 99% while all unsaturated hydrocarbons contained less than 5% impurities. All of the compounds were subjected to appropriate further purification.

The saturated hydrocarbons were shaken with an equal volume of concentrated sulfuric acid for 48 hours at room temperature to remove possible unsaturated impurities, the sulfuric acid being changed every 3—4 hours by means of a separation funnel.

Immediately before use both the saturated and the unsaturated hydrocarbons were distilled from metallic sodium and the corresponding purity checked by capillary gas chromatographic analysis.

The irradiation of the samples was carried out in Rasotherm glass ampoules of 30 cm^3 volume which were approximately half-filled with 12 ± 2 g of hydrocarbon, or of a hydrocarbon mixture, weighed to an accuracy of ± 0.05 g. Before the ampoules were sealed they were evacuated at the temperature of liquid air (final pressure: 10^{-5} mmHg).

The irradiation was carried out in the Institute of Isotopes of the Hungarian Academy of Sciences with a ^{60}Co radiation source [14] of 80,000 Ci nominal activity at 35 ± 3 °C with a dose rate of 2.2 Mrad per hour. The integral dosage was 4.4 Mrad.

After irradiation the ampoules were opened in turn in a closed space and the products not condensed at the temperature of liquid air were collected with a Toepler pump and analyzed gas-chromatographically.

The dose necessary for the determination of the radiation-chemical yield for the hydrogen evolution, G_{H_2}, was obtained with alcoholic chlorobenzene dosimetry, since because of the high dose rate and the design of the radiation source it was not practicable to use the standard Fricke method [15]. Numerous studies were carried out in our laboratory on the applicability of the alcoholic chlorobenzene method, and for relatively small doses they were also carefully checked with the Fricke dosimeter [16].

The G_{H_2} values of the mixtures were determined with one measurement for each composition and with several (in general, three) parallel measurements for the pure components.

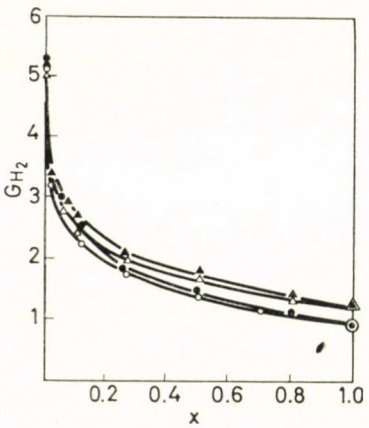

Fig. 1. G_{H_2} *vs. x* curves for C_5 mixtures. *x*, the mole fraction of unsaturated hydrocarbon →. ○ *n*-pentane–1-*n*-pentene, ● cyclopentane–1-*n*-pentene, △ *n*-pentane–cyclopentene, ▲ cyclopentane–cyclopentene

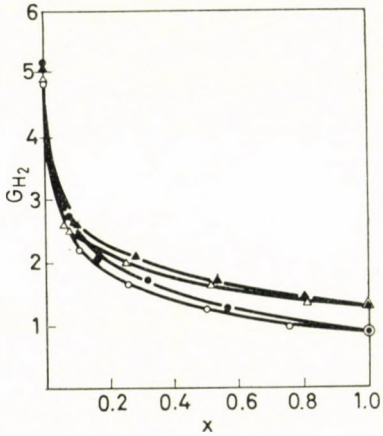

Fig. 2. G_{H_2} *vs. x* curves for C_6 mixtures. *x*, the mole fraction of unsaturated hydrocarbon →. ○ *n*-hexane–1-*n*-hexene, ● cyclohexane–1-*n*-hexene, △ *n*-hexane–cyclohexene, ▲ cyclohexane–cylohexene

In such a way the G_{H_2} values measured for the mixtures were obtained with accuracies of $\pm 4\%$ and those of the pure components with $\pm 2\%$, respectively.

The G_{H_2} values of the alkanes and alkenes studied are given in Table I, while the data for the saturated–unsaturated hydrocarbon mixtures containing members with identical carbon atom numbers are shown in Figs 1—4. The G_{H_2} data for the hydrocarbons of carbon atom numbers 5, 6, 7 and 8, and for their mixtures, are to be found in Figs 1, 2, 3 and 4, respectively.

3. Experimental results

3.1. *Radiation-chemical hydrogen evolution yields for the pure hydrocarbons*

It is obvious from Table I that while the G_{H_2} values of the pure open-chain saturated hydrocarbons (well known from the literature) barely differ from each other [17], the yield values of the cycloalkanes of carbon atom numbers 5—8 increase with increasing carbon atom numbers of the ring and the G_{H_2} values for cycloheptane and cyclooctane are already greater than those of the corresponding open-chain hydrocarbons. In numerous experi-

ments it was checked that the relatively significant differences are not caused by experimental error. FREEMAN and STOVER have also arrived at a similar conclusion. In connection with the extrapolated G_{H_2} values for zero irradiation doses of cyclopentane and cyclohexane (5.4 and 5.6), they found that these increase with increasing carbon atom number of the ring [18].

The radiation-chemical hydrogen evolution yields of the cycloalkenes too take a different shape relative to those of the open-chain 1-*n*-alkenes.

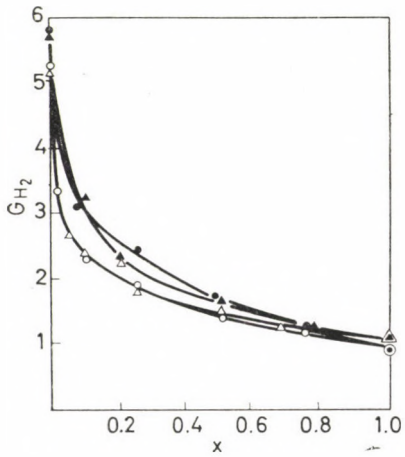

Fig. 3. G_{H_2} *vs. x* curves for C_7 mixtures. *x*, the mole fraction of unsaturated hydrocarbon →. ○ *n*-heptane–1-*n*-heptene, ● cycloheptane–1-*n*-heptene, △ *n*-heptane–cycloheptene, ▲ cycloheptane–cycloheptene

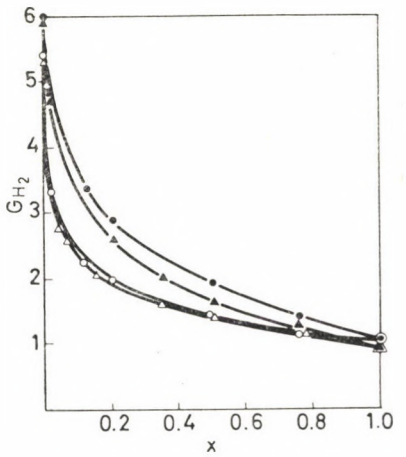

Fig. 4. G_{H_2} *vs. x* curves for C_8 mixtures. *x*, the mole fraction of unsaturated hydrocarbon →. ○ *n*-octane–1-*n*-octene, ● cyclooctane–1-*n*-octene, △ *n*-octane–cyclooctene, ▲ cyclooctane–cyclooctene

While G_{H_2} increases to a small extent with increasing carbon atom number for the aliphatic alkenes, it decreases for the cycloalkenes in the order cyclopentene $\geqslant$ cyclohexene $>$ cycloheptene $>$ cyclooctene.

3.2. G_{H_2} *values of the mixtures*

Figs 1—4 show the measured G_{H_2} values plotted as a function of the mole fractions. It can be seen that the mixture systems studied do not follow the linear mixing rule written for mole fractions. A similar result is obtained if the G_{H_2} values are plotted as a function not of mole fractions but of electron fractions (the differences between the mole fractions and the electron fractions in the mixture systems studied are only small).

The difference in the G_{H_2} values which can be calculated from the linear mixing rule and those found by measurement clearly shows the interaction, called 'protecting action' in the literature occurring during irradiation between the components of the mixtures studied.

The extent of the interaction strongly depends on the structures of the partners concerned. The curves shown in Figs 1—4 differ depending on whether an unsaturated hydrocarbon is mixed with a saturated open-chain hydrocarbon or with a saturated cyclic hydrocarbon of the same carbon atom number. The G_{H_2} curves of the mixtures containing the cyclic saturated hydrocarbon in general lie above the curves relating to the corresponding open-chain hydrocarbons. This difference appears particularly for the 7 and 8 carbon atom cyclic saturated hydrocarbons, while it is barely observable in the case of the 5 and 6 carbon atom rings.

From Figs 1—4 it is difficult to arrive at a definite conclusion as to whether a given unsaturated hydrocarbon has a more pronounced protecting effect in its mixture with the saturated open-chain or with the saturated cyclic hydrocarbon of the same carbon atom number. It is true though that the higher G_{H_2} values refer in all cases to the curves of the mixtures containing the cyclic saturated hydrocarbon rather than to the curves of the corresponding aliphatic saturated hydrocarbons: at the same time, however, the G_{H_2} values of the pure cyclic saturated hydrocarbons are also greater in all cases than those of the corresponding open-chain saturated hydrocarbons.

More clear-cut conclusions can be reached if the concept of '*the extent of the protecting effect*' is introduced. By this is understood the ratio of the hydrogen evolution yield calculated from the linear mixing rule written for electron fractions to that determined from the measurements:

$$\Phi = \frac{e_A G_{H_2,A} + e_E G_{H_2,E}}{G_{H_2}}$$

(If irradiation should not lead to any interaction between the components of the mixtures studied, the value of the fraction would be independent of the concentration and Φ would be equal to 1.)

From the Φ *vs.* x curves in Figs 5—8 it can be seen that in all the cases studied *an unsaturated hydrocarbon exerts a more pronounced protecting action on the open-chain saturated hydrocarbon* of the same carbon atom number than on the saturated cyclic hydrocarbon.

If a given saturated hydrocarbon is mixed with an open-chain or cyclic unsaturated hydrocarbon it appears that for C_5 and C_6 hydrocarbons the protecting effect of 1-*n*-alkenes is greater than that of the corresponding cyclic alkenes, at the same time, however, for the C_7 and C_8 hydrocarbons the protecting action is more pronounced for the cyclic unsaturated hydrocarbons.

An interesting conclusion is obtained if the Φ *vs.* x curves (Fig. 9) of *n-alkane–*1-*n-alkene* mixtures containing merely open-chain hydrocarbons are compared with the curves for the other hydrocarbon mixtures [cycloalkane–1-*n*-alkene (Fig. 10), *n*-alkane–cycloalkene (Fig. 11), cycloalkane–

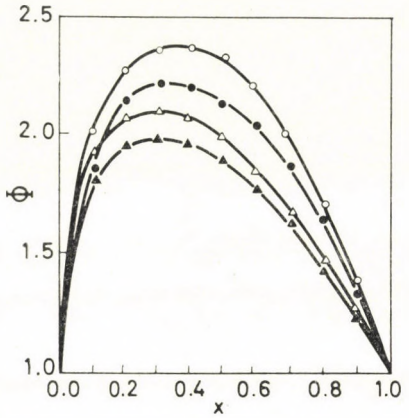

Fig. 5. Φ vs. x curves for C_5 mixtures. *x*, the mole fraction of unsaturated hydrocarbon →. ○ *n*-pentane–1-*n*-pentene, ● cyclopentane–1-*n*-pentene, △ *n*-pentane–cyclopentene, ▲ cyclopentane–cyclopentene

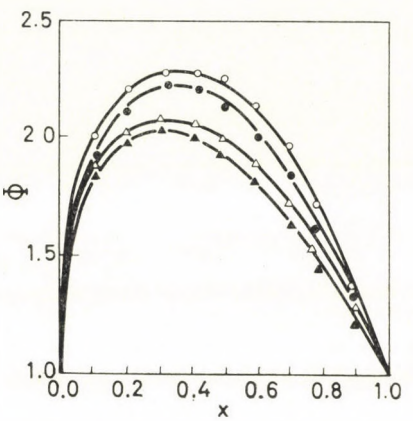

Fig. 6. Φ vs. x curves for C_6 mixtures. *x*, the mole fraction of unsaturated hydrocarbon →. ○ *n*-hexane–1-*n*-hexene, ● cyclohexane–1-*n*-hexene, △ *n*-hexane–cyclohexene, ▲ cyclohexane–cyclohexene

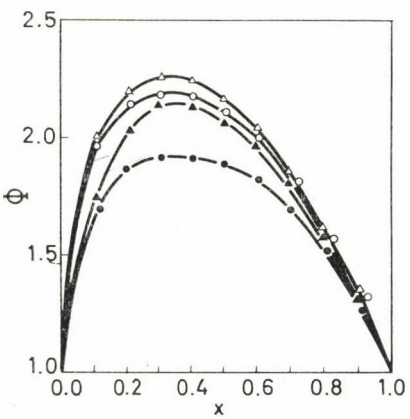

Fig. 7. Φ vs. x curves for C_7 mixtures. *x*, the mole fraction of unsaturated hydrocarbon →. ○ *n*-heptane–1-*n*-heptene, ● cycloheptane–1-*n*-heptene, △ *n*-heptane–cycloheptene, ▲ cycloheptane–cycloheptene

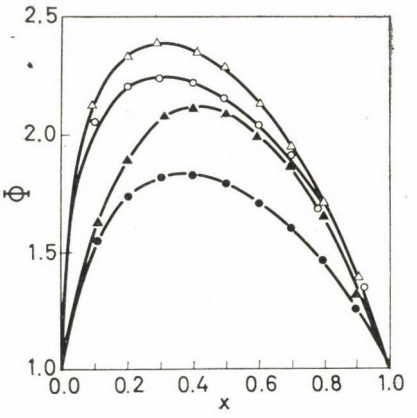

Fig. 8. Φ vs. x curves for C_8 mixtures. *x*, the mole fraction of unsaturated hydrocarbon →. ○ *n*-octane–1-*n*-octene, ● cyclooctane–1-*n*-octene, △ *n*-octane–cyclooctene, ▲ cyclooctane–cyclooctene

cycloalkene (Fig. 12)]. It can be seen that only the corresponding curves of the *n*-alkane–1-*n*-alkene systems agree approximately; this points to the fact that the interactions in these mixtures are roughly of the same nature and extent.

In previous works we reported on studies carried out under other experimental conditions. If the G_{H_2} values for the pure alkenes and for mixtures containing an *n*-alkane and a 1-*n*-alkene or a diene with isolated double bonds were plotted as a function of the 'double bond concentration' *y* defined by us

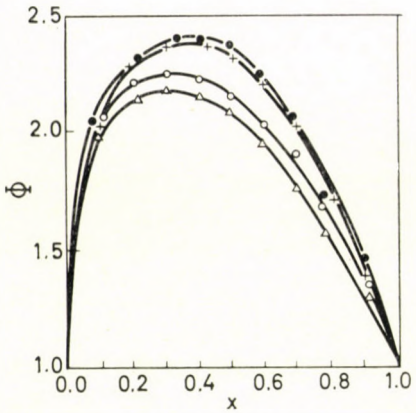

Fig. 9. Φ *vs.* x curves for aliphatic alkane–aliphatic alkene mixtures. x, the mole fraction of unsaturated hydrocarbon →. + *n*-pentane–1-*n*-pentene, ● *n*-hexane–1-*n*-hexene, △ *n*-heptane–1-*n*-heptene, ○ *n*-octane–1-*n*-octene

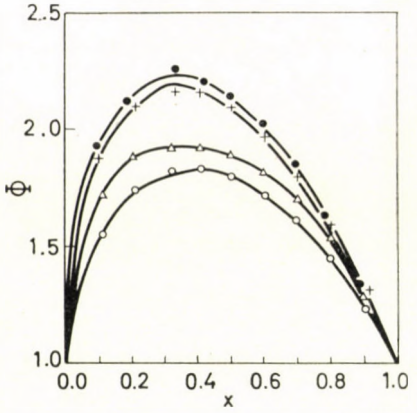

Fig. 10. Φ *vs.* x curves for cyclic alkane–aliphatic alkene mixtures. x, the mole fraction of unsaturated hydrocarbon →. + cyclopentane–1-*n*-pentene, ● cyclohexane–1-*n*-hexene, △ cycloheptane–1-*n*-heptene, ○ cyclooctane–1-*n*-octene

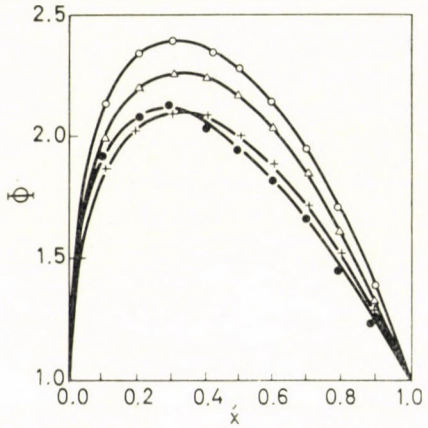

Fig. 11. Φ *vs.* x curves for aliphatic alkane–cyclic alkene mixtures. x, the mole fraction of unsaturated hydrocarbon →.+ *n*-pentane–cyc'opentene, ● *n*-hexane–cyclohexene, △ *n*-heptane–cycloheptene, ○ *n*-octane–cyclooctene

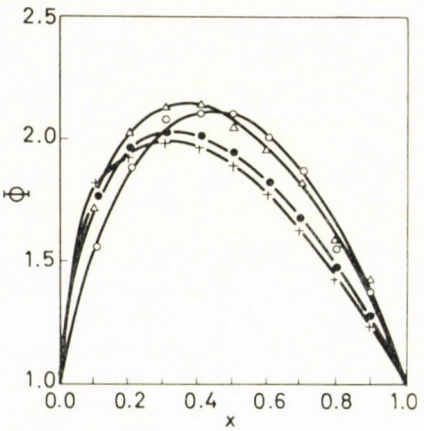

Fig. 12. Φ *vs.* x curves for cyclic alkane–cyclic alkene mixtures. x, the mole fraction of unsaturated hydrocarbon →. + cyclopentane–cyclopentene, ● cyclohexane–cyclohexene, △ cycloheptane–cycloheptene, ○ cyclooctane–cyclooctene

(the formal π-bond number in 1 g of sample), a common curve was obtained [7, 19]. A similar conclusion was reached in the present study (Fig. 13). Also shown in the Figure are the points for *n*-octane–1,7-*n*-octadiene reported in our previous paper, and the G_{H_2} values for 1-*n*-hexadecene [20] and 1-*n*-butene [21] measured by other authors. The average curves obtained in the

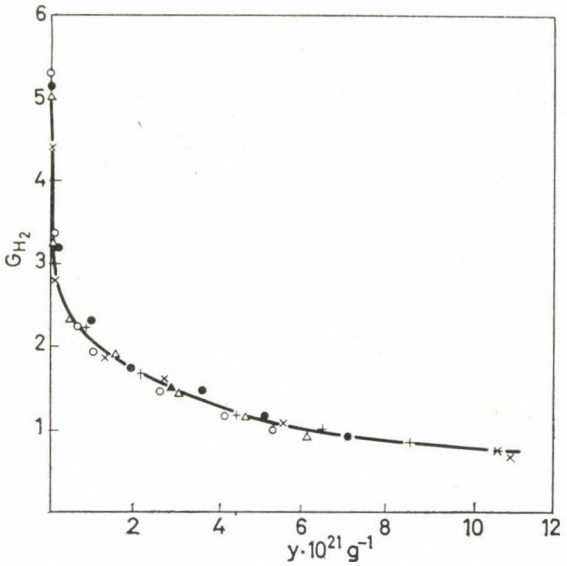

Fig. 13. G_{H_2} values of aliphatic alkane–aliphatic alkene mixtures as a function of y, the 'double bond concentration'. $y \times 10^{21}\ g^{-1}$, the double bond number in 1 g of mixture →. + *n*-pentane–1-*n*-pentene, ● *n*-hexane–1-*n*-hexene, △ *n*-heptane–1-*n*-heptene, ○ *n*-octane–1-*n*-octene, × *n*-octane–1,7-*n*-octadiene [7], ▲ 1-*n*-hexadecene [20], ✳ 1-*n*-butene [21]

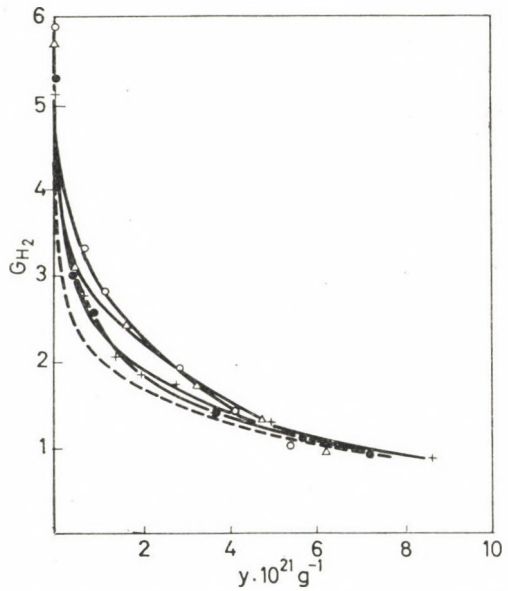

Fig. 14. G_{H_2} values of cyclic alkane–aliphatic alkene mixtures as a function of y, the 'double bond concentration'. $y \times 10^{21}\ g^{-1}$, the double bond number in 1 g of mixture →. + cyclopentane–1-*n*-pentene, ● cyclohexane–1-*n*-hexene, △ cycloheptane–1-*n*-heptene, ○ cyclooctane–1-*n*-octene

earlier and the present studies (the solid curve in Fig. 13) coincide. It appears that the observed phenomenon is a fairly general property of mixtures of open-chain (terminal) monoalkenes and isolated dienes with open-chain saturated hydrocarbons.

The Φ *vs.* x curves of individual cycloalkane–1-*n*-alkene mixtures differ significantly from each other (Fig. 10); at the same time, the G_{H_2} *vs.* y curves are not identical either (Fig. 14). In the latter Figure the curve characteristic of *n*-alkane–1-*n*-alkene mixtures is drawn as a dashed line. Thus, at the same

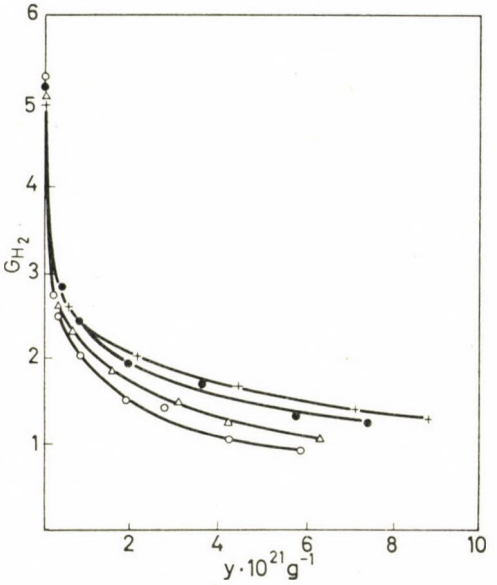

Fig. 15. G_{H_2} values of aliphatic alkane–cyclic alkene mixtures as a function of y, the 'double bond concentration'. $y \times 10^{21}\ g^{-1}$, the double bond number in 1 g of mixture →. + *n*-pentane–cyclopentene, ● *n*-hexane–cyclohexene, △ *n*-heptane–cycloheptene, ○ *n*-octane–cyclooctene

'double bond concentrations' somewhat greater G_{H_2} values relate to mixtures containing a cyclic saturated hydrocarbon than in the case of open-chain saturated hydrocarbon mixtures; this points to a less effective protecting action. According to this, in the radiolysis of their mixtures with unsaturated hydrocarbons the individual cycloalkanes behave differently compared with open-chain molecules; their decomposition leading to the evolution of hydrogen is suppressed less by the double bonds than is that of the normal alkanes.

Significant differences may be observed in the Φ *vs.* x (Figs 11 and 12) and G_{H_2} *vs.* y (Figs 15 and 16) curves for individual open-chain alkane–cyclic alkene and cyclic alkane–cyclic alkene mixtures. With increasing number

of carbon atoms, the G_{H_2} *vs.* y curves for open-chain alkane-cyclic alkene mixtures are displaced towards lower G_{H_2} values; as may be found from Fig. 11, the extent of the protecting action in mixtures of carbon atom numbers 7 and 8 exceeds that observed for mixtures of carbon atom numbers 5 and 6, but at the same time is greater than those observed for aliphatic alkenes (Figs 7 and 8).

The G_{H_2} *vs.* y curves for individual *cyclic alkane–cyclic alkene mixtures* intersect each other, corresponding to the change of the G_{H_2} values of the

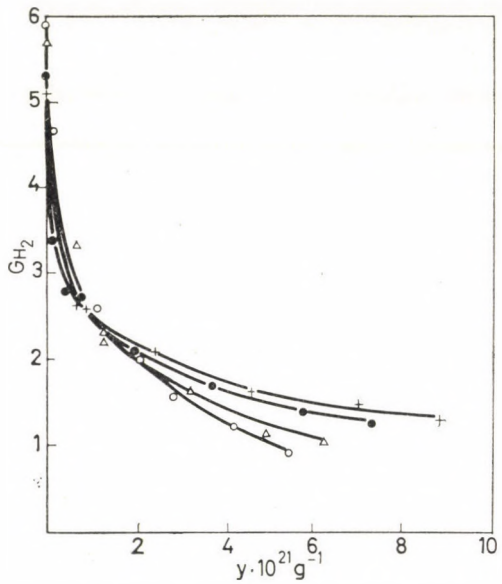

Fig. 16. G_{H_2} values of cyclic alkane–cyclic alkene mixtures as a function of y, the 'double bond concentration'. $y \times 10^{21}$ g^{-1}, the double bond number in 1 g of mixture →. + cyclopentane–cyclopentene, ● cyclohexane–cyclohexene, △ cycloheptane–cycloheptene, ○ cyclooctane–cyclooctene

pure components, at an intermediate concentration value. If the relatively small unsaturated concentrations are disregarded, the extent of the protecting action in C_7 and C_8 mixtures is greater than for C_5 and C_6, similarly to the result for the previous groups.

As has already been considered in detail with regard to Figs 14—16, the '*reducibility to one curve*' observed for mixtures of *n*-alkenes with *n*-alkanes is not found for the G_{H_2} *vs.* y curves of alkane–alkene mixtures containing cyclic hydrocarbons, although the cycloalkane–1-*n*-alkene system does not differ significantly from this.

It follows from the above that both the G_{H_2} values of the pure cycloalkanes and pure cycloalkenes studied, and the behaviour of these shown in

saturated–unsaturated hydrocarbon mixtures, differ from those observed for the pure *n*-alkanes and pure *n*-alkenes and their mixtures, and depend on the carbon atom number; this points to the different behaviour of the individual cyclic hydrocarbons, and to differences in the relative rates of their reactions.

4. Discussion of the results

In the first paper of this series [22], it has already been reported that radiation-chemical hydrogen formation from saturated–unsaturated hydrocarbon mixtures occurs (according to more or less uniform findings in the relevant literature) in bimolecular reactions with the intervention of hydrogen atoms, and the hydrogen formation said to be monomolecular is also *partially* a result of fast hydrogen atom reactions [21, 23—30]. The assumed individual reactions are the following (the saturated molecules are denoted by A and the unsaturated by E):

$A \xrightarrow{\sim\sim} A^x$	(OA)
$E \xrightarrow{\sim\sim} E^x$	(OE)
$A^x \longrightarrow A$ or $A_1 + A_2$	(p)
$E^x \longrightarrow E$ or $E_1 + E_2$	(q)
$A^x \longrightarrow E_A + H_2$	(m)
$E^x \longrightarrow E_B + H_2$	(n)
$A^x \longrightarrow A\cdot + H\cdot$	(s)
$E^x \longrightarrow E\cdot + H\cdot$	(t)
$A^x + E \longrightarrow A + E^x$	(r)
$H\cdot + A \longrightarrow A\cdot + H_2$	(u)
$H\cdot + E \longrightarrow E\cdot + H_2$	(v)
$H\cdot + E \longrightarrow EH\cdot$	(z)

where: A^x and E^x are the excited and ionized molecules formed during the interaction between radiation and matter;

A_1, A_2, E_1 and E_2 are the hydrocarbon radicals (or radical ions) formed by C—C bond rupture; E_A and E_E are the unsaturated molecules (or molecular ions) formed after the loss of a hydrogen molecule from the saturated or unsaturated molecules, respectively;

$A\cdot$ and $E\cdot$ are the saturated or unsaturated hydrocarbon radicals (or radical ions) deprived of one atom of $H\cdot$;

$EH\cdot$ is the semi-hydrogenated hydrocarbon radical. The above reaction possibilities are summarized in Fig. 17. The following remarks apply to the Figure.

(i) The terms written above the individual arrows represent the reaction rates of the relevant processes.

(ii) The 'molecular hydrogen evolution' processes [(m) and (n)] are not shown in the Figure on the strong debatable assumption that the molecular processes are considerably less important than the radical ones;

(iii) The reactions of the saturated hydrocarbons which lead to the rupture of the C—C bonds and to the loss of energy without decomposition accord-

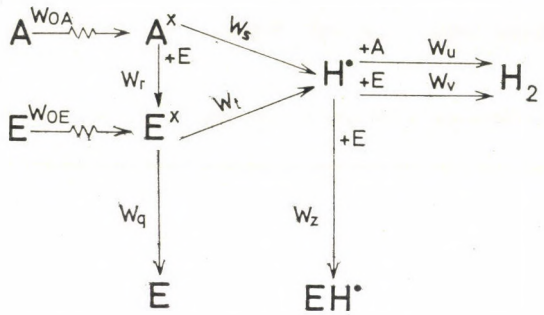

Fig. 17. Proposed hydrogen formation scheme

ing to Eq. (p) do not significantly affect the quasi-stationary concentrations of the reactants that should be considered in the calculations concerning hydrogen evolution.

With the above assumptions, using statistical probabilities in the estimation of the reactions between hydrogen atoms and hydrocarbons, with the help of optimization computer procedures some combinations of reaction rate constants for the hydrogen evolution processes (shown in Table II, columns 3—5) were calculated; these are regarded as characteristic. Our present calculations were carried out using the $\Theta(x)$ functions* reported earlier [31]. The k values in the Table are the appropriate reaction rate constants and the (c)'s are the total molar concentrations of the A and E components with dimensions (mole · lit^{-1}).

* The $\Theta(x)$ function was defined by the relation

$$\Theta(x) = \frac{e_A \, G_{H_2,A}}{G_{H_2}}$$

where:

e_A is the concentration of component A expressed in electron fraction;
$G_{H_2,A}$ is the hydrogen formation yield from pure component A;
G_{H_2} is the measured radiation-chemical yield for the mixture.

Table II

Combination of some characteristic rate constants of the studied saturated–unsaturated hydrocarbon mixtures

Mixture	$\frac{k_r}{k_s}(c)$	$f=\frac{k_t}{k_t+k_q}$	$\frac{k_x}{k_u}$	average f
n-pentane–1-*n*-pentene	29.8±1.5	0.36±0.02	0.50±0.02	0.35
cyclopentane–1-*n*-pentene	25.8±2.0	0.35±0.015	0.50±0.02	
n-pentane–cyclopentene	35.6±2.0	0.39±0.02	0.43±0.02	0.40
cyclopentane–cyclopentene	30.0±1.0	0.40±0.02	0.44±0.02	
n-hexane–1-*n*-hexene	27.0±1.5	0.35±0.01	0.50±0.02	0.35
cyclohexane–1-*n*-hexene	24.2±.10	0.35±0.02	0.48±0.02	
n-hexane–cyclohexene	35.4±1.8	0.39±0.02	0.43±0.02	0.40
cyclohexane–cyclohexene	29.7±1.8	0.40±0.03	0.46±0.02	
n-heptane–1-*n*-heptene	33.8±2.2	0.38±0.02	0.51±0.02	0.39
cycloheptane–1-*n*-heptene	22.7±1.6	0.40±0.03	0.54±0.03	
n-heptane–cycloheptene	34.2±2.0	0.35±0.02	0.50±0.02	0.35
cycloheptane–cycloheptene	19.5±0.8	0.35±0.02	0.48±0.02	
n-octane–1-*n*-octene	33.2±2.0	0.38±0.02	0.50±0.03	0.39
cyclooctane–1-*n*-octene	15.6±0.7	0.40±0.02	0.50±0.02	
n-octane–cyclooctene	32.2±2.0	0.31±0.01	0.50±0.02	0.30
cyclooctane–cyclooctene	10.2±0.6	0.30±0.01	0.46±0.02	

The following more important conclusions arise from these calculations.

The results support our assumption that in the hydrocarbon mixtures shown in Figs 1—4 the radiation-chemical hydrogen evolution proceeds predominantly according to the given hydrogen evolution scheme, *i.e.* the deviation of the G_{H_2} values from the linear mixing rule is the result *both of energy transfer reactions* from the saturated to the unsaturated hydrocarbons, *and of hydrogen atom capture reactions* by the unsaturated hydrocarbons.

It was found above that an unsaturated hydrocarbon exerts a greater protecting effect in its mixture with the open-chain saturated hydrocarbon with the same carbon atom number than in its mixture with the cyclic hydrocarbon. This is supported by the fact that in the mixtures containing the same unsaturated hydrocarbons in Table II, in all cases smaller $\frac{k_r}{k_s}(c)$ values refer to the cycloalkane systems than to the open-chain alkane–alkene mixtures. On the basis of the scheme in Fig. 17, this means that the differences in the protecting action (otherwise following logically from the Φ *vs.* x curves [Figs 5—8)] are attributable to the fact that the energy transfer from the cyclo-

alkane to the aliphatic and cyclic alkenes proceeds with a smaller efficiency relative to the monomolecular decomposition in the mixtures containing cycloalkanes than for the open-chain hydrocarbons. The probable explanation of this is that *because of the strain in the rings* the monomolecular decomposition processes for the cycloalkanes are faster than for the open-chain alkanes and so a relatively *smaller time is available* for bimolecular energy transfer reactions.

In the rate of the monomolecular processes of cycloalkanes, *e.g.* of the reaction according to Eq. (s), a fundamental factor may be the energy requirement of the reaction or, related to this, the energetic stability of the cycloalkyl radical formed during the reaction. In a study of chain reactions (*e.g.* photosulfochlorination) requiring the participation of various cycloalkyl radicals, it was found that the reactivity of the cycloalkanes, and also the energetic stability of the radicals necessary for initiation and propagation of the chain reaction, increases in the order cyclohexane $\approx$ cyclopentane $<$ cycloheptane $<$ cyclooctane [2—4]; this may be paralleled with our observation that the difference in the G_{H_2} *vs.* x and Φ *vs.* x curves for the mixtures containing the open-chain and the cyclic saturated hydrocarbons is most observable in the case of mixtures of C_7 and C_8 hydrocarbons.

From a consideration of the data in Table II, column 3, it may be stated that the $f = \dfrac{k_t}{k_t + k_q}$ *values of mixtures, containing the same unsaturated hydrocarbon*, in boxes separated by a continuous and a dashed line do not differ significantly from each other. Such an agreement of the f values is obvious since on the basis of the reaction scheme in Fig. 17 they are characteristic of the individual unsaturated hydrocarbons. The averaged f values of the various hydrocarbons are to be found in Table II, column 5.

Because of the relatively large imprecision of, and the small differences between the values of the f data in the Table, it is difficult to reach generalizing conclusions. It may be seen, however, that while the f values for the open-chain unsaturated hydrocarbons studied scarcely differ from each other and are not clearly connected with the length of the carbon chain, the differences between these data for the individual cycloalkenes are more significant: the $f = \dfrac{k_t}{k_t + k_q}$ values decrease with increasing carbon atom number of the hydrocarbon rings studied, just as has already been found in the evaluation of the G_{H_2} data. This means therefore that with the increase of the carbon atom number in the cycloalkene ring the relative rate of the reactions leading to hydrogen atom formation, as in Eq. (t), decreases slightly.

Having exposed cycloalkenes to the effect of thermal oxidation under 'mild' conditions, VAN SICKLE et al. observed that the hydrogen atoms of these hydrocarbons may be split off with increasing rate, *i.e.* probability, in the

order cyclooctene < cycloheptene < cyclohexene < cyclopentene [5]. This order corresponds to the order of G_{H_2} and f values observed by us.

The mentioned authors explain the observed phenomenon by the fact that with the removal of one H· atom from cyclopentene or cyclohexene, the structures of which are the closest to planar, there is a possibility for the formation of an allyl type radical which is energetically favourable being closer to the planar structure in which the energy of interaction (resonance energy) of the electrons in the double bond with the unpaired electron of the hydrocarbon radical decreases the energy requirements of the processes leading to hydrogen evolution. On the other hand the structures of cycloheptene and cyclooctene, and also of the radicals formed from them by the removal of a H. atom, differ significantly from planar; as a consequence of the more unfavourable spatial arrangement this leads to a decrease in the resonance energy and also to the fact that the energy necessary for the separation of each hydrogen atom from these cycloalkenes increases [5, 32].

Considering the combinations of rate constants characteristic of the *n*-alkane–1-*n*-alkene mixtures, it may be concluded from Table II that the values corresponding to the individual mixtures differ from each other merely slightly, but in the case of mixtures containing a cyclic hydrocarbon they generally depend significantly on the carbon atom number. This agrees with our earlier finding that while the properties of the hydrocarbons of various carbon atom numbers shown in mixtures are similar for systems containing open-chain hydrocarbons (*n*-alkane–1-*n*-alkene), they are different for mixtures containing a cyclic hydrocarbon.

Our results allow a further interesting conclusion regarding the energy transfer conditions. The energy excess given to the molecules by the radiation, which causes their excitation and/or ionization, can move further either from molecule to molecule, *i.e.* intermolecularly, or within the molecule, *i.e.* intramolecularly. According to general observations, the gross energy transfer is directed towards positions of lower excitational and ionization energy, in the present case the terminal double bonds. Earlier, the question of intermolecular energy transfer was studied essentially in the treatment of our kinetic calculations based on the hydrogen formation scheme of Fig. 17. However, on the basis of literature analogies (*e.g.* observations in the study of alkyl-benzenes [33—35]), the possibility of intramolecular energy transfer directed to the part containing the π bonds from the saturated part of the alkene hydrocarbons must also be considered.

The facts that the G_{H_2} values for the *n*-alkane–1-*n*-alkene mixtures and for the pure 1-*n*-alkenes lie on one and the same curve on the G_{H_2} *vs.* y diagram (Fig. 13), and that the G_{H_2} value of *e.g.* 1-*n*-hexadecene agrees within experimental error with the G_{H_2} value for the mixture of *n*-octane and 1-*n*-octene in a 1 : 1 mole ratio, indicate that the efficiency of intramolecular energy trans-

fer cannot exceed considerably the efficiency of intermolecular energy transfer.

Naturally the result obtained should not be attributed solely to the energy transfer reactions; the other factor contributing to the G value must also be considered, *viz.* the radical capture reactions between the double bonds and hydrogen atoms formed during the radiolysis. As a consequence of the foregoing, it may be assumed that the radical capture properties of the various 1-*n*-alkenes are roughly the same. This picture fits well with what has already been said; the G_{H_2} values on the G_{H_2} *vs.* *y* diagrams (Fig. 13) of aliphatic alkane–aliphatic alkene mixtures and of the pure 1-*n*-alkenes fall into the same curve which is a result of the similar energy transfer and radical capture properties of double bonds of the same type.

According to our data it is also debatable whether truly non-identical reaction steps are involved in the so-called 'intramolecular' and 'intermolecular' protection, *i.e.* whether during the interaction of the radiation and the substance the energy primarily situated in the saturated 'hydrocarbon chain section' of the monoalkenes arrives decisively in the π-bond 'energy trap' of its own molecule or that of a 'neighbouring' molecule, and whether in the radical capture reactions of the hydrogen atoms formed by breaking of the C—H bonds a π-bond in its own molecule means a greater radical capture possibility than does a π-bond of perhaps more favourable geometrical arrangement in a 'neighbouring' molecule.

It is hoped to obtain answers to these questions in our further work.

REFERENCES

1. Turner, R. B., Meador, W. R.: J. Am. Chem. Soc. **79,** 4133 (1957)
2. Huyser, E. S., Schimke, H., Burham, R.: J. Org. Chem. **28,** 2141 (1963)
3. Russel, G. A.: J. Am. Chem. Soc. **80,** 4997 (1958)
4. Overberger, C. G., Biletch, A. B., Finestone, A. B. Lilker, J.; Herbert, J.: J. Am. Chem. Soc. **75,** 2078 (1963)
5. Van Sickle, D. E., Mayo, F. R., Arluck, R. M.: J. Am. Chem. Soc. **87,** 4824 (1965)
6. Gresser, J., Rajbenbach, A., Szwarc, M.: J. Am. Chem. Soc. **83,** 3005 (1961)
7. Wojnárovits, L., Földiák, G.: Acta Chim. Acad. Sci. Hung. **67,** 221 (1971)
8. Manion, J. P., Burton, M.: J. Phys. Chem. **56,** 560 (1952)
9. Freeman, G. R.: Canad. J. Chem. **38,** 1043 (1960)
10. Cramer, W. A., Piet, G. S.: Trans. Faraday Soc. **63,** 1402 (1967)
11. Dyne, P. J., Jenkinson, W. M.: Canad. J. Chem. **39,** 2163 (1961)
12. Freeman, G. R.: J. Chem. Phys. **33,** 71 (1960)
13. Merklin, J. F., Lypsky, S.: J. Phys. Chem. **68,** 3297 (1964)
14. Hirling, J., Stenger, V.: Energia és atomtechnika **22,** 466 (1969)
15. ASTM D 1671—63 Absorbed Gamma Radiation Dose in the Ficke Dosimeter (USA standard)
16. Horváth, Zs., Bányai, É., Földiák, G.: Radiochim. Acta **13,** 150 (1970)
17. Dewhurst, H. A.: J. Phys. Chem. **61,** 1466 (1957)
18. Freeman, G. R., Stover. E. D.: Canad. J. Chem. **46,** 3235 (1968)
19. Földiák, G., Cserép, Gy., Stenger, V., Wojnárovits, L.: Kém. Közl. **31,** 415 (1969)
20. Collinson, E., Dainton, F. S., Walker, D. C.: Trans. Faraday Soc. **57,** 1732 (1961)

21. HATANO, Y. SHIDA, S.: J. Chem. Phys. **46,** 4784 (1967)
22. FÖLDIÁK, G. WOJNÁROVITS, L.: Acta Chim. Acad. Sci. Hung. **67,** 209 (1971)
23. HARDWICK, T. J.: J. Phys. Chem. **65,** 101 (1961)
24. DYNE, P. J.: Canad. J. Chem. **43,** 1080 (1965)
25. HARDWICK, T. J.: J. Phys. Chem. **66,** 291 (1962)
26. DYNE, P. J., JENKINSON, W. M.: Canad. J. Chem. **38,** 539 (1960)
27. DYNE, P. J., JENKINSON, W. M.: Canad. J. Chem. **39,** 2163 (1961)
28. HATANO, Y., SHIDA, S., SATO, S.: Bull. Chem. Soc. Japan **41,** 1120 (1968)
29. HATANO, Y., SHIDA, S.: J. Chem. Phys. **48,** 940 (1968)
30. HATANO, Y.: Bull. Chem. Soc. Japan **41,** 1126 (1968)
31. FEJES, P., WOJNÁROVITS, L.: Acta Chim. Acad. Sci. Hung. **69,** 177 (1971)
32. OHMAE, T., OHNISHI, S., KUWATA, K., SAKURAI, H., NITTA, I.: Bull. Chem. Soc. Japan **40,** 226 (1967)
33. FÖLDIÁK, G., WOJNÁROVITS, L.: Acta Chim. Acad. Sci. Hung. **65,** 59 (1970)
34. JONES, K. H., DUSEN, W., THEARD, L. M.: Rad. Res. **23,** 128 (1964)
35. ZEMAN, A., HEUSINGER, H.: Radiochim. Acta **8,** 149 (1967)

Gábor FÖLDIÁK
László WOJNÁROVITS
} Budapest XII., Konkoly Thege M. út.

Acta Chimica Academiae Scientiarum Hungaricae, Tomus 70 (1—2), pp. 41—54 (1971)

VIBRATIONAL SPECTRA OF ORGANOMERCURY COMPOUNDS, VIII*

INFRARED AND RAMAN SPECTRA OF ALLYLMERCURIC COMPOUNDS

J. MINK and YU. A. PENTIN

(Institute of Isotopes of the Hungarian Academy of Sciences, Budapest, and Department of Chemistry, Moscow State University, Moscow)

Received May 16, 1970

The infrared (3200—200 cm^{-1}) and Raman spectra of allylmercuric chloride and allylmercuric bromide have been recorded in the crystalline phase and in solution.

The observed frequencies were assigned. The normal coordinate analysis performed for the allylmercuric halides with respect to three alternative configurations, *cis*, intermediate, and *trans*, yielded the best fit in the case of the intermediate model.

For allylmercuric chloride and bromide the force field was evaluated by a least squares fit and the force constants of the CHg-stretching were found to be 4.16 and 4.09 $\times 10^6$ cm^{-2} (2.67 and 2.62 mdyn/Å) and those of the HgX-stretching were estimated as 3.01 and 2.87 $\times 10^6$ cm^{-2} (1.93 and 1.84 mdyn/Å), respectively. A frequency assignment was performed for the infrared spectrum of liquid diallylmercury.

Introduction

The infrared spectra of allylmercuric halides and related compounds have been published [1, 2]. Some infrared data on allylmercuric chloride have been also reported [3]. In the reported cases the analysis covered only some of the vibrational bands. No complete analysis has yet been made of the infrared and Raman spectra, nor has the force field of these compounds been investigated so far.

Experimental

Allylmercuric chloride, bromide and diallylmercury were prepared from compounds of the type $CH_2=CHCH_2MgX$ with an equivalent amount of the mercury(II) halide [4] in question.

The allylmercuric halides were purified by recrystallization from methanol. Diallylmercury was distilled at reduced pressure. The analytical data and the other properties are specified in Table I.

Table I

Analytical data for allylmercuric compounds

Compound	Analysis				Melting point; Boiling point (°C)
	Found		Calcd.		
	C%	H %	C %	H %	
$CH_2=CHCH_2HgCl$	13.17	2.06	13.00	1.82	m.p. 109—110
$CH_2=CHCH_2HgBr$	11.31	1.78	11.20	1.57	m.p. 122—123
$(CH_2=CHCH_2)_2Hg$	25.49	3.56	25.71	3.68	b.p. 72—74 (3 mmHg)

*For Part VII, *cf.* Acta Chim. Acad. Sci. Hung. **67**, 435 (1971).

The spectrometers and the methods used for the measurements were the same as those described in an earlier report [5].

The infrared spectra of the crystalline allylmercuric halides and of their solutions in CS_2 and benzene were measured in the wavenumber range from 3200 to 200 cm^{-1}. The spectra are shown in Fig. 1. The infrared spectrum of liquid diallylmercury was measured in the range from 5000 to 400 cm^{-1}. The spectrum recorded in the range between 3500 and 400 cm^{-1} is shown in Fig. 2. The Raman spectra were obtained in dioxan solutions, the depolarization, however, could not be determined because of the almost immediate decomposition of the compounds as a consequence of mercury arc excitation.

The vibrational data of the allylmercuric halides and the infrared frequency data of allylmercuric iodide are summarized in Table II.

Results and discussion

In analogy to allyl halides [6—10] the allylmercuric halides are expected to exhibit torsional isomerism. The possible isomeric forms may be any of the following configurations: *trans* ($\Theta = 0$), *trans-gauche* ($\Theta = 60°$), *cis-gauche* ($\Theta = 120°$) and *cis* ($\Theta = 180°$), where Θ is the azimuthal angle (*i.e.* the angle between the planes of the vinyl and the CCHg groups). The spectroscopic data alone indicate the occurrence of two rotationally isomeric forms in the crystalline state of the allylmercuric halides. Considering the relative intensities, the proportion of the second form, however, is thought to be very small. The weak bands were observed in the vibrational spectra in the environment of the strong bands ν_9, ν_{10}, ν_{12}, ν_{14} and ν_{18} were attributed to a minor isomeric form. The weak bands around ν_9, ν_{10} and ν_{14} observed in the crystalline samples disappear from the spectra of the solutions in which the major isomer seems to be predominant.

The $CH_2{=}CHCH_2HgX$ (X = Cl, Br, I) molecules have 24 fundamental frequencies; 22 bands could be identified in addition to the above mentioned excess bands at wavenumbers above 100 cm^{-1} and attributed to the predominant configuration. Independently of the torsional isomers, all the fundamental vibrations are infrared and Raman active. In the case of planar (*cis* or *trans*) configurations, the allylmercuric halides have C_S symmetry.

Five frequency bands were assigned to the carbon–hydrogen stretching vibrations, of which the three bands, ν_1, ν_2 and ν_3, in the range between 3000 and 3080 cm^{-1}, are attributed to the vinyl group, while the two strong bands below 3000 cm^{-1} to the asymmetric ν_4 and the symmetric ν_5 CH stretching frequencies of the methylene group. The strong band at 3060 cm^{-1} seems to originate from the $\nu_6 + \nu_7$ combination mode.

The C=C stretching frequency ν_6 of the vinyl group is observed in both the infrared and Raman spectra as an intense band at 1630 cm^{-1}.

The wagging ν_{15} and the twisting ν_{13} frequencies of the four deformation modes of the vinyl CH_2 group produce strong bands in the infrared spectra near 900 cm^{-1} and 985 cm^{-1}, respectively. These out-of-plane deformation modes, as expected, are almost or entirely absent from the Raman spectra. Bands which can be attributed to vinyl CH_2, in-plane, bending vibrations

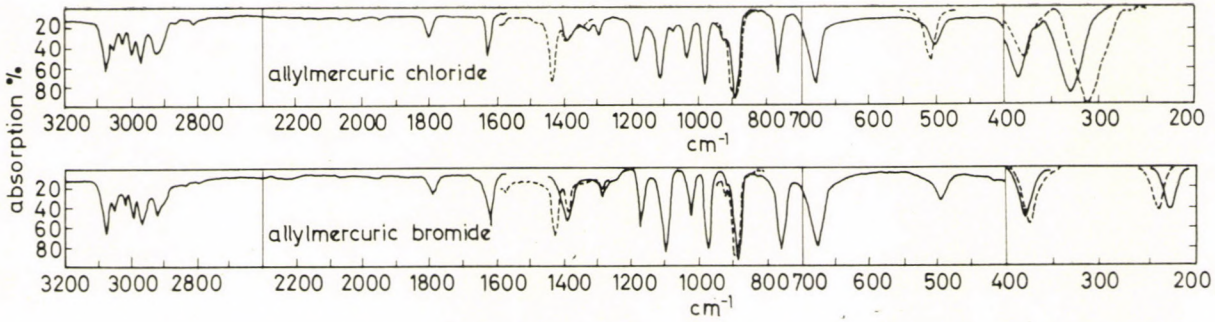

Fig. 1. The infrared spectra of allylmercuric halides. 200—400 cm^{-1} : 0.3 *M* and 0.2 *M* solutions of allylmercuric chloride and bromide in benzene respectively, 1 mm CsI cell; 400—3200 cm^{-1}: 0.16 *M* and 0.19 *M* solutions of allylmercuric chloride and bromide in CS_2, respectively, 1 mm KBr cell. Dashed lines: the spectra of crystalline samples

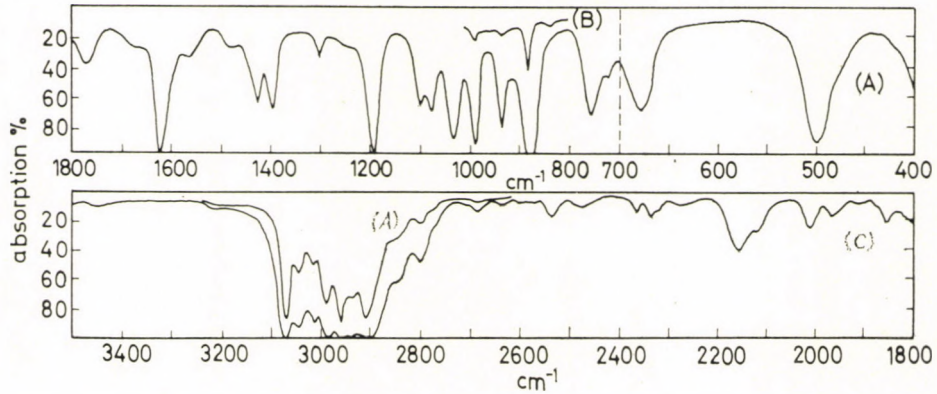

Fig. 2. The infrared spectra of liquid diallylmercury. (*A*) liquid film, (*B*) solution in nujol, (*C*) path length 0.07 mm

Acta Chim. (Budapest) 70, 1971

Table II

Vibrational spectra of allymercuric halides

Allylmercuric chloride			Allylmercuric bromide			Allylmercuric iodide	Assignment
Infrared		Raman	Infrared		Raman	infrared [2]	
solid (cm^{-1})	solution (cm^{-1})	solution (cm^{-1})	solid (cm^{-1})	solution (cm^{-1})	solution (cm^{-1})	solid (cm^{-1})	
1	2	3	4	5	6	7	8
3078 *vs*	3081 *vs*		3078 *vs*	3080 *vs*		3080 *m*	ν_1, A'
3063 *s*	3059 *s*		3061 *s*	3057 *s*		3055 *w*	$\nu_6 + \nu_7$
3030 *s*	3029 *s*		3027 *s*	3027 *s*		3023 *w*	ν_2, A'
3004 *s*	3000 *s*		3002 *s*	3000 *s*		2998 *w*	ν_3, A'
2971 *vs*	2938 *vs*		2973 *vs*	2982 *vs*		2973 *m*	ν_4, A'
2925 *s*	2921 *s*	2910 *w*	2919 *s*	2923 *m*	2906 *m*	2928 *m*	ν_5, A'
2850 *vw*		2858	2850 *vw*	2840 *vw*	2858 *vw*		$\nu_7 + \nu_8$
2808 *vw*	2810 *vw*	2820 *vw*	2811 *w*	2807 *w*	2820 *w*		$2\nu_8$
2780 *vw*			2780 *vw*				$\nu_8 + \nu_9$
2282			2280				
2194			2190				
2162			2160				$\nu_{11} + \nu_{12}$
2033	2031		2031				$\nu_{13} + \nu_{12}$
1968 *vw*	1955 *vw*		1965 *vw*	1955 *vw*			$2\nu_{13}$
1880			1880				$\nu_{15} + \nu_{13}$
1803 *m*	1803 *m*		1801 *m*	1800 *m*			$2\nu_{15}$
1678 *vw*			1677 *vw*	1677 *vw*			$\nu_{16} + \nu_{15}$
1632 *s*	1628 *s*	1618 *s*	1629 *s*	1627 *s*		1623 *m*	ν_6, A'
1590 *vw*		1588	1586 *vw*				$\nu_{17} + \nu_{15}$

1437 *s*			1436 *s*			1432 *m*	ν_7, A'
1400 *m*	1400 *m*	1392 *m*	1398 *m*	1400 *m*	1391 *m*	1396 *w*	ν_8, A'
1346 *vw*	1332 *vw*		1336 *vw*	1331 *vw*			ν_9, A'
1302 *w*	1297 *w*		1301 *w*	1295 *m*			
1225 *vw*			1216 *vw*				
			1190 *s*				
1186 *s*	1186 *s*		1186 *s*	1188 *s*		1192 *m*	ν_{10}, A'
1158 *vw*			1158 *vw*				
1115 *s*	1119 *s*	1114 *vs*	1104 *s*	1111 *vs*	1109 *vs*	1095 *m*	ν_{11}, A''
1076 *m*	1080 *m*		1046 *s*	1037 *s*		1035 *m*	ν_{12}, A'
1049 *s*	1039 *s*						
988 *s*	984 *s*		986 *s*	984 *s*		990 *m*	ν_{13}, A''
933 *w*	932 *w*	939 *w*	936 *w*	931 *w*	938 *w*	938 *w*	ν_{14}, A'
914 *w*, *sh*			916 *s*, *sh*			903 *s*	
902 *vs*	899 *vs*	900 *vw*	900 *vs*	899 *vs*	900 *vw*	898 *s*	ν_{15}, A''
774 *vs*	772 *vs*	770 *w*	771 *vs*	772 *w*	772 *w*	765 *m*	ν_{16}, A''
683 *s*	683 *s*	686 *m*	681 *s*	687 *s*	684 *m*	683 *m*	ν_{17}, A''
		585 *vw*			575 *vw*	487 *w*	ν_{18}, A'
511 *s*	504 *s*	505 *m*	503 *s*	496 *s*	490 *m*		
380 *m*	387 *m*	376 *w*	378 *m*	386 *m*	375 *w*		ν_{19}, A'
312 *s*	329 *s*	308 *vs*	244 *m*	235 *m*	206 *vs*		ν_{20}, A'
		227 *m*		235 m^+			ν_{21}, A'
		143 *vw*			146 *w*		ν_{22}, A''
		120 *vvw*			111 *vvw*		ν_{23}, A''
		88 *vvw*			88 *vvw*		ν_{24}, A'

Note: *s*, strong; *m*, medium; *w*, weak; *v*, very; *sh*, shoulder; $^+$ frequency used twice.

appear at 1400 cm^{-1} (ν_8, scissoring) and at 1045 cm^{-1} (ν_{12}, rocking). The in-plane ν_{15} and out-of-plane ν_{17} deformations of the vinyl hydrogen are thought to be responsible for the bands observed near 1300 cm^{-1} and 680 cm^{-1}, respectively. The latter is observable in the Raman spectra, too.

The assignments to the bending ν_7 and rocking ν_{16} modes of the methylene group are thought to be unambiguous, whereas the frequency assignments to the wagging ν_{10} and twisting ν_{11} vibrations are questionable (Table II). The frequencies specified for the latter are inferred mainly from normal coordinate calculations. The twisting vibration appears in the Raman spectra as an intense band.

Among the skeletal vibrations the C—C stretching ν_{14} can be identified at 930 cm^{-1} in both the infrared and the Raman spectra. Another band appearing in the 903—916 cm^{-1} region of the infrared spectra of crystalline allylmercuric halides can be attributed to the inhomogeneity of the configuration. The appearance of the CCC skeletal bending ν_{19} in the low-frequency region at 380 cm^{-1} reflects the fact that the heavy mercury atom is involved in this deformation mode.

The vibrations involving the mercury atom appear at low frequencies. The CHg stretching ν_{18} frequency decreases in the order chloride, bromide, iodide. The HgCl stretching frequency is observed in the infrared spectrum of the solution in benzene at a frequency higher by 18 cm^{-1} than that measured in the spectrum of the crystalline sample, indicating strong intermolecular interaction (HgCl . . . Hg) in the latter. The HgBr stretching shows a very strong band at 206 cm^{-1} in the Raman spectrum in dioxan solution. This band appears at a considerably lower frequency than in the infrared spectra, which could be attributed to the influence of strongly polar dioxan solvent. The Raman band at 227 cm^{-1} can be assigned to the CCHg skeletal bending frequency, ν_{21}.*

The weak Raman lines near 145 cm^{-1} can be assigned to the torsional mode of the allyl group. The low frequencies which can be assigned to the two (inplane and out-of-plane) deformation modes of the CHgX groups (ν_{24}, ν_{23}) are very difficult to measure by the present technique, thus the assignments are only approximate.

The allyl derivatives of mercury have weak bands in the infrared spectra originating from the overtones $2\nu_8$, $2\nu_{13}$, and $2\nu_{15}$, the latter being especially characteristic of these compounds. The combination tones $\nu_6 + \nu_7$ and $\nu_7 + \nu_8$ are well apparent.

The infrared data of allylmercuric iodide reported by GREEN [2] are in good agreement with the vibrational spectra of the other allylmercuric halides (see Table II).

* This band is difficult to measure in the Raman spectrum of allylmercuric bromide because of the very strong band at 206 cm^{-1}.

Diallylmercury

Diallylmercury is an unstable compound. The infrared spectrum, which to our knowledge has not yet been recorded, was taken on a liquid sample immediately after distillation at reduced pressure. Decomposition of the sample was not observed during the measurement.

The infrared data of diallylmercury are listed in Table III; for their interpretation the spectra of the allylmercuric halides provide a reasonable basis.

The $(CH_2{=}CHCH_2)_2$ Hg molecule has 45 fundamental vibrational modes, of which seven (four skeletal and three torsional modes) are expected to lie in the range above 300 cm^{-1}. In the range of frequencies covered by our investigations only 23 bands of considerable intensity could be observed. The reason for this is the absence or weakness of coupling between most of the vibration of the two allyl groups across the heavy mercury atom. However, a well apparent splitting was observed in the methylene deformation modes ν_{11} and ν_{16}. This phenomenon may be due to either a torsional isomerism within the allyl groups or to vibrational interactions between the two allyl groups. In analogy to the more thoroughly analyzed diethylmercury spectrum [5], the latter seems to be more probable. The symmetric CHg stretching mode ν_{18} was identified at 474 cm^{-1} by the Gauss analysis of the band shape on the low frequency side of the strong band at 495 cm^{-1} assigned to the asymmetric CHg stretching mode. The CCHg asymmetric and symmetric skeletal bending modes have been determined by calculation as approximately at 230 cm^{-1} and 190 cm^{-1}, respectively.

It is difficult to make any definite statement on the molecular symmetry of the diallylmercury on the basis of the available experimental data. The infrared spectra of liquid diallyl mercury are interpretable satisfactorily only with the assumption of a predominant rotationally isomeric form in the allyl groups.

In diallylmercury the rotation about the C—Hg bonds seems to be free and a linear C—Hg—C skeleton can be assumed on the analogy of the other R_2Hg-type compounds [2, 5, 16, 17].

Normal coordinate calculation

The calculations were performed assuming *cis-* and *trans*-configurations of the C_S groups of symmetry and, alternatively, an intermediate-configuration. The plane of the vinyl group is perpendicular to the CCHg plane (between *cis-gauche* and *trans-gauche*) for the intermediate configuration. The internal coordinates are defined in Fig. 3. The coordinates introduced, in addition, are the following: ϱ_1 and ϱ_2, the out-of-plane deformations of the vinyl CH_2 and CH group, $\varkappa_1$ and $\varkappa_2$, the torsions between the CCC plane and the CCHg

Table III

Infrared frequencies of diallylmercury

No.	(cm^{-1})	Assignment	No.	(cm^{-1})	Assignment
	4700 *w*	$\nu_1 + \nu_6$		2260	
	4565			2159 *w*	$\nu_8 + \nu_{16}$
	4490			2122 *vw*	$\nu_{10} + \nu_{14}$
	4460 *w*	$\nu_1 + \nu_8$		2017 *w*	$\nu_{12} + \nu_{13}$
	4370 *vw*	$\nu_4 + \nu_7$, $\nu_3 + \nu_8$		1966 *vw*	$\nu_{13} + \nu_{14}$
	4324 *w*	$\nu_5 + \nu_7$		1915	
	4264 *vw*	$\nu_1 + \nu_{10}$, $\nu_4 + \nu_9$		1861 *w*	$2\,\nu_{14}$
	4154 *vw*	$\nu_1 + \nu_{11}$		1768 *m*	$2\,\nu_{15}$
	4005 *vw*	$\nu_4 + \nu_{12}$, $\nu_1 + \nu_{14}$		1669 *w*	$\nu_{13} + \nu_{17}$
	3225	$2\,\nu_6$	ν_6	1623 *vs*	ν C=C C=C stretching
ν_2	3074 *vs*	ν_{as}=CH_2 vinyl CH_2 stretching		1600 *sh*	$\nu_{14} + \nu_{17}$, $\nu_{11} + \nu_{19}$
	3047 *m*	$\nu_6 + \nu_7$		1560 *w*	$\nu_{15} + \nu_{17}$
ν_1	3014 *w*	ν CH vinyl CH stretching		1480 *w*	$\nu_{13} + \nu_{18}$
ν_3	2989 *s*	ν_s=CH_2 vinyl CH_2 stretching	ν_7	1424 *m*	β_s CH_2 methylene CH_2 bending
ν_4	2960 *vs*	ν_{as} > CH_2 methylene CH_2 stretching	ν_8	1396 *m*	β_s=CH_2 vinyl CH_2 bending
	2938 *vw*	$\nu_6 + \nu_9$	ν_9	1296 *w*	β CH vinyl CH in-plane bending
ν_5	2907 *vs*	ν_s > CH_2 methylene CH_2 stretching		1255	
	2842	$2\,\nu_7$	ν_{10}	1191 *vs*	γ_s > CH_2 methylene CH_2 wagging
	2803 *w*	$2\,\nu_8$	ν_{11}	1099 *m*	γ_{as} > CH_2 methylene CH_2 twisting
	2774			1075 *m*	
	2710		ν_{12}	1032 *s*	β_{as}=CH_2 vinyl CH_2 rocking
	2688 *vw*	$\nu_8 + \nu_9$	ν_{13}	989 *s*	γ_{as}=CH_2 vinyl CH_2 twisting
	2638 *vw*	$\nu_6 + \nu_{12}$	ν_{14}	934 *ms*	ν C—C C—C stretching
	2598		ν_{15}	881 *vs*	γ_s=CH_2 vinyl CH_2 wagging
	2774				
	2580			837	
	2538 *vw*	$\nu_7 + \nu_{11}$	ν_{16}	758 *m*	β_{as} > CH_2 methylene CH_2 rocking
	2484 *w*	$\nu_9 + \nu_{10}$		718 *w*	
	2465 *vw*	$\nu_8 + \nu_{11}$	ν_{17}	678 *ms*	γ CH vinyl CH out-of-plane bending
	2280		ν_{18}	495 *vs*	ν_{as} CHg CHg stretching
				474 *sh*	ν_s CHg
			ν_{19}	390 *s*	β CCC skeletal bending

Notes: see Table II and Table IV.

and the C—CH planes, respectively and finally the out-of-plane deformation of the ChgX. Because of redundancy the coordinates of the angular deformations β_2, β_3 and α_{45} were omitted. Under the operations of C_S point group the symmetry coordinates yield 16 A' and 8 A'' species but the intermediate configuration gives a 24th order eigenvalue problem. The calculation method of the GVFF has been described in Ref. [5]. The geometrical parameters esti-

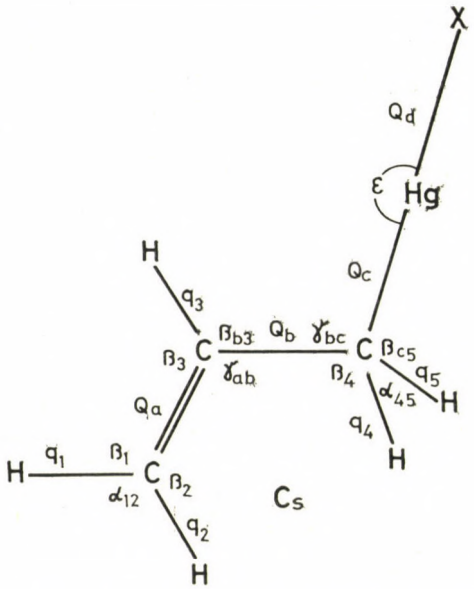

Fig. 3. The internal coordinates of allylmercuric halides.

mated from the data of similar compounds were taken to be the following: $\nu_{C=C} = 1.35$ Å, $\nu_{C-C} = 1.54$ Å, $\nu_{CH_{(vinyl)}} = 1.07$ Å, and $\nu_{CH_{(methylene)}} = 1.09$ Å. The estimated values of $\nu_{CHg} = 2.06$ Å and 2.07 Å and $\nu_{Hg} = 2.28$ Å and 238 Å were used for allylmercuric chloride and bromide, respectively. The bond angles of the vinyl group were taken as 120 °C. Linear CHgX skeleton and tetrahedral methylene angles were assumed.

In zeroth approximation the force field was taken to be equal to that evaluated for allylbromide [8] and propylene [6]. The force constants of the torsional mode $\varkappa_1$ were taken to be 0.12, 0.18 and 0.25 $\times 10^6$ cm^{-2} [11] for the *cis*, intermediate, and *trans* configuration, respectively.

The other force constants were considered to be independent of the configurational motions. The experimental and computed frequencies are listed in Table IV. The vibrational modes ν_{10}, ν_{12}, ν_{14}, ν_{17}, ν_{18}, ν_{19} and ν_{21} were found to be the most sensitive to the configuration. The observed ν_{12}, ν_{14}, and ν_{18} bands indicate the existence of a minor form. The well-defined changes of the

Table IV

Computed fundamental frequencies of allylmercuric chloride for different configurations

No. of fundamentals		Experimental	Calculated (cm^{-1})			Assignment
		(cm^{-1})	*cis*	intermediate	*trans*	
1	2	3	4	5	6	7
in-plane vibrations (A')	ν_1	3081	3099	3100	3099	$\nu_{as}=CH_2$ }
	ν_2	3029	3027	3030	3027	ν CH } vinyl CH stretching
	ν_3	3000	3010	3011	3010	$\nu_s=CH_2$ }
	ν_5	2921	2926	2926	2926	ν_s CH_2 methylene, symmetrical CH_2 stretching
	ν_6	1628	1648	1652	1649	ν C=C C=C stretching
	ν_7	1437	1436	1437	1449	β_s CH_2 methylene CH_2 bending
	ν_8	1400	1420	1427	1407	$\beta_s=CH_2$ vinyl CH_2 bending
	ν_9	1297	1298	1300	1305	β CH vinyl CH in-plane bending
	ν_{10}	1186	1237	1196	1200	γ_s CH_2 methylene CH_2 wagging
	ν_{12}	1039	1073	1040	1092	$\beta_{as}=CH_2$ vinyl CH_2 rocking
	ν_{14}	932	904	913	917	ν C—C C—C stretching
	ν_{18}	504	628	473	632	ν CHg CHg stretching
	ν_{10}	387	406	376	314	β CCC skeletal bending
	ν_{29}	329	331	335	346	ν HgCl HgCl stretching
	ν_{21}	227	138	232	193	β CCHg skeletal bending
	ν_{24}	88	81	77	79	δ CHgCl in-plane deformation
out-of-plane (A'') vibrations	ν_4	2983	2979	2982	2980	ν_{as} CH_2 methylene asymmetrical CH_2 stretching
	ν_{11}	1119	1172	1170	1172	γ_{as} CH_2 methylene CH_2 twisting
	ν_{13}	984	1037	1046	1037	$\gamma_{as}=CH_2$ vinyl CH_2 twisting
	ν_{15}	772	944	945	944	$\gamma_s=CH_2$ vinyl CH_2 wagging
	ν_{16}	899	856	851	845	β_{as} CH_2 methylene CH_2 rocking
	ν_{17}	683	520	640	511	γ CH vinyl CH out-of-plane deformation
	ν_{22}	143	146	137	138	τ torsion
	ν_{23}	120	95	111	93	δ' CHgCl out-of-plane deformation

Designation of the vibrational modes: ν, stretching; β, in-plane-; γ, out-of-plane-; δ, skeletaldeformations; τ, torsion.

G matrix are responsible for the configurational sensitivity of the calculated frequencies. The calculated frequencies are the closest to the experimental values in the case of the intermediate model. In spite of the approximate nature of the normal coordinate calculation, it seems reasonable to assume that allylmercuric chloride and consequently the allylmercuric halides have a major form which is close to the intermediate configuration and a minor,

Table V

Experimental and computed fundamental frequencies for allylmercuric halgenes

N° of fundamentals	Frequencies, cm^{-1}				Assignment	
	Allylmercuric chloride		Allylmercuric bromide			
	exptl.	calcd.	exptl.	calcd.		
ν_1	3081	3081	3081	3081	$\nu_{as}=CH_2$	vinyl, asymmetrical CH stretching
ν_2	3029	3029	3029	3029	ν CH	vinyl, CH stretching
ν_3	3000	3000	3000	3000	$\nu_s=CH_2$	vinyl, symmetrical CH stretching
ν_4	2983	2982	2982	2982	$\nu_{as}>CH_2$	methylene, asymmetrical CH stretching
ν_5	2921	2922	2923	2923	$\nu_s>CH_2$	methylene, symmetrical CH stretching
ν_6	1628	1627	1627	1627	ν C=C	C=C stretching
ν_7	1437	1437	1436	1436	$\beta_s>CH_2$	methylene CH_2 bending
ν_8	1400	1400	1400	1400	$\beta_s=CH_2$	vinyl CH_2 bending
ν_9	1297	1297	1295	1296	β CH	vinyl CH in-plane bending
ν_{10}	1186	1196	1188	1193	$\gamma_s>CH_2$	methylene CH_2 wagging
ν_{11}	1119	1120	1111	1120	$\gamma_{as}>CH_2$	methylene CH_2 twisting
ν_{12}	1039	1036	1037	1036	$\beta_{as}=CH_2$	vinyl CH_2 rocking
ν_{13}	984	988	984	988	$\gamma_{as}=CH_2$	vinyl CH_2 twisting
ν_{14}	932	917	931	919	ν C—C	C—C stretching
ν_{15}	899	899	899	898	$\gamma_s=CH_2$	vinyl CH_2 wagging
ν_{16}	772	765	768	764	$\beta_{as}>CH_2$	methylene CH_2 rocking
ν_{17}	683	662	678	661	γ CH	vinyl CH out-of-plane deformation
ν_{18}	504	504	496	496	ν CHg	CHg stretching
ν_{19}	387	360	386	359	β CCC	skeletal bending
ν_{20}	329	329	206	206	ν HgX	HgX stretching
ν_{21}	227	211	235	236	β CCHg	skeletal bending
ν_{22}	143	137	146	136	τ	torsion
ν_{23}	120	110	111	98	δ' CHgX	out-of-plane deformation
ν_{24}	88	78	88	65	δ CHgX	in-plane deformation

rotationally isomeric form which can be best approximated by the *trans*-model. This assumption is supported also by steric considerations.

The values of the force field were refined using the method of least squares [13] and varying the force constants in the environment of the mercury atom. These calculations were performed for the intermediate model only. After the second or third iteration procedure the calculated frequencies were found to agree well with the observed data (Table V).

Table VI

Force constants of allylmercuric haloides

Force constants	10^6 cm^{-2}
1	2
K_{Q_a}	13.90
K_{Q_b}	7.02
K_{Q_c}	(Cl): 4.16; (Br): 4.09
K_{Q_d}	(Cl): 3.01; (Br): 2.87
$K_{q_1} = K_q$	8.54
K_{q_3}	8.49
$K_{q_4} = K_{q_5}$	8.09
$K_{\alpha_{12}}$	0.51
$K_{\beta_1} = K_{\beta_2} = K_{\beta_3}$	0.77
$K_{\beta_{b_2}}$	0.72
$K_{\gamma_{ab}}$	1.02
$K_{\varepsilon} = K_{\varepsilon'}$	(Cl): 0.60; (Br): 0.48
K_{ϱ_1}	0.30
K_{ϱ_2}	0.48
K_{χ_1}	0.18
K_{χ_2}	0.68
$H_{Q_aQ_b} = H_{Q_aq_{i(1,2,3)}} = H_{Q_cq_{i(1,2)}}$	0.10
$H_{Q_bQ_c}$	(Cl): 0.33; (Br): 0.37
$H_{Q_cQ_d}$	(Cl): 0.27; (Br): 0.26
$H_{q_1q_2}$	0.054
$H_{Q_cq_{i(4,5)}}$	0.075
$h_{q_4q_5}$	0.026
$A_{Q_a\,\beta_{i(1,2,3)}} = A_{q_i\beta_{ci}}$ $(i = 4, 5)$	0.45
$A_{Q_a\gamma_{ab}}$	1.00
$a_{\alpha_{12}q_{i(1,2)}} = A_{Q_b(\beta_{b_3}, \beta_4, \beta_5)}$	0.43
$A_{Q_b\gamma_{ab}}$	0.80
$A_{Q_c\gamma_{bc}}$	0.59
$A_{Q_c\beta_{ci(4,5)}}$	0.71
$a_{q_i\beta_i}$ $(i = 1, 2, 3)$	0.66
$A_{q_1\beta_{b_3}} = a_{q_4(\alpha_{45}, \beta_4)} = a_{q_5\beta_5} = a_{q_5\alpha_{45}}$	0.35
$1_{\beta_1\beta_{b_3}} = 1_{\beta\,\beta_{b_3}}$	0.025
$1_{\beta_1\gamma_{ab}} = 1_{\beta_2\beta_{b_3}}$	0.095
$1_{\beta_{b_3}\gamma_{bc}} = 1_{\gamma_{ab}\gamma_{bc}}$	0.015
$1_{\beta_{b_3}\beta_4} = 1_{\gamma_{ab}\beta_5}$	0.085
$1_{\beta_{b_3}\beta_4} = 1_{\gamma_{ab}\beta_5}$	—0.055
$1_{(\gamma_{bc}, \beta_{c_4}, \beta_{c_5})} = 1_{\varepsilon'\beta_{c_4}}$	—0.020

Table VI (continued)

Force constants	10^6 cm^{-2}
1	2
$1_{\varepsilon'\beta_{c_5}}$	0.020
$u_{Q_1Q_2}$	0.014
$u_{Q_2\chi_{(1,2)}}$	0.120
$u_{Q_1\chi_2}$	0.010
$\delta_{Q_2\beta_4}$	0.008
$\delta_{Q_2\beta_5}$	—0.008
$\delta_{\beta_4\chi_{(1,2)}}$	0.082
$\delta_{\beta_5\chi_{(1,2)}}$	—0.082
$\delta_{\beta_{c_4}\chi_{(1,2)}}$	—0.011
$\delta_{\beta_{c_5}\chi_{(1,2)}}$	0.011

Note: K — diagonal elements; $H(h)$ — elements of valence-valence, $A(a)$ — elements of valence-angle, 1 — elements of angle-angle, u — elements of two out-of-plane, and δ — elements of angle-out-of-plane interactions.
The internal coordinates are shown in Fig. 2 (see text).

The force constants in 10^6 cm^{-2} units as evaluated for the different allylmercuric halides are listed in Table VI. The force constants of the tetrahedral valence angle were obtained in terms of independent (without redundancy) coordinates. This portion of the F-matrix has the form (in 10^6 cm^{-2} units):

γ_{bc}	β_4	β_5	β_{c4}	β_{c5}	
1.78	0.84	0.84	0.44	0.44	γ_{bc}
	1.48	0.94	0.74	0.77	β_4
		1.48	0.77	0.74	β_5
			1.51	0.80	β_{c4}
				1.51	β_{c5}

The force constants which have not been specified in Table VI and above were taken to be equal to zero.

There are only five force constants, namely, the diagonal K_{Qc}, K_{Qd}, K_ε and the valence-valence interaction elements H_{QbQd}, H_{QcQd} that depend on the halogen atom, while the remaining force field is the same for the allylmercuric chloride and bromide. The more characteristic CHg and HgX stretching force constants of the allylmercuric halides were found to be close

to those of the methylmercuric halides [14, 15]. As compared with the allyl halides [8], the major part of the force field shows a slight change. The relatively high value of the force constant $K_{\varrho_2} = 0.48 \times 10^6$ cm^{-2} can be attributed to the higher frequency of the vinyl CH out-of-plane deformation as compared with the allyl halides [7—10].

The X-ray investigation of allylmercuric chloride and the infrared and Raman study of deuterated derivatives have also been performed in order to verify the molecular structure of these compounds inferred from the present analysis.

*

This work has been carried out at the Department of Chemistry, Moscow State University. The authors are grateful to I. P. BELETSKAY, D. Sc., for valuable suggestions and helpful discussions.

REFERENCES

1. NESMEYANOV, A. N., RUBEZNOV, A. Z., LEITES, L. A., GUBIN, S. P.: J. Organometal. Chem., **12,** 187 (1968)
2. GREEN, J. H. S.: Spectrochim. Acta **24A,** 863 (1968)
3. SHORIGIN, P. P., PETUKHOV, V. A., KHOMENKO, A. KH., LOPATIN, B. V.: Zh. Fiz. Khim. **42,** 1584 (1968)
4. MAKAROVA, L. G., NESMEYANOV, A. N.: Methods of Elemental Organic Chemistry, Vol. 4, Mercury. North-Holland, Amsterdam, 1967
5. MINK, J., PENTIN, YU. A.: Acta Chim. Acad. Sci. Hung. **65,** 273 (1970)
6. SVERDLOV, L. M.: Dokl. AN SSSR **106,** 80 (1956)
7. PENTIN, YU. A., SHARIPOV, Z.: Vestnik Mos. Gos. Univ. Ser. Khim. **4,** 30 (1963)
8. PENTIN, YU. A., MOROZOV, E. V., SHARIPOV, Z.: Vestnik Mos. Gos. Univ. Ser. Khim. **2,** 23 (1966)
9. RADCLIFFE, K., WOOD, J. L.: Trans. Faraday Soc. **62,** 2038 (1966)
10. MCLACHLAN, R. D., NYQUIST, R. A.: Spectrochim. Acta **24A,** 103 (1968)
11. VOLKENSTEIN, M. V., ELYASHEVICH, M. A., STEPANOV, B. I.: Kolebanie molekul, Vol. 1, p. 517. Gostechnizdat, 1949
12. MINK, J., MINK, L. M., PENTIN, YU. A.: Zhur. Prikl. Spektr. **9,** 129 (1968)
13. MINK, J., MINK, L. M., PENTIN, YU. A.: Vestn. Mosk. Univ. Khim. (In press)
14. GOGGIN, P. L., WOODWARD, L. A.: Trans. Faraday Soc. **62,** 1423 (1966)
15. MEIC, Z., RANDIC, M.: Trans. Faraday Soc. **64,** 1438 (1968)
16. MINK, J., PENTIN, YU. A.: Acta Chim. Acad. Sci. Hung. **66,** 277 (1970)
17. GUTOVSKY, H. S.: J. Chem. Phys. **17,** 128 (1949)
18. MINK, J., PENTIN, YU. A.: J. Organometal. Chem. **23,** 293 (1970)

JÁNOS MINK; Budapest XII., Konkoly Thege M. út
YU. A. PENTIN; Chemistry Department, Moscow State University, Moscow B—234 USSR.

Acta Chimica Academiae Scientiarum Hungaricae, Tomus 70 (1–2) pp. 55–65 (1971)

MOLECULAR VIBRATIONS AND MEAN SQUARE AMPLITUDES

IV. MEAN AMPLITUDES IN ORGANIC MOLECULES WITH A CARBONYL GROUP

S. J. CYVIN and B. VIZI

(Technical University of Norway, Trondheim, and University of Chemical Industries, Veszprém)

Received April 22, 1970

A survey of mean amplitudes of vibration (l) is given for organic molecules with carbonyl groups, as obtained from electron diffraction and spectroscopic calculations. Characteristic values for l(C=O) are pointed out. The work contains an original contribution to the normal-coordinate analysis of acetone with calculated results of mean amplitudes and atomic vibration mean-square amplitudes. New data are also reported for the mean amplitudes of vibration in three isotopic species of the formic acid monomer.

In the monograph of CYVIN [1], Chapter 12 surveys the existing material on mean amplitudes of vibration. Already at the time when this book was printed it was clear that extensive supplements would be necessary. Some supplementary articles [2, 3] have been published, dealing mostly with inorganic molecules. The present paper is an attempt to survey in part the existing data for organic molecules. It seemed natural to give a special survey of groups of compounds with carbonyl bonds because an appreciable number of papers dealing with such molecules have recently been published, reporting both electron diffraction investigations and spectroscopic computations.

I. Small molecules

Fig. 1 shows the calculated mean amplitudes of vibration for the different atom pairs in (c) formaldehyde [2, 4] and (d) ketene [5], given in a condensed [6] way. The mean amplitudes for (a) carbon dioxide [1] and (b) carbon suboxide [7] are included for the sake of comparison. Similar representations of the mean amplitudes are shown in Fig. 2 for the lowest carboxylic acid, *viz.* formic acid [8], and the lowest dialdehyde, glyoxal [9]. Already a superficial inspection of these figures indicates a characteristic value of the C=O mean amplitude of about 0.039 Å in an aldehyde or carboxyl group, and of 0.035 Å in a =C=O conformation. The value of 0.035 Å is also found as characteristic for C=O in inorganic metal carbonyls [1]; in the CO molecule a mean amplitude of 0.0337 Å has been calculated [1].

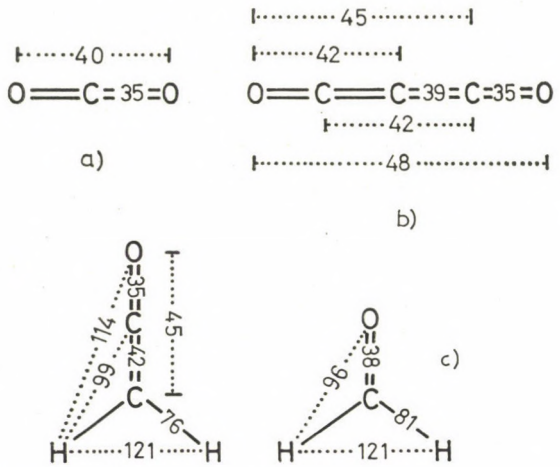

Fig. 1. Mean amplitudes of vibration (10^{-3} Å) at 298 °K for (a) carbon dioxide, (b) carbon suboxide, (c) formaldehyde, and (d) ketene

II. Aldehydes

Calculated mean amplitudes (l) of formaldehyde are shown in Fig. 1(c). They are perfectly consistent with values from electron diffraction data obtained recently by KATO *et al.* [10], *viz.* (in Å units): l(C—H) = $0.088_6 \pm$ $\pm$ 0.041_3, l(C=O) = $0.041_3 \pm 0.004_0$ and l(O . . . H) = $0.0915 \pm 0.036_5$ at 21.5 °C. They also agree with the spectroscopic values reported in the same work [10].

Table I

Mean amplitudes of vibration (Å units) for acetaldehyde

Distance*	From Ref. [11] Spectroscopic		From. Ref. [10] 21.5 °C	
	0 °K	298 °K	Spectr.	Electr. diff.
C_{ald}—H_{ald}	0.0803	0.0803		
C_{meth}—H_i	0.0785	0.0785	0.0778	$0.085_1 \pm 0.015_8$
C_{meth}—H_o	0.0786	0.0786		
C_{ald}=O	0.0389	0.0390	0.0389	$0.038_1 \pm 0.004_0$
C_{ald}—C_{met}	0.0473	0.0477	0.0493	$0.049_7 \pm 0.006_5$
C_{meth}. . .O	0.0574	0.0610	—	$0.060_5 \pm 0.009_0$

* Identification of atoms: C_{ald} and H_{ald} in the aldehyde group; C_{meth}, H_i and H_o in the methyl group; H_i in the aldehyde-group plane.

KATO *et al.* [10] have also reported the observed mean amplitudes for some of the distances in acetaldehyde; *cf.* Table I. They agree very well with the spectroscopic calculations [10, 11]. HAGEN [11] has given a list of calculated mean amplitudes for all of the sixteen distance types in acetaldehyde and several of its deutero isotopes. His work [11] also contains the calculation of mean amplitudes for fluoral (CF_3CHO), chloral (CCl_3CHO) and bromal (CBr_3CHO).

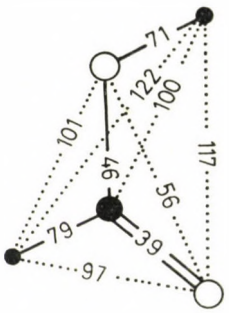

a)

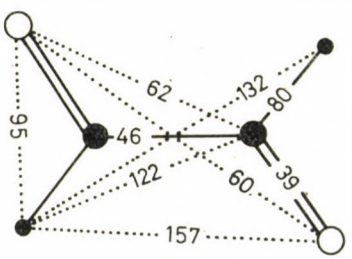

b)

Fig. 2. Mean amplitudes of vibration (10^{-3} Å) at 298 °K for (a) formic acid and (b) glyoxal

For acrolein, an unsaturated aldehyde, see the next section.

For the simplest dialdehyde, *viz.* glyoxal, the calculated mean amplitudes [9] are shown in Fig. 2. In Ref. [9] these values are compared with electron diffraction results [12]; *cf.* Table II. The agreement is found to be satisfactory, except for the (bonded) C—H distance, for which the electron diffraction value appears to be too low. Table II also includes the observed values of l for oxalyl chloride, $C_2O_2Cl_2$ [13]. No spectroscopic values of l for this molecule are known, but it would be feasible to produce such results on the basis of existing spectral data [14—16].

Table II

Mean amplitudes of vibration (with standard deviations in parentheses) from electron diffraction; Å units

Distance	Glyoxal [11]		Oxalyl chloride [13]	
	l	(σ)	l	(σ)
C—H	0.057	(0.010)		
C—Cl			0.058	(0.001)
C=O	0.0371	(0.0030)	0.045	(0.001)
C—C	0.0546	(0.0041)	0.033	(0.003)
C...O	0.0599	(0.0037)	0.058	(0.003)
C...Cl			0.070	(0.004)
O...Cl (short)			0.061	(0.002)
O...Cl (long)			0.090	assumed
O...O	0.0602	(0.0040)	0.070	assumed
Cl...Cl			0.080	assumed

III. Acrolein and p-benzoquinone

JENSEN *et al.* [9] have published the spectroscopic mean amplitudes for glyoxal, acrolein and *p*-benzoquinone, all these molecules having carbonyl bonds in a conjugated system. Table III shows some of their results for acrolein along with electron-diffraction values of l [12, 17] for the same molecule. The agreement is quite satisfactory when taking into account the experimental error limits (about $\pm 3\sigma$) and uncertainties in the spectroscopic calculations.

Table III

Mean amplitudes of vibration (Å units) for acrolein

Distance*	Spectroscopic [9]		Electron diffraction			
			[12]		[17]	
	0 °K	298 °K	l	(σ)	l	(σ)
C_2—H_2	0.078	0.078	0.070	(0.006)	0.0776	(0.0020)
C_3—H_3'	0.078	0.078				
C_3—H_3	0.079	0.079				
C=O	0.039	0.039	0.0360	(0.0045)	0.0382	(0.0006)
C=C	0.041	0.041	0.0477	(0.0038)	0.0439	(0.0008)
C—C	0.048	0.049	0.0422	(0.0032)	0.0548	(0.0010)
C...C	0.056	0.059	0.075	(0.009)	0.0787	(0.0027)
C_2...O	0.060	0.067	0.065	(0.006)	0.0636	(0.0015)
C_3...O	0.057	0.061	0.0494	(0.0037)	0.0722	(0.0024)

*For identification of atoms, see Fig. 3a.

It has been noted [9] that the values of l(C—C) and l(C=C) in Ref. [12] seem to have been interchanged.

In the cited spectroscopic work [9] the structural similarity of acrolein and *p*-benzoquinone is pointed out (*cf.* Fig. 3a) and correlations between the mean amplitudes in the two molecules are discussed. Fig. 3b shows the calculated mean amplitudes for similar distance types in *p*-benzoquinone and acrolein; for the rest of the interatomic distances the mean amplitudes are represented in Fig. 3c.

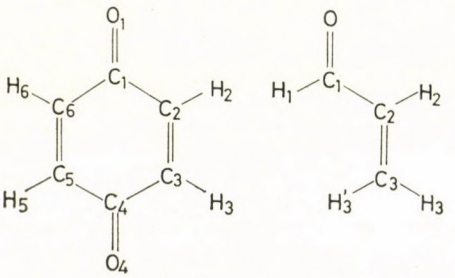

Fig. 3a. Identification and numbering of atoms in *p*-benzoquinone (left) and acrolein (right)

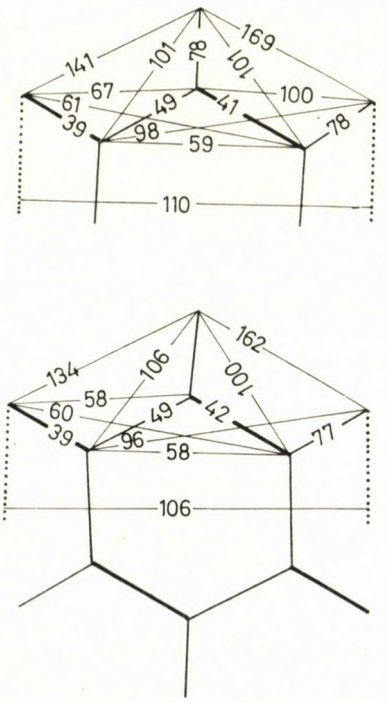

Fig. 3b. Mean amplitudes of vibration (10^{-3} Å) at 298 °K for *p*-benzoquinone and acrolein. Notice the analogy between interatomic distance types in the two molecules

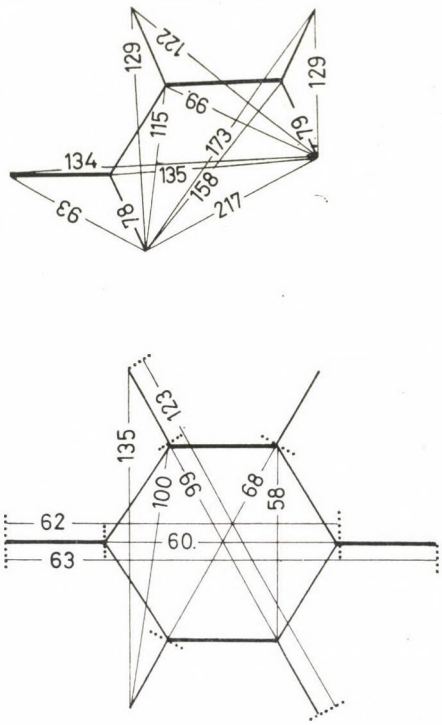

Fig. 3c. Mean amplitudes of vibration (10^{-3} Å) at 298 °K for *p*-benzoquinone and acrolein: the interatomic distance types not included in Fig. 3b

IV. Acetone

Acetone, being the lowest ketone, is naturally an important member within the families of molecules of the present investigation. The report [10] of an electron diffraction work on this molecule contains only some rudimentary results of spectroscopic mean amplitudes. In the present work a complete harmonic force constant analysis with calculations of mean amplitudes for acetone was performed.

An initial approximate force field was set up, and included $f(C{=}O) = 10.0$ mdyne/Å along with a number of force constants transferred from propane [18]. A final force field was adjusted to fit accurately the observed frequencies [19], which are quoted in the following (in cm^{-1}). Species A_1: 3020, 2926, 1738, 1438, 1360, 1067, 779, 483. Species A_2: 2973, 1432, (958 calculated), 105. Species B_1: 2973, 1438, 1093, 384, 105. Species B_2: 3020, 2926, 1456, 1363, 1218, 896, 528. A detailed specification of the applied symmetry coordinates is given elsewhere [20]. Consequently it is an easy matter to give a complete report of the final force field of the present calculations. The force

Table IV

Symmetry force constants (mdyne/Å) for acetone

A_1	1	9.85							
	2	0.15	5.01						
	3	—0.03	—0.01	4.87					
	4	—0.01	—0.03	0.03	4.88				
	5	0.30	—0.26	—0.04	0.01	1.99			
	6	—0.03	—0.02	—0.01	0.01	0.09	1.19		
	7	—0.01	0.03	0.00_3	0.01	—0.02	0.70	1.02	
	8	0.06	—0.04	—0.01	0.01	0.08	0.51	0.36	0.76
A_2	1	4.71							
	2	-0.00_1	0.40						
	3	0.00_2	—0.04	0.41					
	4	0.00_1	-0.00_2	0.00_4	0.0124				
B_1	1	4.70							
	2	-0.00_5	0.40						
	3	-0.00_8	—0.003	0.46					
	4	0.00_1	-0.00_3	-0.00_4	0.032				
	5	0.00_1	0.01	0.00_0	0.024	0.065			
B_2	1	3.75							
	2	—0.01	4.87						
	3	—0.04	0.03	4.89					
	4	0.06	0.00_3	0.00_3	0.62				
	5	0.05	—0.01	0.01	-0.00_1	1.13			
	6	0.01	0.01	0.00_4	-0.00_1	0.62	0.93		
	7	0.12	—0.01	0.02	-0.00_6	0.44	0.37	0.62	

constants in terms of the applied symmetry coordinates [20] are shown in Table IV. The resulting mean amplitudes of vibration are shown in Table V. In this table the values in parentheses are interatomic separations (in Å). They facilitate the identification of atom pairs and simultaneously show implicitly the data here applied as structure parameters. The agreement between calculated and observed [10] values of l(C=O), l(C—C) and l(C . . . O) is excellent. It is also satisfactory for l(C . . . C) in view of the relatively large experimental error limits for this value.

The mean amplitude of vibration for the carbonyl bond in acetone (*viz.* 0.039 Å) confirms the characteristic value of l(C=O) in the aldehyde and carboxyl groups; cf. Section I.

The atomic vibrational mean-square amplitudes have been reported for propane [18]. These quantities from the present calculation for acetone are shown in Table VI. The quantities pertain to the orientation of cartesian axes

Table V

Mean amplitudes of vibration (Å units) for acetone

Distance type	(Equil. dist.)	$i-j$	Spectroscopic		Electr. diff. [10] 21.5 °C
			0 °K	298 °K	
C—H	(1.085)	2—5	0.078	0.078	
C—H	(1.085)	2—7	0.078	0.078	
C=H	(1.222)	1—4	0.039	0.039	$0.039_3 \pm 0.004_8$
C—C	(1.507)	2—4	0.049	0.050	$0.049_1 \pm 0.005_3$
C...C	(2.573)	2—3	0.061	0.065	$0.074_5 \pm 0.025_3$
C...O	(2.384)	1—2	0.057	0.060	$0.062_1 \pm 0.007_5$
O...H	(2.494)	1—5	0.134	0.139	
O...H	(3.092)	1—7	0.136	0.199	
C...H	(2.122)	4—5	0.108	0.109	
C...H	(2.147)	4—7	0.108	0.108	
C...H	(3.476)	2—6	0.104	0.105	
C...H	(2.855)	2—9	0.153	0.212	
H...H	(1.764)	5—7	0.129	0.129	
H...H	(1.764)	7—8	0.129	0.129	
H...H	(4.240)	5—6	0.144	0.145	
H...H	(3.821)	5—9	0.164	0.195	
H...H	(2.710)	7—9	0.215	0.287	
H...H	(3.233)	7—10	0.264	0.459	

Table VI

Atomic vibration mean-square amplitudes ($Å^2$ units) for acetone

Atom* (i)	Temp. (°K)	$\langle x_i^2 \rangle$	$\langle y_i^2 \rangle$	$\langle z^2 \rangle$	$\langle x_i y_i \rangle$	$\langle y_i z_i \rangle$	$\langle z_i x_i \rangle$
C(2)	0	0.00058	0.00124	0.00100	0	—0.00013	0
	298	0.00113	0.00138	0.00110	0	—0.00011	0
C(4)	0	0.00341	0.00095	0.00086	0	0	0
	298	0.00762	0.00097	0.00091	0	0	0
O(1)	0	0.00133	0.00088	0.00087	0	0	0
	298	0.00503	0.00102	0.00096	0	0	0
H(5)	0	0.05104	0.01032	0.01162	0	—0.00467	0
	298	0.17539	0.01056	0.01223	0	—0.00491	0
H(7)	0	0.02044	0.02229	0.03756	0.00884	0.01309	0.02139
	298	0.06324	0.04510	0.12560	0.03903	0.05649	0.08238

* C(2) and C(4) are the methyl and carbonyl carbon atoms, respectively. H(5) lies in the CCC plane.

as in Ref. [20], *viz.* the x-axis is perpendicular to the CCC plane, z is the two-fold symmetry axis, and consequently y is parallel to the connecting line of C(3)—C(2).

V. Ketenes

The mean amplitudes of vibration for ketene (CH_2CO) are shown in Fig. 1(d). Complete harmonic-vibration analyses with calculations of mean amplitudes have also been performed for methylketene [5, 21] and dimethylketene [5].

All these calculations confirm the characteristic value of $l(C{=}O) = 0.035$ Å for the ketene-type carbonyl bond.

VI. Carboxylic acids

Fig. 2(a) shows the calculated mean amplitudes for the formic acid monomer (HCOOH) [8]. The final force field from that work was used to cal-

Table VII

Mean amplitudes of vibration (Å units) for isotopic species of formic acid

Distance type	DCOOH	HCOOD	DCOOD
O—H′ (hydroxyl)	0.071		
O—D′		0.060	0.060
C—H		0.079	
C—D	0.067		0.067
C—O (hydroxyl)	0.046	0.046	0.046
C—O (carbonyl)	0.039	0.039	0.039
C...H′	0.100		
C...D′		0.087	0.087
O...O	0.056	0.056	0.056
O...H		0.101	
O...D	0.087		0.087
O...H		0.097	
O...D	0.085		0.085
O...H′	0.117		
O...D′		0.102	0.102
H...D′		0.113	
D...H′	0.112		
D...D′			0.103

culate the mean amplitudes also for the isotopic species DCOOH, HCOOD and DCOOD. The results at 298.16 °K are given in Table VII. There is no secondary isotope effect on the mean amplitudes within the decimals reported here. Some data of mean amplitudes for the formic acid monomer from electron diffraction have been reported [22, 23]. From the latter work [23] (in Å and with standard deviations in parentheses):

$$l(\text{C—O}) = 0.042\ (0.0014)$$

$$l(\text{C—O}) = 0.032\ (0.0010)$$

$$l(\text{O...O}) = 0.054\ (0.0018)$$

at a nozzle temperature of (175 ± 10) °C.

The cited spectroscopic work [8] is part of a series of papers dealing with carboxylic acids. They include molecular vibration analyses with computations of mean amplitudes for the acetic acid monomer [24], oxalic acid monomer [25] and formic acid dimer [26]. These computations confirm a characteristic value around 0.039 Å for the C=O mean amplitude in a carboxyl group (*cf.* Section I). Specifically the obtained values at 298 °K are (in Å): 0.039 for HCOOH [8], 0.040_5 for CH_3COOH [24], 0.037 for $(COOH)_2$ [25] and 0.040 for $(HCOOH)_2$ [26]. Some mean amplitudes for the oxalic acid monomer [27] and formic acid dimer [23] have been measured by electron diffraction.

REFERENCES

1. CYVIN, S. J.: Molecular Vibrations and Mean Square Amplitudes, Universitetsforlaget, Oslo, and Elsevier, Amsterdam, 1968
2. CYVIN, S. J.: Kgl. Norske Videnskab. Selskabs Skrifter, No. 1 (1969)
3. CYVIN, S. J.: Z. anorg. allgem. Chem. **378,** 117 (1970)
4. MÜLLER, A., KREBS, B., FADINI, A., GLEMSER, O., CYVIN, S. J., BRUNVOLL, J., CYVIN, B. N., ELVEBREDD, I., HAGEN, G., VIZI, B.: Z. Naturforsch. **23a,** 1656 (1968)
5. CYVIN, S. J., ALFHEIM, I.: Indian J. Pure Appl. Phys. **8,** 629 (1970)
6. CYVIN, B. N., CYVIN, S. J., HAGEN, G.: Chem. Phys. Letters **1,** 211 (1967)
7. BRUNVOLL, J., CYVIN, S. J., ELVEBREDD, I., HAGEN, G.: Chem. Phys. Letters **1,** 566 (1968)
8. CYVIN, S. J., ALFHEIM, I., HAGEN, G.: Acta Chem. Scand. **24,** 3038 (1970)
9. JENSEN, H. H., HAGEN, G., CYVIN, S. J.: J. Mol. Structure **4,** 51 (1969)
10. KATO, CH., KONAKA, S., IIJIMA, T., KIMURA, M.: Bull. Chem. Soc. Japan **42,** 2148 (1969)
11. HAGEN, G.: Acta Chem. Scand. (In press)
12. KUCHITSU, K., FUKUYAMA, T., MORINO, Y.: J. Mol. Structure **1,** 463 (1967—68)
13. HJORTAAS, K. E.: Acta Chem. Scand. **21,** 1379 (1967)
14. SAKSENA, B. D., KAGARISE, R. E.: J. Chem. Phys. **19,** 987 (1951)
15. ZIOMEK, J. S., MEISTER, A. G., CLEVELAND, F. F., DECKER, C. E.: J. Chem. Phys. **21,** 90 (1953)
16. HENCHER, J. L., KING, G. W.: J. Mol. Spectry, **16,** 158 (1965)
17. TRAETTEBERG, M.: Acta Chem. Scand. **24,** 373 (1970)
18. CYVIN, S. J., VIZI, B.: Acta Chim. Acad. Sci. Hung. **64,** 357 (1970)
19. COSSEE, P., SCHACHTSCHNEIDER, J. H.: J. Chem. Phys. **44,** 97 (1966)
20. VIZI, B., CYVIN, S. J.: Acta Chim. Acad. Sci. Hung. **64,** 351 (1970)

21. CYVIN, S. J., CHRISTENSEN, D. H., NICOLAISEN, F.: Chem. Phys. Letters **5,** 597 (1970); erratum: ibid. **6,** 552 (1970)
22. KARLE, I. L., KARLE, J.: J. Chem. Phys. **22,** 43 (1954)
23. ALMENNINGEN, A., BASTIANSEN, O., MOTZFELDT, T.: Acta Chem. Scand. **23,** 2848 (1969)
24. ALFHEIM, I., CYVIN, S. J.: Acta Chem. Scand. **24,** 3043 (1970)
25. CYVIN, S. J., ALFHEIM, I.: Acta Chem. Scand. **24,** 2648 (1970)
26. ALFHEIM, I., HAGEN, G., CYVIN, S. J.: J. Mol. Structure (In press)
27. NAHLOVSKA, Z., NAHLOVSKY, B., STRAND, T. G.: Acta Chem. Scand. **24,** 2617 (1970)

Sven Josef CYVIN; N-7034 Trondheim NTH, Norway
Béla VIZI; Veszprém, Schönherz Z. u. 12, Hungary

Acta Chimica Academiae Scientiarum Hungaricae, Tomus 70 (1—2), pp. 67—69 (1971)

SOLANUM GLYCOSIDES, VII*

QUALITATIVE AND PREPARATIVE SEPARATION OF METHYLATED MONOSACCHARIDES

M. M. SHABANA** and P. BITE

(Research Institute for Pharmaceutical Chemistry, Budapest)

Received April 16, 1970

Rapid and effective thin-layer and column chromatographic procedures were elaborated for the qualitative and preparative separation of 2,3,4-tri-O-methyl-L-rhamnose and 2,3,4,6-tetra-O-methyl-D-glucose, as well as of 3,4,6-tri-O-methyl-D-glucose and 4,6-di-O-methyl-D-galactose.

The hydrolysis of the permethylated derivative of solaradixin occurring in the root bark of *Solanum laciniatum* and *Solanum aviculare* gives four methylated monosaccharides [1]: 2,3,4-tri-O-methyl-L-rhamnose (**I**), 2,3,4,6-tetra-O-methyl-D-glucose (**II**), 3,4,6-tri-O-methyl-D-glucose (**III**) and 4,6-di-O-methyl-D-galactose (**IV**).

KUHN et al. [2] attempted the paper chromatographic separation and characterization of **I** and **II** with the *n*-butanol–ethanol–water 4 : 1 : 5 mixture of HIRST et al. [3], but they could not obtain two separate spots even after 18 hrs of developing. After many experiments with different adsorbents and solvent mixtures, we now report a rapid and effective separation method for these two compounds, with a 3 : 1 ether–toluene mixture and a silica gel + gypsum adsorbent. With double development, the R_f values of **I** and **II** are 0.46 and 0.26, respectively. The time requirement of the procedure is about 1 hr. on 20×5 cm plates, and 20 min. on microscope plates.

The preparative separation of **I** and **II** was performed by KUHN et al. [2] on columns filled with a 50 wt.% mixture of Darco G 60 and Celite 535 adsorbents, as described by LINDBERG and WICKBERG [4]. Though the method is effective, the preparation of the column is time-consuming and its capacity is small. Experiments in our laboratory have shown that the good and preparative separation of **I** and **II** can be accomplished within 3—5 hrs with the above 3 : 1 ether–toluene mixture on a silica gel column. A further considerable advantage of the present method is that anhydrous solutions are to be concentrated after the chromatographic separation, in contrast to the aqueous methylethylketone solutions of KUHN et al.

* Part VI: Acta Chim. Acad. Sci. Hung. **65,** 101 (1970).
** United Arab Republic Scholar from Cairo University, Faculty of Pharmacy.

For the paper chromatographic separation of methylated monosaccharides **III** and **IV** obtained from the permethylated solaradixin, we successfully applied1 [1] the 4 : 1 : 5 *n*-butanol–ethanol–water mixture of HIRST et al. [3] on Whatman 1 paper, using the ascending technique. However, this procedure is rather devious. We have elaborated a thin-layer chromatographic separation of these compounds (**III** and **IV**) on silica gel—gypsum adsorbent with 3 : 1 benzene–ethanol. With double development, the R_f values of **III** and **IV** were 0.54 and 0.30, respectively.

The preparative separation of **III** and **IV** was carried out earlier [1] in our laboratory with the solvent mixture of HIRST et al. on Whatman 3 paper, a slow and cumbersome procedure. Though the solvent mixture which had proved to be suitable in the thin-layer chromatographic technique could not be applied directly in this case for the silica gel column, it was found that these two compounds can satisfactorily be separated on silica gel column by starting with a 9 : 1 mixture of benzene and ethanol, and then switching to a 4 : 1 mixture of these same solvents.

Experimental

The thin-layer chromatographic analyses were carried out with silica gel G adsorbent (Merck) on 5 × 20 and 20 × 20 cm plates, and on microscope plates 3 × 8 cm in size. The start-front distance was 15 and 6 cm, respectively. Coloured products were obtained with aniline phthalate.

Column chromatographic separations were performed on Woelm silica gel.

Separation of 2,3,4-tri-O-methyl-L-rhamnose (I) and 2,3,4,6-tetra-O-methyl-D-glucose (II)

a) Thin-layer procedure

The chloroform solution obtained in the workup of the hydrolysis product of permethylated solaradixin was applied to silica gel + gypsum thin-layer in the usual amount. Subsequent to removal of the chloroform, developing was made with a freshly prepared 3 : 1 mixture of ether and toluene. After the first developing the plate was dried with a stream of 50 °C air until the odour of toluene disappeared and the developing procedure was repeated with another, freshly prepared mixture of the same composition. Authentic materials (**I** and **II**) and their mixtures were also developed on the same plates. The spots of trimethylrhamnose and tetramethylglucose were grey and red, respectively, after visibilization.

b) Column procedure

A column of 1.6 cm in diameter was made of 36 g silica gel with a 3 : 1 mixture of ether and toluene. 1 g of the residue of the evaporated chloroform solution was applied in 3 ml of the same solvent mixture. Fractions of 5 ml volume were collected. The results are shown in Table I.

Separation of 3,4,6-tri-O-methyl-D-glucose (III) and 4,6-di-O-methyl-D-galactose (IV)

a) Thin-layer procedure

The aqueous phase obtained in the hydrolysis of permethylated solaradixin was dropped, after extraction with chloroform to remove **I** and **II**, on a silica gel G thin-layer. Subsequent to drying of the spot, developing was made with a 3 : 1 mixture of benzene and ethanol. The second developing was made with the same solvent mixture as described above for **I** and **II**. Both **III** and **IV** appeared as red spots on visibilization.

Table I

Chromatography of methylated monosaccharides **I** *and* **II** *on a silica gel column*

Fraction	Content (mg)	Component (on basis of TLC)
1—10	50.0	—
11—19	300.0	**I**
20—33	100.0	**I**+**II**
34—60	360.0	**II**

I = 2,3,4-tri-O-methyl-L-rhamnose
II = 2,3,4,6-tetra-O-methyl-D-glucose

b) Column procedure

A column of 1.6 cm in diameter was made of 22 g silica gel with benzene, and a mixture of 0.7 g of the residue of the evaporated aqueous phase (previously extracted with chloroform) with silica gel was applied to it. Fractions of 5 ml volume were collected. The results are summarized in Table II.

Table II

Chromatography of methylated monosaccharides **III** *and* **IV** *on a silica gel column*

Solvent mixture	Fraction	Weight of evaporation residue (mg)	Component (on basis of TLC)
benzene	1— 7	—	—
benzene–ethanol			
9 : 1	8—19	40.0	—
	20—48	180.0	**III**
benzene–ethanol			
4 : 1	49—57	50.0	**III**+**IV**
	58—83	150.0	**IV**

III = 3,4,6-tri-O-methyl-L-glucose
IV = 4,6-di-O-methyl-D-galactose

*

The authors express their thanks to Dr. Irmentraut Löw (Max Planck Institute, Heidelberg) and Professor Sir Edmund HIRST (University of Edinburgh) for authentic methylated monosaccharides.

The authors also thank Mrs. Eva BABOS-SZEBENYI for her technical assistance.

REFERENCES

1. BITE, P., SHABANA, M. M., JÓKAY, L., PONGRÁCZ-STERK, L.: Acta Chim. Acad. Sci. Hung. **63,** 343 (1970)
2. KUHN, R., LÖW, I., TRISCHMANN, H.: Chem. Ber. **88,** 1690 (1955)
3. HIRST, E. L., HOUGH, L., JONES, J. K. N.: J. Chem. Soc. **1949,** 928
4. LINDBERG, B., WICKBERG, B.: Acta Chem. Scand. **8,** 569 (1954)

M. Marruan SHABANA
Pál BITE
} Budapest IV., Szabadságharcosok útja 47—49

Acta Chimica Academiae Scientiarum Hungaricae, Tomus 70 (1–2) pp. 71–78 (1971)

CHEMISTRY OF 4*H*-1,3-BENZOTHIAZINE DERIVATIVES, III

HYDROLYSIS OF 2-PHENYL-3-ETHYL-6,7-DIMETHOXY-4*H*-1,3-BENZOTHIAZINIUM BROMIDE*

J. SZABÓ, I. VARGA, E. VINKLER and É. BARTHOS

(Department for Pharmaceutical Chemistry, Medical University, Szeged)

Received April 22, 1970

The hydrolysis of 2-phenyl-3-ethyl-6,7-dimethoxy-4*H*-1,3-benzothiazinium bromide was examined and it was found that under the effect of equivalent amount of alkali the compound is converted through 2-phenyl-3-ethyl-6,7-dimethoxy-4*H*-1,3-benzothiazinium hydroxide into 2-phenyl-2-hydroxy-3-ethyl-6,7-dimethoxy-2,3-dihydro-4*H*-1,3-benzothiazine, which, under the effect of excess alkali, reacts further to give *N*-benzoyl-*N*-ethyl-4,5-dimethoxy-2-mercaptobenzylamine. The acid hydrolysis of 2-phenyl-3-ethyl-6,7-dimethoxy-4*H*-1,3-benzothiazinium bromide gives *S*-benzoyl-*N*-ethyl-4,5-dimethoxy-2-mercaptobenzylammonium bromide in the first step, which is transformed via intermolecular transacylation to *N*-ethyl-4,5-dimethoxy-2-mercaptobenzylammonium bromide and *S*,*N*-dibenzoyl-*N*-ethyl-4,5-dimethoxy-2-mercaptobenzylamine. Upon the effect of alkali, *S*-benzoyl-*N*-ethyl-4,5-dimethoxy-2-mercaptobenzylammonium bromide undergoes intramolecular transacylation to give *N*-benzoyl-*N*-ethyl-4,5-dimethoxy-2-mercaptobenzylamine. The $S \rightarrow N$ acyl migration is a reversible process because *N*-benzoyl-*N*-ethyl-4,5-dimethoxy-2-mercaptobenzylamine is converted in the presence of acid into the corresponding *S*-benzoyl derivative. This hydrolysis proved the structure of 2-phenyl-3-ethyl-6,7-dimethoxy-4*H*-1,3-benzothiazinium bromide and made also possible the preparation of the *N*-ethyl derivative of 4,5-dimethoxy-2-mercaptobenzylamine.

During an examination of the chemistry of 2-phenyl-3-ethyl-6,7-dimethoxy-4*H*-1,3-benzothiazinium bromide (**I**) obtained by quaternization of 2-phenyl-6,7-dimethoxy-4*H*-1,3-benzothiazine [2] it was found that compound **I** is readily dissolved in water and its saturated aqueous solution is acidic (pH 3.5). Accordingly, compound **I** undergoes partial hydrolysis in aqueous solution to 2-phenyl-3-ethyl-6,7-dimethoxy-4*H*-1,3-benzothiazinium hydroxide (**II**) and hydrogen bromide. Subsequently the hydrolysis of the benzothiazine ring, too, occurs at a moderate rate at about 20 °C and considerably faster at elevated temperatures.

After heating an aqueous solution of benzothiazinium bromide (**I**) for 1 hour, the following products could be isolated from the reaction mixture: hydrogen bromide, *N*-ethyl-4,5-dimethoxy-2-mercaptobenzylamine hydrobromide (**VI**), *S*-benzoyl-*N*-ethyl-4,5-dimethoxy-2-mercaptobenzylamine hydrobromide (**IV**) and *S*,*N*-dibenzoyl-*N*-ethyl-4,5-dimethoxy-2-mercaptobenzylamine (**VII**) (experiment No. 1).

* Presented in part at the Session of the Committee of Organic Chemistry, Hungarian Academy of Sciences; February 22, 1966 [1].

When heating of the same aqueous solution was continued for 5—6 hrs, the *S*-benzoyl-2-mercaptobenzylamine derivative (**IV**) could not be detected in the reaction mixture, from which the conclusion was drawn that this compound is merely an intermediate of hydrolysis. The conclusion was further supported by the observation that compound **IV** transformed into compounds **VI** and **VII** in quantitative yield on heating in aqueous solution (experiment No. 2).

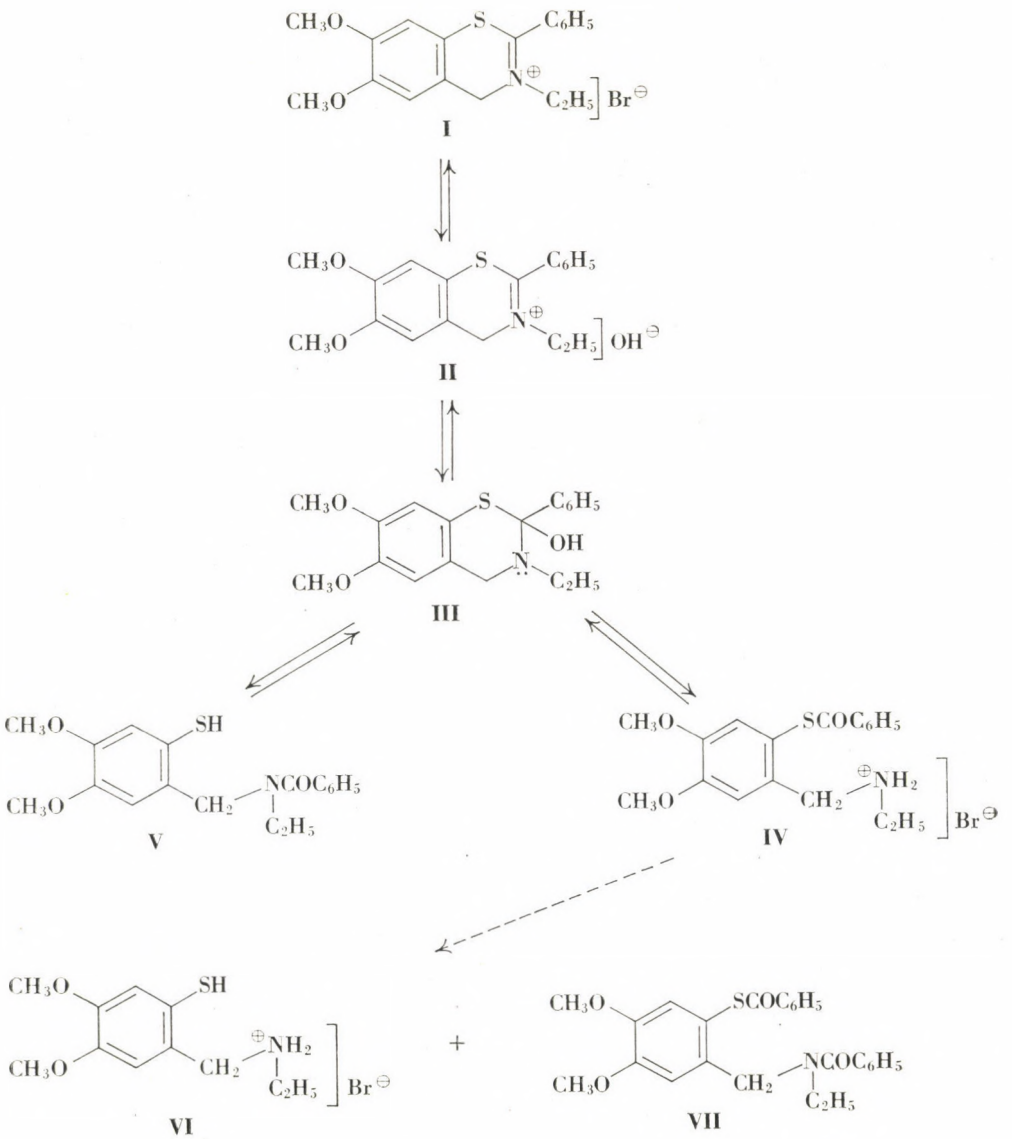

On the basis of these observations, the hydrolysis of quaternary salt **I** proceeds through the following steps; compound **I** hydrolyzes in aqueous solution to a small extent to hydrogen bromide and quaternary base **II**. The quaternary base **II** is transformed into pseudobase **III**, which, in the acidic solution undergoes C—N bond fission to give the *S*-benzoyl-2-mercaptobenzylamine derivative (**IV**). The intermolecular transacylation reaction between two molecules of compound **IV**, which proceeds even under acidic conditions, yields compounds **VI** and **VII**.

S-Benzoyl-*N*-ethyl-4,5-dimethoxy-2-mercaptobenzylamine hydrobromide (**IV**) is transformed in alkaline solution via intramolecular acyl migration, probably through intermediate **III**, into the *N*-benzoyl-2-mercaptobenzylamine derivative (**V**) (experiment No. 3). The $S \rightarrow N$ acyl migration is a reversible process, because on heating with hydrogen bromide the *N*-benzoyl-2-mercaptobenzylamine derivative (**V**) is converted to the corresponding *S*-benzoyl derivative (**IV**), again probably through intermediate **III**, and compound **IV** undergoes further hydrolysis to give compound **VI** (experiment No. 4).

S-Benzoyl-*N*-ethyl-4,5-dimethoxy-2-benzylamine hydrobromide (**IV**) is a stable compound in the solid state, from which the *S*-benzoyl-*N*-ethyl-4,5-dimethoxy-2-mercaptobenzylamine base (**VIII**) cannot be liberated with alkaline agents, because it is immediately transformed into *N*-benzoyl-*N*-ethyl-4,5-dimethoxy-2-mercaptobenzylamine (**V**), as has been seen in experiment No. 3. On treating an aqueous solution of compound **IV** with sodium hydrogen carbonate, an immediate intermolecular transacylation reaction occurs to give *S*,*N*-dibenzoyl-*N*-ethyl-4,5-dimethoxy-2-mercaptobenzylamine (**VII**) and presumably the internal salt of *N*-ethyl-4,5-dimethoxy-2-mercaptobenzylamine in quantitative yield, of which the latter was isolated after acidification of the aqueous solution with hydrogen bromide, in form of the hydrobromide salt (**VI**) (experiment No. 5).

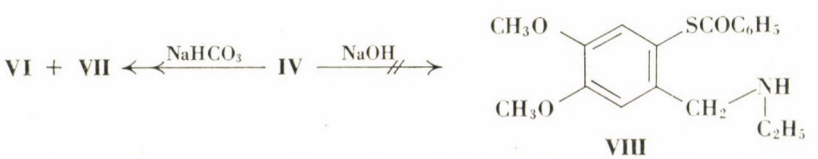

VIII

On the basis of the latter reaction the possibility arises that under the effect of alkali the *S*-benzoyl-2-mercaptobenzylamine derivative (**IV**) is first converted to compounds **VI** and **VII**, and the *N*-benzoyl derivative (**V**) comes about as a result of transacylation between **VI** and **VII**. The intramolecular character of the $S \rightarrow N$ acyl migration process taking place under the effect of alkali is supported by the observation that treatment of compound **IV** with alkali in the presence of 4,5-dimethoxy-2-mercaptobenzylamine hydro-

chloride [3] under the conditions specified in experiment No. 3 gave compound **V** as the only product. The formation of *N*-benzoyl-4,5-dimethoxy-2-mercaptobenzylamine, which might be expected in case of an intermolecular reaction, could not be detected.

The alkaline hydrolysis of 2-phenyl-3-ethyl-6,7-dimethoxy-4*H*-1,3-benzothiazinium bromide (**I**) was also examined. Under the effect of excess alkali, quaternary salt **I** is converted to *N*-benzoyl-*N*-ethyl-4,5-dimethoxy-2-mercaptobenzylamine (**V**), presumably through quaternary base **II** and pseudobase **III** as intermediates (experiment No. 6). By treatment with an equivalent amount of alkali, quaternary base **II** was liberated from quaternary salt **I** in aqueous solution and though our efforts to isolate **II** have failed, it could be transformed back to quaternary salt **I** by immediate treatment with hydrogen bromide.

From the aqueous solution of quaternary base **II**, pseudobase **III** is rapidly precipitated in crystalline form, being sparingly soluble in water (experiment No. 7). Pseudobase **III** is an unstable material, which could not be purified by crystallization, because it was partially transformed to other products already upon dissolution. When dissolved in excess aqueous alkali in the cold, it was quantitatively transformed to the *N*-benzoyl-2-mercaptobenzylamine derivative (**V**), providing a further piece of evidence that alkaline hydrolysis of benzothiazinium bromide (**I**) proceeds through intermediates **II** and **III** (experiment No. 8).

In order to prepare some characteristic derivatives, *N*-benzoyl-*N*-ethyl-4,5-dimethoxy-2-mercaptobenzylamine (**V**) was oxidized with hydrogen peroxide to the corresponding disulfide (**IX**) and, in another experiment, treated with benzoyl chloride in pyridine solution to give the *S*,*N*-dibenzoyl derivative (**VII**) (experiment No. 9). *N*-Benzoyl-*N*-ethyl-2-mercaptobenzylamine

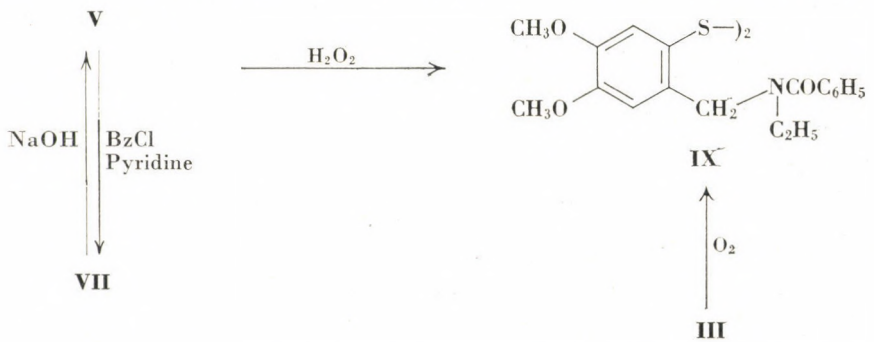

(**V**) was also produced by partial debenzoylation of the *S*,*N*-dibenzoyl derivative (**VII**), one of the hydrolysis products. Disulfide **IX** was also formed by air oxidation, when the solution of pseudobase **III** in ethanol was exposed to air (experiment No. 10).

Surveying the acidic and alkaline hydrolysis of 2-phenyl-3-ethyl-6,7-dimethoxy-4*H*-1,3-benzothiazinium bromide (**I**), it can be established that these processes take place similarly to those observed with 2-phenyl-6,7-dimethoxy-4*H*-1,3-benzothiazine [3]. However, in this case the intermediate pseudobase (**III**) could also be isolated, its IR spectrum being in accord with structure **III** (Fig. 1).

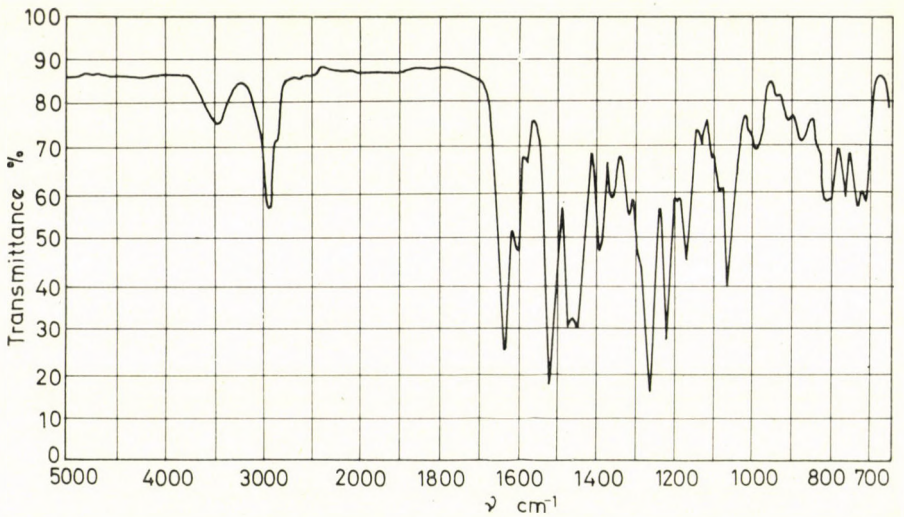

Fig. 1. IR spectrum of 2-phenyl-2-hydroxy-3-ethyl-6,7-dimethoxy-2,3-dihydro-4*H*-1,3-benzothiazine in KBr

Experimental

(Melting points are uncorrected)

1) Hydrolysis of 2-phenyl-3-ethyl-6,7-dimethoxy-4*H*-1,3-benzothiazinium bromide (I)

A solution of 4.95 g (0.01 mole) 2-phenyl-3-ethyl-6,7-dimethoxy-4*H*-1,3-benzothiazinium bromide in 30 ml water was heated for 1 hour on the water bath in a flask provided with a reflux condenser, in carbon dioxide atmosphere. After cooling, the precipitate was separated by decantation, washed with a little water and dried in a vacuum desiccator. Yield: 2.2 g. *S*,*N*-Dibenzoyl-*N*-ethyl-2-mercaptobenzylamine (**VII**) thus obtained was crystallized from ethanol to give colourless needles, m. p. 110—112 °C. The compound shows polymorphism, on repeated crystallization from ethanol it is transformed to another modification with m.p. 166—167 °C. The analysis data of the two modifications are identical.

$C_{25}H_{25}NO_4S$ (435.52). Calcd. C 68.94; H 5.79; N 3.23; S 7.36. Found C 69.30; H 5.52; N 3.25; S 7.49%.

The aqueous solution was saturated with ether, when 0.35 g of *S*-benzoyl-*N*-ethyl-4,5-dimethoxy-2-mercaptobenzylammonium bromide (**IV**) precipitated in the form of colourless needles. The crystals were collected by filtration, dried and crystallized from benzene to give colourless needles, m. p. 135—136 °C (decomposition).

$C_{18}H_{22}BrNO_3S$ (412.35). Calcd. C 52.42; H 5.38; N 3.39. Found C 51.81; H 5.39; N 3.33%.

The aqueous solution was evaporated to dryness in vacuum. The residue, crude *N*-ethyl-4,5-dimethoxy-2-mercaptobenzylammonium bromide (**VI**) (2.15 g) was crystallized from ethanol. Pale yellow prisms, m. p. 193—195 °C (decomposition).

$C_{11}H_{18}BrNO_2S$ (308.24). Calcd. C 42.86; H 5.88; N 4.53; S 10.46. Found C 42.91; H 5.87; N 4.52; S 10.34%.

2) Transformation of *S*-benzoyl-*N*-ethyl-4,5-dimethoxy-2-mercaptobenzylammonium bromide (IV) in aqueous solution

0.41 g (0.001 mole) of *S*-benzoyl-*N*-ethyl-4,5-dimethoxy-2-mercaptobenzylammonium bromide was dissolved in 5 ml water and the solution heated for 30 min. on a water bath in carbon dioxide atmosphere. The material which precipitated on cooling was filtered off, washed with water and dried to give 0.21 g (96.6%) of *S*,*N*-dibenzoyl-*N*-ethyl-4,5-dimethoxy-2-mercaptobenzylamine (**VII**). Colourless needles from ethanol, m. p. 110—112 °C, no m. p. depression was observed with the material obtained in the preceding experiment.

The aqueous solution was evaporated to dryness in vacuum and the residue dissolved in 2 ml ethanol with heating. The solution was diluted with ether to precipitate 0.14 g (91.0%) of *N*-ethyl-2-mercapto-4,5-dimethoxybenzylammonium bromide (**VI**), m. p. 192—195 °C, no m. p. depression with the material obtained in the preceding experiment.

3) Transformation of *S*-benzoyl-*N*-ethyl-4,5-dimethoxy-2-mercaptobenzylammonium bromide (IV) in alkaline media

0.41 g (0.001 mole) of *S*-benzoyl-*N*-ethyl-4,5-dimethoxy-2-mercaptobenzylammonium bromide was dissolved in a mixture of 40 ml ethanol and 2 drops of hydrochloric acid in ethanol. then a solution of 0.5 g potassium hydroxide in 0.5 ml water and 5 ml ethanol was added. The mixture was kept at room temperature for 5 min., slightly acidified with hydrochloric acid in ethanol and titrated with a 0.1 *N* iodinesolution. The analytical procedure revealed the presence of 0.30 g of *N*-benzoyl-*N*-ethyl-4,5-dimethoxy-2-mercaptobenzylamine (**V**), which corresponds to 90% of the theoretical amount. The solution was evaporated to dryness in vacuum, the residue was treated with 10 ml water and extracted with 50 ml ether to remove the [2,2'-*N*,*N*'-diethyl-*N*,*N*'-bis(benzoylaminomethyl)-4,4',5,5'-tetramethoxy]diphenyldisulfide (**IX**) which was formed during iodine oxidation. The ethereal phase was evaporated to dryness and the residue crystallized from 60% ethanol to give 0.25 g (75.5%) of the product. After crystallization from 60% ethanol several times, the m. p. increased to 131—132 °C, pale yellow needles.

$C_{36}H_{40}N_2O_6S_2$ (660.83). Calcd. C 65.43; H 6.10. Found C 65.22; H 5.86%.

4) Acid hydrolysis of *N*-benzoyl-*N*-ethyl-4,5-dimethoxy-2-mercaptobenzylamine (V)

0.33 g (0.001 mole) of *N*-benzoyl-*N*-ethyl-4,5-dimethoxy-2-mercaptobenzylamine was dissolved in 10 ml 5% hydrogen bromide and the solution heated for 6 hrs at 100 °C in carbon dioxide atmosphere. After cooling, the solution was extracted with ether to remove the benzoic acid formed (0.06 g).

The aqueous solution was concentrated in vacuum and cooled to deposit 0.07 g of *S*-benzoyl-*N*-ethyl-4,5-dimethoxy-2-mercaptobenzylammonium bromide (**IV**) in the form of colourless needles, m. p. 133—135 °C (decomposition), no m. p. depression with the material obtained in the first experiment.

The aqueous filtrate was evaporated to dryness in vacuum, the residue heated with a little ethanol, the solution filtered and treated with ether to precipitate 0.17 g of *N*-ethyl-4,5-dimethoxy-2-mercaptobenzylammonium bromide, m. p. 191—193 °C (decomposition). The product showed no m. p. depression with the material obtained in experiment No. 1.

5) Transformation of *S*-benzoyl-*N*-ethyl-4,5-dimethoxy-2-mercaptobenzylammonium bromie (IV) in aqueous sodium hydrogen carbonate solution

0.22 g (0.0005 mole) of *S*-benzoyl-*N*-ethyl-4,5-dimethoxy-2-mercaptobenzylammonium bromide was dissolved in 80 ml water without heating, 0.085 g (0.0005 mole) sodium hydrogen carbonate was added to the solution and the mixture was left standing for 5 min. The solution was acidified with hydrogen bromide and the precipitated *S*,*N*-dibenzoyl-*N*-ethyl-4,5-dimethoxy-2-mercaptobenzylamine (**VII**) was extracted with ethyl acetate. The organic phase was dried over anhydrous sodium sulfate and the solvent removed by distillation. On crystallization from ethanol the residue gave colourless needles, m. p. 110—112 °C, no m. p. depression with the substance obtained in experiment No. 1. Yield: 0.1 g, 96%.

The aqueous solution was evaporated to dryness in vacuum, the residue extracted with ethanol and the solution diluted with ether to precipitate 0.08 g (100%) of *N*-ethyl-4,5-dimethoxy-2-mercaptobenzylammonium bromide (**VI**), m. p. 192—194 °C (decomposition), no m. p. depression with the material obtained in experiment No. 1.

6) Alkaline hydrolysis of 2-phenyl-3-ethyl-6,7-dimethoxy-4*H*-1,3-benzothiazinium bromide (I)

0.2 g (0.0005 mole) of 2-phenyl-3-ethyl-6,7-dimethoxy-4*H*-1,3-benzothiazinium bromide was dissolved in 30 ml water, 5 ml 2*N* sodium hydroxide solution was added and the mixture was left standing for 5 min. The reaction mixture was acidified with hydrochloric acid and the precipitated *N*-benzoyl-*N*-ethyl-4,5-dimethoxy-2-mercaptobenzylamine (**V**) extracted with ethyl acetate. The organic phase was dried and concentrated in vacuum to give an oily residue, which gave a positive mercapto reaction. It was dissolved in ethanol, treated with 1 drop of 1*N* sodium hydroxide and oxidized with hydrogen peroxide to the corresponding disulfide (**IV**). The latter was precipitated by dilution with water. The product was crystallized from 60% ethanol to give 0.16 g pale yellow material (needles), m. p. 129—131 °C; no m. p. depression with the material described in experiment No. 3.

7) Reaction of 2-phenyl-3-ethyl-6,7-dimethoxy-4*H*-1,3-benzothiazinium bromide (I) with one equivalent amount of alkali

0.79 g (0.002 mole) of 2-phenyl-3-ethyl-6,7-dimethoxy-4*H*-1,3-benzothiazinium bromide was dissolved in 60 ml cold water and 2 ml (0.002 mole) 2*N* sodium hydroxide was added with continuous shaking. The solution deposited 0.40 g (60.7%) of 2-phenyl-2-hydroxy-3-ethyl-6,7-dimethoxy-2,3-dihydro-4*H*-1,3-benzothiazine (**III**) in the form of colourless plates. The crystals were washed with water and dried, m. p. 76—80 °C (decomposition). Further purification by crystallization failed.

$C_{18}H_{21}NO_3S$ (331.42). Calcd. C 65.23; H 6.39. Found C 66.52; H 6.19%.

2-Phenyl-3-ethyl-6,7-dimethoxy-4*H*-1,3-benzothiazinium hydroxide (**II**) which remained in the aqueous filtrate was converted with hydrogen bromide to the corresponding bromide (**I**). The aqueous solution was extracted with chloroform several times, the combined organic phase dried over anhydrous sodium sulfate and concentrated to about 1 ml. The residue was diluted with ether to deposit 0.10 g of 2-phenyl-3-ethyl-6,7-dimethoxy-4*H*-1,3-benzothiazinium bromide (**I**), yellow powdery crystals, m. p. 189—191 °C, no m. p. depression with the authentic material [2].

8) Transformation of 2-phenyl-2-hydroxy-3-ethyl-6,7-dimethoxy-2,3-dihydro-4*H*-1,3-benzothiazine (III) in sodium hydroxide solution

0.33 g (0.01 mole) of 2-phenyl-2-hydroxy-3-ethyl-6,7-dimethoxy-2,3-dihydro-4*H*-1,3-benzothiazine was dissolved in a solution of 0.05 g sodium hydroxide in 10 ml ethanol and the solution was left standing for 5 min. The resulting *N*-benzoyl-*N*-ethyl-4,5-dimethoxy-2-mercaptobenzylamine (**V**) was oxidized with hydrogen peroxide to the corresponding disulfide (**IX**). Pale yellow needles from 60% ethanol, m. p. 129—131 °C, no m. p. depression with the product obtained in experiment No. 3.

9) *N*-Benzoyl-*N*-ethyl-4,5-dimethoxy-2-mercaptobenzylamine (V)

2.18 g (0.005 mole) of *S*,*N*-dibenzoyl-*N*-ethyl-4,5-dimethoxy-2-mercaptobenzylamine (**VII**) was dissolved in 30 ml hot ethanol, and a solution of 0.4 g sodium hydroxide in 2 ml water and 5 ml ethanol added. After 3 min. the solution was cooled and acidified with 10 ml 10% hydrochloric acid, 50 ml water was added in small portions to the ice-cold reaction mixture to deposit 1.5 g of *N*-benzoyl-*N*-ethyl-4,5-dimethoxy-2-mercaptobenzylamine, which was filtered off, washed with water and a little ether, and dried. Pale yellow prisms from 50% ethanol, m. p. 120—122 °C.

$C_{18}H_{21}NO_3S$ (331.42). Calcd. N 4.33. Found N 4.20%.

In order to prepare a characteristic derivative, the product was oxidized with hydrogen peroxide to [2,2'-*N*,*N*'-diethyl-*N*,*N*'-bis(benzoylaminomethyl)-4,4',5,5,'-tetramethoxy]-diphenyl disulfide (**IX**). Pale yellow needles from 60% ethanol, m. p. 131—132 °C, no m. p. depression with the material obtained in experiment No. 3.

Compound **V** was benzoylated with benzoyl chloride inpyridine solution to give *S*,*N*-dibenzoyl-*N*-ethyl-4,5-dimethoxy-2-mercaptobenzylamine (**VII**), colourless needles from ethanol, m. p. 166—167 °C, no m. p. depression with the material obtained in experiment No. 1.

10) Formation of [2,2'-*N*,*N*'-diethyl-*N*,*N*'-bis(benzoylaminomethyl)-4,4',5,5'-tetramethoxy]-diphenyl disulfide (IX) from pseudobase (III)

0.20 g of 2-phenyl-2-hydroxy-3-ethyl-6,7-dimethoxy-2,3-dihydro-4*H*-1,3-benzothiazine (**III**) was dissolved in 2 ml ethanol and the solution exposed to air. 0.14 g of [2,2'-*N*,*N*'-diethyl-*N*,*N*'bis(benzoylaminomethyl)-4,4',5,5'-tetramethoxy]diphenyl disulfide was deposited from the solution, yellow prisms, m. p. 130—131 °C, no m. p. depression with the material obtained in experiment No. 3.

*

The authors express their thanks to Dr. J. SZABÓ for his cooperation in the evaluation of the IR spectra.

REFERENCES

1. SZABÓ, J., VINKLER, E., VARGA, I., BARTHOS, É.: Kémiai Közl. **26,** 21 (1966)
2. SZABÓ, J., VARGA, I., VINKLER, E., BARTHOS, É.: Acta Chim. Acad. Sci. Hung. In press
3. SZABÓ, J., VINKLER, E., VARGA, I.: Acta Chim. Acad. Sci. Hung. **58,** 179 (1968)

János SZABÓ
István VARGA
Elemér VINKLER
Éva BARTHOS
Szeged, Eötvös u. 2, Hungary.

Acta Chimica Academiae Scientiarum Hungaricae, Tomus 70 (1–2), pp. 79–82 (1971)

ASSOCIATION STRUCTURE OF 3-HYDROXY-CHROMONES

P. SOHÁR, L. VARGHA † and J. KUSZMANN

(Research Institute for Pharmaceutical Chemistry, Budapest)

Received May 19, 1970

Infrared spectroscopic investigation of the 2-methyl-3-hydroxychromone proved that in the solid state a cyclic dimer is formed instead of a 5-membered chelate ring, with intramolecular hydrogen bonding as supposed earlier. The NMR spectrum excludes the possibility of a tautomer and thus splitting of the carbonyl band in the IR spectrum is presumably caused by FERMI resonance even in solution. The molecules of the corresponding 2-phenyl derivative (flavonol) exist in a state of simple intermolecular (non-cyclic) association.

VARGHA *et al.*, preparing the 2-methyl-3-hydroxy-chromone, suggested for it the intramolecular chelate-like structure **I**, as the compound failed to give reactions characteristic of the oxo and hydroxyl groups (*e.g.* formation of oxonium salts, or reaction with diazomethane).

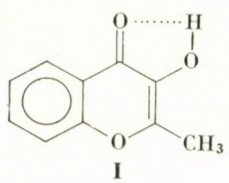

I

To prove this hypothetical structure, the IR spectra of **I** were investigated in the solid state (in KBr pellet) and in 0.1 *M* chloroform solution.

In the spectrum of the solid (Fig. 1), the νOH band at 3295 cm^{-1} is relatively sharp with a weak shoulder at 3385 cm^{-1}, and the γOH band appears at 665 cm^{-1}, too. This indicates [2] the presence of a cyclic, yet weak, con-

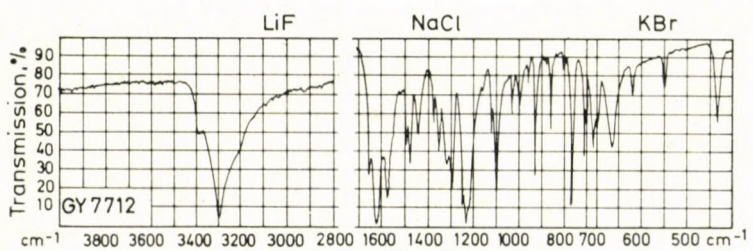

Fig. 1. IR spectrum of **I** in KBr pellet

sequently non-chelate-like hydrogen bond. In the spectrum of the solution (Fig. 2) there is no maximum at 3295 cm^{-1}, and the unsplit νOH band appears

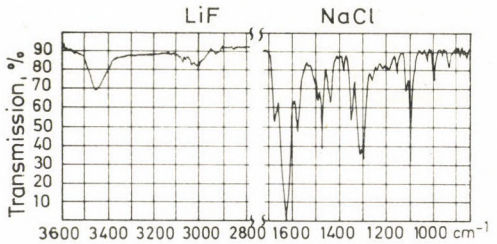

Fig. 2. IR spectrum of **II** in $CHCl_3$

at 3450 cm^{-1}, indicating that the hydrogen bonds are destroyed already in relatively concentrated solutions, proving the intermolecular character of the association [3]. The hypothesis of intramolecular association cannot be maintained even with the restriction that hydrogen bonds are weak, *i.e.*, of non-chelate character. It was obvious to suppose that with the participation of the carbonyl and hydroxyl, a cyclic dimer is formed by two molecules (**II**), motivating the sharp contours of the νOH and γOH bands and the chemical properties of the compound.

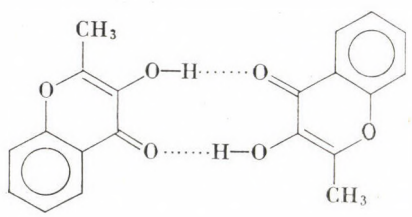

II

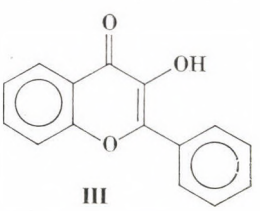

III

For comparison the IR spectra of 3-hydroxy-flavone (**III**) were recorded in the solid state (in KBr pellet) and in 0.1 *M* chloroform solution.

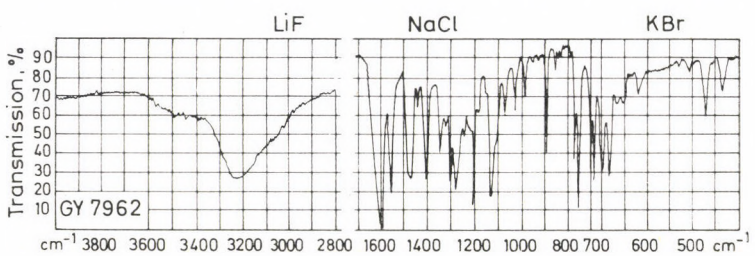

Fig. 3. IR spectrum of **III** in KBr pellet

In the spectrum of the solid (Fig. 3) the broad νOH band appears between 3400—2900 cm^{-1} with a maximum at about 3230 cm^{-1}. The νC=O

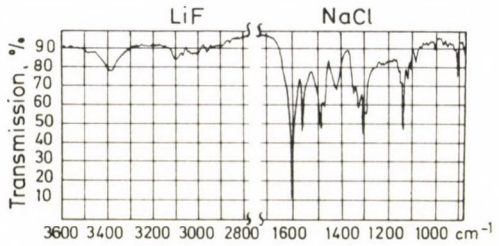

Fig. 4. IR spectrum of **III** in $CHCl_3$

band at 1610 cm^{-1} is not split and the γOH band is very diffuse, appearing between 800—500 cm^{-1} as a broadening-out of the base line. In the spectrum of the solution (Fig. 4), instead of the νOH band at about 3230 cm^{-1}, an absorption maximum appears at 3390 cm^{-1}. This proves that unlike in the case of **II**, compound **III** does not form a cyclic dimer obviously in consequence of the more bulky phenyl group. An intramolecular hydrogen bond that would correspond to structure **I** is also absent, having been replaced by simple intermolecular association.

During the IR investigation of **I** another interesting problem arose, *viz.* that in the spectrum of the solid (Fig. 1) the intense νC=O band at 1625 cm^{-1} is split: at 1650 cm^{-1} a well distinguishable maximum becomes superimposed on the carbonyl band. This maximum remains unchanged after repeated crystallization, and it appears even in the solution spectrum (Fig. 2).

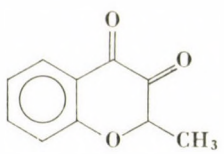

IV

Therefore the splitting of the νC=O band cannot be due to any contamination, or to molecules with association structures different from that given by **II**, or to monomeric structures formed at lower rates in the solid state.

It is possible that, similarly to the phthalides [4], the splitting is caused by the FERMI resonance between the νC=O and an out-of-plane aromatic CH deformation vibration. Nevertheless it was conceivable that a small fraction of the molecules with the diketo-tautomeric (**IV**) form is responsible for the carbonyl band.

To clear up this problem, NMR investigations were performed. In the ^1H spectrum ($CDCl_3$) the δCH_3 signal is a singlet at 2.50 ppm, the OH signal appears at $\delta = 6.53$ ppm, while the aromatic protons give ABCX

type multiplets with the center of the X-part at 8.2 ppm and the ABC-part at about $\delta = 7.4$ ppm. Since neither a doublet, nor a quartet characteristic of the CH—CH_3 group of structure **IV** did appear, the existence of this tautomer can be excluded. Thus, the splitting of the carbonyl band in the IR spectrum is presumably caused by FERMI resonance. This is supported by the fact that in case of **III** where the out-of-plane $C_{Ar}H$ deformation frequencies are modified, the $\nu C{=}O$ band is not split. On the other hand, the position of the OH signal in the NMR spectrum can be considered as further evidence against the chelate structure which would be characterized by significantly larger chemical shifts [5].

Experimental

The IR spectra were recorded with a UR-10 (Jena) double-beam spectrometer in KBr pellets, and in 1 mm NaCl cuvettes using 0.1 *M* $CHCl_3$ solutions. The NMR spectra were recorded with a VARIAN A-60D type spectrometer (60 MHz), in deuterochloroform solution, using tetramethylsilane as internal reference.

REFERENCES

1. VARGHA, L., RAMONCZAI, J., BÁTHORY, J.: J. Am. Chem. Soc. **71**, 2652 (1949)
2a. HOLLY, S., SOHÁR, P.: Infrared Spectroscopy (In Hungarian) p. 73, 74. Műszaki Könyvkiadó, Budapest, 1968
2b. SOHÁR, P., VARSÁNYI, G.: Acta Chim. Acad. Sci. Hung. **55**, 189 (1968)
3a. NAKANISHI, K.: Infrared Absorption Spectroscopy-Practical, p. 32. Holden-Day Inc., San Francisco and Nankodo Co., Ltd., Tokyo, 1962
3b. Cit. 2a. pp. 70, 71.
4a. See Cit. 2a. p. 89.
4b. See Cit 3a. p. 45.
5a. SUHR, H.: Anwendungen der kernmagnetischen Resonanz in der Organischen Chemie, pp. 125, 302. Springer-Verlag, Berlin—Heidelberg—New York. 1965.
5b. SIMON, W., CLERC, TH.: Strukturaufklärung organischer Verbindungen mit spektroskopischen Methoden, p. 78. Akademische Verlagsgesellschaft, Frankfurt am Main, 1967

Pál SOHÁR
László VARGHA †
János KUSZMANN
Budapest IV., Szabadságharcosok útja 47—49.

Acta Chimica Academiae Scientiarum Hungaricae, Tomus 70 (1–2), pp. 83–89 (1971)

PREPARATION OF DL-N-METHYL-N-PROPARGYL-1-PHENYL-2-AMINOPROPANE HYDROCHLORIDE (CARDISON) LABELLED WITH CARBON-14 AND TRITIUM*

I. MEZŐ, B. TANÁCS, I. TEPLÁN, L. BURSICS and J. MÁRTON

(Institute of Isotopes of the Hungarian Academy of Sciences, Budapest)

Received June 12, 1970

Phenylacetone-2-^{14}C was prepared from ethyl acetate-1-^{14}C. The former compound was converted to DL-N-methylphenylisopropylamine-2-^{14}C by means of reductive aminolysis; this substance was propargylated to prepare DL-N-methyl-N-propargyl-1-phenyl-2-amino-propane-2-^{14}C hydrochloride (Cardison-2-^{14}C). Cardison-1-^{3}H and Cardison-2-^{3}H too were prepared by various synthetic procedures.

The psychostimulating effect of phenylisopropylamine (Amphetamine) on the central nervous system has been known since 1933. In the last years several derivatives of this compound were prepared [1a—e, 2a, b, 3] and their pharmacological properties examined [4a—e]. Of these, DL-N-methyl-N-propargyl-1-phenyl-2-aminopropane hydrochloride (Cardison) seemed to be the most potent one (Fig. 1).

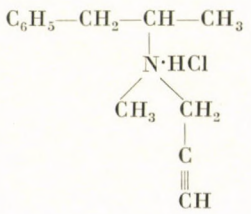

DL-N-methyl-N-propargyl-1-henyl-2-amino-propane hydrochloride
Cardison

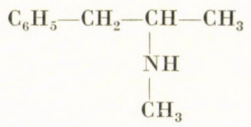

DL-N-methylphenylisopropyl-amine
methylanara

Fig. 1

Our purpose was to prepare ^{14}C and tritium labelled Cardison for use in studies on the mechanism of its action. Theoretically, various syntheses were available for the preparation of labelled Cardison. After trying several synthetic paths,** the preparation of an important intermediate, DL-N-methyl-phenylisopropylamine (methylanara) (Fig. 1), by the reductive condensation of phenylacetone and methylamine and its subsequent conversion to labelled Cardison, was found to be the most suitable method.

From the literature, two synthetic methods are known for the preparation of labelled phenylacetone. WILSON [5, 6] utilized the reaction taking place

* In part reported at the Conference of the Hungarian Chemical Society, Pécs, 1967.
** In our work the experience gained by Dr. Z. ECSERI in the preparation of the inactive compound was extensively used.

between labelled phenylacetyl chloride and ethoxy magnesium diethyl malonate; labelled phenylacetone was obtained on hydrolysis and decarboxylation of the intermediate malonic ester derivative. This synthesis, involving several steps, gives low yield and the purity of the product is not satisfactory. Another synthetic method was developed by EBERSON [7] obtaining the product in one step, namely in the reaction of labelled phenylacetic acid with methyl lithium. This procedure seems to be very advantageous, however, BLATT's method [8] provided a simpler possibility. In our work the labelled phenylacetone-2-^{14}C (Fig. 2) was, therefore, prepared in analogy with this method, using ethyl acetate labelled in its carboxyl group as starting material.

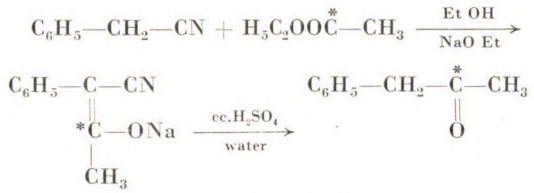

Fig. 2

The sodium salt of labelled α-phenylaceto-acetonitrile obtained from the reaction of inactive benzyl cyanide and ethyl acetate-1-^{14}C in alcoholic medium in the presence of sodium ethylate is readily crystallized; this is important with respect to the purity of the product. In order to obtain a higher radiochemical yield, the condensation was carried out with labelled ethyl acetate until incipient precipitation of the sodium salt, then completed by addition of inactive ethyl acetate to the reaction mixture in an amount required by the molar ratio. The sodium salt separated was hydrolyzed and decarboxylated; phenylacetone-2-^{14}C was obtained on extraction and this crude product was used in the subsequent steps.

According to the synthetic methods given in the literature, inactive DL-N-methylphenylisopropylamine was prepared by means of the aluminium amalgam reduction of phenylacetone in aqueous alcoholic solution of methylamine [1a, 2a]. This procedure is not suitable for preparation of labelled compounds because of the large volumes involved and the highly adsorptive character of the aluminium hydroxide formed. According to another procedure, phenylacetone and secondary amine can be reduced to tertiary phenylisopropylamine in the presence of palladium [1], but this method cannot be applied to methylpropargylamine.

In our work, sodium borohydride reduction of the Schiff base formed by crude phenylacetone-2-^{14}C and methylamine in alcoholic solution was utilized for a very simple preparation of DL-N-methylphenylisopropylamine (Fig. 3).

The Schiff base formed was not separated. In the course of preparation, purification was carried out by making use of the basic character of methyl-

anara to avoid fractional distillation in vacuum giving rise to considerable losses. To check the procedure, hydrochloride salt was precipitated from an aliquot of the crude DL-N-methylphenylisopropylamine-2-^{14}C, in 80% yield. Its melting point was identical with that given in the literature. Cardison was prepared by propargylation of the labelled crude methylanara.

In propargylation of methylanara, the procedures given in the literature [1a, b, c] recommend the use of methylanara as acid-binding agent; after making the mixture alkaline the Cardison base is separated from methylanara

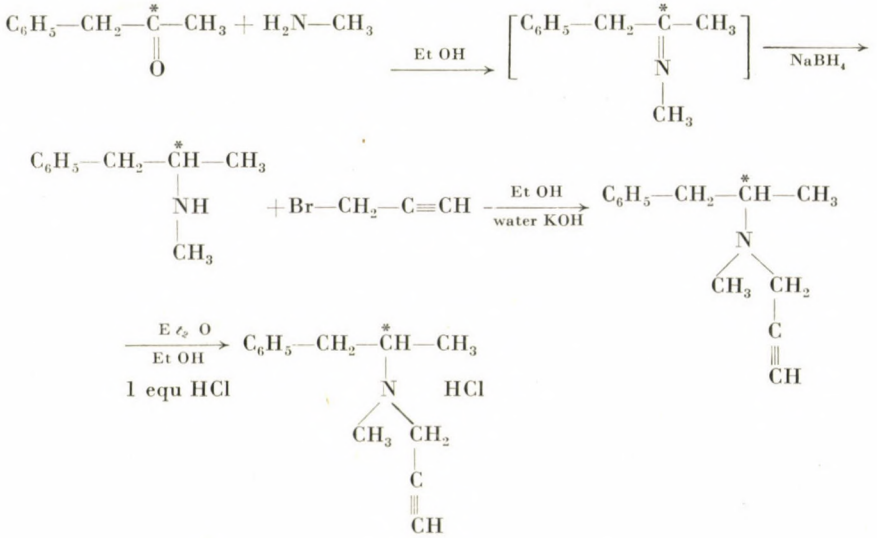

Fig. 3

by means of fractional distillation in vacuum. This procedure cannot be applied with micro quantities of labelled compounds. The crude labelled methylanara was reacted with propargyl bromide in aqueous alcoholic solution, potassium hydroxide being used as an acid-binding agent. The Cardison base was purified by means of distillation in vacuum. No volatile compounds other than Cardison were obtained. Cardison-2-^{14}C was precipitated by addition of a calculated amount of hydrochloric acid in ethanol to the ethereal solution of the distilled Cardison base. This substance was DL-N-methyl-N-propargyl-1-phenyl-2-aminopropane-2-^{14}C hydrochloride. The melting point of the product was in good agreement with that of an authentic sample.

Accomplishment of the above synthesis with ethyl acetate labelled with ^{14}C in position 2, resulted in phenylacetone-3-^{14}C as an intermediate product; this was converted to Cardison-3-^{14}C. For the purpose of extended pharmacological investigation, DL-N-methylphenylisopropylamine-1-^{3}H (methylanara-1-^{3}H), DL-N-methylphenylisopropylamine-2-^{3}H (methylanara-2-^{3}H) as well

as the corresponding tritium-labelled Cardison derivatives, obtained by means of propargylation of the former ones, were prepared.

By analogy with EMDE's method [9], methylamara-1-^{3}H (DL-deoxyephedrine-1-^{3}H hydrochloride) was prepared by catalytic tritio-dehalogenation of DL-chloropseudoephedrine hydrochloride obtained from DL-ephedrine hydrochloride [10] (Fig. 4). The catalytic tritium—halogen exchange was carried out on 0.1 mmole scale with carrier free tritium gas in the presence of palladium charcoal, at a pressure of 675 mm Hg, in 15 min. The molar activity of methylanara-1-^{3}H was 13.2 Ci/mmole.

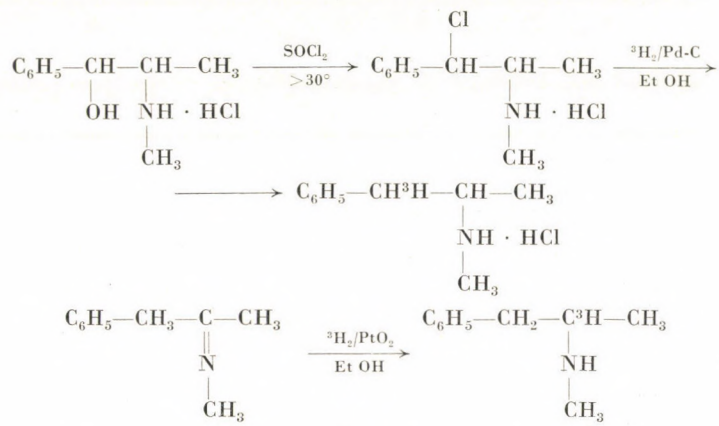

Fig. 4

Methylanara-2-^{3}H was prepared according to the procedure developed for the radiocarbon synthesis, however, the reduction was carried out by means of two different methods. A Schiff base was formed from phenylacetone in an alcoholic solution of methylamine. This Schiff base was reduced with carrier free tritium gas in an alcoholic medium in the presence of Adams' platinum catalyst, at a pressure of 695 mm Hg (Fig. 4). Owing to the isotope exchange occurring during the longer reaction period (45 min), the specific activity of the formed DL-N-phenylisopropylamine-2-^{3}H was relatively low, 1.0 Ci/mmole.

The use of sodium borotritide proved to be a more convenient method, making possible the preparation of a product of molar activity equal to that expected on the basis of the molar activity of sodium borotritide, under the conditions of the synthesis developed for incorporation of radiocarbon (Fig. 3).

In order to achieve a simpler processing and reduced radiolytical decomposition, the crude products were diluted with inactive methylanara hydrochloride. Both methylanara-1-^{3}H and methylanara-2-^{3}H were isolated as hydrochloride salts.

Labelled Cardison derivatives containing tritium in the required positions were prepared from methylanara-1-^{3}H and methylanara-2-^{3}H, under conditions identical to those of the radiocarbon synthesis.

Experimental

Preparation of phenylacetone-2-^{14}C

Sodium ethylate was prepared from 2.4 g (104.2 mmoles) of metallic sodium in absolute ethanol in a three-neck flask equipped with a stirrer, reflux condenser and a separatory funnel. 9.4 g (80 mmoles) of benzyl cyanide was added slowly to the sodium ethylate solution, then it was heated to 55—60 °C and 3.088 g of ethyl acetate-(carboxyl-^{14}C) added under continuous stirring. (Specific activity: 49.5 mCi/g; activity introduced: 152.9 mCi.) After about 5 hrs, when precipitation of the salt started, 4.05 g of inactive ethyl acetate was added slowly to the reaction mixture. (Total weight of ethyl acetate added: 7.138 g; 81 mmoles). About 20 minutes later, 1.30 g of ethyl acetate was added to ensure an excess of ethyl acetate in the reaction mixture while heating it to 100 °C. The mixture was allowed to stand at this temperature for 2 hrs. Then it was cooled and 80 ml of ether was added to the cold suspension. After standing overnight, the salt was filtered off, washed with ether and dried. Its weight was 11.51 g. The sodium salt of α-phenylacetonitrile was suspended in 20 ml of concentrated sulfuric acid under stirring and the reaction mixture heated rapidly to 100 °C. The sodium salt was dissolved in 5—10 min. and the solution was heated further for 5 min. Then it was cooled to 30 °C and after addition of 100 ml of water to the sulfuric acid solution, it was kept in a bath at 110 °C for 2 1/2 hrs. The oily material separated was extracted with ether after cooling. After removing the solvent the weight of the obtained crude phenylacetone-2-^{14}C was 4.5 g; chemical yield: 39%; the substance can be used for further synthetic steps without purification.

Preparation of DL-N-methylphenylisopropylamine-2-^{14}C

4.5 g of crude phenylacetone-2-^{14}C was dissolved in 14 ml of 25% alcoholic methylamine solution; after 15 min., 3.00 g of sodium borohydride was added to the solution. The solution was stirred for 2 hrs after accomplishment of the reduction at room temperature. The alcoholic solution was acidified with 6 *N* hydrochloric acid, diluted by the addition of an equal volume of water and extracted with ether. After this the acidic aqueous portion was evaporated to half volume. 4 *N* sodium hydroxide solution was added to the residue and the base separated was extracted with ether. The ether solution was dried over anhydrous magnesium sulfate. The solvent was distilled off in vacuum; the weight of the residual yellow, oily, crude DL-N-methylphenylisopropylamine-2-^{14}C was 3.573 g. Yield (based on phenylacetone): 76.5%. Specific activity: 15.1 μCi/mg; molar activity: 2.25 mCi/mmole (53.95 mCi), activity yield based on ethyl acetate: 35.3%. In order to check the purity of the crude DL-N-methylphenylisopropylamine-2-^{14}C product, 181.5 mg of the crude base was dissolved in ether and converted to DL-N-methylphenylisopropylamine-2-^{14}C hydrochloride by introduction of gaseous hydrochloric acid. The weight of the obtained white solid substance, DL-N-methylphenylisopropylamine-2-^{14}C hydrochloride, was 176 mg. Yield based on the crude base: 78%; m. p. 131 °C; specific activity: 12.85 μCi/mg; molar activity: 2.38 mCi/mmole.

Preparation of Cardison-2-^{14}C

(DL-N-methyl-N-propargyl-1-phenyl-2-aminopropane-2-^{14}C hydrochloride)

2.976 g (20.0 mmoles) of crude N-methylphenylisopropylamine-2-^{14}C (15.1 μCi/mg; 2.25 mCi/mmole; introduced activity: 45 mCi) was dissolved in 11 ml of absolute ethanol, and 11 ml of 2 *N* potassium hydroxide was added to the solution. The reaction mixture was cooled to —10 °C and 3.38 g (2.25 ml; 20 mmole) of propargyl bromide was added dropwise under continuous stirring of the solution. Stirring and cooling were continued for an hour, then the solution was stirred at room temperature for another two hours. After this the reaction mixture was extracted twice with 75 ml of ether, then the combined ethereal solutions were extracted twice with 25 ml of water. The ethereal solution was dried over anhydrous magnesium sulfate, the solvent evaporated in vacuum. The residual oil was distilled at a pressure of 2 mm Hg at 113—115 °C. The weight of the obtained Cardison-2-^{14}C base was 1554 mg (8.3 mmoles). The Cardison-2-^{14}C base was dissolved in 70 ml of absolute ether; Cardison-2-^{14}C was precipitated by addition of 1.8 ml of 17% alcoholic hydrochloric acid solution under continuous stirring, the substance was filtered off and dried in vacuum. The weight of the white crystalline substance was 1545 mg; m. p. 105—110 °C.

1545 mg of crude Cardison-2-^{14}C was dissolved in 4.0 ml of absolute ethanol and crystallized by addition of 100 ml of absolute ether. The mixture was allowed to stand in a refrigerator for 2 hrs, the crystals were filtered off, washed with ether and dried in vacuum. White crystalline Cardison-2-^{14}C (DL-N-methyl-N-propargyl-1-phenyl-2-aminopropane-2-^{14}C hydrochloride) was obtained, its weight was 1127 mg. M.p. 129—130 °C; specific activity: 10.9 μCi/mg; molar activity: 2.435 mCi/mmole; recovered activity: 12.28 mCi; activity yield (based on methylanara): 27.28 %.

Preparation of DL-N-methylphenylisopropylamine-2-^{3}H hydrochloride

Sodium borotritide method

4.3 g (32 mmoles) of phenylacetone was dissolved in 10 ml of ethanol and 15 ml of 25% alcoholic methylamine solution and 3.46 mg of sodium borotritide dissolved in 9 ml of 0.5 *N* sodium hydroxide (activity of the solution: 21.3 mCi/ml; introduced activity: 192 mCi) were added to the solution under continuous stirring. About 45 min. later, a solution of 2.4 g of sodium borohydride (63.5 mmoles) in 10 ml of 0.5 *N* sodium hydroxide was added to the reaction mixture. Stirring was continued for 2 hrs at room temperature and the solution was allowed to stand overnight. In the next step, a 1 : 1 hydrochloric acid solution was added to it and the acidic aqueous solution was extracted with ether. The ethereal extract was washed with water, dried over anhydrous sodium sulfate and evaporated in vacuum. The residual colourless oil was dissolved in some ethanol and dry hydrochloric acid gas was introduced into the solution after the addition of ether. A solid substance precipitated slowly, it was filtered off, washed with ether and dried. Its weight was 2.467 g. Specific activity: 23.84 μCi/mg.

Methylanara-2-^{3}H was recrystallized from a mixture of 10 ml of ethanol and 100 ml of ether; the obtained white crystalline substance was filtered off, washed with ether and dried. Weight: 1.567 g; m. p. 131 °C. Specific activity: 13.468 μCi/mg. Molar activity: 2.5 mCi/mmole.

1.567 g of the above substance was repeatedly crystallized from 8 ml of methanol by the addition of 80 ml of ether. The weight of the obtained white crystalline methylanara-2-^{3}H hydrochloride was 1.412 g, m. p. 131 °C. Specific activity: 13.161 μCi/mg. Molar activity: 2.44 mCi/mmole.

The incorporation of tritium, calculated for 32 mmoles was 78 mCi, *i.e.* 40.6% of the introduced activity.

Using sodium borohydride-^{3}H of a specific activity of about 10 Ci/mmole as starting material, methylanara-2-^{3}H with a specific activity of 2.4 Ci/mmoles was obtained by an analogous procedure but omitting dilution.

Preparation of DL-N-methylphenylisopropylamine-2-^{3}H hydrochloride

Catalytic hydrogenation method

6.17 g (50 ml) of phenylacetone was dissolved in 10 ml of ethanol and 17 ml of 18.8% alcoholic methylamine solution (approx. 100 mmoles) was added to the solution. The alcohol was removed in vacuum below 20 °C. A yellow, oily substance was obtained, its weight was 7.93 g. Theoretical yield: 7.35 g; this indicates the presence of solvent as contaminant in the crude Schiff base (about 5%). In the following experiments this product was used.

26 mg of the above crude Schiff base was dissolved in 0.5 ml of ethanol and it was tritiated with gaseous tritium applied with carrier free gas in the presence of Adams' platinum catalyst made of platinum oxide, at a pressure of 695 mm Hg for 40 min. Consumption of tritium gas was 3.384 ml (STP) = 8.7984 Ci. Methylanara-2-^{3}H was diluted with methylanara prepared by hydrogenation of the crude Schiff base, *i.e.* the two ethanol solutions were combined after reduction. The combined solution was acidified with a hydrochloric acid solution and evaporated to half volume in vacuum. The acidic aqueous solution was extracted with ether and made alkaline. Methyalanara-2-^{3}H was removed by means of extraction with ether and separated in the form of its hydrochloric acid salt, in accordance with the usual procedure. 252 mg of DL-methylphenylisopropylamine-2-^{3}H hydrochloride was obtained. Specific activity: 442 μCi/mg. The substance was recrystallized from a mixture of 1.5 ml of methanol and 15 ml of ether. Weight of the white, crystalline substance was 172.3 mg, m. p. 130—132 °C. Specific activity: 425 μCi/mg. Molar activity: 78.6 mCi/mmole. Dilution 127 times. Molar activity of DL-N-methylphenylisopropylamine-2-^{3}H hydrochloride was 1.0 Ci/mmole without dilution.

Preparation of DL-N-methylphenylisopropylamine-1-^{3}H hydrochloride

22 mg (0.1 mmole) of chloropseudoephedrine hydrochloride was tritiated with tritium gas (T_2) applied without carrier gas in the presence of activated carbon carrying 10% of palladium in 0.5 ml ethanol for 15 min. Consumption of tritium gas was 1.91 ml (STP) = 4.966 Ci (theoretical consumption of tritium gas: 2.241 ml (STP)). The alcoholic solution was evaporated to dryness after removal of the catalyst and 400 mg of inactive methylanara hydrochloride was added to the residue. After repeatedly distilling methanol off from the material, it wasc rystallized from a mixture of methanol and ether. Weight of the obtained substance: 368 g. Specific activity: 324 mCi/mg. Molar activity: 600 mCi/mmole. Dilution 21.6 times. Molar activity of DL-N-methylphenylisopropylamine-1-^{3}H hydrochloride: 13.2 Ci/mmole, without dilution.

By analogy with the radiocarbon synthetic method, Cardison-2-^{3}H and Cardison-1-^{3}H were obtained from methylanara-2-^{3}H hydrochloride and methylanara-1-^{3}H hydrochloride, respectively, prepared according to the above procedure; the molar activity of Cardison-^{3}H was nearly equal to that of the starting material, methylanara-^{3}H hydrochloride.

*

The authors' thanks are due to Dr. Z. ECSERI for his useful comments, to Dr. T. SZARVAS and Dr. Cs. ÖMBÖLY for the activity measurements, to Mr. A. SZABÓ for preparation of the tritium-labelled compounds and to Mr. L. BARANYAI and Mr. F. HORVÁTH for their technical assistance.

REFERENCES

1. a. Hungarian Pat. 151 090
   b. British Pat. 1 031 452
   c. Austrian Pat. 251 559
   d. Austrian Pat. 251 560
   e. Neth Appl. 6 605 956
2. a. LESPAGNOL, A., DEBAERT, M.: Bull. Soc. Chim. France, **12,** 2744 (1963)
   b. French Pat. M. 2782
3. Swiss Pat. 393 306
4. a. KNOLL, J., ECSERI, Z., NIEVEL, J., KNOLL, B.: Magy. Tud. Akad. Orv. Oszt. Közl., **15,** 231 (1964)
   b. KNOLL, J., ECSERI, Z., KELEMEN, K., NIEVEL, J., KNOLL, B.: Arch. Intern. Pharmacodyn, **155,** 154 (1965)
   c. MAGYAR, K., VIZI, E. S., ECSERI, Z., KNOLL, J.: Kísérl. Orvostud. **19,** 404 (1967)
   d. MAGYAR, K., VIZI, E. S., ECSERI, Z., KNOLL, J.: Acta Physiol. Acad. Sci. Hung. **32,** 377 (1967)
   e. KNOLL, J., VIZI, E. S., SOMOGYI, G.: Arzneimittel-Forsch. (Drug. Res.) **18,** 109 (1968)
5. WILSON, J. W.: J. Am. Pharm. Assoc. Sci. Ed. **39,** 687 (1950)
6. MURRAY, A., WILLIAMS, D. L.: Organic Synthesis with Isotopes. Part. I, p. 512. Interscience Publ., New York 1958
7. EBERSON, L.: Acta Chem. Scand. **17,** 2348 (1963)
8. BLATT, A. H.: Org. Synth. Coll. Vol. II, pp. 391, 487. John Wiley, New York, 1943
9. EMDE, H.: Helv. Chim. Acta, **12,** 365 (1929)
10. EMDE, H.: Helv. Chim. Acta, **12,** 384 (1929)

Imre MEZŐ
Béla TANÁCS
István TEPLÁN
László BURSICS
József MÁRTON

Budapest XII, Konkoly Thege M. út.

Acta Chimica Academiae Scientiarum Hungaricae, Tomus 70 (1—2), pp. 91—96 (1971)

SYNTHESIS OF AN ANALOGUE OF "QUANTRIL" CONTAINING INDOLO-QUINOLIZIDINE RING

L. Novák, Ng. Bang* and Cs. Szántay**

(Organic Chemical Institute, Technical University, Budapest)

Received June 14, 1970

The keto ester **VIb** was prepared by successive reactions of compound **III** with potassium monoethyl malonate, acrylic ester and sodium hydride. The reaction of **VIb** with diethylamine, sodium borohydride and acetic anhydride gave an analogue (**IIb**) of "Quantril" containing the indolo-quinolizidine ring system.

The synthesis of the tranquillant and hypotensive drug represented by Structure I, known as "Quantril" or "Benzquinamide" [1], has been discussed previously [2]. In the present work we aimed at the preparation of an analogue of Compound I containing an indole ring (**IIb**), for the purpose of pharmacological investigation.

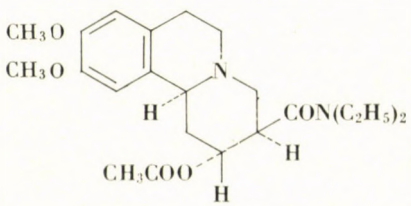

I

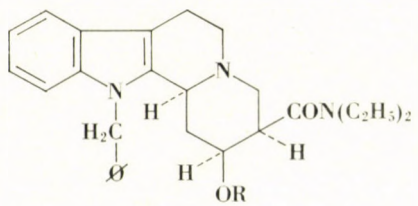

II a R = H
b R = $COCH_3$

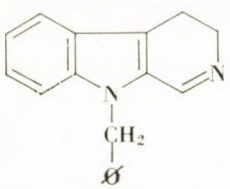

III

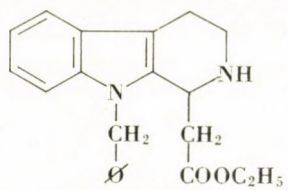

IV

The β-carboline derivative (**III**) prepared by us earlier [3] was allowed to react with potassium monoethyl malonate, similar to the procedure given by Chapman *et al.* [4] for members of the isoquinoline series. Reaction of the resulting ester (**IV**) with ethyl acrylate gave the diester **Vb** in a high yield.

* This paper is part of the Thesis of Ng. Bang.
** To whom enquiries should be addressed.

The keto ester **VIb** was obtained by the Dieckmann condensation of **Vb** by means of sodium hydride in benzene medium, in 70% yield. This reaction deserves some comment. In the case if the NH group of indole in the diester **V**

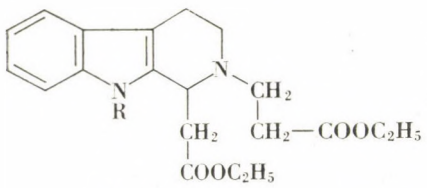

V a R = H
b R = benzyl

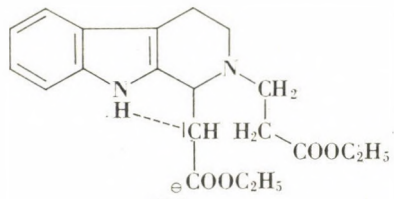

Va′

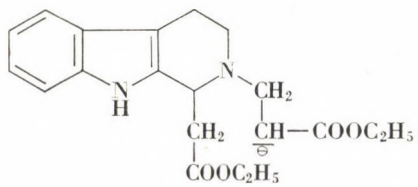

Va″

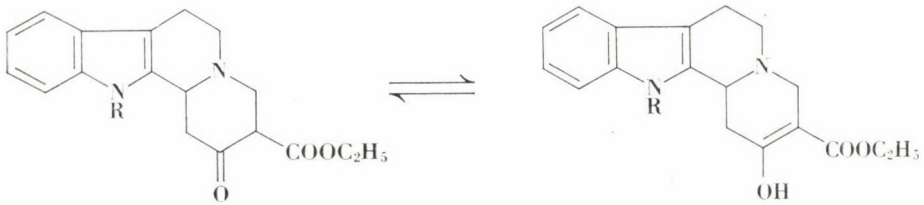

VI a R = H
b R = benzyl

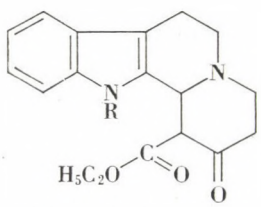

VII a R = H
b R = benzyl

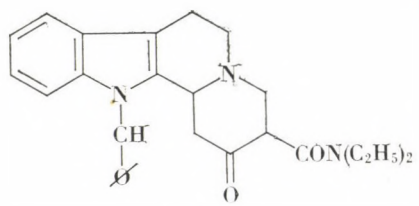

VIII

is not benzylated (**Va**), alternative cyclization results in the keto ester **VIIa** in 90% yield under the above conditions of the reaction providing kinetic control [5]. Dieckmann condensation of the analogous isoquinoline derivatives and the non-benzylated indole derivative **Va** always gives a keto ester of type **VI** under conditions permitting reversible reaction, *i.e.* when thermody-

namical control prevails (*e.g.*, with sodium ethoxide in ethanol). This suggests decisive importance of the presence of the indole-NH group in the formation of the keto ester **VII**. According to KLINE [5], **Va′** is the more stable of the two anions (**Va′** and **Va″**) produced, owing to interaction with the indole-NH group, thus also the activation energy required for its formation is lower. This assumption has been confirmed by our experiences, too. Reaction of the derivative having its indole-NH blocked by means of a benzyl group leads to the more stable product even under conditions providing kinetic control of the reaction (*e.g.* sodium hydride in benzene).

Compound **VIb** undergoes enolisation to a considerable degree. In the solid state both the base and the hydrochloride are completely in the enolic form as shown by the infrared spectra. Integration of the signal of the OH proton present in chelate bond appearing at $\tau - 3$ in the NMR spectrum in $CDCl_3$ solution indicates that about 60% of the compound is present in the enolic form.

Boiling of ester **VIb** with diethylamine in xylene resulted in derivative **VIII**; this crystalline base is present in the ketonic form, while its hydrochloride has the enolic form, as shown by the infrared spectra.

The alcohol **IIa** was obtained by reduction of the acid amide with sodium borohydride, in a high yield. The equatorial position of the hydroxyl group was inferred from the fact that predominant formation of the epimer of this structure in the sodium borohydride reduction has been proved in the literature and in our own former investigations in the case of isoquinoline derivatives of analogous structure [2]. In the course of the reduction, the formation in about 10% of the isomeric alcohol with the hydroxyl group in axial position can be detected by means of thin-layer chromatography. Comparison of the R_f values also confirms the axial position of the hydroxyl group in the latter compound.

Acetylation of **IIa** with acetic anhydride in pyridine gave the expected compound in similarly high yield.

The axial or equatorial position of the acetoxyl group — as shown by the investigations carried out with "Quantril" derivatives [2] — has no decisive pharmacological importance.

Experimental

9-Benzyl-1-(ethoxycarbonylmethyl)-1,2,3,4-tetrahydro-β-carboline (IV), HCl

10.2 g (26 mmole) of 9-benzyl-3,4-dihydro-β-carboline perchlorate [3] was suspended in a mixture of 600 ml water and 30 ml ethanol, and 46.0 g (0.44 mole) of sodium carbonate was added. The mixture was extracted four times with a total of 2400 ml of ether, the ethereal solution was washed with 20 ml of water, dried over magnesium sulfate and the ether was distilled off. The residual 9-benzyl-3,4-dihydro-β-carboline base (6.50 g; 25 mmole; m. p. 134 °C) was heated with 6.63 g (39 mmole) of potassium ethyl malonate in 70 ml of acetic acid at 100 °C for 8 hrs. Acetic acid was distilled off in vacuum on a water bath. The residue was

dissolved in 40 ml of water and 10.6 g (0.10 mole) of sodium carbonate was added to the solution. The solution was extracted three times with a total of 160 ml of ether, the extract washed with 30 ml of water, dried over magnesium sulfate and the ether distilled off. The residue (6.86 g; 62%) was dissolved in 20 ml of absolute alcohol and dry hydrogen chloride was passed into the solution in order to acidify it. 30 ml of absolute ether was added, and the solution was allowed to stand in a refrigerator overnight. The precipitated yellow crystalline substance was filtered off and dried to yield 5.7 g (51.40%) of the product, m. p. 168 °C.

$C_{22}H_{25}N_2O_2Cl$ (384.89). Calcd. C 68.64; H 6.54; N 7.28; Cl 9.20. Found C 68.32; H 6.63; N 7.17; Cl 9.06%.
IR (KBr): 1725 cm^{-1} (CO), 1190, 1170 (C—O—C)
UV $\lambda_{max}^{H_2O}$ = 272 nm (log ε = 3.71)
282 nm (log ε = 3.73).

9-Benzyl-1-(ethoxycarbonylmethyl)-2-(β-carbethoxyethyl)-1,2,3,4-tetrahydro-β-carboline (Vb) HCl

15.4 g (40 mmole) of the hydrochloride **IV** was suspended in a mixture of 38 ml of ethanol and 700 ml of water and 8.40 g (100 mmole) of sodium hydrogen carbonate was added to the solution. The mixture was extracted with ether (total volume: 1000 ml) in two portions. The ethereal solution was washed with 20 ml of water, dried over magnesium sulfate and the ether distilled off. The residue (13.87 g; 39 mmole, m. p. 109—110 °C) was refluxed with 135 ml of ethyl acrylate for 48 hrs. The acryl ester was distilled off in vacuum at 50 °C on a water bath and the residue (18.85 g; 96%) dissolved in 250 ml of absolute ether and treated with dry hydrogen chloride under cooling. The precipitated crystalline substance was filtered off, washed with absolute ether and dissolved in 60 ml of absolute ethanol. The alcoholic solution was mixed with 130 ml of absolute ether and refrigerated for three days. After this, the precipitated crystalline substance was filtered off to obtain 14.82 g (76%), of the product, m. p. 150 °C.

$C_{27}H_{33}N_2O_4Cl$ (485.00). Calcd. C 66.85; H 6.85; N 5.77; Cl 7.31. Found C 66.72; H 6.97; N 5.96; Cl 7.17%.
TLC (8 ml of benzene and 1 ml of methanol) R_f = 0.77 (Kieselgel G)
IR (KBr): 1730 cm^{-1}, 1200 cm^{-1} (CO).
UV λ_{max}^{EtOH} = 282 nm (log ε = 3.93).

2-Oxo-3-(ethoxycarbonyl)-1,2,3,4,6,7,12,12b-octahydro-12-benzylindolo-(2,3-a)-quinolizine(VIb)

4.85 g (10 mmole) of the hydrochloride **Vb** and 1.0 g (12 mmole) of sodium bicarbonate were dissolved in 150 ml of water. This aqueous solution was extracted three times with a total of 160 ml of ether. The ethereal extract was dried over magnesium sulfate and the ether distilled off. The residual oily material was dissolved in 12 ml of absolute benzene and, after the addition of 0.12 g of sodium hydride in 50% oil suspension, the mixture was refluxed for 4 hrs. After cooling, 20 ml of a mixture of ethanol and water (1 : 5) was added, the solution was acidified with 40 ml of 4% acetic acid, and was extracted three times with a total of 160 ml of benzene. The benzene solution was dried over magnesium sulfate and the solvent distilled off in vacuum. The residue (3.75 g; 93%) was dissolved in 10 ml of absolute ethanol, allowed to stand for one day, and the precipitated crystalline substance filtered off, 2.82 g (70%), m. p. 121 °C.

$C_{25}H_{26}N_2O_3$ (402.48). Calcd. C 74.59; H 6.51; N 6.96. Found C 74.51; H 6.64; N 6.97%.
TLC (8 ml of benzene and 1 ml of methanol) R_f = 0.63 (Kieselgel G)
IR (KBr): 1680 (CO), 1630 (C=C), 1200 cm^{-1} (C—O—C), (enolic form)
UV λ_{max}^{EtOH} = 247 nm (log ε = 4.04); 263 (log ε = 4.05); 282 nm (log ε = 3.95); 291 (log ε = 3.87
NMR ($CDCl_3$): 2.6—3 (9H, aromatic protons), 4.68 (2H, CH_2-Ph), 5.55—5.95 quartet J = 8.6.8 Hz (O—CH_2—(CH_3)), 8.7 triplet J = 12, 12 Hz, (CH_3—(CH_2)—, 3H), τ(—)3 (OH) in chelate bond).

Hydrochloride: An ethereal solution of the base was saturated with dry hydrogen chloride and the precipitated salt was filtered off with suction, m. p. 208 °C.

$C_{25}H_{27}N_2O_3Cl$ (438.93). Calcd. C 68.39; H 6.20; N 6.38; Cl 8.07. Found C 68.37; H 6.61; N 6.09; Cl 7.96%.
IR (KBr): 1670 cm^{-1} (CO), 1630 cm^{-1} (C=C), 1210 cm^{-1} (C—O—C), (enolic form).

The sodium salt of the enolic form was obtained by extraction of the mixture with benzene after cyclization. The benzene solution was dried over magnesium sulfate and concentrated in vacuum; crystallization of the residue occurred rapidly, m. p. 305 °C.

$C_{25}H_{25}N_2O_3Na$ (424.46) Calcd. C 70.73; H 5.93; N 6.61; Na (ash) 5.41. Found C 70.67; H 6.13; N 6.38; Na (ash) 4.97%.
IR (KBr): 1640 cm^{-1} (CO), 1540 cm^{-1} (C=C), 1240 cm^{-1} (C—O—C).

2-Oxo-3-(N,N-diethylcarbamoyl)-12-benzyl-1,2,3,4,5,7,12,12b-octahydroindolo-(2,3-a)-quinolizine (VIII)

3.70 g (9.2 mmole) of **VIb** was refluxed with a mixture of 3.8 ml (36 mmole) of diethylamine and 14 ml of xylene for 24 hrs. After cooling, the solution was washed twice with a total of 30 ml of water and dried over magnesium sulfate. The solvent was distilled off in vacuum at 50—60 °C on a water bath and the residue (3.9 g, 96%) recrystallized from 35 ml of absolute alcohol to obtain 2.45 g (62.2%) of the product; m. p. 181 °C.

$C_{27}H_{31}N_3O_2$ (429.54). Calcd. C 75.49; H 7.27; N 9.78. Found C 75.59; H 7.45; N 9.89%.
TLC (8 ml of benzene and 1 ml of methanol) $R_f = 0.78$ (Kieselgel G)
IR (KBr): 1720 cm^{-1}, 1640 cm^{-1} (C=O)
NMR ($CDCl_3$): τ 2.8 (9H aromatic protons), 4.75 (2H, CH_2—Ph), 8.73 and 8.85 (6H, CH_3—(CH_2)—N)
UV $\lambda_{max}^{EtOH} = 283$ nm ($\log \varepsilon = 3.92$), 225 nm ($\log \varepsilon = 4.48$).

2-Hydroxy-3-(N,N-diethylcarbamoyl)-1,2,3,4,6,7,12,12b-octahydroindolo-(2,3-a)-quinolizine (IIa)

1.7 g (4 mmole) of the base **VIII** was dissolved in 22 ml of absolute methanol and after the addition of 0.6 g (16 mmole) of sodium borohydride (20 min.) the solution was stirred for 6 hrs at room temperature. The solvent was distilled off in vacuum, the residue dissolved in 5 ml of 15% HCl, made alkaline with 1 *N* NaOH solution (pH ~ 8) and extracted three times with a total of 150 ml of benzene. The benzene solution was dried over magnesium sulfate, and the benzene distilled off. The residue (1.62 g, 95.3%) was recrystallized from a 1 : 5 mixture of absolute ether and petroleum ether. Of the epimeric alcohols the isomer containing the hydroxyl group in equatorial position crystallized, 1.42 g (83.5%), m. p. 96—97 °C.

$C_{27}H_{33}N_3O_2$ (431.55). Calcd. C 75.13; H 7.70; N 9.48%. Found C 75.00; H 7.64; N 9.78%
TLC (8 ml of benzene and 1 ml of methanol):
axial isomer $R_f = 0.31$
equatorial isomer $R_f = 0.40$
IR (KBr): 3400 cm^{-1} (OH), 1620 cm^{-1} (CO).

2-Acetoxy-3-(N,N-diethylcarbamoyl)-12-benzyl-1,2,3,4,6,7,12,12b-octahydroindolo-(2,3-a)-quinolizine (IIb), HCl

1.3 g (3.0 mmole) of **IIa** was allowed to stand in a mixture of 10 ml of pyridine and 10 ml of acetic acid at room temperature for 18 hrs. The solution was concentrated in vacuum on a water bath, and the residue dissolved in 6 ml of water. The solution was made alkaline by the addition of ammonium hydroxide solution and extracted three times with a total of 60 ml of benzene. The benzene solution was washed with water, dried over magnesium sulfate and the solvent distilled off in vacuum. The residue (1.35 g) was dissolved in 15 ml of absolute ether and the ethereal solution saturated with dry hydrogen chloride. The precipitated hydrochloride was filtered off and washed with absolute ether. The precipitate was dissolved in 1 ml of absolute ethanol with the subsequent addition of 2 ml of absolute ether and the obtained yellow crystalline substance was filtered off, 1.12 g (73.2%), m. p. 211—212 °C.

$C_{29}H_{36}N_3O_3Cl$ (510. 05). Calcd. C 68.28; H 7.11; N 8.23; Cl 6.95. Found C 68.11; H 7.40; N 8.15; Cl 6.75%.
TLC (8 ml of benzene and 1 ml of methanol) $R_f = 0.37$
IR (KBr): 1740 cm^{-1}, 1640 cm^{-1} (CO), 1220 (C—O—C)
UV: $\lambda_{max}^{EtOH} = 226$ nm ($\log \varepsilon = 4.44$); 283 nm ($\log \varepsilon = 3.87$)
NMR: τ 2.7 (9H, aromatic protons), 4.6 (2H, CH_2—Ph),
8 (3H, C—CH_3), 8.7 and 8.8 (6H, (CH_2)—CH_3).

REFERENCES

1. SCRIABINE, A., FINGER, K. F., DELAHUNT, C. S., CONSTANTINE, J. W., SCHNEIDER, J. A.: J. Am. Med. Assoc. **184,** 276 (1963); C. A. **59,** 8024 (1963)
2. SZÁNTAY, Cs., NOVÁK, L., SOHÁR, P.: Acta Chim. Acad. Sci. Hung. **57,** 335 (1968)
3. NOVÁK, L., SZÁNTAY, Cs.: Chem. Ber. **102,** 3959 (1969)
4. CHAPMAN, J. H., HOLTON, P. G., RITCHIE, A. C., WALKER, T., WEBB, G. B., WHITING, K. D. E.: J. Chem. Soc. **1962**, 2479
5. KLINE, G. B.: J. Amer. Chem. Soc. **81,** 2251 (1959)

Lajos NOVÁK
Ng. BANG
Csaba SZÁNTAY; BME Szerves Kémia Tanszék, Bp., XI, Gellért tér 4. Bp. XI,, Zsombolyai út 8.

Acta Chimica Academiae Scientiarum Hungaricae, Tomus 70 (1—2), pp. 97—100 (1971)

THE ACID HYDROLYSIS OF MELIBIOSE*

(SHORT COMMUNICATION)

J. SZEJTLI,** R. D. HENRIQUES and M. CASTIÑEIRA

(Escuela de Bioquimica-Farmaceutica, Universidad de La Habana, La Habana, Cuba)

Received November 6, 1970

The acid hydrolysis of the glucosyl—fructosyl bond (G—F) in raffinose was treated in a previous paper [1]. The rate of hydrolysis of this β-1,2 glycosidic bond is slower by approximately 19% than that of a similar bond in the sucrose molecule, under similar conditions. The greater stability of this bond is probably due to the fact that in raffinose a galactose is joined to the glucose unit. Relatively little is known about the stability to acid hydrolysis of the α-1,6 linkage between galactose and glucose, therefore in the present work the acid hydrolysis of melibiose [6-O-(α-D-galactopyranosyl)-D-glucopyranose] has been investigated.

The first paper [2] dealing with the hydrolysis of melibiose contains only a single k value, determined in sulfuric acid. The first published value of the energy of activation (E_a = 38.6 kcal/mole in HCl) [3] seems to be unlikely high. Some recent data [4, 5] also relate to sulfuric acid hydrolysis, therefore they are not comparable with the hydrolysis characteristics determined in hydrochloric acid. The catalytic activity of sulfuric acid greatly depends on the conditions of hydrolysis, which considerably restricts the possibility of extrapolation to an identical reference basis. Accordingly, hydrolysis-kinetical measurements should be performed in hydrochloric acid [6].

There is no reason for supposing that the acid hydrolysis of the Ga-α-1 → → 6—G in raffinose and melibiose should be different. In principle, it is imaginable that the furanosyl unit may exert some influence on the Ga—G bond in raffinose, however, since the splitting of the G—F bond is about 10^3 times faster than that of the Ga—G bond, such an effect is inobservable. Therefore, within the limits of experimental error, no difference is to be expected in the hydrolysis of the Ga—G bond of the di- and trisaccharide.

* The present paper is a part of a series; the previous part has been published in Acta Chim. Acad. Sci. Hung. **66**, 213 (1970).

** Present address: Chinoin Pharmaceutical and Chemical Works Ltd., Budapest.

Experimental

The above expectation has been justified by the experiments. 1.3 g of melibiose (ME) or raffinose (RAF) was dissolved in 15 ml of hydrochloric acid of appropriate temperature and concentration, and maintaining the desired temperature in a jacketed polarimeter tube by

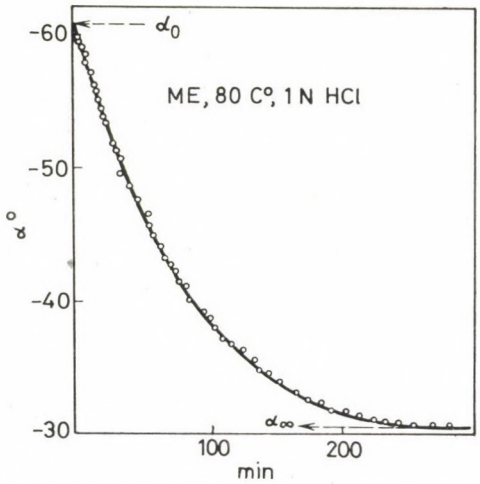

Fig. 1. Variation of the optical rotation as a function of the hydrolysis time

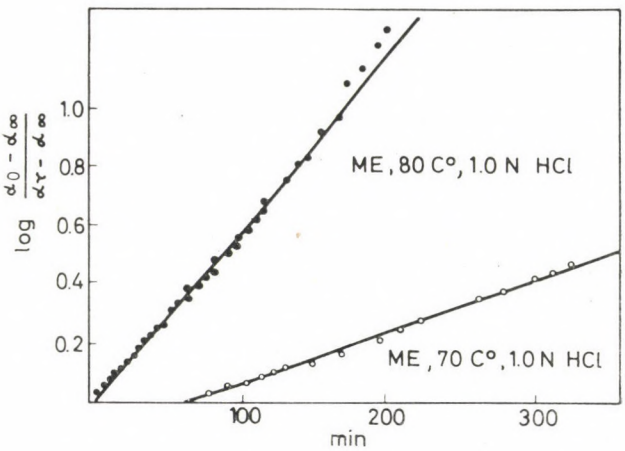

Fig. 2. The values of $\log \frac{\alpha_0 - \alpha_\infty}{\alpha_\tau - \alpha_\infty}$ as a function of the hydrolysis time

means of an ultrathermostate, the optical rotation was registered as a function of time. The values of α_0 and α_∞ which belong to $\tau = 0$ and $\tau = \infty$, respectively, were determined by extrapolation (see Fig. 1) and the values of k (in ln and min^{-1}) were calculated from these results (Table I).

The scattering of the measured points is illustrated in Fig. 2, which shows the log $\frac{\alpha_0 - \alpha_\infty}{\alpha_\tau - \alpha_\infty}$ values as function of the reaction time. The other characteristics (E_a, ΔS^+, d, g, etc.) were calculated as in previous papers [1, 7].

Table I

Characteristics of the hydrolysis of the galactosyl-α ⟶ 6-glucose bond

t °C	[HCl] N	$k \cdot 10^3$ min^{-1}	hydrolysed sugar
60.0	0.977	1.08	RAF
70.0	0.977	4.06	RAF
		4.16	ME
80.0	0.977	17.7	RAF
		14.4	ME
	0.0977	1.32	RAF

Other characteristics: $E_a = 31.9$ kcal/mole, $\Delta S^+ = 12.94$ e.u., $g = 1.011$, $d = 17.820$, $k_{r,100°C} = 0.168$, RAF = raffinose, ME = melibiose

Discussion

According to the determined data, in the presence of HCl catalyst, the hydrolysis rate constant of the Ga-α-1 → 6—G bond can be calculated from the following equation:

$$\log k = 1.011 \cdot \mathrm{pH} + 17.820 - 0.4343 \cdot 31900/(1.987 \cdot T) \qquad (1)$$

Accordingly, we have all data for calculating the extent of hydrolysis of raffinose for any case in which the applied catalyst is hydrochloric acid:

$$p = 1 - 0.5(e^{-k_{G-F} \cdot \tau} - e^{-k_{Ga-G} \cdot \tau}) \qquad (2)$$

The values of k_{Ga-G} can be calculated from Eq. (1), and the values of k_{G-F} as it was published in a previous paper [1].

As it is seen in Table I, the hydrolysis of both RAF and ME furnished practically identical data under similar reaction conditions. The value of $k_{r,100°}$ (the reduced rate constant, which refers to a hydrogen ion activity of unity and 100 °C) is 0.1683; the same value, calculated from the experimental data of MOELWYN-HUGHES [3] is 0.1457. This discrepancy is obviously caused by the different E_a values, which seem to be too high in MOELWYN-HUGHES' paper.

Melibiose — just as gentiobiose and isomaltose — from the viewpoint of hydrolysis kinetics may be regarded as a substituted methylglycoside, since the aglycone moiety is joined to the bridge oxygen atom through a primary carbon atom. Therefore, the hydrolysis characteristics of the Ga—G bonds in ME and in RAF resemble much more the case of Me-α-D-galactopyranose than that of other disaccharides.

REFERENCES

1. Szejtli, J., Henriques, R. D., Castiñeira, M.: Acta Chim. Acad. Sci. Hung. **66,** 213 (1970)
2. Freudenberg, K., Dürr, W., Hochstetter, H.: Chem. Ber. **61,** 1735 (1928)
3. Moelwyn-Hughes, E. A.: Trans. Faraday Soc. **25,** 503 (1929)
4. Timell, T. E.: Canadian J. Chem. **42,** 1456 (1964)
5. Timell, T. E., Enterman, W., Spencer, F., Soltes, E. J.: Canadian J. Chem. **43,** 2296 (1965)
6. Szejtli, J.: Acta Chim. Acad. Sci. Hung. **56,** 175 (1968)
7. Szejtli, J.: Acta Chim. Acad. Sci. Hung. **45,** 141 (1965)

József Szejtli; Budapest IV., Tó u. 1—3.
R. D. Henriques, M. Castiñeira } Escuela de Bioquimica-Farmaceutica, Universidad de La Habana, La Habana, Cuba.

Acta Chimica Academiae Scientiarum Hungaricae, Tomus 70 (1—2), pp. 101—122 (1971)

PIPERAZINDERIVATE, III*

DIÄTHYLCARBAMYL- UND XANTHENDERIVATE

L. Toldy, I. Tóth, J. Borsi und F. Andrási

(Institut für Arzneimittelforschung, Budapest)

Eingegangen am 18. April 1970

Es wurden zahlreiche 1-R'-4-R-piperazine sowie 1-R'-4-β-[4-(R)-piperazinyl-1]-äthylpiperazine hergestellt und ihre antiulcerogene Wirkung wurde untersucht.

Es wurden mehrere neue antiulcerogene Verbindungsgruppen gefunden; am wirksamsten waren die 1-(Xanthen-9-carbonyl)-4-β-[4-(alkyl)-piperazinyl-1]-äthylpiperazine, mit guter peroraler Resorption. Diese Verbindungen üben eine stark hemmende Wirkung auf Versuchsulcera aus, die durch den zentralen Mechanismus entstehen und besitzen zugleich eine anticholinergische Wirkung.

Als potentielles antiulcerogenes Arzneimittel dürfte in erster Reihe das 1-(Xanthen-9-carbonyl)-4-β-[4-(i-butyl)-piperazinyl-1]-äthylpiperazin in Frage kommen.

In den sich mit Piperazinderivaten beschäftigenden Mitteilungen I und II dieser Reihe [1, 2] wurde über antiulcerogene Substanzen berichtet, welche keine anticholinergischen Eigenschaften besitzen und ihre Wirkung vermutlich nach einem zentralen — über den Hypothalamus zur Geltung kommenden — Mechanismus ausüben.

Der neuartige Wirkungsmechanismus dieser Verbindungen gab einen Anlaß zur Herstellung weiterer Piperazinderivate. Als erster Schritt wurden Analoga der in Mitteilung I beschriebenen Piperazine hergestellt, bei denen an Stelle der 3,4,5-Trimethoxygruppe die — bekanntlich ebenfalls über eine sedative Wirkung verfügende — Diäthylcarbamylgruppe [1, 3] verwendet wurde.

In Tabelle I und II sind die aufgrund dieser Überlegungen hergestellten 1-Diäthylcarbamyl-4-R-piperazine** und 1-Diäthylcarbamyl-4-β-[4-(R)-piperazinyl-1]-äthylpiperazine angeführt.

Die Verbindungen wurden ähnlich wie die 3,4,5-Trimethoxybenzamide [1] hergestellt. So wurde bei der Reaktion des 1-(β-Oxyäthyl)-piperazins [5] mit Diäthylcarbamylchlorid [6] das 1-Diäthylcarbamyl-4-(β-oxyäthyl)-piperazin (**I**) gewonnen (Verfahren *A*). Diese Verbindung wurde mit Hilfe von Thionylchlorid zu 1-Diäthylcarbamyl-4-(β-chloräthyl)-piperazin (**II**) umgesetzt (Verfahren *B*). Aus (**II**) gelangten wir mit Hilfe der entstehenden 4-R-Piperazine

* Mitteilung II: Acta Chim. Acad. Sci. Hung. **52**, 283 (1967).

** 1-Diäthylcarbamyl-4-R-piperazine wurden bereits früher eingehend untersucht. Zahlreiche Repräsentanten dieser Gruppe wurden auf ihre Wirkung gegen Lungen- und Darmparasiten von Haustieren geprüft [4]. Das 1-Diäthylcarbamyl-4-methylpiperazin wurde unter der Benennung Pasin in den Handel gebracht. Über die antiulcerogene Wirkung dieser Verbindungen stehen keine Angaben zur Verfügung.

zu den 1-diäthylcarbamyl-4-β-[4-(R)-piperazinyl-1]-äthylpiperazinen **IX, X, XI, XIII, XIV** und **XV** (Verfahren *D*). Die Verbindung **VIII** wurde auf ähnliche Weise aus **II** mit wasserfreiem Piperazin hergestellt (Verfahren D_1). Die Verbindungen **III, V** und **XII** wurden analog wie **I** hergestellt, während die Verbindungen **VI** bzw. **VII** aus **III** bzw. **I** mit 3,4,5-Trimethoxybenzoylchlorid [7] hergestellt wurden (Verfahren *C*).

Im weiteren wurden mit Diäthylcarbamylderivaten auf analoge Weise substituierte Piperazine enthaltende 9-Xanthenylpiperazine hergestellt. Die Wahl dieser Verbindungen wurde auch durch die bekannte günstige antiulcerogene Wirkung der 1-(9-Xanthenyl)-4-carbalkoxypiperazine unterstützt [8].

Bei den durch uns synthetisierten neuen 1-(9-Xanthenyl)-4-R-piperazinen* und den 1-(9-Xanthenyl)-4-β-[4-(R)-piperazinyl-1]-äthylpiperazinen (Tab. III und IV) wurde angenommen, daß in erster Reihe die immobilisierende antiulcerogene Wirkung gesteigert wird.

Die 1-(9-Xanthenyl)-4-R-piperazine (Tab. III) wurden — mit Ausnahme von **XXVI,** welches aus **XX** nach dem Verfahren *C* mit 3,4,5-Trimethoxybenzoylchlorid gewonnen wurde — ebenso hergestellt, wie das bekannte 1-(9-Xanthenyl)-4-carbäthoxypiperazin [8] aus den entsprechenden 4-R-Piperazinen mit Xanthydrol [9] (Verfahren *E*).

Ähnlich wurden die Derivate mit zwei Piperazinringen im Molekül (**XXVII, XXVIII, XXIX, XXX,** Tab. IV) aus 1-Carbäthoxy-4-β-(piperazinyl-1)-äthylpiperazin (siehe im experimentellen Teil), 1-Diäthylcarbamyl-4-β-(piperazinyl-1)-äthylpiperazin (Tab. II, **VIII**) und 1-(*n*-Butyl)-4-β-(piperazinyl-1)-äthylpiperazin mit Xanthydrol bzw. Thioxanthydrol [10] hergestellt. Unter den verwendeten neuen Ausgangsstoffen wurde das 1-α-(2-Pyridyl)-äthylpiperazin (siehe im experimentellen Teil, **XVI**) aus wasserfreiem Piperazin mit 2-(α-Bromäthyl)-pyridin [11], das 1-Carbäthoxy-4-β-(piperazinyl-1)-äthylpiperazin aus den bekannten Verbindungen 1-Carbäthoxy-4-(β-chloräthyl)-piperazin [12] bzw. 1-(*n*-Butyl)-4-(β-chloräthyl)-piperazin [13] mit wasserfreiem Piperazin nach dem Verfahren D_1 hergestellt.

Durch Anwendung der Xanthen-9-carbonylgruppe mit bekanntlich anticholinergischem Charakter [14, 15, 16, 17, 18, 19, 20] wurden 1-(Xanthen-9-carbonyl)-4-R-piperazine** und 1-(Xanthen-9-carbonyl)-4-β-[4-(R)-piperazinyl-1]-äthylpiperazine gewonnen (Tab. V, VI).

Bei diesen Verbindungen wurden für R einerseits in unseren bisherigen Untersuchungen als geeignet gefundene und andererseits hinsichtlich ihrer antiulcerogenen Wirkung noch nicht geprüfte basische Gruppen mit tertiären

* Früher waren nur einige Repräsentanten der 9-Xanthenylpiperazine bekannt; unter diesen befanden sich auch Derivate mit antiulcerogener Wirkung [8].

** Aus dieser Gruppe sind früher nur einige Derivate hergestellt worden [17, 18], bei denen eine parasympatholytische Aktivität gefunden wurde. Besonders bedeutend war ihr spasmolytischer Effekt.

Stickstoffatomen und bekannte normale und verzweigte Alkylgruppen eingesetzt. Es wurde angenommen, daß neben der gesteigerten immobilisierenden antiulcerogenen Wirkung auch die anticholinergische Eigenschaft auftreten wird.

Die Verbindungen **XXXI, XXXIII, XXXIV, XXXV, XXXVI, XXXVII, XXXIX** und **XL** (Tab. V) wurden nach dem Verfahren *A* aus den entsprechenden 4-R-Piperazinen mit Xanthen-9-carbonylchlorid [21] hergestellt. Gemäß der bereits angewendeten Synthese wurde **XXXI** mit Thionylchlorid zu 1-(Xanthen-9-carbonyl)-4-(β-chloräthyl)-piperazin (**XXXII**) umgesetzt und daraus mit dem entsprechenden sekundären Amin die Verbindungen **XLII, XLIII, XLIV, XLVI** erhalten (Verfahren *D*, Tab. V). **XXXVIII** wurde aus N-(β-Oxypropyl)-piperazin [22] mit Xanthen-9-carbonylchlorid hergestellt (Verfahren *F*), während **XLI** und **XLVII** aus den betreffenden Grundverbindungen (**XL** bzw. **XLVI**) mit Methyljodid hergestellt wurden (Verfahren *G*).

Im Zusammenhang mit der Herstellung von **LXIII** wurden die Möglichkeiten einer neuen Synthese der Verbindung geprüft. Aus der Reaktion von 2 Mol N-(β-Oxyäthyl)-piperazin mit 1 Mol i-Butylbromid wurde 1-(i-Butyl)-4-(β-oxyäthyl)-piperazin gewonnen, welches mit Thionylchlorid zu 1-(i-Butyl)-4-(β-chloräthyl)-piperazin umgesetzt wurde. Aus dem letzteren wurde mit wasserfreiem Piperazin 1-(i-Butyl)-4-β-(piperazinyl-1)-äthylpiperazin hergestellt, und daraus mit Xanthen-9-carbonylchlorid, nach dem Verfahren *A*, die Verbindung **LXIII.** Das Produkt war in jeder Beziehung mit dem nach dem allgemeinen Syntheseverfahren erhaltenen identisch.

Die neuen Ausgangsstoffe N-i-Amylpiperazin (siehe im experimentellen Teil) und N-*sec.*-Butylpiperazin wurden auf analoge Weise wie das bekannte N-(*o*-Methylbenzyl)-piperazin [24], aus Piperazin mit dem entsprechenden Alkylhalogenid gewonnen.

Ergebnisse der pharmakologischen Untersuchungen

Die erhaltenen Verbindungen wurden in erster Reihe auf ihre antiulcerogene Wirkung geprüft. Es wurden jedoch auch sonstige pharmakologische Untersuchungen durchgeführt, und zwar hinsichtlich der sedativen und parasympatholytischen Aktivität.*

Es zeigte sich, daß die in Tab. I angegebenen 1-Diäthylcarbamyl-4-R-piperazine nicht wirksamer sind, als das 1-(3,4,5-Trimethoxybenzoyl)-4-(β-oxypropyl)-piperazin-3',4',5'-trimethoxybenzoesäureester-hydrochlorid, bei welchem früher die günstigste antiulcerogene Wirkung festgestellt wurde. Dagegen besitzen unter den zwei Piperazinringe enthaltenden Derivaten

* Diese Untersuchungen wurden mit den in Mitteilung I [1] angeführten Tests durchgeführt.

Tabelle I

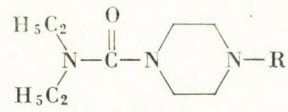

1-Diäthylcarbamyl-4-R-

No.	Bezeichnung*	R	Schmp.	Bruttoformel	Molekulargewicht
I	T19	β-Oxyäthyl	Fumarat 124—126 °C aus Methylcellosolv/abs. Äther 1 : 1	$C_{15}H_{27}N_3O_6$	345,15
II	T296	β-Chloräthyl	Hydrochlorid 182—184 °C aus abs. Äthanol	$C_{11}H_{23}N_3OCl_2$	284,01
III		β-Oxypropyl	Fumarat 122—124 °C aus abs. Äthanol/abs. Äther 1 : 1	$C_{16}H_{29}N_3O_6$	359,16
IV	T291	o-Methylbenzyl	Fumarat 152—154 °C aus abs. Äthanol	$C_{21}H_{31}N_3O_5$	405,21
V	T248	6-Chlorpyridazinyl-3	106—108 °C aus abs. Aceton	$C_{13}H_{20}N_5O^{Cl}$	297,58
VI	T262	β-(3,4,5-Trimethoxybenzoyloxy)-propyl	Hydrochlorid 166—167 °C (Zers.)** aus abs. Aceton	$C_{22}H_{36}N_3O_6Cl$	473,67
VII	R261	β-(3,4,5-Trimethoxybenzoyloxy)-äthyl	Hydrochlorid 160—162 °C (Zers.) aus abs. Äthanol	$C_{21}H_{34}N_3O_6Cl$	459,66

* Im Institut für Arzneimittelforschung, Budapest, übliche Bezeichnungen
** (Zers.) = unter Zersetzung

(Tab. II) **X** und **XI** eine relativ stärkere antiulcerogene Aktivität; ihre anticholinergische Wirkung ist sowohl *in vitro* als auch *in vivo* unbedeutend. Die Verbindungen **VI** und **VII** verursachen eine vorübergehende Hypotension, während **IX** eine schwache Antihistaminwirkung besitzt.

Die 1-(9-Xanthenyl)-4-R-piperazine (Tab. III), besonders **XVII, XVIII, XIX** und **XXI**, sind durch eine starke immobilisierende antiulcerogene Wirkung ausgezeichnet. Zugleich weisen sie *in vitro* keine anticholinergische Aktivität

piperazine

Analyse										Verfahren Bemerkung
Berechnet					Gefunden					
C	H	N	Cl⁻	Cl	C	H	N	Cl⁻	Cl	
52,19	7,82	12,17			52,17	8,11	11,98			*A* $Kp_{1\,mm}$ der Base: 160—165 °C Ausgangsverbn dun gen nach [5, i6]
		14,78	12,76	25,06			14,51	12,37	24,96	*B*
53,50	8,07	11,69			53,61	8,22	11,65			*A* $Kp_{1\,mm}$ der Base: 168—170 °C Ausgangsverbindung nach [22]
62,24	7,62	10,36			62,20	7,91	10,1			*A* Ausgangsverbindung nach [24]
52,46	6,72	23,52			52,31	6,91	23,30			*A* Ausgangsverbindung nach [26]
55,78	7,60	8,85	7,50		55,52	7,88	8,54	7,61		*C* Ausgangsverbindung nach [7]
54,86	7,39	9,13	7,71		55,03	7,42	8,48	7,53		*C*

auf. Eine mäßige Hemmung der Magensekretion *in vivo* zeigte sich allein bei **XVII.**

Es ist interessant, daß die Derivate mit zwei Piperazinringen bei den Diäthylcarbamylpiperazinen größenordnungsmäßig wirksamer sind, als die Verbindungen mit nur einem Piperazinring, während unter den 1-(9-Xanthenyl)-4-β-[4-(R)-piperazinyl-1]-äthylpiperazinen (Tab. IV) allein die Verbindung **XXVII** eine annähernd ähnliche Aktivität besitzt, wie die 1-(9-Xanthenyl)-4-R-piperazine.

Tabelle II

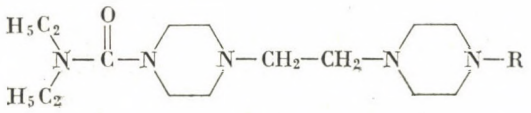

1-Diäthylcarbamyl-4-β-[4-(R)-piperazinyl

No.	Bezeichnung	R	Schmp.	Bruttoformel	Molekulargewicht
VIII	T401	H	Trihydrochlorid 260—261 °C (Zers.) mit heißem abs. Methanol behandelt	$C_{15}H_{34}N_5OCl_3$	406,50
IX	T407	Diäthylcarbamyl	Dihydrochlorid 277—280 °C (Zers.) mit heißem abs. Methanol behandelt	$C_{20}H_{42}N_6O_2Cl_2$	469,10
X	T293	Carbäthoxy	Dihydrochlorid 270—272 °C (Zers.) mit heißem abs. Methanol behandelt	$C_{18}H_{37}N_5O_3Cl_2$	442,08
XI	T294	Carbobenzyloxy	Dihydrochlorid 253—255 °C (Zers.) mit heißem abs. Methanol behandelt	$C_{23}H_{39}N_5O_3Cl_2$	504,13
XII	T402	3,4,5-Trimethoxybenzoyl	Dihydrochlorid 248—250 °C (Zers.) aus abs. Äthanol	$C_{25}H_{43}N_5O_5Cl_2$	564,15
XIII	T419	Methyl	Trihydrochlorid 263—265 °C (Zers.) mit heißem abs. Methanol behandelt	$C_{16}H_{36}N_5OCl_3$	420,51
XIV	20220	i-Butyl	Trihydrochlorid 285—286 °C (Zers.) mit heißem abs. Methanol behandelt	$C_{19}H_{42}N_5OCl_3$	462,54
XV	T405	*o*-Methylbenzyl	Trihydrochlorid 267—269 °C (Zers.) mit heißem abs. Methanol behandelt	$C_{23}H_{42}N_5OCl_3$	510,58

Unter den 1-(Xanthen-9-carbonyl)-4-R-piperazinen (Tab. V) waren jene Derivate hinsichtlich ihrer antiulcerogenen Wirkung am aktivsten, welche außer dem Piperazinring noch ein tertiäres Stickstoffatom enthielten. Eine besonders starke antiulcerogene Wirkung zeigte sich bei **XLVI,** welches dabei *in vivo* auch eine bedeutende anticholinergische Aktivität zeigte.

Die Verbindungen **XXXVII** und **XLIII** besaßen eine mäßige immobilisierende antiulcerogene und Antihistaminwirkung. **XXXV** und **XXXVI** wirken

-1]-äthylpiperazine

Analyse								Verfahren Bemerkung
Berechnet				Gefunden				
C	H	N	Cl⁻	C	H	N	Cl⁻	
44,31	8,36	17,22	26,60	44,19	8,29	17,01	25,94	D_1 $Kp_{0,2\ mm}$ der Base: 180—186 °C
51,20	8,95	17,90	15,11	51,36	9,09	17,92	15,26	*D* Ausgangsverbindung nach [4]
48,90	8,36	15,83	16,03	49,03	8,52	15,81	16,00	*D* Ausgangsverbindung nach [27]
54,79	7,73	13,88	14,06	54,62	7,81	13,76	13,97	*D* Ausgangsverbindung nach [28]
53,22	7,62	12,40	12,56	53,32	7,55	12,21	12,6	*A*
45,64	8,56	16,46	25,29	45,79	8,69	16,56	26,23	*D* Ausgangsverbindung nach [27]
49,33	9,08	15,13	23,00	48,98	9,27	14,82	23,37	*D* Ausgangsverbindung nach [29]
54,10	8,22	13,70	20,82	54,38	8,38	13,83	20,68	*D*

schwach sedativ. Die Aktivität des aus **XLVI** hergestellten quaternären Derivats **XLVII** erwies sich als geringer, als die der Grundverbindung.

Unter den 1-(Xanthen-9-carbonyl)-4-β-[4-(R)-piperazinyl-1]-äthylpiperazinen (Tab. VI) sind die Verbindungen **XLVIII** und **XLIX** durch eine stärkere antiulcerogene Wirkung und — besonders *in vitro* — durch eine bedeutendere parasympatholytische Wirkung gekennzeichnet, als die bereits erwähnten Derivate mit zwei Piperazinringen; *in vivo* zeigte sich jedoch diese Wirkung

Tabelle III

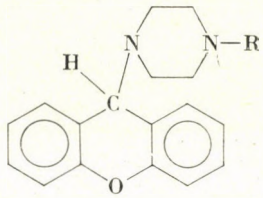

1-(9-Xanthenyl)-4-

No.	Bezeichnung	R	Schmp.	Bruttoformel	Molekulargewicht
XVI	T459	*n*-Butyl	83—84 °C aus abs. Methanol	$C_{21}H_{26}N_2O$	322,21
XVII	T386	*o*-Methylbenzyl	134—136 °C aus abs. Aceton	$C_{25}H_{26}N_2O$	370,25
XVIII	T608	β-Phenyl-i-propyl	110—112 °C aus abs. Aceton	$C_{26}H_{28}N_2O$	384,26
XIX	T597	α-(2-Pyridyl)-äthyl	134—135 °C aus abs. Aceton	$C_{24}H_{25}N_3O$	371,24
XX	T421	β-Oxyäthyl	125—126 °C aus abs. Benzol/ abs. Hexan 1 : 1	$C_{19}H_{22}N_2O_2$	310,19
XXI	T385	Diäthyl-carbamyl	124—126 °C aus Benzol/ Hexan 1 : 1	$C_{22}H_{27}N_3O_2$	365,22
XXII	T445	Carbobenzyl-oxy	153—155 °C aus Benzol/ Hexan 1 : 1	$C_{23}H_{24}N_2O_3$	400,25
XXIII	T446	3,4,5-Trimethoxy-benzoyl	145—147 °C aus abs. Äthanol	$C_{27}H_{28}N_2O_5$	460,27
XXIV	T488	9-Xanthenyl	253—254 °C aus Benzol/ Hexan 1 : 1	$C_{30}H_{26}N_2O_2$	446,30
XXV	T449	6-Chlorpyridazinyl-3	216—218 °C aus abs. Aceton	$C_{21}H_{19}N_4OCl$	378,66
XXVI	T447	β-(3,4,5-Trimethoxybenzoyloxy)-äthyl	134—135 °C aus abs. Aceton	$C_{29}H_{32}N_2O_6$	504,29

R-piperazine

Analyse								Verfahren Bemerkung
Berechnet				Gefunden				
C	H	N	Cl	C	H	N	Cl	
78,27	8,06	8,68		78,12	8,12	8,72		*E* Ausgangsverbindung nach [25], [9]
81,04	7,02	7,56		81,00	7,22	7,36		*E*
81,26	7,28	7,28		81,01	7,42	7,14		*E* Ausgangsverbindung nach [1]
77,64	6,73	11,31		77,65	6,86	11,22		*E*
73,56	7,09	9,02		73,62	7,16	8,87		*E*
72,34	7,39	11,49		72,51	7,28	11,35		*E*
75,01	5,99	6,99		85,15	6,09	6,98		*E*
70,45	6,08	6,08		70,56	6,13	6,28		*E* Ausgangsverbindung nach [1]
80,73	5,82	6,27		80,51	5,90	6,40		*E* Mit 2 Mol Xanthydrol
66,38	5,01	14,78	9,40	66,38	5,19	14,90	9,30	*E*
69,06	6,34	5,55		69,28	6,50	5,54		*C*

Tabelle I V

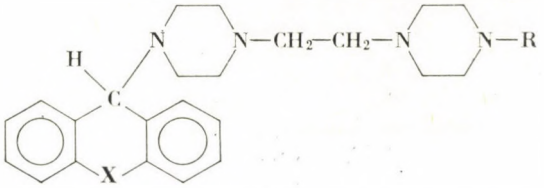

1-(9-Xanthenyl)-4-β-[4-(R)-

No.	Bezeichnung	R	X	Schmp.	Bruttoformel	Molekulargewicht
XXVII	T444	Carbäthoxy	O	131—133 °C aus Benzol/Hexan 1 : 1	$C_{26}H_{34}N_4O_3$	450,26
XXVIII	T452	Diäthyl-carbamyl	O	94—96 °C aus Benzol/Hexan 1 : 1	$C_{28}H_{39}N_5O_2$	477,26
XXIX	T469	*n*-Butyl	O	104—106 °C aus abs. Aceton	$C_{27}H_{38}N_4O$	434,27
XXX	T486	*n*-Butyl	S	105—106 °C aus abs. Aceton	$C_{27}H_{38}N_4S$	450,27

kaum. Eine bedeutende anticholinergische Wirkung *in vivo* konnte endlich durch eine aliphatische R-Substitution erreicht werden. In dieser Gruppe erwies sich die Verbindung **LXIII** sowohl hinsichtlich der Wirkungsstärke als auch der Toxizität und der Resorption als das günstigste Derivat.

Zusammenfassend kann festgestellt werden, daß eine bemerkenswerte antiulcerogene Wirkung bei zwei Verbindungsreihen, namentlich bei den 1-(9-Xanthenyl)-4-R-piperazinen und bei den 1-(Xanthen-9-carbonyl)-4-β--[4-(alkyl)-piperazinyl-1]-äthylpiperazinen gefunden wurde. Darunter zeichnet sich in erster Reihe das 1-(Xanthen-9-carbonyl)-4-β-[4-(i-butyl)-piperazinyl-1]-äthylpiperazin **LXIII** durch gute perorale Resorption, starke antiulcerogene Wirkung bei durch einen zentralen Mechanismus entstehenden Versuchsulcera und bedeutende anticholinergische Eigenschaft aus. Die antisekretorischen und antiulcerogenen Eigenschaften der Verbindung beruhen — gemäß EEG-Untersuchungen — außer der mäßigen peripherischen anticholinergischen Wirkung auch auf der zentralen parasympatholytischen Komponente.

Experimenteller Teil*

N-i-Amylpiperazin

233 g Piperazin-hexahydrat werden in 480 ml Äthylalkohol gelöst und unter Rühren im Laufe von 30 Minuten werden 1,2 Mol HCl in Form einer konzentrierten wäßrigen Lösung

* Unkorrigierte Temperaturen.

piperazinyl-1]-äthyl-piperazine

Analyse								Verfahren Bemerkung
Berechnet				Gefunden				
C	H	N	S	C	H	N	S	
69,35	7,55	12,43		69,60	7,62	12,22		*E*
70,45	8,17	14,66		70,67	8,26	14,50		*E*
74,67	8,75	12,89		74,55	8,86	13,04		*E*
72,01	8,43	12,43	7,10	71,98	8,54	12,29	7,35	*E*

(104 ml 11,5 *n* HCl) portionsweise zugegeben. Danach werden 71 g i-Amylbromid bei 65 °C im Laufe von anderthalb Stunden portionsweise zugegeben. Das Gemisch wird 1 Stunde lang bei 65 °C gerührt und über Nacht im Kühlschrank stehen gelassen. Das ausgeschiedene Salzgemisch Piperazinhydrochlorid-hydrobromid wird abgesaugt und die alkoholische Lösung auf dem Wasserbad unter Vakuum zu einem dicken Brei eingedampft. Dieser wird abgekühlt, mit 70 ml 40%iger wäßriger Natriumhydroxydlösung vermischt und mit 2×150 ml Benzol ausgeschüttelt. Die über Natriumsulfat getrocknete benzolische Lösung wird eingedampft und der Rückstand unter Vakuum fraktioniert.

$Kp_{8-10\ mm}$: 85—86 °C. Ausbeute: 38 g.

Mit Perchlorsäure titriert, erwies sich das Produkt als 99,3%ig.

3 g des obigen Produktes werden in 50 ml abs. Äthanol gelöst und das N-i-Amylpiperazin-dihydrochlorid (3,6 g) mit in abs. Alkohol gelöstem HCl abgeschieden. Aus 40 ml abs. Methanol umkristallisiert schmilzt das Produkt bei 280—282 °C unter Zersetzung.

$C_9H_{22}N_2Cl_2$ (228,9). Berechnet: C 47,20; H 9,60; N 12,22; Cl^- 30,96. Gefunden: C 46,93; H 9,81; N 12,01; Cl^- 30,76%.

N-*sec.*-Butylpiperazin

Diese Verbindung wurde auf analoge Weise wie N-i-Amylpiperazin, aus Piperazinhexahydrat mit *sec.* Butylbromid hergestellt.

$Kp_{15\ mm}$: 84—86 °C.

$C_8H_{18}N_2$ (142,08). Berechnet: C 67,62; H 12,67; N 19,70% Gefunden: C 67,13; H 12,88; N 19,91%.

1-α-(2-Pyridyl)-äthylpiperazin

43 g wasserfreies Piperazin werden in 400 ml abs. Benzol unter Sieden gerührt und im Laufe von 3 Stunden wird die Lösung von 40 g 2-(α-Bromäthyl)-pyridin [11] in 60 ml abs. Benzol portionsweise zugegeben. Das Gemisch wird 2 Stunden lang im Sieden gehalten und

Tabelle V

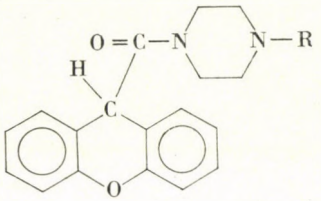

1-(Xanthen-9-carbonyl)

No.	Bezeichnung	R	Schmp.	Bruttoformel	Molekulargewicht
XXXI	T350	β-Oxyäthyl	Hydrochlorid 245—247 °C (Zers.) aus abs. Methanol	$C_{20}H_{21}N_2O_3Cl$	374,65
XXXII	T400	β-Chloräthyl	127—129 °C aus abs. Benzol/Petroläther 2,5 : 1	$C_{20}H_{21}N_2OCl$	356,65
XXXIII	T470	*n*-Butyl	Hydrochlorid 260—262 °C (Zers.) aus abs. Methanol	$C_{22}H_{27}N_2O_2Cl$	386,67
XXXIV	T381	*o*-Methylbenzyl	182—184 °C aus abs. Äthanol	$C_{26}H_{26}N_2O_2$	398,26
XXXV	T382	Carbäthoxy	144—145 °C aus abs. Äthanol	$C_{21}H_{22}N_2O_4$	366,21
XXXVI	T383	Carbobenzyloxy	153—155 °C aus abs. Äthanol	$C_{26}H_{24}N_2O_4$	428,26
XXXVII	T384	Diäthyl-carbamyl	153—155 °C aus abs. Äthanol	$C_{23}H_{27}N_3O_3$	393,23
XXXVIII	T367	β-(Xanthen-9-carbonyloxy)-propyl	155—157 °C aus abs. Äthanol/abs. Aceton 1 : 1	$C_{35}H_{32}N_2O_5$	560,35
XXXIX	T428	β-(Xanthen-9-carbonyl-amino)-äthyl	243—245 °C mit heißem abs. Methanol behandelt	$C_{34}H_{31}N_3O_4$	545,34

-4-R-piperazine

Analyse										Verfahren Bemerkung
Berechnet					Gefunden					
C	H	N	Cl⁻	J	C	H	N	Cl⁻	J	
64,11	6,13	7,74	9,46		64,28	6,27	7,29	9,30		*A* Ausgangsverbindung nach [21]
67,34	5,88	7,85	9,93		67,38	6,02	7,96	9,93		*B* Reinigung der Base unmittelbar durch Kristallisieren
68,33	6,98	7,22	9,16		68,52	7,03	7,08	9,14		*A* Ausgangsverbindung nach [25]
78,40	6,52	7,03			78,24	6,58	6,92			*A* Ausgangsverbindung nach [24]
68,88	6,00	7,64			69,17	6,08	7,59			*A* Ausgangsverbindung nach [27]
72,90	5,60	6,53			73,12	5,72	6,45			*A* Ausgangsverbindung nach [28]
70,24	6,86	10,69			70,43	7,00	10,41			*A* Ausgangsverbindung nach [22]
75,01	5,71	4,99			75,24	5,84	4,85			*F*
74,87	5,68	7,70			74,71	5,75	7,67			*A* Aus 2 Mol Xanthen-9-carbonylchlorid. Ausgangsverbindung nach [30]

Tabelle V

No.	Bezeichnung	R	Schmp.	Bruttoformel	Molekulargewicht
XL	20064	β-Phthalimidoäthyl	140—142 °C aus i-Propylalkohol	$C_{28}H_{25}N_3O_4$	467,28
XLI	20044	**XL**-Methojodid	223—224 °C (Zers.) aus. abs. Aceton/abs. Äther 1 : 2	$C_{29}H_{28}N_3O_4J$	609,21
XLII	T610	β-Piperidinoäthyl	Dihydrochlorid 294—295 °C (Zers.) mit heißem abs. Methanol behandelt	$C_{25}H_{33}N_3O_2Cl_2$	478,15
XLIII	T527	β-[2-(β-Oxyäthyl)-piperidyl]-äthyl	Dihydrochlorid 193—195 °C (Zers.) aus abs. Aceton/abs. Äthanol 1 : 1	$C_{27}H_{37}N_3O_3Cl_2$	522,17
XLIV	T636	β-[Di-(β-Oxyäthyl)]-aminoäthyl	Dihydrochlorid 227—229 °C (Zers.) aus abs. Methanol	$C_{24}H_{33}N_3O_4Cl_2$	498,14
XLV	T628	β-(*tert.*-Butyl-β-oxypropyl)-aminoäthyl	133—134 °C aus abs. Methanol	$C_{27}H_{37}N_3O_3$	451,27
XLVI	T523	β-(β'-Phenyl-i-propylmethyl)-aminoäthyl	Dihydrochlorid 246—248 °C (Zers.) aus abs. Methanol	$C_{30}H_{37}N_3O_2Cl_2$	542,20
XLVII	T524	**XLVI**-Methojodid	206—208 °C (Zers.) mit heißem abs. Aceton behandelt	$C_{31}H_{38}N_3O_2J$	611,23

das ausgeschiedene Piperazin-hydrobromid nach dem Abkühlen abfiltriert. Nach dem Abdampfen des Benzols wird der Rückstand im Vakuum fraktioniert.

$Kp_{1\ mm}$: 118—120 °C. Ausbeute: 16,5 g.

$C_{11}H_{17}N_3$ (191,11). Berechnet: C 69,12; H 8,89; N 21,97%. Gefunden: C 69,82; H 9,20; N 21,58%.

1-(i-Butyl)-4-(β-oxyäthyl)-piperazin

100 g N-(β-Oxyäthyl)-piperazin werden in 350 ml abs. Aceton bei 45—50 °C gerührt und 52 g i-Butylbromid im Laufe einer Stunde portionsweise zugegeben. Anschließend wird 4 Stunden lang bei 50—60 °C gerührt. Das Gemisch wird über Nacht stehen gelassen, das ausgeschiedene N-(β-Oxyäthyl)-piperazin-hydrobromid abfiltriert und die acetonische Lösung eingedampft. Der Rückstand wird unter Vakuum fraktioniert.

$Kp_{1\ mm}$: 112—116 °C. Ausbeute: 27,4 g.

Mit Perchlorsäure titriert, erwies sich das Produkt als 99,3%ig.

4 g der obigen Base werden in 25 ml abs. Äthanol gelöst und das 1-(i-Butyl)-4-(β-oxyäthyl)-piperazin-dihydrochlorid (5,1 g) mit in abs. Alkohol gelöstem Chlorwasserstoff abge-

(Fortsetzung)

Analyse										Verfahren Bemerkung
Berechnet					Gefunden					
C	H	N	Cl^-	J	C	H	N	Cl^-	J	
74,10	5,34	8,97			73,82	5,10	8,76			*A* Statt Dichloräthan in abs. Äthanol. Ausgangsverbindung nach [23]
57,27	4,59	6,89		20,83	57,36	4,67	6,82		20,50	*G*
62,79	6,90	8,78	14,82		62,54	7,13	8,72	14,87		*D*
62,10	7,08	8,04	13,57		62,16	7,16	7,88	13,42		*D* Ausgangsverbindung nach [31]
57,86	6,62	8,43	14,23		58,14	6,74	8,36	14,11		*D*
71,85	8,19	9,30			71,92	8,35	9,44			*D* Ausgangsverbindung nach [32]
66,45	6,82	7,74	13,07		66,62	6,90	7,68	13,10		*D* Ausgangsverbindung nach [33]
60,91	6,21	6,87		20,76	60,88	6,33	6,81		21,00	*G*

schieden. Aus 100 ml eines 1 : 1 Gemisches von abs. Methanol und abs. Äthanol umkristallisiert schmilzt das Salz unter Zersetzung bei 232—234 °C.

$C_{10}H_{24}N_2Cl_2O$ (259,00). Berechnet: C 46,37; H 9,22; N 10,81; Cl^- 27,37%. Gefunden: C 45,98; H 9,43; N 10,62; Cl^- 27,41%.

1-(i-Butyl)-4-(β-chloräthyl)-piperazin

Diese Verbindung wurde analog zu **II** (Tab. I), nach Verfahren *B*, aus 1-(i-Butyl)-4-(β-oxyäthyl)-piperazin mit Thionylchlorid hergestellt. Aus der 35fachen Menge von abs. Äthanol umkristallisiert schmilzt das Dihydrochlorid unter Zersetzung bei 237—239 °C.

$C_{10}H_{23}Cl_3N_2$ (277,45). Berechnet: C 43,28; H 8,29; Cl^- 25,55; Cl 38,04%. Gefunden: C 42,87; H 8,41; N 9,88; Cl^- 25,83; Cl 38,04%.

1-R-4-β-(Piperazinyl-1)-äthylpiperazine

Diese Verbindungen wurden analog zu **VIII** (Tab. II) nach Verfahren D_1, aus wasserfreiem Piperazin und dem entsprechenden 1-R-4-(β-Chloräthyl)-piperazin hergestellt.

Tabelle VI

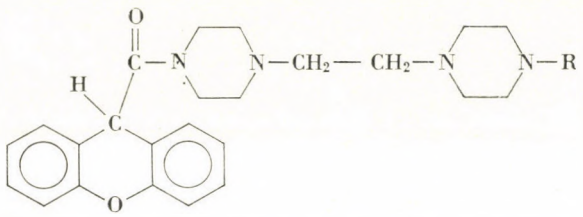

1-(Xanthen-9-carbonyl)-4-β-[4-(R)-

No.	Bezeichnung	R	Schmp.	Bruttoformel	Molekulargewicht
XLVIII	T369	Carbäthoxy	Dihydrochlorid 275—276 °C (Zers.) mit heißem abs. Methanol behandelt	$C_{27}H_{36}N_4O_4Cl_2$	551,17
XLIX	T370	Carbobenzoyloxy	Dihydrochlorid 265—267 °C (Zers.) mit heißem abs. Methanol behandelt	$C_{32}H_{38}N_4O_4Cl_2$	613,22
L	T408	Diäthyl-carbamyl	Dihydrochlorid 272—274 °C (Zers.) mit heißem abs. Methanol behandelt	$C_{29}H_{41}N_5O_3Cl_2$	578,19
LI	T387	*o*-Methylbenzyl	Trihydrochlorid 256—258 °C (Zers.) mit heißem abs. Methanol behandelt	$C_{32}H_{41}N_4O_2Cl_3$	619,17
LII	T584	β-Phenyl-i-propyl	Trihydrochlorid 268—270 °C (Zers.) mit heißem abs. Methanol behandelt	$C_{33}H_{43}N_4O_2Cl_3$	633,68
LIII	T604	α-(2-Pyridyl)-äthyl	Tetrahydrochlorid 250—252 °C (Zers.) mit heißem abs. Methanol behandelt	$C_{31}H_{41}N_5O_2Cl_4$	657,11
LIV	T410	β-Oxypropyl	Trihydrochlorid 266—268 °C (Zers.) mit heißem Methanol behandelt	$C_{27}H_{39}N_4O_3Cl_3$	573,62
LV	T411	β-(3,4,5-Trimethoxybenzoyloxy)-propyl	Trihydrochlorid 227—229 °C (Zers.) aus abs. Methanol	$C_{37}H_{49}N_4O_7Cl_3$	767,62
LVI	20043	Methyl	Trihydrochlorid 263—265 °C (Zers.) mit heißem Methanol behandelt	$C_{25}H_{35}N_4O_2Cl_3$	529,60
LVII	T487	Äthyl	Trihydrochlorid 268—269 °C (Zers.) mit heißem Methanol behandelt	$C_{26}H_{37}N_4O_2Cl_3$	543,61

piperazinyl-1]-äthylpiperazine

Analyse										Verfahren Bemerkung
Berechnet					Gefunden					
C	H	N	Cl−	J	C	H	N	Cl−	J	
58,81	6,53	10,16	12,86		58,56	6,67	10,10	12,79		*D*
62,67	6,19	9,13	11,56		62,50	6,29	9,28	11,68		*D*
60,23	7,09	12,10	12,26		60,26	7,11	11,85	12,33		*D*
62,02	6,61	9,03	17,16		62,02	6,80	9,13	17,29		*D*
62,54	6,78	8,83	16,78		62,38	6,90	8,69	16,58		*D*
56,65	6,23	10,65	21,57		56,61	6,20	10,58	21,35		*D*
56,53	6,79	9,76	18,54		56,28	7,00	9,81	18,34		*D*
57,88	6,38	7,29	13,85		57,65	6,47	7,22	13,75		*B*
56,90	6,60	10,57	20,08		56,69	6,61	10,47	19,85		*D* Ausgangsverbindung nach [27]
57,44	6,80	10,30	19,56		57,62	6,95	10,26	19,48		*D* Ausgangsverbindung nach [34]

Tabelle VI

No.	Bezeichnung	R	Schmp.	Bruttoformel	Molekulargewicht
LVIII	T460	*n*-Propyl	Trihydrochlorid 271—272 °C (Zers.) mit heißem Methanol behandelt	$C_{27}H_{39}N_4O_2Cl_3$	557,62
LIX	T468	Allyl	Trihydrochlorid 271—272 °C (Zers.) mit heißem Methanol behandelt	$C_{27}H_{37}N_4O_2Cl_3$	555,62
LX	T467	i-Propyl	Trihydrochlorid 260—262 °C (Zers.) mit heißem Methanol behandelt	$C_{27}H_{39}N_4O_2Cl_3$	557,62
LXI	T413	*n*-Butyl	Trihydrochlorid 287—290 °C (Zers.) mit heißem Methanol behandelt	$C_{28}H_{41}N_4O_2Cl_3$	571,63
LXII	T485	**LXI**-Dimethojodid	239—241 °C (Zers.) mit heißem Aceton behandelt	$C_{30}H_{44}N_4O_2J_2$	746,14
LXIII	T451	i-Butyl	Trihydrochlorid 273—275 °C (Zers.) mit heißem Methanol behandelt	$C_{28}H_{41}N_4O_2Cl_3$	571,63
LXIV	T588	*sec.*-Butyl	Trihydrochlorid 268—270 °C (Zers.) mit heißem Methanol behandelt	$C_{28}H_{41}N_4O_2Cl_3$	571,63
LXV	T466	*n*-Amyl	Trihydrochlorid 282—284 °C (Zers.) mit heißem Methanol behandelt	$C_{29}H_{43}N_4O_2Cl_3$	585,64
XVI	20020	i-Amyl	Trihydrochlorid 280—282 °C (Zers.) mit heißem Methanol behandelt	$C_{29}H_{43}N_4O_2Cl_3$	585,64

a) 1-(i-Butyl)-4-β-(piperazinyl-1)-äthylpiperazin.
$Kp._{1\ mm}$: 152—154 °C.
Tetrahydrochlorid: Schmp. 270—272 °C unter Zersetzung (mit 20fachem abs. Methanol ausgekocht).
$C_{14}H_{34}Cl_4N_4$ (399,92).
Berechnet: C 42,04; H 8,50; N 14,00; Cl^- 35,06%.
Gefunden: C 42,21; H 8,70; N 14,10; Cl^- 35,06%.
Ausgangsmaterial 1-(i-Butyl)-4-(β-Chloräthyl)-piperazin: siehe experimenteller Teil.
b) 1-(*n*-Butyl)-4-β-(piperazinyl-1)-äthylpiperazin.
$Kp._{2\ mm}$: 122—124 °C.
Tetrahydrochlorid: Schmp. 276—278 °C unter Zersetzung. (Mit 20fachem abs. Methanol ausgekocht.)
$C_{14}H_{34}Cl_4N_4$ (399,44).
Berechnet: C 42,04; H 8,50; N 14,00; Cl^- 35,25%.
Gefunden: C 41,87; H 8,61; N 13,92; Cl^- 35,25%.
c) 1-Carbäthoxy-4-β-(piperazinyl-1)-äthylpiperazin.
$Kp._{0,4\ mm}$: 170—173 °C.

(Fortsetzung)

Analyse										Verfahren Bemerkung
Berechnet					Gefunden					
C	H	N	Cl⁻	J	C	H	N	Cl⁻	J	
58,15	6,99	10,04	19,07		58,45	7,12	10,06	18,84		*D* Ausgangsverbindung nach [29]
58,36	6,65	10,07	19,14		58,49	6,73	10,19	19,32		*D* Ausgangsverbindung nach [35]
58,15	6,99	10,04	19,07		58,06	7,12	9,79	18,91		*D* Ausgangsverbindung nach [29]
58,82	7,17	9,79	18,60		58,68	7,25	9,69	18,48		*D*
48,28	5,89	7,50		34,02	47,92	6,11	7,39		33,84	*E*
58,82	7,17	9,79	18,60		58,67	7,26	9,71	18,50		*A* und *D* Ausgangsverbindung nach [29]
58,82	7,17	9,79	18,60		58,63	7,28	9,66	18,56		*D*
59,47	7,34	9,56	18,15		59,32	7,45	9,64	18,06		*D* Ausgangsverbindung nach [36]
59,47	7,34	9,56	18,15		59,32	7,45	9,64	18,06		*D*

Trihydrochlorid: Schmp. 258—260 °C, unter Zersetzung. (Mit 20fachem abs. Methanol ausgekocht.)

$C_{13}H_{29}Cl_3N_4O_2$ (379,38). Berechnet: C 41,14; H 7,64; N 14,75; Cl^- 28,02%. Gefunden: C 41,78; H 7,63; N 14,85; Cl^- 27,90%.

Ausgangsstoff 1-Carbäthoxy-4-(β-chloräthyl)-piperazin [12].

Verfahren A

1-Diäthylcarbamyl-4-(β-oxyäthyl)-piperazin, I

(Tab. I, T 19)

14,4 g N-(β-Oxyäthyl)-piperazin [5] und 20 ml Triäthylamin werden in 100 ml trockenem Dichloräthan gelöst. Unter Rühren und Kühlen mit Eiswasser wird im Laufe von anderthalb Stunden die Lösung von 16,25 g Diäthylcarbamylchlorid [6] in 40 ml trockenem Dichloräthan portionsweise zugegeben. Anschließend wird 4 Stunden lang bei Zimmertemperatur

gerührt und über Nacht stehen gelassen. Das abgeschiedene Triäthylamin-hydrochlorid wird abfiltriert und das Filtrat mit 20 ml 7%iger wäßriger $KHCO_3$-Lösung und 30 ml Wasser ausgeschüttelt. Die Dichloräthanphase wird über Natriumsulfat getrocknet, das Lösungsmittel wird abgedampft und der Rückstand unter Vakuum fraktioniert.

$Kp_{1\ mm}$: 160—165 °C. Ausbeute: 9,6 g.

Mit Perchlorsäure titriert, erwies sich das Produkt als 99,5%ig.

3 g der obigen Base werden in 10 ml heißem abs. Äthanol gelöst und mit der Lösung von 1,6 g Fumarsäure in 17 ml heißem abs. Alkohol vermischt. Nach Stehen über Nacht wird das ausgeschiedene 1-(Diäthylcarbamyl-4-(β-oxyäthyl)-piperazinfumarat (3,8 g) filtriert. Aus der dreifachen Menge Methylcellosolv/abs. Äther (1 : 1) umkristallisiert ist der Schmelzpunkt 124—126 °C. Ausbeute: 3,2 g.

Die Analysenergebnisse sind in Tab. I angeführt.

Verfahren B

1-Diäthylcarbamyl-4-(β-chloräthyl)-piperazin, II

(Tab. I, T 296)

6 g 1-Diäthylcarbamyl-4-(β-oxyäthyl)-piperazin (**I**) (Tab. I, T 19) werden mit 40 ml trockenem Chloroform bei Siedehitze gerührt und im Laufe von anderthalb Stunden wird die Lösung von 2,82 ml Thionylchlorid in 10 ml trockenem Chloroform portionsweise zugegeben. Nach 3stündigem Sieden wird das Chloroform größtenteils (30 ml) unter Vakuum abgetrieben und der Rückstand mit 20 ml abs. Aceton versetzt. Schmelzpunkt des ausgeschiedenen 1-Diäthylcarbamyl-4-(β-Chloräthyl)-piperazin-hydrochlorids (6,9 g). Ausbeute: 3,05 g.

Die Analysenergebnisse sind in Tab. I angeführt.

Verfahren C

1-Diäthylcarbamyl-4-(β-oxypropyl)-piperazin-3,4,5-trimethoxybenzoesäureester, VI

(Tab. I, T 262)

4,86 g 1-Diäthylcarbamyl-4-(β-oxypropyl)-piperazin (Tab. I, III) und 4 ml Triäthylamin werden in 70 ml trockenem Dichloräthan gelöst. Unter Rühren und Kühlen mit Eiswasser werden im Laufe von 10 Minuten 5 g 3,4,5-Trimethoxybenzylchlorid [7] in 20 ml trockenem Dichloräthan gelöst, portionsweise zugegeben und 8 Stunden lang im Sieden gehalten. Das Gemisch wird über Nacht stehen gelassen, das ausgeschiedene Triäthylamin-hydrochlorid abfiltriert, das Filtrat mit 25 ml 7%iger wäßriger $NaHCO_3$-Lösung und mit 25 ml Wasser ausgeschüttelt, die Lösung über Natriumsulfat getrocknet, das Dichloräthan abgedampft und der Rückstand (7,1 g) in 100 ml abs. Äthanol/abs. Äther 1 : 10 gelöst. Daraus wird das Hydrochlorid der Verbindung **VI** mit abs. alkoholischer Salzsäure abgeschieden (5,1 g); aus 56 ml abs. Aceton umkristallisiert schmilzt das Produkt bei 166—167 °C unter Zersetzung. Ausbeute: 2,8 g.

Die Analysenergebnisse sind in Tab. I angeführt.

Verfahren D

1-Diäthylcarbamyl-4-β-[4-(diäthylcarbamyl)-piperazinyl-1]-äthylpiperazin, IX

(Tab. II, T 407)

12,4 g 1-Diäthylcarbamyl-4-(β-chloräthyl)-piperazin (Tab. I, II, T 296), welches aus dem Hydrochlorid mit Chloroform und der wäßrigen Lösung von $NaHCO_3$ freigemacht wurde, wird 3 Stunden lang bei 130 °C mit 22,12 g N-Diäthylcarbamylpiperazin [4] gerührt. Nach dem Abkühlen wird das Gemisch mit 60 ml 10%iger wäßriger K_2CO_3-Lösung und anschließend mit 60 ml Wasser durch Dekantieren gewaschen und der Rückstand in 80 ml Chloroform aufgenommen. Die Lösung wird über Natriumsulfat getrocknet, das Chloroform abgedampft, der Rückstand (19,5 g) in 80 ml abs. Methanol gelöst und das Dihydrochlorid der Verbindung **IX** (16,5 g) unter Kühlen mit Eiswasser mit abs. alkoholischer Salzsäure abgeschieden. Nach Auskochen mit 180 ml abs. Methanol schmilzt das Produkt bei 277—280 °C unter Zersetzung. Ausbeute: 9,8 g.

Die Analysenergebnisse sind in Tab. II angeführt.

Verfahren D_1

1-Diäthylcarbamyl-4-β-(piperazinyl-1) äthylpiperazin, VIII

(Tab. II, T 401)

16,2 g wasserfreies Piperazin werden bei 105 °C gerührt und im Laufe einer Stunde werden 12,4 g 1-Diäthylcarbamyl-4-(β-chloräthyl)-piperazin (Tab. I, II, T 246) portionsweise zugefügt. Anschließend wird das Gemisch 2 Stunden lang bei 130 °C gerührt, nach dem Abkühlen mit 30 ml 10%iger wäßriger K_2CO_3-Lösung vermischt und mit 2×40 ml Chloroform ausgeschüttelt. Nach Trocknen über Natriumsulfat wird das Chloroform abgedampft und der Rückstand unter Vakuum fraktioniert.

$Kp_{0,2\ mm}$: 180—186 °C. Ausbeute: 3,9 g.

Mit Perchlorsäure titriert erwies sich das Produkt als 99,6%ig.

3,9 g der obigen Base werden in 20 ml abs. Äthanol gelöst und das Trihydrochlorid der Verbindung **VIII** (3 g) wird mit abs. alkoholischer Salzsäure abgeschieden. Mit 50 ml abs. Methanol ausgekocht schmilzt das Produkt bei 260—261 °C unter Zersetzung. Die Analysenergebnisse sind in Tab. II angeführt.

Verfahren E

1-(9-Xanthenyl)-4-(*n*-butyl)-piperazin, XVI

(Tab. III, T 459)

14,2 g N-(*n*-Butyl)-piperazin [25], 19,8 g Xanthydrol [9] und 6 g Essigsäure werden in 100 ml abs. Toluol, unter Anwendung eines wasserabtrennenden Aufsatzes 18 Stunden lang im Sieden gehalten und das als azeotrope Mischung abdestillierende Wasser wird abgetrennt. Nach dem Eindampfen der toluolischen Lösung wird der Rückstand in 80 ml Chloroform aufgenommen und mit 40 ml Wasser abgeschüttelt. Nach dem Trocknen über Natriumsulfat wird das Chloroform abgedampft und der Rückstand (32,1 g) in 100 ml warmem Aceton gelöst. Das beim Stehen über Nacht ausgeschiedene **XVI** (22,1 g) schmilzt nach Umkristallisieren aus der fünffachen Menge abs. Aceton bei 83—84 °C. Ausbeute: 8,6 g.

Die Analysenergebnisse sind in Tab. II angeführt.

Verfahren F

1-(Xanthen-9-carbonyl)-4-β-(xanthen-9-carbonyloxy)-propylpiperazin, XXXVIII

(Tab. V, T 367)

1,44 g N-(β-Oxypropyl)-piperazin [22] und 3,7 ml Triäthylamin werden in 20 ml trockenem Dichloräthan gelöst. Unter Rühren bei Zimmertemperatur wird die Lösung von 5,79 g Xanthen-9-carbonylchlorid in 30 ml trockenem Dichloräthan im Laufe einer Stunde portionsweise zugegeben. Anschließend wird 6 Stunden lang im Sieden gehalten, das beim Stehen über Nacht ausgeschiedene Triäthylamin-hydrochlorid abfiltriert und das Filtrat mit 30 ml 7%iger wäßriger $NaHCO_3$-Lösung und mit 40 ml Wasser ausgeschüttelt. Nach dem Trocknen der Lösung über Natriumsulfat wird das Dichloräthan abgedampft und der Rückstand (6,6 g) in 20 ml abs. Äthanol gelöst. Die beim Stehen über Nacht ausgeschiedene Verbindung **XXXVIII** (4 g) schmilzt — aus 50 ml abs. Äthanol/abs. Aceton (1 : 1) umkristallisiert — bei 155—157 °C. Ausbeute: 2,5 g.

Die Analysenergebnisse sind in Tab. V enthalten.

Verfahren G

1-(Xanthen-9-carbonyl)-4-(β-phthalimidoäthyl)-piperazinmethojodid, XLI

(Tab. V, 20 044)

2,5 g 1-(Xanthen-9-carbonyl)-4-(β-phthalimidoäthyl)-piperazin (Tab. V, XL) werden in 70 ml abs. Aceton gelöst und 1,42 g Methyljodid zugegeben. Anschließend wird drei Stunden lang am Wasserbad im Sieden gehalten. Das beim Stehen über Nacht ausgeschiedene **XLI** (2,3 g) schmilzt — nach dem Umkristallisieren aus der 30fachen Menge abs. Aceton/abs. Äther (1 : 2) — bei 223—224 °C unter Zersetzung. Ausbeute: 1,2 g.

Die Analysenergebnisse sind in Tab. V angeführt.

LITERATUR

1. TOLDY, L., TÓTH, I., BORSY, J.: Acta Chim. Acad. Sci. Hung. **49,** 265 (1966)
2. TOLDY, L., TÓTH, I., BORSY, J.: Acta Chim. Acad. Sci. Hung. **52,** 283 (1967)
3. NONAS, G., STATE, N. Y.: J. Med. **50,** 1257 (1950)
4. KUSHNER, S. et al.: J. Org. Chem. **13,** 144 (1948)
5. MCELVAIN, S. M., BANISTER, L. W.: J. Am. Chem. Soc. **76,** 1129 (1954)
6. LUMIERE, PERRIN: Bull. Soc. Chim. Fr. **31,** 689 (1904)
7. MARSH, J. T., STEPHEN, H.: J. Chem. Soc. **1925,** 1635
8. US Patent 3 157 658 (1964)
9. Org. Synth. Coll. Vol. I. p. 554. 2nd ed. New York—London, 1941
10. OEHLSCHLAEGER, H. F., MCGREGOR, J. R.: J. Am. Chem. Soc. **72,** 5332 (1950)
11. WALKER, B. H.: J. Org. Chem. **25,** 1047 (1960)
12. MORREN, H. et al.: Ind. Chim. Belg. **19,** 1176 (1954)
13. Britisches Patent 780 193 (1957)
14. FODOR, G., NÁDOR, K., TORGOV, I. V.: Recent Developments in the Chemistry of Natural Carbon Compounds. Vol. 1, pp. 176—232, Akadémiai Kiadó, Budapest 1965
15. BURGER, A.: Medicinal Chemistry. 2nd ed. Interscience Publishers Inc. pp. 463—492, New York—London, 1960
16. NEGWER, M.: Organische-chemische Arzneimittel und ihre Synonyma. Akademie-Verlag, Berlin, 1966
17. US Patent 2 742 472 (1956)
18. Belgisches Patent 636 430 (1964)
19. US Patent 3 200 120 (1965)
20. US Patent 3 284 449 (1966)
21. US Patent 2 650 130 (1953)
22. KITCHEN, L. J., POLLARD, C. B.: J. Org. Chem. **8,** 338 (1943)
23. HIDEG, K., HANKOVSZKY, O.: Acta Chim. Acad. Sci. Hung. **39,** 391 (1964)
24. STECK, E. A.: J. Org. Chem. **27,** 308 (1962); australisches Patent 229 238 (1960)
25. HAMLIN, K. E. et al.: J. Am. Chem. Soc. **71,** 2731 (1949)
26. BOISSIER, J. R. et al.: J. Med. Chem. **6,** 541 (1963)
27. STEWART, H. W. et al.: J. Org. Chem. **13,** 134 (1948)
28. GOLDMAN, L., WILLIAMS, J. H.: J. Org. Chem. **18,** 815 (1953)
29. Britisches Patent 834 300 (1960)
30. US Patent 2 965 609 (1960)
31. LAVAGNINO, E. R. et al.: J. Am. Chem. Soc. **82,** 2609 (1960)
32. BOIVIN, J. L.: Can. J. Chem. **36,** 1405 (1958)
33. MINGOIA, Q.: Ann. chim. pharm. **4,** 11 (1940); Bull. Sci. pharm. **48,** 202 (1941)
34. MOORE, T. S. et al.: J. Chem. Soc. **1929,** 39
35. Belgisches Patent 563 610 (1958)
36. Britisches Patent 840 358 (1960)

Lajos TOLDY
István TÓTH
József BORSY
Ferenc ANDRÁSI

Budapest IV., Szabadságharcosok útja 47—49.

Acta Chimica Academiae Scientiarum Hungaricae, Tomus 70 (1—2), pp. 123—127 (1971)

PREPARATION OF 2,4,6-TRI-ARYLPYRYLIUM FLUOROBORATES FROM AROMATIC ALDEHYDES AND ACETOPHENONE DERIVATIVES, II*

PREPARATION OF PYRYLIUM FLUOROBORATES WITH BORON TRIFLUORIDE CATALYST

Z. CSŰRÖS, GY. DEÁK** and P. SALLAY

(Department of Organic Chemical Technology, Technical University, Budapest)

Received May 8, 1970

A number of triarylpyrylium fluoroborate salts were synthesized from benzaldehyde and acetophenone, and their derivatives substituted in the aromatic nucleus, in acetic acid solution in the presence of boron trifluoride catalyst. The maximum yield was obtained with a ratio of the reactants aldehyde : ketone : boron trifluoride 1 : 2 : 4; the yield also depended on the substituents. It was found that the Michael addition of acetophenone to benzylydeneacetophenone is rate-determining in the three-step reaction.

The first synthesis of pyrylium salts from aromatic aldehydes and acetophenone derivatives was accomplished by DILTHEY [1], who reacted two moles of aryl methyl ketone with one mole of aromatic aldehyde in acetic anhydride medium in the presence of iron(III) chloride. Later on, iron trichloride was replaced by sulfuric acid [2], phosphoryl chloride [3], while recently perchloric acid has been applied in toluene medium [4].

Triarylpyrylium fluoroborates have been prepared either from the corresponding chloroferrate with fluoroboric acid [5] or by analogous reactions with boron trifluoride etherate catalyst [6].

All these methods of preparation are common in that the reactions are accomplished under vigorous conditions (intense refluxing for several hours).

Examination of the reactions between benzaldehyde and acetophenone in abs. acetic acid medium with boron trifluoride catalyst [7] rendered possible the elaboration of a new method for the synthesis of pyrylium salts in good yields under milder conditions, at room temperature. As it was pointed out, the pyrylium salt is formed under such conditions, provided that acetophenone is present in excess. Since all the relevant publications [1—6] report a molar ratio of acetophenone—benzaldehyde 2:1, we have chosen the same ratio of the reactants.

The yields of pyrylium salts formed in these reactions also depend upon

* Part I: Z. CSŰRÖS, GY. DEÁK and P. SALLAY: Periodica Polytechnica. (In press.)

** Present address: Research Institute for Experimental Medicine, Hungarian Academy of Sciences, Budapest.

the amount of boron trifluoride added. It was found that maximum yield is attained when four moles of boron trifluoride are applied to each mole of benzaldehyde. With less boron trifluoride the yield is reduced considerably, while greater excesses do not influence the yield (*cf.* Fig. 1).

Accordingly, our investigations revealed that the optimum ratio of the reactants for the preparation of triarylpyrylium fluoroborates is benzaldehyde : acetophenone : boron trifluoride 1 : 2 : 4 and under such conditions a yield of 68% can be reached at room temperature.

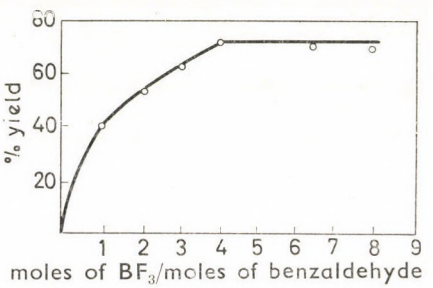

Fig. 1. Dependence of the yield of pyrylium salt, based on benzaldehyde, on the amount of boron trifluoride applied

The reaction was also carried out with a number of substituted aromatic aldehydes and acetophenones and seven new substituted triarylpyrylium salts were prepared (*cf.* Table I). The obtained pyrylium salts contained the benzaldehyde substituents in the 4-phenyl ring of the product, while the acetophenone substituents were found in the 2- and 6-phenyl rings.

The reaction of *p*-chloro-, *p*-methyl- and *p*-methoxybenzaldehydes with acetophenone gave the expected pyrylium salts, while the analogous reaction of *o*- and *p*-nitrobenzaldehydes led to the formation of the corresponding chalcones only. Substituted acetophenones resulted in the expected pyrylium salt in each case.

The yields of pyrylium salts obtained from *p*-substituted acetophenone and benzaldehyde derivatives are summarized in Table II.

It is seen that among substituted benzaldehydes the highest yield is obtained with *p*-methoxybenzaldehyde, the *p*-methyl- and *p*-chlorobenzaldehydes react to a smaller extent, while *p*-nitrobenzaldehyde is not transformed to a pyrylium salt at all.

The same substituents have just the opposite effect when present in the acetophenone reactant; the maximum yield is obtained with the nitroacetophenone derivative and in parallel with the increasing electron donor character of the substituent the yield decreases.

The further experiments aimed at the determination of the slowest one

Table I

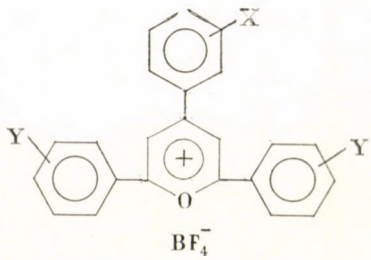

The new pyrylium fluoroborates prepared by the boron trifluoride method

X	Y	M.p. (°C)	Found/Calcd.		
			C %	H %	N or Cl %
p-Cl	H	266—8	64.42	3.69	7.90
			64.10	3.72	8.07
m-Cl	H	216—7	63.81	3.78	8.50
			64.10	3.72	8.07
o-Cl	H	225—6	63.97	3.39	7.59
			64.10	3.72	8.07
p-CH_3	H	280—2	70.16	4.47	
			70.20	4.63	
H	*p*-CH_3	268—9	70.74	4.48	
			70.70	4.95	
H	*m*-CH_3	214—6	69.95	4.54	
			70.70	4.95	
H	*m*-NO_2	302—4	57.38	3.14	5.50
			56.60	3.09	5.83

Table II

Dependence of the yield of pyrylium salt upon the substituents of the starting compounds

Substituent of benzaldehyde	Substituent of acetophenone	% yield of pyrylium salt
p-NO_2	H	0
p-Cl	H	54—56
p-CH_3	H	58—62
p-OCH_3	H	62—66
H	*p*-OCH_3	31
H	*p*-CH_3	50
H	*p*-Cl	60
H	*p*-NO_2	68—78

of the three consecutive reaction steps: (1) Claisen–Schmidt condensation, (2) Michael addition, and (3) ring closure, in the presence of a fourfold molar amount of boron trifluoride catalyst.

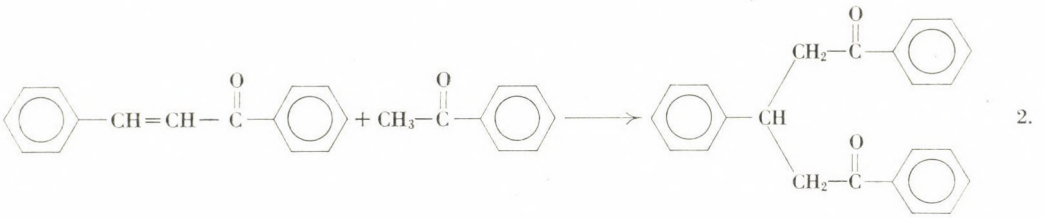

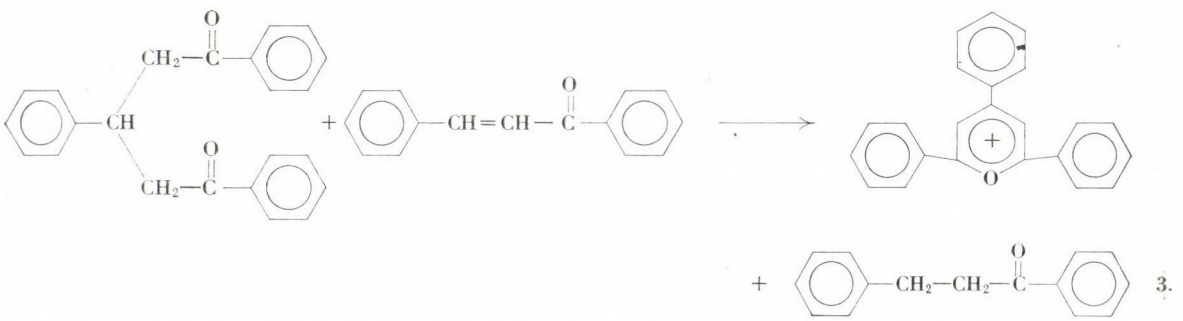

We have measured the rate of formation of the pyrylium salt from benzaldehyde and acetophenone, chalcone and acetophenone and finally chalcone and benzylydene-bisacetophenone, respectively.

Curve a in Fig. 2 corresponds to the reaction of acetophenone with benzaldehyde, while curve b to the reaction starting of chalcone with acetophenone.

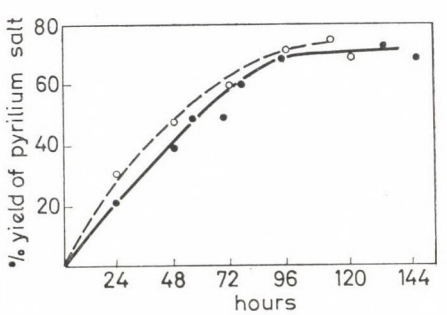

Fig. 2. Rate of formation of the pyrylium salt with different starting materials; ●: acetophenone and benzaldehyde; ○: benzylydeneacetophenone and acetophenone

Taking into account that preparative yields are encountered, the time-course of the two reactions can be considered as identical. Hence it is not the first one of the above three reaction steps which is rate-determining. Since, moreover, the rate of ring closure of benzylydene-bisacetophenone is very fast compared to the other two steps (73% within 5 minutes), it can be concluded that the Michael addition is rate-controlling in the above series of consecutive reactions.

Experimental

A mixture of 10 mmoles of benzaldehyde or substituted benzaldehyde, 20 mmoles of acetophenone or substituted acetophenone and 40 mmoles of boron trifluoride acetic acid complex in 10 ml abs. acetic acid was kept for 90 hours at room temperature and then added to a mixture of 50 ml water and 20 ml benzene. The pyrylium salt precipitated at the interface of the two phases. It was filtered, washed with benzene and then with water until neutral and dried at 100 °C. The crude products were crystallized from ethanol. Further data are shown in T b$^{l.}$ II.

REFERENCES

1. DILTHEY, W.: J. Pract. Chem. **94**, 53 (1916)
2. DAVIS, T., ARMSTRONG, J.: J. Am. Chem. Soc. **57**, 1583 (1935)
3. WIZINGER, R., LOSINGER, S., ULRICH, P.: Helv. Chim. Acta **39**, 5 (1956)
4. DOROFEENKO, G. N., KRIVUM, S. V.: Zh. Obshch. Khimii **32**, 2386 (1962); **34**, 2386 (1964)
5. DIMROTH, K.: Angew. Chem. **72**, 331 (1960)
6. LOMBARD, R., STEPHAN, J. P.: Bull. Soc. Chim. France **1958**, 1458
7. CSŰRÖS, Z., DEÁK, GY., SALLAY, P.: Periodica Polytechnica (In press)

Zoltán CSŰRÖS, Péter SALLAY: Budapest XI., Műegyetem rkp. 3.
Gyula DEÁK: Budapest VIII., Szigony u. 43.

Acta Chimica Academiae Scientiarum Hungaricae, Tomus 70 (1–2), pp. 129–132 (1971)

HYDROLYSIS OF ACETYLCHOLINE STUDIED BY A QUANTUM CHEMICAL METHOD, II

EXPERIMENTAL VERIFICATION OF THE MECHANISM OF HYDROLYSIS

(SHORT COMMUNICATION)

M. FARKAS,* J. TAMÁS and GY. DEÁK*

*(*Institute of Experimental Medicine and Centre for Chemical-Structural Studies, Hungarian Academy of Sciences, Budapest)*

Received May 30, 1970

It is well known from the investigation of NACHMANSON [1] that acetylcholine acting as a mediator has an important role in the process of transfer of stimuli in the vegetative nervous system. In the course of mediation, acetylcholine undergoes rapid enzymatic hydrolysis on the effect of cholinesterase. *In vitro* experiments showed perfect accomplishment of the hydrolysis within a 10^{-3} sec period.

In our previous paper [2] quantum chemical calculations were published. Their purpose was to find a physical process manifesting itself chemically in hydrolysis, in the case of acetylcholine.

The Hoffmann (extended Hückel) method was applied in our calculations and our results can be summarized as follows:

(1) According to the calculations, acetylcholine existing in its ground state does not undergo hydrolysis even in the presence of cholinesterase.

(2) Hydrolytic decomposition of the acetylcholine–cholinesterase complex takes place only with the uptake of the first excitation energy.

(3) On the basis of these facts the unusually high speed of hydrolysis of acetylcholine can be explained. The first step is the uptake of the first electron excitation energy; after this the second step, accompanied by the liberation of energy, takes place spontaneously.

(4) Our calculations indicated alkyl -O- splitting in the course of hydrolysis.

DAVIS and ROSS [3] studied the hydrolysis of ethyl acetate, β-dimethylaminoethyl acetate and acetylcholine at 50 °C in 80% aqueous acetone containing acid and alkali, respectively. In their opinion, the significant increase in the rate of the hydrolysis of acetylcholine under alkaline conditions is due to the presence of a positive charge on the β-nitrogen atom and the formation of an activated complex (**I**) having sterically favoured structure.

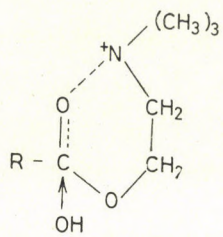

I

ZASLOWSKY and FISHER [4] studied the hydrolysis of β-dimethylaminoethyl acetate in the pH range between 5.5 and 8.4; the increased rate at acid pH values was explained similarly as above.

The results of CHIOU *et al.* [5] obtained with compounds which may be regarded as analogues of acetylcholine but possess conformationally rigid structures, seem to be contradictory to the former assumption. In a study of *cis* and *trans* isomers of 2-acetoxycyclopropyl trimethyl ammonium iodide, the rate of enzymatic hydrolysis of the *trans* isomer incapable to form the activated complex I, was found to be of the same order of magnitude as that of acetylcholine.

Hydrolysis of acetylcholine in water labelled with oxygen isotope seemed to be a suitable method for the experimental verification of the mechanism of this reaction. In earlier studies, STEIN and KOSHLAND [6] carried out the hydrolysis of acetylcholine in water containing labelled oxygen and the carbon dioxide obtained in the pyrolysis of the silver salt of acetic acid was examined by mass spectrometry. On the basis of their results they concluded that under the action of the positive charge present in choline the intermediate adduct formed in the first step of hydrolysis will have an increased ratio of the rates of splitting of the C—OR and C—OH bonds, and essentially each adduct will decompose to acetic acid and choline. Our intention was to use a different method utilizing mass spectrometry for the determination of choline in the course of the hydrolysis, considering that in the case of alkyl —O— splitting the labelled oxygen must be contained in the choline.

Hydrolysis was carried out according to the following procedure. 0.005 mole of acetylcholine was dissolved in 2 ml of water containing 4% of $H_2{}^{18}O$, and 0.01 mole of sodium hydroxide was added to this solution. It was then boiled for 15 minutes in a flask equipped with a reflux condenser. After cooling, the solution was acidified by the addition of 10% aqueous HCl and evaporated to dryness in vacuum. The residue was dried over phosphorus pentoxide in a vacuum desiccator for two days, then the mass spectrum of the substance was recorded. For comparison, 0.005 mole of choline was boiled in 2 ml of water containing 4% of $H_2{}^{18}O$ for 1 hr. and the choline was isolated as described above and studied by mass spectrometry.

Fig. 1 shows the mass spectrum of choline chloride obtained with 20 eV ionization energy. As it can be seen, the mass spectrum of choline chloride corresponds to that of a mixture of dimethylaminoethanol, methyl chloride and a small amount of hydrogen chloride, *i.e.* in the course of recording the spectrum, choline chloride was converted on heating to these neutral molecules before evaporation. Thus the thermal decomposition of choline chloride involves primarily demethylation and some Hoffmann degradation. Several quaternary alkyl ammonium halides show similar fragmentation processes in the course of recording the mass spectra (*e.g.*, [7]).

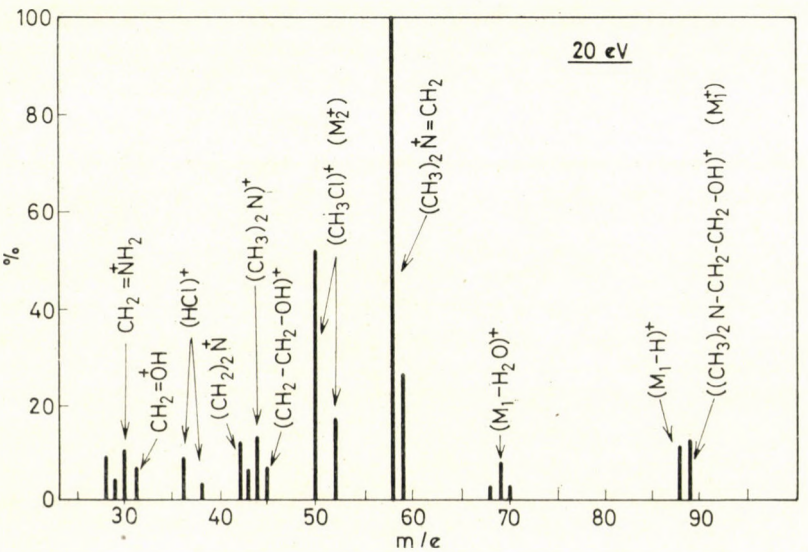

Fig. 1

The main process of decomposition of dimethylaminoethanol on electron bombardment is the splitting of the bond of the CH_2—CH_2-group having β position with respect to the N and O atoms, resulting in the formation of fragments with mass numbers 58 and 31 (Fig. 1).

Relatively low ionization energies are favourable for the appearance of the dimethylaminoethanol molecular ion.

The ^{18}O content of the choline chloride samples can be determined by the mass spectrometric investigation of the salt: the ^{18}O content can be calculated from the measured intensities of the isotope peaks of any of the ion species containing oxygen and producing relatively intense peaks in the mass spectrum. For this purpose, determination of the I_{91}/I_{89}, I_{47}/I_{45} or the I_{33}/I_{31} intensity ratio is equally suitable.

In the case of choline chloride of natural isotope composition these ratios

were between 0.002 and 0.005, giving a good approximation of the natural ratio of $^{18}O/^{16}O = 0.002$.

The same values were obtained with choline chloride samples prepared by refluxing choline chloride of natural isotope content in water containing 4% of $H_2{}^{18}O$ in the presence of 0.01 mole of sodium hydroxide for 1 hr., followed by evaporation of the solution to dryness.

In the case of choline chloride samples obtained by the hydrolysis of acetylcholine in water containing 4% of $H_2{}^{18}O$, these ratios ranged between 0.042 and 0.045, corresponding to the ^{18}O content of the labelled water.

The measurements were carried out by means of a MH-1303 mass spectrometer; the samples were introduced into the instrument through a direct feeding system, at 200—220 °C.

Summing up the above facts, we can state that the base-catalyzed hydrolysis of acetylcholine in water containing $H_2{}^{18}O$ results in the formation of choline containing ^{18}O, verifying the B_A mechanism of the reaction, in agreement with our previous calculations [2].

REFERENCES

1. NACHMANSON, D.: Chemical and Molecular Basis of Nerve Activity. Academic Press, New York, 1959.
2. FARKAS, M., KRUGLYAK, J. A.: Nature **223,** 523 (1969)
3. DAVIS, W., ROSS, W. C. J.: J. Chem. Soc. **1950,** 3056. **1951,** 2706
4. ZASLOWSKY, J. A., FISHER, E.: J. Phys. Chem. **67,** 959 (1963)
5. CHIOU, C. Y., LONG, J. P., CANNON, J. G., ARMSTRONG, P. D.: J. Pharm. Exp. Ther. **166,** 243 (1969)
6. STEIN, S. S., KOSHLAND, D. E., jun.: Arch. Biochemistry and Biophysics **45,** 467 (1953)
7. BUDZIKIEWICZ, H., DJERASSI, C., WILLIAMS, D. H.: Mass-Spectrometry of Organic Compounds pp. 330—333. Holden-Day Inc., San Francisco, 1967

Marianne FARKAS
Gyula DEÁK } Bp. VIII., Szigony u. 43.
József TAMÁS Bp. VIII., Puskin u. 11—13.

Acta Chimica Academiae Scientiarum Hungaricae, Tomus 70 (1–2), pp. 133–142 (1971)

THE CHEMISTRY OF 1,3-BIFUNCTIONAL SYSTEMS, XII*

KINETIC STUDY OF THE TRANSFORMATION OF 2-MONOSUBSTITUTED DERIVATIVES OF TRIMETHYLENECHLOROHYDRIN IN ALKALINE MEDIA

M. BARTÓK, K. LÁNG-LAKOS and G. BOZÓKI-BARTÓK

(Department of Organic Chemistry, A. József University, Szeged)

Received September 11, 1969. In revised form July 15, 1970

The kinetics of alkaline hydrolysis of trimethylenechlorohydrin **(I)** and of some 2-monosubstituted homologues of the latter [2-methyl **(II)**, 2-isopropyl **(III)**, 2-butyl **(IV)**, 2-phenyl **(V)**, 2-cyclohexyl **(VI)** trimethylenechlorohydrin] were studied. Under the applied experimental conditions mainly the corresponding oxacyclobutane homologues were formed. In the case of compound **(V)** the main conversion direction is, due to the 1,2-elimination process, the formation of 2-phenylallyl alcohol. From the experimental data the rate constants, activation energies and entropies and the pre-exponential factors were determined. The experimental results confirmed the validity of the reaction mechanism suggested earlier for this type of compounds too.

In Part VII [1] we have analyzed the main characteristics of the transformation of 1,3-chlorohydrins in alkaline media and have pointed out the importance of such a study. Our work was based on the experimental fact that 1,3-chlorohydrins containing chlorine atoms in the primary position are converted into cyclic ethers in the presence of alkali. The kinetic study of these processes opens a possibility to obtain information about the mechanism of cyclization. In our previous work [1] we suggested a reaction mechanism for 2,2-diethyl-3-chloropropanol as model substance and wish now to confirm the general validity of this mechanism for 1,3-chlorohydrins. At the same time we intend to investigate the effect of substituents in various positions on the kinetic parameters.

In this work we report a kinetic study of the transformation of the following model substances in alkaline media:

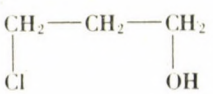

I

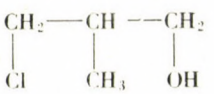

II

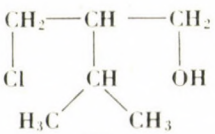

III

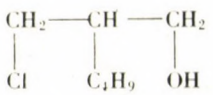

IV

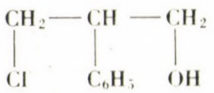

V

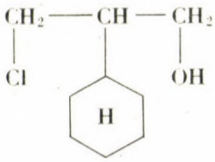

VI

* Part XI: Acta Phys. et Chem. Szeged. **11**, 39 (1970)

In earlier preparative work, we were able to confirm that the above compounds and their acetates are converted mainly into oxetanes in concentrated alkaline media [2, 3]. According to our more recent experiments in a 0.2 *M* aqueous barium hydroxide solution, too, the main reaction is oxetane formation:

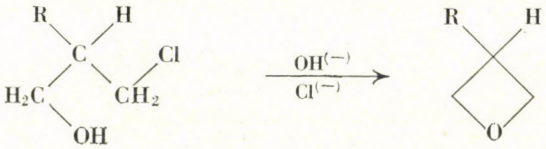

where R represents a methyl, isopropyl, butyl or cyclohexyl group.

This direction of the conversion is not valid for 1-chloro-2-phenylpropanol-3 (**V**) and trimethylenechlorohydrin (**I**). The formation of trimethylene oxide is accompanied by the formation of a large amount of allyl alcohol (about 30%), while with (**V**) mainly 2-phenylallyl alcohol is formed beside a smaller quantity (20 to 30%) of 3-phenyl-oxacyclobutane. These 1,2-eliminations are represented, without details, by the following reaction scheme:

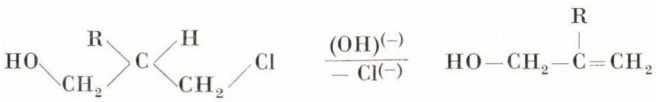

where R is a hydrogen atom or a phenyl group.

The formation of 3-monosubstituted oxetanes may be explained on the basis of the following mechanism suggested in our earlier work [1]:

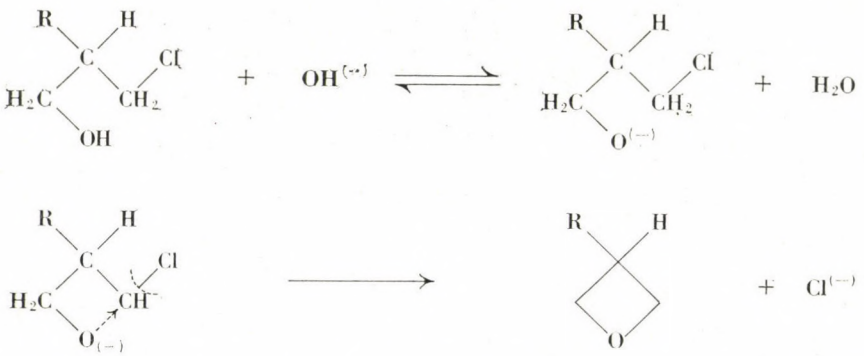

The kinetic results for the six model substances are summarized in Table I. The rate constants were calculated in accordance with [1] from a second order rate equation. Beside the experimental conditions, the table also shows the rate constants (k), activation energies ($\Delta H^{\ddagger}$), pre-exponential factors (A) and the activation entropies ($\Delta S^{\ddagger}$).

Table I

Kinetic data for the alkaline hydrolysis of 1,3-chlorohydrins of the type:

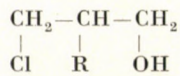

Symbol of compound	t °C	Chlorohydrin conc. mol/l	[OH⁻] geq/l	k l · mol⁻¹ · · min⁻¹	$\Delta H^{\ddagger}$ kcal · · mol⁻¹	A l · mol⁻¹ · · min⁻¹	$\Delta S^{\ddagger}$ e.u.
I	80	0.00988	0.01814	0.024			
	85	0.01005	0.01743	0.036			
	90	0.01009	0.01730	0.052	20.2		
	95	0.01144	0.01855	0.073		5.6×10^{10}	—17.9
II	80	0.01015	0.02063	0.013			
	95	0.00935	0.01257	0.051			
	125	0.00907	0.01302	0.405	21.1	1.8×10^{11}	—15.6
	125	0.00925	0.01257	0.454			
III	80	0.01054	0.02063	0.030			
	95	0.00938	0.01273	0.111	21.0	3.6×10^{11}	—14.1
	125	0.01002	0.01813	1.126			
	125	0.01002	0.01862	0.955			
IV	80	0.01412	0.01775	0.022			
	85	0.01009	0.01623	0.033			
	90	0.01010	0.01623	0.049	21.0		
	95	0.01003	0.01610	0.074		2.0×10^{11}	—15.4
V	85	0.01004	0.01623	0.090			
	90	0.01002	0.01623	0.127	23.5		
	90	0.01015	0.01806	0.136			
	95	0.01008	0.01806	0.219		1.9×10^{13}	— 6.3
	100	0.01008	0.01834	0.345			
VI	80	0.01001	0.01814	0.030			
	85	0.01003	0.01743	0.040			
	90	0.00997	0.01743	0.065	20.2		
	95	0.01002	0.01855	0.097		9.4×10^{10}	—16.9

The experimental data in the Table are in satisfactory agreement with a second order rate equation which confirms the validity of the reaction mechanism suggested in Ref. [1] also for chlorohydrins of this type. The proposed reaction mechanism is further supported by the values of $\Delta H^{\ddagger}$ and $\Delta S^{\ddagger}$ calculated from the kinetic data.

Table II

Symbol of compound	Boiling point		n_D^{20}	Cl (%)	
	t (°C)	mmHg		calcd.	found
I	65	18	1.4467	37.60	37.18
II	60	15	1.4460	32.66	32.27
III	110	30—40	1.4540	25.96	25.34
IV	125	30—40	1.4520	23.54	22.96
V	122	8	1.5431	20.75	20.38
VI	130	8	1.4902	20.00	19.77

Table III

Compound (**I**): $CH_2(Cl)—CH_2—CH_2(OH)$

80 °C
$a = 0.01814$
$b = 0.00988$

No.	t	x	k
1	10	0.00011	0.064
2	35	0.00030	0.048
3	120	0.00049	0.024
4	155	0.00062	0.024
5	235	0.00093	0.024
6	305	0.00119	0.024
7	395	0.00147	0.023

$k_{3-7} = 0.024$

85 °C
$a = 0.01743$
$b = 0.01005$

No.	t	x	k
1	30	0.00038	0.074
2	60	0.00050	0.049
3	120	0.00076	0.038
4	180	0.00104	0.036
5	240	0.00142	0.037
6	300	0.00166	0.036
7	360	0.00190	0.034
8	380	0.00201	0.036

$k_{3-8} = 0.036$

90 °C
$a = 0.01730$
$b = 0.01009$

No.	t	x	k
1	30	0.00035	0.068
2	65	0.00059	0.054
3	120	0.00106	0.055
4	170	0.00139	0.052
5	220	0.00179	0.052
6	270	0.00207	0.052
7	320	0.00237	0.052
8	365	0.00261	0.051

$k_{2-8} = 0.052$

95 °C
$a = 0.01855$
$b = 0.01144$

No.	t	x	k
1	30	0.00055	0.091
2	70	0.00114	0.084
3	120	0.00177	0.079
4	170	0.00231	0.077
5	220	0.00284	0.076
6	250	0.00304	0.076
7	280	0.00336	0.074
8	300	0.00361	0.077

$k_{3-8} = 0.077$

Table IV

Compound (II):

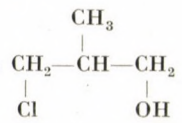

80 °C
$a = 0.02063$
$b = 0.01015$

No.	t	x	k
1	40	0.00014	0.017
2	110	0.00029	0.013
3	180	0.00042	0.011
4	240	0.00064	0.013
5	300	0.00074	0.012
6	360	0.00088	0.012
7	420	0.00098	0.012
8	480	0.00113	0.012

$k_{1-3} = 0.013$

95 °C
$a = 0.01257$
$b = 0.00935$

No.	t	x	k
1	64	0.00049	0.056
2	183	0.00116	0.050
3	245	0.00151	0.051
4	303	0.00183	0.051
5	490	0.00276	0.054
6	605	0.00294	0.015

$k_{2-4} = 0.051$

125 °C
$a = 0.01301$
$b = 0.00907$

No.	t	x	k
1	43	0.00169	0.40
2	82	0.00291	0.41
3	114	0.00377	0.43
4	144	0.00411	0.40
5	178	0.00460	0.39

$k_{1-5} = 0.41$

125 °C
$a = 0.01257$
$b = 0.00925$

No.	t	x	k
1	20	0.00051	0.23
2	46	0.00182	0.41
3	69	0.00282	0.48
4	94	0.00337	0.45
5	119	0.00407	0.48
6	150	0.00488	0.52

$k_{2-5} = 0.45$

Table V

Compound (III):

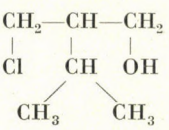

80 °C
$a = 0.02063$
$b = 0.01054$

No.	t	x	k
1	45	0.00037	0.038
2	105	0.00071	0.033
3	170	0.00106	0.031
4	230	0.00128	0.028
5	290	0.00167	0.030
6	350	0.00199	0.030

$k_{2-8} = 0.030$

95 °C
$a = 0.01273$
$b = 0.09386$

No.	t	x	k
1	77	0.00094	0.111
2	124	0.00143	0.120
3	183	0.00196	0.109
4	243	0.00249	0.111
5	306	0.00298	0.113
6	352	0.00321	0.106

$k_{1-6} = 0.111$

125 °C
$a = 0.01862$
$b = 0.010024$

No.	t	x	k
1	4	0.00039	0.524
2	8	0.00100	0.713
3	12	0.00162	0.825
4	16	0.00223	0.900
5	20	0.00277	0.941
6	24	0.00328	0.979
7	28	0.00384	1.042

$k_{3-8} = 0.955$

125 °C
$a = 0.01813$
$b = 0.01002$

No.	t	x	k
1	4	0.00060	0.853
2	8	0.00130	0.985
3	12	0.00199	1.078
4	16	0.00278	1.221
5	22	0.00343	1.171
6	25	0.00369	1.142
7	28	0.00405	1.166

$k_{2-7} = 1.126$

Table VI

Compound (IV): $CH_2(Cl)—CH(C_4H_9)—CH_2(OH)$

80 °C
$a = 0.01775$
$b = 0.01412$

No.	t	x	k
1	60	0.00041	0.025
2	120	0.00079	0.026
3	180	0.00096	0.021
4	240	0.00124	0.021
5	420	0.00218	0.024
6	625	0.00271	0.021
7	1420	0.00428	0.016
8	1445	0.00432	0.016

$k_{1-8} = 0.022$

85 °C
$a = 0.01623$
$b = 0.01009$

No.	t	x	k
1	30	0.00014	0.027
2	75	0.00035	0.030
3	120	0.00063	0.034
4	200	0.00099	0.032
5	280	0.00135	0.033
6	360	0.00168	0.032
7	357	0.00207	0.033
8	563	0.00234	0.031

$k_{3-8} = 0.033$

90 °C
$a = 0.01623$
$b = 0.01010$

No.	t	x	k
1	65	0.00051	0.047
2	143	0.00106	0.049
3	220	0.00156	0.049
4	300	0.00197	0.048
5	360	0.00229	0.048
6	420	0.00261	0.048
7	480	0.00289	0.048
8	545	0.00326	0.050

$k_{1-8} = 0.049$

95 °C
$a = 0.01610$
$b = 0.01003$

No.	t	x	k
1	70	0.00085	0.078
2	140	0.00148	0.074
3	210	0.00214	0.075
4	240	0.00229	0.072
5	280	0.00265	0.074
6	330	0.00299	0.074
7	390	0.00333	0.072
8	450	0.00364	0.071

$k_{1-8} = 0.074$

Table VII

Compound (V): $CH_2(Cl)—CH(C_6H_5OH)—CH_2$

85 °C
$a = 0.01623$
$b = 0.01004$

No.	t	x	k
1	30	0.00039	0.059
2	75	0.00105	0.095
3	120	0.00154	0.091
4	170	0.00201	0.087
5	220	0.00253	0.089
6	270	0.00298	0.089
7	315	0.00336	0.090
8	360	0.00369	0.090

$k_{2-8} = 0.090$

90 °C
$a = 0.01623$
$b = 0.01002$

No.	t	x	k
1	40	0.00092	0.154
2	92	0.00172	0.134
3	112	0.00201	0.132
4	145	0.00242	0.128
5	178	0.00278	0.124
6	210	0.00322	0.125
7	240	0.00351	0.126

$k_{2-7} = 0.128$

90 °C
$a = 0.01806$
$b = 0.01015$

No.	t	x	k
1	30	0.00066	0.126
2	65	0.00143	0.134
3	95	0.00199	0.135
4	121	0.00247	0.137
5	155	0.00306	0.141
6	190	0.00350	0.137
7	225	0.00388	0.134
8	260	0.00444	0.142

$k_{1-8} = 0.137$

95 °C
$a = 0.01806$
$b = 0.01008$

No.	t	x	k
1	25	0.00095	0.221
2	50	0.00173	0.219
3	70	0.00225	0.214
4	90	0.00281	0.219
5	110	0.00331	0.222
6	130	0.00370	0.210
7	160	0.00431	0.222
8	180	0.00453	0.217

$k_{1-8} = 0.219$

100 °C
$a = 0.01834$
$b = 0.01008$

No.	t	x	k
1	22	0.00135	0.379
2	43	0.00229	0.349
3	62	0.00306	0.349
4	83	0.00378	0.348
5	101	0.00422	0.337
6	122	0.00483	0.343

$k_{2-6} = 0.345$

Table VIII

Compound **(VI)**:

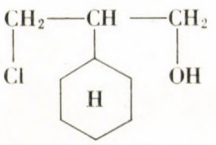

VI

80 °C
$a = 0.01814$
$b = 0.01001$

No.	t	x	k
1	10	0.00009	0.045
2	35	0.00023	0.035
3	95	0.00047	0.028
4	155	0.00089	0.033
5	215	0.00107	0.030
6	275	0.00138	0.031
7	335	0.00159	0.030
8	395	0.00179	0.029

$k_{3-8} = 0.030$

85 °C
$a = 0.01743$
$b = 0.01003$

No.	t	x	k
1	30	0.00024	0.046
2	60	0.00040	0.040
3	120	0.00081	0.041
4	180	0.00119	0.041
5	240	0.00135	0.036
6	300	0.00185	0.041
7	360	0.00206	0.039
8	380	0.00218	0.040

$k_{1-8} = 0.040$

90 °C
$a = 0.01743$
$b = 0.00997$

No.	t	x	k
1	40	0.00052	0.077
2	75	0.00075	0.061
3	130	0.00129	0.063
4	180	0.00167	0.062
5	230	0.00218	0.066
6	280	0.00254	0.065
7	330	0.00286	0.065
8	375	0.00319	0.065

$k_{2-8} = 0.065$

95 °C
$a = 0.01855$
$b = 0.01002$

No.	t	x	k
1	30	0.00050	0.092
2	70	0.00118	0.099
3	120	0.00196	0.102
4	170	0.00250	0.102
5	220	0.00305	0.097
6	250	0.00334	0.097
7	280	0.00357	0.095
8	300	0.00373	0.094

$k_{1-8} = 0.097$

It could be expected from the reaction mechanism suggested earlier that the substituents on the carbon atom not participating directly in the reaction (in the present case carbon atom No. 2) will have no significant influence on the kinetic parameters. In this series it is only the phenyl group that causes a rather marked change compared to the parent compound and this may be explained by a reaction direction differing from that for the other members of the series. In the case of the other substances (*cf.* Table I, *e.g.* the data for 95 °C) the kinetic parameters vary within the following, rather narrow interval:

k: 0.05—0.11 $1 \cdot mol^{-1} \cdot min^{-1}$
$\Delta H^{\ddagger}$: 20—21 kcal $\cdot mol^{-1}$
A: 6×10^{10}—4×10^{11} $1 \cdot mol^{-1} \cdot min^{-1}$
$\Delta S^{\ddagger}$: between —14 and —18 e.u.

In our subsequent work on some other 1,3-chlorohydrins we obtained far more data which, together with the determination of the equilibrium constant of the first process and with proof of the formation of an intermediate gave a deeper insight into the mechanism of the reaction.

Experimental

The 1,3-chlorohydrins were prepared by deacetylation of the corresponding chloroacetates [2, 4] in the presence of methanol. The yield was about 90%. The purity of the starting materials was checked by gas-liquid chromatography.

The methods of kinetic measurements and the calculations have been described in full details in our earlier communication [1].

Experimental data

The following symbols were used:
t: time (min)
a: initial concentration of hydroxide ions [$Ba(OH)_2$ g eq/l]
b: initial concentration of the chlorohydrin (mol/l)
x: quantity of chlorohydrin converted in time t (mol/l)
k: second order rate constant of the reaction ($l \cdot mol^{-1} \cdot min^{-1}$)

REFERENCES

1. BARTÓK, M., BOZÓKI-BARTÓK, G., KOVÁCS, K.: Acta Chim. Acad. Sci. Hung. (In press)
2. BARTÓK, M., APJOK, J.: Acta Phys. et Chim. Szeged. **8,** 133 (1962)
3. BARTÓK, M., KOZMA, B., SHUIKIN, N. I.: Izv. AN USSR, Ser. Khim. 1966, 1241
4. BARTÓK, M., KOZMA, B., GILDE, A. S.: Acta Phys. et Chim. Szeged. **11,** 35 (1965)

Mihály BARTÓK
K. LÁNG-LAKOS
G. BOZÓKI-BARTÓK
Szeged, Dóm tér 8, Hungary.

Acta Chimica Academiae Scientiarum Hungaricae, Tomus 70 (1—2), pp. 143—154 (1971)

ЭЛЕКТРОННОМИКРОСКОПИЧЕСКИЕ ИССЛЕДОВАНИЯ ПОВЕРХНОСТИ И ФИБРИЛЛЯРНОЙ СТРУКТУРЫ МОДИФИЦИРОВАННЫХ ХЛОПКОВЫХ ВОЛОКОН*

Х. У. УСМАНОВ, К. Х. РАЗИКОВ и И. И. ИСАМУХАМЕДОВА

(Научно-исслебовательский институт химии и технологии хлопковой целлюлозы — НИИТЦ, г. Ташкент, СССР)

Поступила: 20 V 1970 г.

Настоящая статья посвящена результатам электронномикроскопических исследований поверхности и внутренней фибриллярной структуры хлопковых волокон, модифицированных путём радиационно-химической прививки ряда виниловых мономеров: акрилонитрила (привес 12,5%), винилпиридина (привес 16%), винилиденхлорида (привес 14%), метакриламида (привес 56%), метакриловой кислоты (привес 60%) и стирола (привес- 3,4%, 13,4% и 21,5%).

Выявлены особенности структуры, как поверхности, так и фибриллярных участков (вторичной стенки) хлопкового волокна в зависимости от природы прививаемого к нему мономера и привеса, а также от условий процесса радиационно-химической прививки.

На основе полученных данных предположено, что при проведении процесса прививки из паровой фазы и, особенно, если до акта прививки хлопковое волокно не подвергнуто каким-либо набухающим обработкам, то в реакции привитой сополимеризации участвуют главным образом те макромолекулы целлюлозы, которые расположены на поверхности структурных элементов — микрофибрилл, фибрилл и т. д. Если же процесс прививки осуществляется из паровой фазы, но с предварительным набуханием хлопкового волокна, то в реакции привитой сополимеризации могут участвовать и те макромолекулы целлюлозы, которые расположены внутри структурных элементов.

Известно, что в настоящее время в ряде химических лабораторий мира найдены эффективные методы модификации свойств полимерных волокон, в том числе и целлюлозных. Одним из них является процесс привитой сополимеризации целлюлозы с различными мономерами. Известно также, что для этой цели успешно применено радиационное инициирование. Последнее получило значительное развитие и в работах нашего института.

Установлено, что в процессе привитой сополимеризации целлюлозы с рядом виниловых мономеров происходит улучшение ее многих физико-химических характеристик, например, целлюлозные волокна начинают устойчиво окрашиваться, приобретают эластичность, повышается их устойчивость к действию микроорганизмов, химикатов, температуры и т. д. [1—3].

Следует указать, что с химическим превращением целлюлозы непременно происходит и ее структурное превращение, причем последнее может иметь место как на молекулярном, так и на надмолекулярном уровне. Подтверждением этого могут служить результаты наших исследований и исследований

* Материал был доложен на Международном симпозиуме по макромолекулярной химии, Будапешт, (Венгрия) 25—30 августа 1969 года, доклад 9/02.

ряда других авторов (4—11). Показано, что прививка инородных макромолекул к целлюллозе существенно изменяет взаимную упаковку целлюлозных цепей друг с другом, а это, в свою очередь, приводит к изменению формы и размеров структурных элементов (микрофибрилл, фибрилл), а также слоев вторичной стенки целлюлозы. В наших работах (4—7) обнаружено изменение структуры поперечных и продольных ультратонких срезов хлопкового волокна до и после прививки к нему ряда виниловых полимеров. Нужно полагать, что проводя тщательные электронномикроскопические исследования, с применением комплекса методов препарирования, можно получить необходимые данные, которые позволят судить о механизме прививки синтетических полимеров к целлюлозе на надмолекулярном уровне.

В данной работе нами использованы методы реплик и механического диспергирования (в сочетании с ультразвуковым воздействием) для электронномикроскопического исследования структуры поверхности радиационно-химически привитых сополимеров целлюлоза с различными виниловыми мономерами, как из паровой фазы, так и из раствора.

Объектами исследований были:

1. хлопковые волокна, очищенные от различных спутников целлюлозы (пектинов, гемицеллюлоз, жировосковых веществ) известным методом Корея-Грея (экстракция щелочью, спиртом и эфиром) — исходные волокна;

2. волокна хлопка, очищенные вышеуказанным способом, привитые полиакрилонитрилом — ПАН из паровой фазы, привес 12,5%;

3. то же, поли-2-винилпиридином — ПВП из паровой фазы, привес 16%;

4. то же, поливинилиденхлоридом — ПВДХ из раствора, привес 14%;

5. то же, полиметакриламидом — ПМАА из раствора, привес 56%;

6. то же, полиметакриловой кислотой — ПМАК из раствора, привес 60%;

7. то же, полистиролом — ПС из раствора, нов разных привесах: 3,4%, 13,4%, 21,5%.

При получении этих образцов использовано гамма-излучение Co^{60} с целью инициирования реакции привитой сополимеризации целлюлозы с виниловыми мономерами при мощности излучения 70 р/сек. Дозы облучения были в таких пределах (не более 1 м. рад), при которых целлюлоза не претерпевает существенных изменений. Подробные условия получения вышеуказанных образцов, их физико-химические характеристики, а также способы очистки от гомополимеров, образующихся в процессе привитой сополимеризации виниловых мономеров к целлюлозе, приведены в других работах [1—3].

На рис. 1а, б представлены электронные микрофотографии реплик поверхности и фрагмент вторичной стенки исходного (непривитого) хлопкового волокна. На них видны многочисленные складки на поверхности волокна, их расположение, а также исключительно фибриллярный характер вторичной

стенки хлопка. Видно, что складки на поверхности волокна расположены под некоторым углом (рис. 1а). Фибриллярные же образования, являющиеся сложными организациями макромолекул целлюлозы расположены внутри волокна достаточно плотно и преимущественно параллельно друг к другу, образуя слои, т. е. еще более крупные надмолекулярные структуры. На рис. 1б виден фрагмент фибриллярного слоя.

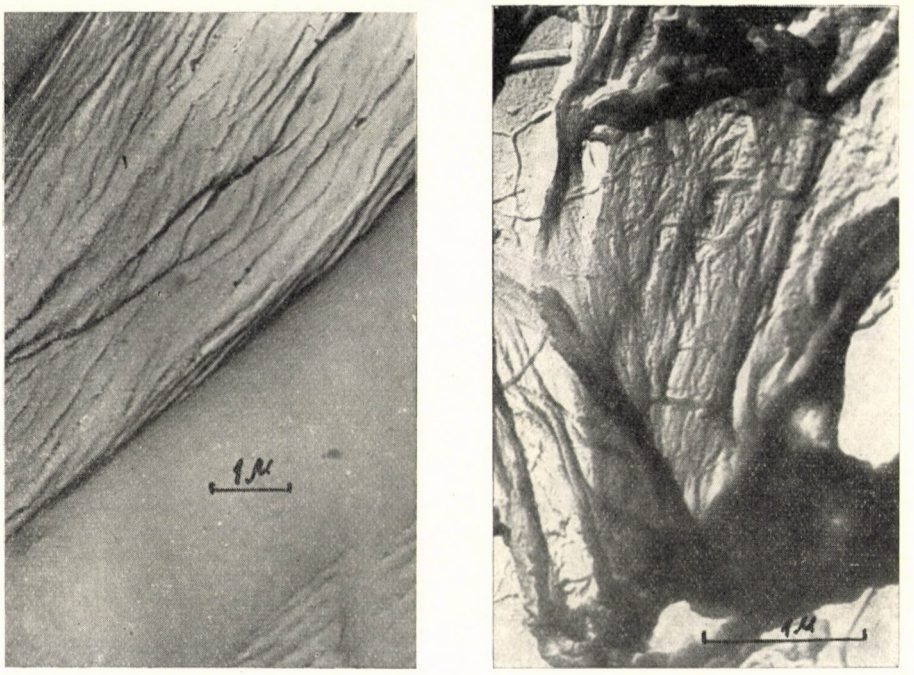

Рис. 1. Электронные микрофотографии (ЭМ) исходного (немодифицированного) хлопкового волокна (ХВ) (а) реплика поверхности; (б) фрагмент фибриллярной структуры

Нами ранее детально была изучена слоистая структура хлопкового волокна по его ультратонким срезам [2]. Ниже рассмотрены изменения в структуре поверхности и фибриллярных участков хлопкового волокна при прививке к нему того или иного винилового полимера.

На рис. 2а, б, в, г, соответственно, показаны электронномикроскопические картины поверхностной структуры и фибриллярных участков (фрагментов) вторичной стенки волокон хлопка после прививки ПАН и ПВН. Можно отметить, что процесс прививки существенно влияет на картины поверхности и фибриллярных структур хлопковой целлюлозы, причем это в значительной степени зависит от природы прививаемого полимера. Так, в случае ПАН, в частности, на поверхности волокна наблюдаются мельчайшие сферические образования, глобулы, расположенные преимущественно вдоль складок

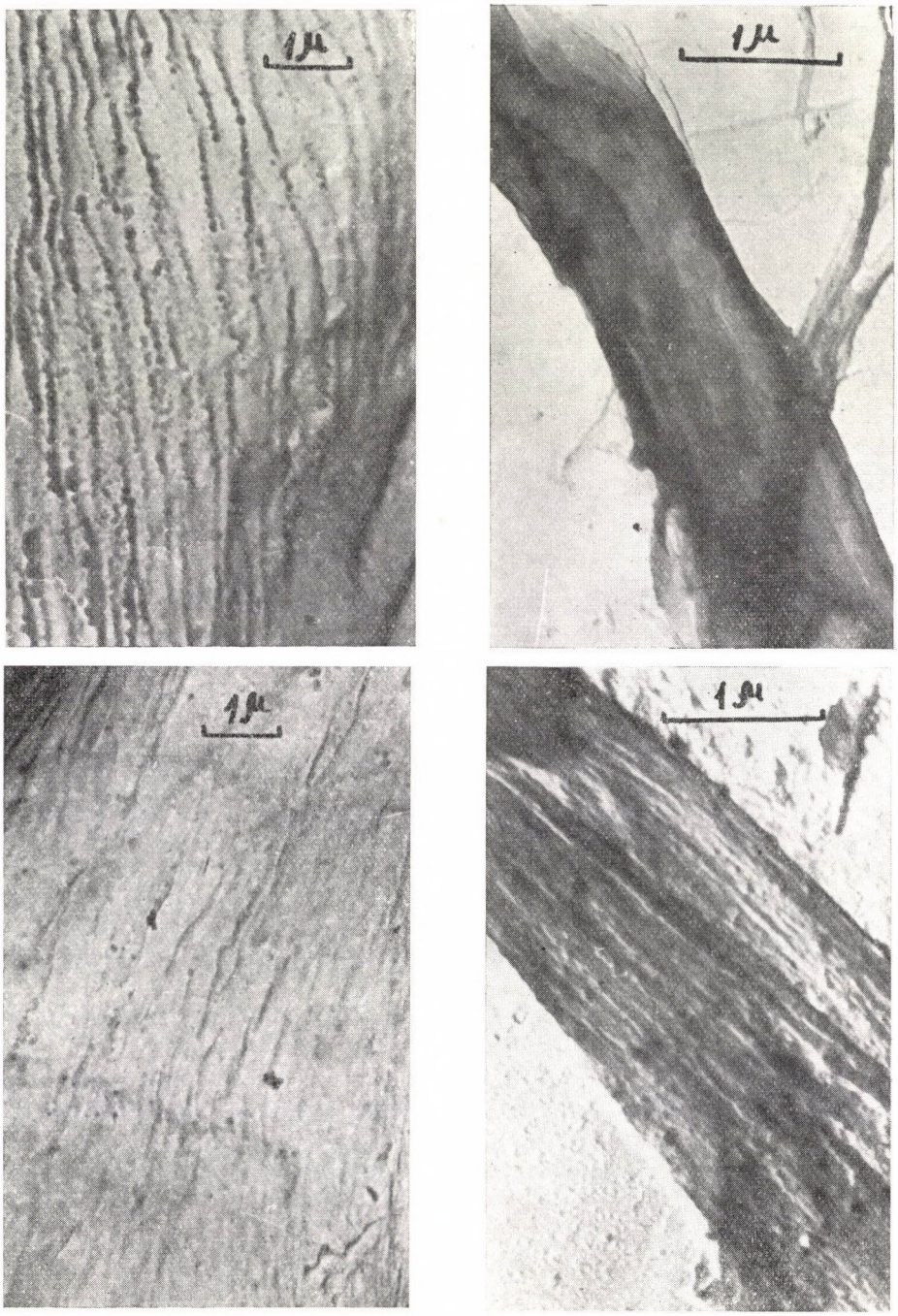

Рис. 2. ЭМ ХВ, модифицированных путем прививки ПАН (привес 12,5%). (а) реплика поверхности; (б) фрагмент фибриллярной структуры; ПВП (привес 16%), (в) реплика поверхности; (г) фрагмент фибриллярной структуры

(рис. 2а). Это — структурные элементы привитого ПАН. Видно, что прививка ПАН не сглаживает складчатой структуры, а наоборот, подчеркивает. Если внимательно рассмотреть, то можно заметить, наличие еще более мелких образований ПАН, расположенных между складками поверхности волокна. Отсюда следует, что прививка шла по всей поверхности, но в местах складок — в большей степени; глобулярные частицы ПАН в этих участках значительно крупнее (более 1000 Å в диаметре).

Прививка ПАН так же сильно влияет на картину фибриллярных образований (вторичной стенки) хлопкового волокна (рис. 2б). В отличие от исходных волокон в привитых ПАН образцах наблюдаются фибриллярные участки с более плотной взаимной упаковкой фибрилл друг относительно друга, в результате чего трудно отчетливо судить о форме и размерах отдельных фибрилл, будто они склеены друг с другом. Очевидно, что прививка ПАН к фибриллярным образованиям целлюлозы способствует более прочному связыванию их друг с другом.

Результаты электронномикроскопических исследований показывают, что в случае ПВП обнаруживаются несколько отличные картины. Количество складок поверхности волокна привитого ПВП стало значительно больше, по-видимому, это связано с тем обстоятельством, что в последнем случае поверхность волокна покрывается ровным слоем ПВП (глобулярные частицы здесь не наблюдаются, что очевидно, не является характерным для данного полимера) и, в результате, создаются некоторые напряжения, под действием которых образуются новые складки (рис. 2в). Фибриллярная структура волокна при этом также несколько отличается (рис. 2г). Тонкая структура фрагментов вторичной стенки волокна — фибриллярность здесь выражена более отчетливо и в этом образце также значительная взаимная упорядоченность фибрилл друг относительно друга.

Далее наши исследования показали, что структура поверхности и фибриллярных участков хлопкового волокна, привитого ПВДХ, существенно отличается от таковых предыдущих модифицированных образцов (рис. 3а, б). Видно, что в этом случае наряду с процессом прививки ПВДХ (она составляет 14% по отношению к исходному весу волокна) происходит как-бы травление волокна, т е. некоторое разрушение его рыхлых участков в процессе привитой сополимеризации с винилиденхлоридом. Хотя поверхностные складки волокна после прививки не исчезают, тем не менее из-за «травления» общая картина структуры поверхности волокна сильно изменяется. Нами замечено, что эффект травления имеет место и во внутренней части — фибриллярной структуре хлопкового волокна. При механическом диспергировании такого препарата обнаруживаются фрагменты вторичной стенки волокна с разрушенной фибриллярной структурой (рис. 3б).

Структура поверхности хлопкового волокна и его внутренние фибриллярные участки (вторичная стенка) будут иметь отличный вид при прививке

таких виниловых полимеров, как ПМАА и ПМАК, особенно, при больших привесах (соответственно 56% и 60%). На рис. 4а, б, в, г приведены результаты электронномикроскопических наблюдений их структуры (рис. 4а, — бдля привитых ПМАА волокон и рис. 4в, г — для случая ПМАК).

Видно, что в случае прививки ПМАА складчатый характер поверхностной структуры хлопкового волокна несколько видоизменяется (рис. 4а). При фрагментации обнаруживаются слои с высокой упорядоченностью

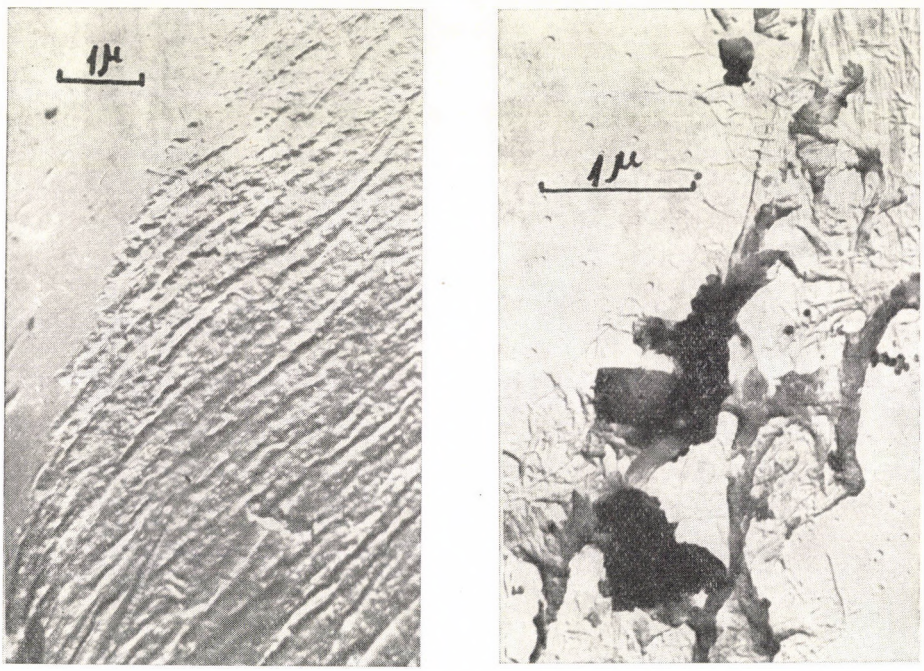

Рис. 3. ЭМ ХВ, модифицированного путём прививки ПВДХ (привес 14%). (а) реплика поверхности; (б) фрагмент фибриллярной структуры

(рис. 4б). Это, по-видимому, обусловлено тем, что благодаря прививке ПМАА к целлюлозе увеличиваются силы сцепления структурных элементов (микрофибрилл, фибрилл) целлюлозы друг с другом, как в случае ПАН.

Несколько иные картины обнаруживаются в случае ПМАК. Хотя складчатость поверхностной структуры хлопкового волокна при этом полностью сохраняется, но она из-за большой прививки полимера (рис. 4в) имеет более гладкий вид. И фибриллярная структура, несмотря на возможность образования довольно больших фибриллярных слоев (рис. 4г) при фрагментации такого волокна имеет отличный вид, по сравнению с таковой привитого ПМАА образца, например, отсутствуют бугорки. При ПМАК фибриллы, образующие слои вторичной стенки волокна, не имеют сильно натянутых форм.

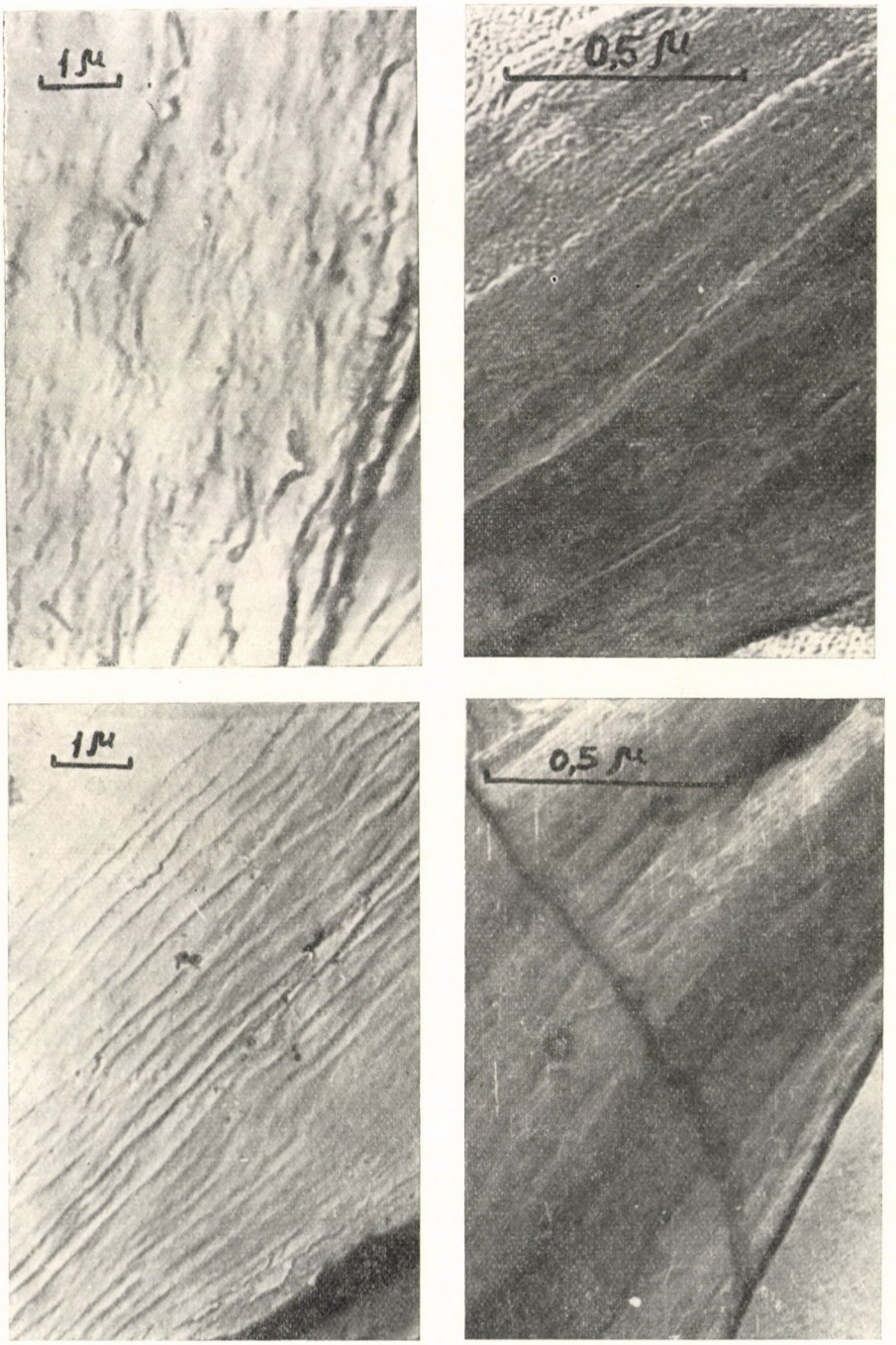

Рис. 4. ЭМ ХВ, модифицированных путём прививки ПМАА (привес 56%). (а) реплика поверхности; (б) фрагмент фибриллярной структуры; ПМАК (привес 60%); (в) реплика поверхности; (г) фрагмент фибриллярной структуры

Местами они переходят в соседние участки. Отсюда можно заключить, что силы сцепления фибриллярных образований друг с другом, в боковом направлении, в случае ПМАК выражены несколько слабее, чем при прививке ПМАА.

Вышеприведенные результаты свидетельствуют о том, что структура поверхности и фибриллярных участков хлопкового волокна приобретает различный вид в зависимости от типа прививаемого к нему винилового полимера. Общим для всех исследованных случаев является, очевидно, то обстоятельство, что в процессе радиационно-химической привитой сополимеризации хлопковой целлюлозы с виниловыми мономерами, бесспорно, происходит отложение синтетического полимера в целлюлозе. Когда этот процесс осуществляется из паровой фазы и до акта прививки волокно не подвергается каким-либо процессам набухания (в случае ПАН, ПВП), прививка макромолекул к целлюлозе осуществляется преимущественно на поверхности структурных элементов — микрофибриллах, фибриллах.

Данные, полученные при исследовании привитых образцов целлюлозы с ПВДХ, ПММА и ПМАК свидетельствуют о том, что структурные превращения целлюлозы в этих случаях проявляются в наибольшей степени. Как видно из полученных электронных микрофотографий, в этих образцах и поверхностная структура волокна и его участки с фибриллярной упаковкой (вторичная стенка) видоизменяются более отчетливо. Отсюда следует, что в случае прививки из раствора структурные элементы целлюлозы в растворе значительно набухают, следовательно, в реакции привитой сополимеризации могут принять участие и те целлюлозные цепи, которые расположены внутри структурных элементов, т. к. в последнем случае доступность прививаемого реагента значительно больше.

Представляет интерес выявить характер структурных превращений хлопковой целлюлозы в зависимости от степени прививки винилового полимера. Нами изучены волокна, привитые ПС при различных привесах, а именно: 3,4%, 13,4%, 21,5%. На рисунках 5а, б; 7а, б приведены, соответственно, электронные микрофотографии поверхности и фибриллярной структуры вышеуказанных образцов.

Как видно из электронномикроскопических наблюдений, при привесе ПС 3,4% уже заметны изменения в структуре хлопкового волокна. Складки исчезают, картина поверхности волокна становится более однородной. Кроме того, можно заметить наличие мельчайших сферических образований (глобул), расположенных преимущественно на местах складок волокна, которые представляют привитой ПС (рис. 5а). Можно предположить, что при привесе 3,4% ПС покрывает поверхность волокна уже в такой степени, что складчатая структура сглажена и возникают структурные образования — глобулы, характерные для ПС. Установлено, что диаметр глобул колеблется от 150 до 300 Å. При фрагментации (механическом диспергировании) такого препарата

наблюдается картина фибриллярной структуры целлюлозы (рис. 5б), аналогичная той, которая наблюдалась, обычно, для привитых образцов с ПМАА, ПМАК. Отсюда можно заключить, что даже малый привес ПС к целлюлозе (3,4%) является вполне достаточным, чтобы связывать фибриллы целлюлозы друг с другом. Благодаря этому обстоятельству и наблюдаются фрагменты фибриллярной структуры со сплошной упаковкой (рис. 5б).

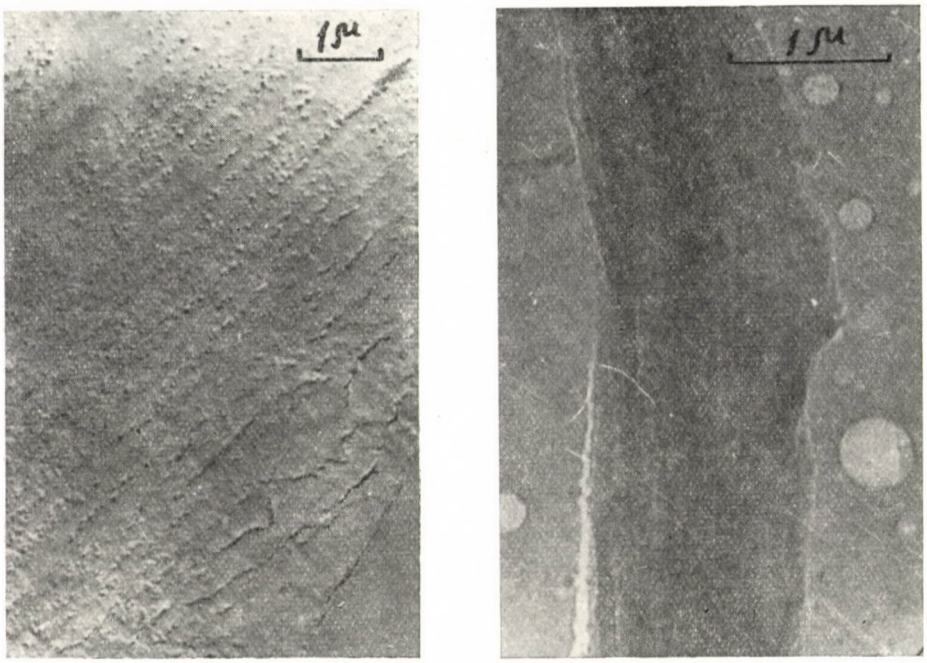

Рис. 5. ЭМ ХВ, модифицированного путём прививки ПС, привес 3,4%. (а) реплика поверхности; (б) фрагмент фибриллярной структуры

С увеличением привеса картина становится все более отличной. Так, при привесе ПС 13,4% в местах складок на поверхности волокна наряду с глобулярными агрегатами начинают возникать анизодиаметричные частицы типа микрофибриллы (рис. 6а). При тщательном рассматривании электронномикроскопических картин можно заметить, что некоторые из таких образований состоят из глобул. Но это, по-видимому, не означает, что все фибриллярные агрегаты ПС возникли за счет укладки глобул в одну линию, вероятно, они могут образовываться и в результате плотной упаковки нескольких распрямленных глобулярных агрегатов. Наблюдаемые в последнем случае длинные агрегаты имеют форму лент; ширина ленточных структур от 500 до 1500 Å. Это более отчетливо видно при привесе 21,5%, где поверхностная структура волокна состоит исключительно из т. н. „ленточных" структур (рис. 7а).

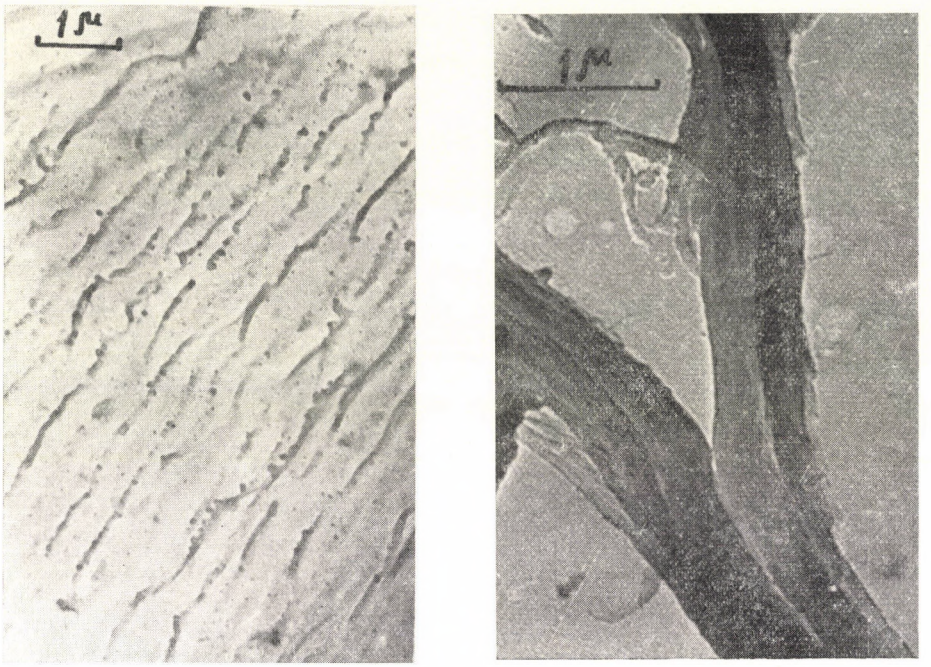

Рис. 6. ЭМ ХВ, модифицированного путём прививки ПС, привес 13,4%. (а) реплика поверхности; (б) фрагмент фибриллярной структуры

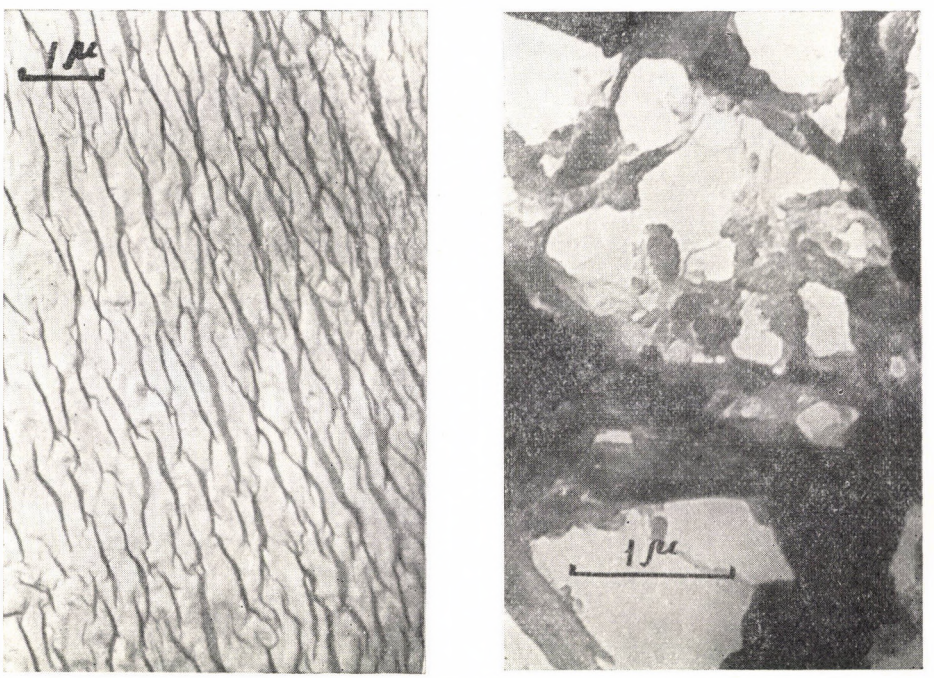

Рис. 7. ЭМ ХВ, модифицированного путём прививки ПС, привес 21,5%. (а) реплика поверхности; (б) фрагмент фибриллярной структуры

Результаты проведенных исследований показали, что увеличение привеса ПС в хлопковой целлюлозе также сильно влияет на характер ее фибрилляции (рис. 6б, 7б). При больших привесах фибрилляция привитой целлюлозы значительно ухудшается, это особенно сильно заметно при привесе 21,5% (рис. 7б), что можно объяснить тем, что прививка ПС к целлюлозе ведет к появлению гидрофобных свойств. С увеличением степени прививки препарат приобретает все больше и больше гидрофобное свойство, вследствие чего, при проведении фрагментации в воде, нам не удалось наблюдать характера фибриллярной структуры привитой целлюлозы с ПС, особенно, при наибольшем привесе.

Таким образом, электронномикроскопические исследования структуры поверхности и фибриллярных участков (вторичной стенки) хлопковых волокон, модифицированных путём радиационно химической прививки ряда виниловых полимеров позволили выявить их структурные особенности. Для всех исследованных образцов удалось установить их специфические отличия, вызванные природой прививаемого полимера, а также условиями процесса прививки (из раствора мономеров и из паровой фазы), на надмолекулярном уровне.

Выводы

Результатами электронномикроскопических исследований показано, что прививка различных виниловых полимеров к хлопковому волокну поразному влияет на структуру его поверхности и фибриллярных участков.

Установлено, что степень структурных изменений волокна зависит как от природы прививаемого полимера и степени прививки, так и от условий получения привитого образца — из паровой фазы или из раствора.

Предположено, что при проведении процесса прививки виниловых полимеров к хлопковому волокну из паровой фазыи, особенно, в случае малых привесов, в реакции привитой сополимеризации участвуют в основном те макромолекулы целлюлозы, которые расположены на поверхности структурных элементов — микрофибрилл, фибрилл. В случае же, когда процессу прививки предшествует набухание хлопковых волокон в растворе мономеров, то в реакции могут участвовать и те макромолекулы, которые расположены внутри структурных элементов целлюлозы.

На основании полученных экспериментальных данных также можно заключить, что если прививка винилового полимера к волокну осуществляется в достаточно большой степени, то на поверхности волокна можно заметить возникновение глобулярных или асимметричных (фибриллярных, ленточных) структур, характерных привитому полимеру.

И, наконец, изучая фрагментацию привитого образца, из результатов электронномикроскопических наблюдений будет возможно судить о некоторых физико-химических свойствах модифицированного образца, например, о повышении гидрофобности волокон.

SUMMARY

Results are presented of the electron microscopic examination of the surface and internal structure of cotton fibres modified by radiation-chemical grafting of various vinyl monomers onto the fibre: acrylonitrile (12.5% increase of weight), vinylpyridine (16%), vinylidene chloride (14%), methacrylic acid (60%) and styrene (3.4; 13.4 and 21.5% increase of weight).

The structural features of both the surface and the fibrillar portions (secondary walls) of the cotton cellulose were studied as a function of the following factors: the monomer used for grafting; the increase in weight; and the conditions of the radiation-chemical treatment.

The results suggest that the grafting process should be carried out by treatment in the vapour phase. If the cotton fibre had not been treated in any way causing swelling before grafting, graft copolymeryzation involves mainly the macromolecules on the surface of the cellulose microfibrils, fibrils, etc. If the process is carried out with solutions of the monomers, or by grafting in the gaseous phase but after preliminary swelling, also macromolecules situated in the internal structural elements of the cellulose fibre can take part in the graft copolymerization.

ЛИТЕРАТУРА

1. K. U. Usmanov. U. Azizov J. Polymer Sci. Part C, 579 (1964)
2. K. U. Usmanov, Celluloza Si Hirtie, *14*, N. 7—8—9, 363 (1965)
3. Усманов, Х.« У., Азизов, У., Садыков, М. У.: Сб. «Радиационная химия полимеров», Москва, Наука», 1966 г. 153—156, дискуссия 156—157.
4. Разиков, К. Х., Усманов, Х. У.: Высокомол. соедин., *8*, 387 (1966).
5. Разиков, К. Х., Усманов, Х. У.: Высокомол. соедин., *69*, 742 (1967).
6. Разиков, К. Х., Исамухамедова, И. И., Усманов, Х. У.: Сб. «Совещание по радиационному модифицированию полимеров», г. Обнинск, 9—13 декабря 1968 г., «Наука», 1968 г. стр. 60.
7. Усманов, Х. У., Разиков, К. Х., Исамухамедова, И. И., Азизов, У.: Intern. Simposium on Macromol. Chem., Budapest, 25—30th August 1969. Preprints Vol. 4, p. 165.
8. M. L. Rollins, A. T. Noore, et al, Amez. Dyestuff Reporter, *54*, 36, (1965).
9. Лившиц, Р. М., Сыдыков, Т. С., Роговин, З. А.: Cellulose Chem. Tecknol., *2*, 3 (1968).
10. Роговин, З. А., и др.: Высокомол. соедин., *Б10*, 46 (1968).
11. Разиков, К. Х., Тягай, Э. Д., Садовникова, В. И., Усманов, Х. У.: Высокомол. соедин., *А11*, 1717 (1969).

Х. У. Усманов
К. Х. Разиков
И. И. Исамухамедова

Научно-исследовательский институт химии и технологии хлопковой целлюлозы — «НИИХТЦ», г. Ташкент, СССР.

Acta Chimica Academiae Scientiarum Hungaricae, Tomus 70 (1—2), pp. 155—166 (1971)

ИССЛЕДОВАНИЕ ВЗАИМОСВЯЗИ СТРУКТУРНЫХ И ХИМИЧЕСКИХ ПРЕВРАЩЕНИЙ В ЦЕЛЛЮЛОЗЕ*

К. Х. РАЗИКОВ, Э. Д. ТЯГАЙ и Х. У. УСМАНОВ

(Научно-исследовательский институт химии и технологии хлопковой целлюлозы — НИИТЦ, г. Ташкент, СССР)

Поступила: 20 V 1970 г.

В данной работе тщательно изучен вопрос структурной и химической модификации хлопковой целлюлозы как в отдельности, так и во взаимосвязи друг с другом. Чтобы проследить изменения структуры исследуемых препаратов, были использованы методы световой и электронной микроскопии.

С целью структурной модификации целлюлозы нами были проведены следующие обработки: 18%-ным едким натром, то же с последующей инклюдацией изоамиловым спиртом, смесью глицерин-вода (1 : 1). Наблюдения, проведенные с помощью светового микроскопа, показали, что хлопковые волокна различным образом изменяются в форме и размерах под влиянием вышеуказанных обработок. В некоторых случаях исчезает извитость (скрученность) хлопкового волокна и его поперечное сечение становится почти круглым. В других же случаях скрученность сохраняется, но средний диаметр волокна заметно увеличивается. Электронно-микроскопическими наблюдениями как реплик поверхности, так и ультратонких срезов установлены два типа изменения структуры волокна — внутрифибриллярное и междуфибриллярное набухание.

Далее эти препараты хлопковой целлюлозы подвергались химическим превращениям — реакция цианэтилирования и радиационно-химической привитой сополимеризации с акрилонитрилом. Были выявлены особенности надмолекулярной структуры полученных препаратов-цианэтилированных и привитых полиакрилонитрилом волокон хлопка. Кроме того, установлено наличие взаимосвязи структурных и химических превращений в исследуемых образцах целлюлозы.

В настоящее время большое внимание уделяется процессам переработки природной целлюлозы и получению на её основе материалов с более ценными физико-химическими и механическими свойствами. В связи с этим важное значение приобретает вопрос о повышении реакционной активности целлюлозы в тех или иных реакциях химического превращения.

Известны многочисленные работы [1—6], в которых для химической модификации целлюлозы используются предварительные активационные процессы (обработки аминами, аммиаком, ледяной уксусной кислотой и др.).

Для проявления высокой реакционной способности целлюлозы необходимо общее ослабление межмолекулярного взаимодействия по всей глубине структуры, наличие развитой сети тончайших субмикроскопических капилляров, а также большой активной внутренней поверхности, гидроксильные группы которой являются доступными для молекул реакционной среды

* Материал доложен на Международном симпозиуме по Макромолекулярной химии Будапешт, 25—30 августа 1969 г. Доклад 10/26.

[7]. Этого можно добиться путем изменения надмолекулярной структуры целлюлозы, т. е. путем структурной модификации.

Для проведения целенаправленной структурной модификации нативной целлюлозы необходимо предварительное исследование всех возможных типов превращений целлюлозы как в отдельности, так и во взаимосвязи друг с другом.

С целью установления взаимосвязи между структурными и химическими превращениями в природной целлюлозе хлопковые волокна подвергали некоторым активирующим процессам (обработка едким натром, инклюдация высшими спиртами, кипячение в смеси глицерина с водой) с последующей химической модификацией (цианэтилированием и радиационно-привитой сополимеризацией с акрилонитрилом).

Объекты исследования и методика эксперимента

Объектами исследования были:

1. Хлопковая целлюлоза, обработанная 18%-ным раствором едкого натра при 0°С в течение 2-х часов;

2. Хлопковая целлюлоза, обработанная едким натром (п. 1) с последующей инклюдацией изоамиловым или гептиловым спиртом;

3. Хлопковая целлюлоза, обработанная смесью глицерин-вода (1 : 1) при кипячении, в течение 1 часа;

4. Активированные образцы (п. 1, 2, 3), подвергнутые реакции цианэтилирования;

5. Активированные образцы (п. 1, 2, 3), подвергнутые радиационно-привитой сополимеризации с акрилонитрилом из паровой фазы под действием γ-лучей Co^{60} при дозе облучения 1 Мрад и мощности 70 р/сек.

Выход продуктов, полученных при химической модификации предварительно активированных целлюлозных образцов, позволяет судить об их реакционной активности. В таблице приведены данные по выходу производных целлюлозы.

Основными методами исследования были световая и электронная микроскопия.

С помощью светового микроскопа МБИ-6 были изучены форма и размеры исследуемых волокон, а также их поперечных сечений.

Электронномикроскопические наблюдения проводили с помощью приборов УЭМВ-100 и «Тесла» при различных прямых электронно-оптических увеличениях. Для контрастирования препаратов использовали оттенение палладием и хромом.

При электронномикроскопических исследованиях применялись многие из существующих способов препарирования (получение ультратонких срезов, механическое и гидролитическое диспергирование, метод реплик).

Таблица 1

Выход производних целлюлозы после обработки

№/№ п/п	Исследуемые образцы	выход производных (%)	
		содержание азота в циан-этилированных препаратах	содержание азота в привитых сополимерах
1.	Исходная хлопковая целлюлоза	2,8	1,6
2.	Хлопковая целлюлоза, обработанная 18%-ным раствором едкого натра.	5,0	2,0
3.	Хлопковая целлюлоза, обработанная 10%-ным раствором едкого натра с последующей инклюдацией изоамиловым спиртом.	7,5	7,0
4.	Хлопковая целлюлоза, обработанная смесью глицерин-вода (1:1)	3,2	3,4

Полученные результаты и их обсуждение

Микроскопические исследования показали, что проведенные нами физико-химические обработки приводят к изменению формы и размеров волокна [8]. Одним из характерных признаков изменения хлопкового волокна при щелочной обработке является увеличение его диаметра и сокращение длины. Кроме того, сплющенная эллиптическая форма поперечного сечения переходит в сферическую. Все эти изменения обусловлены процессом набухания целлюлозы в щелочи. Дальнейшая инклюдация изоамиловым спиртом приводит к еще большему увеличению диаметра волокна.

После обработки смесью глицерин-вода средний диаметр хлопкового волокна заметно увеличивается, однако форма его, по сравнению с исходной, не меняется. Все это свидетельствует о том, что механизм небухания волокна в этом случае иной.

Электронномикроскопические исследования ультратонких срезов хлопкового волокна, обработанного едким натром, показали, что элементы надмолекулярной структуры целлюлозы — микрофибриллы, фибриллы и их слои — имеют набухший вид. При последующей инклюдации эти изменения проявляются в большей степени.

На рис. 1а, б представлены электронные микрофотографии поперечного и продольного ультратонких срезов хлопкового волокна, обработанного едким натром с последующей инклюдацией изоамиловым спиртом. Вторичная стенка такого образца состоит из плотноупакованных набухших микрофибриллярных слоев. Исследования показали, что структурные изменения, вызванные щелочной обработкой, не только закрепляются при последующей инклюдации, но и в некоторой степени углубляются.

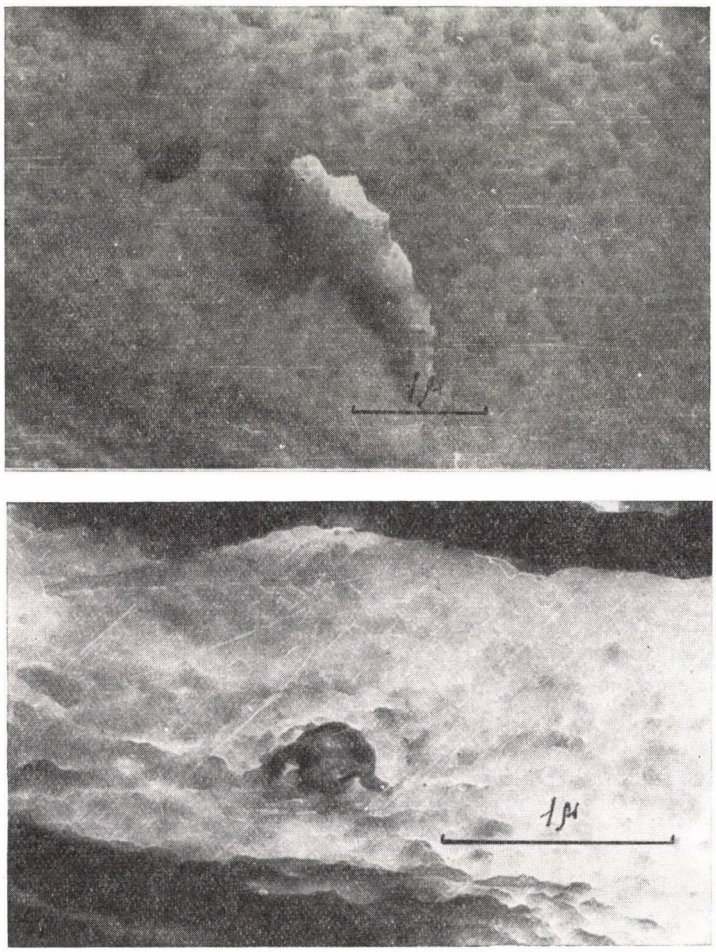

Рис. 1. ЭМ ультратонких срезов хлопкового волокна, обработанного едким натром с последующей инклюдацией изоамиловым спиртом. (а) поперечный срез; (б) продольный срез

Измерения ширины отдельных микрофибрилл дали следующие результаты: если для исходного хлопкового волокна ширина микрофибрилл составляет 100 Å, то для хлопкового волокна, инклюдированного изоамиловым спиртом, она порядка 170 Å°.

Видоизменение структуры хлопкового волокна при соответствующих обработках было выявлено также при изучении реплик его поверхности и диспергированных препаратов [9]. Было установлено, что обработка едким натром и последующие процессы инклюдации способствуют набуханию фибриллярных элементов целлюлозы, расположенных во всех частях волокна.

Итак, нами было показано, что обработка щелочью, а также последующие процессы инклюдации изоамиловым спиртом вызывают внутрифибрил-

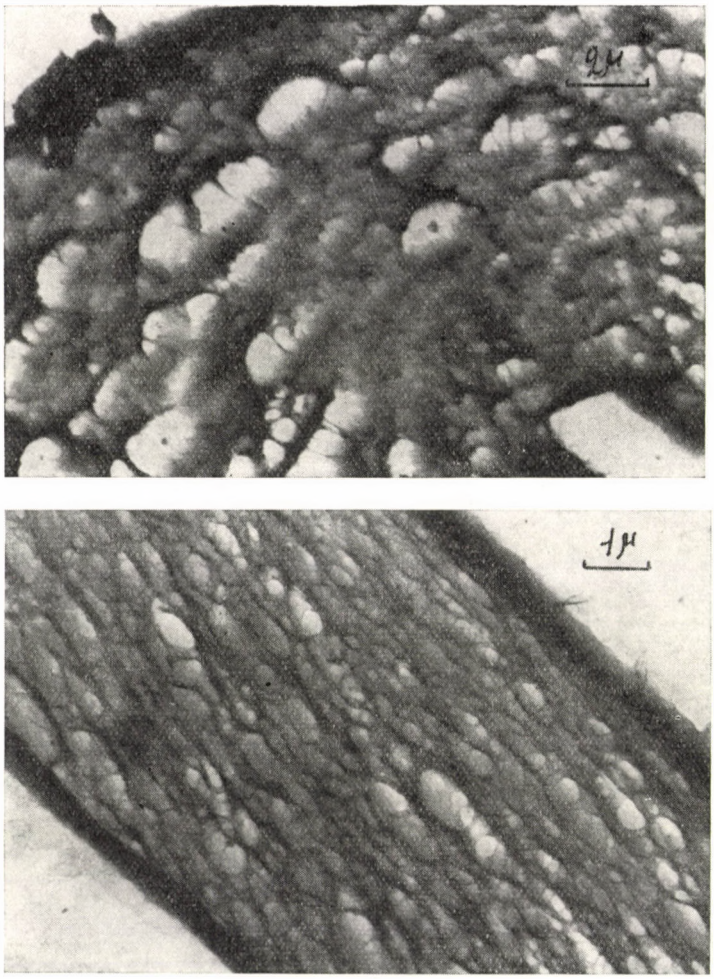

Рис. 2. ЭМ ультратонких срезов хлопкового волокна после обработки смесью глицерин-вода (1 : 1). (а) поперечный срез; (б) продольный срез

лярное набухание целлюлозы, что хорошо согласуется с ранее произведенными рентгенографическими исследованиями [10].

Совершенно иная картина была обнаружена при обработке хлопковой целлюлозы смесью глицерин-вода. На рис. 2 а, б приведены характерные электронномикроскопические снимки поперечных и продольных срезов этого образца. Как видно из снимков, эффекту набухания в этом случае подвергаются только рыхлые (межслоевые и межфибриллярные) области, вследствие чего происходит нарушение слоевой и фибриллярной упаковки.

Размеры индивидуальных микрофибрилл тонкого образца те же, что и у необработанного хлопкового волокна [9].

Изучение реплик с поверхности этого образца показало, что данная обработка способствует более отчетливому выявлению фибриллярной структуры первичной стенки. Это происходит вследствие травления рыхлого слоя на поверхности волокна.

Проведенные исследования показали, что молекулы глицерина, в отличие от молекул щелочи, не могут проникнуть в плотные участки целлюлозных микрофибрилл, вследствие чего обработка смесью глицерин-вода вызывает межфибриллярное набухание целлюлозы.

Далее структурно-модифицированные препараты (обработанные едким натром, водным раствором глицерина, инклюдированные изоамиловым спиртом) подвергали химическим превращениям, а именно, реакциям цианэтилирования и радиационно-привитой сополимеризациис акрилонигрилом.

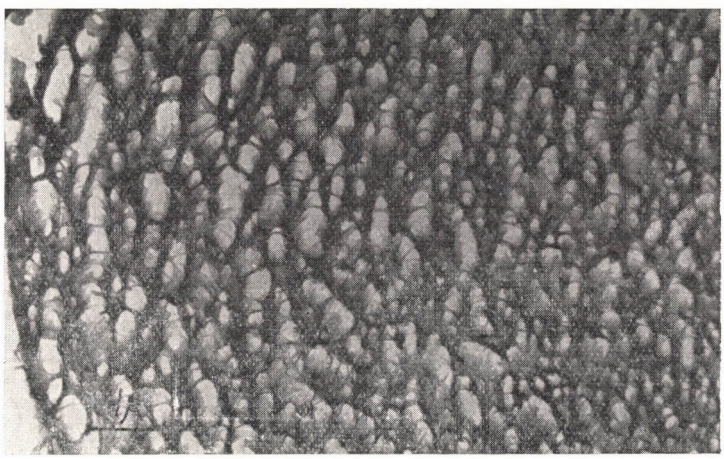

3. а

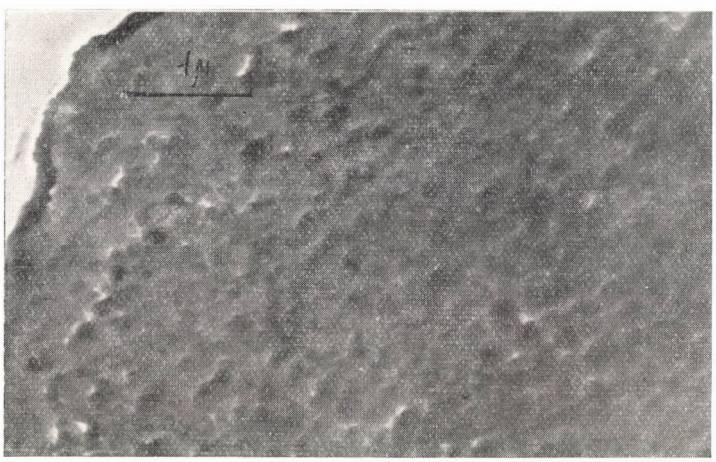

3. б

Исследования, проведенные с помощью светового микроскопа, показали, что форма и размеры модифицированных волокон зависят как от типа химической реакции, так и от характера предварительной обработки [8].

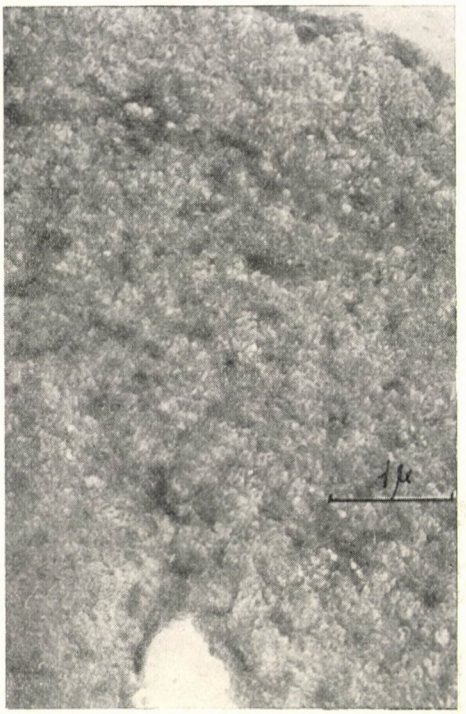

3. в

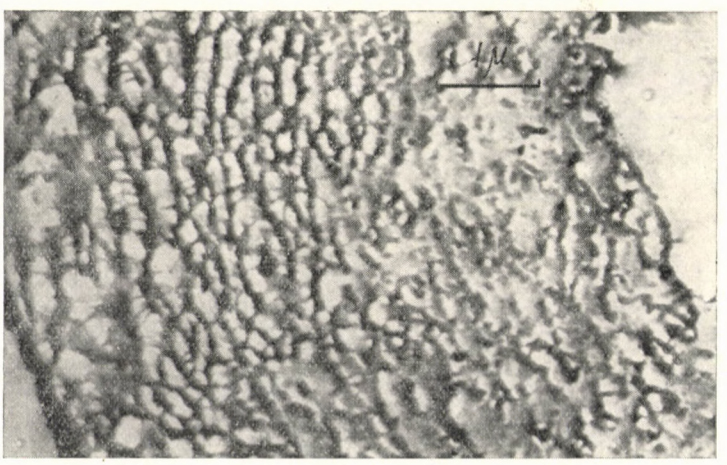

3. г

Рис. 3. ЭМ ультратонких поперечных срезов различных цианэтилированных волокон. (а) исходного (необработанного) хлопкового волокна; (б) обработанного едким натром; (в) обработанного сначала едким натром, затем изоамиловым спиртом; (г) обработанного смесью глицерин-вода (1 : 1)

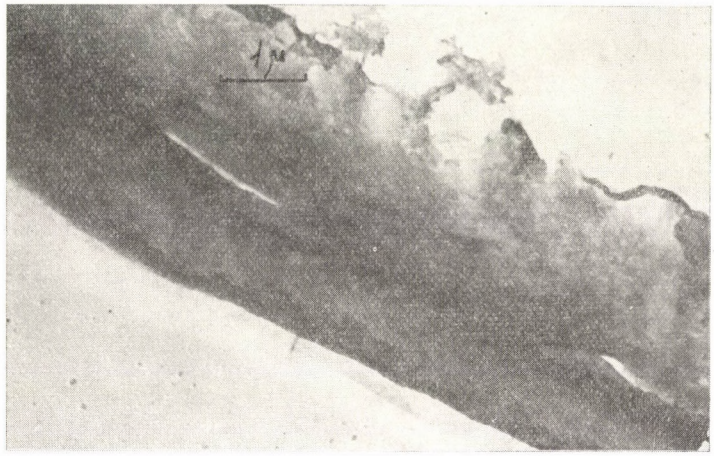

4. а

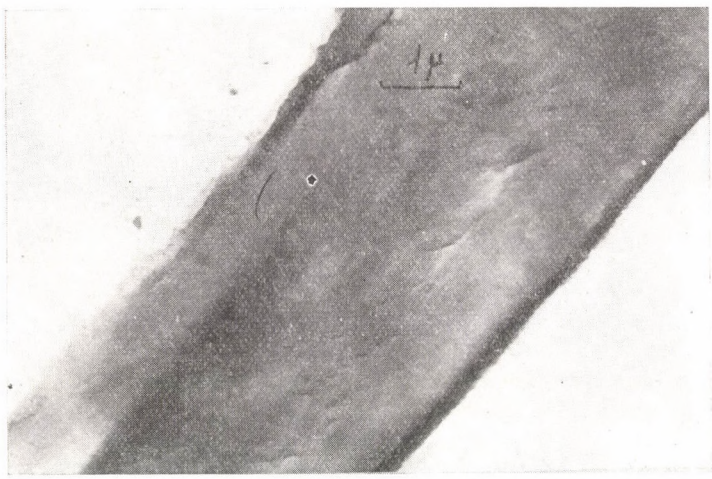

4. б

Электронномикроскопические исследования предварительно активированных и затем цианэтилированных образцов (рис. 3 а, б, в, г) позволили выявить специфические особенности их надмолекулярной структуры.

Наблюдаемое расслоение вторичной стенки на срезах исходного цианэтилированного волокна (рис. 3 а) является, очевидно, следствием химического превращения целлюлозы, т. е. замещения гидроксильных групп в макромолекулах целлюлозы на цианэтильные.

Равномерный характер распределения слоев вторичной стенки на поперечных срезах цианэтилированного волокна свидетельствует о равномерном протекании процесса цианэтилирования по всему поперечному сечению хлопкового волокна.

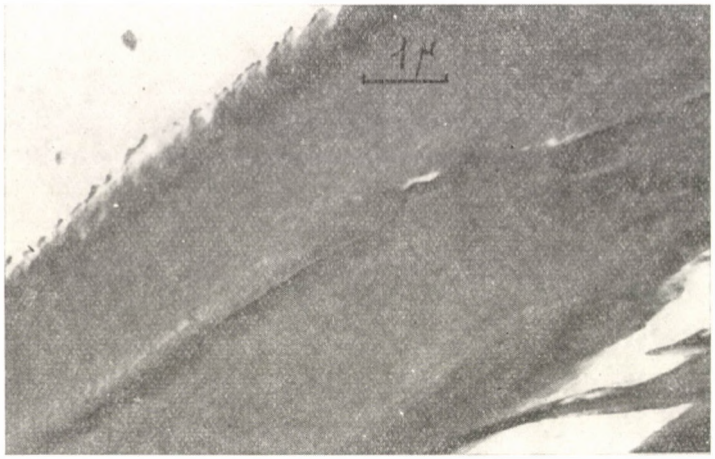

4. в

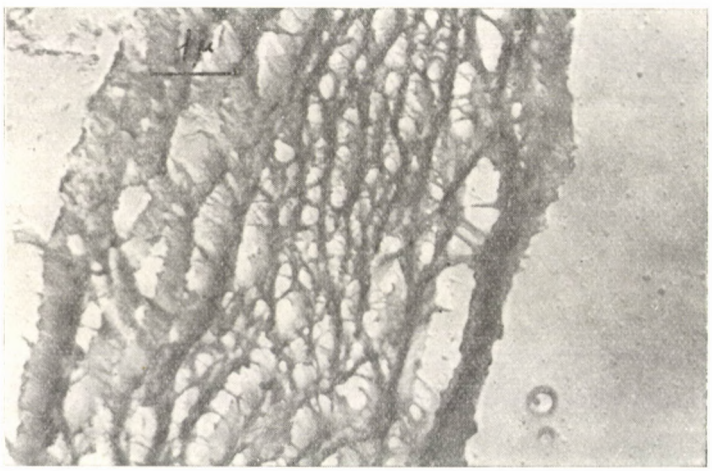

4. г

Рис. 4. ЭМ ультратонких продольных срезов различных привитых ПАН волокон хлопка. (а) исходного волокна; (б) обработанного едким натром; (в) обработанного едким натром и затем изоамиловым спиртом; (г) обработанного смесью глицерин-вода (1: 1)

При цианэтилировании предварительно мерсеризованной целлюлозы (рис. 3б) четко выраженная слоевая картина на её ультратонких срезах не наблюдается. Это объясняется тем, что процессу цианэтилирования предшествовала щелочная обработка, вызывающая внутрифибриллярное набухание целлюлозы.

Эффект внутрифибриллярного набухания приводит к увеличению степени замещения гидроксильных групп на цианэтильные в процессе цианэтили-

рования (содержание азота в исходном цианэтилированном волокне —2,8%, а в предварительно мерсеризованном цианэтилированном волокне —5%).

В случае цианэтилированных волокон, предварительно инклюдированных изоамиловым спиртом (рис. 3в), указанные различия в структуре волокон проявляются более отчетливо (содержание азота —7,0%).

Для цианэтилированного хлопкового волокна, предварительно обработанного смесью глицерина-вода, наблюдается разупорядочение элементов надмолекулярной структуры, позволяющее судить о характере распределения слоев вторичной стенки (содержание азота —3,2%).

Следует отметить, что поскольку при обработке целлюлозы смесью глицерина с водой имеет место лишь межфибриллярное набухание, а тонкая структура её микрофибрилл остается незатронутой, то можно предположить, что при цианэтилировании такого препарата в реакции участвуют преимущественно те макромолекулы, которые расположены на поверхности микрофибрилл или их агрегатов.

Предварительно активированные цианэтилированные препараты устойчивы к гидролизу.

На рис. 4а, б, в, г приведены электронные микрофотографии продольных ультратонких срезов радиационно-привитых сополимеров целлюлозы с полиакрилонитрилом (ПАН).

Набухание структурных элементов во вторичной стенке исходного привитого ПАН хлопкового волокна обусловлено прививкой полиакрилонитрильных молекул к целлюлозной цепи. Прививка ПАН происходит, очевидно, в наиболее доступных участках волокна.

К предварительно активированным хлопковым волокнам прививка ПАН идет гораздо интенсивнее, чем к исходной целлюлозе.

Электронномикроскопические исследования привитых ПАН волокон, предварительно обработанных едким натром, а также инклюдированных изоамиловым спиртом, показали, что на продольных срезах их видны укрупненные структурные элементы, плотно упакованные друг относительно друга.

Предварительная обработка целлюлозы едким натром при низкой температуре, а также последующий процесс инкюдации привели к сильному набуханию микрофибрилл и их плотных участков. Поэтому прививка в этом случае протекает, по-видимому, как в рыхлых, так и в плотных участках структуры целлюлозы.

В случае привитого ПАН хлопкового волокна, предварительно обработанного смесью глицерин-вода, сохраняется эффект межслоевого и межфибриллярного набухания, вызванный предварительной обработкой. В этом случае прививка ПАН идет, в основном, к тем целлюлозным цепям, которые расположены на поверхности микрофибрилл и их агрегатов. Происходит как бы обволакивание микрофибрилл цепочками ПАН.

Предварительно активированные хлопковые волокна, привитые ПАН, устойчивы к кислотному гидролизу, что объясняется, очевидно, экранирующим действием цепей ПАН.

Подобные исследования (структурные и химические превращения) были проведены и на гидролизованной целлюлозе, т. е. на её плотных участках. Полученные результаты подтверждают наши высказывания относительно взаимосвязи различных превращений в целлюлозе.

Резюмируя результаты микроскопических и электронномикроскопических исследований структуры модифицированных хлопковых волокон, можно отметить следующее: при том или ином типе химических превращений целлюлозы, наряду с модификацией её свойств, происходят изменения и в надмолекулярной структуре целлюлозы. Причем характер этих изменений зависит как от типа предварительной структурной модификации, так и от последующего химического превращения целлюлозы.

Следовательно, структура цианэтилированных и радиационно-химически привитых ПАН волокон хлопка всецело зависит от их первоначальной физической структуры. Это свидетельствует о наличии прямой зависимости между структурными и химическими превращениями в целлюлозе.

Выводы

1. Комплексом структурных методов исследования показано, что обработка хлопковой целлюлозы щелочью и последующие процессы инклюдации приводят к внутрифибриллярному разрыхлению целлюлозы, а обработка смесью глицерин-вода (1 : 1) — к межфибриллярному разрыхлению.

2. Установлено, что характер структурных изменений при химической модификации активированной целлюлозы зависит как от типа предварительной структурной модификации, так и от последующего химического превращения целлюлозы.

3. Детально изучена взаимосвязь структурных и химических превращений в хлопковой целлюлозе, в том числе и на её плотных участках. Показано, что характер и степень предшествовавших структурных модификаций целлюлозы всецело отражаются на надмолекулярной структуре её цианэтилированных и привитых полиакрилонитрилом препаратов.

SUMMARY

The structural and chemical changes occurring in cotton cellulose were studied both independently and in correlation with each other. In order to observe the changes in structure, light- and electron microscopic methods were used.

Structural modifications were effected by treatment of the cellulose with 18% sodium hydroxide solution, isoamyl alcohol, and a mixture of glycerol and water. Examination with a light microscope showed that this treatment produced different changes in the cotton fibre to a varying degree. In some cases the coiled (twisted) structure of the cotton fibre disappeared and its transverse section became almost round. In other cases the twist was retained, but

there was a noticeable increase in the mean diameter of the fibre. The electronmicroscopic observations of ultra-thin cuts confirmed that there were two types of structural changes in the fibre: intrafibrillary and interfibrillary swelling.

In other experiments, the cellulose preparations were treated chemically with ethyl cyanide followed by radiation graft copolymerization with acrylonitrile. The supermolecular structural features of the cyanoethylated and graft-polyacrylonitrile fibres of cotton were established. A relationship was found between the structural and chemical changes of the cellulose samples investigated.

ЛИТЕРАТУРА

1. Staudinger H. Eischer T.: Makramol. Chem. **10**, 254 (1958).
2. Krassig H. Schrott E.: Makromol. Chem. **13**, 179—193 (1954).
3. Кленкова, Н. И., Кулакова, О. М., Матвеева, Н. А., Волкова, А. А.: ЖПХ, *38*, 919 (1965).
4. Кленкова, Н. И., Кулакова, О. М., Матвеева, Н. А., Волкова, А. А., Цимара, Н. Д.: ЖПХ, *38*, 1077 (1965).
5. Кленкова, Н. И.: В сб. «Химия и технология производных целлюлозы», 1964, стр. 151.
6. Юльчибаева, С. Г.: Кандидатская диссертация, ТашГУ, Т., 1966.
7. Кленкова, Н. И.: ЖПХ, *40*, 2191 (1967).
8. Тягай, Э. Д., Разиков, К. Х., Усманов, Х. У.: Высокомол. соедин., *Б10*, 301 (1968).
9. Разиков, К. Х., Тягай, Э. Д., Ларин, П. П., Усманов, Х. У.: Высокомол. соедин., *А9*, 393 (1967).
10. Разиков, К. Х., Тягай, Э. Д., Ташпулатов, Ю. Т., Усманов, Х. У.: ЖПХ, *41*, 2706 (1968).

К. Х. Разиков,
Э. Д. Тягай,
Х. У. Усманов

Научно-исследовательский институт химии и технологии хлопковой целлюлозы — «НИИХТЦ», г. Ташкент, СССР.

RECENSIONES

International Compendium of Numerical Data Projects, XXIII

295 p. Produced by CODATA, Springer-Verlag, Berlin—Heidelberg—New York, 1969

The studies in chemistry, physics and technology are immensely branching out recently. For being conversant at least with one's own field of research, one needs a lot of time to study a tremendous number of reviews and collect systematically the data coming from several places. The effort against backwardness takes a considerable time originally devoted to research work.

The research work is aided to a great extent by the present Compendium, the material of which attempts to answer the following general questions:

What compilations containing critically evaluated data are now available, what centers or organizations produce or aid production of such data for publication on a continuing basis, what national programs exist for financial support and encouragement of data compilation work, and what guidelines are available to compilers of all countries so that their products may be compatible.

The Compendium is divided into six chapters:

In the first chapter, the national data programs and the national committees for CODATA are enumerated. In the second, the centers covering a number of areas of science are discussed. The topics of the third chapter:

Nuclear properties (General nuclear properties, properties of neutrons, properties of nucleides, indexes); *Atomic properties and molecular properties* (Atomic properties including spectra, molecular properties including spectra, infrared and microwave spectra, Raman spectra, electronic spectra, ultraviolet and visibles, mass spectra, NMR spectra, other atomic and molecular projects, indexes to compilations); *Solid state* (Crystallographic, mineralogical, electrical and magnetic, and related properties); *Thermodynamic and transport properties* (including thermophysical and solution properties, indexes to compilations); *Chemical kinetics*; *Gas Chromatographic Data*; *Optical properties* (Optical rotatory power: steroids, triterpenes, amino acids, alkaloids).

The entries in chapter 3 of the Compendium, which is the most important part, are organized under the following headings: 1) Organization, 2) Coverage, 3) Analysis, and 4) Publications. The first heading presents brief information about the organization under which the work is done, the second gives facultal information as to the substances covered and their states, the properties covered and the range of variables if appropriate, and the period of time covered. Under the term "Analysis" an effort is made to present facts and observations that reflect the aims of the compiler in evaluating and distributing the results of his work. Under "Publications" information is given leading the user to the source of the publication and its cost.

In the fourth chapter, the Compendium enumerates those new and secondary centers, which have had insufficient time to make their products available to the public. Some of these will in due course publish tables of data. Others are concerned, at least initially, in preparing complete bibliographies of pertinent papers for various fields. Just to mention the main topics: Secondary nuclear data centers, colloid and surface properties, other specialized centers (high pressures, radiation chemistry, diffusion in metals and alloys, equilibrium constants of molten steel, molecular weights of polymers, electrolyte solutions).

In the fifth chapter there are handbooks enumerated, giving only the necessary data without any evaluation. The sixth chapter (physical quantities, units and symbols, basic

physical constants, nomenclature and related matters) gives the survey of those national and international organizations, which play a leading role in the international scientific life concerning the topics mentioned in the title. The most important issues are enumerated as well.

The volume is supplemented by detailed author and subject indexes.

We greet the Compendium of ICSU—CODATA with great pleasure and should like to call the attention of every library, and research institute of natural sciences to this issue, which is indispensable in science and industry alike, and can give significant support to research work by its vast amount of information.

We should like to quote the lines from the Foreword written by Frederick D. ROSSINI, President of ICSU—CODATA, which perfectly throw light upon the aim of CODATA and the Compendium: "At the time of its establishment in 1966, by the International Council of Scientific Unions (ICSU), the Committee on Data for Science and Technology (CODATA) was given the basic mission of promoting and encouraging, on a worldwide basis, the production and distribution of compendia and other forms of collections of critically selected numerical data on substances of interest and importance to science and technology."

L. LÁNG

N. ANAND, J. S. BINDRA and S. RANGANATHAN: *Art in Organic Synthesis*

Holden-Day Inc., San Francisko, London, Amsterdam, 1970

The spiritual similarity between the activity of the creative scientist and artist has been the dominant idea of several studies discussing scientific results. Obviously, the same thought stimulated the authors of the present work in preparing a survey of the brilliant achievements in modern organic chemistry.

Naturally, neither a textbook nor a study, summarizing without omission the results, can be written on the 'art' of organic chemistry. However, a representative publication, similar to an album illustrating the products of a given artistic period can be compiled. This seems to have been the leading principle of the authors in the compilation of their material, selected from recent decades of organic chemistry.

The limited extent of a book makes inevitable the use of some guiding principle. This is shown here in the fact that the 100 examples presented were taken from the domain of the synthesis of natural organic substances. This selection is fortunate, because in this way the most useful knowledge can be given in a rather concise form. Indeed, this field gives, *e.g.*, the most useful thesaurus of examples on the selective conversion of polyfunctional compounds. In this respect the book can serve therefore as a source of guiding principles in selecting reaction conditions and reagents. Thus, for younger chemists it is a summary of possibilities, whereas for those who did active research during the period when organic chemistry achieved its recent spectacular successes, it is a summarizing recapitulation of the results of these decades.

The syntheses described in the book represent without exception the highest level in organic chemistry, but the intention of the authors to present an interesting material selected from a broad field can also be seen. There have been many other achievements in recent decades in organic chemistry which deservedly might have been included in this work. However, the authors had to make use of their privilege to choose from equals. The book makes very useful and thought-provoking reading.

L. TOLDY

S. J. BARKER and M. B. PRICE: *Polyacetals*

175 pp. Iliffe Books, London, 1970

The polymerization of formaldehyde was first oberved by BUTLEROV in 1859. STAUDINGER studied the process of polyoxymethylene formation and the properties of the polymer. Nevertheless, production on an industrial scale began only in 1956. The reason for this can be ascribed to the technical difficulties of the industrial purification of formaldehyde, required for the formation of the polymer, and to steps necessary for the stabilization of the polymer formed. The book by S. J. BARKER and M. B. PRICE gives an excellent survey of the chemistry of polyacetals, the principle and technical realization of their preparation and of the mechanical,

electric and chemical properties of the polymers. In the characterization of the mechanical properties, the description of characteristics observed under prolonged load is of particular interest. The second part of the book deals with the processing methods of polyacetals, machines and tools required for this purpose. Finally, the conditions of efficient use and application are discussed, among others, the problems pertinent to the cementing, fastening together, dyeing and imprinting of polyacetals, and to the modification of the properties of polyacetals by various reinforcing substances. The last chapter of the book describes the polyacetals of aldehydes with a higher number of carbon atoms. The book will be very useful to those experts who wish to process and use polyacetals. These products are relatively expensive, which makes a careful consideration of their technical properties absolutely necessary in their application. This is a precondition of their optimum technical and economic application and spreading use. The book gives valuable and reliable help in this task.

Gy. HARDY

Advances in Macromolecular Chemistry, Vol. 2

267 pp. Edited by Wallace M. PASIKA. Academie Press, London, New York, 1970

The book comprises five studies on actual problems in macromolecular chemistry and physics. The first study (Jett C. ARTHUR, Jr.: Graft Polymerization onto Polysaccharides) gives an excellent survey of the methods of graft polymerization, and of the chemical and physical characterization and use of the products. The modification of the properties of natural fibres on cellulose basis by synthetic methods to suit given technical requirements, attaches particular actuality to this method. The second study (B. CHU: Critical Opalescence and the Macromolecule) discusses problems in connection with the light-scattering method used widely in the physical investigation of polymers, the phenomenon of the critical opalescence of macromolecular solutions and its applicability to the structural investigation of polymer solutions and macromolecules. Recent technical developments in the examination of the phenomenon permit the study of the configuration and dynamic behaviour of liquids and macromolecular solutions. Thus, *e.g.* the diffusion constant of dissolved particles, the translational and rotational diffusion constants of biomacromolecules, laminar and turbulent flow profiles and the duration of turbulent fluctuations can be determined by means of this method. The third study (A. BLUMSTEIN: Polymerization in Preoriented Media) discusses the rules of polymerization reactions in preoriented systems and those ordered in one, two and three dimensions. Since an extensive review has been published in the first volume of this series on solid phase polymerization, this study is concerned mainly with processes occurring in liquid-crystalline, mono- and multilayer systems. Many new results are to be expected particularly in the field of syntheses in macromolecular matrices simulating biosynthesis. The fourth study of the volume (H. L. FRISCH and D. KLEMPNER: Topological Isomerism and Macromolecules) discusses in detail the topological isomerization of macromolecules, the corresponding synthetic methods and their interpretation, a problem of actuality with both synthetic and bio-polymers. The last, fifth study of the book (M. M. KOTON: High-Temperature Polymers Containing Cyclic Functions) is a systematic description of the methods of preparation of cyclic polymer chains of high thermal resistance. The author, Professor M. M. KOTON, is one of the leading experts in this field in the Soviet Union, and is therefore the most qualified interpreter of the results achieved in Soviet chemical schools for those who read only English.

Gy. HARDY

Fortschritte der chemischen Forschung. Topics in Current Chemistry, Band 14, Heft 1

126 Seiten. Inorganic and Analytical Chemistry. Springer-Verlag, Berlin, Heidelberg, New York, 1970

Die beim Springer-Verlag erschienene Reihe begann 1951 und gibt kurze Übersichte meist zusammenfassenden Charakters über neuere Ergebnisse auf verschiedenen Gebieten der Chemie (organische Chemie, anorganische Chemie, analytische Chemie, Komplexchemie, Radiochemie, Photochemie, Chemie der Naturstoffe, Stereochemie, Elektrochemie, organische

Synthesen, neue Methoden in der chemischen Forschung, Spektren und Molekülstruktur usw). Das Prinzip der Folge widerspiegelt die bereits verbreitete Erkenntnis, daß die Zeit der umfangreichen Monographien (umfassenden Charakters) allmählich vergeht und zwar besonders auf Wissenschaftsgebieten mit starkem Entwicklungstempo. Wegen des hohen Zeitbedarfs für die Bearbeitung der einschlägigen Literatur und für das Schreiben ausführlicher Monographien sowie wegen der längeren Durchlaufszeit in der Druckerei (bei umfangreichen Büchern) sind nämlich viele Monographien bereits im Zeitpunkt ihres Erscheinens als veraltet zu betrachten. Die vorliegende Bücherfolge ist eine solche, bei der die in kürzeren Perioden wiederholte Information, der up-to-date-Charakter gegenüber den immer schwieriger realisierbaren ausführlichen Darlegungen bevorzugt wird.

Heft 1 des 14. Bandes der Reihe enthält drei Arbeiten vom Gebiet der anorganischen und analytischen Chemie.

In seiner 43 Seiten umfassenden Arbeit "Localized Molecular Orbitals and Bonding in Inorganic Compounds" erörtert H. A. BENT die Eigenschaften des Bindungssystems der Moleküle durch elektrostatische Wechselwirkungen. Sein Grundprinzip ist, daß eine Analogie zwischen den ionischen und kovalenten Verbindungen besteht. In den kovalenten Verbindungen spielt der aus dem Atomkern und den abschirmenden, jedoch an der Bindung nicht beteiligten Elektronen bestehende Atomrumpf die Rolle der Kationen, während die Anionen die "elektriden Ionen" sind, die durch die Sphäre je eines in der äußeren Elektronenhülle befindlichen Elektronenpaars charakterisiert werden. Der Autor ordnet jedem Elektronenpaar und jedem Atomrumpf je eine negativ bzw. positiv geladene Kugel zu. Seiner Auffassung nach sind die bei Kristallen erkannten Zusammenhänge auf analoge Art auf die aus Atomrümpfen und elektriden Ionen aufgebauten Moleküle übertragbar, woraus er zu zahlreichen interessanten Folgerungen gelangt. Die Nutzbarkeit dieser Konzeption besteht darin, daß qualitative Feststellungen bei solchen — hauptsächlich anorganischen — chemischen Systemen ermöglicht werden, deren quantitative quantenmechanische Behandlung gar nicht in Frage käme.

Es könnte eingewendet werden, daß der auf die lokalisierten Molekülbahnen hinweisende Titel nicht mit dem durch den Autor beschriebenen, im wesentlichen elektrostatischen Prinzip im Einklang steht.

In der 43 seitigen Übersicht mit dem Titel "Non-Destructive Techniques in Activation Analysis" führt W. D. EHMAN die Entwicklung und Leistungsfähigkeit der zerstörungsfreien aktivierungsanalytischen Verfahren vor.

Bei der Behandlung der Neutronenaktivierungsanalyse (14 MeV bzw. thermische Neutronen) wird der Leser auch über die Meßtechnik und Meßgenauigkeit informiert. Unter den sonstigen aktivierungsanalytischen Verfahren werden die in biologischer Hinsicht wichtige, zur Bestimmung von ^{16}O, ^{14}N und ^{12}C besonders geeignete Photoaktivierungsanalyse, die Aktivierung mit geladenen Teilchen (Protonen, Deuteronen, Tritonen, Helium(III)-Ionen, Alphateilchen), die für die Bestimmung von leichten Elementen angewendet wird und die prompte Gammastrahlenanalyse, deren Anwendung die Bestimmung von Radionukliden mit äußerst geringer Halbwertszeit ermöglicht, kurz behandelt.

Die Anwendbarkeit der Verfahren wird mit verschiedenen Beispielen illustriert. Die Arbeit ist in erster Reihe für die Informierung von auf diesem Gebiet noch nicht bewanderten Fachleuten zu empfehlen.

In der 33 Seiten umfassenden Arbeit von R. B. KING unter dem Titel "Transition Metal Organometallic Compounds in the Mass Spectrometer" werden die Ergebnisse der massenspektrometrischen Untersuchung von metallorganischen, hauptsächlich Carbonylverbindungen der Übergangsmetalle behandelt, die in vielen Fällen zur Klärung der Struktur führten. Es werden reichlich Beispiele angegeben, aus denen hervorgeht, wie aus der bei mehreren Verbindungsgruppen durchgeführten systematischen Forschung auf die Struktur gefolgert werden konnte. So kann z. B. aus dem Massenspektrum der Metallcarbonylhaloide und der Metallcarbonylhydride die Brücken- oder terminale Liganden-Stellung eindeutig bestimmt werden. Die Untersuchung der M_x Clusterionen, die im Spektrum der Metallcarbonyle auftreten, zeigte, daß die Stärke der Bindung zwischen verschiedenartigen Metallatomen mit zunehmendem Unterschied der Elektronegativität dieser Metalle ansteigt. Die Schrift führt die Anwendungsmöglichkeit der Massenspektrometrie zur Strukturuntersuchung der Metallcarbonyle in einer auch für Nicht-Spezialisten dieses Gebiets leicht verständlichen Form und dennoch anspruchsvoll vor.

Der up-to-date-Charakter aller drei Arbeiten des Bandes wird durch das mit dem Jahr 1969 abgeschlossenen Literaturverzeichnis demonstriert (der Band erschien im Februar 1970).

Das Niveu der Bearbeitung der drei Themen ist unterschiedlich. Unter Berücksichtigung des Übersichtcharakters, der voneinander völlig unabhängigen Themen und der verschiedenen Autoren, scheint dies jedoch unvermeidlich. Es wäre nicht richtig, diese Arbeiten als Abschnitte eines Buches zu betrachten und demgemäß einheitliche Ausführung und homogene Anschauung

zu erwarten. Um eine solche Einheitlichkeit zu erreichen, müßte eine Tätigkeit des Herausgebers eingeschaltet werden, die die Durchlaufzeit der Manuskripte wesentlich verlängern würde; demgemäß müßte auf den größten Vorteil der Folge, auf seinen up-to-date-Charakter verzichtet werden.

B. CSÁKVÁRI

A kémia újabb eredményei (Neuere Ergebnisse der Chemie)

Herausgegeben von: Béla CSÁKVÁRI. Akadémiai Kiadó, Budapest

Beispielen aus dem Ausland folgend, angeregt durch die Abteilung der chemischen Wissenschaften der Ungarischen Akademie der Wissenschaften, erschienen vor kurzem die ersten drei Bände dieser neuen Kleinmonographiefolge. Mit ihrer Herausgabe soll das Ziel verfolgt werden, den Chemikern zusammenfassende Arbeiten über einige engere Fachgebiete der Chemie zur Verfügung zu stellen, in denen die erreichten Ergebnisse aufgrund der neuesten Literaturangaben behandelt werden. Bekanntlich werden in unseren Tagen deshalb an Stelle der Fachbücher vom alten Typ die Monographien und hauptsächlich die sog. Kleinmonographien bevorzugt, weil zwischen dem Tempo der Veröffentlichung der wissenschaftlichen Ergebnisse und dem Erscheinen der diese Ergebnisse zusammenfassend darstellenden Fachbüchern sich Asynchronisation eingestellt hatte. Das gestörte Gleichgewicht kann nur so hergestellt werden, wenn Bände mit höchstens 2—3 Arbeiten herausgegeben werden, deren Verfasser — auf dem engen Fachgebiet arbeitende und folglich mit der neuesten Literatur vertraute Spezialisten — die endgültige Formulierung sozusagen unmittelbar vor der Drucklegung vornehmen und wenn auch der Verlag sein Möglichstes tut, um das Buch schnell erscheinen zu lassen. Solche Monographien sind — außer den Pflegern des engen Fachgebietes — auch für die in den Grenzgebieten arbeitenden Fachleute von Interesse. Es ist jedoch fraglich, ob Chemiker, die auf anderen Fachgebieten arbeiten, ebenfalls Anspruch auf diese Art von Zusammenstellungen erheben; meiner Ansicht nach sind für diese auch heute noch die umfassenderen, eher Zusammenhänge als Teilergebnisse enthaltenden Bücher von größerer Bedeutung.

Die ersten drei Bände der durch Béla CSÁKVÁRI herausgegebenen neuen Folge — in Leinen gebundene, gefällige Büchlein — enthalten je 2—4 selbständige Arbeiten, deren Umfang 30—120 Seiten beträgt. Der erste Band beschäftigt sich größtenteils mit anorganischer Chemie, während der zweite Band analytisch-chemische Aufsätze und der dritte eine organisch-chemische und eine komplexchemische Arbeit enthält.

A kémia újabb eredményei (Neuere Ergebnisse der Chemie). Band 1

Herausgegeben von: Béla CSÁKVÁRI. Akadémiai Kiado, Budapest, 1970· Preis Ft. 23.—

Zoltán SZABÓ: *Ergebnisse der modernen anorganischen Chemie*

Die Vergangenheit und Gegenwart der anorganischen Chemie vergleichend, führt der Verfasser aus, daß der Leitfaden dieser heute wiederauflebenden Disziplin die Strukturchemie ist, deren Grundlage die elektronische anorganische Chemie bildet. Von diesem Gedanken ausgehend werden die auf der Feinverteilung der Elektronen beruhenden periodischen Funktionen erwähnt, wonach der Verfasser auf die Elektronegativität übergeht. Die Konzeptionen, die zur quantitativen Formulierung des Begriffs führen, werden in großen Zügen behandelt und ihr gemeinsamer physikalischer Inhalt wird nachgewiesen. Der Begriff wird auf zusammengesetzte Radikale und Ionen ausgedehnt und es wird betont, daß der Wert der Elektronegativität im allgemeinen auch vom Oxydationszustand und vom Partner abhängig ist. Auf die Anwendung übergehend behandelt der Verfasser die Bindungsenergie, den Bindungsabstand, den ionischen Charakter der Bindung und dessen Wirkung auf die Löslichkeit ausführlicher- Die Theorie der Ionenpolarisation wird als gute Annäherung von der Seite der ionischen Bin. dung her erwähnt. Abschließend wird die Säure—Basen-Theorie kurz charakterisiert.

Zoltán Szabó—Kálmán Burger—Endre Kőrös: *Über die Pearsonsche Interpretation der Lewisschen Säure—Basen-Reaktionen*

In der Einleitung wird darauf hingewiesen, daß die leicht memorierbaren Regeln, die auf der unmittelbaren Systematisierung der Erfahrungen beruhen, wobei von der exakten wissenschaftlichen Ableitung Abstand genommen wird, für den praktischen Chemiker recht nützlich sind. Da auf dem Gebiete der Reaktionsfähigkeit die Pearsonsche Konzeption trotz ihrer Einfachheit als die umfassendste betrachtet werden kann, nahmen die Verfasser mit ihrer Themenwahl eine recht dankbare Aufgabe auf sich. Nach einem Überblick über die Vorgeschichte werden die Gesichtspunkte der Pearsonschen Kategorisierung diskutiert. Die Einteilung der Lewis-Säuren und Lewis-Basen in die Kategorien 'hard' und 'soft' ist tabellarisch angegeben, wobei die Grenzfälle separat angeführt wurden. Die Regel, daß "hard-Säuren mit hard-Basen und soft-Säuren mit soft-Basen stabilere Komplexe bilden bzw. mit höherer Geschwindigkeit reagieren", wird durch zahlreiche Beispiele unterstützt. Die anorganischen und organischen Reaktionen werden gesondert behandelt; danach wird auf einige Fragen der Stabilität und der Reaktionskinetik eingegangen. Die Bestrebungen, deren Ziel die theoretische Fundierung der Pearsonschen Konzeption ist, werden weitgehend erläutert.

Pál Szarvas: *Neure Ergebnisse in der Chemie der anorganischen Polysäuren*

Die zusammenfassende Arbeit von Pál Szarvas widerspiegelt und betont die Änderung in der Methodik und Anschauung, die sich im letzten Jahrzehnt in der Chemie der Polysäuren abgespielt hat. Obwohl der Verfasser einige Gesichtspunkte der Aufteilung der Polysäuren erwähnt, wobei er die tieferen Zusammenhänge als wichtiger beurteilt, verpflichtet er sich zu keinem dieser Gesichtspunkte. Er weist jedoch darauf hin, daß — unabhängig von ihrem Charakter — sowohl unter Metallen als unter Nichtmetallen allein diejenigen Elemente zur Bildung von Polysäuren neigen, deren Elektronegativität nicht geringer als 1,6 und nicht höher als 2,1 ist. Ausführlicher werden die Ergebnisse auf dem Gebiet der Polyborate, Polyphosphate und Vanadium-, Molybdän- und Wolframsäuren behandelt. Jener Teil des Aufsatzes, den die kritische Bearbeitung charakterisiert, gibt dem Leser einen Eindruck über die Kompliziertheit der untersuchten Systeme und beweist die Notwendigkeit und die Vorteile der vielseitigen Untersuchungen. Ein frappantes Beispiel der Schwierigkeiten bei der Klärung der tatsächlichen Verhältnisse ist die nur in den letzten Jahren erkannte Tatsache, daß der saure Charakter der *Ortho*borsäure nicht auf elektrolytischer Dissoziation, sondern auf der Addition von Hydroxydionen beruht.

Ferenc Török: *Analoge Züge der Schwingungstheorie von Molekülen und Kristallen*

Die Rolle, die auf die Schwingungstheorie in der Festkörperforschung wartet, ist ebenso wichtig wie ihre grundlegende Rolle in der Klärung der Molekülstruktur. Die Abhandlung von Ferenc Török führt die Schwierigkeiten der Anwendung auf Kristalle und zeigt den gangbaren Weg vor. Der Verfasser geht von der Schwingungstheorie der Moleküle aus, die er als bekannt voraussetzt. Er beweist, daß die analoge Determinante für Kristalle unendlicher Ordnung und für praktische Berechnungen ungeeignet ist. Dann führt er vor, wie die Schwingunglsgeichungen durch Berücksichtigung der Symmetrien vereinfacht werden können. Er weist auf die Unterschiede hin, die zwischen Molekülen und Kristallen hinsichtlich der Auswahlregeln vorliegen und führt verschiedene Methoden zur Klassifizierung der Kristallschwingungen an. Die Anwendung von polarisiertem Licht, die eine geradezu für Kristalle prädestinierte Methode zu sein scheint, wird gesondert behandelt. Zum Abschluß der wertvollen Abhandlung werden die Berechnungsprobleme der Kristallspektren dargestellt.

A kémia újabb eredményei (Neuere Ergebnisse der Chemie) Band 2

Herausgegeben von: Béla Csákvári

László Erdey—László Pólos: *Die Gravimetrie als Grundlage der chemischen Analyse*

In der Einleitung erörtern die Verfasser ausführlich, daß die Gravimetrie — wie auch der Titel ahnen läßt — trotz außerordentlicher Entwicklung der Instrumentation und Automatisierung keineswegs restlos ersetzbar ist; sie bleibt nach wie vor die Methode der letzten Kontrolle der Etalone. Ihre Entwicklung wird durch die Ergebnisse bewiesen, die auf dem Gebiet der Gravimetrie durch die Vervollkommnung ihrer Verfahren und durch die Klärung der Teilvorgänge erreicht wurde. All dies wird durch die Verfasser in einer logischen Kette der Zusammenhänge vorgeführt, wobei als Ausgangspunkt die Theorie der übersättigten Lösungen dient. In diesem Rahmen wird gezeigt, daß der Charakter der Nukleation in der metastabilen und in der labilen Zone verschieden ist. Es wird die Temperatur- und pH-Abhängigkeit der Breite der metastabilen Zone behandelt und ihre Bedeutung am Beispiel der Abscheidung von Bariumsulfat demonstriert. Anschließend wird die Abhängigkeit des Keimwachstums von der Diffusionsgeschwindigkeit und der Absorption sowie der Kossel-Stranskische Mechanismus und der Mechanismus des spiralen Kristallwachstums erläutert. Der Mechanismus wird im allgemeinen erfolgreich durch Anwendung des Dissolutionsverfahrens untersucht, oft mit dem Ausglühen der Niederschläge kombiniert. Der Teil der Abhandlung über die komplexe Untersuchung der Niederschläge ist recht wertvoll. Die Vorteile der gemeinsamen Anwendung der Differentialthermoanalyse, der Thermogravimetrie und der Dilatometrie werden an Hand mehrerer Beispiele vorgeführt. Der Derivatograph ist jedoch keineswegs nur ein Hilfsmittel im analytischen Laboratorium, sondern ermöglicht — wie die angeführten Beispielen zeigen — auch die unmittelbare Lösung analytischer Probleme.

Ernő Pungor—Ágnes Szász: *Neuere Entwicklungen der Flammenphotometrie*

Als Einführung wird ein kurzer Auszug der Theorie der Flammen gegeben; diesen möchte ich als höchst interessanten und knapp gefaßten Beitrag auch jenen Chemikern empfehlen, die die Flammenphotometrie weder weiterentwickeln noch anwenden möchten. Ausführlicher werden die Bildung und die Gleichgewichte der Radikale sowie die zur Bestimmung ihrer Konzentration dienenden Methoden ausgeführt. Auch das Ionisationsgleichgewicht und die Elektronenkonzentration der Flammen werden behandelt. Das verständlicherweise kurze Kapitel "Entwicklung der Meßtechnik" gibt den Zeitpunkt und die Umstände der Entwicklung der drei grundlegenden Meßmethoden, namentlich des Emissions-, Absorptions- und Atomfluoreszenzverfahrens an und schildert kurz ihre Verbreitung. Die Orientierung hinsichtlich der Nachweisgrenzen wird durch eine nützliche Tabelle gefördert. Bezüglich der Empfindlichkeit geben die Verfasser außer den informativen Angaben eine beachtenswerte Definition, deren Geist sich auch auf die Kapitel "Genauigkeit" und "Auswertung" auswirkt. Die Erfahrungen bezüglich der praktischen Ausführung werden kurz aber gut gegliedert mitgeteilt. Die knapp zusammengefaßten Kapitel behandeln die Fragen der Lösungsmittelwirkung, der Messung extrem hoher Konzentrationen, der Störwirkungen, der Instrumentation, der Lichtquellen, der Flammenzusammensetzung, der Monochromatoren; zwei Kapitel beschäftigen sich mit Fragen der Zerstäubung. Bezüglich der Anwendung in der Analyse betrachten die Verfasser jenen Umstand als wesentlichste Änderung, daß die Flammenphotometrie sich auch zur unmittelbaren Bestimmung von Nichtmetallen als geeignet erwiesen hat.

Wenn man berücksichtigt, wie wirtschaftlich die Verfasser den zur Verfügung gestellten Umfang durch kurze und treffende Charakterisierung der Literaturangaben trotz deren großer Zahl (1130 Hinweise) ausnützen und wie erfolgreich sie den Leser informieren, darf man wohl ruhig behaupten, daß die Arbeit: "Neuere Entwicklungen der Flammenphotometrie" für ähnliche Kleinmonographien als Vorbild dienen kann.

A kémia újabb eredményei (Neuere Ergebnisse der Chemie) Band 3.

Herausgegeben von: Béla Csákvári

Kálmán Medzihradszky: *Neueste Ergebnisse auf dem Gebiet der Synthese natürlicher Peptide*

Die durch ungarische Forscher durchgeführte und vor kurzem mit dem Staatspreis gewürdigte Synthese des menschlichen Adrenocorticotrop-Hormons (ACTH) erweckte das Interesse breiter Fachkreise für die Synthese natürlicher Peptide. Die sprunghafte Entwicklung, die auf diesem Gebiet — ähnlich anderen Zweigen der organischen Chemie — einsetzte, konnte vom organischen Chemiker in den heimischen und ausländischen Fachzeitschriften längere Zeit hindurch noch verfolgt werden. Die Anzahl der auf diesem Gebiet publizierten Arbeiten steigt jedoch neuerdings — in Übereinstimmung mit der Theorie über die "Informationsexplosion" — derart steil an, daß nur der auf dem eng genommenen Fachgebiet Arbeitende fähig ist, die Ergebnisse überblicken zu können. Es ist erfreulich, daß ein Mitglied der oben erwähnten ungarischen Forschergruppe es unternommen hat, die neuesten Ergebnisse der Synthesen natürlicher Peptide zusammenfassend zu beschreiben.

Zunächst behandelt der Verfasser die Methoden der Peptid-Synthese. Nach der kritischen Bewertung der verschiedenen Schutzgruppen erörtert er die Verfahren zur Bildung der Peptidbindung. Das Merrifieldsche Verfahren und seine neueren Varianten werden ausführlich dargelegt, wobei erwähnt wird, daß diese in ihrer gegenwärtigen Form nur einer "mechanisierten" Peptidsynthese entsprechen, woraus sich prinzipielle Probleme ergeben.

Der zweite Teil der Abhandlung befaßt sich mit der Synthese natürlicher Polypeptide und Proteine. Zuerst werden mit größter Ausführlichkeit die Versuche zur Synthese der Hypophysenhormone, des ACTH, des MSH (melanocidstimulierende Hormone), des β-LPH (β-Lipotrophormon), der Hinterlappenhormone und der Pankreashormone dargelegt. Im weiteren werden die neueren Versuche der Synthese der blutdruckregulierenden Hormone, der Polypeptidhormone des Darmtrakts, der jüngst entdeckten Polypeptidhormone, der Calcitonine, des Apoferredoxins und ganz kurz die Herstellung der Polypeptid-Antibiotika behandelt.

Im abschließenden Teil erhält der Leser ein Bild über die bisher größte Leistung auf dem Gebiet der Synthese der natürlichen Polypeptide und Proteine, über die erste Enzymsynthese: über die Totalsynthese des Ribonuklease A-Enzyms.

Der Wert der vorzüglich abgefaßten Arbeit wird durch die Hinweise auf zusammenfassende Mitteilungen und durch das auch die neuesten Ergebnisse enthaltende Literaturverzeichnis gesteigert.

László Markó—Gábor Speier: *Stickstoff-Fixierung in synthetischen Systemen unter milden Reaktionsbedingungen*

Die Abhandlung von László Markó und Gábor Speier berichtet über ein neues, noch im Anfangsstadium befindliches, jedoch vor einer großen Zukunft stehendes Gebiet der organischen Komplexchemie. Bekanntlich geht der Vorgang der Umwandlung des elementaren Stickstoffs in gebundenen Stickstoff in Mikroorganismen und Pflanzen unter milden Bedingungen, im Temperatur- und Druckbereich der Umgebung der Lebewesen (0—40°, 0.8 Atm · p_{N_2}) vor sich, während die Haber-Boschsche Ammoniaksynthese, deren Funktion letzten Endes die gleiche ist, nur bei hoher Temperatur (400—500 °C) und bei hohem Druck (250—1000 Atm.) realisierbar ist. Deswegen sind die Ergebnisse der Untersuchungen von Reaktionen zwischen nichtbiologischen Systemen und Stickstoff unter milden Bedingungen von äußerstem Interesse.

Im ersten Teil werden die zwischen Stickstoff und metallorganischen Mischkatalysatoren verlaufenden Reaktionen diskutiert. Der zweite, umfangreichere Teil befaßt sich mit molekularen Stickstoff enthaltenden Übergangsmetallkomplexen. Es wird eine ausführliche Beschreibung der Herstellung solcher Komplexe und ihrer Reaktionen in folgender Gliederung gegeben: Reaktionen, in denen Stickstoffmoleküle freigesetzt werden; Reaktionen, in denen das Stickstoffmolekül chemisch umgesetzt wird; Substitution und Reaktionen der im Komplex gebundenen sonstigen Liganden; katalytische Aktivität der Komplexe. Anschließend werden die Faktoren behandelt, die die Stabilität der Übergangsmetall-Stickstoff-Komplexe beeinflussen. Zum Abschluß werden die gemischten Systeme der Stickstoff-Fixierung erörtert.

Die Abhandlung lenkt die Aufmerksamkeit auf ein Gebiet, das auch für Forscher mit verhältnismäßig bescheidenen Mitteln zugänglich ist und im Falle von Erfolg eine unabsehbare praktische Bedeutung erlangen kann.

Gy. Deák

INDEX

INORGANIC AND ANALYTICAL CHEMISTRY – ANORGANISCHE UND ANALYTISCHE CHEMIE – НЕОРГАНИЧЕСКАЯ И АНАЛИТИЧЕСКАЯ ХИМИЯ

PHYSICAL CHEMISTRY – PHYSIKALISCHE CHEMIE – ФИЗИЧЕСКАЯ ХИМИЯ

ORGANIC CHEMISTRY – ORGANISCHE CHEMIE — ОРГАНИЧЕСКАЯ ХИМИЯ

Printed in Hungary

A kiadásért felel az Akadémiai Kiadó igazgatója — Műszaki szerkesztő: Várhelyi Tamás

A kézirat nyomdába érkezett: 1971. V. 24. — Terjedelem: 15,5 (A/5) ív, 74 ábra

71.71844 Akadémiai Nyomda, Budapest — Felelős vezető: Bernát György

ACTA CHIMICA

ТОМ 70 — ВЫП. 1–2.

РЕЗЮМЕ

Получение и свойства боротрипирролила

П. САРВАШ, Б. ДЬЁРИ и Й. ЭМРИ

Были изучены некоторые реакции, приводящие к образованию боротрипирролила. Было найдено, что взаимодействие BF_3, BCl_3 и B_2H_6 с $K(NC_4H_4)$, а также $K[BH(NC_4H_4)_3]$ с BF_3 и HCl, при соответствующем молярном отношении компонентов, приводит к образованию боротрипирролила.

Для получения и выделения боротрипирролила был разработан пригодный препаративный метод.

Химическое поведение боротрипирролила характеризуется следующими реакциями: быстро реагирует с водой, метанолом и уксусной кислотой, образуя при этом $B(OH)_3$, $B(OCH_3)_3$ и $B_2O(OOCCH_3)_4$, соответственно. С аммиаком и пиридином дает комплексы соответствующего состава. С LiH, NaH, LiC_6H_5 и $K(NC_4H_4)$ образует стабильные анионные комплексы. Однако, в противоположность вышесказанному, реагируя с $K(OCH_3)$ и $K(OC_6H_5)$, дает $K[B(NC_4H_4)_4]$ и соответствующие сложные эфиры борной кислоты.

Были получены следующие новые соединения: $B(NC_4H_4)_3$, $B(NC_4H_4)_3NH_3$, $B(NC_4H_4)_3NC_5H_5$, $Cs[BH(NC_4H_4)_3]$, $K[B(C_6H_5)(NC_4H_4)_3]$, а также новым методом был синтезирован $K[B(NC_4H_4)_4]$.

На основе химических и спектроскопических исследований было установлено, что $(NBC_4H_4)_3$ является относительно сильной кислотой Льюиса.

Описание с помощью потенциальной теории фазовых переходов первого рода

Л. МЕЗЕИ

Были обсуждены некоторые основные результаты, полученные при рассмотрении фазовых переходов с точки зрения статистической термодинамики, а также сделаны некоторые обобщения. В согласии с литературными данными, делались допущения для распределения нулевых положений фазовых интегралов, а затем рассматривалось заключение, вытекающее из формализма инверсной трансформации Лапласа. После этого определялась связь между функциями, характерными для «двухразмерного» электростатического поля, и полем, описываемым «статистическими термодинамическими комплексными потенциалами». При анализе этой связи объяснялся физический смысл формализма, предложенного впервые Ли и Янгом. Инверсия использованного хода рассуждений показывает, как возникает из расхождений между строением отдельных фаз, широко распространенный в настоящее время математический формализм в обсуждении фазовых переходов.

Радиационная химия систем насыщенных и несасыщенных углеводородов, IV

Влияние циклической структуры на радиационно-химический выход водорода из углеводородов с пятью-восьмью углеводородными атомами

Г. ФЕЛЬДИАК и Л. ВОЙНАРОВИЧ

Определялись величины $Чn_2$ для смесей между алканами с 5—8 атомами углерода (н-пентан, н-гексан, и-гептан- н-октан; циклопентан, циклогексан, циклогептан, циклооктан) и алкенами с одинаковым числом углеродных атомов (1-н-пентен, I-н-гексен, I-н-октен; циклопентен, циклогексен, циклогептен, циклооктен), а также величины G_{H_2} истых компонентов при температуре 35 ± 3°С и при интегральной дозе 4,4 Мрад. Было установлено, что напряжение, возникающее вследствие закрытия кольца, а также характерные свойства, определяемые строением молекулы сильно влияют на выход водорода в случае циклических углеводородов. Величины G_{H_2} для смесей, содержащих насыщенные линейные углеводороды, во всех случаях ниже величин, полученных для смесей насыщенных-ненасыщенных углеводоров, содержащих циклический алкан. Наблюдаемое явление объяснялось тем, что в случае циклоалканов мономолекулярные процессы, вследствие напряженности в кольце, протекают быстрее, чем в случае алифатических алканов, и т. о. для протекания бимолекулярных процессов «защиты» остается относительно меньшее время.

Колебательные спектры ртутноорганических соединений, VIII

ИК- и раман-спектры аллильных ртутных соединений

Я. МИНК и Ю. А. ПЕНТИН

Изучались ИК- (3200—200 см $^{-1}$) и Раман-спектры хлористой и бромистой аллильртути в твердой фазе и в растворах.

Проводилось отнесение измеренных полос. Колебательный расчет для галогенидов аллильртути проводился для трех конфигураций: цис, промежуточная и транс. Наилучшее приближение наблюдалось в случае промежуточной модели.

Силовое поле хлористой и бромистой аллильртути уточнялось с помощью метода наименьших квадратов. Были получены следующие значения валентных силовых постоянных хлористой и бромистой аллильртути: для $CH_д$ — 4,16 и 4,09. 10^6 см$^{-2}$ [2, 67 и 2,62 мдин/А], а для $НдХ$ — 3,01 и 2,87. 10^6 см$^{-2}$ [1,93 и 1,84 мдин/А], соответственно. Было проведено отнесение полос ИК-спектра жидкой диаллильртути.

Молекулярные колебания и средние квадратичные амплитуды

Средние амплитуды в органических молекулах, содержащих карбонильную группу

С. Й. СИВИН и Б. ВИЗИ

Сообщение представляет собой обзор средних амплитуд колебаний (l) органических молекул с карбонильной группой, полученных на основе электроннодиффракционных измерений и сректроскопических расчетов. Приводятся характерные величины средних амплитуд колебаний (С = 0) карбонильных групп. В сообщении приводятся также новые данные для анализа ацетона методом нормальных координат, а также приводятся расчетные величины средних квадратичных амплитуд колебаний атомов и средних амплитуд. Помимо этого, здесь могут быть найдены новые данные относительно средних амплитуд колебаний трех изотопных производных мономерной муравьиной кислоты.

Гликозиды семейства Solanum, VII

Качественное и препаративное разделение метилированных простых сахаров

М. М. ШАБАНА и П. БИТЕ

Был разработан простой и быстрый метод качественного и препаративного разделения 2,3,4-три О-метил-L-рамнозы и 2,3,4,6-тетра-О-метил-D-глюкозы, а также 3,4,6-три-О-метил-D-глюкозы и 4,6-ди-О-метил-D-галактозы с помощью тонкослойной и колонной хроматографий.

Химические свойства производных 4H-1,3-бензтиазина, III

Гидролиз бромистого 2-фенил-3-этил-6,7-диметокси-4H-1,3-бензтиазиния

Й. САБО, И. ВАРГА, Э. ВИНКЛЕР и Е. БАРТОШ

При гидролизе бромистого 2-фенил-3-этил-6,7-диметокси-4H-1,3-бензтиазиния было обнаружено, что под влиянием расчетного количества щелочи он превращается через гидроокись 2-фенил-3-этил-6,7-диметокси-4H-1,3-бензтиазиния в 2-фенил-2-гидрокси-3-этил-6,7-диметокси-2 3-дигидро-4H-1,3-бензтиазин, который под влиянием избытка щелочи превращается дальше в N-(бензоил)-N-(этил)-4,5-диметокси-2-меркапто-бензиламин. При кислом гидролизе бромистого 2-фенил-3-этил-6,7-диметокси-4H-1,3-бензтиазиния на первой ступени образуется бромистый S-(бензоил)-N-(этил)-4,5-диметокси-2-меркапто-бензил-аммоний, который с дальнейшим межмолекулярным переацилированием превращается в бромистый N-(этил)-4,5-диметокси-2-меркапто-бензил-аммоний и S,N-(дибензоил)-N-(этил)-4,5-диметокси-2-меркапто-бензиламин. Бромистый S-(бензоил)-N-(этил)-4,5-диметокси-2-меркапто-бензил-аммоний превращается под влиянием щелочи за счет внутримолекулярного переацилирования в N-(бензоил)-N-(этил)-4,5-диметокси-2-меркапто-бензиламин. S,N-ациловая перегруппировка является обратимой, т. к. N-(бензоил)-N-(этил)-4,5-диметокси-2-меркапто-бензиламин, реагируя с кислотой, дает S-бензоиловое производное. С помощью этого гидролиза была подтверждена структура бромистого 2-фенил-3-этил-6,7-диметокси-4H-1,3-бензтиазиния и была открыта возможность получения N-этиловых производных 4,5-диметокси-2-меркапто-бензиламина.

Ассоциационная структура 3-гидроксихромонов

П. ШОХАР, Л. ВАРГА и Й. КУСМАНН

ИК-спектроскопическими исследованиями было доказано, что в твердой фазе 2-метил-3-гидроксихромон находится в форме циклического димерного ассоциата, вместо хелатной структуры с 5-членным циклом за счет внутримолекулярной водородной связи, как полагалось ранее. Спектр ЯМР исключает возможность образования таутомера, и, таким образом, расщепление карбонильной полосы в ИК-спектре даже в растворе является, вероятно, результатом резонанса Ферми. Молекулы соответствующего 2-фенил-производного (флавонола) находятся в состоянии простого межмолекулярного (не циклического) ассоциата.

Получение DL-N-метил-N-пропинил-1-фенил-2-аминопропангидрохлорида (Cardison), меченного изотопом C^{14} и тритием

И. МЕЗЁ, Б. ТАНАЧ, И. ТЕПЛАН, Л. БУРШИЧ и Й. МАРТОН

Из этилацетата-1-C^{14} синтезировался фенилацетон-2-C^{14}. Из последнего с помощью восстанавливающего аминолиза приготовлялся DL-N-метил-фенил-изопропиламин-2-C^{14}-пропаргилированием которого был получен DL-N-метил-N-пропинил-1-фенил-2-амино, пропан-2-C^{14}-гидрохлорид (Cardison-2-C^{14}). Различными путями были синтезированы такеж Cardison-1-H^3 и Cardison-2-H^3.

Синтез аналога «Квантрила», содержащего индоло-хинолизидиновое кольцо

Л. НОВАК, Н. БАНГ и Ч. САНТАИ

Исходя из соединения I при взаимодействии с полуэфиром калия малоната и по следующей реакцией с эфиром акриловой кислоты и гидридом натрия, был приготовлен кетоэфир VIIb. Реакция последнего с диэтиламином, натрийборогидридом и ангидридом уксусной кислоты приводит к образованию аналога «Квантрила», содержащего циклическую систему индоло-хинолизидина (IIb).

Производные пиперазина, III

Диэтилкарбамильные и ксантеновые производные

Л. ТОЛДИ, Й. ТОТ, Й. БОРШИ и Ф. АНДРАШИ

Были синтезированы многочисленные 1-R'-4-R-пиперазины, а также 1-R'-4-β-[4-(R)-пиперазинил-1]-этилпиперазины и изучалось их влияние на язву желудка.

Было найдено несколько групп соединений, обладающих антиульцерогенным действием, среди которых наибольшие преимущества, вследствие хорошего перорального рассасывания, имеют 1-(ксантен-9-карбонил)-4-β-[4-)алкил)-пиперазинил-1]-этилпиперазины. Эти соединения сильно препятствуют возникновению экспериментальных язв, образующихся по центральному механизму, и в то же самое время обладают антихолинергным влиянием. Так в качестве потенциального противоязвенного лекарства, в первую очередь, может быть использован 1-(ксантен-9-карбонил)-4-β-[4-(изобутил)-пиперазинил-1]-этилпиперазин.

Изучение синтеза 2,4,6-триарил-пирилий-фтороборатов из ароматических альдегидов и производных ацетофенона II

Получение пирилий-фтороборатов с помощью катализа

З. ЧЮРЁШ, ДЬ. ДЕАК и П. ШАЛЛАИ

Были синтезированы некоторые триарил-пирилийфтороборатов из бензальдегида и ацетофенона, а также их замещенных в кольце производных, в растворе абс. уксусной кислоты и в присутствии трехфтористого бора. Максимальный выход был достигнут при молярном отношении альдегид : кетон : $BF_3 = 1 : 2 : 4$; выход зависит от природы заместителя. Было установлено, что самой медленной ступенью этой трехступенчатой реакции является присоединение по Михаэлю ацетофенона к бензилиден-ацетофенону.

Химия 1,3-бифункциональных систем, XII

Изучение кинетки реакций превращения триметиленхлоргидрина и его 2-монозамещенных производных в щелочных средах

М. БАРТОК, К. ЛАНГ-ЛАКОШ и Г. БОЗОКИ-БАРТОК

Исследовалась кинетика реакции щелочного гидролиза триметиленхлоргидрина (I), а также его некоторых 2-монозамещенных гомологов [2-метил- (II), 2-изопропил- (III), 2-н-бутил- (IV), 2-фенил- (V) и 2-циклогексил-тргиметиленхлоридринов (VI)]. При изученных условиях в основном образуются соответствующие гомологи оксациклобутана. В случае соединения V основным направлением превращения является образование 2-фенил-аллилового спирта в результате процесса 1,2-элиминации. На основе экспериментальных данных были рассчитаны константы скоростей, энергии активации, энтропии активации, а также предэкспоненциальные множители. Данными экспериментальными результатами подтверждалась справедливость механизма реакции, предложенного авторами ранее, и для данного типа соединений.

The Acta Chimica publish papers on chemistry in English, German, French and Russian.

The Acta Chimica appear in volumes consisting of four parts of varying size, 4 volumes being published a year.

Manuscripts should be addressed to

Acta Chimica
Budapest 112/91 Műegyetem

Correspondence with the editors should be sent to the same address.

The rate of subscription is $ 16.00 a volume.

Orders may be placed with "*Kultúra*" Foreign Trade Company for Books and Newspapers (Budapest I., Fő utca 32. Account No. 43-790-057-181) or with representatives abroad.

Les Acta Chimica paraissent en français, allemand, anglais et russe et publient des mémoires du domaine des sciences chimiques.

Les Acta Chimica sont publiés sous forme de fascicules. Quatre fascicules seront réunis en un volume (4 volumes par an).

On est prié d'envoyer les manuscrits destinés à la rédaction à l'adresse suivante:

Acta Chimica
Budapest 112/91 Műegyetem

Toute correspondance doit être envoyée à cette même adresse.

Le prix de l'abonnement est de $ 16.00 par volume.

On peut s'abonner à l'Entreprise pour le Commerce Extérieur de Livres et Journaux «*Kultúra*» (Budapest I., Fő utca 32. Compte-courant No. 43-790-057-181) ou à l'étranger chez tous les représentants ou dépositaires.

«*Acta Chimica*» издают трактаты из области химической науки на русском, французском, английском и немецком языках.

«*Acta Chimica*» выходят отдельными выпусками разного объема. 4 выпуска составляют один том. 4 тома публикуются в год.

Предназначенные для публикации рукописи следует направлять по адресу:

Acta Chimica
Budapest 112/91 Műegyetem

По этому же адресу направлять всякую корреспонденцию для редакции.

Подписная цена — $ 16.00 за том.

Заказы принимает предприятие по внешней торговле книг и газет «*Kultúra*» (Budapest I., Fő utca 32. Текущий счет № 43-790-057-181) или его заграничные представительства и уполномоченные.

Reviews of the Hungarian Academy of Sciences are obtainable at the following addresses:

ALBANIA

Drejtorija Qändrone e Pärhapjes dhe Propagandimit të Librit
Kruga Konferenca e Päzes
Tirana

AUSTRALIA

A. Keesing
Box 4886, GPO
Sydney

AUSTRIA

GLOBUS
Höchstädtplatz 3
A-1200 Wien XX

BELGIUM

Office International de Librairie
30, Avenue Marnix
Bruxelles 5
Du Monde Entier
5, Place St. Jean
Bruxelles

BULGARIA

HEMUS
11 pl Slaveikov
Sofia

CANADA

Pannonia Books
2, Spadina Road
Toronto 4, Ont.

CHINA

Waiwen Shudian
Peking
P. O. B. 88

CZECHOSLOVAKIA

Artia
Ve Smečkách 30
Praha 2
Poštovní Novinová Služba
Dovoz tisku
Vinohradská 46
Praha 2
Mad'arská Kultura
Václavské nám. 2
Praha I
SLOVART A. G.
Gorkého
Bratislava

DENMARK

Ejnar Munksgaard
Nörregade 6
Copenhagen

FINLAND

Akateeminen Kirjakauppa
Keskuskatu 2
Helsinki

FRANCE

Office International de Documentation et Librairie
48, rue Gay Lussac
Paris 5

GERMAN DEMOCRATIC REPUBLIC

Deutscher Buch-Export und Import
Leninstraße 16
Leipzig 701
Zeitungsvertriebsamt
Fruchtstraße 3—4
1004 Berlin

GERMAN FEDERAL REPUBLIC

Kunst und Wissen
Erich Bieber
Postfach 46
7 Stuttgart S.

GREAT BRITAIN

Blackwell's Periodicals
Oxenford House
Magdalen Street
Oxford
Collet's Subscription Import Department
Dennington Estate
Wellingsborough. Northants.
Robert Maxwell and Co. Ltd.
4—5 Fitzroy Square
London W. I

HOLLAND

Swetz and Zeitlinger
Keizersgracht 471—487
Amsterdam C.
Martinus Nijhof
Lange Voorhout 9
The Hague

INDIA

Hind Book House
66 Babar Road
New Delhi I

ITALY

Santo Vanasia
Via M. Macchi 71
Milano
Libreria Commissionaria Sansoni
Via La Marmora 45
Firenze
Techna
Via Cesi 16.
40135 Bologna

JAPAN

Kinokuniya Book-Store Co. Ltd.
826 Tsunohazu 1-chome
Shinjuku-ku
Tokyo
Maruzen and Co. Ltd.
P. O. Box 605
Tokyo-Central

KOREA

Chulpanmul
Phenjan

NORWAY

Tanum-Cammermeyer
Karl Johansgt 41—43
Oslo I

POLAND

RUCH
ul. Wronia 23
Warszawa

ROUMANIA

Cartimex
Str. Aristide Briand 14—18
Bucureşti

SOVIET UNION

Mezhdunarodnaya Kniga
Moscow G—200

SWEDEN

Almquist and Wiksell
Gamla Brogatan 26
S—101 20 Stockholm

USA

F. W. Faxon Co. Inc.
15 Southwest Park
Westwood Mass. 02090
Stechert Hafner Inc.
31. East 10th Street
New York, N. Y. 10003

VIETNAM

Xunhasaba
19, Tran Quoc Toan
Hanoi

YUGOSLAVIA

Forum
Vojvode Mišića broj 1
Novi Sad
Jugoslovenska Knjiga
Terazije 27
Beograd

29. X. 1971

Index: 26.007

ACTA CHIMICA

ACADEMIAE SCIENTIARUM HUNGARICAE

TOMUS 70 FASCICULUS 3

AKADÉMIAI KIADÓ, BUDAPEST

1971

ACTA CHIM. (BUDAPEST) ACASA 2 70 (3) 175—289 (1971)

ACTA CHIMICA

A MAGYAR TUDOMÁNYOS AKADÉMIA KÉMIAI TUDOMÁNYOK OSZTÁLYÁNAK IDEGEN NYELVŰ KÖZLEMÉNYEI

Az Acta Chimica német, angol, francia és orosz nyelven közöl értekezéseket a kémia tudományok köréből.

Az Acta Chimica változó terjedelmű füzetekben jelenik meg, egy-egy kötet négy füzetből áll. Évente átlag négy kötet jelenik meg.

A közlésre szánt kéziratok a szerkesztőség címére (Budapest 112/91 Műegyetem) küldendők.

Ugyanerre a címre küldendő minden szerkesztőségi levelezés. A szerkesztőség kéziratokat nem ad vissza.

Megrendelhető a belföld számára az „Akadémiai Kiadó"-nál (Budapest V., Alkotmány utca 21. Bankszámla 05-915-111-46), a külföld számára pedig a „Kultúra" Könyv- és Hírlap Külkereskedelmi Vállalatnál (Budapest I., Fő utca 32. Bankszámla: 43-790-057-181) vagy annak külföldi képviseleteinél és bizományosainál.

Die Acta Chimica veröffentlichen Abhandlungen aus dem Bereiche der chemischen Wissenschaften in deutscher, englischer, französischer und russischer Sprache.

Die Acta Chimica erscheinen in Heften wechselnden Umfanges. Vier Hefte bilden einen Band. Jährlich erscheinen 4 Bände.

Die zur Veröffentlichung bestimmten Manuskripte sind an folgende Adresse zu senden:

Acta Chimica
Budapest 112/91 Műegyetem

An die gleiche Anschrift ist auch jede für die Redaktion bestimmte Korrespondenz zu richten. Abonnementspreis pro Band: $16.00.

Bestellbar bei dem Buch- und Zeitungs-Außenhandels-Unternehmen »*Kultúra*« (Budapest I., Fő utca 32. Bankkonto No. 43-790-057-181) oder bei seinen Auslandsvertretungen und Kommissionären.

Acta Chimica Academiae Scientiarum Hungaricae, Tomus 70 (3), pp. 175—184 (1971)

KINETICS AND MECHANISM OF SUBSTITUTION REACTIONS OF COMPLEXES, XXXVI

FORMATION OF THE *CIS*-$[CoBR(en)_2(\beta\text{-PICOLINE})]^{2+}$ AND *CIS*-$[CoBR(en)_2(\gamma\text{-PICOLINE})]^{2+}$ COMPLEX IONS AND THEIR AQUATION IN ACID SOLUTIONS

J. ZSAKÓ, Cs. VÁRHELYI and S. BLEOCA
(Faculty of Chemistry, Babeş-Bolyai University, Cluj, Rumania)

Received June 12, 1970

The syntheses of *cis*-$[CoBr(en)_2(\beta\text{-picoline})]^{2+}$, *cis*-$[CoBr(en)_2(\gamma\text{-picoline})]^{2+}$ and of 24 new salts of these ions are reported. The UV, visible and IR spectra are discussed. The aquation kinetics of these complex ions are studied in acid solutions and activation enthalpy and entropy values are reported. An S_N1 mechanism is suggested. The results are compared with the kinetic behaviour of the analogous chloro derivatives. The inductive effect of the coordinated amine upon the release of the halide ion is discussed.

The number of the $[CoBr(en)_2(amine)]^{2+}$-type complexes is much smaller than that of the analogous chloro derivatives. Several complexes with aromatic and aliphatic amines have been described [1—4]. The synthesis of complexes of the above type, containing pyridine and pyridine derivatives, has been reported in our previous paper [5].

In the present paper the β- and γ-picoline derivatives are described. The composition of the new complex cations was checked by isolating 24 products of double exchange reactions. These complexes are isomeric compounds, owing to the position or structural isomerism of the ligands. This is why the properties of their salts, such as solubility, absorption spectra, thermal stability, etc. are very similar. The behaviour of the complex ions studied is very close also to that observed in the case of the analogous pyridine derivative [5]. Concentrated aqueous solutions of $NaNO_3$, NaI, $NaClO_3$, $NaClO_4$ and $Na[BF_4]$ precipitate readily soluble crystalline products from the aqueous solutions of $[CoBr(en)_2(\beta\text{-picoline})]\,Br_2$ and $[CoBr(en)_2(\gamma\text{-picoline})]\,Br_2$. The products of the double exchange reaction with picric acid, with Erdmann's salt and especially with Reinecke's salt, similarly to those described in Ref. [6], are sparingly soluble. Complex acids of the $H[Co(dioxime)_2X_2]$ type do not precipitate the complex cations studied even from their concentrated aqueous solutions.

With colourless anions both complex cations form red salts. The absorption spectra of the nitrates in the visible and UV region are given in Fig. 1.

The characteristic spectral data are the following:
cis-$[CoBr(en)_2(\beta\text{-picoline})]\,(NO_3)_2$:

λ_1 (nm)	log ε_1	λ_2 (nm)	log ε_2	λ_3 (nm)	log ε_3	λ_4	log ε_4
530—540	2.39	370_i	2.70	300_i	3.65	250	4.57

cis-$[CoBr(en)_2(\gamma\text{-picoline})]\,(NO_3)_2$:

λ_1 (nm)	log ε_1	λ_2 (nm)	log ε_2	λ_3 (nm)	log ε_3	λ_4	log ε_4
530—545	2.28	360_i	2.80	300_i	3.65	240	4.40

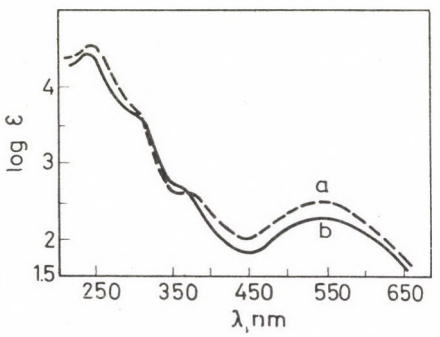

Fig. 1. Visible and UV absorption spectra of $[CoBr(en)_2(\beta\text{-picoline})]\,(NO_3)_2$ *(a)* and of $[CoBr(en)_2(\gamma\text{-picoline})]\,(NO_3)_2$ *(b)*

The IR spectra have been recorded, too, one example being given in Fig. 2.

These spectra enable us to make a choice between the *cis* and *trans* configurations, on the basis of the CH_2-rocking frequencies of the cobalt-ethylenediamine rings. These frequencies are presented in Table I for the complexes studied in comparison with some alkylamine derivatives examined

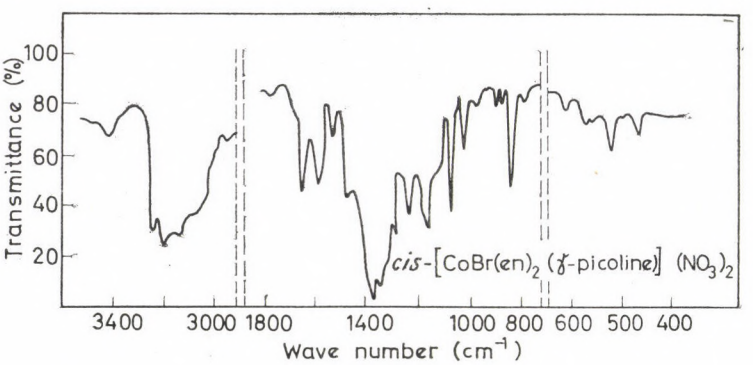

Fig. 2. IR spectrum of $[CoBr(en)_2(\beta\text{-picoline})]\,(NO_3)_2$

by BALDWIN [7] and by CHAN *et al.* [8]. Since in the 870—900 cm^{-1} region two rocking frequencies appear, the studied complexes must be of the *cis* configuration. The 512 (499) cm^{-1} and 462 (466) cm^{-1} absorption bands, which appear in the case of $[Co(NH_3)_6]\ Cl_3$, too, can be assigned probably to the Co–N stretch which is consistent with the covalent character of the Co–N bond. The N—H stretching frequencies (3220—30, 3130—40 cm^{-1}) are indicative of the strong covalent character of the Co–N bond.

Table I

CH_2-rocking frequencies (cm^{-1}) in the infrared spectra of some $[Co(en)_2XY]X$ type complexes

Formula	Frequency	Reference
trans-$[CoCl(en)_2NH_3]\ (ClO_4)_2$	888	[7]
cis-$[CoCl(en)_2NH_3]\ (NO_3)_2$	900, 893	[7]
trans-$[Co(en)_2(NH_3)(H_2O)]\ (NO_3)_3$	888	[7]
cis-$[CoCl(en)_2(pyridine)]\ (NO_3)_2$	899, 883	[10]
$[CoBr(en)_2(\beta\text{-picoline})]\ (NO_3)_2$	900, 880	
$[CoBr(en)_2(\gamma\text{-picoline})]\ (NO_3)_2$	902, 882	

The aquation kinetics of $[CoBr(en)_2(amine)]^{2+}$ type complexes are scarcely studied. The solvolytic aquation, *i.e.* the aquation in neutral solutions, has been studied by CHAN *et al.* [8] for several complexes with amine (isopropylamine, *n*-propylamine, allylamine, prop-2-ynylamine, ethylamine and methylamine). Since under such conditions the base hydrolysis is not entirely suppressed, their experimental data could not lead to reliable activation enthalpy and entropy values. As shown in our previous papers [5, 9, 10], a hydrogen ion concentration of at least $10^{-3}M$ is needed to suppress base hydrolysis. The aquation of $[CoBr(en)_2\ (pyridine)]^{2+}$ in acid solutions has been described in our previous paper [5] and the aquation rate has been found to be about 3 times larger than in the case of the analogous chloro derivative. This result is consistent with literature data concerning the aquation rate of bromopentamine and chloropentamine type complexes [8, 11—13]. The activation enthalpy has been found to be less than that for the analogous chloro derivatives.

In the present paper the aquation of the $[CoBr(en)_2(\beta\text{-picoline})]^{2+}$ and $[CoBr(en)_2(\gamma\text{-picoline})]^{2+}$ complex ions has been studied. The same aquation reaction occurs as in the case of the $[CoBr(en)_2(pyridine)]^{2+}$ ion [5], and the analogous chloro derivatives [9, 10], studied earlier, *viz.* the halide ion is replaced by a water molecule in an apparently first order reaction:

$$[CoBr(en)_2(amine)]^{2+} + H_2O = [Co(en)_2\ H_2O(amine)]^{3+} + Br^- \qquad (1)$$

The substitution of Br ions has been followed by titration with a silver nitrate solution. The plot of log C_0/C against time showed good linearity, which enabled us to derive apparent first order rate constants. The influence of perchloric acid upon the reaction rate has been studied. This influence is the same as in the case of the $[CoCl(en)_2(amine)]^{2+}$ type complexes [9,10], and of $[CoBr(en)_2(pyridine)]^{2+}$ [5], *i.e.* the rate constant decreases with increasing

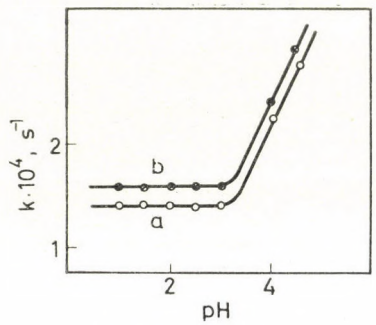

Fig. 3. Influence of perchloric acid upon the rate of reaction (1). $t = 60$ °C, a — $[CoBr(en)_2(\beta\text{-picoline})]^{2+}$, b — $[CoBr(en)_2(\gamma\text{-picoline})]^{2+}$

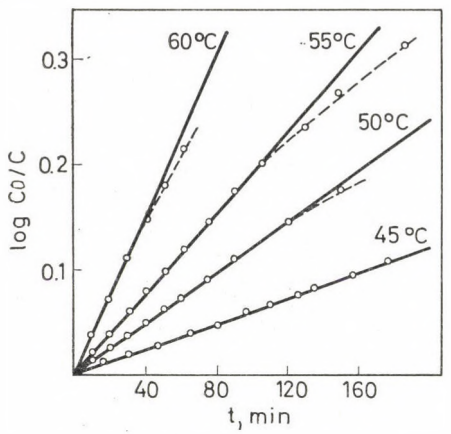

Fig. 4. Determination of the first order rate constants of reaction (1) for $[CoBr(en)_2(\beta\text{-picoline})]^{2+}$

acidity, until $[H^+]$ reaches the value of about 10^{-3} M, and then remains practically constant in spite of further increases in $[H^+]$. This effect is illustrated in Fig. 3.

The influence of the temperature has been studied in order to determine the activation enthalpy and entropy values. All the kinetic runs were carried out in solutions with $[H^+] = 10^{-3}$ M and at a constant ionic strength of $\mu = 0.1$ M. The plot of log C_0/C against time for several runs is given in Fig. 4.

As seen from the figure good linearity is observed at the beginning of the aquation but at higher conversion degrees negative deviations appear, indicating the reversible character of the aquation reaction, reported also by CHAN *et al.* [8] in the case of other $[CoBr(en)_2(amine)]^{2+}$ type complexes. From the slopes of the straight lines, corresponding to the linear portion of the log C_0/C *vs.* t curves, first order rate constants have been calculated. Mean values of these rate constants are given in Table II (k_{Br}).

Table II

First order rate constants of reaction (1) in acid solutions for $[CoBr(en)_2(amine)]^{2+}$ type complexes (k_{Br}), as compared with the same data for $[CoCl(en)_2(amine)]^{2+}$ complexes (k_{Cl})

Amine	t (°C)	$k_{Br} \cdot 10^4$ (s^{-1})	$k_{Cl} \cdot 10^4$ (s^{-1})*	k_{Br}/k_{Cl}
β-picoline	45	0.24	—	—
	50	0.46	0.13	3.54
	55	0.77	—	—
	60	1.41	0.41	3.44
γ-picoline	50	0.53	0.15	3.53
	55	1.00	—	—
	60	1.62	0.47	3.45
	65	2.80	0.92	3.04

* taken from Ref. [10]

The plot of log k against $1/T$ shows good linearity, as seen in Fig. 5. By means of the least square method, the following activation enthalpy and entropy values have been calculated

$[CoBr(en)_2(\beta\text{-picoline})]^{2+}$: $\Delta H^{\ddagger} = 23.6 \pm 0.5$ kcal/mole; $\Delta S^{\ddagger} = -5.5 \pm 1.2$ e.u.

$[CoBr(en)_2(\gamma\text{-picoline})]^{2+}$ $\Delta H^{\ddagger} = 23.2 \pm 0.6$ kcal/mole; $\Delta S^{\ddagger} = -6.4 \pm 1.5$ e.u.

Errors have been calculated in the usual statistical way, on the basis of the standard deviations, using tabulated $t_{0\,95}$ values.

By comparing the kinetic behaviour of the complexes studied with that of the analogous chloro complexes, one can see that the aquation rate of the bromo derivatives is about 3 times larger than that of the chloro derivatives (*cf.* Table II). This is in agreement with the above mentioned literature data concerning the aquation of bromo- and chloropentamine type complexes [5, 8, 11—13].

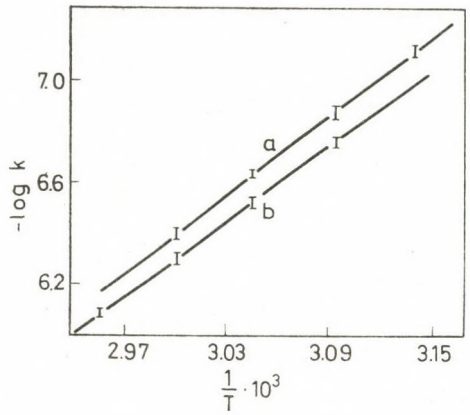

Fig. 5. Determination of the activation enthalpy and entropy of reaction (1) in acid solutions. *a* — $[CoBr(en)_2(\beta\text{-picoline})]^{2+}$, *b* — $[CoBr(en)_2(\gamma\text{-picoline})]^{2+}$

It is interesting to compare the activation enthalpies and entropies with values obtained earlier. All these values are presented in Table III, together with the pK_b values of the corresponding amines [14].

Table III

Activation parameters of reaction (1) for $[CoX(en)_2(amine)]^{2+}$ type complexes

Amine	pK_b at 25°	$\Delta H^{\ddagger}$ (kcal/mole)		$\Delta S^{\ddagger}$ (e.u.)	
		X = Br	X = Cl	X = Br	X = Cl
pyridine	8.57	23.8	24.4	−5.1	−5.0
β-picoline	8.26	23.6	24.4	−5.5	−5.0
γ-picoline	7.94	23.2	24.3	−6.4	−5.0
benzylamine	4.63	—	24.2	—	−8.6

It can be seen that the activation enthalpy values are smaller for the bromo complexes than for the corresponding chloro derivatives. This can be explained easily if we assume an S_N1 mechanism for reaction (1). In this case only bond breaking is involved in the formation of the transition state, and so the activation enthalpies are expected to be in the order Br < Cl [8], *i.e.* the same as for the dissociation energies of the cobalt–halogen bonds. The assumed S_N1 mechanism is consistent also with the obtained activation entropy values. In all the cases studied $\Delta S^{\ddagger}$ has small negative values. Since the release of the halide ion leads to an increased electric charge, *i.e.* to stronger hydration, the negative activation entropy values are understandable.

The activation enthalpies reported by CHAN *et al.* [8] cannot be compared with the present values since the corresponding kinetic measurements have

been made in neutral solutions. Under such conditions the apparent activation enthalpies can be much larger than the real ones. Thus, for the aquation of $[CoCl(en)_2(\gamma\text{-picoline})]^{2+}$ we have found $\Delta H^{\ddagger} = 26.1$ kcal/mole in neutral solutions [15], while in acid solutions only 24.3 kcal/mole [10]. Since in neutral solutions the base hydrolysis is not entirely suppressed, the physical significance of the apparent activation enthalpy is rather obscure. CHAN *et al.* [8] have found in two cases the activation enthalpy of the bromo complex to be smaller than that of the chloro derivative, the opposite having been observed in 4 other cases. These authors assume an S_N1 mechanism in the former, and an S_N2 mechanism in the latter case. We consider the activation enthalpy values reported by CHAN *et al.* for both the bromo and chloro derivatives to be too large and we are of the opinion that the larger values for the bromo derivatives, as compared with the chloro complexes, can result also from the superposition of the aquation reaction and of base hydrolysis, thus they are certainly not due to an S_N2 mechanism.

The pK_b values of the amine ligands have been included in Table III, in order to check on the existence of an inductive effect of the amine molecule. It is obvious that the pK_b and $\Delta H^{\ddagger}$ values vary in parallel. Since the increasing basic character corresponds to a decreasing electron-withdrawing character, the stronger the coordinated base, the weaker the cobalt–halogen σ bond, and the smaller the activation enthalpy for the release of the halogen in an S_N1 reaction. This inductive effect is quite insignificant in the case of the chloro derivatives, and not exceeding the expected experimental error, but it is more definite in the case of the bromo complexes. The higher sensitivity of the Co–Br bond towards this inductive effect can be assigned to its stronger covalent character relative to the Co–Cl bond.

Experimental

Synthesis of *cis*-$[CoBr(en)_2(\beta\text{-picoline})]\ (NO_3)_2$ (I) and *cis*-$[CoBr(en)_2(\gamma\text{-picoline})]\ (NO_3)_2$ (II)

42 g (0.1 mole) of *trans*-$[CoBr_2(en)_2]$ Br, completely acid-free, are dissolved in 150 ml water and 10 g (0.11 mole) of β-picoline (or γ-picoline) are added dropwise. The yellow-green solution becomes gradually violet-red. After standing for about 12 hrs, the solution is filtered and mixed with a concentrated aqueous solution of 100 g $NaNO_3$. After a short time a brilliant, reddish-violet precipitate, consisting of irregular plates, appears.
After 15—20 min. the substance is filtered, washed with ice water and dried in air.

Yield:	**I**	45%
	II	60%
Found	**(I)**	Co 12.20; NO_3 25.90%
	(II)	Co 12.32; NO_3 26.10%.

Calcd. $[CoBr(C_2H_8N_2)_2(CH_3C_5H_4N)]\ (NO_3)_2$ (475.98): Co 12.38; NO_3 26.05%.

Synthesis of the new products. 25 ml of an aqueous solution, containing 5 mmoles of *trans*-$[CoBr_2(en)_2]$ Br are treated with 5 mmoles of β-picoline (γ-picoline) in the above described manner, then one of the following solutions is added: 25 ml 25% solution of NH_4Br; 25 ml 20% solution of NaI, 15 ml conc. solution of $NaBF_4$; 25 ml 30% solution of $HClO_4$;

Table IV

New derivatives of the type $[CoBr(en)_2(\beta\text{-picoline})]X_2$ *and* $[CoBr(en)_2(\gamma\text{-picoline})]X_2$

No.	Isomer	X	Mol. weight calcd.	Yield %	Appearance	Analysis		
						Calcd.		Found
1.	β	Br	511.8	40	red-violet prisms	Co Br^-	11.51 31.23	11.43 31.03
2.	γ	Br	511.8	50	red-violet prisms	Co Br^-	11.51 31.23	11.36 30.94
3.	β	I	605.8	55	red-brown prisms	Co I	9.73 41.90	9.52 41.10
4.	γ	I	605.8	63	red-brown dendrites	Co I	9.73 41.90	9.61 42.20
5.	β	BF_4	525.6	50	red-violet rectangular prisms	Co	11.21	11.14
6.	γ	BF_4	525.6	55	red-violet rectangular prisms	Co	11.21	11.24
7.	β	ClO_4	550.9	60	thick, regular plates	Co ClO_4	10.70 36.10	10.53 35.70
8.	γ	ClO_4	550.9	70	red-violet irregular dendrites	Co ClO_4	10.70 36.10	10.44 35.24
9.	β	$1/2\ S_2O_8$	544.1	30	red-violet hexagonal plates	Co S_2O_8	10.83 35.31	10.52 35.14
10.	γ	$1/2\ S_2O_8$	544.1	25	red-violet rectangular prisms	Co S_2O_8	10.83 35.31	10.66 35.22

11.	β	1/2 Cr_2O_7	568.0	70	brown hexagonal plates	Co + 2 Cr N	28.70 12.33	28.40 12.18
12.	γ	1/2 Cr_2O_7	568.0	80	brown rhombohedral plates	Co + 2 Cr N	28.70 12.33	28.29 12.24
13.	β	picrate	808.2	80	yellow prisms	Co	7.29	7.21
14.	γ	picrate	808.2	85	yellow needles	Co	7.29	7.18
15.	β	$[Co(NO_2)_4(NH_3)_2]$	906.1	50	brilliant, yellow-brown irregular plates	Co N	19.52 26.28	19.45 26.33
16.	γ	$[Co(NO_2)_4(NH_3)_2]$	906.1	70	irregular brown prisms	Co N	19.52 26.28	19.36 26.02
17.	β	$[Cr(NCS)_4(aniline)_2]$	1293.1	90	light red microcrystals	Co + 2 Cr N	12.60 18.42	12.45 18.60
18.	γ	$[Cr(NCS)_4(aniline)_2]$	1293.1	92	light red microcrystals	Co + 2 Cr N	12.60 18.42	12.70 18.20
19.	β	$[Cr(NCS)_4(p\text{-toluidine})_2]$	1349.2	90	light red-brown microcrystals	Co + 2 Cr N	12.08 17.65	11.90 17.36
20.	γ	$[Cr(NCS)_4(p\text{-toluidine})_2]$	1349.2	95	light red-brown microcrystals	Co + 2 Cr N	12.08 17.65	12.22 17.88
21.	β	$[Cr(NCS)_4(p\text{-anisidine})_2]$	1381.2	85	light red-violet microcrystals	Co + 2 Cr N	11.80 17.24	11.54 17.01
22.	γ	$[Cr(NCS)_4(p\text{-anisidine})_2]$	1381.2	88	light red-violet microcrystals	Co + 2 Cr N	11.80 17.24	12.01 17.37

25 ml 10% solution of $K_2Cr_2O_7$; 25 ml conc. solution of $Na_2S_2O_8$; 500 ml 1% solution of picric acid; 500 ml 1% solution (in 1 : 4 ethanol–water) of NH_4 [$Cr(NCS)_4$ (aniline)$_2$]. H_2O; 500 ml 1% solution (in 1 : 3 ethanol–water) of (*p*-toluidine · H) [$Cr(NCS)_4$(*p*-toluidine)$_2$]; or 500 ml 1% solution (in the same ethanol–water mixture) of (*p*-anisidine · H) [$Cr(NCS)_4$(*p*-anisidine)$_2$]. The precipitate is filtered off after standing for 20—30 min., then washed several times with water, and dried in air. at room temperature for 3—4 days.

In Table IV are given the synthesis and analysis data for 22 new complexes of this type.

Analysis. Cobalt was determined complexometrically, after decomposing the sample with sulfuric acid and some crystals of KNO_3, in the presence of murexide as indicator. The sum of the metals was determined by weighing Co_3O_4 + Cr_2O_3, obtained after a 2 hr heating of the complex at 900—920 °C. Sulfur was determined gravimetrically as $BaSO_4$.

The anions Br^-, I^-, NO_3^- and ClO_4^- were determined volumetrically. A 0.400—0.600 g sample of the complex salt was dissolved in 50 ml water. The solution was passed through an ion exchange column (with Amberlit IR 120, R—H form) and the HBr, HI, HNO_3 or $HClO_4$ n the eluent titrated with 0.05 *M* NaOH.

Spectra. The visible and UV spectra were obtained on a Beckmann Model DB recording spectrophotometer, using aqueous solutions in 1 cm cell. The concentration of the solution was $2 \cdot 10^{-3}$ and $1 \cdot 10^{-4}$ *M*, respectively. The IR spectrum was obtained using a "UR-10-Carl Zeiss Jena" infrared spectrophotometer. Measurements were made in potassium bromide pellets.

Kinetic measurements. The weighed samples of the complexes were dissolved at the desired temperature in distilled water, and the acidity and ionic strength adjusted with $HClO_4$ and $NaNO_3$ solutions (all preheated to the temperature of the experiment). The liberation of Br^- ions was followed by potentiometric titration. 10 ml samples were cooled quickly to 0 °C, 20 ml 0.1 *M* HNO_3 was added (cooled to 0 °C too) and the bromide ion was titrated with 0.01 *M* $AgNO_3$ solution, using a silver wire as indicator electrode.

At each temperature at least three parallel runs were made with different initial concentrations of the complex ion, varying between $3 \cdot 10^{-3}$ and $6 \cdot 10^{-3}$ *M*.

REFERENCES

1. MEISENHEIMER, H., KIDERLEN, E.: Liebigs Ann. **438,** 217 (1924)
2. BAILAR, J., WORK, B. J.: J. Amer. Chem. Soc. **67,** 176 (1945)
3. BAILAR, J., CLAPP, L. B.: J. Amer. Chem. Soc. **67,** 171 (1945)
4. ABLOV, A. V.: Bull. Soc. Chim. France **4,** 1783 (1937)
5. VÁRHELYI, Cs., ZSAKÓ, J.: Revue roum. chim. **16,** 1185 (1971)
6. VÁRHELYI, Cs., GĂNESCU, I.: Monatshefte **98,** 472 (1967)
7. BALDWIN, M. E.: J. Chem. Soc. **1960,** 4369
8. CHAN, S. C., CHENG, C. Y., LEH, F.: J. Chem. Soc. (A) **1967,** 1586
9. ZSAKÓ, J., VÁRHELYI, Cs., BANICI, L.: Studia Univ. Babeş-Bolyai, Chem. **13** (2), 21 (1968)
10. ZSAKÓ, J., VÁRHELYI, Cs., DOBOCAN, D.: J. Inorg. Nucl. Chem. **31,** 1459 (1969)
11. LAMB, A., MARDEN, F.: J. Amer. Chem. Soc. **33,** 1908 (1911)
12. BUSHNELL, G. W., LALOR, G. C.: J. Inorg. Nucl. Chem. **30,** 219 (1968)
13. DAVIES, M. B., LALOR, G. C.: J. Inorg. Nucl. Chem. **31,** 799 (1969)
14. LANDOLT—BÖRNSTEIN: Zahlenwerte und Funktionen aus Physik, Chemie, Astronomie, Geophysik, Technik. II. Band, 7. Teil, Elektrische Eigenschaften, II, pp. 898—917. Springer Verlag, 1960
15. ZSAKÓ, J., VÁRHELYI, Cs., MOSTIS, J.: Studia Univ. Babeş-Bolyai, Chem. **12** (2), 127 (1967)

János ZSAKÓ
Csaba VÁRHELYI
Stela BLEOCA
Cluj, str. Arany János, 11. Rumania.

Acta Chimica Academiae Scientiarum Hungaricae, Tomus 70 (3), pp. 185–188 (1971)

SEPARATION OF TRACE ELEMENTS BY PRECIPITATION, IX

FURTHER STUDY OF THE SORPTION OF URANIUM(VI) IN CARBONATE MEDIA

E. UPOR and GY. NAGY

(Mecsek Ore Mining Enterprise, Pécs)

Received June 13, 1970

As a supplement to earlier work, a study was made of how the pH-dependence of the sorption of uranium(VI) on $Fe(OH)_3$ in carbonate media changes with the concentration of the carbonate. It was found that at low carbonate concentration (1×10^{-3} *M*), sorption is complete below pH 11 and the curve is identical with that obtained in an NaOH medium. In the case of macro amounts of uranium, however, desorption above pH 12 in carbonate solution does not occur. The slope of the log $[CO_3^{2-}]$ *vs.* log D_U straight line at different pH values is $-(1.0 \pm 0.2)$; this necessitates the further clarification of the desorption mechanism.

Introduction. Experimental methods

In earlier communications [1—3] results were reported on the sorption of uranium(VI) on metal hydroxide and other precipitates in carbonate media. The roles of the most important factors (pH, carbonate concentration, temperature, etc.) which affect the sorption were described. In the present paper we wish to report the results of some supplementary studies.

In our experiments the $Fe(OH)_3$ precipitated from 100 mg of iron(III) was used as carrier. The volume of the solution was 100 ml. $NaHCO_3$ and NaOH were used to adjust the pH. If the pH was maintained at a given value in an experiment, this was achieved with the use of a buffer solution. A pH of 9.2 was produced with a 0.2 *M* H_3BO_3 + 0.1 *M* NaOH solution, and pH's of 10.8—12.2 with 0.1 *M* glycine and 0.1 *M* NaOH solutions mixed in various ratios. The buffer solution capacity proved adequate even in 1 *M* Na_2CO_3. The pH was measured with an LPU–1 pH-meter to an accuracy of $\pm$ 0.05 pH using an NNT glass and silver–silver chloride electrode.

Uranium was determined with Arsenazo III, photometrically or by a luminescence method. Analyses were carried out at times on both the precipitate and the solution, but in general only on the phase containing the smaller amount of uranium.

Variation of uranium(VI) sorption with the pH and carbonate concentration

Experiments were carried out to decide how the applied carbonate concentration affects the pH-dependence of the sorption. In Fig. 1 it can be seen that above a certain limit, changes in the carbonate concentration affect the pH-dependence of the sorption primarily quantitatively.

However, it can be observed that with the decrease of the CO_3^{2-} concentration the position of the maximum of the curve between pH 11 and pH 13 is shifted to lower values. The minimum value of sorption increases with decreasing carbonate concentration until finally the curve becomes identical

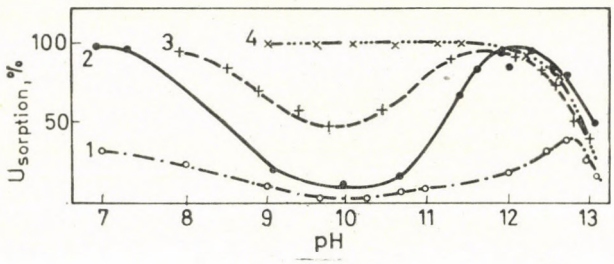

Fig. 1. Dependence of the sorption of uranium(VI) on pH at different carbonate concentrations (100 mg Fe^{3+}; 100—500 μg uranium; precipitated at 25 °C in a volume of 100 ml; filtered after 30 minutes' standing). Na_2CO_3 concentration: 1. 0.20 *M*; 2. 0.03 *M*; 3. 0.01 *M*; 4. 0.001 *M*

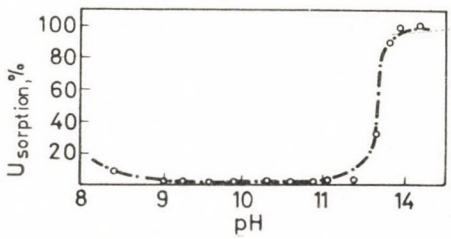

Fig. 2. Dependence of the sorption of macro amounts of uranium on the pH in Na_2CO_3 solution (100 mg Fe^{3+}; 100 mg uranium; precipitated at 25 °C in a volume of 100 ml with 0.20 *M* Na_2CO_3; filtered after 1 hour's standing)

with that obtained in an alkali metal hydroxide solution [4]. Accordingly below pH 12 the sorption will become complete through the decomposition of the carbonato complex, whereas at higher pH the uranium goes into solution as a colloid. The change of the carbonate concentration thus finally causes a qualitative change in the pH-dependence of the sorption. However, the course of the curve is affected by the uranium concentration too. In our earlier papers it was shown that for the sorption the Freundlich isotherm is valid in the region (pH = 9—10) where the sorption is caused by the hydrolytic decomposition of the carbonatouranyl complex. As has already been mentioned, above pH 12 the sorption is affected by the hydroxide ion concentration, and a result of this is the colloidal dissolution of uranium. This dissolution, however, does not take place at higher uranium concentrations [4]. This is also reflected by the pH curve (Fig. 2) with 100 mg of uranium in a carbonate medium, which differs qualitatively from the curve for an identical concentration of

Na_2CO_3 but with 100 μg of uranium (Fig. 1, curve 1). Below pH 11.4 the hydrolytic sorption of $[UO_2(CO_3)_3]^{4-}$ is relatively insignificant, while at higher pH the colloidal dissolution of uranium does not occur.

Dependence of the distribution of uranium on the carbonate concentration

From our experimental results it was possible to demonstrate a linear relation between the carbonate concentration and the uranium distribution if logarithmic values are plotted for each. In Fig. 3 can be seen the log $[CO_3^{2-}]$ *vs.* log D_U plot at four different pH values. The slopes of the straight lines are

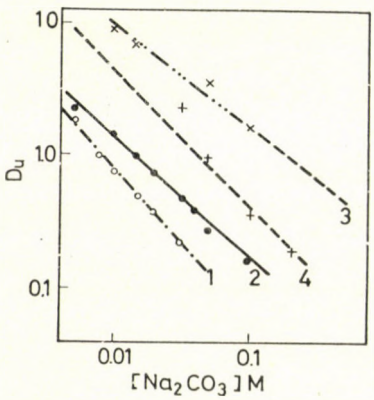

Fig. 3. Dependence of the distribution quotient for uranium(VI) sorption on the carbonate concentration at various pH values (100 mg Fe^{3+}; 500 μg uranium; precipitated at 25 °C in a volume of 100 ml; filtered after 30 minutes' standing). 1. pH = 9.2; 2. pH = 11.3; 3. pH = 11.5; 4. pH = 12.1

$-(1.0\pm0.2)$. The explanation of these values requires further considerations. The interpretation accepted for the desorption of uranium is the formation of soluble carbonato complexes and the hindrance of the hydrolytic decomposition of the complex. According to the stability constant data available in the literature [5, 6], however, under the experimental conditions quoted, the vast majority of the $[UO_2(CO_3)_3]^{4-}$ is to be found in solution. On the basis of the following schematic reaction equation:

$$M{-}UO_{2(ppt)} + n\,CO_3^{2-} \rightleftharpoons UO_2(CO_2)_n^{2-2n}{}_{(sol)} + M_{(ppt)}$$

(where $M_{(ppt)}$ is the sorbent polymeric metal hydroxide and $M{-}UO_{2(ppt)}$ is the sorbed uranium complex) this would require a value of -3 for the slope of the straight line.

From the results obtained, either it must be assumed that the local formation of monouranyl carbonate (UO_2CO_3), as the compound with the lowest

carbonate content formed in the series of complexes, is sufficient for the desorption process (in accordance with the slope of the straight line), or the explanation must be sought with a different initial consideration.

Dependence of the extent of sorption on the amount of adsorbent

Exploratory experiments were carried out to find out how the extent of sorption depends on the quantity of $Fe(OH)_3$ applied as carrier. As can be seen in Fig. 4, the logarithm of the uranium distribution quotient is a linear function of the logarithm of the amount of $Fe(OH)_3$.

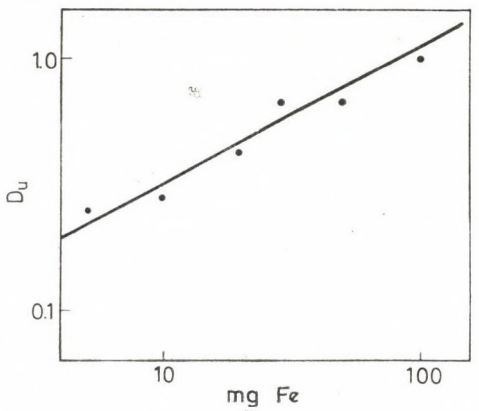

Fig. 4. Dependence of the sorption of uranium(VI) on the amount of $Fe(OH)_3$ (5—100 mg Fe^{3+}; 100 μg uranium; precipitated at 25 °C in a volume of 100 ml; pH = 12.05; Na_2CO_3 concentration = 0.1 *M*; filtered after 30 minutes' standing)

On the basis of more detailed studies, these results may assist in the determination of the mechanism of sorption and of the degree of polymerization of $Fe(OH)_3$ [7].

REFERENCES

1. Upor, E., Nagy, Gy.: Acta Chim. Acad. Sci. Hung. **28,** 287 (1961)
2. Upor, E., Nagy, Gy.: Acta Chim. Acad. Sci. Hung. **50,** 5 (1966)
3. Upor, E.: Acta Chim. Acad. Sci. Hung. **51,** 119 (1967)
4. Upor, E.: Acta Chim. Acad. Sci. Hung. **51,** 139 (1967)
5. Paramonova, V. I.: Radiokhimiya **4,** 84 (1962)
6. Tchernyaev, I. I.: Komplexnie Soyedinieniya Urana. Izd. Nauka, Moscow, 1964
7. Kolarik, Z., Szlaun, J.: Coll. Czech. Chem. Comm. **28,** 1993 (1963)

Endre Upor; Pécs, 39-es dandár út 3/a
Gyula Nagy; Pécs, Páfrány u. 27, Hungary.

Acta Chimica Academiae Scientiarum Hungaricae, Tomus 70 (2), pp. 189—205 (1971)

APPLICATION OF SUPERHEATED BENZENE VAPOUR DISTILLATION IN THE SEPARATION OF AMINES*

I. GYENES

Physical Chemistry Research Laboratory, Chemical Works of Gedeon Richter Ltd., Budapest

Received July 3, 1970

It is a precondition of the superheated benzene vapour distillation method developed earlier [1—4] that the relative volatility of the volatile amine must be known for the separation of binary or multicomponent amine mixtures. For this a model experiment is suitable, but an empirical distillation formula may also be used the terms in which are known (*e.g.* the molecular weight and boiling point (°C) of the amine), the other terms having been determined empirically in the course of a series of distillation experiments. In the interest of this, 134 different amines were distilled with superheated benzene vapour and the amount of superheated benzene vapour needed for the distillation (condensed benzene expressed in ml = V) was determined as was the probable connection of this with the material properties of the amines. The smaller the amount of benzene vapour necessary to distil over an amine, the more volatile is the amine; the selected expression $1000/V$ is suitable for judging this. The volatility sequence of the amines studied was determined.

The study of interactions in non-aqueous media has made possible the elaboration of a new type of analytical method of separation. This method, "superheated benzene vapour distillation", has proved suitable for the separation under water vapour-free conditions of volatile and non-volatile, binary or multicomponent amine mixtures. At the end of the operation, the non-volatile amine may be titrated in anhydrous solvents with a standard solution of perchloric acid or toluene-*p*-sulfonic acid (0.01—0.005 M). (For the relevant literature and a detailed description of the analytical application, see Refs. [1—4].)

The objectives of the present work were the following:

1. The distillation with superheated benzene vapour of a homologous series of amines, and the determination of an empirical numerical relation between the material constants of an amine (*e.g.* boiling point, molecular weight, the presence of certain functional groups) and the amount of superheated benzene vapour necessary for the distillation, which makes possible the derivation and the application of an empirical distillation formula in the calculation of the relative volatility of a volatile amine to be separated.

2. The determination of the relative volatility sequence of the amines studied.

* Extracted from thesis for the D. Sc. degree.

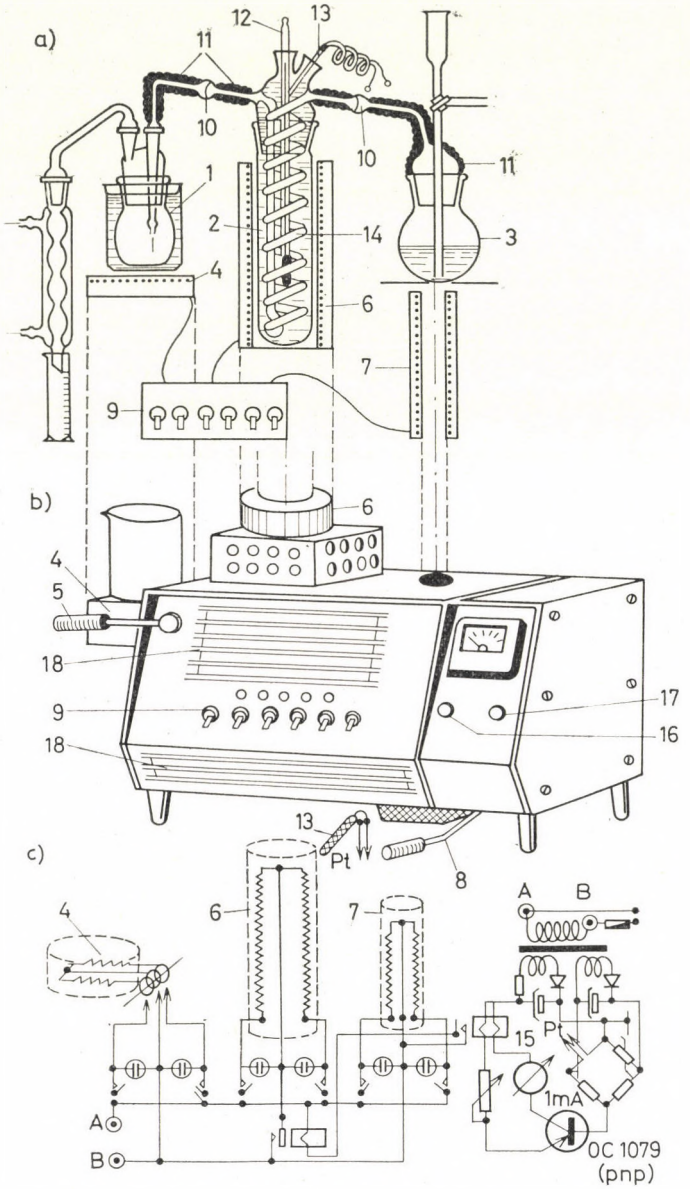

Fig. 1. Apparatus for superheated benzene vapour distillation. *a:* Outline scheme; *b:* frontal view; *c:* heaters and automatic temperature control. 1: Titration flask in 100 °C water bath; 2: 185 °C silicone oil bath; 3: 300 ml spherical flask; 4, 6 and 7: heater; 4 can be tilted through an angle of 90° with the arm 5, and 7 can be tilted through an angle 25° behind the plane of the diagram with the help of the arm 8; 9: switch panel; 10: spherical joints; 11: insulation; 12: control thermometer; 13: Pt resistance for the thermostatic control of superheater 14; 15: circuit diagram of the automatic control; 16: rough adjustment; 17: fine adjustment; 18: air grid

Experimental

An apparatus was designed for the separation of volatile and non-volatile components of amine mixtures; this was also used for the measurement of the relative volatilities of the amines (Fig. 1).

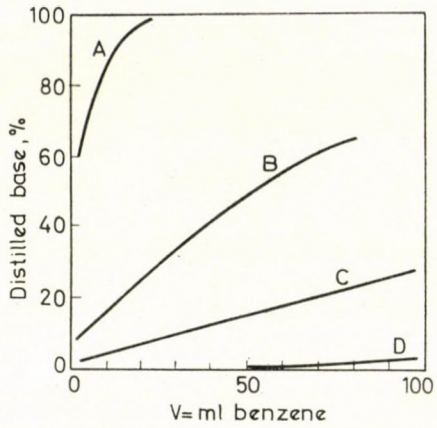

Fig. 2. Idealized curves of superheated benzene vapour distillation. A: volatile amine, *e.g.* heptylamine; B: slightly volatile amine (not linear), *e.g.* triethanolamine; C: slightly volatile amine (linear), *e.g.* 1-piperidino-2-methyl-3-*p*-toluyl-propanone-3 [3]; D: non-volatile amine, *e.g.* atropine [2]

Table I

The relative volatilities of some high-boiling amines

$1000/V$, where V is the volume of condensed benzene in ml equivalent to the volume of superheated benzene vapour necessary for the distillation

Amine	b.p. °C	$1000/V$
diethanolamine	272	12
(±)norephedrine	270	21
1,5-dimethyltropine	258	31
(±)ephedrine	255	34
4-ethoxyaniline	254	48
N-ethyldiethanolamine	251	33
N-methyldiethanolamine	247	25
2-methylquinoline	245	50
N-*n*-butylaniline	238	57
4-methoxybenzylamine	237	54
2,4,6-trimethylaniline	230	62
tropine	229	37
5-aminopentanol	215	111
2-aminopyridine	204	128

A solution of $(2 \pm 5) \times 10^{-5}$ gram equivalents of a mono- or bifunctional amine in 5 ml of chloroform was evaporated in a titration flask immersed in the boiling water bath of the apparatus; the film-like residue was subjected to superheated benzene vapour distillation. The amine remaining in the flask was dissolved in 5 ml of chloroform and titrated with 0.01 *M* perchloric acid prepared with a 1 : 1 mixture of carbon tetrachloride and acetic acid, using one drop of 0.1% Crystal Violet indicator solution.

Table II

Primary aliphatic amines

No.	Amine	c	x	k	ΔC	X	ml benzene		$1000/V$ rel. volatility
							calcd.*	found	
1	*n*-propylamine	0.96	0	0	—	0	0.85	0.7	1430
2	*n*-butylamine	1.12	0	0	1	1	1.5	1.8	556
3	isobutylamine	0.88	0	0	1	1	1.2	1.2	853
4	*t*-butylamine	0.50	0	0	1	1	0.45	0.7	1430
5	*n*-pentylamine	1.48	0	0	2	2	3.0	3.6	278
6	*n*-hexylamine	1.62	0	0	3	3	4.9	5.4	185
7	*n*-heptylamine	1.77	0	1	4	5	12.1	11.0	91
8	*n*-octylamine	1.90	0	1	5	6	19.5	18.5	54
9	1-amino-2-ethylhexane	1.62	0	1	5	6	16.6	15.5	64
10	*n*-nonylamine	1.74	0	1	6	7	26.8	27.0	37
11	*n*-decylamine	1.81	0	1	7	8	41.7	40.0	25

* Calculated with the empirical distillation formula:

$$\text{ml benzene} = V = c \times 1.5^{(x+\Delta C+k)} \times 0.9$$

where c is the square of the quotient of the molecular weight and the boiling point of the amine, x is the X value of the basis compound (in this case *n*-propylamine), ΔC is the carbon atom number difference, and k is a supplementary factor.

Table III

Secondary aliphatic amines

No.	Amine	c	x	k	ΔC	X	ml benzene		$1000/V$
							calcd.	found	
12	N-methyl-*n*-butylamine	1.07	0	0	2	2	2.2	2.5	400
13	di-*n*-propylamine	1.31	0	0	3	3	4.0	3.9	256
14	diisopropylamine	0.67	0	0	3	3	2.1	2.6	385
15	N-methyl-*n*-hexylamine	1.45	0	1	4	5	10.0	10.1	99
16	di-*n*-butylamine	1.50	0	1	5	6	15.4	15.0	67
17	diisobutylamine	1.13	0	1	5	6	11.6	12.0	83
18	N-methyl-*n*-octylamine	1.66	0	1	6	7	25.6	27.5	36
19	di-*n*-pentylamine	1.66	0	1	7	8	38.2	39.5	25
20	di-*n*-hexylamine	1.69	0	1	9	10	87.7	87.0	12
21	bis(2-ethylhexyl)amine	1.35	0	?	13	?	*	158.0	6

* If $X = 12$, the calculated volume of benzene is 159 ml.

Table IV

Tertiary aliphatic amines

No.	Amine	c	x	k	ΔC	X	ml benzene		$1000/V$
							calcd.	found	
22	triethylamine	0.78	0	0	3	3	2.4	2.8	357
23	N,N-dimethyl-*n*-pentylamine	1.34	0	1	4	5	9.2	8.0	125
24	tri-*n*-propylamine	1.10	0	1	6	7	16.9	15.0	67
25	N,N-dimethyl-*n*-octylamine	1.44	0	1	7	8	33.2	34.0	29
26	tri-*n*-butylamine	1.37	0	1	9	10	70.9	73.0	14
27	N,N-diisopropylethylamine	0.96	0	−1	5	4	4.4	4.8	208

The benzene vapour formed in the benzene vapour generator passes through the coil of the superheater heated at 185 °C, and flows into the flask at high speed through a nozzle of 2 mm internal diameter. Depending on the amount of benzene vapour, the volatile amine distils over in part or without residue and condenses in the cooler together with the benzene. The rate of flow of the superheated benzene vapour is 0.77 l/min.

The distillation curves of the amines were so drawn that the amount of benzene vapour was shown on the abscissa, expressed in ml of benzene condensed (25 ± 2 °C), while the percentage of the amine distilled over appeared on the ordinate. Several (idealized) characteristic curves are illustrated in Fig. 2.

Experimental data of 6—30 individual distillations were used for the construction of the distillation curve of each amine.

134 amines belonging to 11 compound groups were distilled with superheated benzene vapour (the "basis compounds" of the compound groups, *i.e.* the amine series, are given in parentheses below): **I.** Primary, secondary and tertiary aliphatic amines (*n*-propylamine). **II.** Cyclohexylamine derivatives (cyclohexylamine). **III.** Piperidine derivatives (piperidine). **IV.** Morpholine derivatives (morpholine). **V.** Aniline derivatives (aniline). **VI.** Benzylamine derivatives (benzylamine). **VII.** Phenylethylamine derivatives (*β*-phenylethylamine). **VIII.** Pyridine and quinoline derivatives (pyridine and quinoline). **IX.** Ethylenediamine derivatives

Table V

Cyclohexylamine and its derivatives.
Cyclopentylamine, cycloheptylamine and dicyclohexylamine

No.	Amine	c	x	k	ΔC	X	ml benzene		$1000/V$
							calcd.	found	
28	cyclohexylamine	1.78	3	—	0	3	5.4	6.0	167
29	N-methylcyclohexylamine	1.66	3	—	1	4	7.6	7.2	139
30	N-ethylcyclohexylamine	1.66	3	—	2	5	11.3	11.2	89
31	N-propylcyclohexylamine	1.70	3	—	3	6	17.4	18.0	18
32	N,N-dimethylcyclohexylamine	1.58	3	—	2	5	10.8	10.0	100
33	N,N-diethylcyclohexylamine	1.50	3	—	4	7	23.1	21.5	46
34	cyclopentylamine	1.71	2	—	0	2	3.5	3.2	312
35	cycloheptylamine	2.26	3	—	0	3	6.9	7.0	143
36	dicyclohexylamine	1.86	6	—	0	6	19.0	19.0	53

Note: Amines No. 34, 35 and 36 may be considered as new "basis compounds", and at the same time the X value of dicyclohexylamine is twice that of cyclohexylamine.

Table VI

Piperidine and its derivatives. Tropine and 1,5-dimethyltropine

No.	Amine	c	x	k	ΔC	X	ml benzene		1000/V
							calcd.	found	
37	piperidine	1.69	3	0	—	3	5.1	4.5	222
38	2-methylpiperidine	1.42	3	0	—	3	4.3	4.3	233
39	4-methylpiperidine	1.64	3	0	—	3	5.0	5.7	175
40	2-ethylpiperidine	1.52	3	0	—	3	4.6	5.0	200
41	4-*n*-propylpiperidine	1.98	3	0	—	3	6.0	6.6	152
42	N-methylpiperidine	1.21	3	0	—	3	3.7	3.5	279
43	N-ethylpiperidine	1.28	3	0	—	3	3.9	4.5	222
44	N-(2-hydroxyethyl)piperidine	2.30	3	0	—	3	7.3	7.0	143
45	N-ethyl-3-aminopiperidine	1.90	3	0.5	—	3.5	7.1	7.2	139
46	4-hydroxypiperidine	4.38	3	0	—	3	13.3	12.8	78
47	2,6-dimethylpiperidine	1.23	3	1	—	4	5.6	5.7	175
48	tropine	2.66	6	0	—	6	27.3	27.0	37
49	1,5-dimethyltropine	2.32	6	1	—	7	35.5	32.5	31

Note: Amine No. 48 may be considered as a new "basis compound". With reference to 2,6-dimethylpiperidine, 2,6-dimethylmorpholine and 1,5-dimethyltropine see Table XIV.

Table VII

*Morpholine and its derivatives**

No.	Amine	c	x	k	ΔC	X	ml benzene		1000/V
							calcd.	found	
50	morpholine	2.17	2	0	—	2	4.4	4.2	238
51	2-methylmorpholine	1.82	2	0	—	2	3.7	3.7	270
52	N-methylmorpholine	1.33	2	0	1	3	4.0	4.0	250
53	N-ethylmorpholine	1.41	2	0	2	4	6.4	6.8	147
54	N-(2-hydroxyethyl)morpholine	2.76	2	0	2	4	12.6	12.4	81
55	2,6-dimethylmorpholine	1.54	2	1	—	3	4.8	5.0	200

* *cf.* Table XV.

and propylenediamine (*n*-propylamine). **X.** Piperazine derivatives (piperazine free of water of crystallization). **XI.** Aminoalcohols (one hydroxy group, aminoethanol). The purity of the amines was checked by determination of the boiling point, titration in non-aqueous media, and at times by gas-chromatography.

The characteristics of the method are the following:

a) The distillation of water-vapour-free benzene vapour superheated to 95 °C into the titration flask at a speed of about 4 m/sec.

b) During the distillation the amines separate corresponding to their relative volatilities.

c) High-boiling amines also become volatile (Table I).

d) The less the benzene vapour necessary to distil over an amine (the volume of the benzene condensed expressed in ml = V), the more volatile is the amine. Under our experimental conditions, the value $1000/V$ was selected for the numerical description of the "relative volatility". With the object of comparison, those points on the distillation curves of the individual amines where the amine distils with 90% efficiency were taken as the basis. V is the volume ml of benzene condensed corresponding to this. The experimental data are given in Tables II—XIII.

Table VIII

Aniline and its derivatives

No.	Amine	c	x	k	ΔC	X	ml benzene		$1000/V$
							calcd.	found	
56	aniline	3.91	1	0	0	1	5.3	6.0	167
57	4-methylaniline	3.49	1	0.5	1	2.5	8.7	8.7	115
58	4-ethylaniline	3.15	1	0.5	2	3.5	11.7	12.0	83
59	4-*n*-propylaniline	2.79	1	0.5	3	4.5	15.6	15.5	64
60	2,4-dimethylaniline	3.01	1	0.5	2	3.5	11.5	9.6	104
61	2,4,6-trimethylaniline	2,96	1	0.5	3	4.5	16.5	16.2	62
62	4-methoxyaniline	3.95	1	1.75	1	3.75	16.2	16.0	62
63	4-ethoxyaniline	3.42	1	1.75	2	4.75	21.1	21.0	48
64	N-methylaniline	3.25	1	0	1	2	6.6	7.4	135
65	N-ethylaniline	2.86	1	0	2	3	8.7	10.0	100
66	N-*n*-propylaniline	2.67	1	0	3	4	12.2	13.0	77
67	N-*n*-buthylaniline	2.56	1	0	4	5	17.5	17.6	57
68	N,N-dimethylaniline	2 54	1	0	2	3	7.7	7.8	128
69	N,N-diethylaniline	2.14	1	0	4	5	14.6	13.4	75
70	N,N-dimethyl-4-methylaniline	2.31	1	0.5	3	4.5	12.9	12.1	83

Table IX

Benzylamine and its derivatives

No.	Amine	c	x	k	ΔC	X	ml benzene		$1000/V$
							calcd.	found	
71	benzylamine	2.95	2	0	0	2	6.0	6.0	167
72	4-methylbenzylamine	2.57	2	0.5	1	3.5	9.5	9.6	104
73	2,4-dimethylbenzylamine	2.61	2	0.5	2	4.5	14.6	13.0	77
74	4-methoxybenzylamine	3.02	2	1.75	1	4.75	18.7	18.4	54
75	N-methylbenzylamine	2.23	2	0	1	3	6.8	7.0	143
76	N-ethylbenzylamine	2.04	2	0	2	4	9.3	8.7	115
77	N,N-dimetylbenzylamine	1.88	2	1	2	5	12.9	13.5	74
78	N,N-dietylbenzylamine	1.68	2	1	4	7	25.8	25.0	40
79	N-isopropylbenzylamine	2.01	2	—1	3	4	10.2	9.5	105
80	dibenzylamine	2.34	10	—	—	10	121.5	120	8

Table X

Phenylethylamine and its derivatives. Norephedrine and ephedrine

No.	Amine	c	x	k	ΔC	X	ml benzene		1000/V
							calcd.	found	
81	(±) α-phenylethylamine	2.39	3	3	0	0	7.3	6.8	147
82	β-phenylethylamine	2.62	3	0	0	3	8.0	8.0	125
83	(±) 2-amino-1-phenylpropane	2.24	3	0	1	4	10.2	10.4	96
84	N-methyl-β-phenylethylamine	2.28	3	−0.5	1	3.5	8.5	8.3	120
85	(±) 2-methylamino-1-phenylpropane	1.85	3	−0.5	2	4.5	10.3	10.0	100
86	1-phenyl-2-aminopropanol-1 (norephedrine)	3.19				6.9*		47.0	21
87	1-phenyl-2-methylamino-propanol-1 ((±) ephedrine)	2.38				6.4*		29.0	34

* Found X values; the X difference of amines No. 86 and 87 is 0.5. *Cf.* amines No. 82 and 84, and 83 and 85.

Table XI

Pyridine and its derivatives. Quinoline, isoquinoline and methylquinoline

No.	Amine	c	x	k	ΔC	X	ml benzene		1000/V
							calcd.	found	
88	pyridine	2.16	1	0	0	1	2.9	2.9	345
89	2-methylpyridine	1.88	1	+0.25	1	2.25	4.2	4.4	227
90	3-methylpyridine	2.32	1	−0.25	1	1.75	4.3	4.5	222
91	4-methylpyridine	2.29	1	−0.25	1	1.75	4.2	4.5	222
92	2-ethylpyridine	1.90	1	−0.25	2	2.75	5.2	5.4	185
93	4-ethylpyridine	2.40	1	−0.25	2	2.75	6.6	6.6	152
94	2-*n*-propylpyridine	1.96	1	−0.25	3	3.75	8.1	8.2	122
95	2-methoxypyridine	1.58	1	−0.25	1	1.75	2.9	3.6	278
96	2-(β-methoxyethyl)-pyridine	2.35	1	−0.25	3	3.75	9.7	10.0	100
97	2,4-dimethylpyridine	2.02	1	+0.25 −0.25	2	3	6.1	6.0	167
98	2,6-dimethylpyridine	1.71	1	+0.25 −0.25	2	3	5.2	5.0	200
99	2-methyl-4-ethylpyridine	2.08	1	+0.25 −0.25	3	4	9.5	9.1	110
100	2,4,6-trimethylpyridine	2.04	1	+0.25 −0.25	3	4	9.3	9.0	111
101	2-aminopyridine	4.65	1	+0.5	0	1.5	7.7	7.8	128
102	2-amino-3-methylpyridine	4.22	1	+0.5 −0.25	1	2.25	9.5	8.8	114
103	4-*n*-propylpyridine	2.31	1	−0.25	3	3.75	9.5	7.5	133
104	quinoline	3.38	4	0	0	4	15.4	15.0	67
105	2-methylquinoline	2.91	4	0	1	5	19.9	20.0	50
106	isoquinoline	3.51	4	0	0	4	16.0	14.4	69

Table XII

Compounds containing two nitrogen atoms per molecule: ethylenediamine derivatives, propylenediamine, piperazine and its derivatives

No.	Amine	c	x	k	ΔC	X	ml benzene		1000/V
							calcd.	found	
107	N,N'-dimethylethylenediamine	1.75	0	0.5	−1 +2	1.5	2.9	3.5	286
108	N,N-dimethylethylenediamine	1.49	0	0.5	−1 +2	1.5	2.5	2.8	357
109	(±)1,2-diaminopropane	2.61	0	0.5	0	0.5	2.9	2.8	357
110	piperazine (anhydrous)	2.79	3.5	0	—	3.5	10.4	10.0	100
111	N-methylpiperazine	1.78	3.5	0	—	3.5	6.6	6.2	161
112	N,N'-dimethylpiperazine	1.30	3.5	0	—	3.5	4.8	5.2	192
113	N-*n*-propylpiperazine	1.82	3.5	0	—	3.5	6.8	6.8	147
114	N-(2-aminoethyl)piperazine	2.77	3.5	0	—	3.5	10.3	10.2	98
115	N-(2-hydroxyethyl)piperazine	3.18				8.5*		100	10

* Calculated from ml benzene.

Table XIII

Aminoalcohols

No.	Amine	c	x	k	ΔC	X	ml benzene		1000/V
							calcd.	found	
116	ethanolamine	7.94	−3	0	0	−3	2.1	2.0	500
117	3-aminopropanol-1	6.05	−3	2	1	0	5.4	5.0	200
118	1-aminopropanol-2	4.38	−3	1	1	−1	2.6	2.8	357
119	4-aminobutanol-1	5.31	−3	2	2	1	7.2	7.6	132
120	2-aminobutanol-1	3.91	−3	2	2	1	5.3	5.2	192
121	5-aminopentanol-1	4.34	−3	2	3	2	8.8	9.0	111
122	(±) leucinol	2.88	−3	2	4	3	8.8	10.0	100
123	N-methylaminoethanol	4.41	−3	2	1	0	4.0	3.4	294
124	N-ethylaminoethanol	3.15	−3	2	2	1	4.9	5.2	192
125	N,N-dimethylaminoethanol	2.24	−3	3	2	2	4.5	4.2	238
126	N,N-diethylaminoethanol	1.91	−3	3	4	4	8.7	8.2	122
127	1-dimethylaminopropanol-2	1.46	−3	3	3	3	4.4	4.6	217
128	1-diethylaminopropanol-2	1.53	−3	3	5	5	10.4	11.6	86
129	(±) N,N-diethylleucinol	1.47	−3	3	8	8	34.0	36.0	28
130	3-dimethylaminopropanol-1	2.70	−3	1	3	1	3.6	4.0	250
131	3-diethylaminopropanol-1	2.08	−3	1	5	3	6.3	6.8	147

Discussion

Two working hypotheses were used in the formation of the empirical distillation formula. The first was that, by means of the statistical comparison of the data found in the distillation of many amines, a relation may be found between the relative volatility and certain fundamental properties of the amine molecule. Therefore the structural properties of the amine molecule must be reflected in one term of the empirical formula. The second hypothesis was that the relative volatility is an inherent property of an amine which comes to the surface in the given case, *e.g.* in connection with the effect of a superheated solvent vapour.

> The object of the molecular (structure) theory is the determination of exact correlations between the physical properties of a material and the intermolecular forces. At present the determination of such a relation is possible only in two extreme cases, with gases at low density and in the case of solid materials at low temperature, *i.e.* in the regions of complete disorder or of complete order. In the intermediate region, with liquids, the properties of liquids are applicable only with rough approximations to throw direct light on the forces acting between molecules [5].

Statistical comparison of the series of distillation experiments led to an empirical distillation formula which serves the simplification of analytical amine separation in a study of binary or multicomponent amine mixtures where the relative volatility of the volatile amine is unknown. Thus in the case of simpler amines the amount of benzene vapour necessary to distil over the volatile amine may be precalculated. In this case a model experiment is unnecessary.

Under the experimental conditions of superheated benzene vapour distillation, by "relative volatility" is understood that that amine is more volatile, for the distillation of $(2 \pm 5) \times 10^{-5}$ gram equivalents of which less benzene is necessary (condensed and expressed as ml of benzene at 25 ± 2 °C, *i.e.* V). The empirical distillation formula is:

$$V = c \times 1.5^{X} \times 0.9$$

where V is the volume of benzene in ml, c is the square of the quotient of the molecular weight of the amine and its boiling point: $(\text{M.W./b.p.})^2$; 1.5 and 0.9 are empirical constants. X is an empirical value depending on the molecular structure.

According to our studies, the power X changes from amine to amine but not randomly; it reflects periodic relationships. Thus in complete generality the formula is:

$$V = c \times 1.5^{(x+\Delta C+k)} \times 0.9$$

where x is the X value of the basis compound. This latter is modified for the amines included in the basis compound groups by the difference in carbon

Table XIV

Variation of the k factor and its application

k factor	Application
−1	With N,N-diisopropylethylamine and N-benzylisopropylamine
−0.5	With N-methyl substituted phenylethylamine derivatives (see norephedrine and ephedrine, Table X)
−0.25	With pyridine derivatives, alkyl substitution (exception: 2-methyl substitution)
+0.25	2-methyl substitution in pyridine derivatives
+0.5	C-alkyl substitution in aniline and benzylamine derivatives; with amines containing a second nitrogen atom in the molecule; in the basic x value of piperazine
+1	With aliphatic amines if $C \geqslant 4$; with benzylamine derivatives in the case of a tertiary nitrogen atom; with 2,6-dimethylpyridine, 2,6-dimethylmorpholine and 1,5-dimethyltropine; in the case of 1-aminopropanol-2 and N,N-dialkyl derivatives of 3-aminopropanol-1
+1.75	With methoxy or ethoxy substituted aniline and benzylamine
+2	With aminoalcohols containing a primary or secondary nitrogen atom (exception: 1-aminopropanol-2)
+3	With aminoalcohols containing a tertiary nitrogen atom (exceptions: 1-diethylaminopropanol-2 and N,N-diethylleucinol)

atom number (ΔC), and by the supplementary factor k corresponding to the nature of the functional groups. Such factors are summarized in Table XIV. The use of the basic x, ΔC and the k factor is illustrated in Table XV. The x can be calculated from the number of ml of benzene found experimentally, using the above formula. The smaller the value of the basic x, the more volatile is the basis compound. Table XVI illustrates this, showing the boiling points of the basis compounds, the values of c, the values of the basic x (and the average difference from the mean value), and also the $1000/V$ values expressing the relative volatility. In place of the experimentally found basic x values, rounded numbers were used in the empirical distillation formula; these, in order of their appearance in Table XVI, are: 0, 3, 3, 2, 1, 2, 3, 1, 3.5, and —3. The value of the basic x of the basis compound was found experimentally:

$$x = \frac{\log \frac{V}{c \times 0.9}}{\log 1.5}$$

The experimental data and the factors derived from them make it possible to arrange the amines in a numerical series according to their volatilities (see for example Table XVII).

Table XV

Application of the basic x and the k factor in some basis compounds and in groups of amines

Basis compound	Basic x	With derivatives, do calculations involve	
		ΔC ?	k factor?
n-propylamine	0	yes	yes
cyclohexylamine	3	yes	no
piperidine	3	no	no[1]
morpholine	2	yes[2]	no[3]
aniline	1	yes	yes[4]
benzylamine	2	yes	yes[5]
phenylethylamine	3	yes	yes[6]
pyridine	1	yes	yes
piperazine	3.5	no	no
ethanolamine	−3	yes	yes

[1] Exception: N-ethyl-3-aminopiperidine ($k = 0.5$, second nitrogen atom in the molecule) and 2,6-dimethylpiperidine.
[2] With N-alkyl substitution.
[3] Exception: 2,6-dimethylmorpholine.
[4] C-alkyl substitution.
[5] With C-alkyl substitution and in the case of a tertiary nitrogen atom.
[6] With N-methyl derivatives.

Table XVI

Data of the "basis compounds"

Basis compound	b.p. (°C)	c	Basic x	Relative volatility $1000/V$
n-propylamine	49.5	0.96	0.03 ± 0.29	1430
cyclohexylamine	134	1.78	2.97 ± 0.17	167
piperidine	106.5	1.69	3.05 ± 0.21	222
morpholine	129	2.17	2.00 ± 0.11	238
aniline	184.4	3.91	1.03 ± 0.21	167
benzylamine	185.4	2.95	1.93 ± 0.11	167
phenylethylamine	197	2.62	2.95 ± 0.03	125
pyridine	115.5	3.96	1.05 ± 0.17	345
piperazine (anhydrous)	145.5	2.79	3.48 ± 0.12	100
ethanolamine	171	7.94	-2.97 ± 0.17	500

Table XVII

Examples from the relative volatility sequence of amines

Amine	1000/V	Amine	1000/V
n-propylamine	1430	N-ethylaniline	100
ethanolamine	500	2-methylquinoline	50
N-methyl-*n*-butylamine	400	*n*-decylamine	25
N-methylaminoethanol	294	N-(2-hydroxyethyl)piperazine	10
2-ethylpiperidine	200		

There is no simple relation between the volumes of benzene needed to distil over the amines, or the relative volatility, and the boiling points. This can be seen in Fig. 3. In general, the higher the boiling point the more benzene vapour is necessary for the distillation, but there are obvious exceptions too: aniline (No. 56), benzylamine (No. 71), β-phenylethylamine (No. 82), quinoline (No. 104), ethanolamine (No. 116) and 1-aminopropanol-2 (No. 118). The relative volatilities of amines with almost identical boiling points may be different (see Table XVIII).

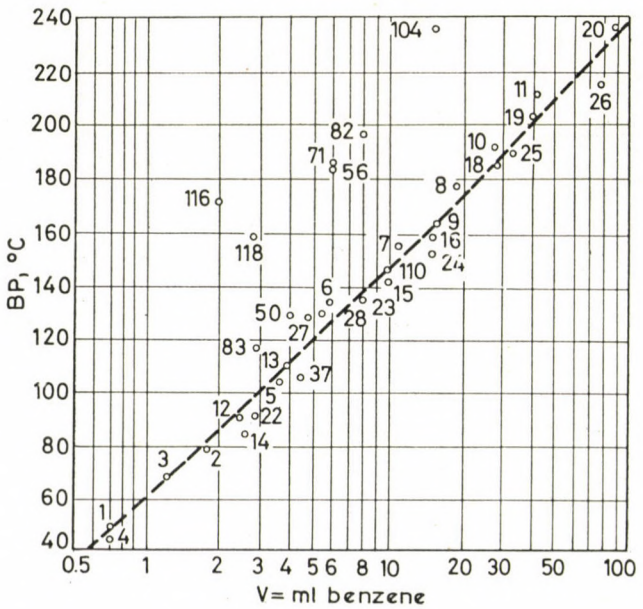

Fig. 3. Interdependence of the boiling points of the amines and the amounts of superheated benzene vapour necessary for their distillation (expressed as ml of condensed benzene). See the numeration in Tables II—XIII

Table XVIII

Relative volatilities of amines with almost identical boiling points

Amine	b.p. (°C)	c	$1000/V$
3-aminopropanol-1	185	6.05	200
aniline	184.4	3.91	167
benzylamine	185.4	2.95	167
4-*n*-propylpyridine	184.4	2.31	133
N,N-dimethylbenzylamine	185.5	1.88	74
N-propylcyclohexylamine	185	1.70	56
N-methyl-*n*-octylamine	185	1.66	36

With aminoalcohols, where significant intermolecular binding forces may be presumed (in many cases H-bridging has been confirmed), the c value is large. This latter permits conclusions on the association of the amine molecules. Nevertheless, 3-aminopropanol-1 for example is more than six times as volatile as N-methyloctylamine although their boiling points are identical.

Superheated benzene vapour distillation is not similar to steam distillation; the characteristics of the latter are given in parentheses.

In superheated benzene vapour distillation the solvent is inert and apolar (polar), the solvent vapour is superheated (at the boiling point), the compound distilled over dissolves in the solvent (it does not dissolve well in water), the distilling system is a water-vapour-free solvent vapour with a turbulent benzene vapour flow and with an amine–solvent film (steam led under the surface of the liquid), the molar ratio of the carrier vapour and the codistillate, *e.g.* in the case of aniline, is 13,600 : 1 (in the case of nitrobenzene 38 : 1).

A comparison of the amount of benzene vapour needed to distil over the amines and the evaporation enthalpy values known from the literature [6] shows a relation similar to that in Fig. 3 (Fig. 4). In this case too, *e.g.* aniline (No. 56) or 1-aminopropanol-2 (No. 118), some values stand out. Both figures show that the amount of benzene vapour needed to distil over individual amines ($\log V$ = log ml of benzene) is only approximately proportional to the boiling point (°C) or to the ΔH_v and kJ/mole values. Significant deviations appear which may be attributed to structural relations (*e.g.* the ability of aminoalcohols to form H-bridges, and their high degree of association). Despite both the high boiling point and the high enthalpy value, 1-aminopropanol-2 and aniline are easily distilled with superheated benzene vapour.

A consideration of the empirical data in Tables XIV and XV shows that the experimental points of the distillations lie on a straight line (Fig. 5; the experimentally found volume of benzene was taken as basis on the abscissa).

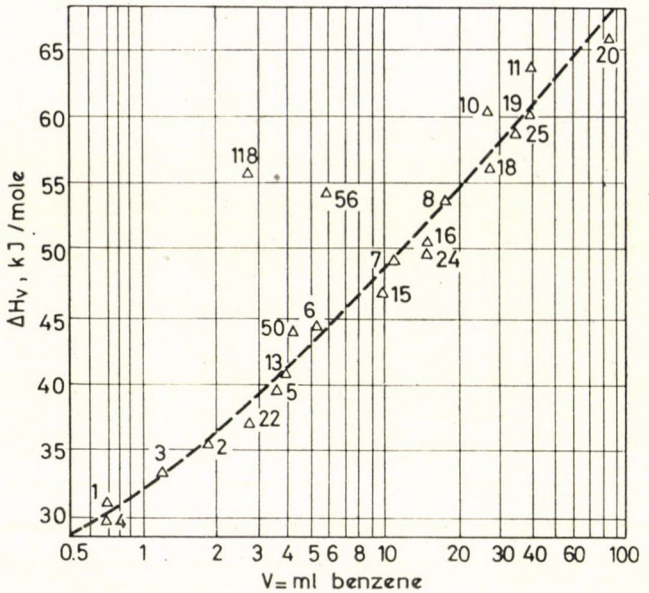

Fig. 4. Interdependence of the evaporation enthalpy values of the amines and the amounts of superheated benzene vapour necessary for their distillation. See numeration in Tables II—XIII

Under the experimental conditions of superheated benzene vapour distillation the binding forces between the amine molecules assert themselves by various means because the rapidly flowing benzene vapour hinders or decreases the association of amine molecules on the amine film surface with those in the vapour space. The amines thus show their inherent volatilities which are not in linear connection with their boiling points. This is obvious for those anomalous liquids in which H-bridge formation has been proved. The possibility that amine molecules which reach the vapour space from the surface of the liquid film can return to the liquid phase in the form of new associations decreases since the rapidly moving, superheated, turbulent benzene vapour hinders it in this and drives it towards the cooler. Thus the superheated solvent vapour has an important effect in those cases when significant binding energies are involved owing to the formation of molecular associations (*e.g.* H-bonding). Its effect is moderate when the intermolecular forces are also weaker (*e.g.* the polarization arising from the π-electron system of an aromatic group). Superheated benzene vapour has an insignificant effect where the internal binding forces are of very low strength. In this respect the c value has proved useful as a relative number (cf. Table XVI).

The V values obtained from the empirical distillation formula (dashed line) and those found experimentally (volume of benzene) show good agree-

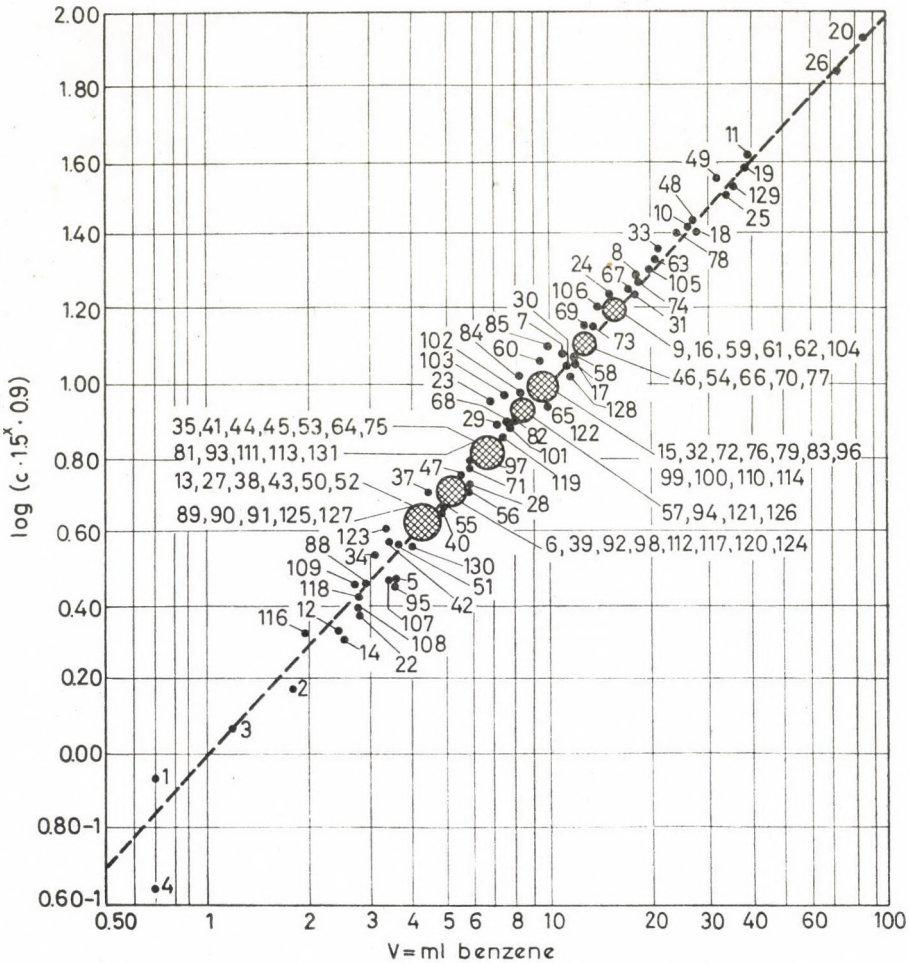

Fig. 5. Correlation of the amine distillation data with the value $\log (c \times 1.5^X \times 0.9)$. The dashed line indicates the theoretical volume of benzene in ml

ment in Fig. 5; this has proved to be of use in the case of binary or multicomponent amine mixtures in the programming of distillation experiments of unknown volatile amines.

The preconditions of the analytical application of the method of superheated benzene vapour distillation are the following ([1—4] and this work); *a)* in a mixture of two amines one must be volatile; *b)* an amine to be determined volumetrically in multicomponent systems must be non-volatile or only slightly volatile; *c)* the relative volatility of the volatile component must be known: from model experiments, from calculations with the empirical distillation formula or with the help of Fig. 5; *d)* the amines should be soluble

in chloroform and benzene and their titration in anhydrous media should be possible; *e)* the non-volatile amine should not undergo thermal decomposition during the time necessary for the distillation of the volatile amine.

*

The author wishes to thank Mrs. L. DESEŐ and Mrs. P. LANTOS who carried out many distillations, Mr. Gy. HÖRÖMPŐ for valuable discussions, and Mr. Gy. LUKÁCS for the construction of the apparatus.

REFERENCES

1. GYENES, I.: Titration in Non-Aqueous Media, p. 384 ff. Akadémiai Kiadó, Budapest, 1967; Iliffe Books Ltd., London, 1967; D. Van Nostrand Co., Inc., Princeton, New Jersey, 1967
2. GYENES, I.: Magy. Kém. Foly. **59,** 12 (1953)
3. GYENES, I.: Acta Chim. Acad. Sci. Hung. **26,** 403 (1961)
4. GYENES, I.: Acta Pharm. Acad. Sci. Hung. **34,** 99 (1964)
5. ROWLINSON, J. S.: Intermolecular forces and some properties of matter, Quart. Rev. **8,** 168 (1954)
6. Date of Dreisbach in Gould: Physical Properties of Organic Compounds, Vols I, II, III, Advances in Chemistry Series 29, American Chemical Society, Washington, 1961

István GYENES; Budapest X., Gyömrői út 19.

Acta Chimica Academiae Scientiarum Hungaricae, Tomus 70 (3), pp. 207—214 (1971)

VOLTAMMETRIC DETERMINATION OF SOME DRUGS USING SILICONE RUBBER BASED GRAPHITE ELECTRODE

E. PUNGOR, ZS. FEHÉR* and G. NAGY*

(Department of Analytical Chemistry, University of Chemical Industries, Veszprém)

Received July 20, 1970

The authors report on the voltammetric assay of a few basic materials of the pharmaceutical industry. The concentration of the solutions of phenothiazine and dioxyphenyl derivatives, amidopyrine, phenacetine, etc. could be measured in general with an accuracy of a few tenths of a per cent. In some of the cases, the determination was carried out in supporting electrolytes prepared with nonaqueous solvents. The authors show on a few examples that the method can be used for the determination of the active components of pharmaceutical preparations also without separation.

The analysis of the basic substances of the pharmaceutical industry, meaning in the majority of the cases the quantitative determination of organic substances of higher molecular weight, is undertaken mostly by classical methods. The determination of drugs present in the pharmaceutical preparations in the form of halides is prescribed in the Pharmacopoeiae often through the determination of the anion. The determination of bases containing nitrogen is carried out in most cases by titration with perchloric acid in nonaqueous media. For supplementing and replacing classical methods, increasing use is made of various instrumental techniques. Thus, for example, ion-selective membrane electrodes can be used directly or in combination with Schöniger's method for the quantitative determination of compounds used in the form of halides mentioned above, and of drugs containing halogens [1, 2].

Classical polarography at the dropping mercury electrode is often used in pharmaceutical analysis for following various processes and for the quality control of products. However, the determination of several electroactive substances at the dropping mercury electrode is complicated by the fact that mercury is dissolved already at relatively low positive potentials. The polarographic determination of some compounds can be undertaken after chemical treatment, which converts quantitatively the compound, inactive in the negative potential range, into a form reducible at the dropping mercury electrode (*e.g.* [3—10]).

* Permanent place of work: EGYT Pharmacochemical Works

The quantitative analysis of organic compounds, which cannot be determined by oxidative reactions at the dropping mercury electrode, is carried out most expediently by means of solid electrodes.

BILLON [11, 12] used a Pt electrode, KABASKALLIAN and MCGLOTTEN [13] a gold electrode for the determination of phenothiazine. LUGOVOY and RYZANOV [14] determined amidopyrine, DEYS [15] morphine derivatives, by means of a Pt microdisc electrode.

Using solid electrodes, difficulties are encountered because of possible memory phenomena of the electrode, owing to the fact that its surface is not renewed. In the determination of organic compounds, this may be due to two causes. During successive polarizations the surface of the electrode may be contaminated by the oxide layer formed, and by the binding of the reaction products. Both factors result in a gradual decrease of the activity of the electrode surface. The error caused by this contamination can be eliminated only by renewal of the electrode surface. Procedures known for the regeneration of the electrode surface complicate the handling of the electrode and involve possible sources of error. This explains why the use of solid electrodes in the analysis of the basic materials of pharmaceutical industry is not as widespread as that of the dropping mercury electrode.

PUNGOR and SZEPESVÁRY reported on the development of an electrode of novel type, the silicone rubber based graphite electrode [16]. They showed experimentally that a highly accurate oxidative determination of several organic compounds can be performed with this electrode without regeneration of the surface. (The standard deviation of the peak current values is $<0.2\%$.) Good reproducibility, and the fact that the electrode does not exhibit memory phenomena with the majority of substances investigated so far, permit to conclude that polarization does not give rise to processes in the surface layer, which would change the activity of the electrode. Memory phenomena were observed only in a few cases by the authors (phenol, resorcinol, naphthylamine). These phenomena can be explained by the binding on the surface of non-conducting polymers formed from the products of the electrode reaction.

The quantitative analysis of several basic substances of the pharmaceutical industry has been already performed with the silicone rubber based graphite electrode [16]. The present work reports on further results.

Determinations carried out so far concerned the measuring of concentration in aqueous solutions. However, the fact that high molecular electroactive substances are often poorly soluble in water, limited the applicability of the method.

Investigations carried out in other fields [17] showed that the silicone rubber based graphite electrode operates well also in various nonaqueous solvents. In some of the cases, insofar as it became necessary, determinations were carried out in supporting electrolytes prepared with a nonaqueous solvent.

Experimental method

Silicone rubber based graphite electrode was used as indicator electrode, and Ag/AgCl as a reference electrode. If determinations are made in aqueous solutions, there is no need for the pretreatment of the indicator electrode. However, when using nonaqueous solvents, the indicator electrode must be soaked before the measurement for about 30 minutes in the given solvent. In most of the cases, KCl in a concentration of 10^{-1} mole was used as supporting electrolyte, so that the supporting electrolyte proper served as the solution phase of the reference electrode. This permitted to use a beaker as the measurement cell.

The voltammograms were recorded in a static solution polarizing the electrode at a rate of 2 V/min in the positive direction. Between the single recordings, the solution was stirred for 30 sec with a magnetic stirrer.

A Radelkisz Polarograph Type OH 101/1 was used for the measurements.

The reagents used were of analytical grade or of pharmacopoeial purity.

Experimental results

The formulas of the drugs investigated, the supporting electrolyte used for the determination, the concentration range investigated, and the values of the halfwave potential, against the saturated calomel electrode, are shown in Table I. Figs. 1 and 2 show, by way of example, the calibration line of diethazine and phenothiazine, respectively.

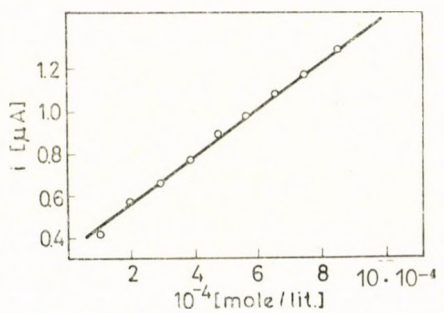

Fig. 1. Voltammetric calibration curve of diethazine. Supporting electrolyte: 10^{-1} mole/l KCl. Sensitivity: 2×10^{-8} A/mm

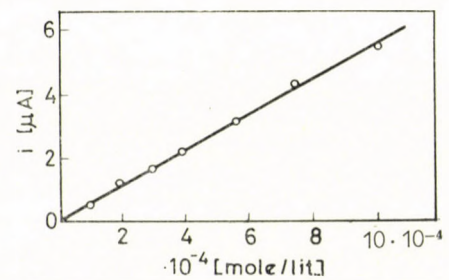

Fig. 2. Voltammetric calibration curve of phenothiazine. Supporting electrolyte: methanol saturated with KCl. Sensitivity: 8×10^{-8} A/mm

Table I

Name of the drug	Formula of the drug	Supporting solution	Concentration range investigated [mole/l]	Current constant $\left[\frac{\mu A}{\text{mole/l}}\right]$	Half-peak potential (V)
Isoprenaline	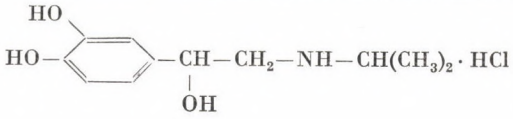	10^{-1} mole/l KCl	10^{-5}—10^{-3}	583*	+0.54
α-methyl-DOPA	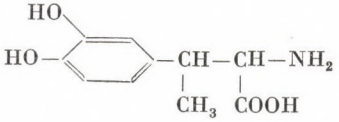	10^{-1} mole/l KCl	10^{-4}—10^{-3}	547	+0.60
Phenothiazine	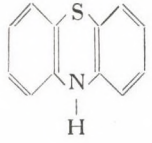	Methanol saturated with KCl	10^{-4}—10^{-3}	571	+0.68
		Acetonitrile saturated with tetramethyl-ammonium perchlorate	5×10^{-4}—5×10^{-3}	1430	+0.95
Chlorpromazine	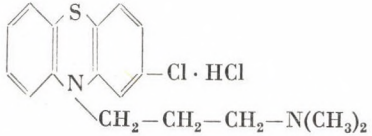	10^{-1} mole/l KCl containing 2% of HCl	10^{-4}—10^{-3}	338	+0.80

Frenolon	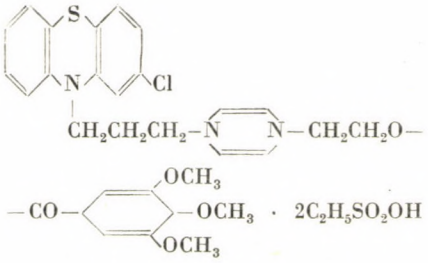	Methanol, saturated with KCl	10^{-4}—10^{-3}	923*	+0.54
Diethazine	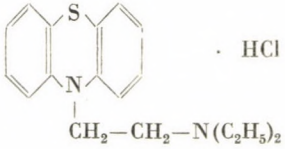	10^{-1} mole/l KCl	10^{-4}—10^{-3}	1140	+0.75
Tisercin	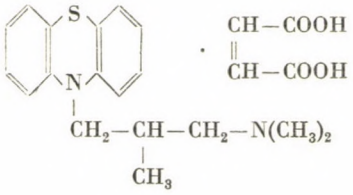	10^{-1} mole/l KCl	5×10^{-5}—5×10^{-3}	690	+0.62
Gastrixon	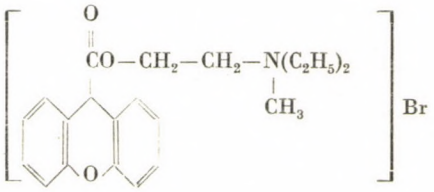	10^{-1} mole/l KCl	10^{-3}—10^{-2}	727*	+0.95

Table I (Continued)

Name of the drug	Formula of the drug	Supporting solution	Concentration range investigated [mole/l]	Current constant $\left[\frac{\mu A}{\text{mole/l}}\right]$	Half-peak potential (V)
Phenacetine	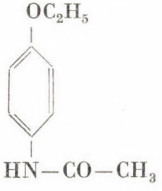	1 : 1 mixture of glacial acetic acid and water, 10^{-1} mole/l with respect to KCl	10^{-3}—10^{-2}	537	+1.35
p-Aminosalicylic acid	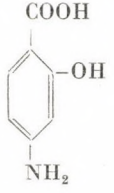	10 : 1 mixture of methanol and 10^{-1} mole/l NaOH saturated with tetramethylammonium perchlorate, and containing 0.5 g/l of Tween 20	5×10^{-3}—5×10^{-2}	182	+1.15
Amidopyrine	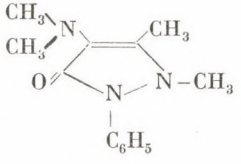	10^{-1} mole/l KCl	10^{-4}—10^{-3}	360	+0.45 and +0.7 respectively
		DMSO saturated with TMAP	10^{-4}—10^{-3}	254	+0.85
		DMF saturated with KCl	10^{-3}—5×10^{-3}	3570	+1.06 and +1.53 respectively
		Acetonitrile saturated with TMAP	10^{-3}—5×10^{-3}	90	+0.90 and +1.25 respectively

TMAP = tetramethylammonium perchlorate
DMSO = dimethylsulfoxide
DMF = dimethylformamide

It should be mentioned that only the determinations marked with asterisks were made with the same electrode, so that a comparison of the current constant values is justified only for these cases.

Though of the compounds listed in Table I, *p*-aminosalicylic acid is very sparingly soluble in water, the surface of the electrode becomes gradually contaminated during the electrochemical reaction in aqueous medium, and

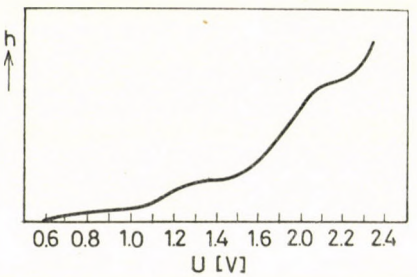

Fig. 3. Voltammogram of a solution containing amidopyrine and phenacetine. Supporting electrolyte: 1 : 1 mixture of glacial acetic acid and water, containing 10^{-1} mole/l of KCl. Amidopyrine concentration: 4.30×10^{-3} mole/l Phenacetine concentration: 2.52×10^{-3} mole/l. Sensitivity: 6×10^{-8} A/mm

becomes inactive after the recording of a few voltammograms. However, in a supporting electrolyte of the composition given in Table I, reproducible results are obtained.

Voltammetry is suitable also for the analysis of several pharmaceutical preparations. The task is simple if the preparation contains only one component which participates in the electrode reaction in the potential range used.

Dopegyt tablets, manufactured by EGYT, were investigated from this aspect. It was found that only the active substance, α-methyl-DOPA exhibits voltammetric activity, and the other components have no effect on the magnitude of the voltammetric current. Thus, the active substance of the tablet can be determined directly in the aqueous solution without previous separation.

Of the active substances of Antineuralgica tablets (amidopyrine, phenacetine, caffeine) amidopyrine and phenacetine show voltammetric activity in the positive potential range applied.

According to our investigations, in a 1 : 1 mixture of glacial acetic acid and water, containing 10^{-1} mole/l of KCl, the two drugs can be measured without separation in the presence of each other.

Amidopyrine gives both in aqueous solution and in glacial acetic acid–water mixture two voltammetric waves. When phenacetine is added, the height of the second wave increases, to give the curve of the shape shown in Fig. 3.

It should be mentioned that the height of the second voltammetric wave is not equal to the sum of the magnitude of the two waves, characteristic

of phenacetine and amidopyrine, respectively, at this concentration, but is slightly larger. This must be taken into consideration when plotting the calibration curve.

The amidopyrine concentration can be calculated from the first peak of the voltammogram, and knowing this value, the phenacetine concentration can be determined from the calibration curve plotted for phenacetine.

The mean error of the peak current values, calculated from the voltammograms recorded in aqueous solutions, was a few tenths of a per cent (calculated from 5 voltammograms); with nonaqueous solvents, this error was slightly higher. For example, in the case of amidopyrine, the mean error was 0.5% in the aqueous solution, 0.9% in acetonitrile, 0.6% in dimethyl formamide, and 1.1% in dimethyl sulfoxide.

REFERENCES

1. PUNGOR, E., PAPP, E.: Z. Anal. Chem. **250**, 31 (1970)
2. DESSOUKY, Y. M., TÓTH, K., PUNGOR, E.: Analyst **95**, 1027 (1970)
3. MASLOVA, A. F.: Biokhimiya **24**, 181 (1959)
4. DEZELIC, M., TRKOVMIK, M., POPOVIC, R., DIMITRIJEVIC, D.: Acta Pharm. Jugoslav. **17**, 81 (1967)
5. SVATEK, E., VACHEK, J.: Czech. patent No. 115.980 (1965)
6. DANEK, A., STROZIK, H.: Diss. Pharm. Pharmacol. **18**, 519 (1966)
7. ZHANTALAI, B. P.: Biokhimiya **29**, 1009 (1964)
8. SKORA, M.: Diss. Pharm. Pharmacol. **15**, 433 (1963)
9. BOZSAI, G., VASTAGH, G.: Pharm. Zentralhalle **103**, 250 (1964)
10. BROCKELT, G.: Pharmazie **20**, 136 (1965)
11. BILLON, J. P.: Bull. Soc. Chim. France **1961**, 1423
12. BILLON, J. P.: Ann. Chim. **7**, 183 (1962)
13. KABASKALLIAN, P., MCGLOTTEN, J.: Anal. Chem. **31**, 431 (1959)
14. LUGOVOY, S. V., RYZANOV, I. P.: Zh. Anal. Khim. **22**, 1093 (1967)
15. DEYS, H. P.: Pharm. Weekblad **99**, 737 (1964)
16. PUNGOR, E., SZEPESVÁRY, É.: Anal. Chim. Acta **43**, 289 (1968)
17. PUNGOR, E., FEHÉR, ZS., NAGY, G.: in preparation

Ernő PUNGOR; Budapest XI., Gellért tér 4.
Zsófia Fehér, Géza NAGY } Budapest, X. Keresztúri u. 30—38, Hungary.

Acta Chimica Academiae Scientiarum Hungaricae, Tomus 70 (3), pp. 215–224 (1971)

ASSOCIATION OF PROPIONIC ACID IN VAPOUR PHASE

J. Liszi

(Department of Physical Chemistry, University of Veszprém, and Electrochemical Research Group, Hungarian Academy of Sciences, Veszprém)

Received June 12, 1970

A method of calculation is presented for the determination of the association equilibrium constant of A–A_2–B type mixtures. This method allows direct determination of the equilibrium vapour pressure for the monomeric component. As application of this method, the association equilibrium constant of propionic acid referring to the vapour phase and expressed in partial pressures has been determined as a function of the temperature. This functional relationship has the following form:

$$\lg K_p = -10.484 + \frac{3227.7}{T} \qquad (K_p: \text{mmHg}^{-1})$$

Introduction

The nominal ("chemical") composition of mixtures containing associative components is different from their true composition. Due to the association, the mixture has more components than the nominal ones. Let us consider a nominally binary mixture in which only one component (*e.g.* a carboxylic acid) is capable of association. Let the other component be a nonpolar substance (*e.g.* carbon tetrachloride) unable of self-association, mixed association being also excluded. Neglecting the products of association higher than dimeric, the nominally binary mixture should be treated as a ternary mixture consisting of the following components: the monomer of the associating substance (A), its dimer (A_2), and the non-polar substance (B). The monomer and the dimer of the associating substance are connected through the following dimerization equilibrium:

$$2A \rightleftharpoons A_2 \qquad (1)$$

Such mixtures are referred to in the literature as ternary mixtures of the type A–A_2–B [1]. If the non-ideal behaviour of the nominal mixture is due solely to association, the term "ideally associated mixture" is used [1, 2].

In this paper a method of calculation is presented by which the equilibrium constant of a dimerization reaction occurring in the vapour phase can be obtained from the vapour–liquid equilibrium data if the association equilibrium constant in the liquid phase is known. The method to be presented is valid for ideally associated A–A_2–B mixtures. As an application of the

method, the association equilibrium constant for vapour-phase propionic acid (expressed in partial pressures) will be calculated as a function of the temperature.

1. Determination of the association equilibrium constant for A–A_2–B type ideal mixtures in the vapour phase

Let us assume that there is no association in the mixture, *i.e.* it is composed of the monomeric associating substance and the non-polar substance only. Further, we assume the mixture to be free of any special molecular interaction resulting in non-ideal behaviour of the binary mixture. This defines a hypothetic mixture, which is an ideal binary mixture of ideal components and which is composed of monomers of the associating substance and of the non-polar substance. This hypothetic mixture will be used as an auxiliary system. For this mixture the Gibbs–Duhem equation can be written as follows:

$$x_A \, \partial \ln \, p_A^* + x_B \, \partial \ln \, p_B^* = 0 \tag{2}$$

In Eq. (2) x_A is the nominal mole fraction of the associating substance in the liquid phase, x_B is the same for the non-polar component, p_A^* and p_B^* are the partial pressures of the monomeric associating substance and the non-polar component, respectively, in the hypothetic mixture. (The two latter quantities are, of course, hypothetic pressures without any real sense.) Dalton's law can be written for the hypothetic components as follows:

$$p_A^* = p^* y_A \tag{3}$$

$$p_B^* = p^* y_B \tag{4}$$

where p^* is the total pressure of the hypothetic mixture, y_A the nominal mole fraction of the associating component in the vapour phase, y_B the nominal mole fraction of the non-polar substance in the vapour phase. From Eqs. (2), (3) and (4) the following expression can be derived:

$$\left(\frac{\partial \ln p^*}{\partial y_B} \right)_T = \frac{y_B - x_B}{y_A y_B} \tag{5}$$

According to our initial assumption, Eq. (5) holds true only if the nominal mixture considered is an ideal mixture of non-associating ideal components. In the case of the A–A_2–B ternary system the above condition is fulfilled only in one point of the total concentration range, namely if $x_B = 1$. (The association equilibrium is shifted towards dissociation as the concentration of the non-polar components is increased; see reaction (1).)

In the case of an ideal mixture of ideal components, the total pressure of the binary mixture is, in agreement with Raoult's law, a linear function of the mole fractions in the liquid phase. In order that this property of the total pressure curve could be used, it is convenient to rearrange the right-hand side of Eq. (5) by introducing the mole fraction of the liquid phase instead of the vapour phase:

$$\left(\frac{\partial \ln p^*}{\partial x_B}\right)_T = \left(\frac{\partial \ln p^*}{\partial y_B}\right)_T \left(\frac{\partial y_B}{\partial x_B}\right)_T \tag{6}$$

Eq. (6), similarly to Eq. (5), is valid for the real A–A_2–B mixture only in the point where $x_B = 1$.

The above considerations permit to determine the total pressure of the hypothetic mixture as a function of the nominal composition. Since Eqs. (5) and (6) are valid for a real mixture only at $x_B = 1$, the first step to be performed is the extrapolation of the function

$$\frac{y_B - x_B}{y_A x_B} = f(y_B) \tag{7}$$

to the value of $x_B = 1$, using experimental data for x_B and y_B. Thus the partial derivative $\left(\frac{\partial \ln p^*}{\partial y_B}\right)_{T,x_B=1}$ is obtained. From the experimental values of x_B and y_B, the quantity $\left(\frac{\partial y_B}{\partial x_B}\right)_{T,x_B=1}$ can also be determined. The product of these two quantities gives the value of $\left(\frac{\partial \ln p^*}{\partial x_B}\right)_{T,x_B=1}$. Since we have a pure non-polar substance at $x_B = 1$, the following expression can be written:

$$\left(\frac{\partial \ln p^*}{\partial x_B}\right)_{T,x_B=1} = \frac{1}{P_B^0}\left(\frac{\partial p^*}{\partial x_B}\right)_{T,x_B=1} \tag{8}$$

where P_B^0 stands for the equilibrium vapour pressure of the non-polar substance referring to temperature T. Eq. (8) gives the slope of the total pressure curve of the hypothetic mixture and the total pressure at $x_B = 1$ since $(p^*)^{x_{B=1}} = P_B^0$. The total pressure of the hypothetic mixture is a linear function of the liquid phase mole fractions. Thus the two latter data unambiguously determine the total pressure curve of the hypothetic mixture. (See Fig. 1 which contains the data on the propionic acid–carbon tetrachloride mixture at 30 °C.) We have to point out again that the hypothetic mixture has been defined as an ideal binary mixture free of association. If there were no association in the mixture, then the point $x_B = 0$ would correspond to the monomeric associat-

ing component. Thus the hypothetic total pressure curve (p^*) (Fig. 1) intersects the ordinate ($x_B = 0$) at the value of the equilibrium vapour pressure (p_1^0) of the monomeric associating substance referring to temperature T. The equilibrium vapour pressure of the monomeric associating substance at temperature T can also be calculated from the following equation

$$\left(\frac{\partial p^*}{\partial x_B}\right)_{T,x_B=1} = p_B^0 - p_1^0. \tag{9}$$

On the basis of what was said above, the equilibrium vapour pressure of the monomeric associating substance can be determined as a function of temperature from vapour–liquid equilibrium data. Assuming an ideally associated mixture model the following expression can be written:

$$p_1^0 x_1 = p y_1 \tag{10}$$

where p is the total pressure of the mixture (a measured value), p_1^0 is the equilibrium vapour pressure of the monomeric associating substance (its calculation has been described above), and x_1 is the mole fraction of the monomer of the associating substance in the liquid phase. Given the value x_1, y_1 can be calculated. On the basis of the true composition of the vapour phase, the association equilibrium constant expressed in partial pressures can be determined:

$$K_p = \frac{p_2}{p_1^2} = \frac{y_2}{p y_1^2} \tag{11}$$

In the next part the application of the method outlined above will be demonstrated on the example of the propionic acid–carbon tetrachloride mixture.

2. Association equilibrium constant of propionic acid in the vapour phase

The calculations have been performed for systems at five different temperatures. For the sake of brevity, the detailed calculations will be presented only for one temperature, 30 °C, and only the initial data and the results will be given for the others. The vapour-liquid equilibrium data at 30 °C, used in the calculations, are collected in Table I. More detailed vapour–liquid equilibrium data for the propionic acid–carbon tetrachloride mixture in the entire concentration range can be found in an earlier paper [3].

Table I

Vapour–liquid equilibrium data for the propionic acid–carbon tetrachloride mixture at 30 °C

x_B	y_B	p (mmHg)
0.495	0.975	85
0.512	0.977	81
0.630	0.982	94
0.782	0.993	108
0.927	0.997	116
0.950	0.998	117
1.000	1.000	121

On the basis of Table I and the relationships derived in the previous section, the following values are obtained:

$$\left(\frac{\partial \ln p^*}{\partial y_B}\right)_{303\ °K,\ x_B=1} = 25.0$$

$$\left(\frac{\partial y_B}{\partial x_B}\right)_{303\ °K,\ x_B=1} = 0.022$$

$$\left(\frac{\partial \ln p^*}{\partial x_B}\right)_{303\ °K,\ x_B=1} = 0.5501$$

$$\left(\frac{\partial p^*}{\partial x_B}\right)_{303\ °K,\ x_B=1} = 67\ \text{mmHg}$$

Using the above results in Eq. (9) we obtain:

$$p_1^0 = p_B^0 - \left(\frac{\partial p^*}{\partial x_B}\right)_{T,x_B=1} = 121 - 67 = 54\ \text{mmHg}$$

Thus a 30 °C the equilibrium vapour pressure of monomeric propionic acid is almost ten times higher than that of propionic acid.

To illustrate the proportions between the pressures, the experimentally determined total pressure of the propionic acid–carbon tetrachloride mixture at 30°C and the total pressure of the hypothetic mixture used as an auxiliary system are shown in Fig. 1 as a function of the nominal mole fraction of carbon tetrachloride. The experimental data shown in Fig. 1 were taken, in part, from a previous paper [3].

The mole fraction of monomeric propionic acid is $x = 0.033$ at 30 °C [3, 4]. The equilibrium vapour pressure of propionic acid at this temperature

is $p_A^0 = 6$ mmHg [3]. Using the above data in Eq. (10) the mole fraction of monomeric propionic acid in the equilibrium vapour phase at 30 °C is found to be $y_1^0 = 0.297$. Hence for the value of the association equilibrium constant expressed in partial pressures we obtain $K_p = 1.328$.

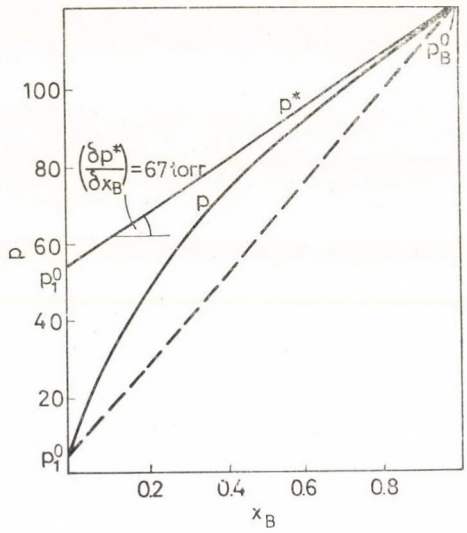

Fig. 1. Total pressure of the propionic acid–carbon tetrachloride mixture at 30 °C as a function of the nominal mole fraction of carbon tetrachloride. p — experimental data, p^* — total pressure of the hypothetic mixture; the dotted line represents the ideal mixture of the nominal components

In the following section the results referring to 40, 50, 60 and 70 °C will be outlined. The vapour–liquid equilibrium data used in the calculations are collected in Tables II, III, IV and V.

Table II

Vapour–liquid equilibrium data for the propionic acid–carbon tetrachloride mixture at 40 °C

x_B	y_B	p (mmHg)
0.552	0.981	147
0.582	0.983	153
0.627	0.986	160
0.681	0.989	175
0.895	0.996	190
0.960	0.998	197
0.967	0.999	199
1.000	1.000	208

Table III

Vapour–liquid equilibrium data for the propionic acid–carbon tetrachloride mixture at 50 °C

x_B	y_B	p mmHg)
0.505	0.972	213
0.526	0.974	216
0.539	0.975	219
0.550	0.997	221
0.771	0.990	268
0.783	0.992	274
0.892	0.995	293
0.960	0.998	299
1.000	1.000	306

Table IV

Vapour–liquid equilibrium data for the propionic acid–carbon tetrachloride mixture at 60 °C

x_B	y_B	p (mmHg)
0.454	0.956	267
0.476	0.959	274
0.481	0.960	279
0.570	0.972	305
0.813	0.991	376
0.977	0.999	404
1.000	1.000	413

Table V

Vapour–liquid equilibrium data for the propionic acid–carbon tetrachloride mixture at 70 °C

x_B	y_B	p mmHg)
0.550	0.968	440
0.625	0.976	478
0.732	0.985	514
0.827	0.992	550
0.880	0.995	570
0.974	0.998	590
1.000	1.000	605

The data referring to vapour phase association were determined on the basis of Tables II—VI. The method of calculation was described in detail for the mixture at 30 °C. The results are listed in Table VII. (For the sake of completeness, the data referring to 30 °C were also included into Table VII.)

Table VI

Mole fractions of monomeric propionic acid in the liquid phase and the equilibrium vapour pressure of propionic acid at various temperatures [3, 4]

T (°K)	x_1^0	p_A^0 (mmHg)
303.16	0.033	6
313.16	0.043	10
323.16	0.053	18
333.16	0.064	32
343.16	0.079	49

Table VII

Characteristic data on the vapour phase association of propionic acid as a function of the temperature

T (°K)	p_1^0 (mmHg)	y_1^0	K_p (mmHg^{-1})
303.16	54	0.297	1.328
313.16	71	0.305	0.745
323.16	116	0.342	0.313
333.16	172	0.344	0.173
343.16	248	0.400	0.077

The data summarized in Table VII are valid as far as the propionic acid–carbon tetrachloride mixture behaves like an A–A_2–B type ideal ternary mixture. A check on these results is obtained by plotting the logarithm of the association equilibrium constant, expressed in partial pressures, against the reciprocal absolute temperature (Fig. 2). In the Figure, the data obtained by TAYLOR and BRUTON [5] and MACDOUGALL [6] are shown for comparison. TAYLOR and BRUTON have determined the equilibrium constant from P–V–T data whereas MACDOUGALL used the results of vapour density measurements. The comparison of the values obtained by different methods permits the conclusion that the propionic acid–carbon tetrachloride mixture can actually be regarded as a ternary mixture of the A–A_2–B type, *i.e.* the method outlined in the first part of this paper gives reliable results. Using the data in

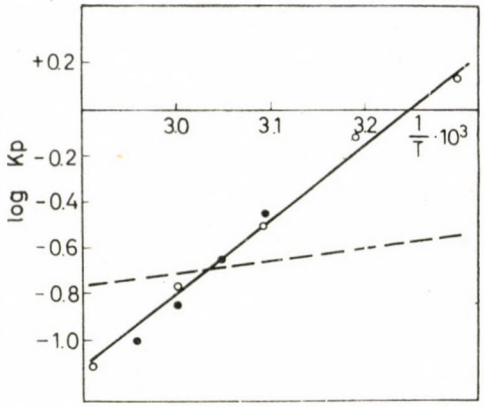

Fig. 2. The log K_p *vs.* $1/T$ diagram for propionic acid. ○ — experimental data of the present work, ● — MACDOUGALL's data, — — — data of BRUTON and TAYLOR, ——— a least-squares fit to the author's data

Table VII we obtained the following expression for the temperature dependence of the association equilibrium constant of propionic acid, referring to the vapour phase and expressed in partial pressures:

$$\lg K_p = -10.484 + \frac{3227.7}{T} \quad (K_p: \text{ mmHg}^{-1})$$

An advantage of this method of calculation is that it allows direct determination of the equilibrium vapour pressure of the monomeric substance. A drawback to be mentioned is that its application is restricted to ideally associated mixtures.

Symbols

A — monomer of the associating substance,
A_2 — dimer of the associating substance,
B — non-polar component,
K — association equilibrium constant,
p — pressure,
V — volume,
T — absolute temperature,
x — mole fraction in the liquid phase,
y — mole fraction in the vapour phase.

Subscripts

1 — monomeric substance in the real mixture,
2 — dimeric substance in the real mixture,
A — associating substance in the nominal mixture,
B — non-polar substance in the nominal mixture,
p — the indexed quantity expressed with partial pressures.

Upper indexes

o — pure substance,
* — the hypothetic mixture used as an auxiliary system.

REFERENCES

1. KEHIAIAN, H., SOSNKOWSKA, K., Bull. Acad. Polon. Sci. Sér. sci. chim. **11**, 583 (1963)
2. LISZI, J.: Acta Chim. Acad. Sci. Hung. **62**, 263 (1969)
3. LISZI, J.: (In press)
4. PIMENTAL, G. C. MCCLELLAN, A. L.: The Hydrogen Bond Appendix B. Freeman, New York, 1960
5. TAYLOR, M. D., BRUTON, J.: J. Am. Chem. Soc. **74**, 4151 (1952)
6. MACDOUGALL, F. H.: J. Am. Chem. Soc. **63**, 3420 (1941)

János LISZI; Veszprém, Schönherz Z. u. 12, Hungary.

Acta Chimica Academiae Scientiarum Hungaricae, Tomus 70 (3), pp. 225—234 (1971)

CHEMISTRY OF FREE RADICALS, VIII

ESR INVESTIGATION OF PHENYL NITROXIDE-N-SULFONATE TYPE FREE RADICALS

B. LAKATOS, B. TURCSÁNYI and F. TÜDŐS

(Central Research Institute for Chemistry, Hungarian Academy of Sciences, Budapest)

Received June 18, 1970

Similarly to isoelectronic aromatic aldehydes, aromatic nitroso compounds form addition compounds with bisulfites and dithionites. These addition products can be oxidized into radicals, whose ESR spectra are similar to those of alkylphenyl nitroxide free radicals. The dependence on the temperature and solvent of the coupling constants of nitrogen (a_N) suggest the formation of phenyl nitroxide-N-sulfonate upon the addition of bisulfite, and the formation of phenyl nitroxide-N-sulfinate in the reaction with dithionite.

The a_N values show both inductive and steric effects, similarly to alkylphenyl nitroxide free radicals.

The functional groups of organic nitroso and oxo compounds show considerable structural similarity. The two groups are isoelectronic, the hybridization state of participating atoms as well as the number of σ- and π-electrons are identical and the polarization properties of the groups are similar. These facts offer reasonable grounds for comparison between the chemical properties of the two types of compounds.

It can be established that in certain reaction types there is a marked difference in the behaviour of the two groups. As regards the addition of free radicals, *e.g.*, the nitroso group is extremely reactive, while the reactions between the oxo group and even the most reactive radicals proceed only very slowly. This difference in behaviour may be attributed to the nonbonding electron pair of the nitrogen atom which allows the formation of energetically highly favourable reaction products: nitroxide type free radicals with a three-π-electron structure. With oxo compounds, however, there is no possibility for stabilization of the unpaired electron. At the same time, it is a well-known fact that the behaviour of nitroso compounds toward oxo reagents is similar to that of aldehydes and ketones: their reactivities are comparable and their reactions result in addition or condensation products with analogous structures.

Hydrosulfite ion may, *e.g.*, be considered as a typical oxo reagent which readily gives addition products with aldehydes and under suitable steric conditions even with ketones. In addition to chemical evidence [1], X-ray diffraction studies [2] also prove that the reaction leads to an α-hydroxysulfonic acid. Thus with benzaldehyde the reaction product is the salt of α-hydroxybenzylsulfonic acid (**I**).

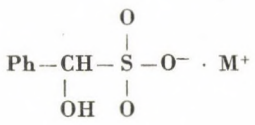

I

Nitrosobenzene corresponding to benzaldehyde also reacts with bisulfite ion. Detailed kinetic measurements showed that the reaction is first order with respect to each reactant and the overall rate is inversely proportional to the first power of the hydrogen ion concentration [3]. However, only secondary conversion products were isolated, which did not allow unequivocal determination of the structure of the primary product.

In the course of our investigations, we have observed that the oxidation of a reaction mixture containing nitrosobenzene or its derivatives and alkali bisulfite gives relatively stable paramagnetic products, which may be characterized as phenyl nitroxide-N-sulfonate free radicals (**III**). These radicals were formed during oxidation of the primary addition product: phenylhydroxylamine-N-sulfonic acid (**II**)

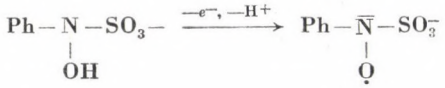

II III

The presence of phenyl nitroxide-N-sulfonate radicals proves that the bisulfite addition to nitroso compounds is entirely analogous with the corresponding reaction of oxo compounds. In addition, the radicals (**III**) prepared by us may themselves be of interest owing to their particular structure since they represent a transition between the well-known organic nitroxide radicals [4a, b, c] and the inorganic nitrosyldisulfonate radical ion (the anion of FREMY's salt [5a—l]).

Experimental

The preparation of the nitroso compounds followed the reaction course: nitro compound → hydroxylamine → nitroso compound. Purification was carried out by steam distillation and subsequent crystallization [6]. The N,N-dimethyl-4-nitroso-aniline (a "purum" quality Riedel product) was repeatedly recrystallized. Purity of the compounds was checked by m.p. measurements and infrared spectra. Solvents and inorganic reagents were of analytical purity.

Owing to the different solubility of reactants, bisulfite addition was carried out in a mixture of solvents. The methanol, dioxan, acetone, or dimethyl sulfoxide (DMSO) solutions of the nitroso compounds were mixed with the aqueous solution of sodium bisulfite containing a phosphate buffer. The concentration of both the nitroso compound and sodium bisulfite was 2.5×10^{-2} mole/l, the ratio of water to the organic solvent was generally 50 : 50 vol.%. The hydrogen ion concentration of the solution was adjusted so as to obtain an optimum radical concentration (the optimum pH values obtained by trial and error are given in Table I). The mixtures were allowed to react for 10 min, then oxidized by shaking with lead (IV) oxide.

ESR measurements were carried out with a JEOL JES-P-10 type X-band spectrometer. Owing to the high dielectric constants of the solvents, thin glass capillary cells (1.5 mm dia) were used. The solutions were deoxygenated by bubbling pure nitrogen gas through the capillaries. The distances between spectral lines were converted into field strength values by means of the nitroxyl disulfonate radical ion as standard ($a_N = 13.13 \pm 0.09$ Øe [5g].

On oxidizing the reaction mixture, we obtained orange-red solutions. This colour suggested visible light absorption characteristic of organic nitroxide radicals [7], but since we failed to isolate the radical products, these radicals could not be unequivocally identified. Accordingly, our investigations on the radical structure were also limited to direct ESR studies of the oxidized products.

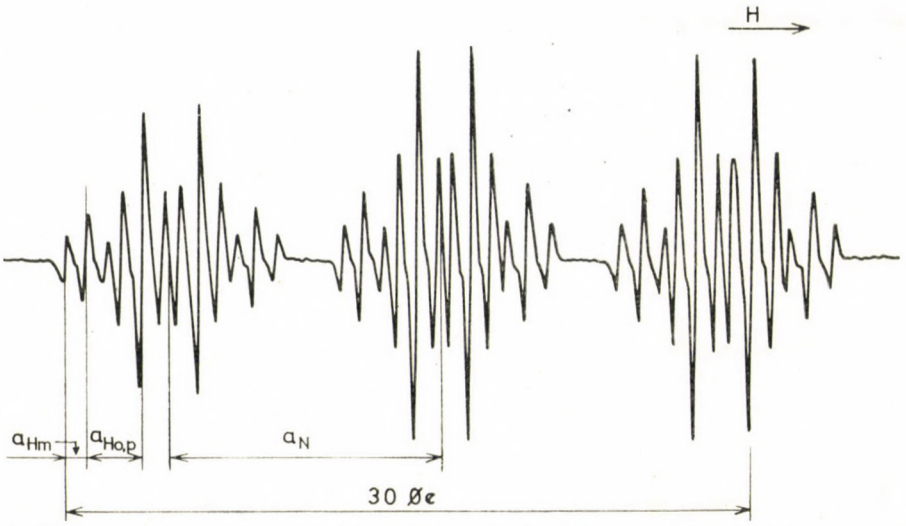

Fig. 1. ESR spectrum of the radical ion obtained in 1 : 1 dioxan–water by oxidation of the addition product of nitrosobenzene and sodium hydrogen sulfite

The ESR spectra of solutions containing dissolved oxygen show a broad triplet with an intensity ratio of 1 : 1 : 1, which indicates the presence of a high spin density nitrogen atom (**I** = 1). In certain cases (when the small excess of sulfite consumes dissolved oxygen) further hyperfine structure is observed. The oxygen-free solution [8] almost always gave well-resolved spectra.

The hyperfine structure of the spectra could be unequivocally related to structural factors. In the spectrum of the radical formed from nitrosobenzene, the line groups brought about by the nuclear spin of nitrogen are split into quadruplets (intensity ratio 1 : 3 : 3 : 1) and triplets (intensity ratio 1 : 2 : 1). This pattern is characteristic of the phenyl group linked to the radical center. The quadruplet splitting, characterized by a higher coupling constant, may be assigned to approximately equivalent *ortho* and *para* protons, while the triplet splitting with lower coupling constants may be attributed to *meta* protons (Fig. 1).

The spectra of the radicals prepared from substituted derivatives of nitrosobenzene are modified in accordance with the structural differences. Substitution of chlorine and bromine in *para* or *meta* position led to a decrease in the number of lines. The splitting brought about by the substituent was not observable. A fluorine substituent in the *para* position, on the other hand, resulted in strong doublet splitting.

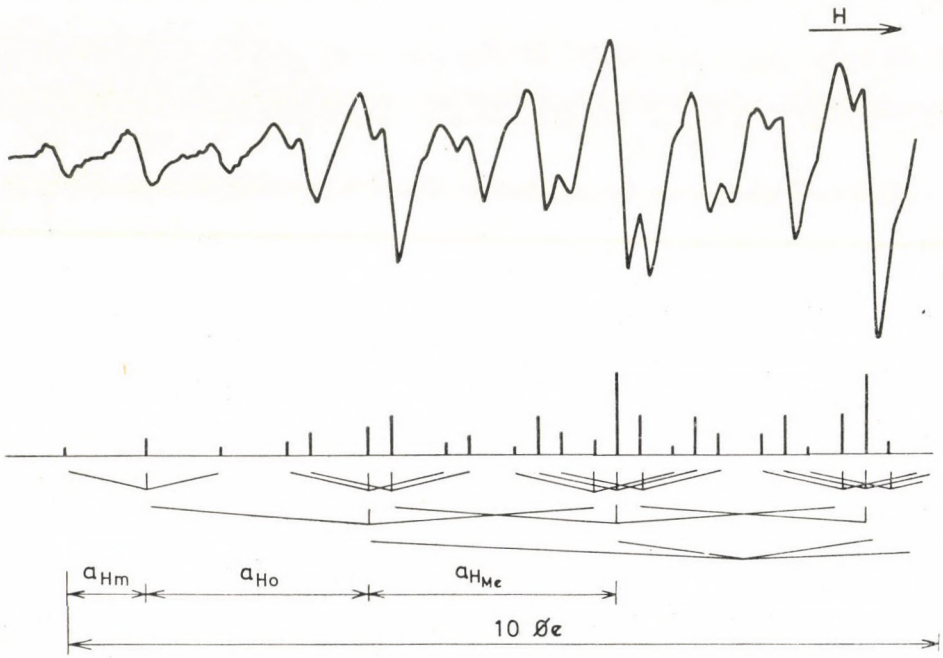

Fig. 2. Part of the ESR spectrum of the radical ion obtained in 1 : 1 methanol–water by oxidation of the addition product of *p*-nitrosotoluene and sodium hydrogen sulfite

The spectrum of the radical obtained from *p*-nitrosotoluene gave nearly equal coupling constants for protons in the *p*-methyl group and in the *ortho* position. On the basis of well-resolved spectra, we were able to determine separately the coupling constants of protons in various positions (*cf.* Fig. 2). Considering the order of lines with different intensities, the higher of the two nearly equal values may be ascribed to the methyl protons.

In the ESR spectrum of *o*-nitrosotoluene, we failed to observe further hyperfine structure in addition to the primary splitting. Neither could we observe well-resolved spectra of N,N-dimethylamino-4-nitrosobenzene. The concentration of radicals obtained from the latter compound was rather low, which indicated the formation of non-radical oxidation products, too.

The coupling constant values for radicals studied in detail are listed in Table I.

Table I

Coupling constants of phenyl nitroxide-N-sulfonate radicals (in Øe) (in methanol–water mixture at 25 °C)

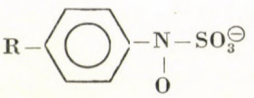

R	pH	a_N	a_{Ho}	a_{Hp}	a_{Hm}	
H	8.3	12.21	2.38	2.38	0.90	
2-CH_3	6.1	13.33	—	—	—	
4-CH_3	4.5	12.16	2.47	—	0.90	$a_{H\,CH_3} = 2.74$
4-F	7.0	12.29	2.49	—	0.91	$a_F = 5.71$
4-Cl	6.8	11.78	2.47	—	1.00	
4-Br*	4.5	11.58	2.45	—	0.94	
3-Br	4.5	11.60	2.39	2.39	0.87	

* Solvent: dioxan–water 1 : 1.

In the case of the radical prepared from nitrosobenzene, we studied the dependence of the coupling constants on the solvent. The change in the coupling constant values of phenyl protons was found to be within the limits of measurement errors, while the coupling constant of the nitrogen atom showed considerable changes (Table II).

Table II

Coupling constants of phenyl nitroxide-N-sulfonate radicals (in Øe) in different solvents at 25 °C

Solvent mixture		Dielectric constant	a_N	$a_{Ho,p}$	a_{Hm}
methanol–water	1 : 1	65.5	12.21	2.38	0.90
acetone–water	1 : 1	48.2	12.03	2.42	0.91
dioxan–water	1 : 1	35.9	11.85	2.41	0.88
dimethyl sulfoxide–water	4 : 6	70.0	11.69	2.36	0.88

Some other reagents with similar structures were investigated to establish whether their reaction with nitrosobenzene leads to products easily oxidizable to radicals as observed in the case of bisulfite addition. With sodium dithionite, we obtained radicals in high concentration whose ESR spectrum was very similar to that of the radical formed from the bisulfite adduct. The cor-

responding coupling constants were found to be almost identical, however, owing to the reproducible differences in the nitrogen coupling constants at different temperatures, the identity of the two radicals is questionable (Table III).

Table III

Nitrogen coupling constants of radicals prepared by the reaction of nitrosobenzene with bisulfites (A) and dithionites (B) (a_N, in Øe), in a mixture of methanol–water (1 : 1)

Temperature °C	A	B
25	12.21	12.09
0	12.08	11.88
−25	11.77	11.73
−45	11.74	11.67

The presence of paramagnetic species could also be detected after oxidizing the reaction products of nitrosobenzene with benzenesulfinic acid,* or phosphite and hypophosphite ions. The concentration of these radicals was, however, not high enough to obtain well-resolved ESR spectra with our equipment, therefore, no detailed study could be made. It has been established, on the other hand, that selenite ion, which is very similar to bisulfite ion, fails to produce radicals in a measurable amount.

Discussion

The radicals obtained in the reaction of nitrosobenzene with bisulfite ion suggest the phenyl nitroxide-N-sulfonate structure (**III**). This structure is in agreement with both our ESR results and the chemical properties of compounds with similar structures.

The patterns of ESR spectra and the relative values of the individual coupling constants unequivocally point to the phenyl nitroxide structure. This assumption is definitely confirmed by the fact that the coupling constants of the nitrogen atom of radicals obtained from different substituted nitrosobenzenes change strictly parallel to the corresponding coupling constants of aromatic nitroxide radicals with well-known and chemically verified structures.

The increased coupling constants of radicals containing an *ortho*-methyl substituent on the phenyl group, as well as the complete lack of splitting caused by aromatic protons owing to steric hindrance, is rather remarkable.

* *Note added in proof.* After sending the present paper the work of De Boer *et al.* had been communicated dealing with the ESR examination of free radicals obtained by the reaction of C-nitroso compounds with benzenesulfinic acid (Rec. Trav. Chim. **89,** 696 (1970)).

Table IV

Nitrogen coupling constants of phenyl nitroxide radicals (a_N, in Øe) at 25 °C

R_1 \ R_2	$-SO_3^-$	$-C(CH_3)_2CN$ [4a]	$-C(CH_3)_3$ [4b]
H	12.21	11.25	12.32
2-CH_3	13.33	13.24	13.37
4-CH_3	12.16	11.29	11.66
4-F	12.29	11.53	—
4-Cl	11.78	10.94	—
4-Br	11.58*	10.84	11.80
3-Br	11.60	10.87	—
Solvent	methanol–water	toluene	toluene

* Solvent: dioxan–water 1 : 1.

This fact unambiguously proves that the radicals studied are N,N-disubstituted nitroxide derivatives and that the steric requirements of the second substituent are similar to those of the *tert.*-butyl or cyanopropyl group.

The nitrogen coupling constants of aromatic nitroxide radicals are affected by two factors. One is the degree of π-electron delocalization in the system containing the unpaired electron. In case the π-electron system of the N—O bond interacts with further π-electron systems, the probability of finding the unpaired electron in the vicinity of the nitrogen atom will be lower than in the absence of such interaction, owing to steric hindrance or the lack of appropriate groups. Consequently, the coupling constant values will also be lower. The other factor is the degree of polarization of the π-electron system in the N—O bond. Mesomeric structures **IV**—**V** clearly show that the N → O drift of the π-electron system results in an increased spin density on the nitrogen atom:

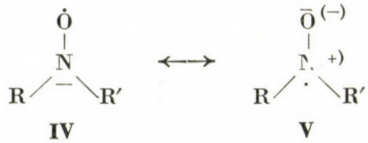

IV **V**

The polarization degree of the N—O bond may be affected both by structural factors and the environment. Electron-withdrawing substituents increase the contribution of mesomeric structure **IV**, which leads to a decrease in coupling constants. Similar changes can be observed with the radicals under investigation (*cf.* Table I), although the coupling constants plotted against the Hammett substituent parameters failed to give a good linear dependence.

One explanation for this fact may be that the solvatation properties of the radicals compared are not quite identical.

According to the theory, the increasing polarity of the solvent results in an increasing polarization of the N—O bond, which leads to an increased nitrogen coupling constant. However, the macroscopic polarity characteristics of the solvent mixtures applied (*e.g.* the dielectric constant [9c]), cannot be simply related to the measured coupling constants. The nitrogen coupling constants of the phenyl nitroxide-N-sulfonate radical show a change parallel to the dielectric constant of the three solvent mixtures. The corresponding values of the dimethyl sulfoxide–water mixture, however, cannot be fitted into this sequence (Table II). This indicates that in each particular case, the value of the coupling constant may also be affected by specific interactions.

On extrapolation from the values obtained in polar solvent mixtures, we find that without external polar effects, the nitrogen coupling constants of the above radicals are close to the corresponding values for phenylcyanopropyl nitroxide radicals [4a]. This suggests that in the present case, the sulfo group is a weak electron-withdrawing substituent since the effect of high polarity S—O bonds is mostly compensated by the free electric charge of the group. It should be noted that the solubility of these radicals in water is also due to their electric charge.

In our experiments, the formation of phenyl nitroxide-N-sulfonate radicals occurred in two steps. The formation of the bisulfite adduct of nitroso compounds was entirely analogous to the corresponding reaction of oxo compounds. In both cases, the nonbonding electron pair of the bisulfite ion becomes attached to the low electron density N or C atom. This reaction with a nitroso compound leads to an N-disubstituted hydroxylamine. The oxidation of these compounds to free radicals is a well-known process with both organic and inorganic substituents. Since the nitroso group is a considerably stronger electron acceptor than the oxo group, its reactivity in this reaction is also extremely high. This fact is supported by our observation that the reaction proceeds smoothly also in a mixture of acetone and water while such reaction would be impossible if the reactivities of the nitroso and oxo compound were comparable. References concerning similar addition reactions between organic nitroso compounds and reagents containing nonbonding electron pairs, like sulfinic acids, phosphites and hypophosphites, are in full agreement with our own findings. Finally, the above mechanism of the reaction is consistent with our observation that selenite ion, which has no nucleophilic electron pair, is incapable of such reaction.

The reaction of dithionite ions with nitroso compounds is much more complicated. According to literature data [10], radicals are directly formed in this reaction. This phenomenon was not observed under the conditions of our experiments. We found, however, that subsequent oxidation of the reaction

mixture yielded radicals identical with those described in [10]. The ESR spectra of these compounds were very similar to those of phenyl nitroxide-N-sulfonate radicals.

RUSSEL *et al.* [10] assume a redox reaction between nitrosobenzene and dithionite. The expected reduction product of nitrosobenzene, the nitrosobenzene radical-anion or its protonated form, the phenyl nitroxide radical, was, however, not detected in the ESR spectra. Therefore, structure **VI** was assumed for the radicals formed:

VI

Structure **VI** cannot be verified either experimentally or theoretically. The radical may be considered as an adduct of a nitrosobenzene molecule and a phenyl nitroxide radical. If this adduct were a truly stable formation, the addition of another nitrosobenzene molecule would presumably lead again to a stable product. Such polymerization phenomena are, however, not known with nitroso compounds. Furthermore, the spectrum described in Ref. [10] is not observed in mixtures containing phenylhydroxylamine and nitrosobenzene, where the reaction between phenyl nitroxide radicals formed and the excess of nitrosobenzene also could have led to structure **VI.**

In our opinion, the reaction of nitrosobenzene with dithionite may follow two pathways, depending on the experimental conditions. Direct formation of the radicals is due to the addition of $\dot{S}O_2^-$ radical ions [11] formed in the dissociation of dithionite ions. Thus, the radicals derived from phenylhydroxylamine-N-sulfinic acid are obtained (**VII**):

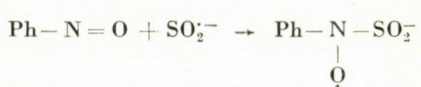

VII

In the other process, the following reaction takes place:

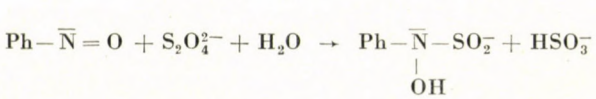

The phenylhydroxylamine-N-sulfinic acid formed may be oxidized to radical **VII.** The great similarity between the structure of radical **VII** and that of phenyl nitroxide-N-sulfonate gives an explanation for the highly similar ESR spectra.

*

One of the authors (B. LAKATOS) wishes to express his acknowledgement to the Department of Chemical Sciences of the Hungarian Academy of Sciences as well as to the Central Research Institute for Chemistry, Hungarian Academy of Sciences, for offering him the possibility to work in the Institute as a visiting scientist. Thanks are also due to B. MOHOS for helpful suggestions regarding ESR investigations and to L. JÓKAY for preparing the nitroso compounds.

REFERENCES

1. STEWART, T. D., DONALLY, L. H.: J. Amer. Chem. Soc. **54,** 3559 (1932)
2. KURODA, T. *et al.*: Bull. Chem. Soc. Japan **40,** 1377 (1967)
3. KRESSE, G., MANTHEY, H.: Chem. Ber. **89,** 1412 (1956)
4a. KENDE, I., TÜDŐS, F., SÜMEGI, L.: Acta Chim. Acad. Sci. Hung. **54,** 315 (1967); Magy. Kém. Foly. **74,** 260 (1968)
4b. MOHOS, B., TÜDŐS, F.: Private communication, Budapest, 1965
4c. MACKOR, A., WAJER, TH. A. J. W., DE BOER, T. H. J.: Tetrahedron Letters **1967,** 385
5a. FREMY, E.: Ann. Chim. Phys. **15,** 408 (1845)
5b. SINGH, R. P.: Canad. J. Chem. **44,** 1994 (1966)
5c. PAKE, G. E., TOWSAND, J., WEISSMAN, S. I.: Phys. Rev. **85,** 682 (1952); **89,** 606 (1953); J. Amer. Chem. Soc. **75,** 2534 (1953)
5d. WINDLE, J. J., WIERSEMA, A. K.: J. Chem. Phys. **39,** 1139 (1963)
5e. POWLES, J. G., MOSLEY, M. H.: Proc. Phys. Soc. **77,** 729 (1961)
5f. LUTZ, Z. *et al.*: J. Chem. Phys. **44,** 4421 (1966); Quart. Rev. **21,** 458 (1966)
5g. VALENZUELA, J. A., BAIRD, A. J.: J. Phys. Chem. **72,** 286 (1968)
5h. DRAGO, R. S.: J. Amer. Chem. Soc. **79,** 2049 (1957)
5i. YAMADA, S., TSUHIDA, R.: Bull. Chem. Soc. Japan **32,** 72 (1959)
5j. FILLMORE, D. L., WILSON, B. V.: Inorg. Chem. **7,** 1952 (1968)
5k. MOSER, W., HOWIE, R. A.: J. Chem. Soc. **A, 1968,** 3039
5l. HOWIE, R. A., GLASER, L. S. D., MOSER, W.: J. Chem. Soc. **A, 1968,** 3043
6. TÜDŐS, F., KENDE, I., AZORI, M.: MTA KKKI Közleményei **7,** 15 (1962)
7. KEUSSLER, V., LÜTTKE, W.: Z. Elektrochem. **63,** 614 (1959)
8. HAUSSER, K. H.: Naturwissenschaften **47,** 251 (1960)
9a. Zahlenwerte und Funktionen aus Physik. Chemie, Astronomie, Geophysik und Technik. 6. Aufl. II. Band Teil 6, p. 750. Springer Verlag, Berlin—Göttingen—Heidelberg, 1959
9b. MARTIN, D. *et al.*: Angew. Chem. **79,** 340 (1967)
9c. SCHLAFER, H. L. *et al.*: Angew. Chem. **72,** 618 (1960)
10. RUSSEL, G. A. *et al.*: J. Amer. Chem. Soc. **89,** 3821 (1967)
11. BURLAMACCHI, L. *et al.*: Trans. Faraday Soc. **65,** 496 (1969)

Béla LAKATOS
Béla TURCSÁNYI
Ferenc TÜDŐS
Budapest II., Pusztaszeri út 59/67.

Acta Chimica Academiae Scientiarum Hungaricae, Tomus 70 (3), pp. 235–246 (1971)

INVESTIGATION OF THE REACTION OF CHROMIUM(III) AND ETHYLENEDIAMINETETRAACETIC ACID, I

J. GÉHER-GLÜCKLICH and M. T. BECK

(Research Institute of Leather Industry, Budapest, Institute of Physical Chemistry, Kossuth Lajos University, Debrecen 10, Hungary)

Received July 15, 1970

The factors influencing the rate of the chromium(III)-EDTA reaction have been investigated by a spectrophotometric method. The reaction rate was studied as a function of the ligand concentration; it was found that, in contrast to literature data, the rate does depend on the ligand concentration. The interdependence was interpreted by a reaction mechanism in which the rate-determining step is the entry of the ligand from the outer sphere into the inner sphere.

The effect of pH on the reaction-rate was investigated. It was found that a known linear relation between the apparent rate constant and the pH holds only between narrow limits. The pH effect has been explained in terms of several factors. Possible reaction paths throughout the entire pH range were considered as a consequence of the hydrolysis of the chromium(III) ion and the dissociation of EDTA. The different types of chromium(III)-EDTA outer-sphere complexes are reported, together with the probability of their formation and the role of the different protonated outer-sphere complexes in the establishment of the chromium(III)-EDTA reaction rate. The experimentally determined pH dependence of the reaction rate was accounted for on the basis of theoretical considerations.

As an illustration the determination of the probable reaction paths at a given pH is presented.

Introduction

Since the turn of the century, there have been many publications on the chemistry of chromium(III) complexes. However, in spite of this, only a few papers may be found which deal with quantitative aspects.

The great interest may be attributed, at least in part, to the fact that trivalent chromium compounds play an important role in leather production as tanning agents. In the technical literature of the leather industry the works published cover a very wide field and in many cases lead to the solution of important practical problems. Since, however, in general they do not go further than qualitative statements, it is barely possible to use their results in systematic coordination chemistry research; therefore this field of the technical literature is not considered here.

The investigation of equilibrium and kinetic problems of chromium(III) compounds raises many difficulties which are not unambiguously soluble with the aid of the available experimental data and the conceptions of the reaction mechanisms. Especially little work deals with the mechanism of formation of chromium(III) complexes or the kinetics of their formation and decomposition

reactions. The most complete such investigation was published in ten papers by HAMM *et al.* in the period 1951—63.

In this series of papers HAMM considers in detail the kinetics of formation of complexes between chromium(III) and organic acid anions, and also the reaction mechanism. The investigation includes the oxalate, malonate, acetate, glycolate, lactate, phthalate, citrate and tartrate ions [1, 2]. The study of the reaction of chromium(III) with ethylenediaminetetraacetic acid (EDTA) was published in a separate paper [3].

According to HAMM, the reactions between chromium(III) and oxalate ion [4], and between chromium(III) and EDTA take place according to a single mechanism. In the first, relatively fast step one of the carboxylate groups replaces one of the water molecules of the hexaquochromium(III) ion, and an intermediate, *B*, is formed:

$$[Cr(H_2O)_6]^{3+} + H_2Y^{2-} \xrightarrow{\text{fast}} B \qquad (1)$$

(H_2Y^{2-} represents undissociated EDTA.)

This is followed by the reversible reaction:

$$B \rightleftarrows B' + H^+ \qquad (2)$$

and then by the rate-determining step in which the first chelate ring is formed:

$$B' \xrightarrow{k} C \qquad (3)$$

This mechanism for mono- and dicarboxylic acids and for oxyacids was later amended by HAMM himself [2]. According to the newer hypothesis, the rate-determining step is the formation of a five-coordinated intermediate. Since, however, he did not amend the conclusions concerning the chromium(III)-EDTA reaction, as a first step it is necessary to re-examine these.

For the reaction between EDTA and chromium(III) HAMM found the following:

1. The rate of reaction depends linearly on the concentration of chromium(III).

2. The rate of reaction is independent of the ligand concentration.

3. The apparent rate constant of the reaction is inversely proportional to the hydrogen ion concentration over a considerable pH range.

It is clear that statement 1 is in agreement with the proposed mechanism; however, the experimental conditions used by HAMM give rise to doubts with regard to the correctness of statements 2 and 3.

The constancy of the pH during the reaction was ensured by the use of a large, 40—50-fold, excess of the ligand. With such an excess, however, the

dependence of the reaction rate on the ligand concentration is naturally not ascertainable. Even this amount is not sufficient to really ensure a constant pH during the reaction and therefore in statement 3 the quoted pH can only be considered as the initial value. This necessitates the further consideration that HAMM found the linear pH-dependence of the reaction rate valid up to pH 1.6 under the above experimental conditions, although the solubility of EDTA rapidly decreases with decreasing pH and at pH 1.8 reaches such a low minimum value that it is impossible to use it in the quoted concentration [5]. (The 40-fold excess means a 0.2 *M* EDTA solution.)

Experimental

The chromium(III)-EDTA complex has an absorption maximum in its visible absorption spectrum at 545 nm. Since the other components of the system do not absorb at this wavelength the reaction may be followed spectrophotometrically. The measurements were made with a Zeiss VSU 1 spectrophotometer; extinctions of solutions were measured in 1 cm glass cells.

The pH was measured with a Radiometer PHM 4d instrument, using a glass-calomel electrode pair.

The reactants were placed, separated from each other, in a two-compartment glass vessel and the reaction was started by shaking the vessel. The reaction time was measured with a stopwatch.

The reaction rates were determined at 25 ± 0.1 °C. The temperature was kept constant by means of a Höppler ultrathermostat.

Chromium(III) perchlorate was prepared by the reduction of chromium(VI) oxide with hydrogen peroxide in a perchloric acid medium. The reduced solution contained 1 *M* chromium(III) perchlorate and 1 *M* perchloric acid (to prevent hydrolysis). A 0.025 *M* solution was used for the measurements. The chromium content was checked iodometrically.

A 0.125 *M* EDTA-disodium salt solution was used for the measurements. The EDTA content was determined with nickel sulfate.

A 2.5 *M* sodium perchlorate solution, prepared from sodium hydroxide and perchloric acid, was used to adjust the ionic strength.

The pH was adjusted with 0.1 *M* sodium hydroxide.

The final reaction mixtures contained 0.0025 *M* chromium(III) perchlorate and 1 *M* sodium perchlorate.

Calculation of the apparent rate constant

The chromium(III) ion reacts with EDTA in several steps; of these we deal only with the study of the rate-determining step. Reference [3] gives in detail the method of determining the rate constant. The mechanism comprising Eqs. (1), (2) and (3) forms the basis of the calculation. The reaction rate is given by the differential equation:

$$\frac{\mathrm{d}[C]}{\mathrm{d}t} = k\,[B'] \tag{4}$$

The boundary condition of the solution of the equation is that at $t = 0$ the concentration of the chelated complex, C, is zero.

Since at the wavelength of measurement all of the components with the exception of the Cr(III)-EDTA complex have negligible absorbance, the extinction E at time t is given by:

$$E_t = a_c b[C]_t \tag{5}$$

where a_c is the molar extinction coefficient of C, b is the cell length and $[C]$ the concentration of the chelated complex.

The equilibrium constant of reaction (2) is

$$K = \frac{[H^+]}{[B]} \cdot [B'] \tag{6}$$

Using these relations (4) becomes:

$$2.303 \lg \frac{E_\infty - E_t}{E_\infty} = -\frac{kK}{[H^+]+K} t \tag{7}$$

where k is the true rate constant. If the left-hand side is plotted as a function of time (t), we obtain from the slope the apparent rate constant:

$$k' = \frac{kK}{[H^+] + K} \tag{8}$$

Many mechanisms fit this mathematical model, and the apparent rate constants calculated on this basis may also be correct if the mechanism is interpreted in another way.

In several series of 5—7 parallel measurements the average mean error in the negative logarithm of the apparent rate constant ($p_{k'}$) was calculated; this amounted to $\pm$ 0.09.

Experimental results

The first step in the study of the chromium(III)-EDTA reaction was to re-examine whether at a given pH the reaction rate is actually independent of the ligand concentration. In the series of measurements the Cr(III) : EDTA ratio varied between 1 : 0.5 and 1 : 15. The pH of the solution was adjusted to between 4.4 and 4.5. Fig. 1 shows the dependence of the negative logarithm of the apparent rate constant on the EDTA : Cr(III) ratio. The graph clearly demonstrates that the apparent rate constant is strongly dependent on the ligand concentration if the latter is present only in a slight excess, while with a larger excess a change of rate constant is scarcely perceptible.

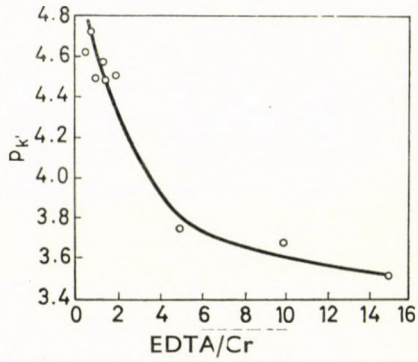

Fig. 1. $p_{k'}$ as a function of the EDTA : chromium(III) ratio

The pH dependence of the reaction rate was examined in solutions containing Cr(III) : EDTA ratios of 1 : 5, 1 : 10 and 1 : 15. Fig. 2 shows $p_{k'}$ values calculated from the measurements as a function of pH.

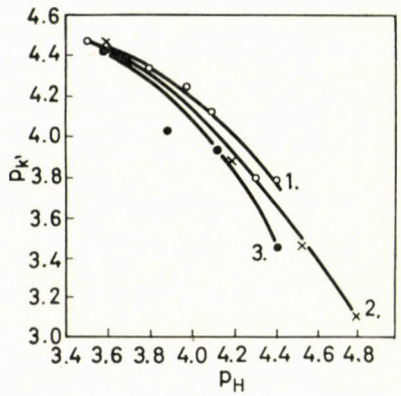

Fig. 2. The reaction rate as a function of pH. 1. 1 chromium : 5 EDTA; 2. 1 chromium : 10 EDTA; 3. 1 chromium : 15 EDTA

Analysis of the experimental results

The mechanism described by Eqs. (1), (2) and (3) means that the reaction rate of the chromium(III)-EDTA reaction is independent of the ligand concentration. Since this is disproved by the experimental data, the mechanism must be reconsidered.

According to HAMM, reaction (1) is fast and irreversible and hence there can be no hexaquochromium(III) ions present in the system if there is an excess of EDTA. If, however, it is postulated that the reaction is reversible:

$$[Cr(H_2O)_6]^{3+} + H_2Y^{2-} \rightleftharpoons B \qquad (9)$$

then the amount of B is not independent of the amount of H_2Y^{2-}. Since,

according to HAMM, the reaction-rate is determined by the chelation step $B' \rightarrow C$, and this rate is given by differential equation (4), then the rate cannot be independent of the H_2Y^{2-} concentration.

A further question is whether the rate-determining step is indeed the step of ring-closure. In the formation of nickel(II) malonate the rate is determined by the ring-closure according to NICKEL *et al.* [6]. Since, however, the reaction between a different metal ion and a different ligand is under consideration, and moreover the formation of nickel malonate is a considerably faster reaction than that of the chromium(III)-EDTA complex, it is not possible to extend the conclusions regarding the former reaction unreservedly to the latter. It seems likely that in the chromium(III)-EDTA reaction the entry of the ligand into the inner sphere is a slower process than chelate-ring formation.

It has already been mentioned that HAMM *et al.* [2] modified their proposed mechanism in the case of certain ligands. However, this modified version is still questionable from many aspects.

In our opinion the first step is a rapid equilibrium reaction:

$$[Cr(H_2O)_6]^{3+} + H_2Y^{2-} \rightleftharpoons Cr(H_2O)_6H_2Y^{+} \qquad (10)$$

The product is probably an outer-sphere type complex. (Direct experimental proof of the existence of outer-sphere type cobalt complexes with EDTA was recently found [7].)

The subsequent dissociation reaction can proceed in two ways because the hydrogen ion may dissociate from either the aquo group or from the H_2Y^{2-} loosely bound in the outer sphere:

$$\underset{B_1'}{Cr(H_2O)_6HY} + H^{+} \rightleftharpoons \underset{B}{Cr(H_2O)_6H_2Y^{+}} \rightleftharpoons \underset{B_2'}{Cr(OH)(H_2O)_5H_2Y} + H^{+} \qquad (11)$$

It is not possible to distinguish between the two reaction paths and therefore the reaction is more simply written as Eq. (2), $B \rightleftharpoons B' + H^{+}$.

This step has the result that the reaction rate depends on the pH; this point will be returned to later.

According to our assumption, the rate-determining step of the chromium(III)-EDTA reaction is the entry of the EDTA into the inner sphere:

$$\underset{B_2'}{Cr(H_2O)_6HY} \xrightarrow{k_1} \underset{C_1'}{Cr(H_2O)_5HY} + H_2O \xrightarrow{fast} \underset{C}{Cr(H_2O)HY} + 4H_2O \qquad (12a)$$

or

$$\underset{B_2'}{Cr(OH)(H_2O)_5H_2Y} \xrightarrow{k_2} \underset{C_2'}{Cr(OH)(H_2O)_4H_2Y} + \qquad (12b)$$

$$+ H_2O \xrightarrow{fast} \underset{C}{Cr(H_2O)HY} + 4\ H_2O$$

Since these reaction paths likewise cannot be distinguished the reaction is written in the following general form:

$$B' \xrightarrow{k} C' \xrightarrow{\text{fast}} C \tag{13}$$

where C is the chelated inner sphere complex. In the chromium(III)-EDTA complex the EDTA acts as a pentadentate ligand.

The reaction rate is given in this case by differential equation (4) which formally corresponds with the HAMM equation and since the boundary condition is the same ($C = 0$ at time $t = 0$) its solution is also identical.

On the basis of the measured data HAMM determined from Eq. (8) the true rate constant k and the equilibrium constant K at 31.0 °C; however, this calculation can only be accepted with reservation. It is questionable whether, in the light of the order of magnitude of the measured data, it is theoretically correct to calculate the equilibrium constant from the kinetic data.

Eq. (8) may be solved for K with the use of two values each of k' and $[H^+]$ to give an expression:

$$K = \frac{1}{k_2' - k_1'} (k_1'[H^+]_1 - k_2'[H^+]_2) \tag{14}$$

Since the error in the determination of k' is fairly large the scatter of the pk' values in our measurements was ± 0.09; if we suppose a scatter of only 10% in k' the difference in the small values may easily be negative. In view of the fact that K is calculated from the quotient of the differences, a scatter within the measurement error can also give a negative value of K.

Neither does a graphical evaluation of the results lead to the desired end. If Eq. (8) is rearranged, we obtain

$$\frac{1}{k'} = \frac{1}{kK} [H^+] + \frac{1}{k} \tag{15}$$

in which the reciprocal of the apparent rate constant is a linear function of the hydrogen ion concentration. If the measured k', $[H^+]$ pairs are plotted and the straight line is drawn, the intercept will be $1/k$ and the slope $1/kK$. However, this solution has the same uncertainty as the above-mentioned calculation.

Interpretation of the pH effect

According to Fig. 2, the dependence of the $p_{k'}$ on the hydrogen ion concentration only approximates linearity over a narrow pH range.

The interpretation of the pH effect is a very complex problem. At low pH the possibility of investigation is restricted by the very limited solubility

of EDTA. At high pH, on the other hand, metastable hydroxochromium(III) complexes are formed which readily precipitate above pH 5.

It may be presumed that the linear dependence is the resultant of a number of effects. In order to explain these, the system must be examined more closely.

The reactants may be in various hydrolyzed or ionic forms in the solution depending upon the pH. With increasing pH the chromium(III) forms hydroxo complexes; the hexaquochromium(III) ion is in equilibrium with these:

$$\underset{\text{I}}{[Cr(H_2O)_6]^{3+}} \rightleftharpoons \underset{\text{II}}{[Cr(OH)(H_2O)_5]^{2+}} \rightleftharpoons \underset{\text{III}}{[Cr(OH_2)(H_2O)_4]^{+}}$$

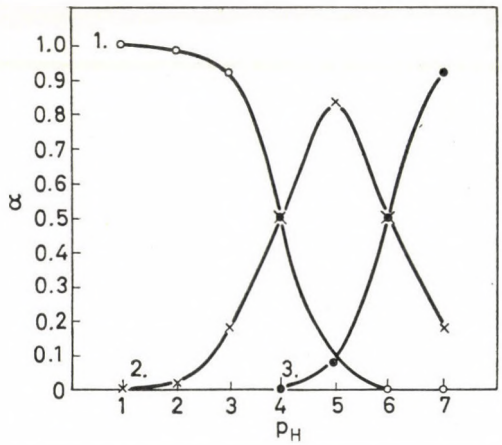

Fig. 3. Mole fractions of the chromium(III) ionic species as a function of pH. 1. $[Cr(H_2O)_6]^{3+}$; 2. $[Cr(OH)(H_2O)_5]^{2+}$; 3. $[Cr(OH_2)(H_2O)_4]^{+}$

The equilibrium constant of process I $\rightleftharpoons$ II is 10^{-4}, and that of II $\rightleftharpoons$ III is 10^{-6}. The variation of the mole fractions of these ionic species with pH is shown in Fig. 3.

EDTA is present in the solution in seven different ionized forms depending upon the pH:

$$H_6Y^{2+},\ H_5Y^{+},\ H_4Y,\ H_3Y^{-},\ H_2Y^{2-},\ HY^{3-},\ Y^{4-}$$

The corresponding equilibrium constants are [5, 8]:

$$K_1 = 1.2\times10^{-1} \qquad K_2 = 2.4\times10^{-2} \qquad K_3 = 1.0\times10^{-2}$$
$$K_4 = 2.1\times10^{-3} \qquad K_5 = 6.9\times10^{-7} \qquad K_6 = 5.5\times10^{-11}$$

The mole fraction of the ionic species is shown in Fig. 4.

Hence there is the possibility of 21 reaction paths between the hydrolyzed and dissociated reactants over the whole pH range; at each pH naturally only a few of these play an important role and make perceptible contributions to the conversion.

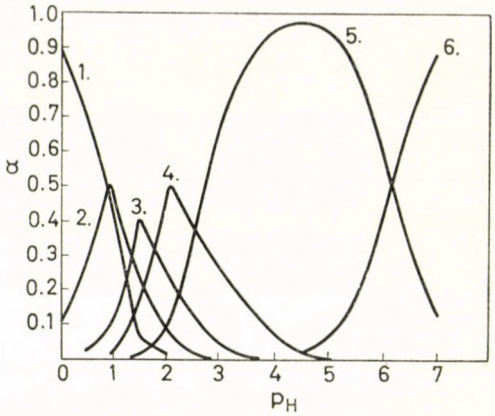

Fig. 4. Mole fractions of EDTA ionic species as a function of pH. 1. H_6Y^{2+}; 2. H_5Y^{+}; 3. H_4Y; 4. H_3Y^{-}; 5. H_2Y^{2+}; 6. HY^{3-}

In Table I the possible combinations can be seen by which the three chromium(III) and the seven EDTA species can form an outer-sphere type complex. The figures refer to how many protons there are altogether in the outer-sphere complexes formed from the species in the respective horizontal and vertical rows. The presence of a hydroxo group is regarded as equivalent to the loss of one proton.

Table I

	H_6Y^{2+}	H_5Y^{+}	H_4Y	H_3Y^{-}	H_2Y^{2+}	HY^{3-}	Y^{4-}
$[Cr(H_2O)_6]^{3+}$	6	5	4	3	2	1	0
$[Cr(OH)(H_2O)_5]^{2+}$	5	4	3	2	1	0	−1
$[Cr(OH_2)(H_2O)_4]^{+}$	4	3	2	1	0	−1	−2

The formation of some of the possible 21 types, although favoured electrostatically (*e.g.* $Cr^{3+} + Y^{4-}$), need not be taken into consideration because the components are present in different pH regions: $Cr(H_2O)_6^{3+}$ is present in insignificant concentration above pH 5, and the Y^{4-} likewise below pH 7. The reaction of certain types (*e.g.* $Cr(H_2O_6)^{3+} + H_6Y^{2+}$) is improbable purely from electrostatic reasons.

It can be seen in Table I that the extent of protonation of many com-

plexes is the same; although there are nine different ionic species in the pH range used (pH 3.3—4.7) only outer-sphere complexes with 3, 2 or 1 proton need be considered. From a kinetic and equilibrium viewpoint the identically protonated ionic species (*e.g.* CrH_3Y, $Cr(OH)H_4Y$ and $Cr(OH_2)H_5Y$) are indistinguishable. For the mole fractions of these ions we have the following expressions:

$$\alpha_{CrH_3Y} = K_{31}^* \frac{[H^+]^5}{\Sigma \cdot \Sigma'}$$

$$\alpha_{Cr(OH)H_4Y} = K_{32}^* \frac{[H^+]^5}{\Sigma \cdot \Sigma'}$$

$$\alpha_{Cr(HO_2)H_5Y} = K_{33}^* \frac{[H^+]^5}{\Sigma \cdot \Sigma'}$$

where

$$\Sigma = [H^+]^2 + K_1^{Cr}[H^+] + K_1^{Cr}K_2^{Cr}$$

$$\Sigma' = [H^+]^6 + K_1^Y[H^+]^5 + K_1^Y K_2^Y[H^+]^4 + K_1^Y K_2^Y K_3^Y[H^+]^3 + + K_1^Y K_2^Y K_3^Y K_4^Y[H]^2 + K_1^Y K_2^Y K_3^Y K_4^Y K_5^Y[H^+] + + K_1^Y K_2^Y K_3^Y K_4^Y K_5^Y K_6^Y$$

Due to the indistinguishability of the three ionic species, the mole fraction of triprotonated ions may be written simply as

$$\alpha_3 = \alpha_{CrH_3Y} + \alpha_{Cr(OH)H_4Y} + \alpha_{Cr(OH_2)H_5Y} = K_3^* \frac{[H^+]^5}{\Sigma \cdot \Sigma'}$$

Similarly the mole fractions of the di- and monoprotonated complexes are:

$$\alpha_2 = K_2^* \frac{[H^+]^4}{\Sigma \cdot \Sigma'}$$

$$\alpha_1 = K_1^* \frac{[H^+]^3}{\Sigma \cdot \Sigma'}$$

Since equilibrium data for the outer-sphere complexes, K_1^*, K_2^* and K_3^*, are unknown, α_1, α_2 and α_3 cannot be calculated. The solution of the problem becomes a little nearer if the values of

$$\frac{[H^+]^5}{\Sigma \cdot \Sigma'}, \quad \frac{[H^+]^4}{\Sigma \cdot \Sigma'}, \quad \frac{[H^+]^3}{\Sigma \cdot \Sigma'}$$

are calculated at different pH's, and their logarithms plotted as a function of the pH (Fig. 5). The positions of the maxima are independent of the unknown constants; only their magnitude depends on them.

With regard to these considerations, the pH dependence of the chromium(III)-EDTA reaction rate appears in a different light. According to HAMM, the reaction rate between pH 1.65 and 4.45 is inversely proportional to the hydrogen ion concentration and its pH dependence is attributable solely

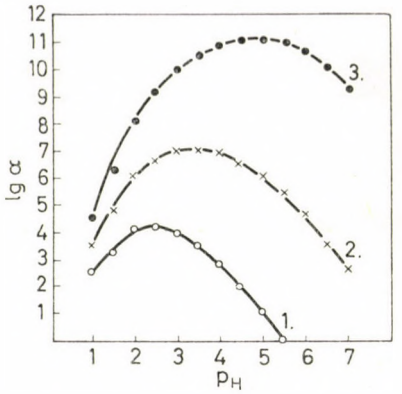

Fig. 5. Distribution of outer-sphere complexes as a function of pH. 1. Triprotonated outer sphere complex; 2. diprotonated outer-sphere complex; 3. monoprotonated outer-sphere complex

to the dissociation equilibrium $B \rightleftarrows B' + H^+$. It has been seen that the reaction mechanism is much more involved than presupposed; the state of protonation of the outer-sphere complexes formed in the pre-equilibrium depends on the pH. It is highly probable that the outer-sphere complexes with various degrees of protonation become inner-sphere complexes at different rates. The reaction of the triprotonated CrH_3Y type complexes is considerably slower than that of the diprotonated isomeric complexes present in greater concentration at higher pH; the monoprotonated CrHY type isomers react more rapidly than these. Such an explanation of the pH effect makes it more easy to understand that the dependence of the reaction rate on the hydrogen ion concentration is linear in only a narrow range of pH. It may be supposed that with decreasing protonation the rate does not increase linearly.

We shall illustrate the establishment of the probable reaction path by an example with the aid of Fig. 6 which summarizes the relations already described.

If the establishment of the probable reaction path at pH 3.3 is required, it can be seen from Fig. 6a that at this pH the hexaquochromium(III) ion and the hydroxopentaquochromium(III) ion are present in considerable amounts while the mole fraction of the dihydroxotetraquochromium(III) ion may be neglected. Fig. 6b shows that at pH 3.3 the mole fraction of the diprotonated CrH_2Y type complexes is near to the maximum. From Fig. 6c it

may be observed that the reaction of the diprotonated complexes may be realized through the Cr^{3+}—H_2Y^{2-}, $Cr(OH)^{2+}$—H_3Y^- and $Cr(OH)_2^+$—H_4Y routes.

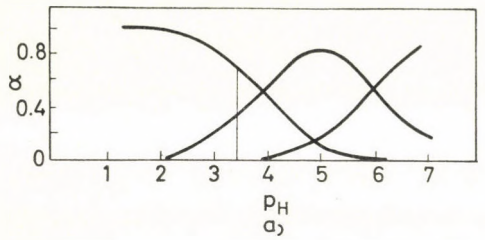

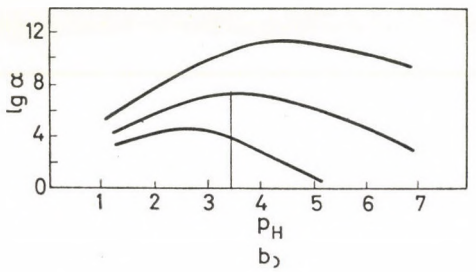

	H_6Y^{2+}	H_5Y^+	H_4Y	H_3Y^-	H_2Y^{2-}	HY^{3-}	Y^{4-}
Cr^{3+}	6	5	4	3	2	1	0
$Cr(OH)^{2+}$	5	4	3	2	1	0	−1
$Cr(OH)_2^+$	4	3	2	1	0	−1	−2

c)

Fig. 6. Evaluation of the probable reaction path

REFERENCES

1. HAMM, R. E., PERKINS, R. H.: J. Am. Chem. Soc. **77,** 2083 (1955)
2. HAMM, R. E., JOHNSON, R. L., PERKINS, R. H., DAVIS, R. E.: J. Am. Chem. Soc. **80,** 4469 (1958)
3. HAMM, R. E.: J. Am. Chem. Soc. **75,** 5670 (1953)
4. HAMM, R. E., DAVIS, R. E.: J. Am. Chem. Soc. **75,** 3085 (1953)
5. BECK, M. T., GÖRÖG, S.: MTA Kém. Tud. Oszt. Közl. **12,** 265 (1959)
6. NICKEL, U., HOFFMANN, H., JAENICKE, W.: Ber. Bunsenges. phys. Chemie **72,** 526 (1968)
7. ILCHEWA, L., BECK, M. T.: Proc. 3rd Symp. Coord. Chem., p. 89. Akadémiai Kiadó, Budapest, 1970
8. SCHWARZENBACH, G., ACKERMANN, H.: Helv. Chim. Acta **30,** 1978 (1947)

Judit GÉHER-GLÜCKLICH; Budapest IV., Paksi József u. 43.
Mihály T. BECK; Debrecen 10, Hungary.

Acta Chimica Academiae Scientiarum Hungaricae, Tomus 70 (3), pp. 247—253 (7971)

INVESTIGATION OF THE REACTION OF CHROMIUM(III) AND ETHYLENEDIAMINETETRAACETIC ACID, II

J. GÉHER-GLÜCKLICH and M. T. BECK

(Research Institute of Leather Industry, Budapest; Institute of Physical Chemistry, Debrecen 10, Hungary)

Received July 15, 1970

The reaction between binuclear chromium(III) complexes and EDTA has been examined by a spectrophotometric method. It was found that the hydrolysis occurring in dilute aqueous solutions of chromium(III) perchlorate, the formation of bi- and polynuclear complexes, and their decomposition with acid may be followed by the change in rate of the chromium(III)-EDTA reaction. With this method of measurement a new possibility is opened for the investigation of the behaviour of polynuclear complexes.

The reactions of mono- and binuclear complexes with EDTA have been compared; it was found that the binuclear complex reacts very much more slowly, and the pH dependence of the reaction rate, especially at higher excesses of EDTA, is much smaller than that of the mononuclear complex.

Introduction

In boiled or aged solutions of chromium(III) salts polynuclear hydrolysis products are present; these react very slowly with acid, and remain unchanged for a long time even in strongly acidic solutions. This was first noted by BJERRUM during a study of the formation of hexaquochromium(III) chloride from dichlorotetraquochromium(III) chloride [1—3].

The possible structures of chromium(III) compounds with two or more nuclei have been dealt with by many authors. In 1931 STIASNY summarized the changes occurring during the boiling of chromium(III) sulfate and chloride solutions [4]. He assumed that during the boiling binuclear complexes with two bridging hydroxo groups are formed; as a result of continued boiling the hydroxo bridges are transformed into oxo bridges. A re-examination of this proposed simple picture only followed about twenty years later when HALL and EYRING titrated chromium(III) salts with hexammonium heptamolybdate; it followed from the amount of molybdenum consumed per chromium atom that many types of bi- or polynuclear complexes must be present together in the solution [5].

LASWICK and PLANE [6] separated three main components from a boiled chromium(III) perchlorate solution by ion-exchange chromatography:

1. the unchanged hexaquochromium(III) ion,

2. a polynuclear bluish-green product which was formed rapidly on boiling; its amount did not change after a few minutes,

3. a polynuclear green product which was formed much more slowly than the former.

ARDON and PLANE [7] established that a binuclear complex is formed from chromium(II) by 2-electron oxidizing agents; this is a homogeneous substance according to chromatographic study, and corresponds to fraction 2 obtained from a boiled solution as in Ref. [6].

It has been established by an ion-exchange method that the substance obtained by the oxidation of the chromium(II) salt is a binuclear complex; bearing in mind that the charge per chromium atom is 2, two types of structure are possible:

I. $[(H_2O)_5Cr-O-Cr(H_2O)_5]^{4+}$

II. 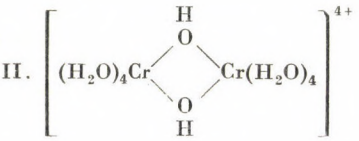

KOLACZKOWSKI and PLANE [8] established by exchange studies using $H_2{}^{18}O$ that the structure of the binuclear complex present in the solution corresponds to the second formula. For the time being it remains an open question whether the reason for this is the greater thermodynamic stability of the hydroxo bridged complex or it has only a kinetic origin.

The kinetics and mechanism of the formation and decomposition of the diol bridges were studied by GRANT and HAMM [9, 10] during the dimerization reaction of *cis*-hydroxodioxalatoaquochromium(III) and the decomposition of tetraoxalato-μ,μ-dihydroxodichromium(III); they found that both the formation and decomposition of the diol bridges occur according to a dissociation mechamisn.

So far only the formation and decomposition reactions of the binuclear acidochromium(III) complexes have been examined; the question of how the binuclear hydroxochromium(III) complexes react with ligands has not been dealt with.

During our experimental work it was observed that the chromium(III) perchlorate — EDTA reaction is considerably slower if the chromium(III) perchlorate solution stands diluted for several days before the starting of the reaction. It seemed likely that in the dilute solution the chromium(III) perchlorate hydrolyses and the hydroxo complexes give rise to binuclear complexes on ageing. These react more slowly not only with acids but also with EDTA. To clear up this phenomenon we have examined how much the reaction slows down as a result of the hydrolysis, and whether the slowing-down may also be observed when the dilution is not accompanied by a change in pH. A binuclear complex was prepared and the rates of reaction of the mono- and binuclear complexes with EDTA were compared. Finally the EDTA reaction

was followed during the decomposition of the binuclear complex to prove whether the decomposition reaction is accompanied by an increase in the rate of the chromium(III)-EDTA reaction.

Experimental

The chromium(III)-EDTA complex has a sharp absorbance maximum at 545 nm; as the other components of the system do not absorb at this wavelength, the reaction may be followed spectrophotometrically. The measurements were made with a Zeiss VSU 1 spectrophotometer; the extinctions of solutions were measured in 1 cm glass cells.

The measurement conditions were described in detail in the first paper of this series [11]. The reaction rate was determined at 25.0 ± 0.1 °C (Höppler ultrathermostat). The pH of reaction mixtures was measured with a Radiometer PHM 4d pH-meter, using a glass—calomel electrode pair.

The apparent rate constant of the reactions was calculated by the method used also by HAMM [12]. This calculation was considered in detail in Ref. [11], and only the expression serving as the basis of the calculations is given here:

$$k' = \frac{\lg (E_\infty - E_{t_2}) - \lg (E_\infty - E_{t_1})}{t_2 - t_1}$$

where E_∞ is the extinction measured for the equilibrium solution, and E_{t_1} and E_{t_2} are the extinctions measured at times t_1 and t_2 after the beginning of the reaction.

Chemicals

The homogeneous, binuclear complex containing two diol bridges was prepared as in Ref. [6]: chromium(III) perchlorate was reduced electrolytically and the chromium(II) perchlorate formed oxidized with atmospheric oxygen. The chromium content of the resulting solution was 0.025 *M*.

0.025 *M* chromium(III) perchlorate was used as a comparison solution; this was made by the reduction of chromium(VI) oxide with hydrogen peroxide [11].

A 0.125 *M* solution of EDTA-disodium salt was used.

The constant ionic strength was adjusted with 2.5 *M* sodium perchlorate: this solution was prepared by the neutralization of perchloric acid.

The pH was adjusted with 0.1 *M* sodium hydroxide solution.

Experimental results

The effect of the ageing of the chromium(III) perchlorate solution on the rate of the chromium(III)-EDTA reaction was studied in a solution with a Cr : EDTA ratio of 1 : 10. The concentration of chromium(III) was 2.5×10^{-3} *M*, the ionic strength was 1.0 (with sodium perchlorate) and the pH was adjusted to 4.0—4.1 with sodium hydroxide.

The reaction was so arranged that in one half of a two-compartment reaction vessel, the chromium(III) perchlorate solution, the sodium perchlorate solution and the amount of water required to make up the final volume were allowed to stand before the beginning of the reaction. After some hours or some days the chromium(III)-EDTA reaction is progressively slowed down. The negative logarithms of the apparent rate constants ($p_{k'}$) calculated from the measurements are shown in Fig. 1 as a function of the standing period. Accord-

ing to the graph, after standing for 72 hours the chromium(III) perchlorate reacts with the EDTA as slowly as does an equal concentration of the binuclear chromium(III) complex at the same pH.

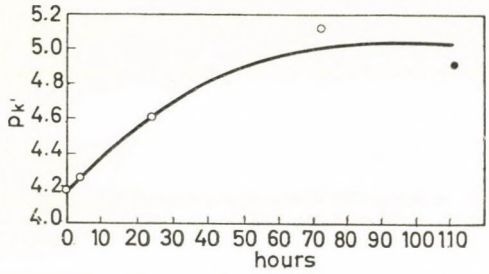

Fig. 1. Effect of the ageing of chromium(III) perchlorate solution on the rate of the chromium(III)-EDTA reaction; ○ binuclear complex

The pH of the 2.5×10^{-2} *M* chromium(III) perchlorate solution was 2.0. After a 7—8-fold dilution as in the above experiment, the pH became 3.77. In order to demonstrate the effect of the change of pH, the reaction with EDTA of a solution diluted with water was compared with that of a solution diluted with 0.01 *M* perchloric acid.

The experiments were carried out with a 1 Cr : 5 EDTA ratio and an ionic strength of 1.0. The pH of the solution diluted with water was 3.77 and that of the acid-diluted solution 2.37. The pH of both solutions was adjusted to 4.4 with sodium hydroxide before the beginning of the chromium(III)-EDTA

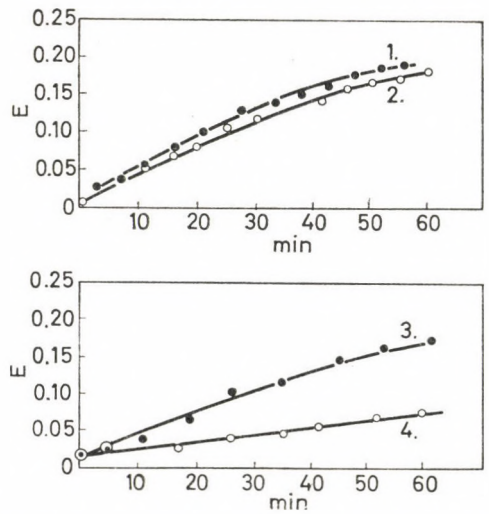

Fig. 2. Effect of the pH of the diluted solution on the rate of the chromium(III)-EDTA reaction
Immediately: 1. dilution with perchloric acid; 2. dilution with water. After 2 days of standing: 3. dilution with perchloric acid; 4. dilution with water

reaction. Fig. 2 shows the time *vs.* extinction graphs for both types of solution measured immediately after dilution and after standing for 2 days. While the measured data are in agreement in the freshly prepared solutions, the two curves for the solutions which stood for 2 days differ markedly from each other. The reaction with EDTA of the water-diluted solution is much slower than that of the acid-diluted solution.

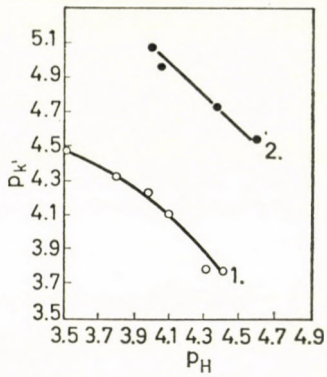

Fig. 3. $p_{k'}$ as a function of the pH (1 chromium : 5 EDTA); 1. mononuclear complex; 2. binuclear complex

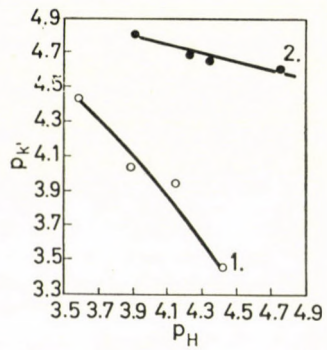

Fig. 4. $p_{k'}$ as a function of the pH (1 chromium : 15 EDTA) 1. mononuclear complex; 2. binuclear complex

Next the pH dependence of the chromium(III)-EDTA reaction rate was studied in a solution of the pure binuclear complex with Cr : EDTA ratios of 1 : 5, 1 : 10 and 1 : 15. Solutions with Cr : EDTA ratios of 1 : 5 and 1 : 15 containing mononuclear complexes were also studied. The pk' values found in the 1 Cr : 5 EDTA and 1 Cr : 15 EDTA solutions are plotted in Figs 3 and 4 as a function of the pH. In the 1 Cr : 5 EDTA solutions the two curves run almost parallel; the mononuclear complex reacts with EDTA about

ten times faster than the binuclear complex. The difference is even greater in the 1 Cr : 15 EDTA solutions; in this case the pH increase scarcely affects the rate of the binuclear complex — EDTA reaction, while the rate with the mononuclear complex rapidly increases with increasing pH.

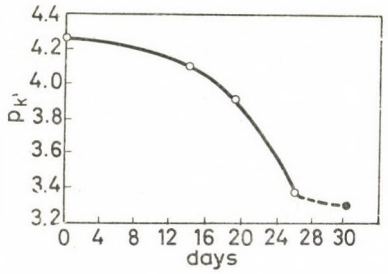

Fig. 5. Effect of the degradation of the binuclear complex on the rate of the chromium(III)-EDTA reaction; ○ chromium(III) perchlorate

Further experiments were carried out to prove that decomposition of the binuclear complex with acid accelerates the reaction with EDTA, which finally attains the rate measured in a chromium(III) perchlorate solution.

Although it is known from the literature that the binuclear complex is stable for several days even in strong acids, the decomposition cannot be effected in very strongly acidic solution because the adjustment of the ionic strength would lead to difficulties. Therefore the binuclear complex solution containing 0.025 *M* chromium(III) was mixed in a 1 : 1 ratio with 0.5 *M* perchloric acid. The mixture was allowed to stand at room temperature for 4 weeks, but from time to time samples were taken out and the reaction rate was measured in a 1 Cr : 5 EDTA solution at pH 4.7—4.8. Fig. 5 shows the pk' values calculated from the measurements, as a function of the decomposition time.

The results support the assumption that the reaction of the binuclear complex with EDTA becomes gradually faster as the decomposition with acid proceeds. After standing for about 4 weeks the reaction rate attains that of the chromium(III) perchlorate solution; consequently, during this time the binuclear complex is completely transformed into the mononuclear complex.

Many authors have dealt with the formation and decomposition of bi- and polynuclear complexes, but until now it has not been observed that the binuclear hydroxo complexes exhibit a decreased tendency to react with complex-forming compounds such as EDTA.

In the diluted state chromium(III) perchlorate which has been aged for several days reacts much more slowly with EDTA than the freshly prepared solution. This phenomenon led to the idea that the "olation" process taking place during standing, and the acid decomposition of the bi- and polynuclear complexes may be followed by the change in rate of the chromium(III)-EDTA

reaction. The expected processes may be represented schematically as follows:

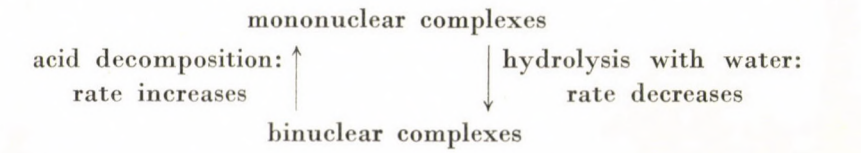

In the experimental section this conception was verified by the reported results. These also supported the literature data according to which the aged or boiled solutions also resist strong acids for several days: only after a week did the reaction rate of the binuclear complex in perchloric acid solution begin to increase slowly, and nearly 4 weeks were necessary for the rate to attain that of the mononuclear complex.

The reaction of the binuclear complex with EDTA differs also in other respects from those of the mononuclear complexes. While the pH dependence of the reaction rate at a slight excess of EDTA is similar to that of the mononuclear complexes, at a greater excess of EDTA the pH scarcely affects the reaction rate.

It is very probable that the binuclear complexes react with EDTA according to a mechanism different than that of the mononuclear complexes. Since the values of the apparent rate constant were calculated on the basis of the mechanism for the reaction of the mononuclear complexes, the data should be considered only as indicative.

The problems concerning binuclear complexes are still far from solved. The work completed so far throws light on the fact that there are fundamental differences from mononuclear complexes. Following the formation and decomposition reactions by the method reported in this paper affords a new possibility for the study of the binuclear complexes and brings closer the elucidation of the mechanism and kinetics.

REFERENCES

1. BJERRUM, N.: Z. physik. Chem. **59,** 336 (1907)
2. BJERRUM, N.: Z. physik. Chem. **73,** 724 (1910)
3. BJERRUM, N.: Z. physik. Chem. **110,** 656 (1924)
4. STIASNY, E.: Gerbereichemie. Verlag Th. Steinkopff, Dresden, 1931
5. HALL, H. T., EYRING, H.: J. Am. Chem. Soc. **72,** 782 (1950)
6. LASWICK, J. A., PLANE, R. A.: J. Am. Chem. Soc. **81,** 3564 (1959)
7. ARDON, M., PLANE, R. A.: J. Am. Chem. Soc. **81,** 3197 (1959)
8. KOLACZKOWSKI, R. W., PLANE, R. A.: Inorg. Chem. **3,** 322 (1964)
9. GRANT, D. M., HAMM, R. E.: J. Am. Chem. Soc. **78,** 3006 (1956)
10. GRANT, D. M., HAMM, R. E.: J. Am. Chem. Soc. **80,** 4166 (1958)
11. GÉHER, J., BECK, M. T.: Acta Chim. Acad. Sci. Hung. **70,** 235 (1971)
12. HAMM, R. E.: J. Am. Chem. Soc. **75,** 5670 (1953)

Judit GÉHER-GLÜCKLICH; Budapest IV., Paksi József u. 43.
Mihály T. BECK; Debrecen 10, Hungary.

Acta Chimica Academiae Scientiarum Hungaricae, Tomus 70 (3), pp. 255—261 (1971)

SYNTHESIS OF SOME L-ASPARTIC AND L-GLUTAMIC ACID DERIVATIVES

J. TOMASZ*

(Reanal, Factory of Laboratory Chemicals, Budapest)

Received July 1, 1970

The synthesis of α-benzyl *N-t*-butyloxycarbonyl-L-aspartate (**VIa**), α-*t*-butyl *N-t*-butyloxycarbonyl-L-aspartate (**IVa**) and α-*t*-butyl *N-t*-butyloxycarbonyl-L-glutamate (**IVb**) is described. In addition, simplified preparations of α-benzyl *N-t*-butyloxycarbonyl-L-glutamate (**VIb**) and *N-t*-butyloxycarbonyl-L-glutamine (**VIII**) are reported.

α-Benzyl *N-t*-butyloxycarbonyl-L-aspartate (**VIa**), α-*t*-butyl *N-t*-butyloxycarbonyl-L-aspartate (**IVa**) and α-*t*-butyl *N-t*-butyloxycarbonyl-L-glutamate (**IVb**) were synthesized. These compounds may be useful intermediates in the synthesis of oligopeptides containing β-aspartyl or γ-glutamyl residues, respectively.

In addition, an improved, large-scale procedure was elaborated for the synthesis of *N-t*-butyloxycarbonyl-L-glutamine (**VIII**), and α-benzyl-*N-t*-butyloxycarbonyl-L-glutamate (**VIb**) was prepared by a simpler method than described earlier [1].

Synthesis of α-t-butyl N-t-butyloxycarbonyl-L-aspartate (IVa) and α-t-butyl N-t-butyloxycarbonyl-L-glutamate (IVb)**

IVa and **IVb** were prepared in the following way:

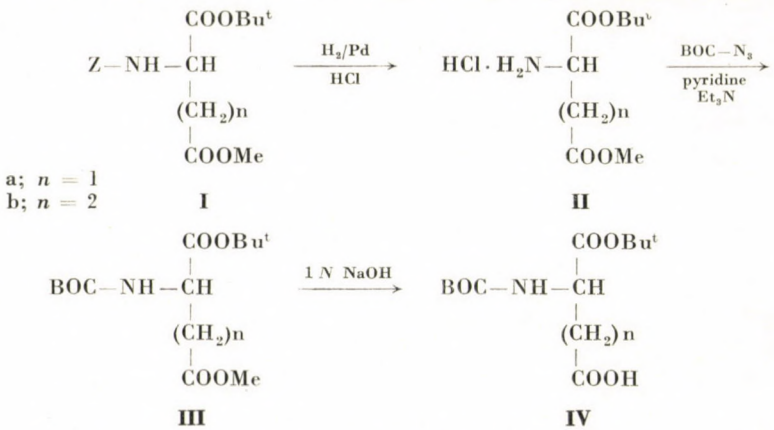

* Present address: Institute of Biochemistry, Biological Research Center, Hungarian Academy of Sciences, Szeged, Hungary.

** Abbreviations used in this paper conform to those recommended by the 5th European Peptide Symposium [2].

The α-*t*-butyl ω-methyl esters of the appropriate *N*-benzyloxycarbonyl-L-amino acids (**Ia**) and (**Ib**) [3, 4] were hydrogenated in absolute methanol in the presence of equivalent hydrogen chloride using 10% palladium on charcoal as catalyst to give the mixed ester hydrochlorides **IIa** and **IIb**. After neutralization with equivalent triethylamine, **IIa** and **IIb** were acylated by treatment with *t*-butyloxycarbonyl azide in pyridine solution at room temperature over a period of 72 hrs. to give α-*t*-butyl β-methyl *N*-*t*-butyloxycarbonyl-L-aspartate (**IIIa**) as well as α-*t*-butyl γ-methyl *N*-*t*-butyloxycarbonyl-L-glutamate (**IIIb**). Selective hydrolysis of **IIIa** and **IIIb** with 1*N* sodium hydroxide in acetone solution at room temperature gave the desired crystalline **IVa** and **IVb** in overall yields of 41.3% and 32.8%, respectively.

Attempts were made to obtain **IIa** and **IIb** directly from the respective ω-methyl esters according to ROESKE's method [5]. It was found that ω-methyl esters of both aspartic and glutamic acid gave clear solutions with isobutylene in dioxan–conc. sulfuric acid mixture after a few days' shaking at room temperature, but considerable reaction occurred only in the case of γ-methyl L-glutamate. However, for preparative purposes, the procedure is useless in this case, too, since the otherwise low yield was diminished further during the neutralization of the reaction mixture, owing to a cyclization reaction giving *t*-butyl pyroglutamate [6].

Synthesis of α-benzyl N-t-butyloxycarbonyl-L-aspartate (VIa) and α-benzyl N-t-butyloxycarbonyl-L-glutamate (VIb)

VIa and **VIb** were synthesized by treatment of the corresponding α-benzyl esters (**Va** and **Vb** [8]) with *t*-butyloxycarbonyl azide in dimethyl formamide solution in the presence of triethylamine at room temperature according to Ref. [7]. **VIa** and **VIb** were obtained as crystalline free acids in yields of 51.8% and 54.8%, respectively.

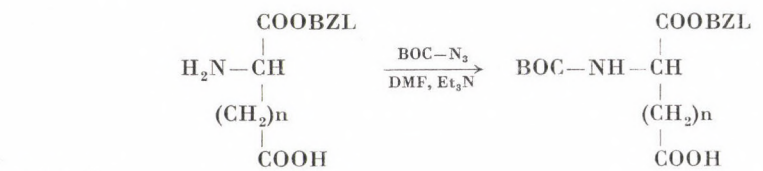

a; $n = 1$
b; $n = 2$

V **VI**

VIb was accessible hitherto either from **Vb** by the "magnesium oxide procedure" in low yield, or indirectly from *N*-*t*-butyloxycarbonyl L-glutamic acid *via* the selective fission of *N*-*t*-butyloxycarbonyl-L-glutamic acid anhydride with benzyl alcohol [1]. **Va** was prepared by the selective debenzylation of

dibenzyl L-aspartate *p*-toluenesulfonate (**VII**) according to Ref. [8]. To obtain **VII**, a procedure was adapted with slight modifications which had been elaborated for the synthesis of the glutamate analogue [9].

Synthesis of N-t-butyloxycarbonyl-L-glutamine (VIII)

The first synthesis of **VIII** was elaborated by HOFMANN *et al.* [10]. The substance was prepared by the reaction of L-glutamine with *t*-butyloxycarbonyl azide in aqueous dioxan containing equivalent triethylamine at 45—50 °C, in 24 hrs. with a yield of 58%. However, the unusually tedious and time-consuming isolation procedure (*e.g.* 27 extractions during a single work-up) due to the excellent water solubility of **VIII**, makes large-scale preparations impossible.

SCHNABEL synthesized the substance with the same acylating agent according to his "pH-stat method" (aqueous dioxan, pH = 10.3, room temperature, 24 hrs.) in a yield of 82%, but he did not describe the isolation and purification of the product [11].* It was found that working under SCHNABEL's conditions but at 50 °C, the reaction time could be reduced to one fourth of that described. [It is our general observation that working at a somewhat higher temperature (50—55 °C), but otherwise under SCHNABEL's conditions, the time of *t*-butyloxycarbonylation is reduced about 4-fold without any racemization of the amino acids.] On the other hand, upon decreasing the pH, the water solubility of **VIII** is significantly reduced. This rendered possible the complete omission of HOFMANN's complicated isolation procedure. After the reaction had been finished, the product could be isolated from the strongly acidified (pH $\sim$ 0.5) aqueous dioxan mixture by a single extraction with ethyl acetate. **VIII** was obtained in a yield of 59%, as a crystalline dicyclohexylamine salt.

Experimental

Melting points are uncorrected and were determined on a Tottoli apparatus (W. Büchi, Flavil, Switzerland). All evaporations were carried out on a rotary evaporator ("Rotavapor", W. Büchi, Flavil, Switzerland) at about 15 mm Hg and a bath temperature of 40 °C. Before microanalysis, the samples were dried in a vacuum desiccator over phosphorus pentoxide at room temperature. Pyridine was dried by distillation from phosphorus pentoxide and stored over calcium hydride. Dimethyl formamide was distilled from phosphorus pentoxide under reduced pressure, *t*-butyloxycarbonyl azide was prepared from *t*-butyloxycarbonyl hydrazide (EGA-Chemie KG., Steinheim) according to Ref. [14]. Thin-layer chromatography was performed on silica gel layers (Kieselgel HR, Merck) in the following solvent systems:

a) chloroform–methanol–glacial acetic acid (95 : 5 : 3),
b) *n*-butanol–glacial acetic acid–water (4 : 1 : 1),

* Other methods for the preparation of **VIII** have been described as well. These, however, differ from the above mentioned ones in the nature of the acylating agents applied; *e.g.* *t*-butyloxycarbonyl fluoride [12] or *t*-butyl 2,4,5-trichlorophenyl carbonate [13] are employed instead of the commonly used *t*-butyloxycarbonyl azide.

c) ethyl acetate–pyridine–glacial acetic acid–water (60 : 5 : 1.5 : 3),
d) *n*-butanol–pyridine–glacial acetic acid–water (30 : 20 : 6 : 11),
e) *s*-butanol–3% ammonium hydroxide (3 : 1),
f) ethyl acetate–pyridine–glacial acetic acid–water (20 : 60 : 6 : 11),
g) benzene–ethyl acetate–glacial acetic acid–water (20 : 20 : 8 : 3),
h) ethanol–water (7 : 3),
i) carbon tetrachloride–ethanol (4 : 1).

Spots were detected by ninhydrin spray after preheating for 15—20 min. at 120—130 °C [15].

α-t-Butyl β-methyl L-aspartate hydrochloride (IIa)

Ia (168.5 g; 0.51 mole) [3] was hydrogenated in absolute methanol (870 ml) containing hydrogen chloride (18 g; 0.51 mole) in the presence of 10% palladium on charcoal (5 g) catalyst until the carbon dioxide evolution ceased (about 1 hr). The catalyst was filtered off and the solution was evaporated. The remaining crystalline substance was mixed with absolute ether (500 ml), filtered, washed with absolute ether (2×200 ml) and dried. 96 g (78%) of white, crystalline, chromatographically homogeneous material (in solvents a), b) and i)) was obtained; m.p. 135.5—137 °C; $[\alpha]_D^{25}$ +7.5° (c = 1.0, methanol).

$C_9H_{17}NO_4 \cdot HCl$ (239.62). Calcd. C 45.11; H 7.15; N 5.84; Cl 14.79. Found C 45.02; H 6.95; N 5.78; Cl 14.63%.

α-t-Butyl β-methyl N-t-butyloxycarbonyl-L-aspartate (IIIa)

Triethylamine (55.5 ml; 0.4 mole) was added dropwise at 0 °C to a vigorously stirred solution of **IIa** (96 g; 0.4 mole) in pyridine (620 ml). Then *t*-butyloxycarbonyl azide (125 ml; 0.88 mole) was added, and the reaction mixture was stirred at room temperature for 3 days. The precipitated pyridine hydrochloride was removed by filtration and washed with pyridine. The combined filtrate and washing was evaporated. The oily, reddish-brown residue (138 g) was dissolved in ethyl acetate (1000 ml). The ethyl acetate solution was washed with 10% aqueous citric acid (5×250 ml), water (5×250 ml), then dried (Na_2SO_4) and evaporated.

The residue (119 g; 98%) began to crystallize after a short standing at room temperature. The crude product could be used for the next step without any further purification. An aliquot after recrystallization from aqueous methanol was homogeneous in solvents a), b) and i) and had a m.p. of 56—58 °C.

$C_{14}H_{25}NO_6$ (303.36). Calcd. C 55.44; H 8.30; N 4.61; "acido labile CO_2" [16] 14.50. Found C 55.32; H 8.16; N 4.68; "acido-labile CO_2" 14.75%.

α-t-Butyl N-t-butyloxycarbonyl-L-aspartate (IVa)

1 *N* sodium hydroxide was added dropwise to a solution of **IIIa** (119 g; 0.39 mole) in a mixture of acetone (1500 ml) and water (250 ml) at room temperature, under stirring. The rate of addition of alkali was controlled so as to keep the pH of the solution at 8.0—8.5. In the course of about 2 hrs. 360 ml 1 *N* sodium hydroxide was consumed. The solution was evaporated to about 800 ml and extracted with ether (3×200 ml). Ether (500 ml) was layered above the aqueous phase and the pH was brought to 2.5 with 1 *N* sulfuric acid under ice-cooling and stirring. After separation of the phases the aqueous layer was extracted with ether (3×200 ml). The combined ethereal solution was washed with water (3×150 ml) and dried (Na_2SO_4). The solution was evaporated to a slightly coloured solid which was contaminated with a trace of *N*-*t*-butyloxycarbonyl-L-aspartic acid (in solvents a), b) and i)). Crude yield: 85 g. The material was dissolved in methanol (6 parts) at room temperature. Water was added to the filtered solution until initial turbidity. (About twice the volume of the employed methanol was necessary.) After one day's standing at room temperature, the crystals were filtered, washed with a little ice-cold methanol–water (1 : 2) mixture and dried. A second portion could be isolated from the mother liquor. The chromatographically homogeneous, white, crystalline substance weighed 61 g (54.2%); m.p. 106 °C; $[\alpha]_D^{25}$ —30.0° (c = 1.0, methanol). The overall yield based on **Ia** was 41.3%.

$C_{13}H_{23}NO_6$ (289.33). Calcd. C 53.96; H 8.36; N 4.84; "acido-labile CO_2" [16] 15.55. Found C 54.23; H 8.27; N 4.77; "acido-labile CO_2" 15.47%.

α-t-Butyl γ-methyl L-glutamate hydrochloride (IIb)

10% palladium on charcoal catalyst (8 g) was added to a solution of **Ib** (450 g; 1.28 mole) [4] in absolute methanol containing hydrogen chloride (43.8 g; 1.20 mole). The suspension was shaken in a stream of hydrogen until no more carbon dioxide could be detected in the departing gas (about 4 hrs.). The catalyst was filtered off and the solution was evaporated. The oily residue was dissolved in absolute ether (2000 ml) and the solution was cooled for a few hours. The separated crystals were collected, washed with some ice-cold absolute ether and dried. Yield: 165 g (51.0%) of white, crystalline substance contaminated with a trace of γ-methyl glutamate (in solvents a), d) and f)). M.p. 132—136 °C; $[\alpha]_D^{25}$ +20.0° (c = 2.0, ethanol) (literature values: m.p. 135—135.5 °C; $[\alpha]_D^{25}$ +21.7° (c = 2.0, ethanol) [17]). The material was used without further purification in the next step.

α-t-Butyl γ-methyl N-t-butyloxycarbonyl-L-glutamate (IIIb)

Triethylamine (57 ml; 0.41 mole) was added dropwise to a stirred solution of **IIb** (105.5 g; 0.41 mole) in pyridine (200 ml) at 0 °C. *t*-Butyloxycarbonyl azide (80 ml; 0.55 mole) was then added and the reaction mixture was stirred at room temperature for 3 days. The separated pyridine hydrochloride was filtered with suction and washed with pyridine. The combined filtrate and washing was evaporated. The remaining reddish-brown oil (142 g) was taken up in ethyl acetate (800 ml). The ethyl acetate solution was extracted with 10% aqueous citric acid (4×200 ml), 10% salt solution (3×200 ml), water (1×100 ml), then dried (Na_2SO_4) and evaporated. The solid residue (114 g; 87.8%) was used without further purification in the next step.

An aliquot was recrystallized from methanol–water to give a chromatographically homogeneous (in solvents a), c) and e)), white substance melting at 62—63.5 °C, $[\alpha]_D^{25}$ —25.0° (c = 1.0, methanol).

$C_{15}H_{27}NO_6$ (317.33). Calcd. C 56.77; H 8.57; N 4.41; "acido-labile CO_2" [16] 13.86. Found C 56.52; H 8.54; N 4.56; "acido-labile CO_2" 13.99%.

α-t-Butyl N-t-butyloxycarbonyl-L-glutamate (IVb)

1 *N* sodium hydroxide was added dropwise to a stirred solution of **IIIb** (114 g; 0.36 mole) in acetone (1700 ml) at room temperature and such a rate that the pH of the solution never exceeded 8.5. The consumption of 1 *N* sodium hydroxide was 364 ml. The solution was evaporated to about 800 ml and extracted with ethyl acetate (3×200 ml), and ether 1×200 ml). Ether (500 ml) was layered above the aqueous phase, then the pH was brought to 2.5 with 1 *N* sulfuric acid under ice-cooling and strirring. The phases were separated and the aqueous layer was extracted with ether (1×800 ml and 1×400 ml). The combined ethereal solution was washed with water (2×300 ml), dried (Na_2SO_4) and evaporated. The crystalline, cream-coloured residue, which was contaminated with some *N*-*t*-butyloxycarbonyl-glutamic acid (in solvents a), c) and e)) weighed 99 g. The crude product was dissolved in methanol (2.5 parts) at room temperature. The solution was decolourized with charcoal and filtered. Water was added to slight turbidity (about the same volume was necessary as the employed methanol), and the solution was allowed to stand overnight at room temperature. The separated mass of colourless crystals was collected by suction, washed with some ice-cold methanol–water (1 : 1) mixture and dried. A second portion could be isolated from the combined mother liquor and washings.

Yield: 83 g (73.7%); m.p. 110—114 °C; $[\alpha]_D^{25}$ —30.2° (c = 1.0, methanol). The substance was chromatographically homogeneous in the above mentioned three solvent systems. The overall yield based on **Ib** was 32.8%.

$C_{14}H_{25}NO_6$ (303.35). Calcd. C 55.43; H 8.31; N 4.62; "acido-labile CO_2" [16] 14.50. Found C 55.26; H 8.35; N 4.73; "acido-labile CO_2" 14.77%.

Dibenzyl L-aspartate p-toluenesulfonate (VII)

VII was produced according to Ref. [9], described for the preparation of the glutamate analogue, but *p*-toluenesulfonic acid was used instead of benzenesulfonic acid.

A mixture of L-aspartic acid (1080 g; 8.1 moles), benzyl alcohol (6000 ml) and *p*-toluenesulfonic acid monohydrate (1710 g; 9.0 moles) was stirred for 6 hrs. at 110 °C in

an open stainless steel vessel, then the reaction mixture was allowed to stand overnight at room temperature. The separated crystals were filtered with suction, washed with ether (7000 ml) and dried.

Yield: 3230 g (82.3%); m.p. 156—158 °C (literature values 155 °C [18], 156—158 °C [19] and 158—160 °C [20, 21]).

α-Benzyl L-aspartate (Va)

Va was obtained according to the procedure described for the synthesis of **Vb** [8]. Yield: 60.5%; m.p. 174—176 °C (literature value 174—175 °C [22]).

α-Benzyl N-t-butyloxycarbonyl-L-aspartate (VIa)

A suspension of **Va** (72 g; 0.32 mole) in dimethyl formamide (600 ml) containing triethylamine (89 ml; 0.64 mole) and *t*-butyloxycarbonyl azide (55 ml; 0.38 mole) was shaken at room temperature until a clear solution was obtained (2—3 days). The solvent was evaporated and ice-cold water (550 ml) was added to the residue. A viscous yellow oil was settled out. It was dissolved by adjusting the pH to 8.0 with small portions of 2 *N* sodium hydroxide under ice-cooling and mixing. The yellow solution obtained was extracted with ether (3×200 ml). The aqueous phase was cooled to 0 °C, overlayered with ethyl acetate (500 ml) and the pH was brought to 3.0 by addition of 20% aqueous citric acid under stirring. After the phases had separated, the aqueous layer was extracted with further amounts of ethyl acetate (2×200 ml). The combined ethyl acetate solution was washed with 10% salt solution (3×100 ml), dried (Na_2SO_4) and evaporated. The residue was a solid and weighed 77 g (74.5%). The crude product was taken up in two volumes of methanol at room temperature. The resulting solution was decolourized with charcoal and filtered. Water was added until the solution became turbid. (About two thirds of the employed methanol were necessary.) The mixture was allowed to stand overnight at room temperature. The separated colourless crystals were collected, washed with some ice-cold methanol–water (3 : 2) mixture and dried. Yield: 53.5 g (51.8%); m.p. 102—104 °C; $[\alpha]_D^{25}$ —25.0° (c = 1.0 methanol).

The substance was homogeneous in solvents a), c) and g).

$C_{16}H_{21}NO_6$ (323.33). Calcd. C 59.43; H 6.55; N 4.33; "acido-labile CO_2" [16] 13.61. Found C 59.60; H 6.78; N 4.42; "acido-labile CO_2" 13.82%.

α-Benzyl N-t-butyloxycarbonyl-L-glutamate (VIb)

VIb was prepared from **Vb** [8] by exactly the same procedure as described above for the synthesis of **VIa**. Yield: 54.8%; m.p. 96.5—99 °C; $[\alpha]_D^{25}$ —32.5° (c = 1.0, methanol) (literature values: m.p. 93—93.5 °C, 92—93 °C, $[\alpha]_D^{20}$ —29.2—30.2° (c = 1.0, methanol) [1]).

For chromatography solvents a), c) and g) were employed.

$C_{17}H_{23}NO_6$ (337.38). Calcd. C 60.52; H 6.87; N 4.15; "acido-labile CO_2" [16] 13.04. Found C 60.38; H 6.99; N 4.25; "acido-labile CO_2" 12.90%.

N-t-Butyloxycarbonyl-L-glutamine·dicyclohexylamine salt (VIII)

t-Butyloxycarbonyl azide (800 ml; 5.5 moles) was added to a suspension of L-glutamine (730 g; 5.0 moles) in 50% aqueous dioxan (1000 ml). The mixture was warmed up to 50—55 °C under vigorous stirring. 4 *N* sodium hydroxide was added dropwise to the reaction mixture at such a rate as to keep the pH value between 10.0—10.5. In the course of 6—7 hrs. the consumption of sodium hydroxide was about 10% more than the calculated value of 2500 ml. A clear, pale-yellow solution was obtained. It was cooled to 0 °C and acidified with concentrated hydrochloric acid to pH 0.5. The separated thick oil was immediately extracted with ice-cold ethyl acetate (5000 ml) and the ethyl acetate solution was dried (Na_2SO_4). The solvent and the azoimide dissolved in ethyl acetate were distilled off.*

* The complete removal of azoimide is of great importance since it forms a well crystallizing dicyclohexylamine salt rendering the purification of the product more difficult.

The oily residue (1000 g) was taken up in ethyl acetate (2000 ml). The solution was filtered off and mixed with dicyclohexylamine (1000 g; 5.0 moles) in ethyl acetate (2000 ml) at 0 °C. The mixture was allowed to stand overnight at room temperature. The precipitate was filtered, washed with cold ethyl acetate and petroleum ether, and dried. Yield: 1400 g (66.0%); m.p. 162—163 °C.

The crude product was dissolved in two volumes of ethanol on a steam bath. To the filtered solution petroleum ether was added at room temperature until it became turbid. (About 4—6 times the volume of employed ethanol was necessary.) The solution was allowed to stand overnight at room temperature. The separated crystals were filtered with suction, washed with ethanol–petroleum ether (1 : 1) mixture, then with petroleum ether, and dried. Yield: 1260 g (59.0%) of white, chromatographically homogeneous substance (in solvents a), b) and h)); m.p. 157 °C; $[\alpha]_D^{25}$ +8.5° (c = 1.0, dimethyl formamide) (literature values m.p. 158—160 °C; $[\alpha]_D^{25}$ +8.5 (c = 1.0 dimethyl formamide) [11]).

$C_{22}H_{41}N_3O_5$ (427.59). Calcd. C 61.80; H 9.67; N 9.83. Found C 61.66; H 9.48; N 9.78%.

*

The author is indebted to the Management of REANAL Factory for permission to publish this work. The microanalyses performed in the Analytical Laboratory of the Institute of Organic Chemistry, L. Eötvös University (Head Mrs. H. Medzihradszky-Schweiger), as well as the valuable technical assistance of Mr. T. Gál and Mr. B. Horváth are gratefully acknowledged.

REFERENCES

1. Schröder, E., Klieger, E.: Ann. **673,** 196 (1964)
2. 5th European Peptide Symposium, Oxford, 1962 (Ed. G. T. Young). The MacMillan Co., New York, 1963
3. Gregory, H., Morley, J. S., Smith, J. M., Smithers, M. J.: J. Chem. Soc. **C, 1968,** 715
4. Camble, R., Purkayastha, R., Young, G. T.: J. Chem. Soc. **C, 1968,** 1219
5. Roeske, R.: J. Org. Chem. **28,** 1251 (1963)
6. Hollósi, M., Kajtár, M.,Ráthonyi, Z., Tomasz, J.: Acta Chim. Acad. Sci. Hung. (In the press)
7. Polzhofer, K. P.: Tetrahedron Letters **1969,** 2305
8. Sachs, H., Brand, E.: J. Am. Chem. Soc. **75,** 4610 (1953)
9. Bruckner, V., Szekerke, M., Kovács, J.: Z. physiol. Chem. **309,** 25 (1957)
10. Hofmann, K., Haas, W. L., Smithers, M. J., Wells, R. D., Wolman, V. Yanaihara, N., Zanetti, G.: J. Am. Chem. Soc. **87,** 620 (1965)
11. Schnabel, E.: Ann. **702,** 188 (1967)
12. Schnabel, E., Herzog, H., Hoffmann, P., Klauke, E., Ugi, J.: Ann. **716,** 175 (1968)
13. Broadbent, W., Morley, J. S., Stone, B. E.: J. Chem. Soc. **C, 1967,** 2632
14. Carpino, L. A.: J. Am. Chem. Soc. **79,** 4427 (1957)
15. Wolman, V., Klausner, Y. S.: J. Chromatog. **24,** 277 (1966)
16. Kutassy, S., Kajtár, J., Medzihradszky-Schweiger, H.: Acta Chim. Acad. Sci. Hung. **57,** 123 (1968)
17. Taschner, E., Chimiak, A., Bator, B., Sokotowska, T.: Ann. **646,** 134 (1961)
18. Velluz, L., Amiard, G., Bartos, J., Coffinet, B., Heymes, R.: Bull. Soc. Chim. France **1956,** 1464
19. Mazur, R. H.: Canad. J. Chem. **40,** 1098 (1962)
20. Gibian, H., Schröder, E.: Ann. **642,** 145 (1961)
21. Zervas, L., Winitz, M., Greenstein, J. P.: J. Org. Chem. **22,** 1515 (1957)
22. Bryant, P. M., Moore, R. H., Pimlott, P. J., Young, G. T.: J. Chem. Soc. **1959,** 3868

Jenő Tomasz; Szeged, Odesszai krt. 62, Hungary.

Acta Chimica Academiae Scientiarum Hungaricae, Tomus 70 (3), pp. 263—266 (1971)

A FURTHER SIMPLIFIED HARDEGGER METHOD FOR THE SYNTHESIS OF 2-DEOXY-D-RIBOSE

J. TOMASZ*

(Reanal, Factory of Laboratory Chemicals, Budapest)

Received July 1, 1970

A simplified, large-scale procedure is described for the synthesis of 2-deoxy-D-ribose (**II**) starting from 1,2 : 5,6-di-0-isopropylidene-3-0-*p*-tolylsulfonyl-α-D-glucose (**III**).

One of the most widely used synthesis of 2-deoxy-D-ribose (**II**) applied on large-scale is based on the alkaline degradation of 3-O-methylsulfonyl-D-glucose (**I**). The process (elimination and hydrolysis) may be formulated as follows [1]:

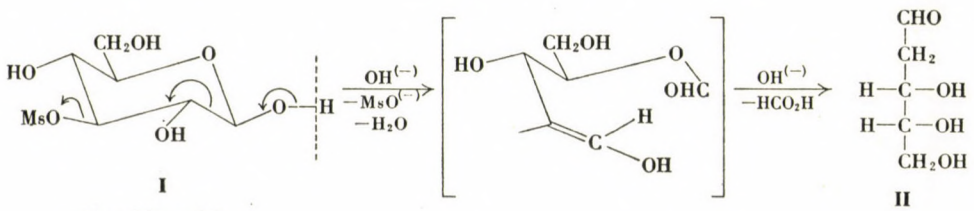

I **II**

Ms = $CH_3—SO_2—$

In the up-to date procedures [2—4] **I** is prepared *in situ* in the reaction mixture by acid hydrolysis of the easily accessible 1,2 : 5,6-di-O-isopropylidene-3-O-methylsulfonyl-α-D-glucose. Subsequent alkaline degradation by dilute sodium hydroxide [2, 3], or by solid sodium carbonate [4] under controlled pH values (8.6—8.9) and temperature (50—60 °C) gives 2-deoxy-D-ribose. The product is isolated from the reaction mixture as its well-crystallizable N-phenylglycosylamine (**V**) in a yield of about 45%.

3-O-*p*-tolylsulfonyl-D-glucose (**IV**) seems to be a more economical starting material for a large-scale synthesis, than **I**. However, HARDEGGER and HUWYLER observed that when 3-O-*p*-tolylsulfonyl-D-glucose (**IV**) is used instead of **I**, the yields are about 50% lower [3]. Contrary to this finding, we observed that a reaction *via* **IV** may be an equally suitable route for the preparation of **II** without any significant decrease in the yield, if the experimental conditions are modified. This is in good agreement with the observations of KENNER

* Present address: Institute of Biochemistry, Biological Research Centre, Hungarian Academy of Sciences, Szeged.

and RICHARDS, who obtained better yields from **IV** than from **I**, carrying out the splitting with calcium hydroxide in water [5].

The starting material of our procedure is 1,2 : 5,6-di-O-isopropylidene-3-O-*p*-tolylsulfonyl-α-D-glucose (**III**). **III** is hydrolyzed with four volumes of dilute (1 : 10) aqueous hydrochloric acid at 90—100 °C for 10—15 min. After neutralization of the resulting solution with solid potassium carbonate, the arising **IV** is decomposed to **II** by treatment with two equivalents of potassium hydrogen carbonate at 60—65 °C in the course of 2 hrs. **II** is isolated from the reaction mixture as its N-phenylglycosylamine (**V**) in a yield of 42.5%. The conversion of **V** to **II** is carried out by a modified SOWDEN's method [6].

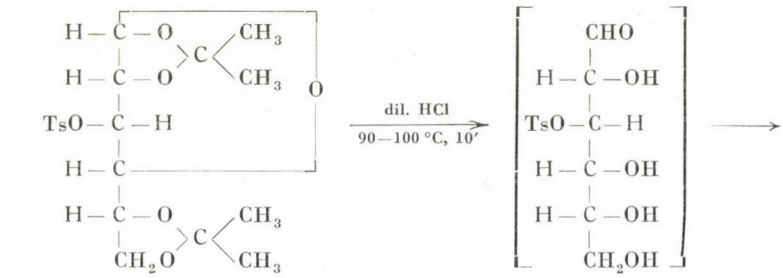

III **IV**

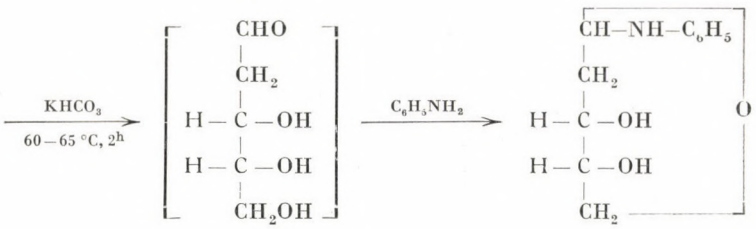

II **V**

III was prepared from 1,2 : 5,6-di-O-isopropylidene-α-D-glucose (**VI**) according to the literature [7], while the latter compound was obtained by a modification of LEVENE's procedure [8].

Experimental

All melting points are uncorrected and were determined with a Tottoli apparatus (W. Büchi, Flavil, Schweiz). Evaporations were carried out under diminished pressure at a bath temperature of max. 45 °C. D-Glucose, acetone and anhydrous cupric sulfate were commercial products. *p*-Tolylsulfonyl chloride was purified in the following way: its saturated solution in acetone was poured into ten volumes of water, with stirring. The separated mass of crystals was collected by filtration with suction and dried at room temperature first in air, then under reduced pressure over phosphorus pentoxide. Pyridine was distilled from phosphorus pentoxide and stored over calcium hydride. Aniline and benzaldehyde were freshly distilled before use.

1,2 : 5,6-Di-O-isopropylidene-α-D-glucose (VI)

VI was prepared by a slight modification of LEVENE's procedure [8].

A suspension of D-glucose (3.6 kg) and anhydrous cupric sulfate (9.0 kg) in acetone (36 l) containing conc. sulfuric acid (59 ml) was vigorously stirred at 40 °C over a period of 24 hrs. with the exclusion of moisture. The unchanged D-glucose and cupric sulfate were collected by suction, thoroughly washed with acetone and the combined filtrate and washings were decolourized with charcoal (300 g) at room temperature. The clear solution was neutralized with conc. aqueous ammonium hydroxide, and the precipitated ammonium sulfate was filtered off. After evaporation the dried, crystalline, pale-yellow residue weighed 3.15 kg (~60%) and needed no further purification for the next step; m.p. 94—98 °C (*cf.* m.p. 95—101 °C for a crude product, 105—109 °C [9], 108—110 °C [4], 109—111 °C [10]).

1,2 : 5,6-Di-O-isopropylidene-3-O-p-tolylsulfonyl-α-D-glucose (III)

III was prepared from 1,2 : 5,6-di-O-isopropylidene-α-D-glucose at 0—10 °C as described in the literature [7]. Yield: 96% (crude product), m.p. 118 °C (after recrystallization from 3 volumes of methanol; *cf.* m.p. 120—121 °C [7]).

2-Deoxy-N-phenyl-D-ribosylamine (V)

A suspension of recrystallized **III** (1035 g; 2.5 moles) was stirred for 10—15 min. on a steam bath in dilute (1 : 10) aqueous hydrochloric acid (4000 ml) warmed previously to 90—100 °C. The evolving acetone was collected by a condenser. A dark-brown solution resulted containing some undissolved resin-like material. The mixture was immediately cooled to 60 °C and neutralized cautiously with small portions of solid potassium carbonate (about 400—450 g were necessary). Potassium hydrogen carbonate (500 g; 5.0 moles) was added and stirring was continued at 60—65 °C for 2 hrs. The reaction mixture was cooled to room temperature and neutralized with conc. hydrochloric acid (about 300—400 ml were necessary). The solution was evaporated as far as possible. The semi-solid residue was brought onto a large Buchner funnel by several portions of methanol and the oily product was eluted from the large crystalline mass of the different potassium salts by further portions of methanol. (For the whole process not more than 4 l of methanol was required.) The filtrate was evaporated as above. The residue was taken up in methanol (1500—1750 ml) and filtered. Aniline (230 ml) and water (200—250 ml) were added to the filtrate and, after seeding, the solution was allowed to stand overnight in a refrigerator.

The separated pale-yellow crystals were collected, washed successively with distilled water (3×500 ml), 50% aqueous methanol (1×500 ml), methanol (3×500 ml) and ether (2×500 ml), then dried at room temperature under diminished pressure over phosphorus pentoxide. Yield: 240 g (42.5%); m.p. 166 °C, with decomposition (*cf.* m.p. 166—177 °C, *e.g.* [2, 3, 4], for crude products).

2-Deoxy-D-ribose (II)

A mixture of crude **V** (1200 g; 6.0 moles), benzoic acid (120 g), benzaldehyde (1200 ml; 12 moles) and distilled water (10 l.) was shaken at room temperature for 24 hrs. in a well-stopped stainless steel reaction vessel. Benzalanilide separated as a dark oily layer and was extracted with ether (3×3000 ml). The aqueous phase was evaporated to about half of its volume, and decolourized by stirring with charcoal (120 g) for 1 hr. at room temperature.

The filtered solution was evaporated to a weight of 720±60 g. The resulting viscous, colourless or pale-yellow sirup was dissolved in a 1 : 6 mixture of 2-propanol–acetone (480 ml) at room temperature, seeded and kept at —5 °C overnight. The crystals were crushed, collected by suction, washed with some ice-cold 2-propanol–acetone mixture and dried in a vacuum desiccator over phosphorus pentoxide. A second crop could be isolated by repeated working-up of the combined mother liquor and washing.

Yield: 660 g (85%) of 2-deoxy-D-ribose as a mixture of the α- and β-anomers, m.p. 78—88 °C, $[\alpha]_D^{25}$ —59.1° (at equilibrium, $c = 1.1$, water). The m.p. of the pure β-anomer is 95—97 °C [3].

The overall yield from D-glucose is 10.4%.

*

Thanks are offered to the Management of Reanal Factory for permission to publish this work. The valuable technical assistance of Mr. T. GÁL is gratefully acknowledged.

REFERENCES

1. SMITH, D. C. C.: Chem. Ind. **1955,** 92; J. Chem. Soc. **1957,** 2690
2. HARDEGGER, E., SCHELLENBAUM, M., HUWYLER, R., ZÜST, A.: Helv. Chim. Acta **40,** 1815 (1957)
3. HARDEGGER, E.: Methods Carbohydr. Chem. **1,** 177 (1962)
4. RECONDO, E., RINDERKNECHT, H.: Helv. Chim. Acta **43,** 1653 (1960)
5. KENNER, J., RICHARDS, G. N.: J. Chem. Soc. **1957,** 3019
6. SOWDEN, J. C.: J. Am. Chem. Soc. **76,** 3541 (1954)
7. FREUDENBERG, K., IVERS, O.: Chem. Ber. **55,** 929 (1922)
8. MEYER, G. M., LEVENE, P. A.: J. Biol. Chem. **92,** 257 (1931); LEVENE, P. A., RAYMOND, A. L.: J. Biol. Chem. **92,** 757 (1931)
9. GLEN, W. L., MYERS, G. S., GRANT, G. A.: J. Chem. Soc. **1951,** 2568
10. LODER, D. J., LEWIS, W. L.: J. Am. Chem. Soc. **54,** 1041 (1932)

Jenő TOMASZ; Szeged, Odesszai krt. 62, Hungary.

Acta Chimica Academiae Scientiarum Hungaricae, Tomus 70 (3), pp. 267—270 (1971)

ON THE CRYSTALLIZATION OF 2,4,6-TRIBENZOYLOXYPROPIOPHENONE $C_{30}H_{22}O_7$ FROM SOLUTIONS IN DIFFERENT SOLVENTS

K. SASVÁRI and T. SZÉLL

(Central Research Institute for Chemistry, Hungarian Academy of Sciences, Budapest, and Department of Applied Chemistry, A. József University, Szeged)

Received July 3, 1970

2,4,6-tribenzoyloxypropiophenone crystals obtained from solutions in different solvents (methanol, ethanol, benzene and toluene), almost always show a gradually decreasing melting point. The crystals contain one solvent molecule per one molecule of $C_{30}H_{22}O_7$ and most probably form clathrate type compounds. Crystals with no trace of the solvent could also be obtained from a solution in ethanol. In this case, however, the unit cell contained 8 molecules of $C_{30}H_{22}O_7$ instead of 4 as was found for the crystals containing solvent.

2,4,6-Tribenzoyloxypropiophenone samples prepared and crystallized from solutions of four different solvents as described in the experimental part of this paper, show a decreasing melting point. Immediately after crystallization the melting point was found to be about 85 °C. If the crystals are kept in air at room temperature, depending on the solvent used, the melting point will decrease at different rates and the crystals will simultaneously turn opaque. This alteration is relatively fast for crystals obtained from solutions in methanol and ethanol in comparison with the crystals from the other two solvents. The opaque crystals keep their original morphology but are plastic and can easily be bent and smeared. After a longer period in air at room temperature even their morphology changes and a shapeless opaque mass remains, the melting point of which is indefinite.

On crystallization from an ethanolic solution it was found that besides the crystals with the behaviour just described, depending on the circumstances of crystallization which, however, are not yet completely clarified, also colourless transparent stubby crystals could be obtained, which were stable in air. As can be established at present it is easier to obtain these stable crystals than metastable ones, which are mostly obtained by a slightly speeded crystallization. At the same time, however, only one of the two types of crystals will appear and so far we have not obtained the two types mixed. When the metastable crystals were kept in the solution and especially if in the meantime the solution was also diluted, stable crystals could be found in the solution after a day or two.

In any case metastable crystals can always be retained for an optional time without any alteration if they are kept in the saturated vapour space of

the solvent. From this fact we concluded that in all cases the metastable crystals contain in their crystal lattices a certain amount of solvent molecules and have a stability depending on the kind of solvent.

For preliminary study of the crystals mentioned above and to determine their real composition, the crystals have been investigated by X-ray diffraction. To avoid alteration of the crystals, while taking X-ray photographs, the crystals were put in closed capillary above a little amount of the solvent to maintain saturation pressure. The cell parameters and symmetry of the above crystals were determined from Buerger precession and Weissenberg X-ray photographs. The data are summarized in Table I. From the systematic absences of reflections ($0k0$) if $k = 2n+1$ and ($h0l$) if $h+l = 2n+1$ the space group $P2_1/n$ could be established for all metastable crystals. From the systematic absences of reflections ($0k0$) if $k = 2n+1$ and ($h0l$) if $l = 2n+1$, the space group of the stable crystal, obtained from the solution in ethanol, proved to be $P2_1/c$.

Table I

Crystal data of 2,4,6-tribenzoyloxypropiophenone crystallized from solutions in four different solvents

The last two rows give the measured and calculated weight reductions effected by heat-treatment

Solvent	Methanol	Ethanol		Ligroine*	
		(metastable)	(stable)	benzene	toluene
a (Å)	16.619	16.841	9.532	16.634	16.761
b	8.586	8.547	26.005	8.443	8.549
c	21.479	21.493	20.674	21.515	21.229
β (°)	92.70	92.00	96.73	93.17	93.42
Z	4	4	8	4	4
V (Å^3)	3058.17	3091.85	5089.51	3016.84	3036.42
D_m (g · cm^{-3})	1.146	1.151	1.293	1.255	1.227
D_x (g · cm^{-3})	1.143	1.161	1.290	1.260	1.283
Space group	$P2_1/n$	$P2_1/n$	$P2_1/c$	$P2_1/n$	$P2_1/n$
ΔG % (meas.)	5.89	8.25	0	13.25	15.26
ΔG % (calc.)	6.09	8.52	0	13.64	15.71

* Boiling range: 100—120 °C.

All five modifications, as can be seen in Table I, have the same crystal symmetry, and the cell dimensions of the four metastable crystals show only slight differences. The measured densities (by flotation in aqueous KI solution, and with a pycnometer in water containing 0.1% of the detergent "ultra") of the metastable crystals can very well be approximated by the calculated ones (Table I) if we take four molecules per unit cell with the composition

$C_{30}H_{22}O_7 \cdot R$, where R represents a molecule of the solvent. Thus we may consider it proved that metastable crystals contain in their lattices one molecule of solvent per molecule of 2,4,6-tribenzoyloxypropiophenone. The same can be stated on the basis of measuring the weight reduction upon thermal treatment. Well developed crystals, previously dried in air at room temperature for a period of 50 min, were taken and treated in vacuum at 65 °C for a period of 27 hrs. This thermal treatment resulted in weight reductions as listed in Table I, and compared with the calculated ones. The agreement is satisfactory if we consider that some slight weight reduction, which cannot be avoided, was already effected by the process of drying the crystals.

The stable crystal obtained from ethanol solution has a considerably larger unit cell than the metastable ones but keeps the same symmetry. In this case the calculated density equals the measured one if we take 8 molecules of 2,4,6-tribenzoyloxypropiophenone to be contained in the unit cell without any trace of the solvent molecules.

It seems probable that for metastable crystals with solvent molecules in their lattices, the POWELL [1] conditions may be satisfied for the formation of clathrate type compounds. To attain certainty, complete crystal structure determination is contemplated for one of the metastable crystals as well as for the stable crystal. This work is in progress.

Experimental

2,4,6-tribenzoyloxypropiophenone has been prepared from 6 moles of 2,4,6-trihydroxypropiophenone dissolved in 5 ml of pyridine by gradually adding 20 moles of benzoylchloride to the solution at 0 °C. The solution was kept for one night in a refrigerator below 0 °C, then 200 ml of water was added and the mixture was stirred for a period of about 15 min. The suspension was extracted three times with 50 ml diethylether and the combined solution washed three times with 50 ml water and finally dried (Na_2SO_4). In the end the ether was removed by distillation in vacuum. The end product is 2,4,6-tribenzoyloxypropiophenone $C_{30}H_{22}O_7$ which is soluble in methanol or ethanol as well as in mixtures of ligroine + benzine or ligroine + toluene (1 : 3). From the solutions, colourless transparent crystals can be obtained with well defined planes and edges mostly with a shape of laths.

Analysis of the compound dried in vacuum, gave C 72.9 and H 4.6%. (Calcd. C 72.9 and H 4.5%). The i.r. spectrum taken by Dr. P. SOHÁR [2] is in accordance with the tribenzoate structure.

*

The authors wish to express their thanks to Mr. Cs. KERTÉSZ for his valuable help in collecting X-ray data and also to Mrs N. AGÓCS and Mrs N. BARTÓK for measuring densities.

REFERENCES

1. POWELL, H. M., RAYNER, J. H.: Nature, (Lond.) **163**, 566 (1949)
2. SOHÁR, P.: Private communication (1970)

Kálmán SASVÁRI
Tamás SZÉLL
Budapest II., Pusztaszeri út 57—69.

Acta Chimica Academiae Scientiarum Hungaricae, Tomus 70 (3), pp. 271—282 (1971)

STEREOCHEMICAL STUDIES, IX* CYCLIC AMINOALCOHOLS AND RELATED COMPOUNDS, III*

SYNTHESIS OF SOME N-ACYLAMINOMETHYLCYCLOPENTANE AND CYCLOHEXANE DERIVATIVES AND RELATED COMPOUNDS**

G. BERNÁTH, E. CSÓKÁSI, I. HEVÉR, L. GERA and K. KOVÁCS

(Institute of Organic Chemistry, A. József University, Szeged)

Received July 5, 1970

The synthesis of some derivatives of N-acylaminomethylcyclohexane (**I—VII**), of *cis*- and *trans*-N-acylaminomethylcyclohexan-2-ol (**VIII—XIX**), N,N'-diacyl-*cis*-1,4-diaminomethylcyclohexane (**XX—XXII**), of N-acylaminomethylcyclopentylamine (**XXIII—XXVI**), N-acyl-*cis*-2-aminomethylcyclopentanol (**XXVII—XXXI**), N-acyl-*cis*-2-hydroxymethylcyclohexylamine (**XXXII—XXXIV**), N-acylaminomethylcyclohexene-1 (**XXXV—XXXIX**), and N-substituted *cis*-2-acetoxycyclohexanecarboxamide (**XL—XLIII**) is described.

Several N-acylated derivatives of *cis*- and *trans*-2-aminomethylcyclohexanol, of *cis*- and *trans*-2-hydroxymethylcyclohexylamine, and of related compounds with cyclopentane structure [4] have been prepared for our stereochemical studies on cyclic 1,3-aminoalcohols [1—3]. Since some of the aminoalcohols and their derivatives are known to possess properties interesting from a pharmacological point of view, it seemed advisable to study the pharmacological aspects of these compounds, too. As we had prepared a number of analogous compounds earlier, this added incentive to such studies promising further data on correlations between chemical structure and physiological effects. Since many compounds were *cis* and *trans* derivatives prepared in stereospecific syntheses, a comparison of the pharmacological effect of compounds with different configurations also seemed to be feasible. Furthermore, since analogous compounds with cyclohexane, cyclopentane, and with bicyclic skeleton obtained from these compounds [5] became available, pharmacological effects could be also studied as a function of configuration and conformation [6].

The pharmacological studies have shown [6] that, among the aminoalcohols mentioned, the N-acyl derivatives of 2-aminomethylcyclohexanol are valuable pharmacons affecting the central nervous system; this suggested the synthesis of some further analogous compounds.

It is surprising that while the N-alkyl and N-dialkyl derivatives of cyclo-

* Part VIII (II): G. BERNÁTH, K. KOVÁCS, K. L. LÁNG: Acta Chim. Acad. Sci. Hung. **65**, 347 (1970).

** Some of the compounds described here form the subject of Hung. Pat. No. 156 542, requested Sept. 11, 1967, by G. BERNÁTH, K. KOVÁCS, E. PÁLOSI, P. GÖRÖG, L. SZPORNY (accepted: July 4, 1971).

hexylmethylamine and of its analogues substituted in the skeleton are systematically and widely explored analgesics, the related N-acyl compounds are but rarely mentioned. In connection with studies on analgesics with structures simpler than that of morphine, the synthesis of numerous N-alkyl derivatives of cyclohexylmethylamine [7—11] has been worked out. The local anaesthetic effect of related substances [12—14] as well as their effect upon blood pressure [15, 16] have been studied. Though N-benzoylcyclohexylmethylamine has been known for a long time [17, 18], no preparation of the series of related acid amides has been reported. It was only recently [19] that a few N,N'-disubstituted cyclohexane-1,4-bismethylamine derivatives, among them acid

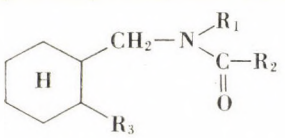

I-XIX
(See: Table I)

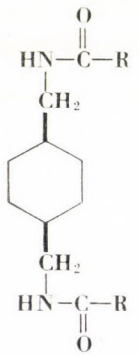

XX-XXII
(See: Table II)

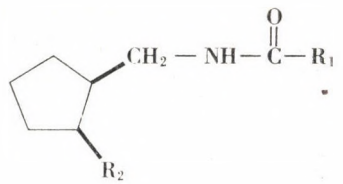

XXIII-XXXI
(See: Table III)

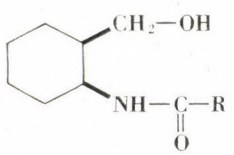

XXXII-XXXIV
(See: Table IV)

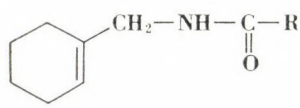

XXXV-XXXIX
(See: Table V)

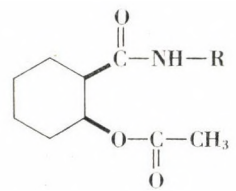

XL–XLIII
(See: Table VI)

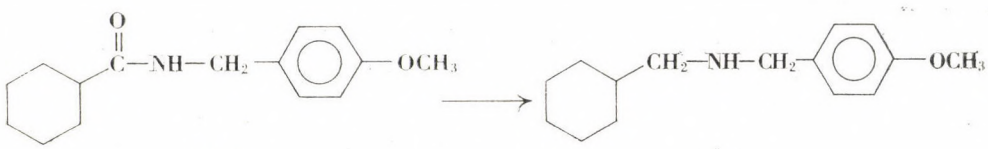

XLIV **XLV**

Fig. 1

Table I

Melting points and analyses of N-*acylaminomethylcyclohexane derivatives* **I – XIX**

No.	R_1	R_2	R_3	Configuration	Formula, molecular weight	M.p (°C); solvent of crystallization	Analysis (%) Calcd./Found			Note
							C	H	N	
I	H	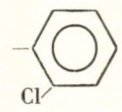	H	—	$C_{41}H_{18}ONCl$ 251.76	122.5—123 ethanol	66.77 67.18	7.23 6.87		
II	H	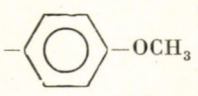	H	—	$C_{15}H_{21}O_2N$ 274.34	116—116.5 ethanol	72.85 72.90	8.55 8.24	5.66 5.74	
III	H	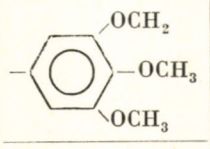	H	—	$C_{17}H_{25}O_4N$ 307.40	140—141 ethanol	66.43 66.70	8.20 7.74	4.55 4.86	*a)*
IV	H	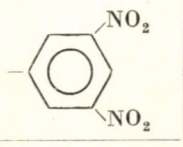	H	—	$C_{14}H_{17}O_5N$ 307.31	160—160.5 ethanol	54.71 54.90	5.58 5.71	13.67 14.00	*b)*
V	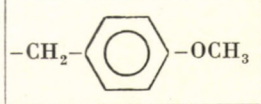	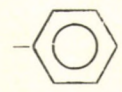	H	—	$C_{22}H_{27}O_4N$ 337.66	79.5—80 ethanol	78.27 78.44	8.07 7.90		
VI	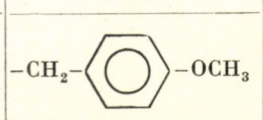	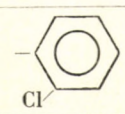	H	—	$C_{22}H_{26}O_2NCl$ 371.50	88.5 ethanol	71.06 71.24	7.00 6.93		
VII	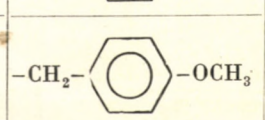	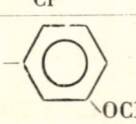	H	—	$C_{25}H_{33}O_5N$ 427.53	84—85 ethanol	70.23 70.15	7.78 8.11		
VIII	H	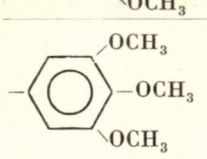	OH	*cis*	$C_{15}H_{21}O_3N$ 263.35	96—96.5 ethanol–water	68.41 68.60	8.04 8.14		*c)*
IX	H	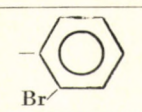	OH	*cis*	$C_{14}H_{18}O_2NBr$ 312.22	111—111.5 ether	53.86 53.97	5.81 5.64		*c)*
X	H	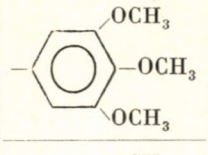	OH	*cis*	$C_{17}H_{25}O_5N$ 323.40	159—159.5 ethanol	63.14 63.07	7.79 7.59		*d)*
XI	H	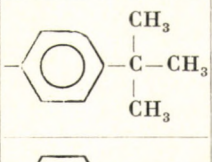	OH	*cis*	$C_{18}H_{27}O_2N$ 289.43	124—124.5 benzene–petroleum ether	74.70 74.48	9.40 8.98		
XII	H	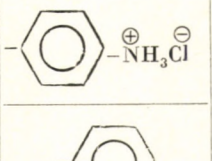	OH	*cis*	$C_{14}H_{21}O_2N_2Cl$ 284.79	191 ethanol–ether	59.04 58.82	7.43 7.53		
XIII	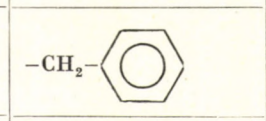		OH	*cis*	$C_{21}H_{25}O_2N$ 323.42	114—115 ethanol	77.99 77.60	7.79 7.73		
XIV	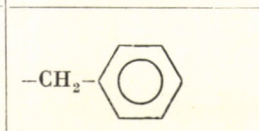	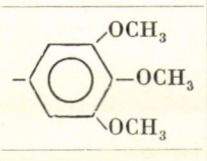	OH	*cis*	$C_{24}H_{31}O_5N$ 413.50	163—163.5 ethanol	69.70 70.02	7.84 7.82		
XV	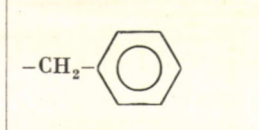	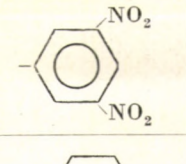	OH	*cis*	$C_{21}H_{23}O_6N_3$ 413.44	140—140.5 ethanol	61.02 61.16	5.66 5.91	10.16 10.37	
XVI	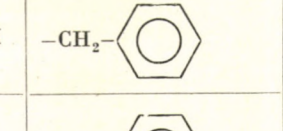	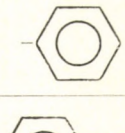	OH	*trans*	$C_{21}H_{25}O_2N$ 323.42	163.5—164.5 ethanol	77.99 77.98	7.19 7.12	4.33 4.59	
XVII	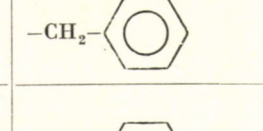	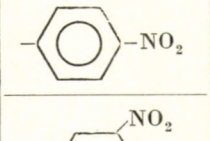	OH	*trans*	$C_{21}H_{24}O_4N_2$ 368.50	144—144.5 ethanol–water	68.48 68.40	6.56 6.70	7.60 8.01	*a)*
XVIII	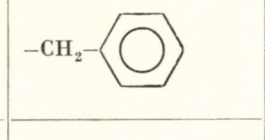	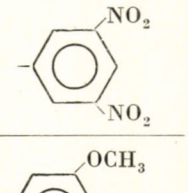	OH	*trans*	$C_{21}H_{23}O_6N_3$ 413.44	162—162.5 ethanol	61.02 61.38	5.60 5.72	10.16 10.02	
XIX	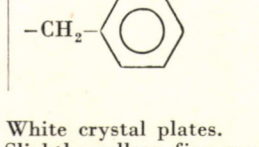	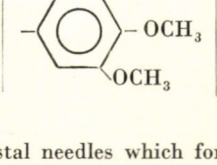	OH	*trans*	$C_{24}H_{31}O_5N$ 413.52	74—75 ethanol	69.70 69.92	7.84 7.92		

a) White crystal plates.
b) Slightly yellow, fine crystal needles which form a fluffy cluster.
c) Very soluble in ethanol.
d) White crystal needles which form a fluffy cluster.

amides were synthesized in the course of studies on substances affecting fat metabolism.

In former communications the stereospecific syntheses of *cis*- and *trans*-2-aminomethylcyclohexanol, of *cis*- and *trans*-2-hydroxymethylcyclohexylamine [1—3], and of the corresponding 1,3-aminoalcohols with cyclopentane structure [4] have been reported. This paper describes syntheses of some further acid amide derivatives, and of some acid amides with related structure, all containing the aminomethylcyclopentane or aminomethylcyclohexane structural moiety. The compounds synthesized are N-acylaminomethylcyclohexanes (**I—VII**, *cf.* Table I), *cis*- and *trans*-N-acylaminomethylcyclohexan-2-oles (**VIII—XIX**, *cf.* Table I), derivatives of N,N'-diacyl-*cis*-1,4-diaminomethylcyclohexane (**XX—XXII**, *cf.* Table II), N-acylaminomethylcyclopentylamine derivatives (**XXIII—XXVI**, *cf.* Table III), N-acyl-*cis*-2-aminomethylcyclopentanol derivatives (**XXVII—XXXI**, *cf.* Table III), N-acyl-*cis*-2-hydroxymethylcyclohexylamine derivatives (**XXXII—XXXIV**, *cf.* Table IV), N-acylaminomethylcyclohexene-1 derivatives (**XXXV—XXXIX**, *cf.* Table V), and *cis*-2-acetoxycyclohexanecarboxamides (**XL—XLIII**, *cf.* Table VI).

Among the many methods [20—25] available for the preparation of aminomethylcyclohexane, used in the synthesis of the N-acylaminomethylcyclohexane derivatives **I—IV**, we selected that proposed by MOUSSERON *et al.* [26] with some modification. The 1-cyanocyclohexene [27] was reduced with sodium in a hot alcoholic solution. The amine thus obtained, containing a very slight contamination of 1-aminomethylcyclohexene (**XXIX**), was hydrogenated in the presence of Adams' PtO_2 catalyst. The catalytic hydrogenation of aminomethylcyclohexene-1 (**L**) prepared by lithium aluminium hydride reduction [18] of 1-cyanocyclohexene proved to be an even more convenient pathway to aminomethylcyclohexane.

Reduction with lithium aluminium hydride of N-hexahydrobenzoyl-*p*-methoxybenzylamine (**XLIV**) obtained by the reaction of cyclohexanecarboxylic acid chloride with *p*-methoxybenzylamine yielded N-*p*-methoxybenzylaminomethylcyclohexane (**XLV**) which was used in the preparation of the N-acyl-N-*p*-methoxybenzylaminomethylcyclohexane derivatives **V—VII** (*cf.* Fig. 2).

cis: **XLVI** *cis*: **XLVIII**
trans: **XLVII** *trans*: **XLIX**

Fig. 2

The starting material in the preparation of derivatives **VIII—XII** of N-acyl-*cis*-2-aminomethylcyclohexanol was *cis*-2-aminomethylcyclohexanol. In order to obtain this compound, *cis*-2-hydroxycyclohexanecarboxamide was reduced with lithium aluminium hydride, as described earlier [2]. The N-acyl

Table II

Melting points and analyses of N,N'-*diacyl-cis-1,4-diaminomethylcyclohexane derivatives* **XX—XXII**

No.	R	Formula; molecular weight	M.p. (°C); solvent of crystallization	Analysis (%) Calcd./Found		Note
				C	H	
XX	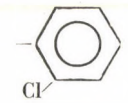	$C_{22}H_{24}O_2N_2Cl_2$ 419.36	238—240 ethanol	63.01 63.39	5.77 5.74	*a)*
XXI		$C_{22}H_{24}O_2N_2F_2$ 386.45	260—261 ethanol	68.38 68.20	6.26 6.10	*a)*
XXII	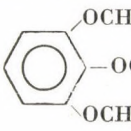	$C_{28}H_{38}O_8N_2$ 530.63	270—273 methanol	63.38 63.33	7.22 7.37	*a)*

a) Melting with decomposition.

compounds **VIII—XI** were prepared by direct acylation with the appropriate acid chloride of *cis*-2-aminomethylcyclohexanol. Reduction with Adams' PtO_2 catalyst of N-*p*-nitrobenzoyl-*cis*-2-aminomethylcyclohexanol [2] yielded N-*p*-aminobenzoyl-*cis*-2-aminomethylcyclohexanol (**XII**). The Schotten–Baumann acylation of *cis*- and *trans*-N-benzyl-2-aminomethylcyclohexanol (**XLVIII**, **XLIX**) afforded the derivatives (**XIII—XV** and **XVI—XIX**) of N-benzyl-N-acyl-*cis*- and N-benzyl-N-acyl-*trans*-2-aminomethylcyclohexanol. The compounds **XLVIII** and **XLIX** were obtained by lithium aluminium hydride reduction of *cis*- and *trans*-N-benzyl-2-hydroxycyclohexanecarboxamides (**XLVI**, **XLVII**) which, in turn, were prepared by a reaction of *cis*- and *trans*-β-hydroxycyclohexanecarboxylic acid with benzylamine (*cf.* Fig. 3). The acyl derivatives **I—XIX** obtained with the usual methods of acylation are shown in Table I.

Some N,N'-diacyl-*cis*-1,4-diaminomethylcyclohexane derivatives (**XX—XXII**) were also prepared (*cf.* Table II). Commercially available (Aldrich) *cis*-1,4-diaminomethylcyclohexane was the starting material in the preparation of these N-acyl compounds.

Cyanocyclopentane (**LIII**) was prepared from cyclopentyl bromide, according to the method described by ROGERS and ROBERTS [29]. Reduction of **LIII** with lithium aluminium hydride [18] yielded aminomethylcyclopentane (**LII**) (*cf.* Fig. 4). A method consisting of the degradation of cyclopentylacetamide [30] and cyclopentyl acetic anhydride [31] might also be considered. Acylation of aminomethylcyclopentane (**LII**) led to derivatives **XXIII—XXV** of N-acylaminomethylcyclopentane (*cf.* Table II).

LIII **LII**

Fig. 3

In an earlier communication [4] we have already described the reduction, with lithium aluminium hydride, of *cis*-2-hydroxycyclopentanecarboxamide leading to *cis*-2-aminomethylcyclopentanol, which is the starting material in the synthesis of derivatives **XXVI—XXXI** of N-acyl-*cis*-2-aminomethylcyclopentanol. *Cis*-2-aminomethylcyclopentanol thus obtained could be converted by Schotten—Baumann acylation into N-acyl compounds **XXVI—XXXI** with fairly good yields (*cf.* Table III).

Reduction, with lithium aluminium hydride, of *cis*-hexahydroanthranilic acid gave *cis*-2-hydroxymethylcyclohexylamine, the acylation [2] of which produced, with very good yields, derivatives **XXXII—XXXIV** of N-acyl-*cis*-2-hydroxymethylcyclohexylamine (shown in Table IV).

Acylation [18] of aminomethylcyclohexene-1, produced by the reduction with lithium aluminium hydride [27] of 1-cyanocyclohexene, yielded the derivatives **XXXV—XXXIX** of N-acylaminomethylcyclohexene-1. Melting points and analytical data of these acid amides are listed in Table V.

A few N-substituted derivatives of *cis*-2-acetoxycyclohexanecarboxamide (**XL—XLIII**) have been prepared, too. The *cis*-2-hydroxycyclohexanecarboxylic acid (**LIV**) was acylated with acetyl chloride according to the method described by PASCUAL *et al.* [28]; the *cis*-2-acetoxycyclohexanecarboxylic acid (**LV**) thus obtained was converted with thionyl chloride into acid chloride (**XLVI**). Treatment of the latter with the appropriate amine produced the N-substituted *cis*-2-acetoxycyclohexanecarboxamides (**XL—XLIII**) (*cf.* Fig. 4). Melting points and analyses of these compounds are listed in Table VI.

Table III

Melting points and analyses of N-*acylaminomethylcyclopentane derivatives* **XXIII—XXXI**

No.	R_1	R_2	M.p. (°C); solvent of crystallization	Formula, molecular weight	Analyses (%) Calcd./Found			Note
					C	H	N	
XXIII	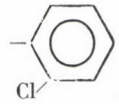	H	88.5—89 ethanol	$C_{13}H_{17}ONCl$ 238.74	65.40 65.16	7.18 7.25	5.86 5.64	*a)*
XXIV	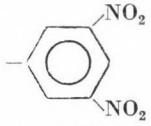	H	151 ethanol	$C_{13}H_{15}O_5N_3$ 295.36	52.88 52.57	5.76 5.30	14.23 13.80	*b)*
XXV	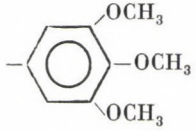	H	148 ethanol	$C_{16}H_{23}O_4N$ 293.22	65.53 65.70	7.85 7.97	4.78 4.80	
XXVI	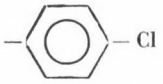	OH	125—125.5 ethanol	$C_{13}H_{16}O_2NCl$ 253.70	61.54 61.96	6.36 6.24		
XXVII	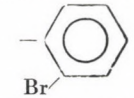	OH	106—106.5 ether	$C_{13}H_{16}O_2NBr$ 298.20	52.36 52.70	5.41 5.50		*c)*
XXVIII		OH	121 ethanol	$C_{14}H_{19}O_2N$ 233.30	72.08 71.75	8.21 7.95		

XXIX	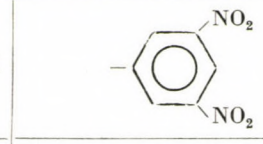	OH	212 ethanol	$C_{13}H_{15}O_6N_3$ 309.28	50.49 50.17	4.89 4.73	13.58 13.16	*b)*
XXX	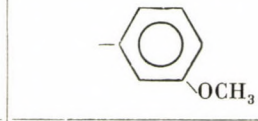	OH	76—76.5 petroleum ether	$C_{14}H_{19}O_3N$ 249.30	67.45 67.16	7.68 7.39	5.56 5.87	
XXXI	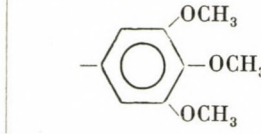	OH	135.5—136 ethanol	$C_{16}H_{23}O_5N$ 309.34	62.12 62.34	7.49 7.47	4.53 4.59	*d)*

a) Chlorine, calcd. 14.85; found 14.90%.
b) Slightly yellow crystals.
c) Very soluble in ethanol.
d) Sparingly soluble in benzene.

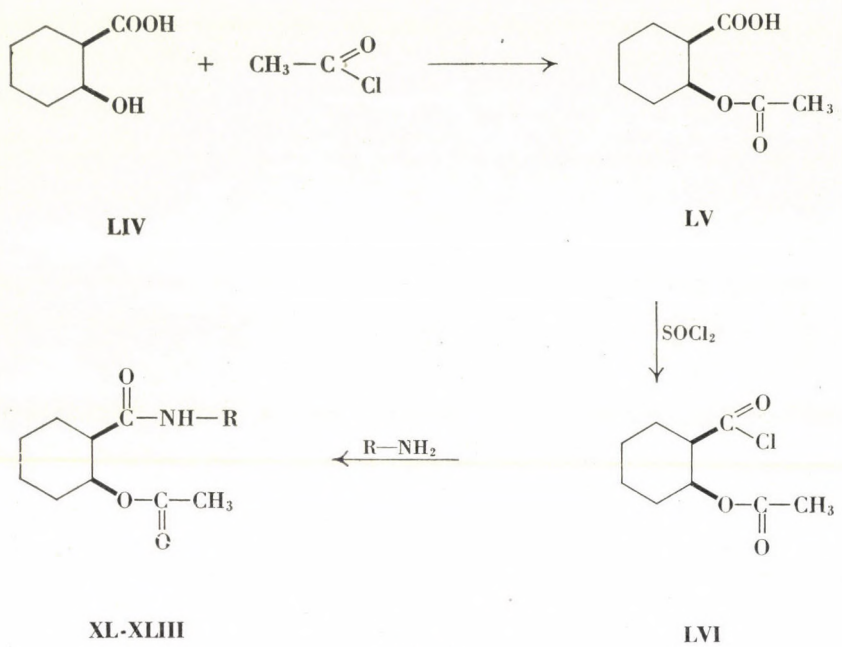

Fig. 4

Table IV

Melting points and analyses of N-acyl-cis-2-hydroxymethylcyclohexylamine derivatives **XXXII—XXXIV**

No.	R	Formula; molecular weight	M.p. (°C); solvent of crystallization	Analyses (%) Calcd./Found		Note
				C	H	
XXXII	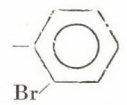	$C_{14}H_{18}O_2NBr$ 312.22	146.5—147 benzene–petroleum ether	53.86 53.84	5.81 5.92	*a)*
XXXIII	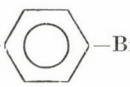	$C_{14}H_{18}O_2NBr$ 312.22	156.5—157 benzene–petroleum ether	53.86 54.00	5.81 5.62	
XXXIV	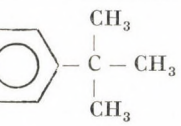	$C_{18}H_{27}O_2N$ 289.43	139.5—140 benzene–petroleum ether	74.70 74.39	9.40 9.35	*b)*

a) White crystal prisms.
b) Fine, white crystal rosettes.

Table V

Melting points and analyses of N-acylaminomethylcyclohexene-1 derivatives **XXXV—XXXIX**

No.	R	Formula; molecular weight	M.p (°C); solvent of crystallization	Analyses (%) Calcd./Found		Note
				C	H	
XXXV		$C_{14}H_{26}O_3N_2$ 260.29	109—110 ethanol	64.61 64.32	6.19 6.05	*a)*
XXXVI	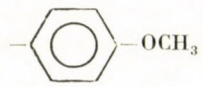	$C_{15}H_{19}O_2N$ 245.33	102—102.5 ethanol	73.45 73.48	7.80 7.81	*a)*
XXXVII	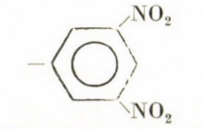	$C_{14}H_{15}O_5N_3$ 305.29	144.5—145 ethanol	55.09 55.23	4.95 5.24	*b)*
XXXVIII	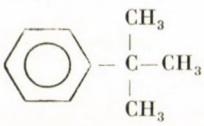	$C_{18}H_{25}ON$ 271.40	97—98 ethanol	79.66 79.45	9.28 9.36	*a)*
XXXIX	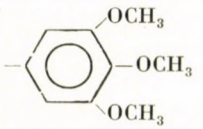	$C_{17}H_{23}O_4N$ 305.37	126—126.5 ethanol	66.84 66.80	7.59 7.69	*c)*

a) Very soluble in ethanol.
b) Slightly yellow crystals.
c) White crystal powder.

Experimental*

N-Hexahydrobenzoyl-*p*-methoxybenzylamine (XLIV)

Cyclohexanecarboxylic acid chloride (29.1 g, 0.20 mole) was added dropwise to abs. pyridine (30 ml) under stirring at 4 °C, then *p*-methoxybenzylamine (32.4 g, 0.23 mole) was added drop by drop in 15 minutes to this reaction mixture. After stirring at room temperature for about 15 minutes, the mixture was diluted with water (40 ml) and filtered on a sintered glass filter. The precipitate was washed with water, then with 5% hydrochloric acid, and with water once again. After drying, the white crystalline substance weighed 40.5 g (81.9%) and was pure enough for the reduction with lithium aluminium hydride. A small portion was crystallized twice from ethanol; the product, N-hexahydrobenzoyl-*p*-methoxybenzylamine (**XXX**), had a m.p. of 118 °C.

$C_{15}H_{21}O_2N$ (247.34).
Calcd. C 72.84 H 8.56 N 5.66;
Found C 72.75 H 8.20 N 5.51%.

* Melting points, determined on a Boetius apparatus, are uncorrected.

Table VI

Melting points and analyses of N*-substituted derivatives* (**XL—XLIII**) *of cis-2-acetoxycyclohexanecarboxamide*

No.	R	Formula; molecular weight	M.p. (°C); solvent of crystallization	Analyses (%) Calcd./Found		Note
				C	H	
XL		$C_{17}H_{23}O_4N$ 305.38	119.5—120 ether	66.86 66.47	7.59 7.34	*a)*
XLI	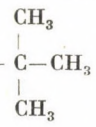	$C_{13}H_{23}O_3N$ 241.33	100—101 ether	64.70 64.41	9.60 9.64	
XLII	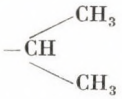	$C_{12}H_{21}O_3N$ 228.31	143.5—144.5 ethanol–water	63.39 63.23	9.31 9.11	
XLIII	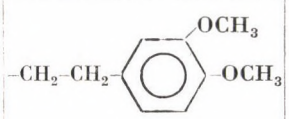	$C_{19}H_{27}O_5N$ 349.43	105—106 ethanol–water	65.31 65.43	7.79 7.90	*b)*

a) White, fluffy crystal mass.
b) Very soluble in ethanol.

N-*p*-methoxybenzylaminomethylcyclohexane (XLV)

Into a 1 l three-necked, round-bottomed flask fitted with a stirrer and with a reflux condenser, abs. ether (500 ml) and N-hexahydrobenzoyl-*p*-methoxybenzylamine (38.0 g, 0.15 mole) were given. To the mixture lithium aluminium hydride (11.4 g, 0.3 mole) was added in portions under stirring, which was continued for 10 hours under slow refluxing of the mixture. After standing overnight at room temperature and another 10 hours' stirring under slow reflux followed by standing overnight, the reaction mixture was decomposed in the usual way [32]. The ethereal phase was dried over potassium hydroxide. Evaporation of the ether left N-*p*-methoxybenzylaminomethylcyclohexane (**XXXI**) (25.1 g, 70.0%) pure enough for use in the preparation of acid amides. Conversion of a small portion into the hydrochloride gave a substance melting at 197 °C.

$C_{15}H_{24}ONCl$ (269.82).
Calcd. C 66.77 H 8.96 N 5.19;
Found C 66.42 H 8.96 N 4.87%.

N-Benzyl-*cis*-2-hydroxycyclohexanecarboxamide (XLVI)

In a 250 ml round-bottomed flask fitted with a condenser, *cis*-2-hydroxycyclohexanecarboxylic acid (18.0 g, 0.125 mole) [2, 28] and benzylamine (50 g, 0.462 mole) were kept in an oil bath at 170 °C for two hours. After this the excess of benzylamine was removed under reduced pressure and the residue was taken up in ethanol (30 ml), wherefrom it crystallized on addition of water. First an oily substance separated which, on friction, congealed as a crystalline mass (21.7 g, 74.5%), m.p. 87—88 °C. Recrystallization of a small portion gave crystals with m.p. 89—90 °C. Analyses were carried out after drying over phosphorus pentoxide.

$C_{14}H_{19}O_2N$ (233.31).
Calcd. C 72.06 H 8.20;
Found C 72.17 H 8.37%.

N-Benzyl-*trans*-2-hydroxycyclohexanecarboxamide (XLVII)

The reaction of benzylamine with *trans*-2-hydroxycyclohexanecarboxylic acid [2, 28], carried out as with the *cis* compound, produced the corresponding *trans* acid amide **XLVIII**, with a yield of 63—71%. Crystal plates (m.p. 142 °C) were obtained from aqueous ethanol.
$C_{14}H_{19}O_2N$ (233.31).
Calcd. C 72.06 H 8.20;
Found C 72.04 H 7.76%.

N-Benzyl-*cis*-2-aminomethylcyclohexanol (XLVIII)

N-Benzyl-*cis*-2-hydroxycyclohexanecarboxamide (**XXXII**) (19.5 g, 0.09 mole) was reduced with lithium aluminium hydride (7.8 g, 0.2 mole) in abs. tetrahydrofurane (600 ml) under reflux for 10 hours. After the decomposition of excess lithium aluminium hydride, the solution was dried over sodium sulfate and evaporated. The residue was converted into the hydrochloride by the addition of dilute hydrochloric acid (300 ml). Impurities were removed by extraction with 3×100 ml ether. The aqueous phase was made alkaline by the addition of sodium carbonate, then the N-benzyl-*cis*-2-aminomethylcyclohexanol was extracted with ether (3×200 ml). The ethereal extract was dried over potassium hydroxide and evaporated. The residue (15.6 g, 85%) was pure enough for use in the preparation of acid amides. A small portion was distilled under reduced pressure (b.p. 128—136 °C at 1 torr), converted into the hydrochloride and analysed. Crystals from abs. acetone had a m.p. of 163—164 °C.
$C_{14}H_{22}ONCl$ (255.79).
Calcd. C 65.74 H 8.67 Cl 13.87;
Found C 65.28 H 8.46 Cl 13.85%.

N-Benzyl-*trans*-2-aminomethylcyclohexanol (XLIX)

This compound was prepared similarly to the *cis*-isomer, with a yield of 71.3%. Its hydrochloride, crystallized from abs. acetone, had a m.p. of 136.5—137 °C.
$C_{14}H_{22}ONCl$ (255.79).
Calcd. C 65.74 H 8.67 Cl 13.87;
Found C 65.67 H 8.51 Cl 14.03%.

Aminomethylcyclohexene-1 (L)

(a) (*cf.* [18]) Lithium aluminium hydride (16 g, 0.423 mole) was taken up in abs. ether (500 ml) and stirred under cooling with salt/ice for 20 min. while 1-cyanocyclohexene (35 g, 0.327 mole) dissolved in abs. ether (50 ml) was added dropwise. Cooling and stirring were continued for further 2 hours, then the reaction mixture was subjected to the usual treatment and the product converted into a hydrochloride. Recrystallized twice from an ethanol–ether mixture, the hydrochloride of aminomethylcyclohexene-1 (31.8 g, 65.9%) was obtained [m.p. 242—250 °C (decomp.)]. Due to decomposition of the sample even in a capillary, the m.p. could not be determined more accurately.
$C_7H_{14}NCl$ (147.65).
Calcd. C 56.85 H 9.55;
Found C 56.58 H 9.43%.

Preparation of the N-acyl derivatives (I—XXXIX)

The slightly modified method of SCHOTTEN and BAUMANN [33] was used for the preparation of the acid amides listed in Tables I—V, from the corresponding amines or aminoalcohols. The general method was as follows.

A solution (in 8—12 ml of benzene) of the amine or aminoalcohol (0.03 mole) is cooled with ice-water under stirring. A solution (in 5—10 ml of benzene) of the aromatic acid chloride (0.035 mole) and 0.05 molar solution of sodium hydroxide are simultaneously added over 10 to 15 min., always keeping the mixture alkaline. This addition completed, the reaction mixture is stirred for another 15 to 25 min. Petroleum ether (30—50 ml) is then added and the mixture allowed to stand at room temperature or under cooling. The white crystals separated are collected by filtration, washed repeatedly with petroleum ether and dried. Recrystallization to constant melting point is carried out in the solvent mentioned. Yields between 65 and 92%.

N-*p*-Methoxybenzyl-*cis*-2-acetoxycyclohexanecarboxamide (XL)

Cis-2-hydroxycyclohexanecarboxylic acid (**LIV**) (30 g, 0.021 mole) in ether (75 ml) was refluxed for 3 hours with acetyl chloride (15 ml). Ether and excess acetyl chloride were removed by distillation. The residue, crude *cis*-2-acetoxycyclohexanecarboxylic acid (**LV**), was boiled under reflux for one hour with freshly distilled thionyl chloride (10 ml). After removing the excess thionyl chloride by distillation, the *cis*-2-acetoxycyclohexanecarboxylic acid chloride (**LVI**) was taken up in abs. ether (100 ml). To the mixture *p*-methoxybenzylamine (6 g, 0.044 mole) in abs. ether (10 ml) was added dropwise under cooling. The precipitate was collected on a glass filter and thoroughly washed with water to remove all the *p*-methoxybenzylamine hydrochloride. The washed product was recrystallized from ether. Yield 4.3 g (67.6%) of a white fluffy crystal mass that had a sharp m.p. of 119.5—120 °C. For the analysis *cf.* Table VI.

REFERENCES

1. BERNÁTH, G., KOVÁCS, K., LÁNG, K. L.: Tetrahedron Letters **1968,** 2713
2. BERNÁTH, G., KOVÁCS, K., LÁNG, K. L.: Acta Chim. Acad. Sci. Hung. **64,** 183 (1970)
3. BERNÁTH, G., KOVÁCS, K., LÁNG, K. L.: Acta Chim. Acad. Sci. Hung. (In the press)
4. BERNÁTH, G., LÁNG, K. L., GÖNDÖS, GY., MÁRAI, P., KOVÁCS, K.: Tetrahedron Letters **1968,** 4441
5. BERNÁTH, G., LÁNG, K. L., KOVÁCS, K.: to be published
6. SZPORNY, L. *et al.:* to be published
7. LEE, J., ZIERING, A., BERGER, L., HEINEMAN, S. D.: The Synthesis of Analgesic Compounds. Jubilee Volume Emile Barell, **1946,** 264—305; C. A. **41,** 6246 (1947)
8. TAKAHASHI, T., HORI, M.: J. Pharm. Soc. Japan **74,** 354 (1954); C. A. **49,** 5322 (1955)
9. TAKAHASHI, T., HORI, M.: J. Pharm. Soc. Japan **74,** 52 (1954); C. A. **49,** 1663 (1955)
10. TAKAHASHI, T., HORI, M.: J. Pharm. Soc. Japan **74,** 1141 (1954); C. A. **49,** 1452 (1955)
11. TAKAHASHI, T., HORI, M., TSURUHA, H.: J. Pharm. Soc. Japan **75,** 1380 (1955); C. A. **50,** 9341 (1956)
12. OGATA, A., NIINOBU, S.: J. Pharm. Soc. Japan **62,** 152 (1942); C. A. **45,** 1728 (1951)
13. OGATA, A., NIINOBU, S.: J. Pharm. Soc. Japan **62,** 160 (1942); C. A. **45,** 1728 (1951)
14. OGATA, A., NIINOBU, S.: J. Pharm. Soc. Japan **62,** 372 (1942); C. A. **45,** 1728 (1951)
15. CASTORINA, G.: Il Farmaco (Pavia) Ed. sci. **9,** 218 (1954); C. A. **49,** 6141 (1955)
16. LEWIS, J. R.: Proc. Soc. Exp. Biol. Med. **61,** 343 (1946); C. A. **40,** 4144 (1946)
17. GUTT, J.: Ber. **40,** 2068 (1907)
18. COLOGNE, J., DAUNIS, H.: Compt. rend. **251,** 1080 (1960)
19. HUMBER, L. G.: Med. Chem. **7,** 826 (1964)
20. QUINN, J. F., TERPSTRA, M. A.: U. S. Pat. 2 945 063 July 12, 1960; C. A. **55,** 9309 (1961)
21. STRICHNOTH, O.: German Pat. 1 072 241, Dec. 31, 1959; C. A. **55,** 11361 (1961)
22. SOLLAZZO, R. GOFFREDO, O., BOSISIO, G.: Il Farmaco (Pavia) Ed. sci. **13,** 175 (1958); C. A. **53,** 2124 (1959)
23. GEIGY, J. R. A. G.: Brit. Pat. 785 108, Oct. 23, 1957; C. A. **52,** 5459 (1958)
24. BAUMGARTEN, H. E., BOWER, F. A., OKAMOTO, T. T.: J. Am. Chem. Soc. **79,** 3145 (1957)
25. COPE, A. C., BAUMGARDNER, C. L., SCHWEIZER, E. E.: J. Am. Chem. Soc. **79,** 4729 (1957)
26. MOUSSERON, M., JACQUIER, R., MOUSSERON-CANET, M.: Bull. soc. chim. France **1952,** 1042
27. RUZICKA, L., BRUGGER, W.: Helv. Chim. Acta **9,** 399 (1926)
28. PASCUAL, J., SISTRARÉ, J., REGÁS, A.: J. Chem. Soc. **1949,** 1943
29. ROGERS, M., ROBERTS, J.: J. Am. Chem. Soc. **68,** 843 (1946)
30. WALLACH, O.: Ann. **353,** 284 (1907)
31. JEWERS, K., MCKENNA, J.: J. Chem. Soc. **1958,** 2209
32. MICOVIĆ, V. M., MIHAILOVIĆ, LJ. M.: J. Org. Chem. **18,** 1190 (1953)
33. WEYGAND—HILGETAG: Organisch-Chemische Experimentierkunst; 3. Aufl., p. 535. Johann Ambrosius Barth Verlag, Leipzig, 1964

Gábor BERNÁTH
Etelka CSÓKÁSI
Imre HEVÉR
Lajos GERA
Kálmán KOVÁCS

Szeged, Dóm tér 8, Hungary.

RECENSIONES

M. PRETTRE et B. CLAUDEL: *Eléments de Cinétique Chimique*

Ed. Gordon and Breach, Paris, London, New York 1969.

Ce texte élémentaire réunit l'information fondamentale sur la cinétique chimique, d'habitude dispersée dans des cours différents, dans une représentation cohérente et systématique.

La première partie de l'ouvrage est divisée en sept chapitres. Le titre «Généralités et Réactions Spontanées» nous parait discutable, car les «Réactions Catalysées» de la seconde partie sont de plusieurs points de vue pas moins spontanées. Aprés un traitement des définitions fondamentales et l'influence de la concentration sur la vitesse de réaction, la matière est d'abord groupée selon les modes d'activation: thermique et par rayonnement, en suite selon le degré de complexitée des réactions, aboutissant aux réactions en chaine. Les cinq chapitres de la seconde partie traitent les généralités de la catalyse, la catalyse homogène, l'adsorption sur les surfaces solides et finalement, théorie et pratique de la catalyse hétérogène ou de contacte.

Le texte très lucide et logique avec des exercices à la fin de chaque chapitre peut-être recommendé a tout étudiant de cours supérieur, voulant aquérir une fondation solide dans ce domaine.

La typographie et les figures de l'ouvrage sont d'une très bonne qualitée.

I. TELCS

G. KLOPMAN and B. O'LEARY: *All-valence electrons SCF calculations.* (Fortschritte der Chemischen Forschung), Topics in Current Chemistry, Band 15, Heft 4. Sept. 1970.

Springer-Verlag, Berlin, Heidelberg, New York.

The development of quantum chemistry progresses in two directions. One is represented by the *ab initio* calculation method in which no experimental data other than the nuclear charge and the number of electrons are taken into account and all the electrons of the system are considered. The other direction known as semiempirical methods is characterized by various simplifying assumptions: *e.g.*, only the electrons of the valence shell are taken into account, certain types of integrals are taken equal to zero, and a number of empirical parameters are used in the calculations.

Research is justified in both directions. The *ab initio* calculations are of great importance because starting with a minimum amount of information they yield reliable quantitative results on the systems studied. Unfortunately, exact calculations cannot be performed on systems containing more than 100 electrons even if the most advanced computer techniques are used. The semiempirical methods can be applied to such many-electron systems, but the results should always be viewed with criticism and conclusions should be drawn with care, keeping in mind the neglections.

KLOPMAN and O'LEARY summarize the theory, field of application and the results of semiempirical methods developed in the course of the last 6 years. In the methods described, all valence electrons are taken into account, *i.e.* in contrast to earlier semiempirical methods (*e.g.* the Hückel method), the σ and π bond systems are treated together.

The theoretical basis of the methods is derived in this review from the most generally used *ab initio* method, the HARTREE—FOCK approach. The authors give an account of the integrals of the HARTREE—FOCK method neglected in the various semiempirical calculations. The individual methods derive their names from the initials of English words representing the integrals neglected.

The following methods are treated in the review:
CNDO: *c*omplete *n*eglect of *d*ifferential *o*verlap (POPLE—SANTRY—SEGAL, 1965);
INDO: *i*ntermediate *n*eglect of *d*ifferential *o*verlap (POPLE—BEVERIDGE—DOBOSH, 1967);
MINDO: *m*odified *i*ntermediate *n*eglect of *d*ifferential *o*verlap (BAIRD—DEWAR, 1969);
EMZDO: *e*xchange *m*odified *z*ero *d*ifferential *o*verlap (DIXON, 1967);
PNDO: *p*artial *n*eglect of *d*ifferential *o*verlap (DEWAR—KLOPMAN, 1967).

After the name of the method, the authors and the year of publication are shown in parentheses.

In a longer chapter of the review, the authors describe the empirical parameters that can be used to calculate some of the integrals which have not been neglected. At the end of this chapter the reader finds a very illustrative and useful table summarizing not only the method of determining the integrals but also indicating the type of compounds (*e.g.* hydrocarbons, heteroaromatic compounds, etc.), to which the method in question can be applied most expediently to achieve a given objective (*e.g.* determination of charge densities, spin densities, heats of formation, etc.)

In the last chapter the authors give an account of the results obtained by the methods in calculating ionization potentials, heats of formation, dipole moments, ultraviolet spectra, and NMR and ESR parameters.

The reader is assumed to be familiar with some linear algebra and quantum chemistry. The style is comprehensive and lucid. Since the application of the methods described does not require extra high-speed computers, numerous publications have appeared in this field during the last years. Therefore this review is useful not only for those intending to perform quantum-chemical calculations, but also for specialists who wish to follow the pertinent literature and obtain information about the applications and reliability of these methods.

F. TÖRÖK

F. TAMÁS and I. PÁL: *Phase Equilibria, Spatial Diagrams* (Phase Diagrams, Their Interpretation and Anaglyph Representation), pp. 234 + 80 bicolour insets.

Akadémiai Kiadó, Budapest, 1970.

The book is a kind of textbook or practical guide, respectively, with the double aim of acquainting the reader with a great variety of different types of phase diagrams and of enabling him to read the information to be derived from them. Its scope is limited insofar as it deals only with the diagrammatic representation of melting and crystallization processes at constant pressure, though it has to be admitted that these constitute a preponderant and most diversified part of phase diagrams of practical interest.

The main and outstanding merit of this book as compared with other existing textbooks dealing with phase diagrams is the anaglyph representation used for visualizing spatial relations, parallel with the usual two-dimensional projections or sequences of isothermal sections, respectively. Anaglyphs are planar diagrams drawn in two complementary colours so that, when viewed through a bicolour spectacle the figures spring into perspective making thus the spatial distributions of the regions belonging to the different phases immediately ostensible together with the surfaces and intersecting lines separating them; this kind of representation is superior even to most real spatial models because the anaglyphs appear completely transparent so that all details in their interior become clearly visible; identification of the slopes of lines and surfaces is greatly aided by incorporation of isothermal lines at regular intervals in the anaglyphs of ternary systems. The book is equipped with eighty anaglyphs in form of insets, all of which are constructed with the utmost care and precision, an achievement to be especially esteemed.

The text is divided into four main parts. Part 1 is a short survey (10 pages altogether) of the principles underlying phase equilibria and their representation. Some of these principles are presented in a somewhat perfunctory and not quite exact way. Thus, the definition of equilibrium from the theoretical or thermodynamic aspect as "the stage in any reversible process when no useful energy passes from or into the system" is anything but exact; the dis-

tinction to be made between extensive and intensive variables, and the fact that only the latter have to be considered in connection with the phase rule, is not mentioned (the text simply states that only the effects of concentrations and of temperature will be discussed); the use of the terms "heating" and "cooling", in connection with isothermal melting and crystallization may be somewhat misleading, "uptake" and "loss of heat" would be more correct, or even better "increase" and "decrease in enthalpy", respectively, with a view that later the author speaks of states of maximum and minimum enthalpy, at the respective end points of an isothermal transformation. Inconsistencies of these kinds will be probably overcome, however, by attentive students without serious difficulties, and on the whole, the survey of part 1 gives a sound foundation for the following ones, which are arranged according to the very clear classification of systems given in this part.

Part 2 (61 pages) deals quite exhaustively with simple and complex binary systems (intermediate compound formation), with different degrees of miscibility in the solid and/or the liquid phases. Eutectic and peritectic invariant points as well as the behaviour of monotectic and syntectic systems are explained very clearly. Spatial representation being superfluous in connection with binary systems when effects of pressure changes are left out of account, the usual planar diagrams are only used in this part, with the exception of § 38, in which a possible transition from eutectic to peritectic behaviour effected by pressure variation is exemplified on a hypothetical system (it has to be noted, however, that the choice of this system may not be very fortunate, because there appears a depression of the melting points with increasing pressure which is a rather exceptional behaviour). It is a very valuable feature of the treatment in this part that it discusses a series of actual systems and that, on the other hand, the use of the lever rule for calculating phase proportions is demonstrated by many actual numerical examples. The lever rule (and more generally, the center of gravity principle) is introduced, however, quasi-axiomatically, and in the opinion of the referee, motivation by material balance considerations would have been expedient. Part 2 includes also a section on the evaluation of phase diagrams in certain cases of non-equilibrium, and this is very satisfactory, with view at the fact that true equilibrium crystallization does not generally occur in practice. An interesting method for making calculations, evolved by one of the authors, for the case when one high melting solid component is present in excess over the equilibrium composition, is discussed in an instructive way.

Part 3 (112 pages) is devoted to the discussion of ternary systems, classified in a very clear way according to the nature of the binary subsystems involved in them. It is here that the anaglyph representation proves extremely useful for a better understanding of the usual planar diagrams (isothermal sections and projections onto the base triangle, respectively), a copious and at the same time judicious selection of which is included into the text. The verbal explanations given in the text being also remarkably lucid, it may be stated that this part of the book will be most helpful to anyone who wishes to become familiar with the use of phase diagrams which do not represent just only the simplest systems occurring in reality. Part 3 ends with a very instructive discussion of non-equilibrium crystyllization exemplified by the system K_2O—Al_2O_3—SiO_2 (porcelain).

Part 4 deals shortly (20 pages altogether) with quaternary systems, first with so-called reciprocal systems (four salts, any pair of them having either a common cation or anion, respectively), then with true quaternary systems. The space allotted to this part does not allow more than a more or less sketchy treatment of the subject, so that the reader may get only a glimpse into the ways in which quaternary systems have to be discussed. It is nevertheless shown that the anaglyph representation in three dimensions is as useful in this case as the two-dimensional diagrams in connection with ternary systems.

The book will be of great value to anyone who wishes to get not only acquainted with phase diagrams but also versed in their use. The excellent get-up, easy legibility, lucidity of the diagrams and careful execution of the bicolour insets will all contribute to this end.

G. SCHAY

J. KORYTA, I. DVOŘÁK and V. BOHÁČKOVÁ: *Electrochemistry*, pp. 339 + index.

Methuen et Co. Ltd., London, 1970.

Persons active in the most varied branches of science, experts working in the most diverse fields of industry are confronted with electrochemical phenomena, and utilize the laws of electrochemistry in their day-to-day activity. Therefore, works dealing with this field of science are of great importance.

The book of KORYTA, DVOŘÁK and BOHÁČKOVÁ gives a short but almost complete survey of theoretical electrochemistry. Owing to its limited extent, some problems can be discussed only very briefly, but the list of references at the end of each chapter, comprising mainly general papers and monographs, partly fills this gap. The subdivision, the structure of the book is lucid, almost symmetrical. Of its four chapters the first two deal with electrolyte solutions (homogeneous electrochemical systems), while the third and fourth chapters discuss heterogeneous electrochemical systems. The first chapter treats the equilibria in electrolyte solutions, the second the transport processes occurring in electrolyte solutions, the third the equilibria in heterogeneous electrochemical systems, and the fourth is concerned with processes in the latter systems (electrode processes).

Accordingly, the first chapter of the book deals with the structure of electrolyte solutions, the Debye—Hückel theory of strong electrolytes, the classical theory of electrolytic dissociation and equilibria, and with the acid–base theories.

In the second chapter ("Transport Phenomena in Electrolyte Solutions") phenomena produced by the passage of electric current through electrolyte solutions are discussed by the authors, with a particular view to the diffusion of electrolytes, the methods for measuring the diffusion coefficient, and problems of convective diffusion. Within the scope of the latter, convective diffusion on the rotating disk and on an increasing sphere (dropping mercury electrode) are described.

The third chapter treats equilibria established at the phase boundaries of electrochemical systems. In addition to metal-electrolyte equilibria, problems concerning membrane equilibria, glass electrodes and potentiometric methods are discussed. The structure of electrical double layers, important from the viewpoint of electrode processes is also treated.

The fourth chapter is concerned with the kinetics of electrode processes. Among others, the authors succeeded in giving a short and lucid summary of transfer and concentration (diffusion) polarizations, and of the most important experimental methods in electrochemical kinetics. Finally, a few important electrode processes are described.

The book of KORYTA, DVOŘÁK and BOHÁČKOVÁ, written in a modern concept, is a valuable contribution to the literature on electrochemistry. It will facilitate students and experts interested in and using electrochemistry to get acquainted with the fundamental theory of modern electrochemistry.

L. KISS

INDEX

Printed in Hungary

A kiadásért felel az Akadémiai Kiadó igazgatója — Műszaki szerkesztő: Várhelyi Tamás

A kézirat nyomdába érkezett: 1971. VI. 7. — Terjedelem: 10 (A/5) ív, 38 ábra, 1 melléklet

71.71916 Akadémiai Nyomda, Budapest — Felelős vezető: Bernát György

ACTA CHIMICA

ТОМ 70 — ВЫП. 3

РЕЗЮМЕ

Кинетика и механизм реакций замещения в комплексах, XXXVI. Образование комплексных ионов 1,2-[Co(en)$_2$ Brβ-пиколин]$^{+2}$ и 1,2-[Co(en)$_2$Br γ-пиколин]$^{+2}$ и их активация в кислотных растворах

ЖЙ.АКО, Ч. ВАРХЕИ и Ш. БЛЕОКА

Приводится синтез 1,2-[Co(en)$_2$Brβ-пиколин]$^{+2}$, 1,2-[Co(en)$_2$Brγ-пиколин]$^{+2}$ и их 24 новых солей. Были сняты и обсуждаются УФ, видимые и ИК-спектры. Изучалась кинетика активации этих комплексов в кислотных растворах. Были определены энтальпии и энтропии активации. Полагалось, что реакция протекает по механизму S_N1. Результаты сравнивались с кинетическим поведением аналогичных хлоропроизводных. Обсуждается индуктивное влияние координированного амина на диссоциацию галогена.

О некоторых вопросах осадительного разделения следов элементов, IX. Дальнейше изучение сорбции урана(VI) в карбонатных средах.

Э. УПОР и Дь. НАДЬ

С целью дополнения предшествующих исследований исследовалось изменение зависимости сорбции урана(VI) на $Fe(OH)_3$ от pH в карбонатных средах с изменением концентрации карбоната. Было установлено, что при низкой концентрации карбоната ($1 \cdot 10^{-3}$M) в интервале pH ниже 11 сорбция является полной и кривая сорбции идентична кривой, полученной в среде NaOH. В случае же макроколичеств урана и в карбонатной среде десорбция не наблюдалась при величинах pH выше 12. Тангенс угла наклона зависимости $\log[CO_3]^{-2}$ — $\log D_u$ при различных pH равен $1{,}0 \pm 0{,}2$; это делает необходимым дальнейшее выяснение механизма десорбции.

Использование перегонки с перегретым бензольным паром для разделения аминов

И. ДЬЕНЕШ

Необходимым условием для разделения бинарных и многокомпонентных смесей аминов с помощью метода перегонки с перегретым бензольным паром, разработанного автором ранее, является знание относительной летучести аминов. Для этой цели может быть проведен опыт на модели, но может быть также использовано экспериментальное уравнение дистилляции, некоторые члены которого известны (напр., молекулярный вес, температура кипения амина), а остальные члены на основе ряда исследований определяются эмпирически. С этой целью 134 различных амина подвергались перегонке с перегретым бензольным паром, и были определены количества перегретого бензольного пара, необходимого для перегонки (в виде количества сконденсированного бензола, в мл) —V —, а также вероятная связь этой величины с характеристиками амина. Чем меньше требуется бензольного пара, тем летучее амин; характеристикой может служить выражение V/1.1000. Был установлен ряд летучести аминов.

Вольтамметрическое определение некоторых фармаконов на графитных электродах на основе силиконовой резины

Э. ПУНГОР, Ж. ФЕХЕР и Г. НАДЬ

Описывается вольтамметрическое определение некоторых основных веществ промышленности лекарственных препаратов. Концентрации растворов производных фенотиазина, производных диоксифенила, амидазофена, фенацетина и др. были определены, как правило, с точностью до некторых десятых процента. Для некоторых веществ определение проводилось в неводных растворах. На нескольких примерах демонстрируется применимость метода для определения содержания эффективных веществ в лекарственных препаратах и без предварительного разделения.

Ассоциация пропионовой кислоты в паровой фазе

Я. ЛИСИ

Приводится расчетный метод определения равновесных констант ассоциации, относящихся к паровой фазе, для смесей типа $A-A_2-B$. Метод позволяет непосредственно определить равновесное давление пара мономерного вещества. Для иллюстрации метода определялась равновесная константа ассоциации, выраженная с помощью парциальных давлений, в зависимости от температуры для случая паровой фазы пропионовой кислоты. Согласно полученным результатам:

$$\lg K_p = -10{,}484 + \frac{3227{,}7}{T} \left(K_p: \text{торр}^{-1}\right)$$

Химия свободных радикалов, VIII. Изучение N-сульфофенил-окиси азота методом ЭПР

Б. ЛАКАТОШ, Б. ТУРЧАНИ и Ф. ТЮДЁШ

Ароматические нитрозосоединения подобно изоэлектронным ароматическим альдегидам образуют аддукты с бисульфитом и дитионитом. Эти продукты присоединения могут быть окислены в радикалы, ЭПР спектры которых подобны спектрам радикалов алкил-фенил-окиси азота.

На основе зависимости константы расщепления на азоте (a_N) от температуры и растворителя в случае бисульфитного присоединения полагалось образование радикала N-сульфо-фенил-окиси азота, а в случае дитионита — N-сульфин-фенил-окиси азота. В случае их производных наблюдались как индуктивный, так и стерический эффекты, подобно радикалам типа алкил-фенил-окись азота.

Изучение реакции хрома(III) с этилендиаминтетрауксусной кислотой, I

Ю. ГЕХЕР-ГЛЮКЛИХ и М. БЕК

Изучались факторы, оказывающие влияние на скорость реакции хрома(III) с этилендиаминтетрауксусной кислотой (ЭДТУ). Измерения проводились с помощью спектрофотометрического метода.

Была исследована скорость реакции в зависимости от концентрации лиганда и было установлено, что в отличие от литературных данных, константа скорости зависит от концентрации лиганда. Найденная зависимость объяснялась на основе такого механизма, согласно которому ступенью, лимитирующей скорость, является переход лиганда из внешней координационной сферы во внутреннюю.

Изучалось влияние pH на скорость реакции. Было установлено, что принятая до сих пор линейной зависимость кажущейся константы скорости от pH является справедливой лишь в очень узком интервале. Влияние pH объяснялось суммой многих факторов. Принимались во внимание все пути реакций, возможные по целому диапазону pH вследствие гидролиза иона хрома(III) и диссоциации ЭДТУ. Приводятся различные типы комплексов хром(III)-ЭДТУ по внешней сфере, вероятности их образования и влияние комплексов типа внешней сферы с различной степенью протонирования на величину скорости реакции хрома(III) с ЭДТУ. Зависимость скорости реакции от pH, найденная экспериментально, объяснялась на основе теоретических соображений.

На примере приводилось определение различных вероятных путей реакций для одного заданного значения pH.

Изучение реакции хрома(III) с этилендиаминтетрауксусной кислотой, II

Ю. ГЕХЕР-ГЛЮКЛИХ и М. БЕК

Рассматривалась реакция двухядерных комплексов хрома(III) с этилендиаминтетрауксусной кислотой (ЭДТУ). За реакцией следили спектрофотометрически.

Было установлено, что в случае перхлората хрома(III) о гидролизе, протекающем в разбавленных водных растворах, об образовании двух- и многоядерных комплексов и об их разложении под влиянием кислоты можно судить по изменению скорости реакции хрома(III) с ЭДТУ. Данный метод открывает новые возможности для изучения поведения многоядерных комплексов.

Сравнивалась реакция одно- и двухядерных комплексов с ЭДТУ и было установлено, что двухядерные комплексы реагируют значительно медленнее, и зависимость скорости реакции от pH — особенно в области значительных избытков ЭДТУ — намного меньше, нежели в случае одноядерных комплексов.

Синтез некоторых производных L-аспарагиновой и L-глутаминовой кислот

Й. ТОМАС

Описывается синтез α-бензилового эфира N-*трет*-бутилоксикарбонил-L-аспарагиновой кислоты (*VIa*), α-*трет*-бутилового эфира N-*трет*-бутилоксикарбонил-L-аспарагиновой кислоты (*IVa*) и α-*трет*-бутилового эфира N-*трет*-бутилоксикарбонил-L-глутаминовой кислоты (*IVb*). Помимо этого, приводится упрощенный синтез α-бензилового эфира N-*трет*-бутилоксикарбонил-L-глутаминовой кислоты (*VIb*) и N-*трет*-бутилоксикарбонил-L-глутамина (VIII).

Дальнейшее упрощение метода Хардеггера для синтеза 2-деокси-D-рибозы

Й. ТОМАС

Описывается упрощенный метод синтеза в больших масштабах 2-деокси-D-рибозы (II) из 1,2 : 5,6-ди-О-изопропилиден-3-О-*п*-толилсульфонил-α-D-глюкозы (III).

О кристаллизации 2,4,6-трибензоилокси-пропиофенона $C_{30}H_{22}O_7$ из растворов в различных растворителях

К. ШАШВАРИ и Т. СЕЛЬ

Кристаллы 2,4,6-трибензоилокси-пропиофенона, полученные из растворов с различными растворителями (метанол, этанол, бензол и толуол) почти всегда дают уменьшающиеся постепенно температуры плавления. Кристаллы содержат одну молекулу растворителя на одну молекулу $C_{30}H_{22}O_7$ и, по всей вероятности, образуют соединения клафратного типа. Кристаллы без следов растворителя могут быть также получены из этанола. В этом случае, однако, элементарная ячейка содержит 8 молекул $C_{30}H_{22}O_7$ вместо 4, как было найдено для кристаллов, содержащих растворитель.

Стереохимические исследования, X. Циклические аминоспирты и их аналоги, IV. Синтез некоторых производных N-ацил-аминометил-циклопентана, -циклогексана и их аналогов

Г. БЕРНАТ, Э. ЧОКАШИ, И. ХЕВЕР, Л. ГЕРА и К. КОВАЧ

Приводится синтез следующих соединений: некоторых производных N-ацил-аминометилциклогексана (I—VII), некоторых 2-замещенных производных *цис-* и *транс-*N-ацил-аминометилциклогексана (VIII—XIX), некоторых производных N,N'-диацил-*цис*-1,4-диаминометил-циклогексана (XX—XXII), некоторых производных N-ацил-аминометил-циклопентиламина (XXIII—XXVI), некоторых производных N-ацил-*цис*-2-аминометил-циклопентанола (XXVI—XXXIV), некоторых N-ацил-*цис*-2-гидроксиметил-циклогексиламинов (XXXII—XXXIV), некоторых N-ацил-аминометил-циклогексенов-1 (XXXV—XXXIX), а также некоторых N-замещенных производных амида О-ацетил-*цис*-2-гидроксициклогексан-карбоновой кислоты (XL—XLIII).

T. Erdey-Grúz

DIE CHEMISCHEN QUELLEN DER ENERGIE

Die ständige Entwicklung der menschlichen Kultur ist auch mit einem stets wachsenden Energieverbrauch verbunden, wodurch die höchst möglichste ökonomische Nutzung der Energiequellen erfordert wird. In der Gegenwart wird dieser Energiebedarf letztlich vorwiegend durch die Chemie bestritten. Die vorliegende Studie beschäftigt sich mit dem Ursprung der Energievorräte für die Menschheit, wobei das eigentliche Wesen der chemischen Energie, die besondere Natur der Wärme bzw. deren Verhältnis zur Arbeit, sowie das wichtige Problem der direkten Umwandlung chemischer in elektrische Energie in allgemein verständlicher Weise behandelt wird.

In deutscher Sprache • Etwa 320 Seiten • 14×21 cm • Ganzleinen

Eine Gemeinschaftsausgabe — vertrieben in den sozialistischen Ländern von KULTURA, Budapest, in allen anderen Ländern von VERLAG CHEMIE, Weinheim

1828

AKADÉMIAI KIADÓ

VERLAG DER UNGARISCHEN AKADEMIE DER WISSENSCHAFTEN

Budapest

J. HOLLÓ – É. KURUCZ – A. BORÓDI

THE APPLICATIONS OF MOLECULAR DISTILLATION

Molecular distillation is the only method for the separation of heat sensitive and slightly volatile materials of high molecular weight by means of distillation in which the decomposition of the materials can be avoided or reduced to a minimum rate. The development of chemistry and of chemical industry has implied the unavoidable fractionation and purification of a constantly increasing number of materials of the said characteristics. The work is destined to give a comprehensive survey of the definite fields of research and the applications of pilot-plant and unit operation character in which molecular distillation has been utilised as a technological method.

To this end, first a brief survey is presented concerning theoretical and apparatus-concentrated problems, and then the possibilities of the application of molecular distillation are described both in laboratory work and in industrial plants.

In English • Approx. 160 pages • 14×21 cm • Cloth

AKADÉMIAI KIADÓ

PUBLISHING HOUSE OF THE HUNGARIAN ACADEMY OF SCIENCES, BUDAPEST

The Acta Chimica publish papers on chemistry in English, German, French and Russian.

The Acta Chimica appear in volumes consisting of four parts of varying size, 4 volumes being published a year.

Manuscripts should be addressed to

Acta Chimica
Budapest 112/91 Műegyetem

Correspondence with the editors should be sent to the same address.

The rate of subscription is $16.00 a volume.

Orders may be placed with "*Kultúra*" Foreign Trade Company for Books and Newspapers (Budapest I., Fő utca 32. Account No. 43-790-057-181) or with representatives abroad.

Les Acta Chimica paraissent en français, allemand, anglais et russe et publient des mémoires du domaine des sciences chimiques.

Les Acta Chimica sont publiés sous forme de fascicules. Quatre fascicules seront réunis en un volume (4 volumes par an).

On est prié d'envoyer les manuscrits destinés à la rédaction à l'adresse suivante:

Acta Chimica
Budapest 112/91 Műegyetem

Toute correspondance doit être envoyée à cette même adresse.

Le prix de l'abonnement est de $16.00 par volume.

On peut s'abonner à l'Entreprise pour le Commerce Extérieur de Livres et Journaux «*Kultúra*» (Budapest I., Fő utca 32. Compte-courant No. 43-790-057-181) ou à l'étranger chez tous les représentants ou dépositaires.

«*Acta Chimica*» издают трактаты из области химической науки на русском, французском, английском и немецком языках.

«*Acta Chimica*» выходят отдельными выпусками разного объема. 4 выпуска составляют один том. 4 тома публикуются в год.

Предназначенные для публикации рукописи следует направлять по адресу:

Acta Chimica
Budapest 112/91 Műegyetem

По этому же адресу направлять всякую корреспонденцию для редакции.

Подписная цена — $16.00 за том.

Заказы принимает предприятие по внешней торговле книг и газет «*Kultúra*» (Budapest I., Fő utca 32. Текущий счет № 43-790-057-181) или его заграничные представительства и уполномоченные.

Reviews of the Hungarian Academy of Sciences are obtainable at the following addresses:

ALBANIA

Drejtorija Qändrone e Pärhapjes
dhe Propagandimit të Librit
Kruga Konferenca e Päzes
Tirana

AUSTRALIA

A. Keesing
Box 4886, GPO
Sydney

AUSTRIA

GLOBUS
Höchstädtplatz 3
A-1200 Wien XX

BELGIUM

Office International de Librairie
30, Avenue Marnix
Bruxelles 5
Du Monde Entier
5, Place St. Jean
Bruxelles

BULGARIA

HEMUS
11 pl Slaveikov
Sofia

CANADA

Pannonia Books
2, Spadina Road
Toronto 4, Ont.

CHINA

Waiwen Shudian
Peking
P. O. B. 88

CZECHOSLOVAKIA

Artia
Ve Smečkách 30
Praha 2
Poštovní Novinová Služba
Dovoz tisku
Vinohradská 46
Praha 2
Mad'arská Kultura
Václavské nám. 2
Praha 1
SLOVART A. G.
Gorkého
Bratislava

DENMARK

Ejnar Munksgaard
Nörregade 6
Copenhagen

FINLAND

Akateeminen Kirjakauppa
Keskuskatu 2
Helsinki

FRANCE

Office International de Documentation
et Librairie
48, rue Gay Lussac
Paris 5

GERMAN DEMOCRATIC REPUBLIC

Deutscher Buch-Export und Import
Leninstraße 16
Leipzig 701
Zeitungsvertriebsamt
Fruchtstraße 3—4
1004 Berlin

GERMAN FEDERAL REPUBLIC

Kunst und Wissen
Erich Bieber
Postfach 46
7 Stuttgart S.

GREAT BRITAIN

Blackwell's Periodicals
Oxenford House
Magdalen Street
Oxford
Collet's Subscription import
Department
Dennington Estate
Wellingsborough. Northants.
Robert Maxwell and Co. Ltd.
4—5 Fitzroy Square
London W. 1

HOLLAND

Swetz and Zeitlinger
Keizersgracht 471—487
Amsterdam C
Martinus Nijhof
Lange Voorhout 9
The Hague

INDIA

Hind Book House
66 Babar Road
New Delhi 1

ITALY

Santo Vanasia
Via M. Macchi 71
Milano
Libreria Commissionaria Sanso
Via La Marmora 45
Firenze
Techna
Via Cesi 16.
40135 Bologna

JAPAN

Kinokuniya Book-Store Co. Ltd.
826 Tsunohazu 1-chome
Shinjuku-ku
Tokyo
Maruzen and Co. Ltd.
P. O. Box 605
Tokyo-Central

KOREA

Chulpanmul
Phenjan

NORWAY

Tanum-Cammermeyer
Karl Johansgt 41—43
Oslo 1

POLAND

RUCH
ul. Wronia 23
Warszawa

ROUMANIA

Cartimex
Str. Aristide Briand 14—18
Bucureşti

SOVIET UNION

Mezhdunarodnaya Kniga
Moscow G—200

SWEDEN

Almquist and Wiksell
Gamla Brogatan 26
S—101 20 Stockholm

USA

F. W. Faxon Co. Inc.
15 Southwest Park
Westwood Mass. 02090
Stechert Hafner Inc.
31. East 10th Street
New York, N. Y. 10003

VIETNAM

Xunhasaba
19, Tran Quoc Toan
Hanoi

YUGOSLAVIA

Forum
Vojvode Mišića broj 1
Novi Sad
Jugoslovenska Knjiga
Terazije 27
Beograd

ACTA CHIMICA

ACADEMIAE SCIENTIARUM HUNGARICAE

TOMUS 70 FASCICULUS 4

AKADÉMIAI KIADÓ, BUDAPEST

1971

ACTA CHIM. (BUDAPEST) ACASA 2 70 (4) 287–418 (1971)

ACTA CHIMICA

A MAGYAR TUDOMÁNYOS AKADÉMIA KÉMIAI TUDOMÁNYOK OSZTÁLYÁNAK IDEGEN NYELVŰ KÖZLEMÉNYEI

SZERKESZTI

LENGYEL BÉLA

TECHNIKAI SZERKESZTŐK

DEÁK GYULA és HARASZTHY-PAPP MELINDA

Az Acta Chimica német, angol, francia és orosz nyelven közöl értekezéseket a kémiai tudományok köréből.

Az Acta Chimica változó terjedelmű füzetekben jelenik meg, egy-egy kötet négy füzetből áll. Évente átlag négy kötet jelenik meg.

A közlésre szánt kéziratok a szerkesztőség címére (Budapest 112/91 Műegyetem) küldendők.

Ugyanerre a címre küldendő minden szerkesztőségi levelezés. A szerkesztőség kéziratokat nem ad vissza.

Megrendelhető a belföld számára az „Akadémiai Kiadó"-nál (Budapest V., Alkotmány utca 21. Bankszámla 05-915-111-46), a külföld számára pedig a „Kultúra" Könyv- és Hírlap Külkereskedelmi Vállalatnál (Budapest I., Fő utca 32. Bankszámla: 43-790-057-181) vagy annak külföldi képviseleteinél és bizományosainál.

Die Acta Chimica veröffentlichen Abhandlungen aus dem Bereiche der chemischen Wissenschaften in deutscher, englischer, französischer und russischer Sprache.

Die Acta Chimica erscheinen in Heften wechselnden Umfanges. Vier Hefte bilden einen Band. Jährlich erscheinen 4 Bände.

Die zur Veröffentlichung bestimmten Manuskripte sind an folgende Adresse zu senden:

Acta Chimica
Budapest 112/91 Műegyetem

An die gleiche Anschrift ist auch jede für die Redaktion bestimmte Korrespondenz zu richten. Abonnementspreis pro Band: $ 16.00.

Bestellbar bei dem Buch- und Zeitungs-Außenhandels-Unternehmen »*Kultúra*« (Budapest I., Fő utca 32. Bankkonto No. 43-790-057-181) oder bei seinen Auslandsvertretungen und Kommissionären.

Acta Chimica Academiae Scientiarum Hungaricae, Tomus 70 (4), pp. 287—299 (1971)

INVESTIGATION OF THE PARTIAL CATALYTIC OXIDATION OF METHANE, I

CONVERSION RATES IN A SINGLE-GRAIN REACTOR

K. HUSZÁR, GY. RÁCZ and GY. SZÉKELY

(Department of Physical Chemistry, Technical University, Budapest)

Received March 25, 1970

In a reactor containing a single nickel catalyst grain on a ceramic carrier, the rate of the partial oxidation of methane has been measured in a methane–air mixture containing 25% of methane, in the temperature range from 760 to 900 °C. For the characterization of the reaction the conversion rate of the reactants and the rate of formation of the products is given in units of cm^3 (25 °C) min^{-1}.

The conversion rate of oxygen depends only very slightly on the temperature, and the conversion rate of oxygen changes proportionally to the concentration of oxygen within the stable range of operation of the catalyst. The principal products of the reaction were hydrogen, carbon monoxide and water vapour even at low conversions of the feed mixture. This kind of partial oxidation of methane is assisted by nickel only in the reduced state. The observed phenomena lead to the conclusion that, owing to the hindering effect of diffusion in the gas phase, the oxygen concentration is practically zero on the surface of the catalyst.

The partial catalytic oxidation of methane yielding hydrogen and carbon monoxide as principal products, has been studied by several authors [1—5]. From the kinetic point of view, these investigations brought no results because the reaction rate could not be measured. A few preliminary investigations indicated that the usual reactor type, containing a bed of granular catalyst, is not suitable for measuring the oxidation rate of methane, therefore we used a reactor containing a single catalyst grain. Single-grain reactors have been described by other investigators for the study of rapid reactions. For example WURZBACHER [7] measured the oxidation rate of hydrogen over a silver catalyst, and OTANI and SMITH [6] the oxidation rate of carbon monoxide over a nickel–oxide alumina catalyst.

Description of the reactor

The reactor is made of quartz, and has a length of 32 cm. The inner diameter of the lower part of the reactor is 17 mm, that of the upper part 8 mm. The part of the thinner tube bent at right angle protruding from the reactor, serves as condenser (Fig. 1). The ground insert fitted into the bottom of the wider tube carries the gas inlet tube and one or two thermometer sleeves of 1—1.5 mm diameter, which reach deep into the wider quartz tube. One of the thermometer sleeves is centered by braces, and the catalyst grain is fastened to the tip of this sleeve. In the middle 15 cm section of the oven used, the temperature was constant within 5 °C in the region of 700 °C. The reactor was arranged in the oven so that the catalyst grain reached into the top part of the zone of constant temperature. A hole was bored at this height into the oven, which permitted the measurement of the temperature also with a pyrometer.

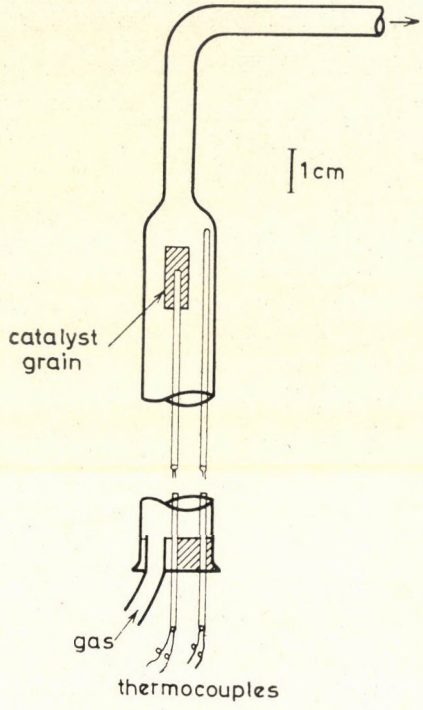

Fig. 1a. Schematic diagram of the single-grain reactor

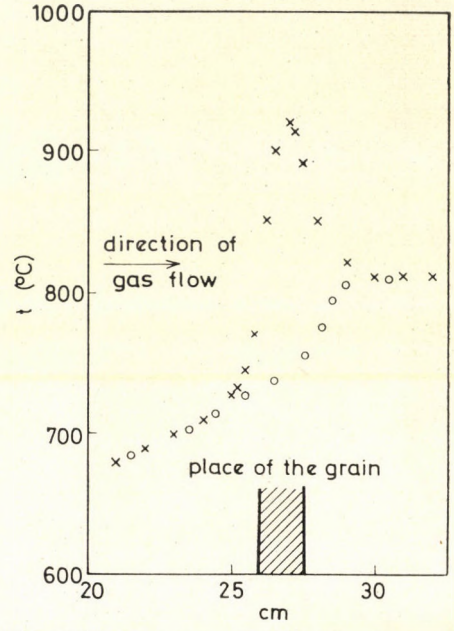

Fig. 1b. Temperature distribution along the reactor. Symbols: × measured with the thermometer passing through the grain; ○ measured with the thermometer alongside the grain

Feeding

The reagents were taken from gas cylinders. Methane was purified by washing with a concentrated alkali solution and by adsorption on active carbon. The principal contaminant of purified methane was nitrogen, the concentration of which was less than 1%. Air and nitrogen, the latter used in certain cases as additive, were not purified. The gas flow rates were measured by means of a wet gasometer. Gas flow rates given in the experimental part refer to room temperature, the gas being saturated with water vapour. The gas mixture was dried with silica gel after mixing, and dry gas was fed into the reactor.

Analysis of the product gas

The outflow rate of the product gas was measured with a wet gasometer. Samples of the product gas were dried over calcium chloride, and analyzed by chromatography. Two chromatographs were used: one was a Polish instrument with a heat conductivity cell and a 1 meter column packed with a molecular sieve (Molfilit 50×). Hydrogen was determined in this column, using argon as carrier gas. The remaining components — carbon dioxide, carbon monoxide, methane, nitrogen and oxygen — were analyzed by a chromatograph designed in our laboratory [8]. It was a two-column system with hydrogen as carrier gas. After separating carbon dioxide on a 3 m column packed with hexamethyl-triphosphamid (HTP) or a 50 cm column packed with Porapak Q, the carbon dioxide was removed and the remaining components were separated on Molfilit 50× at 77 °C. Details of the procedure have been given earlier [8].

Analysis was made by measuring the peak height of the chromatographic waves. With the exception of hydrogen, the change in peak height was proportional to the concentration of the component.

Conversion rates. Calculations

For the characterization of the catalysts, the volumes of methane and oxygen converted in unit time are given (in units of cm^3/min). These characteristic values will be called conversion rates. The conversion rates of the products are obtained by multiplying the product flow rate by the corresponding concentrations. The symbol of the conversion rate of component i is v_i; the conversion rates of the reactants are negative.

We will avoid using the expression reaction rate, as no uniform equation (equations) of reaction was found, so that the conversion rates measured cannot be assigned to equations of reaction.

Calculations were made with computer MINSK 22. The input data were the gas rates, chromatographic peak heights and calibration data of the chromatograph. The computer calculated the conversion rates of components determined chromatographically, gave the scatter of the results, and discarded automatically the results incompatible with the mass balance. (For the details of calculations, see Ref. [9].)

Catalyst

The preparation of a catalyst for methane decomposition does not cause any difficulties. The impregnation of any porous ceramics with nickel nitrate solution, and the subsequent decomposition of the nitrate at 500 °C, yields a catalyst, which is suitable for the decomposition of methane at about 700—800 °C.

On the other hand, it is difficult to prepare a catalyst that would be for years efficient under industrial conditions. The differences between catalysts with various basic constituents can be quickly shown even by the most unpretentious comparative test [10].

The active substance of the catalyst is always nickel, however, the various catalysts differ with respect to the ceramic carrier and additives applied simultaneously with nickel.

This work deals with catalysts on aluminium silicate basis (mullite), for which the carrier substance has been manufactured by the Porcelain Factory of Budapest.* Catalysts made with this carrier proved satisfactory when used in industrial reactors [10]. The catalyst carrier is porous ceramics, containing

* The substance is essentially the same as the carrier called RÉBO 29 by BARSI *et al.* [14].

besides about 80% of mullite, small amounts of α-alumina, silicium dioxide and a vitreous phase. The apparent density of the carrier is 1.75 g/cm^3, its pore volume 0.35 cm^3/g, and its surface measured by the BET method 1.3 m^2/g. From this substance, 15 mm long cylinders, 5.5—6 mm in diameter, have been prepared for the experiments.

The carrier was impregnated with nickel nitrate solutions of various concentrations, depending on the desired nickel content. After impregnation, the grains were dried at 60 °C for 24 hours, and the nickel nitrate was subsequently decomposed at 350 °C by heating with air for 30 min. The catalyst formed was greyish black. The nickel oxide content was determined by chemical analysis and by derivatography [11]. Determinations by the two methods were generally in good agreement (Table I). The catalysts undergo reduction

Table I

Catalyst No.	Nickel surface m^2/g	Nickel content, mg Ni/g carrier method of determination	
		chemical analysis	thermal analysis
1	0.09	10	12
2	0.16	25	25
3	0.23	46	50
4	0.22	63	56
5	0.45	96	101
6	0.44	221	161

at 750 °C in the methane–oxygen mixture and start the partial oxidation. After 10—20 min of operation, the activity of the catalysts becomes constant. Under the experimental conditions used, a lasting and irreversible change in activity was observed only if the catalyst has been oxidized at about 900 °C. In this case reaction started again only after reduction with methane or hydrogen, and the activity was generally (but not reproducibly) lower than before oxidation. The nickel surface of the fresh catalyst was determined by hydrogen chemisorption [15]. The properties of the catalysts are summarized in Table I.

Reaction temperature

The beginning of the conversion of the gas blown on the catalyst grain was indicated by the increase in temperature of the grain. In one of the experiments, the catalyst grain was completely bored through, and the temperature

distribution was measured along the axis of the grain and in the vicinity of the grain (Fig. 1b) in a 25% methane–air mixture at a total flow rate of 2400 cm^3/min. Owing to the high gas velocity, the temperature was not constant in the reactor, increasing before the grain by 5—10 °C per cm. After the grain, the temperature of the gas increased suddenly, due to mixing of the hot product gas and the gas flowing at a greater distance from the grain. The average temperature of the grain cannot be calculated from the temperature distribution curve measured with the thermocouple because sudden temperature increases at the grain–gas boundary are masked by the thermal conductivity of the thermometer sleeve and the wires.

The surface temperature of the grain has been measured by means of a pyrometer. The end of the grain on the gas stream side had a temperature by about 30 °C higher than the other end. The average temperature measured with the pyrometer was the same as the highest temperature measured with the thermocouple inside the grain. In the experiments described in the following, temperatures were measured with a thermocouple reaching to the center of the grain.

Empty reactor

Above 500 °C, the reaction of methane with oxygen can proceed in the homogeneous phase or on the wall of the reactor. If a 25% methane–air mixture is fed into the quartz reactor at a rate of 2300 cm^3/min, above 700 °C, formaldehyde is found in the product. At 710 °C, the concentration of formaldehyde is 0.6, at 800 °C 1.7 and at 850 °C 1.6 mg/l. The other products of the homogeneous reaction, hydrogen and carbon monoxide can be detected from about 900 °C (Table II). The reaction mixture begins to burn at 980 °C, and all the oxygen is consumed in the reaction under formation of substantial quanti-

Table II

*Composition of the product gas of the empty reactor at a feed rate of 2300 cm^3/min**

Maximum temperature measured in the reactor, °C	Vol. %		
	H_2	CO	CO_2
930	0.6	1.3	0
960	1.3	2.7	0.1
980	2.9	5.7	0.2
1130	20.2	15.5	1.3

* Note: Product composition depends on the life-history of the reactor. Data given were measured in a quartz reactor used for a long time.

ties of soot and acetylene. It is interesting that in the homogeneous reaction methane is decomposed mainly into carbon monoxide and hydrogen. This observation is in accord with the findings of BURGOYNE and HIRSCH [12].

The findings discussed so far concerning the homogeneous reaction are not valid for the zone after the catalyst grain in the reactor, because the catalytic reaction changes the composition of the gas mixture. However, the extent of the homogeneous reaction possibly occurring in the zone after the catalyst grain will depend on the volume of this zone. We have made a series of experiments, where the position of the catalyst grain was varied. The situation was characterized by the distance between the narrow part of the reactor and the top of the catalyst grain. The results are listed in Table III. Notwithstanding the fact that the homogeneous reaction zone was increased by a factor of three, the changes in conversion rate did not exceed the experimental error, which indicates that the conversion observed proceeds in the immediate vicinity of the catalyst grain.

Table III

Feed: 25% methane–air mixture
Feed rate: 2200 cm³/min. Grain temperature: 935 ± 5 °C

Position of the grain cm	Conversion rate cm³/min		Rate of formation cm³/min		
	Methane	Oxygen	Carbon monoxide	Carbon dioxide	Hydrogen
1	104	97	84	21	140
3	102	96	82	20	136
5	106	105	85	21	128
7	106	102	84	22	132
Stand. dev.	5	6	5	3	7

Effect of the gas rate

The single-grain reactor furnishes valuable kinetic data, if the degree of conversion of the gas mixture is low. For this, high gas velocities are required. In this case, the composition of the feed can be assigned unequivocally to the reaction rate observed.

The variation of the conversion rate as a function of gas velocity is shown in Fig 2. The conversion rate increases slightly with increasing gas velocity, to an extent corresponding approximately to the change in average concentration of the reagents, due to the decreasing degree of conversion. The ratio of the consumption of the reagents was in each case close to unity ($v_{CH_4}/v_{O_2} = 1$),

indicating that the reaction mechanism is not influenced by the gas velocity. The standard deviation of the conversion rate of methane is 10 cm^3/min, that of oxygen 12 cm^3/min at the highest gas velocity. The error is nearly proportional to the gas velocity. (Limits of error are indicated in Fig. 2.)

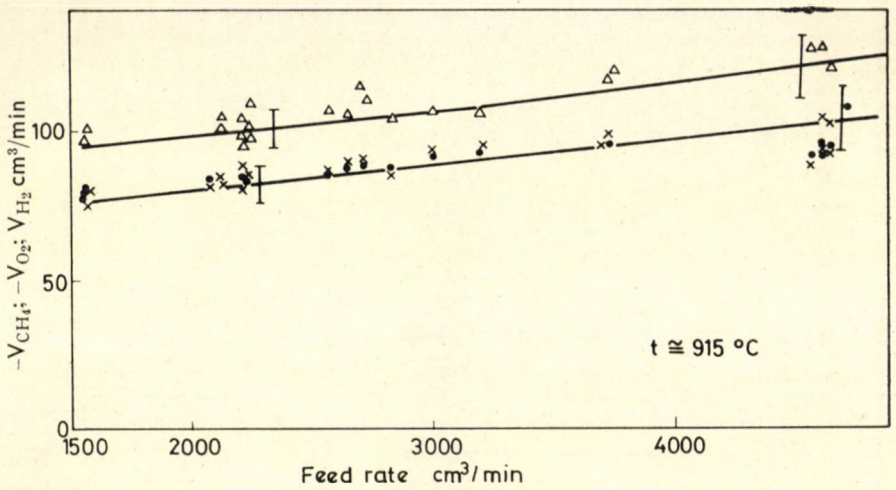

Fig. 2. Variation of the conversion rates of methane and oxygen as a function of the feed rate. Symbols: ● oxygen; × methane; △ hydrogen

Owing to the slight change in conversion rates, the gas velocity can be selected at will. Our experiments were carried out at a gas velocity of 2400 cm^3/min.

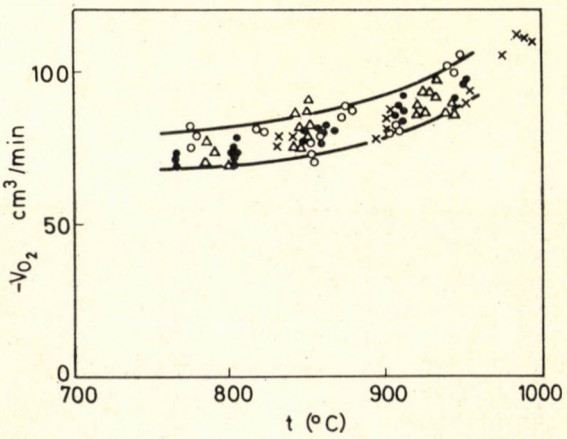

Fig. 3. Conversion rate of oxygen over four catalysts. Catalyst No. Symbols: 3: ×; 4; ○; 5: △; 6: ●

Variation of the reaction rate over catalysts of various nickel content with the temperature

The upper limit of the temperature range of the investigation is given by the ignition of the reaction mixture, the lower limit by the extinction of the catalytic reaction. With the catalysts used, extinction may occur below 760 °C, therefore the measurements were carried out above 760 °C.

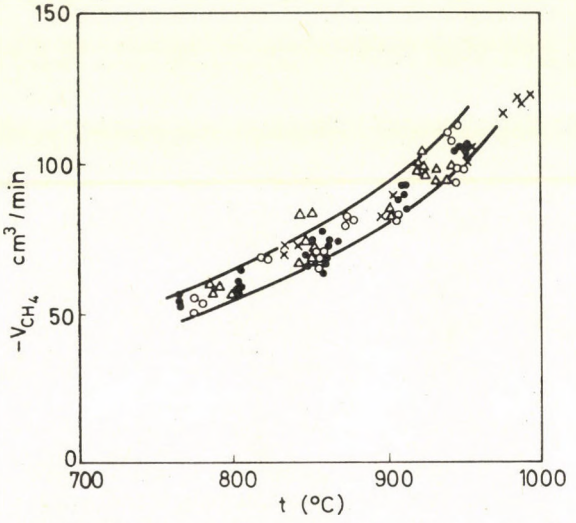

Fig. 4. Conversion rate of methane over four catalysts. Catalyst No. Symbols: 3: ×; 4: ○; 5: △; 6: ●

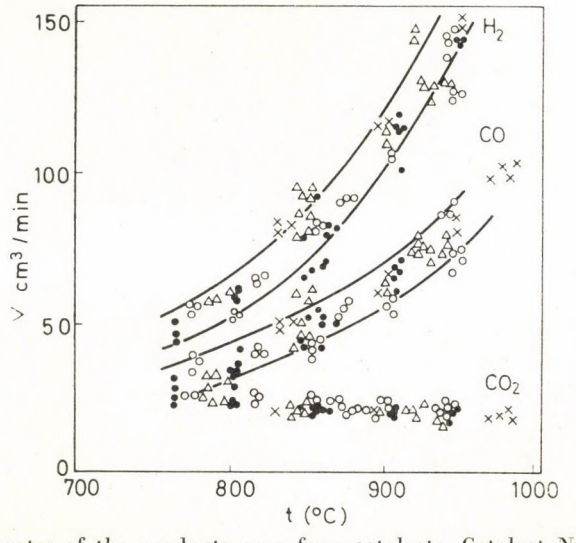

Fig. 5. Conversion rates of the products over four catalysts. Catalyst No. Symbols: 3: ×; 4: ○; 5: △; 6: ●

Results are shown in Figs 3—7. The feed rate was 2400 ± 50 cm³/min, and the mixture contained 25 ± 0.5 *v/v* % of methane. Over catalyst samples No. 3—6, the conversion rates were the same within experimental errors,

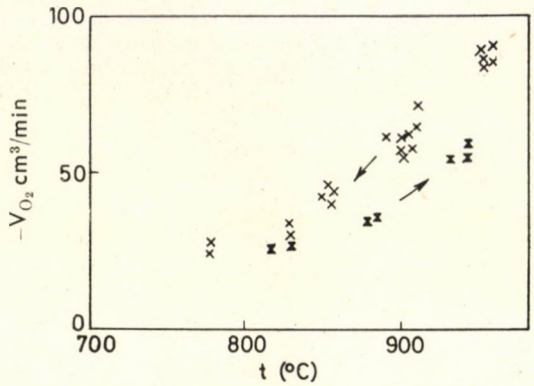

Fig. 6. Conversion rate of oxygen over catalyst No. 1. Symbols: × measured at decreasing temperature, x measured at increasing temperature

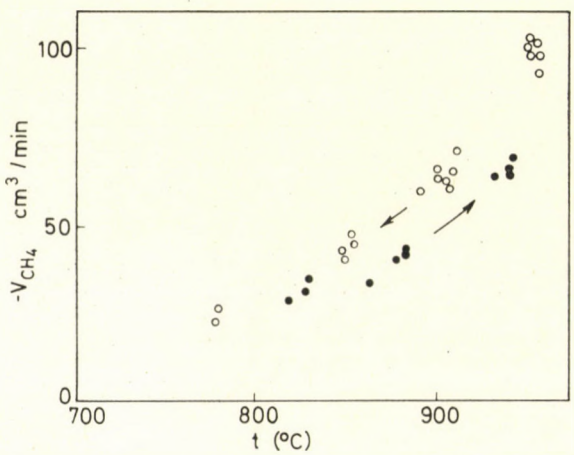

Fig. 7. Conversion rate of methane over catalyst No. 1. Symbols: ○ in the direction of decreasing temperatures, ● in the direction of increasing temperatures

and were therefore plotted on the same figures (Figs 3, 4, 5). As compared to the other catalysts, the conversion rate was lower with catalyst No. 1. It increased more steeply with temperature, and the change exhibited hysteresis, higher rates being measured with decreasing, than with increasing temperatures (Figs 6, 7). The behaviour of catalyst No. 2 represented a transition between catalysts No. 1 and 3. Owing to their non-specific character, these data are omitted.

Dependence of the reaction rate on composition at 890 °C

At a methane concentration of 25 *v/v* % the concentration of oxygen was varied. The results shown in Fig. 8 were obtained with catalyst grain No. 4, at a total gas rate of 2400 cm^3/min.

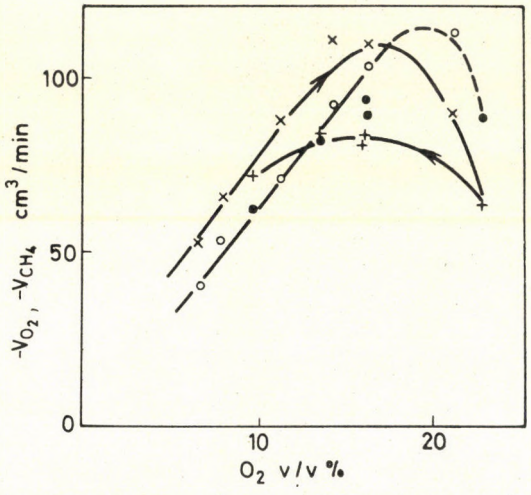

Fig. 8. Variation of the conversion rate of oxygen and methane as a function of oxygen concentration. Symbols: ● — O_2 in the direction of decreasing concentrations; + — CH_4 in the direction of decreasing concentrations; ○ — O_2 in the direction of increasingcon centrations; × — CH_4 in the direction of increasing concentrations

The conversion rates of both methane and oxygen were dependent on oxygen concentration. The stable region of operation was relatively narrow; below an oxygen concentration of about 10 *v/v* %, carbon was deposited on the catalyst grain, and above an oxygen concentration of about 20 *v/v* %, the activity of the catalyst diminished, due probably to the oxidation of nickel. Above 25 *v/v* % oxygen concentration, the methane decomposition stopped.

The conversion rate of oxygen was independent of the life history, and up to about 20 *v/v* % was proportional to the oxygen concentration. If the experiment was started with a mixture containing 6.7 *v/v* % of oxygen, and the concentration of oxygen was subsequently increased, the conversion rate of methane was higher than in the case when the concentration of oxygen was gradually decreased from an initial value of 22.8 *v/v* %.

The effect of changing the methane concentration was investigated on a gas mixture containing 11 *v/v* % of oxygen. It was found (Fig. 9) that the catalyst is inactive in a gas containing less than about 10 *v/v* % of methane. On increasing the methane content, the conversion rates of both oxygen and methane changed towards a limiting value.

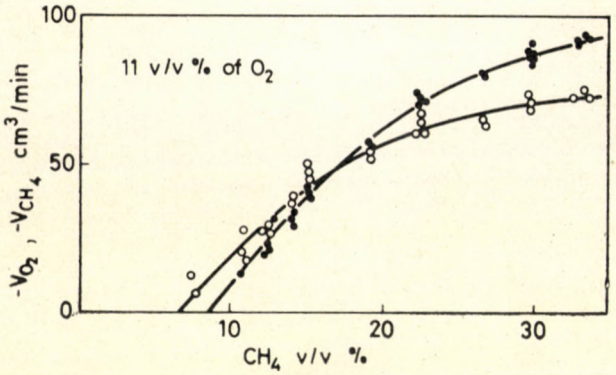

Fig. 9. Variation of the conversion rate of methane and oxygen as a function of the concentration of methane. Symbols: ● methane; ○ oxygen

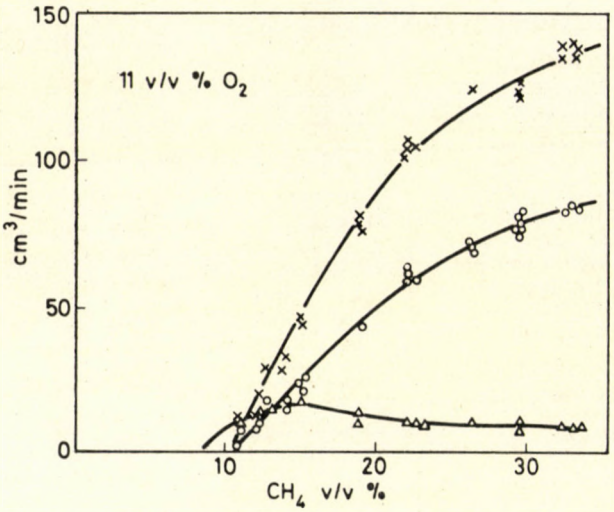

Fig. 10. Rate of formation of the products as a function of methane concentration. Symbols: × hydrogen; ○ carbon monoxide; △ carbon dioxide

Probably soot formation would begin at a sufficiently high methane concentration, which, however, has not been attained in this experimental series. The rates of product formation are shown in Fig. 10.

Evaluation of the results

The experimental results permit to conclude that the reaction rate is determined by the diffusion of oxygen through the gas film surrounding the catalyst grain.

This is supported by the following findings:

1. Mass transport in heterogeneous catalytic reactions is due to diffusion through the gas film surrounding the grain, and through the pores. The apparent activation energy of a surface reaction is in general decreased by diffusion, pore diffusion decreasing it by about 50%, and gas film diffusion to about 5—6 kcal. The slight temperature dependence of the conversion rate of oxygen observed between 760 and 900 °C indicates that the rate is determined by diffusion across the gas film.

2. The nickel surface of the fresh catalysts increases with the nickel content, whereas the catalytic activity exhibited a limiting value from the third member of the series. Assuming that the nickel surface does not shrink while in use or shrinking does not affect the catalytic activity, the phenomenon observed is indicative of the rate determining role of gas film diffusion.

3. During operation, the nickel catalyst must be in the reduced state. PRETTRE et al. [2] activated the catalyst before use by reduction. PETERS and KAPPELMACHER [13] proved that the catalyst remains in the reduced state also during operation. It is known that metallic nickel can be oxidized at high temperatures with molecular oxygen. Should the catalyst nevertheless remain in the reduced state during operation, it becomes inaccessible for molecular oxygen, or should it be accessible, the oxide formed is immediately reduced by methane. When the reaction rate diminishes at low temperatures, or the oxygen content of the gas mixture increases so that the catalyst becomes accessible for oxygen, the nickel is oxidized and the reaction stops. According to the experiments shown in Figs 8 and 9, the oxidation of the catalyst occurs when the concentration of oxygen is about the same as that of methane.

4. The rate-determining role of oxygen diffusion is also consistent with the finding that the conversion rate of oxygen is proportional to the oxygen concentration.

The single-grain method was suitable for clarifying the initial step of the conversion of methane–oxygen mixtures. In the starting mixture, the catalyst grain can remain and function in the reduced state, because during diffusion across the gas film the concentration of oxygen decreases practically to zero before it reaches the surface of the catalyst.

Besides gas film diffusion, the catalyst can be 'protected' from oxygen also by pore diffusion. This is supported by the results obtained with catalysts No. 1 and 2. Indeed, oxygen consumption remains below the limiting diffusion rate in this case, and changes relatively steeply with temperature. The protective action of the pores could not be verified at temperatures substantially lower than 760 °C: and we did not find that catalysts with high nickel content operated permanently below the limiting diffusion rate. This may be due primarily to thermal effects. The ratio of the conversion rates of methane and oxygen decreases with temperature, so that at lower temperatures the reaction

becomes more exothermic and, consequently, the temperature difference between the catalyst and the gas stream will be greater than at higher temperatures (before extinction, it amounts to about 300 °C). It seems that the decrease in reaction rate makes the heat transfer conditions of the catalyst grain unstable below 760 °C, and extinction arises from the fact that rate of heat conduction becomes higher than that of heat evolution.

The temperature of extinction is strongly dependent on the nature of the catalyst. According to a plant method, the catalyst is tested by stopping the heating of the catalyst bed, and by measuring the time of extinction with a cold reactant feed [10]. The extinction temperature of our catalysts is relatively high, so that the catalyst cannot function in a single-grain reactor with a cold feed, and the gas must be preheated to at least 400—450 °C for the catalyst grain to function.

It was observed in the reactor of the Gas Works of Óbuda that in the case of a cold gas feed the thermometer of the catalyst bed indicated a temperature varying between 100 and 800 °C. When the gas was preheated, this variation of temperature ceased.

A periodic fluctuation of catalyst temperature has been observed repeatedly also by us before the extinction of the reaction.

The similarity of the temperatures relevant to stable operation in the case of the industrial and single-grain reactors permits to consider the results obtained for the initial step of the reaction in the single-grain reactor valid also for the industrial reactor.

REFERENCES

1. Ogura, T. Ichimaru, T.: J. Soc. Chem. Ind. Japan **47,** 540 (1944)
2. Prettre, M., Eichner, C., Perrin, M.: Trans. Faraday Soc. **43,** 335 (1946)
3. Peters, K., Rudolf, M., Voetter, H.: Brennstoff-Chem. **36,** 257 (1955)
4. Padovani, C., Salvi, G., Distante, G.: Riv. Combustibile **6,** 175 (1952)
5. Joklik, A., Küninger, K.: Gas, Wasser, Wärme **5,** 112 (1956)
6. Otani, Seiya, Smith, J. M.: J. Catalysis **5,** 332 (1966)
7. Wurzbacher, G.: J. Catalysis **5,** 476 (1966)
8. Székely, Gy., Rácz, Gy., Traply, G.: Periodica Polytechn. **10,** 231 (1966)
9. Huszár, K.: Thesis. Technical University, Budapest, 1969
10. Barsi, L., Bunyitai J., Horváth L.: Energia és Atomtechnika **21,** 229 (1968)
11. Parlagh G., Huszár K., Rácz Gy., Székely Gy.: Magy. Kém. Foly. **77,** 213 (1971)
12. Burgoyne, J. H., Hirsch, H.: Proc. Roy. Soc. **A227,** 73 (1955)
13. Peters, K., Kappelmacher, E.: Brennstoff-Chem. **33,** 296 (1952)
14. Barsi L., Bunyitai J., Horváth L.: Energia és Atomtechnika **20,** 145 (1967)
15. Rácz Gy., Székely Gy., Huszár K., Oláh K.: Periodica Polytechn. **15,** 111 (1971)

Klára Huszár
György Rácz
György Székely

Budapest XI., Budafoki út 8.

Acta Chimica Academiae Scientiarum Hungaricae, Tomus 70 (4), pp. 301–311 (1971)

INVESTIGATION OF THE PARTIAL CATALYTIC OXIDATION OF METHANE, II

THE RATE OF OXYGEN DIFFUSION

GY. RÁCZ and GY. SZÉKELY

(Department of Physical Chemistry, Technical University, Budapest)

Received March 25, 1970

The conversion rate of oxygen has been measured on a single spherical catalyst grain in a mixture containing 25% of methane and 75% of air at different feed rates. In each case, the rate of oxygen conversion was found to be higher than the limiting rate of diffusion that can be calculated from data in the literature. This difference can be explained by the assumption that the conversion of the reactants is not restricted to the surface of the catalyst, but takes place also in the layer surrounding the catalyst. It could be proved by other experiments that the homogeneous reaction is not extended to the flowing medium, but occurs only in the vicinity of the catalyst surface.

The rate of heterogeneous reactions generally increases with temperature. This increase is limited by the fact that the concentration of the reactants decreases at the site of the reactions, the surface, because they can be replaced only at a finite rate by diffusion from the bulk of the gas phase. In steady state, the rate of diffusion is equal to the rate of the surface reaction. This condition determines the concentration of the reactants in the vicinity of the surface. With increasing temperature, the rates of reaction and diffusion increase simultaneously. At the same time the surface concentration of the reactants decreases and at high temperatures, the concentration of the reactant present in substoichiometric quantities approaches zero in the case of a smooth surface. The limiting value of the reaction rate belonging to zero surface concentration is called the diffusion controlled limiting rate.

In principle, the rate of heterogeneous reactions proceeding in porous substances cannot attain the diffusion controlled rate, because the reactants must penetrate to a certain depth into the pores to find an active surface and, therefore, the concentration of the reactants cannot decrease to zero on the enveloping surface of the porous body. If the path-length of diffusion is in the order of millimeters and the pore size in the order of micrometers, the limiting rate of diffusion in the vicinity of a porous solid cannot differ appreciably from that pertinent to the case of the smooth surface.

At such temperatures, where the rate of the heterogeneous catalytic reaction approaches the limiting rate of diffusion, it is to be expected in many cases that the reactants undergo reaction also in the homogeneous phase. If the

direction of the homogeneous reaction is different from that of the heterogeneous reaction, the composition of the product permits conclusions on the homogeneous reaction. If the product composition is not indicative of a homogeneous reaction, separation of the two kinds of reactions can be attempted by the techniques customary in homogeneous reaction kinetics, *i.e.* by varying the ratio of the homogeneous space and the heterogeneous surface. However, the occurrence of the homogeneous reaction may require the presence of a heterogeneous surface, taking place only in the vicinity of the latter in the diffusion layer. In such cases, the presence of the homogeneous reaction can be detected by sampling with a microprobe. RIBAUD and VALENTINE [1] burned a hydrogen–air mixture, originally at room temperature, on a preheated platinum surface. They have shown that at temperatures higher than 700 °C, hydrogen does not reach the surface of platinum, but its concentration decreases to zero already at a certain distance from the surface. Here a relatively simple explanation can be given for the homogeneous reaction of hydrogen. Upon approaching the heated sheet, the temperature increases, and thus the conditions become increasingly favourable for the homogeneous reaction. The reaction of hydrogen occurred always in that zone in which the temperature attained about 700 °C. We know also from other sources that the ignition temperature of air containing a few per cents of hydrogen is in the vicinity of 700 °C [2].

The investigation of the diffusion layer with a microprobe involves great experimental difficulties and it is doubtful whether the gas composition remains unchanged during sampling since secondary reactions may take place. The possible role of rapid homogeneous reactions in homogeneous–heterogeneous mechanisms can be evaluated by a simple method, *viz.* the reaction rate measured should be compared with the limiting rate of diffusion calculated for the given heterogeneous surface. If the reaction rate is higher than the limiting rate of diffusion, the presence of a homogeneous reaction is unequivocally established.

The catalytic reaction of methane with air is very fast, so that PETERS *et al.* [3] could not force a breakthrough of oxygen in their laboratory reactor because oxygen reacted completely even at a residence time as short as 4×10^{-3} s. PETERS *et al.* have concluded from this finding that the reaction is probably partly homogeneous, although they have offered no direct experimental proof.

HOUGEN and WATSON [4] describe a method for the calculation of the limiting rate of diffusion in a granular catalyst bed. By means of this method we calculated that in the experiments reported by PETERS *et al.* a residence time of about 2×10^{-3} s would have been sufficient for the reaction of 99% of the oxygen introduced, if the reaction rate had been equal to the limiting rate of diffusion. Thus, without doubting the likelihood of a homogeneous reaction between methane and air, it can be established that a high reaction rate, as

found in the experiment cited, is not sufficient proof for a homogeneous reaction.

In the first part of this work [5] we have concluded from the characteristic properties of methane partial oxidation that diffusion plays a decisive role in the reaction. We checked this finding by the calculation of the diffusion rate. The method of HOUGEN and WATSON mentioned above cannot be used because it does not apply to a single catalyst grain.

Component transfer to and from a single grain in flowing gas

The rate of component transfer is influenced primarily by the concentration difference of the diffusing component between the flowing gas and the surface of the grain. All the other effects are expressed in the relationship between the rate and the concentrations by a single component transfer coefficient. Thus the definition equation of the component transfer coefficient is:

$$k_A = \frac{N_A}{f(x_A^0, x_A^s)} \tag{1}$$

The function f should be such as to make the component transfer coefficient independent of the concentration of the diffusing component. Unfortunately, the composition influences the component transfer coefficient also indirectly, through the physical properties of the gas mixture, so that the form of the function can be established only by theoretical considerations (*cf.* later).

The component transfer coefficient depends on many factors. A relationship of practical use will be obtained if the variables are taken into consideration in the form of dimensionless parameters that can be deduced from the general differential equations pertinent to the phenomenon.

The Nusselt number expresses the component transfer coefficient in a dimensionless form, being a function of the path-length of diffusion

$$Nu = \frac{\text{Characteristic dimension of the grain}}{\text{Path-length of diffusion}} \tag{2}$$

On the other hand, the path-length of diffusion is a function of the properties of the flowing gas, which can be given by the Reynolds number

$$Re = \frac{v \cdot d}{\nu} \tag{3}$$

and by the Schmidt number

$$Sc = \frac{\nu}{D} \tag{4}$$

Eventually, the results of component transfer measurements can be expressed by the function

$$Nu = g(Re,\ Sc) \tag{5}$$

The form and constants of this function are determined by the shape of the grain.

We searched the literature for component transfer rate measurements with which our own results could be compared.

From the viewpoint of component transfer, the most extensively investigated shape is the sphere. This is due to the fact that spherical grains or droplets, which can be regarded as independent, single particles are involved in many chemical operations. According to Refs [6, 7], the experiments of RANZ and MARSHALL [8] can be considered reliable. These authors measured the evaporation rate of pure liquid drops in air, and summarized their results in the following equation:

$$Nu = 2.0 + 0.6\ Re^{1/2}\ Sc^{1/3} \tag{6}$$

This equation was regarded as the basis of comparison. Since our earlier single-grain experiments had been carried out on a cylindrical grain [5], they had to be repeated with a spherical grain.

In the evaluation of the experimental results, we had to clarify the following problems that arose in the calculation of the above dimensionless parameters for a heterogeneous reaction.

(1) Calculation of the component transfer coefficient;

(2) Interpretation of the physical quantities involved in Re;

(3) Effect of the temperature difference between the grain and the gas stream on the component transfer rate.

Description of the experiments

Spheres were ground from the nickel catalyst on ceramics carrier. The spheres were fixed on the tip of a thin quartz thermoelement sleeve, and introduced into an empty quartz tube with a diameter of 17 mm. The tube was heated in an oven to 750 °C, and a mixture of 25% methane and 75% air was passed through the tube. The oxygen content of the product was determined by gas chromatography. In our experiments the grain size and the flow rate of the gas were varied. Catalyst grains with 0.50; 0.78 and 0.90 cm in diameter have been studied. As the same conclusions could be drawn from the results of all three series, numerical values will be given here only for one series of experiments (Table I). Temperatures were measured with a standard Pt-PtRh thermocouple in the middle of the grain. The gas volume refers to 25 °C and 1 atm.

Table I

Variation of the conversion rate of oxygen as a function of the gas rate

Diameter of the catalyst grain: 0.78 cm					
Catalyst temperature °C	Gas-flow rate cm³/min	Conversion rate of oxygen cm³/min	Error of conversion rate cm³/min	Average mole fraction of oxygen	$k_{O_2} \times 10^6$ mole cm^{-2} s^{-1}
875	1388	88		0.127	265
876	1360	84	±5	0.127	251
875	1374	87		0.127	260
865	2620	75		0.140	206
864	2624	80	±6	0.140	218
865	2623	78		0.141	212
859	2616	80		0.141	217
860	1862	77		0.132	221
865	1866	78		0.132	225
872	960	87		0.110	299
876	960	91		0.109	315
860	3926	65		0.154	164
859	3886	69	+10	0.154	172
858	3920	68		0.155	169
858	2934	67		0.150	172
860	2890	69	+7	0.149	179

Calculation of the component transfer coefficient and Nu

The form of function corresponding to Eq. (1) can be derived from the Stefan—Maxwell equations. Accordingly, in a mixture of K components the relationship between the concentration gradient of component A and the diffusion rates is:

$$\frac{dx_A}{dz} = \sum_{i=1}^{K} \frac{1}{cD_{Ai}} (x_A N_i - x_i N_A) \tag{7}$$

(summation must be carried out with respect to all the components); here c is the total concentration, and D_{Ai} is the diffusion coefficient of the mixture of A and i. Eq. (7) becomes considerably simplified if a mean diffusion coefficient is written instead of the D_{Ai} values. According to HOUGEN and WATSON [4], the mean diffusion coefficient of component A is:

$$D_A(1 - x_A) = \sum_{i=B}^{K} x_i D_{Ai} \tag{8}$$

The relationship between the N_i values is given by the surface reaction. In our case the stoichiometry of the surface reaction cannot be expressed by a simple equation. However, according to experimental data published in our previous communication [5], the following equation is approximately valid in the temperature range between 850 and 900 °C:

$$CH_4 + O_2 = CO + H_2 + H_2O \tag{9}$$

If this reaction proceeds on the catalyst, the diffusion rates are interrelated in the surrounding gas layer as

$$-N_{CO} = -N_{H_2} = -N_{H_2O} = N_{CH_4} = N_{O_2} \tag{10}$$

Considering Eqs (8) and (10), Eq. (7) can be written in the following form:

$$D_{O_2} \cdot c \frac{dx_{O_2}}{dz} = -N_{O_2}(1 + x_{O_2}) \tag{11}$$

The integral of this equation gives the form of the function in question. Integration is performed for the simplest model: the diffusion layer is planar with a tickness of δ, the mole fraction of oxygen at the gas-side boundary of the layer is $x^o_{O_2}$, and at the surface $x^s_{O_2}$.

Integration gives:

$$\frac{c \cdot D_{O_2}}{\delta} = \frac{N_{O_2}}{ln \dfrac{1 + x^o_{O_2}}{1 + x^s_{O_2}}} \equiv k_{O_2} \tag{12}$$

This equation can be rearranged to indicate the mode of calculation of Nu:

$$Nu = \frac{d}{\delta} = \frac{d\, k_{O_2}}{c\, D_{O_2}} \tag{13}$$

Calculation of the physical properties of the gas mixture

The diffusion coefficient of two-component mixtures has been calculated by the formula of GILLILAND [4]:

$$D_{AB} = 0.0043 \frac{T^{3/2}}{P(V_A^{1/3} + V_B^{1/3})^2} \sqrt{\frac{1}{M_A} + \frac{1}{M_B}} \tag{14}$$

Data used for the calculation are summarized in Table II.

Table II

Data used for the calculation of diffusion coefficients

Substance	M_i	V_i
O_2	32	25.6
N_2	28	31.2
CH_4	16	29.6
CO	28	30.7
H_2O	18	18.9
H_2	2	14.3

The average diffusion coefficients of oxygen and methane were calculated from Eq. (8). In accordance with reaction (9) and under the assumption that the mole fraction of oxygen is zero on the surface of the catalyst, the calculations were carried out with the following average mole fractions in the diffusion layer:

$$x_{O_2} = x_{CO} = x_{H_2O} = x_{H_2} = 0.072;$$

$$x_{CH_4} = 0.160; \qquad x_{N_2} = 0.552.$$

The average molecular mass of the diffusion layer is 23.7. The results of the calculations are summarized in Table III.

Table III

Physical properties of the gas film surrounding the catalyst

Temperature K	$\mu \cdot 10^6$ poise	D_{CH_4} $cm^2 \cdot s^{-1}$	D_{O_2} $cm^2 \cdot s^{-1}$	$\varrho \times 10^3$ $g \cdot cm^{-3}$	Sc_{CH_4}	Sc_{O_2}
900	326	1.12	1.02	0.322	0.88	0.99
1000	350	1.31	1.20	0.289	0.92	1.01
1100	369	1.51	1.38	0.263	0.93	1.03
1200	398	1.73	1.57	0.241	0.95	1.06

The viscosities of the diffusion layer and the flowing gas have been calculated by the method of WATSON and UYEHARA [4] (Table III), which is based on the theorem of corresponding states. The error in calculating the viscosity of gas mixtures containing hydrogen is estimated to be about 10%.

Calculation of Nu

According to our assumption [5], in the temperature range between 760 and 900 °C the rate-determining process is the diffusion of oxygen. In other words, the surface concentration of oxygen is zero. This assumption permits to calculate the component transfer coefficient of oxygen by substituting zero in Eq. (12) for the surface mole fraction of oxygen. The mole fraction in the gas phase is replaced by the arithmetic mean value of the mole fractions measured in the feed and in the product gas.

From the experimental conversion rate of oxygen (Table I, Column 3), the average diffusion rate referred to unit surface has been calculated with the following formula:

$$N_{O_2} = \frac{\text{conversion rate of oxygen}}{60.24500 \text{ grain surface}} \frac{\text{mol}}{\text{cm}^2 \text{ s}} \tag{15}$$

Into expression (13) of Nu, the following constants referring to the mean value (1080 °K) of the average gas temperature and the average catalyst temperature (Table I, Column 1) have been inserted:

$$c = 1.13 \times 10^{-5} \text{ mol} \cdot \text{cm}^{-3}; \; d = 0.78 \text{ cm}; \; D_{O_2} = 1.35 \text{ cm}^2 \cdot \text{s}^{-1}.$$

The Nu values calculated from the average results of measurements carried out at the same gas velocity are shown in Column 2 of Table IV; the error of Nu arising from errors in the measurement of the conversion rate are listed in Column 3.

Table IV

Summary of data

Gas rate cm³/min	Nu	Error of Nu	Re	
			max.	min.
1370	13.3	0.8	54	27
2620	10.9	0.9	104	52
1870	11.3	0.7	72	36
960	15.7	0.7	38	19
3900	8.6	1.3	154	77
2910	9.0	1.0	114	57

Diameter of the grain: 0.78 cm

Schmidt number

As can be seen from Table III, the Sc values relative to oxygen are approximately equal to unity within the experimental error.

Reynolds number

In the evaluation of the experiment, the calculation of the Reynolds number, *Re*, presented the most problems since RANZ and MARSHALL [8] determined the component transfer coefficient in a medium which could be considered infinite. This was easily done in their case because they measured the amount evaporating from a liquid drop, and replenished the liquid from a microburette. The error of this method is independent of the magnitude of the gas volume. The above authors substituted into the *Re* formula the flow rate of the gas, flowing pluglike and undisturbed, at a large distance from the grain.

Such a well-defined situation cannot be created in studying the relationship between a heterogeneous reaction and diffusion because the degree of conversion of the gas mixture has to be measured, and the gas : catalyst ratio cannot be increased arbitrarily. The problem is to estimate that gas rate at which an extensive gas flow should be moved (let us call this the equivalent rate) to produce the same component transfer rate on the catalyst placed into the said gas stream as that in the given narrow reactor.

If we would cut out from a medium of very great extent, moving at the equivalent rate in pluglike flow, an imaginary cross-section corresponding to that of the reactor, the average flow rate would be higher in this cross-section than in the annular cross-section of the actual reactor, because friction along the walls of the actual reactor slows down the gas.

Owing to this effect, the estimation of the equivalent rate is rather uncertain. In the calculation of *Re*, the average flow rate in the space between the grain and the reactor wall was taken as the lower limit of uncertainty of the equivalent rate, and the double of this rate as the upper limit.

A further uncertainty in the determination of the velocity arises from the fact that natural convection, due to temperature and density differences, occurs besides forced flow. According to KRISCHER and LOOS [7], the velocity of free convection flow is

$$v = \left[dg \left(\frac{T^s M^o}{M^s T^o} - 1 \right) \right]^{1/2} \tag{16}$$

where the superscript s refers to properties valid at the surface of the grain, and the superscript o to those valid at great distances from the grain. If the direction of the natural convection flow is the same as that of forced flow, the two velocities have to be added. Upon substituting into Eq. (15) $M^o = 25.6$; $M^s = 22.1$; $T^s = 1130$ and $T^o = 1010$ K, one obtains $v = 15$ cm $\cdot$ s^{-1}. This value is about one half of the error of the equivalent gas velocity at the lowest gas-flow rate (960 cm^3 $\cdot$ min^{-1}), and about one tenth of the error at the highest rate, therefore we did not take it into consideration.

Evaluation of the results

The results of calculations are summarized in Table IV. The data were also plotted on a diagram (Fig. 1) with *Nu* values on the ordinate and log *Re* $Sc^{2/3}$ values on the abscissa. The function determined by RANZ and MARSHALL (Eq. 6) is also plotted on the diagram. Data measured at the highest gas

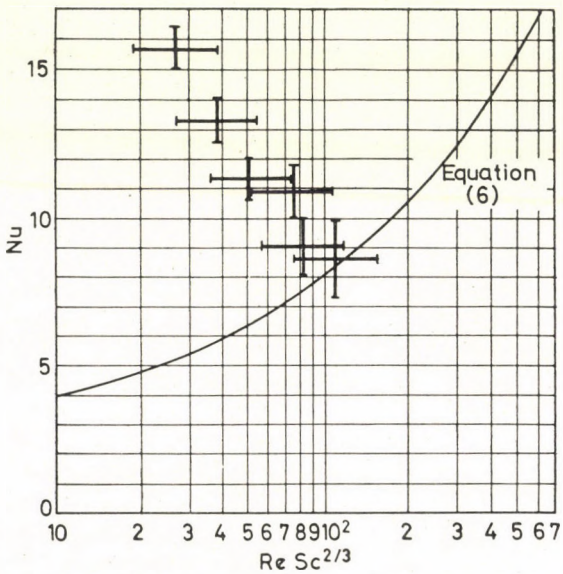

Fig. 1. Graphical representation of the results of component transfer measurements plotted as the relationship of dimensionless parameters

velocities agree within experimental errors with the data published in the literature, whereas at lower velocities a systematic deviation occurs. In the extreme case, the *Nu* number determined by us is two to three times the calculated value, *i.e.* the reaction rate of oxygen is 2—3 times higher than would be possible in a pure surface reaction.

The results of calculations on diffusion can be explained solely by the fact that besides a heterogeneous reaction (occurring on the surface) there is also a homogeneous reaction.

The question arises, what connection exists between this homogeneous reaction and the heterogeneous reaction. A closer connection can be assumed between the two reactions if the homogeneous one proceeds only in the vicinity of the surface. A looser connection is to be expected between the homogeneous and the heterogeneous reactions if the homogeneous reaction extends over the whole reactor. To elucidate this problem, we repeated the experiments in which the position of the grain was varied (for the description of the experiment *cf.*

Ref. [5]). Under the conditions of this experiment the measured rate of oxygen conversion was about twice as high as the calculated limiting rate of diffusion, and the rate of oxygen consumption was independent of the position of the grain. This means that the predominant part of the homogeneous reaction takes place within a few millimeters from the grain surface.

At the temperature and gas velocity used, the gas feed does undergo reaction without a catalyst in the homogeneous phase. It is therefore to be assumed that the homogeneous reaction observed in connection with the heterogeneous reaction was initiated by the catalyst.

Notations and dimensions

A, B	notation of the selected component
c	total concentration (mol · cm^{-3})
d	grain diameter (cm)
D	diffusion coefficient (cm^2 s^{-1})
g	gravitational acceleration (cm s^{-2})
i	general notation of the component
k_i	component transfer coefficient (mol cm^{-2} s^{-1})
K	number of components
M_i	molecular mass (g mol^{-1})
N_i	diffusion rate (mol cm^{-2} s^{-1})
Nu	Nusselt number
Re	Reynolds number
Sc	Schmidt number
T	absolute temperature (K)
V_i	molecular volume for the calculation of the diffusion constant
v	gas velocity
z	distance
x_i	mole fraction
δ	thickness of the diffusion layer (cm)
μ	dynamic viscosity (g/cm^{-1} s^{-1})
ν	kinematic viscosity (cm^2 s^{-1})
ϱ	density
o	value at the external boundary of the gas film
s	value at the enveloping surface of the catalyst grain

REFERENCES

1. RIBAUD, G., VALENTINE, P.: Compt. rend. **243,** 463 (1956)
2. BURGOYNE, J. H., HIRSCH, H.: Proc. Roy. Soc. A **227,** 73 (1955)
3. PETERS, K., RUDOLF, M., VOETTER, H.: Brennstoff-Chem. **36,** 257 (1955)
4. HOUGEN, O. A., WATSON, K. M.: Chemical Process Principles, Part III. Wiley, New York, 1949
5. HUSZÁR, K., RÁCZ GY., SZÉKELY GY.: Acta Chim. Acad. Sci. Hung. **70,** 287 (1971)
6. BIRD, R. B., STEWART, W. E., LIGHTFOOT, E. N.: Transport Phenomena. Wiley, New York, 1960
7. KRISCHER, O., LOOS, G.: Chem. Ing. Techn. **30,** 31 (1958)
8. RANZ, W. E., MARSHALL, W. R.: Chem. Eng. Progress **48,** 141, 173 (1952)

György RÁCZ
György SZÉKELY } Budapest XI., Budafoki út 8.

Acta Chimica Academiae Scientiarum Hungaricae, Tomus 70 (4), pp. 313—318 (1971)

STUDY ON THE PASSIVATION OF IRON IN WATER-ACETIC ACID MIXTURE

L. KISS, DO NGOC LIEN and M. L. VARSÁNYI

(Departments of Physical Chemistry and Radiology, L. Eötvös University, Budapest)

Received May 8, 1970

The anodic behaviour of iron was studied by a potentiostatic method in sodium acetate, perchloric acid and sodium perchlorate solutions prepared either with anhydrous acetic acid or acetic acid–water mixtures. In sodium acetate solutions passivation is observed only in the presence of water. However, in solutions of perchloric acid and its sodium salt passivation occurs only in anhydrous media. This phenomenon can be explained by the different properties of ion pairs formed in the solutions.

In a previous paper [1] we reported our study on the anodic dissolution of activated iron in anhydrous acetic acid. It has been established, among others, that under the conditions studied the rate of the anodic dissolution of iron increases with increasing acetate ion concentration. This paper deals with the passivation of iron in anhydrous acetic acid and in water–acetic acid mixtures. Water is known to play an important role in the passivation of metals. This fact was emphasized by several authors [2—9] and was confirmed by some experiments relating to the passivation of metals in non-aqueous solvents [6—9]. In the latter studies the absence of passivation has been established on the basis of potentiostatic curves in anhydrous solvents. The appearance and development of passivation are significantly affected by anions present in the solution [4, 6, 10—12] and deformations in the metals [13].

So far, the passivation of iron in acetic acid solutions has not been studied in detail. A short reference to such investigations can be found in a recent paper by HEITZ [14].

Experimental

The potentiostatic current-potential curves were obtained using a Type IP-410B potentiostat. The potential set by the potentiostat was checked by a Radelkisz Type OP 205 precision pH-Titrimeter. The potential was usually changed in steps of 50 or 100 mV and after a waiting period of 3 min the value of the current across the electrodes was read. Usually no change in the current across the electrodes was observed after this period. The electrode potentials given below (φ) refer to the saturated aqueous calomel electrode. Since it was the form of the potentiostatic curves that served as a basis of our conclusions, the diffusion potentials could be neglected.

The measurements were performed in vessels described earlier [1, 15]. The quality of iron and other chemicals as well as the method of preparing the experimental materials were similar to those described in a previous paper [1].

Results and discussion

The potentiostatic φ *vs.* lg i curves (i is the current density) determined for an iron electrode immersed into a water–acetic acid mixture containing 0.5 M sodium acetate are shown in Fig. 1. It can be seen that the iron electrode is passivated in all cases except in the solution prepared with anhydrous acetic acid.

With increasing the acetic acid content of the solution the rate of dissolution measured in the passive region is increased. The rate of anodic dissolution

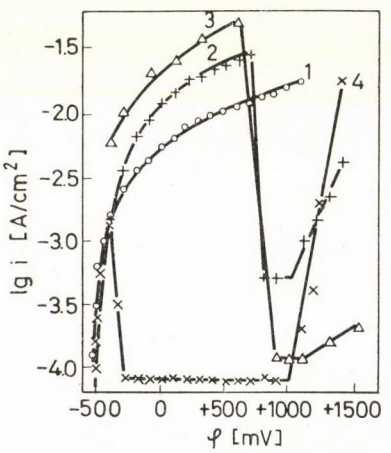

Fig. 1. Potentiostatic polarization curves for iron electrodes immersed into a 0.5 M CH_3COONa solution. Composition of the solvent: 1 — anhydrous acetic acid, 2 — 90% acetic acid + 10% water, 3 — 50% acetic acid + 50% water, 4 — 100% water

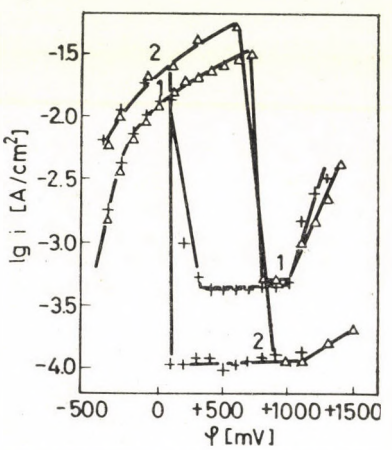

Fig. 2. Potentiostatic polarization curves recorded by sweeping the potential in positive (△) and (+) opposite directions in a 0.5 M CH_3COONa solution. Solvents: 1 — 90% CH_3COOH + 10% H_2O, 2 — 50% CH_3COOH + 50% H_2O

in the active state at sufficiently positive potentials is, however, increased upon increasing the water content (at the examined compositions of solutions). The curves shown in Fig. 1 were obtained by passing from negative to positive electrode potentials. Upon varying the potential in the opposite direction, hysteresis is observed in the cases represented by curves 2 and 3 shown in Fig. 2.

In Fig. 3 the potentiostatic curves obtained in a 0.15 M sodium acetate solution are shown. The shape of the curves depends upon the water content similarly to the cases shown in Fig. 1.

From the exprerimental results the conclusion can be drawn that the passivation of iron in acetic acid solution of sodium acetate is observed only in the presence of water, in agreement with the results of other authors [6—9] relating to non-aqueous solutions.

In Fig. 4 are shown the potentiostatic curves obtained for iron immersed in anhydrous and aqueous acetic acid solutions containing 0.5 *M* $HClO_4$. It can be seen that, in contrast to literature data referring to non-aqueous solvents

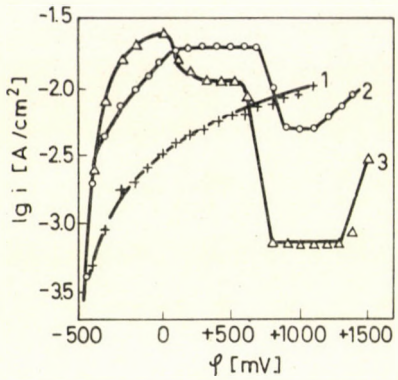

Fig. 3. Potentiostatic polarization curves recorded in a 0.15 *M* sodium acetate solution. Solvents: 1 — anhydrous acetic acid, 2 — 96.7% CH_3COOH + 3.3% H_2O, 3 — 90% CH_3COOH + 10% H_2O

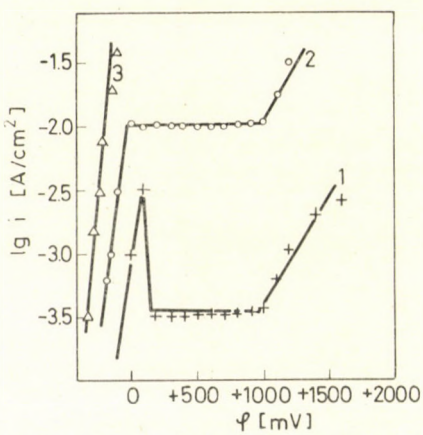

Fig. 4. Potentiostatic polarization curves recorded in a 0.5 *M* perchloric acid solution. Composition of the solvent: 1 — anhydrous acetic acid, 2 — 98% CH_3COOH + 2% H_2O, 3 — 90% CH_3COOH + 10% H_2O

as well as our results on sodium acetate solutions, the shape of the potentiostatic curve obtained in anhydrous solution indicates passivation, whereas the presence of water eliminates passivation, *i.e.* iron cannot be passivated. In the region corresponding to the dissolution of activated iron the rate of anodic dissolution increases with increasing water concentration in agreement with the data reported in a previous paper [1].

Potentiostatic polarization curves of similar shape can be obtained by changing the concentration of perchloric acid in the range of 0.1—0.5 *M*.

The potentiostatic curves obtained in 0.2 *M* sodium perchlorate solutions prepared with acetic acid are shown in Fig. 5. Thus a slight passivation is observed in anhydrous media as the potential becomes positive. This passivation is, however, eliminated by adding 2% of water.

To study the behaviour of the iron electrode immersed into a solution containing sodium acetate, perchloric acid and its sodium salt, the effect of stirring the polarization curves was examined using a rotaring disc electrode. It was found in these experiments that the speed of rotation practically does

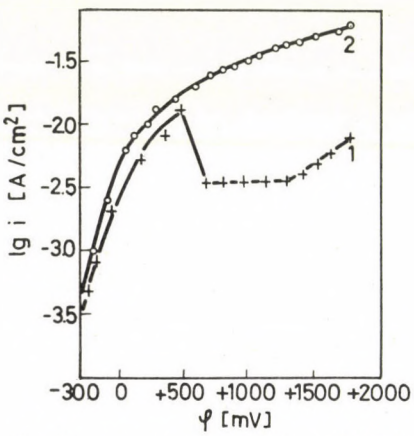

Fig. 5. Potentiostatic polarization curves recorded in a 0.2 *M* $NaClO_4$ solution. Solvents: 1 — anhydrous acetic acid, 2 — 98% CH_3COOH + 2% H_2O

not affect the shape of the potentiostatic curves. If perchloric acid or sodium perchlorate is used, the shape of the potentiostatic curve does not change with the speed of rotation of the electrode in the active region; in the passive region, however, the current intensity increases significantly and no current density drop, characteristic of passivation, can be observed when the potential becomes positive. This phenomenon can be seen in Fig. 6, where potentiostatic curves are shown recorded at various rpm values of a disc electrode immersed into a 0.2 *M* $HClO_4$ solution.

On the basis of these results the following can be established: in the first case (CH_3COONa solution) the passivation, occurring when water is added to the solution, is probably caused by an oxide layer formed on the iron surface; the dissolution of this layer is independent of the hydrodynamic conditions. However, in the second case (anhydrous solution of perchloric acid and its sodium salt), passivation is due to the accumulation and slow removal of the product of dissolution at the electrode surface as well as to the low rate at which the component promoting dissolution (*e.g.*, acetate ions) arrives upon the surface. In this case the situation is similar to the dissolution of iron in aqueous NaCl

solutions, applying high current densities, where the appearance of passivation is controlled by convective diffusion [16, 17].

As for the role of water, it increases the rate of dissolution in the active state in all cases. This effect can probably be explained by the adsorption of water on the surface and by its contribution to the formation of the solvate shell promoting anodic dissolution. On the other hand, water increases the concentration of acetate ions in the solutions, as has been shown in an earlier paper [1]. This process increases the rate of active dissolution. In solutions con-

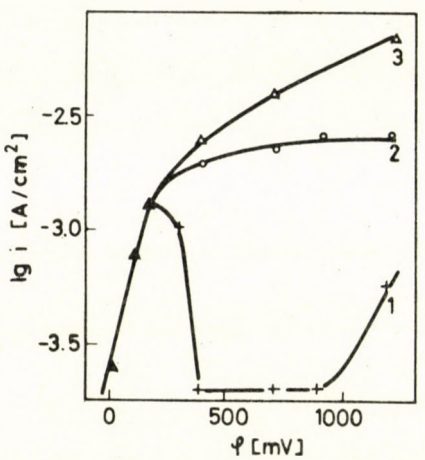

Fig. 6. Effect of speed of rotation of the electrode on the shape of the potentiostatic curve recorded on 0.2 *M* $HClO_4$ solution prepared with anhydrous acetic acid. The rpm of the rotating disc electrode: 1 — $f = 0$ min^{-1}, 2 — $f = 230$ min^{-1}, 3 — $f = 1320$ min^{-1}

taining perchloric acid and sodium perchlorate a similar effect prevails at potentials corresponding to passivation; however, it is probably combined with the increased solubility of the product of anodic dissolution upon the addition of water. This assumption is supported by the significant increase in the solubility of iron(II) acetate in the presence of water. Thus, according to our preliminary measurements the solubility of iron(II) acetate in anhydrous acetic acid containing 0.5 *M* $HClO_4$ is 0.46 g/100 ml, whereas in a mixture of 90% acetic acid + 10% water, 0.5 *M* $HClO_4$ added, the solubility is 3.5 g/100 ml. A similar increase of solubility upon the addition of water is observed in sodium acetate solutions.

The results obtained in these experiments are probably affected by the difference between the character of interaction of water and the dissolved components in the two solutions. In the first case $[(CH_3COOH)_2Na^+CH_3COO^-]$ complexes (ion pairs) are probably present in the solution. The addition of water to the solution does not destroy these complexes. In anhydrous perchloric acid solutions $[(CH_3COOH)_2H^+ClO_4^-]$ complexes are present. When water is added

to the solution the following reaction may take place [1], since the proton is more strongly bounded by water than it is in the complex,

$$[(CH_3COOH)_2H^+ClO_4^-] + H_2O \rightleftarrows (CH_3COOH)_2 + (H_3O^+ClO_4^-).$$

In this case the ion pair contains hydroxonium ion, which makes passivation impossible. However, in sodium acetate solutions, at certain potentials, the water adsorbed on the electrode surface permits the formation of a protective layer whose rate of dissolution is independent of the hydrodynamic conditions.

From the results reported above and in our previous paper [1], the conclusion can be drawn that the anodic dissolution of iron takes place by an electrochemical mechanism, in agreement with HEITZ's assumption [14].

However, our results appear to be at variance with the remark of the above author according to which the passivation observed in monocarboxylic acids is due to a $Me(Carb)_n$ protective layer. Our view is supported by the experimental fact that in sodium acetate solutions passivation can be observed only in the presence of water (see Figs 1, 2).

REFERENCES

1. KISS, L., DO NGOC LIEN, VARSÁNYI, L.: Magyar Kém. Foly. **76**, 371 (1970)
2. SCHWABE, K.: Werkstoffe u. Korrosion **18**, 961 (1967)
3. SCHWABE, K.: Proceedings of the 3rd Int. Congr. on Met. Corr. Vol. 1. Moscow, p. 54, 1968
4. KOLOTYRKIN, YA. M.: Zashchita Metallov **3**, 131 (1967)
5. HOAR, T. P.: Corrosion Sci. **7**, 341 (1967)
6. FREIMAN, L. I., KOLOTYRKIN, YA. M.: Zashchita Metallov **5**, 139 (1969)
7. KOLOTYRKIN, YA. M., KOSSY, G. G.: Zashchita Metallov **1**, 271 (1965)
8. SHMIDT, V.: Zashchita Metallov **5**, 608 (1969)
9. TSINMAN, A. I., KARTEVICH, A. N.: Zashchita Metallov **5**, 517 (1969)
10. FREIMAN, L. I., KOLOTYRKIN, YA. M.: Zashchita Metallov **1**, 161 (1965); Doklady AN SSSR **162**, 376 (1965); **171**, 1138 (1966)
11. KOLOTYRKIN, YA. M., KONONOVA, M. D., FLORIANOVICH, G. M.: Zashchita Metallov **2**, 609 (1966)
12. NOBE, K., TOBIAS, R. F.: Corrosion **20**, 262 (1964)
13. FREIMAN, L. I., KOLOTYRKIN, YA. M., GIVENTAL, A. YA.: Zashchita Metallov **1**, 286 (1965)
14. HEITZ, E.: Berichte Bunsenges phys. Chemie **73**, 1085 (1969)
15. KISS, L., KŐRÖSI, A., FARKAS, J.: Magy. Kém. Foly. **73**, 551 (1967)
16. DAVIDOV, A. D., KASCHEEV, V. D., KABANOV, B. N.: Elektrokhimia **5**, 221 (1969)
17. KABANOV, B. N.: 20th Meeting of CITCE, Strasbourg 1969, Extended Abstracts, p. 215

László KISS
DO NGOC LIEN
Magda L. VARSÁNYI

Budapest VIII., Puskin u. 11—13.

Acta Chimica Academiae Scientiarum Hungaricae, Tomus 70 (4), pp. 319–327 (1971)

POLYMERIZATION OF ACRYLAMIDE WITH THE REDOX SYSTEM $K_2S_2O_8$–ASCORBIC ACID IN AQUEOUS SOLUTION AT ROOM TEMPERATURE*

I. GÉCZY** and H. I. NASR***

(Textile Research Institute, Budapest)

Received May 20, 1970

Acrylamide was polymerized in aqueous solution at room temperature with the redox system potassium persulfate–ascorbic acid. The kinetical course of polymerization was followed iodometrically. The effect of monomer and initiator concentrations on the rate of the reaction was studied and a kinetical equation for the over-all rate was established. The role of the solvent as a chain transfer agent was also investigated.

Finally, the dependence of the number average degree of polymerization on the initial monomer concentration as well as the initiator–activator concentration and temperature were determined.

Recently polyacrylamide has found use in many fields, *e.g.* as a flocculant or sizing agent. Therefore polymerization studies on acrylamide monomer are of great importance.

The aim of our investigation was to polymerize acrylamide in aqueous solution with redox systems at room temperature. Preliminary studies were made to find redox systems which are effective at room temperature. Table I illustrates such redox systems.

Table I

Redox systems effective at 25 °C

Initiator \ Activator	Ascorbic acid	$NaHSO_3$	Na_2SO_3	$Na_2S_2O_4$	$H_2NCH_2CH_2NH_2$	$C_6H_5NHNH_2$	$FeSO_4(NH_4)_2SO_4$
H_2O_2	+	+	+	+	+	+	
$K_2S_2O_8$	+			+	+	+	+
$(NH_4)_2S_2O_8$	+	+	+	+	+	+	

* Presented at the IUPAC International Symposium on Macromolecular Chemistry Budapest, 27th August, 1969. (*Cf.* Kinetics and Mechanism of Polyreactions 5/12.)

** Present address: Central Research Laboratory for Colouristics, Budapest, Hungary.

*** Present address: National Research Centre, Cairo, UAR.

All these systems successfully initiated the polymerization at room temperature.

The redox system potassium persulfate–ascorbic acid proved to be the most effective, therefore it was subjected to detailed kinetical investigations. The kinetic course of polymerization was followed iodometrically. Fig. 1 shows the instantaneous monomer concentration at time t as a function of the different powers of the monomer concentration.

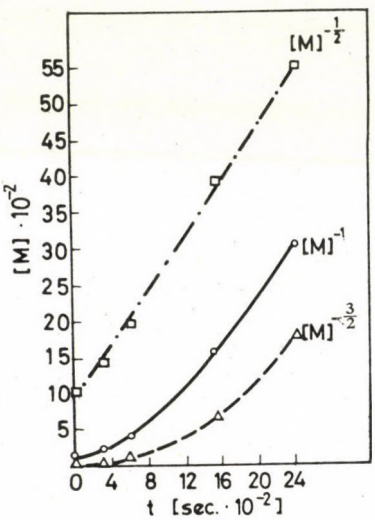

Fig. 1. Kinetical course of the polymerization of acrylamide. $[M_0] = 2.816$ mole/l; $[K_2S_2O_8] = 1.5 \times 10^{-2}$ mole/l; [ascorbic acid] $= 1 \times 10^{-2}$ mole/l; pH $= 4.5$; temp. $= 25\,^{\circ}C$

As can be seen in Fig. 1, a linear relationship exists only at $[M]^{-1/2}$, therefore

$$[M]^{-1/2} = k_1 t + c \tag{1}$$

where k_1 = the slope

c = the intercept of the straight line.

By differentiating we get:

$$-\frac{d[M]}{dt} = 2k_1 [M]^{3/2} \tag{2}$$

The dependence of the rate of polymerization on the concentration of the redox system is shown in Table II and in Fig. 2. The rate of polymerization has half-order dependence on the concentration of the redox system.

The value of the over-all rate constant proved to be fairly constant, $K = 0.15 \pm 0.04$ l/mole.sec.

Table II

Dependence of the rate of polymerization on the concentration of the redox system $K_2S_2O_8$–ascorbic acid

($[M_0] = 1.408$ mole/l; pH = 4.5; temp. = 25 °C)

$[I] \times 10^3$ mole/l	Time, min.	Rate, % min.	K $l \cdot mole^{-1} \cdot sec^{-1}$
3.06	15	2.46	0.19
6.16	15	3.15	0.14
12.3	10	3.82	0.11
24.5	10	4.58	0.16

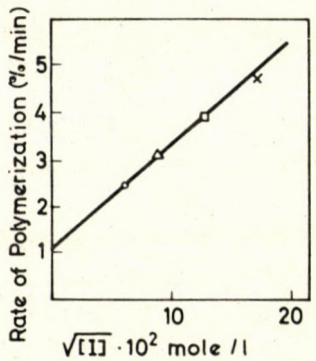

Fig. 2. Initial rate of polymerization of acrylamide as a function of the square root of the concentration of the initiator system. $[M_0] = 1.408$ mole/l; pH = 4.5; temp. = 25 °C

These results can be explained assuming that a steady state condition exists, as follows:

$$v_i = k_i[I][M] \tag{3}$$

$$v_p = k_p[R\cdot][M] \tag{4}$$

$$v_t = k_t[R\cdot]^2 \tag{5}$$

where k_i, k_p, k_t are the rate constants for the initiation, propagation and termination, respectively.

Under stationary-state conditions, the rate of initiation equals that of the termination, *i.e.*:

$$v_i = v_t$$

$$k_i[I][M] = k_t[R\cdot]^2$$

$$[R\cdot]^2 = \frac{k_i}{k_t}[I]\ [M]$$

$$[R\cdot] = \sqrt{\frac{k_i}{k_t}}[I]^{0.5}[M]^{0.5} \tag{6}$$

By substituting the value of $[R\cdot]$ obtained from Eq. (6) into Eq. (4) we get:

$$v_p = v_{br} = -\frac{d[M]}{dt} = k_p \sqrt{\frac{k_i}{k_t}} [I]^{0.5}[M]^{1.5} \tag{7}$$

It can be concluded that in the polymerization of acrylamide in aqueous solution initiated by potassium persulfate–ascorbic acid, the monomer participates in the initiation, and termination takes place between two growing radicals.

The number average molecular weights ($\bar{M}_n$) of the polymers were determined in order to investigate their dependence on the initial monomer and initiator concentrations as well as the temperature.

Viscosity measurements were carried out in $1N$ sodium nitrate solution at 30 °C, according to Eq. (8) [1]

$$[\eta]_{30°C} = 6.8 \times 10^{-4} \ \bar{M}_n^{0.66} \tag{8}$$

Table III shows the pertinent data and Fig. 3 represents the relation between the initial monomer concentration and number average molecular weights of the resulting polymers; it can be seen that a proportionality exists between them having a first order dependence. This is in good agreement with RODRIGUEZ's statements concerning persulfate–metabisulfite and persulfate–thiosulfate redox systems [2, 3].

Table III

The number average molecular weight of polyacrylamide ($\bar{M}_n$) versus the initial monomer concentration $[M_0]$
($[I] = 6.16 \times 10^{-3}$ mole/l; pH = 4.5; temp. = 25 °C)

$[M_0]$ mole/l	$\bar{M}_n \times 10^{-5}$	$\bar{P}_n$	$\frac{1}{\bar{P}_n} \times 10^{-3}$	$[S]/[M]$ mole/l
0.704	0.388	547	1.83	78.8
1.408	0.689	970	1.03	39.4
2.112	0.809	1140	0.88	26.3
2.816	1.427	2010	0.49	19.7

The chain transfer to the solvent was determined according to MAYO [4]:

$$\frac{1}{\bar{P}_n} = \frac{1}{\bar{P}_0} + C_s \frac{[S]}{[M]} \tag{9}$$

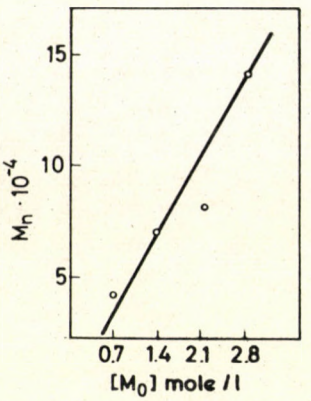

Fig. 3. The number average molecular weight of polyacrylamide (M_n) plotted against the initial monomer concentration $[M_0]$. $[I] = 6.16 \times 10^{-3}$ mole/l; pH = 4.5; temp. = 25 °C

where $\frac{1}{\bar{P}_0}$ is the reciprocal value of the number average degree of polymerization in the absence of a transfer agent, and C_s is the transfer constant to the solvent, $[S]$ being the concentration of the solvent. The values of C_s and $\frac{1}{\bar{P}_0}$ were calculated on the basis of Table III and Fig. 4, by the mean value method.

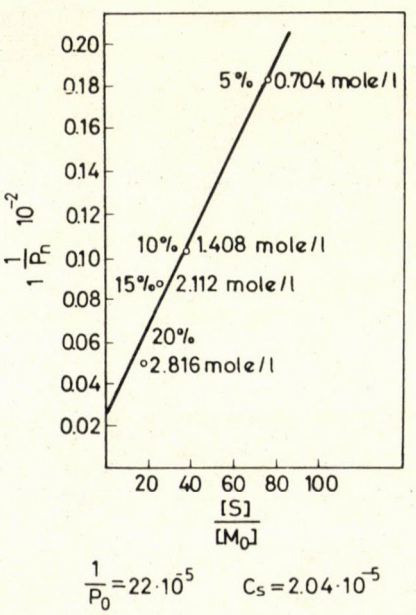

Fig. 4. Effect of chain transfer of water on the molecular weight of polyacrylamide. $[I] = 6.16 \times 10^{-3}$ mole/l; $\frac{1}{P_0} = 0.022 \times 10^{-2}$, $C_s = 2.04 \times 10^{-5}$

C_s was found to be equal to 2.04×10^{-5}, whereas $\frac{1}{\overline{P}_0}$ was 2.2×10^{-4}, and hence $\overline{P}_0 = 4.545$, which value represents the maximum theoretical degree of polymerization that can be attained in the absence of a transfer agent under the given experimental conditions. This value corresponds to the number average molecular weight $\overline{M}_n = 322.695$.

The effect of initiator concentration on the molecular weight of polyacrylamide formed in the presence of redox systems has been reported by different authors to be of a complex controversial nature [2, 3, 5, 6], therefore this question was investigated in detail in the present work.

The dependence of the number average molecular weight of polyacrylamide on the persulfate–ascorbic acid concentration is given in Table IV and Fig. 5.

Table IV

Dependence of the number average molecular weight of polyacrylamide on the persulfate–ascorbic acid concentration

($[M_0] = 1.408$ mole/l; pH = 4.5; temp. = 25 °C)

$\sqrt{[I]}/[M_0] \times 10^{-3}$	$\overline{M}_n \times 10^{-5}$	$\overline{P}_n$	$\frac{1}{\overline{P}} \times 10^3$
2.17	1.85	2610	0.38
4.36	1.75	2469	0.40
8.73	0.69	970	1.03
17.46	0.69	970	1.03

The relation between the molecular weight and the concentration of potassium persulfate–ascorbic acid is inversely proportional, *i.e.* the plotting of the reciprocal molecular weight and number average degree of polymerization against the square root of the initiator–activator concentration gives a straight line*.

Its intercept is k_{tr}/k_p, and the slope $\sqrt{2k_i k_t}/k_p$, where k_{tr} is the rate constant for the chain transfer; thus the above mentioned terms can be estimated. The former value was found to be 1.78×10^{-4}, while the latter equals 6.51×10^{-2}, both calculated by the mean value method. The intercept also represents $1/\overline{P}_0$ and hence the theoretical number average molecular weight ($\overline{M}_n$) that can be reached equals 3.9×10^5. This value is in good agreement with that of the chain transfer to the solvent.

* The mathematical relationship is as follows:

$$\frac{1}{\overline{P}_n} = \frac{k_{tr}}{k_p} + \frac{\sqrt{2k_i k_t}}{k_p} \cdot \frac{\sqrt{[I]}}{[M_0]}$$

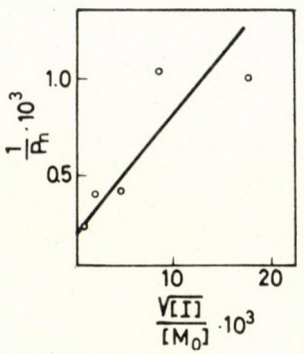

Fig. 5. Reciprocal of the number average degree of polymerization $\left(\frac{1}{\overline{P}_n}\right)$ against $\frac{\sqrt{[I]}}{[M_0]}$

The effect of temperature on the molecular weight was examined within the range 25 to 60 °C, as shown in Table V and Fig. 6. (In the experiments the possible network reactions were neglected.)

Table V

The effect of temperature on the molecular weight of the resulting polymer ($[M_0] = 1.408$ mole/l; $[I] = 6.16 \times 10^{-3}$ mole/l; pH = 4.5)

Temperature, °C	$1/T \times 10^3$, °K^{-1}	$\overline{M}_n \times 10^{-5}$
25	3.35	0.69
35	3.24	0.59
50	3.09	0.29
60	3.00	0.06

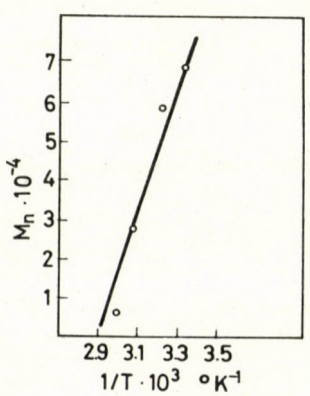

Fig. 6. Effect of temperature on the molecular weight ($\overline{M}_n$). $[M_0] = 1.408$ mole/l; $[I] = 6.16 \times 10^{-3}$ mole/l; pH = 4.5

In one of his papers [2] on acrylamide polymerization initiated by persulfate–metabisulfite, RODRIGUEZ stated that the temperature had no effect on the molecular weight, whereas in one of his other publications [3] where persulfate–thiosulfate redox system was used, results different from the former one were obtained. In our investigations as indicated in Fig. 6, the molecular weight is inversely proportional to the temperature in a system initiated by potassium persulfate–ascorbic acid. A plot of the number average molecular weights against the reciprocal absolute temperatures gives a straight line.

Finally endeavours were made to estimate the rate of initiation of the polymerization under consideration.

In principle, the velocity of initiation of a free radical polymerization can be obtained from studies of the over-all rate of the polymerization and number average molecular weight of the resulting polymer [7]. The following two equations can be applied:

$$v_{br} = -\frac{d[M]}{dt} = k_p \sqrt{\frac{v_{\text{init}}}{k_t}}\,[M] \tag{10}$$

and

$$\frac{1}{\bar{P}_n} = \frac{(k_t\, v_{\text{init}})^{1/2}}{k_p[M]} + \frac{k_{tr}}{k_p} \tag{11}$$

In the cases where chain transfer to the monomer can be considered negligible, elimination of $k_p[M]/k_t^{1/2}$ from Eqs (10) and (11) gives the following relation [7]:

$$\frac{v_{br}}{P_n} = v_{\text{init}} \tag{12}$$

Table VI

Change of the rate of initiation with the monomer concentration
($[I] = 6.16\times10^{-3}$ mole/l; pH = 4.5; temp. = 25 °C)

$[M_0]$, mole/l	v_{br}			$v_{\text{init}}\times10^6$ mole/l.sec
	% min	mole/l.sec$\times10^4$		
0.704	2.32	2.72	547	0.5
1.408	3.82	8.96	970	0.9
2.112	6.84	24.0	1140	2.1
2.816	9.74	45.9	2010	2.3

Table VII

Change of the rate of initiation with the concentration of the redox system ($[M_0] = 1.408$ mole/l; pH = 4.5; temp. = 25 °C)

$[I]$ mole/l $\times 10^3$	v_{br}		$\bar{P}_n$	$v_{init} \times 10^6$ mole/l.sec
	%/min	mole/l.sec $\times 10^4$		
1.54	2.46	5.76	2610	0.21
3.08	3.15	7.38	2469	0.3
6.16	3.82	8.96	970	0.9
12.32	4.58	10.75	970	1.1

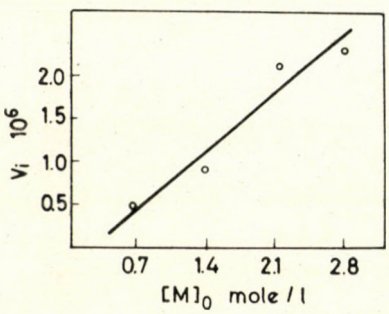

Fig. 7. Change of the rate of initiation with the monomer concentration. $[I] = 6.16 \times 10^{-3}$ mole/l; pH = 4.5; temp. = 25 °C

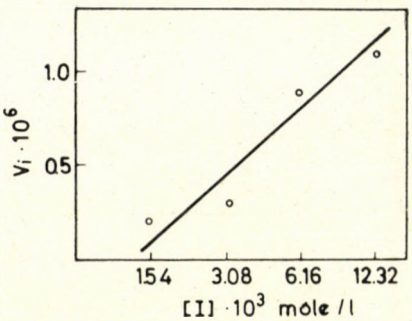

Fig. 8. Change of the rate of initiation with the concentration of the redox system. $[M_0] = 1.408$ mole/l; pH = 4.5; temp. = 25°C

Assuming that chain transfer to the monomer is negligible (which is the most general case), the rate of initiation can be determined from Eq. (12). Tables VI and VII as well as Figs 7 and 8 show the obtained data from which it can be seen that the rate of initiation is proportional to the initial monomer and initiator concentration as a consequence of Eq. (3). It amply supports the fact that the monomer is also taking part in the initiation step.

REFERENCES

1. Collinson, E., Dainton, F. S., McNaughton, G. S.: Trans. Farad. Soc. **53,** 476 (1957)
2. Rodriguez, F., Givey, R. D.: J. Polymer Sci. **55,** 713 (1961)
3. Riggs, J. P., Rodriguez, F.: J. Polymer Sci. (A-1) **5,** 3167 (1967)
4. Mayo, F. R.: J. Am. Chem. Soc. **65,** 2324 (1943)
5. Riggs, J. P., Rodriguez, F.: J. Polymer Sci. (A-1) **5,** 3151 (1967)
6. Suen, T. J., Yuan, Jen., Lockwood, J. V.: J. Polymer Sci. **31,** 481 (1958)
7. Priest, W. J.: Polymerization and Polymer Reactions, p. 483

István Géczy; Budapest IV., Váci út 71.
Hussein Ibrahim Nasr; National Research Centre, Cairo, UAR.

Acta Chimica Academiae Scientiarum Hungaricae, Tomus 70 (4), pp. 329—341 (1971)

MÖSSBAUER STUDY OF FROZEN FERRIC PERCHLORATE SOLUTIONS AT DIFFERENT pH

I. DÉZSI,* V. D. GOROBCHENKO,** M. KOMOR,*** I. I. LUKASHEVICH,** A. VÉRTES*** and K. F. TSITSKISHVILI**

(Central Research Institute for Physics, Budapest, ** Kurchatov Atomic Energy Institute, Moscow, USSR and *** L. Eötvös University, Budapest)*

Received June 12, 1970

Mössbauer measurements have been performed on frozen ferric perchlorate solutions down to 2.8 °K. The presence of different types of ions as a function of pH was observed. The hydrolysis was found to be enhanced by preheating the solution before freezing. The magnetic structures of the polymeric ions are inferred from the Mössbauer data and the results are compared with those obtained by other authors from spectrophotometric and magnetic susceptibility measurements.

Introduction

The hydrolysis of Fe(III) ions has been extensively studied. Simultaneously with the pH dependence, a decrease in the magnetic susceptibility of the ferric perchlorate solutions could be observed [1, 2, 3]. The formation of dimeric $Fe_2(OH)_2^{4+}$ ions prior to complete hydrolysis of the solutions was inferred from potentiometric data by HEDSTRÖM [4]. The decrease in the magnetic moment from 5.8 to 3.8 BM (Bohr magneton) per Fe(III) ion, observed in magnetic susceptibility measurements on solutions at high pH, was attributed by MULAY and SELWOOD [5] to the diamagnetic structure of the dimeric ions. The formation of dimeric ions during the hydrolysis of Fe(III) ions was recently confirmed by the thorough investigations of SCHUGAR *et al.* [6]. In solutions at high values of pH, polymeric ions containing more than 2000 ferric ions per molecule were detected by SPIRO *et al.* [7].

In earlier investigations on the Mössbauer effect in frozen ferric perchlorate solutions at different pH values, ferric ions with different structures have been identified [8, 9, 10]. It seemed of interest to continue the study of these solutions in wider ranges of pH and temperature. Though the structure of the frozen solutions has not yet been fully established, it was thought to be useful to find a correlation between the Mössbauer data in frozen solutions and the data on ionic structure obtained in the liquid phase by other methods.

Experimental

For the experiments, metallic iron enriched to 80% in ^{57}Fe, and reagent grade Merck chemicals were used. The stock solution of $Fe(ClO_4)_3$ was prepared by the dissolution of metallic iron in hot 35% perchloric acid and evaporation until onset of crystallization. The stock solu-

tion was diluted with distilled water. In addition to 0.04 *M* $Fe(ClO_4)_3$ + 3 *M* $NaClO_4$ solutions described in Ref. [5], 0.04 *M* $Fe(ClO_4)_3$ solutions were also prepared, which contained $NaClO_4$ as a result of pH adjustment. The pH was adjusted by the addition of perchloric acid or sodium bicarbonate, to an accuracy of ± 0.02 pH units by Radelkis type Titri-pH-meter. The spectrophotometric curves were taken on a Unicam SP 700 spectrophotometer, using an optical path length of 0.05 mm.

The Mössbauer spectra were determined with a spectrometer operated in 'time mode' and with ^{57}Co radiation source diffused in Pd. The Mössbauer equipment was calibrated with natural iron and $^{57}Fe_2O_3$. Zero velocity was evaluated from the tabulated data of MUIR *et al.* [11]. In the low temperature measurements, a He cryostat was used which generated 2.8 °K by reduced pressure over liquid helium.

Results

The experimental solutions were first used for reproducing the spectrophotometric experiments of MULAY and SELWOOD [5]. The Mössbauer spectra were studied on solutions with a $NaClO_4$ concentration much lower than 3 *M* since in frozen solutions the low relative concentration of other than Fe ions is preferable for Mössbauer experiments. The optical absorption spectra are shown in Figs 1a—b. It is apparent that their shape is not sensitive to the variation of the $NaClO_4$ concentration. Two absorption peaks are observed, the first at 240 nm in the pH range from 0.0 to 1.8 and the second at 335 nm, appearing at pH > 1 with increasing intensity at the expense of the 240 nm

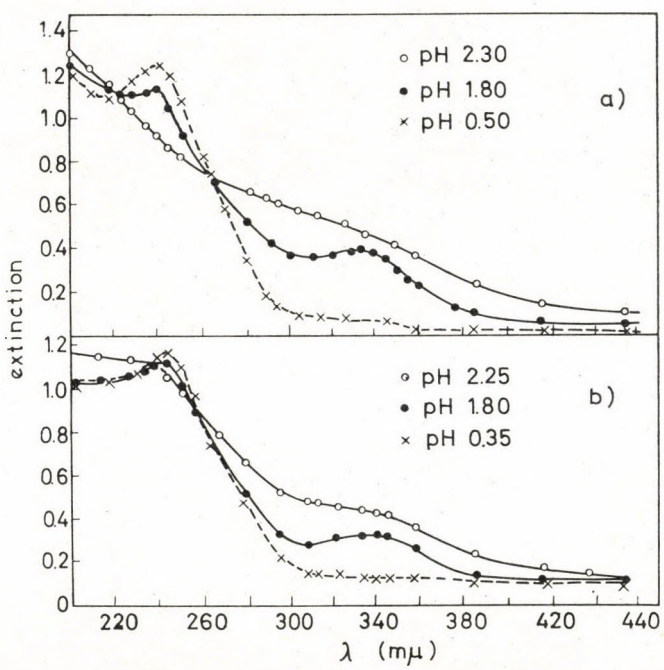

Fig. 1. Variation of spectrophotometric curves with the pH of solutions a) in 3 *M* $NaClO_4$, b) $\ll 3$ *M* $NaClO_4$ in ferric perchlorate solution

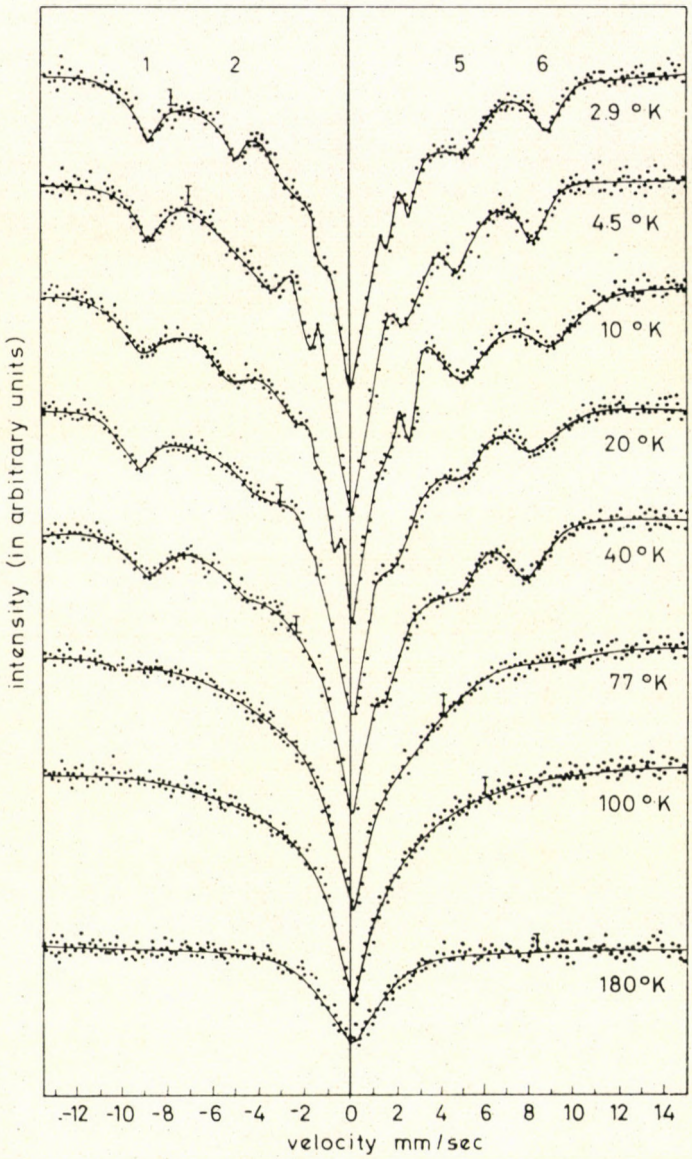

Fig. 2. Variation of Mössbauer spectra with temperature in solutions at different values of the pH. a) pH = 0.40

peak as the pH increases. The first peak was assigned by MULAY and SELWOOD to the $Fe(H_2O)_6^{3+}$ ion, the second to the $[Fe_2(OH)_2 \cdot 8H_2O]^{4+}$ dimeric ion.

Table I

Mössbauer parameters as a function of the pH and temperature in frozen solutions

Sample	2.85	4.5	10	20	40	77	T°K
pH = 0.40	575	577	575	571	571		H kOe
	571	565					H kOe
pH = 1.45	0.39 1.59	0.34 1.59					2ε mm/sec
pH = 2.20		494		491		479	H kOe
				0.64		0.73	2ε mm/sec
pH = 2.35	497	487	490	487	487	474	H kOe
			0.53	0.53	0.71	0.71	2ε mm/sec

H = values of internal magnetic field calculated from the two extreme lines.
Error: $\Delta H = \pm 5$ kOe
2ε = values of the quadrupole splitting calculated from the two central lines.
Error: $\Delta 2\varepsilon = \pm 0.05$ mm/sec.

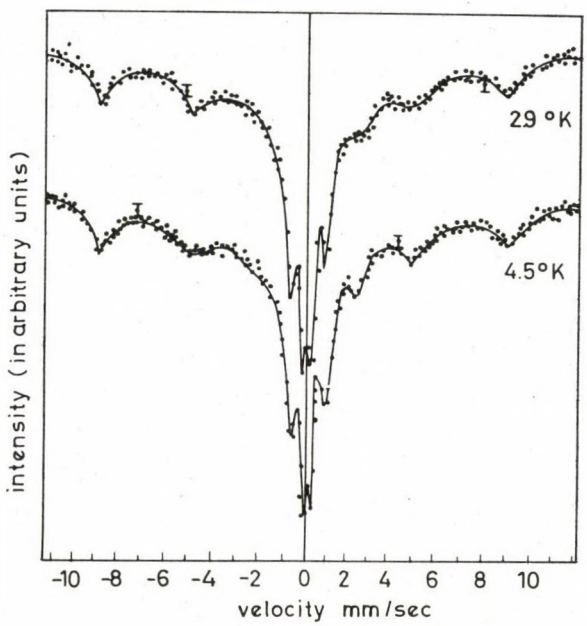

Fig. 2b. pH = 1.45

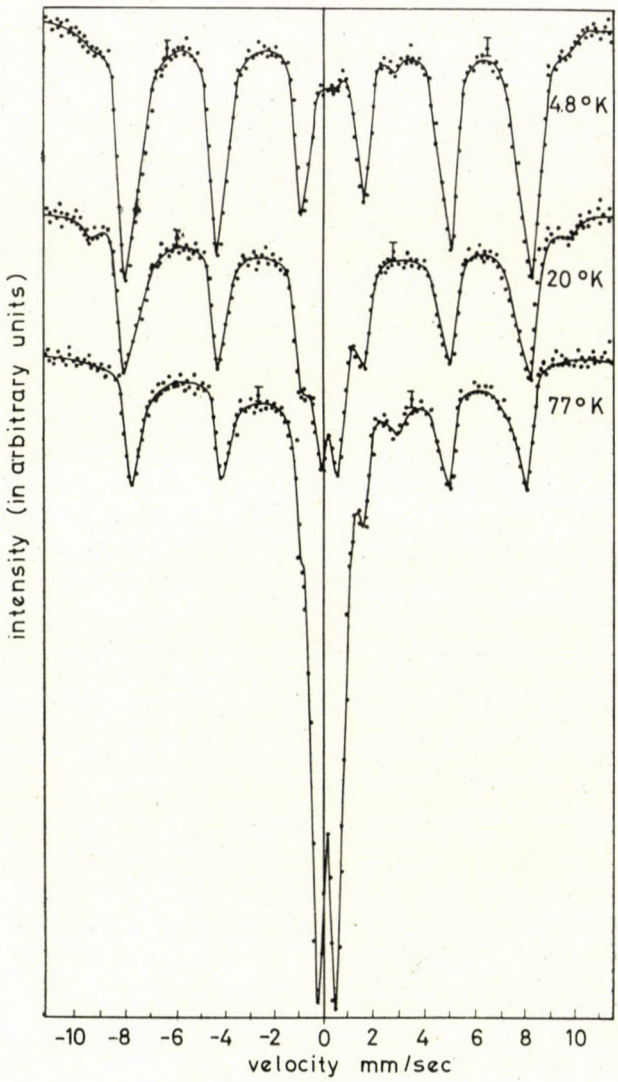

Fig. 2c. pH = 2.20

The Mössbauer spectra were taken on solutions of pH adjusted successively to 0.40; 1.40; 1.45; 2.20; 2.35. The liquid samples were first cooled down, in about 3 min, to 77 °K in a cryostat filled with liquid nitrogen, then to 4.8 °K by the addition of liquid helium. The temperature was increased by gradual heating of the samples. The Mössbauer patterns as a function of temperature are to be seen in Figs 2a—b—c—d. The Mössbauer parameters measured as a function of pH and temperature are summarized in Table I.

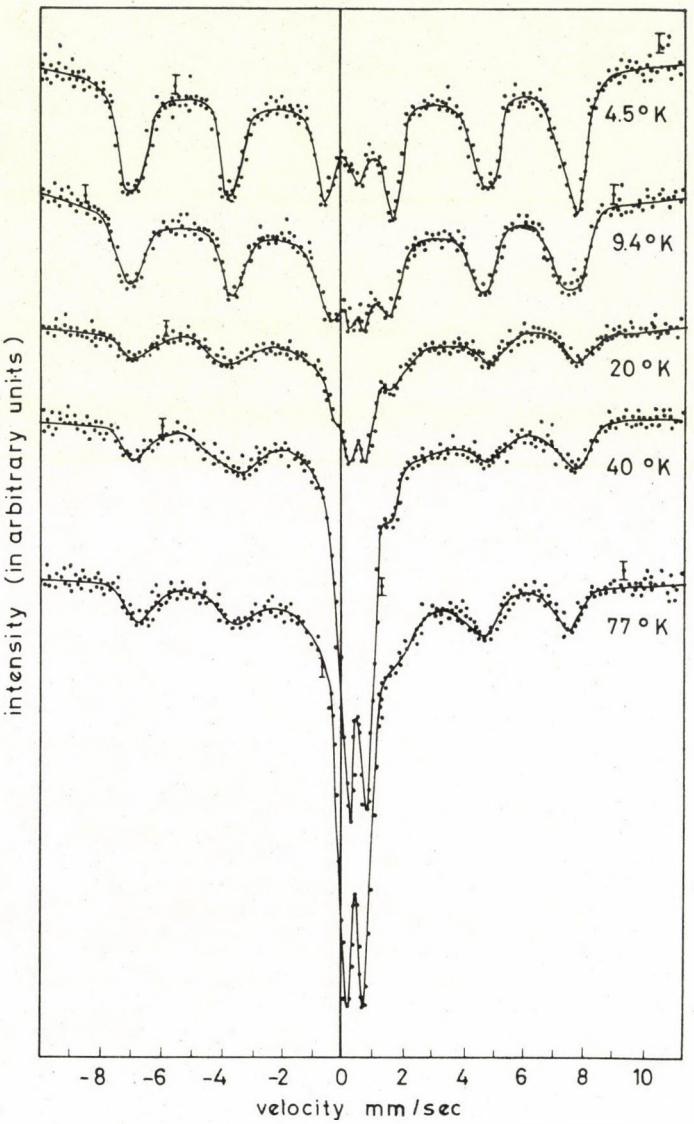

Fig. 2d. pH = 2.35

In order to take account of the temperature dependence of hydrolysis, some samples were heated in the liquid phase up to 60 °C and kept at this temperature for various periods before freezing. The Mössbauer spectra taken under these conditions are shown in Figs 3 and 4. The effect of preheating is apparent in Fig. 4 from the increase in the area below the magnetically split lines after longer periods of preheating. The time behavior of the pH dependence of hydrolysis was studied by taking the Mössbauer spectrum of the same sample,

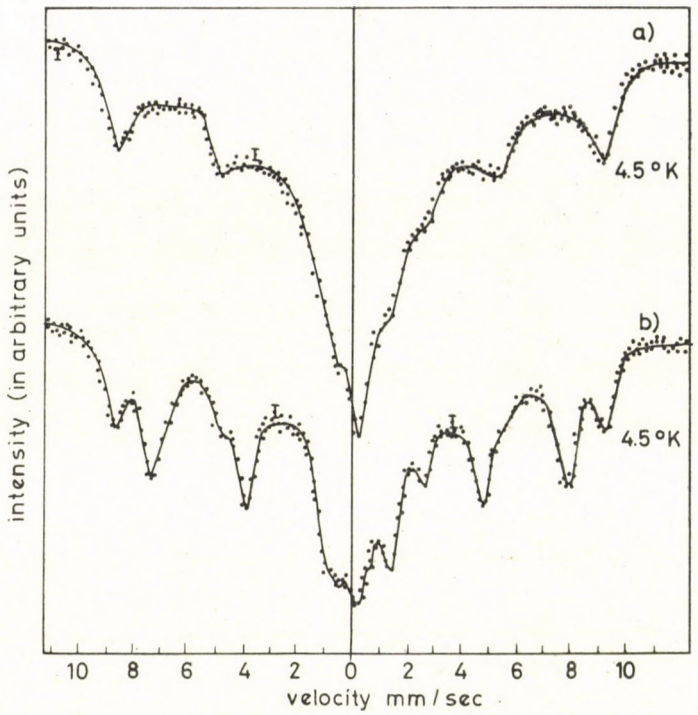

Fig. 3. Mössbauer spectra of frozen solutions with pH = 1.40. a) without preheating, b) solution preheated at 60 °C for 45 min before freezing

first immediately after the pH adjustment, then after its standing for 26 days at room temperature (Figs 5a and 5b).

Discussion

Isomer shift

In the presence of magnetic splitting it is rather difficult, sometimes even impossible, to identify the quadrupole splitting in the complex spectra and thus to evaluate the isomer shift. From the central, magnetically unsplit part of the spectra the isomer shift could be evaluated as $\delta = 0.2$ to 0.4 mm/sec. This range of δ is the same as that observed for high-spin ferric ions and indicates a 3 d^5 electron configuration in these ions [12].

Quadrupole splitting

The Fe^{3+} ion has an *S*-type ground state, thus the quadrupole splitting can be attributed to the asymmetric charge distribution due to the neighbouring atoms.

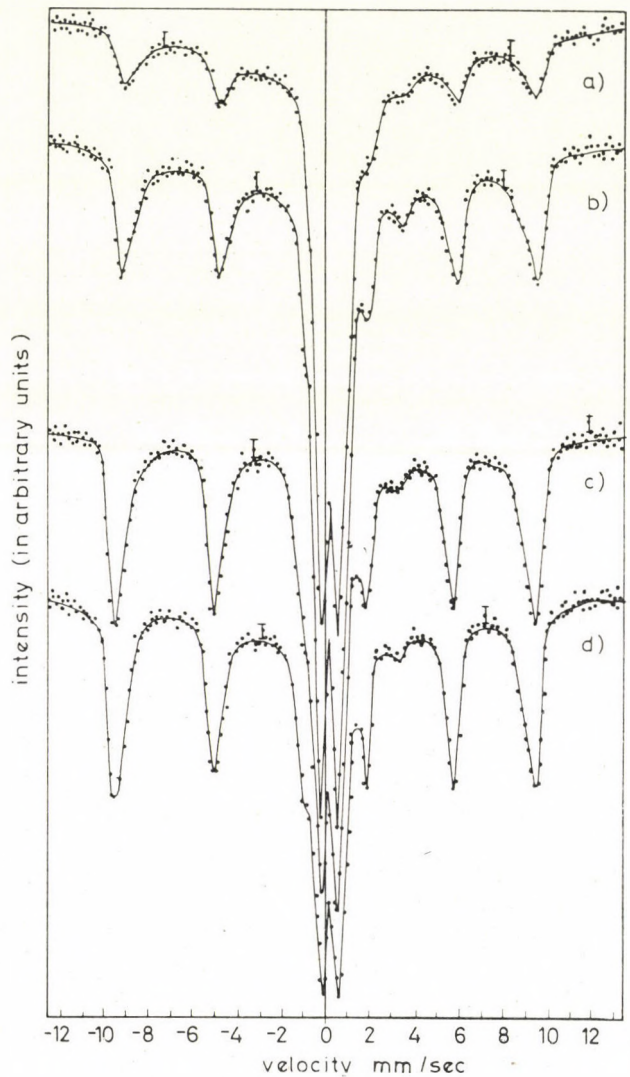

Fig. 4. Effect of preheating at 60 °C on the Mössbauer spectrum measured at 77 °K in a solution with pH = 2.20. a) without preheating. Time of preheating b) 45 min; c) 2h; d) spectrum *c* measured after 20 days

As a function of solution pH the presence of different ionic structures, like $Fe(H_2O)_6^{3+}$, $[Fe(H_2O)_5OH]^{2+}$ $[Fe(H_2O)_4(OH)_2]^{+}$ and the dimeric (and polymeric) $[(H_2O)_4\,Fe\text{-}(OH)_2\text{-}Fe(H_2O)_4]^{4+}$ can be expected [5]. The measured spectra were analyzed in terms of assignment to these ions of different structures. In the sample with pH 0.4, the highly complex spectrum does not exhibit any splitting in the central line (the broadening can be attributed to

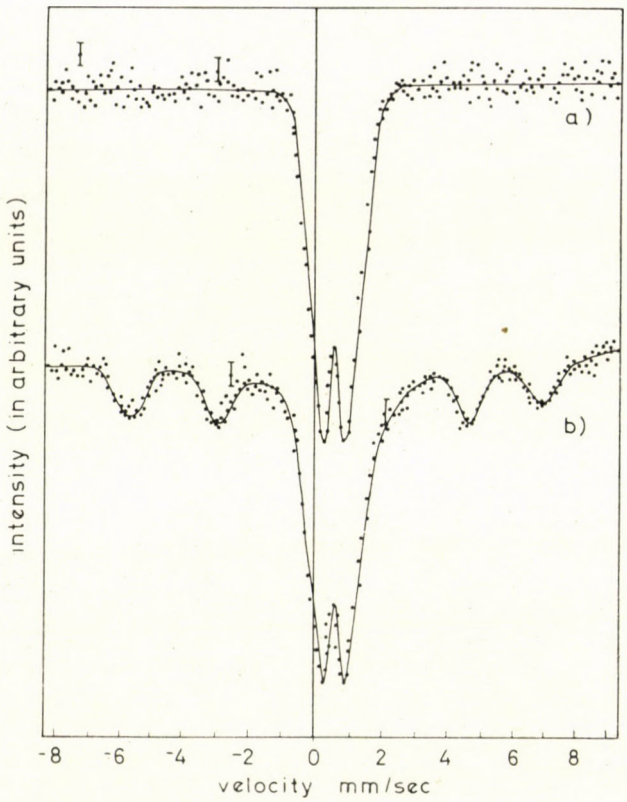

Fig. 5. Mössbauer spectrum of a solution of pH = 2.35, measured at 77 °K a) immediately after pH adjustment; b) after standing for 26 days

hyperfine relaxation effects). This is consistent with the presence of $Fe(H_2O)_6^{3+}$ ions with an octahedral first-neighbour configuration, and consequently, without electric field gradient. In the sample with pH 1.45, the quadrupole splitting exhibited by the central part of the spectra produces two sets of lines (Fig. 2b). The two values of the quadrupole splitting, differing by a factor of 4, suggest the simultaneous presence of two types of ferric ions. Their formation could be explained in several ways. One of them might be the presence of two structurally different phases of the solution during freezing. The different environments of ferric ions could produce electric field gradients leading to different quadrupole splittings. Alternatively, ions of different structures might be formed and homogeneously distributed in the solution. Neither of these mechanisms can be definitely confirmed by the Mössbauer measurement under the given conditions. It seems, however, highly probable that the electric field gradient is generated primarily by the first neighbours and that the different values of the field gradient can be attributed to the appearance of the

OH^- ion in the first co-ordination sphere of the ferric ion. It is the negative charge of the OH^- ion that is thought to be mainly responsible for the change in the field gradient. As estimated in [4], about 90% of the ions is still in the $Fe(H_2O)_6^{3+}$ form at pH 1.40 to 1.45 while the rest has the above dimeric structure. This 10% cannot cause a great change in the Mössbauer spectrum. The estimate from magnetic susceptibility data [5] gives 80% of $Fe(H_2O)_6^{3+}$ and 20% of dimeric ions. In this case, however, it is not impossible that the 80% includes a relatively high concentration of $[Fe(H_2O)_5OH]^{2+}$ and $[Fe(H_2O)_4(OH)_2]^+$ ions which contribute to the magnetic susceptibility in the same measure as the $Fe(H_2O)_6^{3+}$ ions. These three types of ions will be considered in the analysis of the observed quadrupole splitting. In the case of ^{57}Fe the quadrupole splitting 2ε can be expressed as [13]

$$2\varepsilon = e^2 Qq \left[\left(1 + \frac{1}{3} \eta^2 \right) \right]^{1/2} ,$$

where Q is the quadrupole moment of the nucleus, e is the electronic charge, q is the field gradient and η is the asymmetry parameter.

$$q = \frac{V_{zz}}{e}$$

with V_{zz} given as in [14]

$$V_{zz} = \sum_i Z_i \frac{3z_i^2 - r_i^2}{r_i^5} ,$$

z_i is the co-ordinate of the Z_i-th charge, r_i is the radius vector of the i-th charge. With this formula, it is possible to evaluate the quadrupole splitting if *e.g.* the OH^- group is regarded as a point charge in the first co-ordination sphere. For a reasonable distance of 2.2 Å between the ferric ion and its first neighbours, with $Q = 0.28$ barn [13], and the Sternheimer factor $(1-\gamma_\infty) = 9.14$ [15], the predicted values of 2ε are 0.8 mm/sec for one OH^- group in the octahedron, 1.6 mm/sec for two OH^- groups in opposite vertices of the octahedron, and 0.8 mm/sec for two OH^- groups in adjacent positions. η is zero in every case. The values differ only by a factor of 2, thus a factor of 4 cannot be accounted for by this simple picture.

The measured $2\varepsilon = 0.66$ mm/sec (see Figs 2c and 2d) can be attributed to the dimeric (or polymeric) molecules present. This value of 2ε agrees with that measured for precipitated ferric hydroxide gels. Consequently, the microstructure of polymeric ions does not seem to change appreciably upon coagulation.

Magnetic splitting

The internal magnetic field evaluated from the two extreme lines was found to be 580 kOe in the solidified solution of pH 0.40, containing monomeric ions. Both the shape of the spectrum and the value of the internal magnetic field agree with those obtained in the Mössbauer effect measurement performed by NOZIK and KAPLAN [16] on $FeCl_3$ solutions of low pH. The hyperfine splitting can be attributed to the increase in the spin-spin relaxation time at low concentrations of the paramagnetic component [17]. Under the action of the crystal field, the $^6S_{5/2}$ state may split into three Kramer doublets characterized by $S_z = \pm 5/2, \pm 3/2$ and $\pm 1/2$. In this case the two outer lines in the measured spectra (Fig. 2a) would reflect the hyperfine interaction of the $S_z = 5/2$ state, the lines 2 and 5 that of $\pm 3/2$, while the central complex part of the spectrum could be caused simultaneously by all three states. The two outer lines reflecting the internal magnetic field of 580 kOe appear even for samples with higher pH (pH = 1.40 and 1.45 in Figs 3a and 2b). This is consistent with earlier observations indicating that monomeric ions are present at higher pH values, too. At pH > 2 the spectra have an entirely different hyperfine structure. The value of internal magnetic field decreases to 480 kOe and, though slightly, it varies with the temperature within the covered range. As the temperature rises, the intensity of the central paramagnetic lines gradually increases. This phenomenon is very similar to that observed in the Mössbauer spectra of very fine-grained superparamagnetic Fe_2O_3 [18] and ferric oxyhydroxide [19] samples. Such small ferric oxyhydroxide particles may have been present in the experimental solutions at high pH values. This suggests that not only dimeric but polymeric molecules, containing a large number of ferric ions, do exist.

The spin values of the ferric ions in the polymeric molecule can be estimated from the magnetic hyperfine structure of the Mössbauer spectrum. The calculations of WATSON and FREEMAN [20] show that in the case of a 3 d^5 electron configuration the electron spin, $S = 1/2$, corresponds to an internal magnetic field of 125 kOe. This would give $S > 3/2$ for the measured 480 kOe. The spin values of the polymeric molecules obviously cannot be inferred from the present measurements, but it is reasonable to assume that a fraction of the *d*-electron spins of the ferric ions have anti-parallel orientation in the polymeric molecules. The orientation is affected by the variation of chain length, too.

Effect of heating before freezing

The preheating of solution leads to appreciable changes in the Mössbauer spectra. Lines appearing normally only at higher pH values (sample with pH = 1.40, Fig. 3) could be detected. The intensity ratio of magnetically split

and unsplit hyperfine lines in samples with pH = 2 and above, increases as a result of preheating. The relative intensity of the magnetically split lines did not change even after keeping the sample for a long time at room temperature (Fig. 4). The 1 : 1 intensity ratio obtained on preheating could be observed even at 77 °K, *i.e.* at a temperature where, as a rule, no magnetic splitting appears in the spectra taken immediately after the adjustment of pH. This fact suggests that the magnetic structure cannot be attributed exclusively to the increased length of the polymeric chains, but may be influenced also by magnetic ordering with increasing temperature.

It has been shown by OOSTERHOUT [21] that the magnetic structure of the polymeric ions may change with the standing time of the solution. It was observed by this author that the almost normal paramagnetic susceptibility measured on rapidly precipitated ferric hydroxide at temperatures from 80 °K to 300 °K becomes very low if the solution is left standing for a long time at room temperature before precipitation of the ferric hydroxide. This observation is fully confirmed by our data discussed above.

Conclusions

It remains to be seen to what extent the ionic equilibrium is modified during the freezing of ferric perchlorate solutions at different pH values. In addition to the thermal effect, the local variations in solute concentration during the relatively slow cooling may also be important.

The experiments described above show that the Mössbauer data reflect the pH-dependent formation of ions with different structures in ferric perchlorate solutions, as observed earlier by other methods. It was also observed that hydrolysis is enhanced at higher temperatures. The smaller distance between the ferric ions in the polymeric chains seems to lead to magnetic exchange interactions. The decrease in the magnetic moment per ion can be attributed primarily to the ordering of spins. Further information about the nature of the intramolecular magnetic interactions could be obtained from the study of exchange interactions in chains of restricted (specifically, dimeric) length.

REFERENCES

1. BOSE, A.: Proc. Ind. Acad. Sci. **A1**, 754 (1934)
2. AUMERAS, M., MOUNIC, M.: Bull. Soc. Chim. France **4**, 523, 536 (1937)
3. CHEVALIER, R., MATHIEU, S.: Compt. rend. **206**, 1955 (1938)
4. HEDSTRÖM, B. O. A.: Ark. Kemi. **6**, 1 (1953)
5. MULAY, L. N., SELWOOD, P. W.: J. Am. Chem. Soc. **77**, 2693 (1955)
6. SCHUGAR, H., WALLING, C., JONES, R. B., GRAY, H. B.: J. Am. Chem. Soc. **89**, 3712 (1967)
7. SPIRO, T. G., ALLERTON, S. A., RENNER, J., TERZIS, A., BILS, R., SALTMAN, P.: J. Am. Chem. Soc. **88**, 2721 (1966)
8. DÉZSI, I., KESZTHELYI, L., MOLNÁR, B., PÓCS, L.: Report, Central Research Institute for Physics, 9/1967

9. Dézsi, I., Vértes, A., Komor, M.: Inorg. Nucl. Chem. Letters **4,** 649 (1968)
10. Dézsi, I., Gorobchenko, V. D., Lukashevich, I. I., Vértes, A.: Chem. Phys. Letters **2,** 665 (1968)
11. Muir, A. H., Ando, K. J., Coogan, H. M.: Mössbauer Effect Data Index 1958—1965, p. 26. Interscience Publishers, New York, 1966
12. Walker, L. R., Wertheim, G. K., Jaccarino, V.: Phys. Rev. Letters **6,** 98 (1961)
13. Ingalls, R.: Phys. Rev. **133,** A787 (1964)
14. Bersohn, R.: J. Chem. Phys. **29,** 326 (1958)
15. Sternheimer, R. M.: Phys. Rev. **130,** 1423 (1963)
16. Nozik, A. J., Kaplan, M.: Yale University (U.S.A.). Report 3219-19, 1968
17. Wertheim, G. K., Remeika, J. P.: Phys. Letters **10,** 14 (1964)
18. Kündig, W., Bömmel, H., Gonstabaris, G., Lindquist, R. H.: Phys. Rev. **142,** 327 (1966)
19. Shinjo, T.: J. Phys. Soc. Japan **21,** 917 (1966)
20. Watson, R. E., Freeman, A. J.: Phys. Rev. **123,** 2027 (1961)
21. Oosterhout, G. W. v.: in Proceedings of the International Conference on Magnetism, p. 529. Nottingham 1964. Edited by The Institute of Physics and Physical Society, London

István Dézsi; Budapest XII., Konkoly Thege M. út
V. D. Gorobchenko; Kurchatov Atomic Energy Institute Moscow, USSR
Mária Ranogajec-Komor; Budapest VIII., Puskin u. 11—13.
I. I. Lukashevich; Kurchatov Atomic Energy Institute Moscow, USSR
Attila Vértes; Budapest VIII., Puskin u. 11—13.
K. F. Tsitskishvili; Kurchatov Atomic Energy Institute, Moscow, USSR

Acta Chimica Academiae Scientiarum Hungaricae, Tomus 70 (4), pp. 343–354 (1971)

ÉTUDE DES PROPRIÉTÉS CHIMIQUES ET ÉLECTROCHIMIQUES DES INDICATEURS D'OXYDORÉDUCTION FONCTIONNANT EN MILIEUX NON-AQUEUX, I

GÉNÉRALITÉS ET CAS DE LA PERSANTINE

L. LADÁNYI

(Institut de Chimie Anorganique et Analytique de l'Université L. Eötvös, Budapest)

Reçu le 10 juillet 1970

L'oxydation électrochimique de la Persantine dans l'acétonitrile neutre non-tamponné se fait en deux étapes monoélectroniques parfaitement reversibles ($P \rightleftarrows R^{+\cdot} + e$; $R^{+\cdot} \rightleftarrows Q^{++} + e$. $R^{+\cdot}$ et Q^{++} mono et dications sont des espèces oxydées stables; P est le produit de départ).

Les différences d'absorptions de P et $R^{+\cdot}$ permettent d'utiliser ce système oxydoréducteur rapide comme indicateur d'oxydo-réduction dans le milieu décrit.

A la base de ce modèle, chaque système oxydoréducteur à deux électrons, s'oxydant (ou se réduisant) en deux étapes monoélectroniques et ayant

(1) des propriétés électrochimiques semblables à celles de la Persantine

(2) des couleurs visiblement différentes pour la forme réduite (ou oxydée) et le radical

(3) une stabilité suffisante pour l'espèce oxydée (ou réduite) à un électron

peut être considéré, comme indicateur d'oxydoréduction réversible dans le milieu étudié.

Des systèmes ayant de telles propriétés ont été déjà décrits. Parmi eux, on peut citer les familles de bases suivantes:

Phénothiazine, 5,10-dihydro-Phénazine, N,N,N′,N′-Tétraméthylbenzidine, 2,2′-Dipyridile, 4,4′-Dipyridile, Benzoxazole, Benzthiazole et Benzdithiole.

Introduction

L'application analytique des titrages d'oxydoréduction en milieu non-aqueux a débuté il y a quelque vingt ans et il est encore difficile de prévoir le rôle et l'importance de telles méthodes dans l'avenir. Toujours est-il, que l'exploitation des possibilités théoriques offertes par les solvants n'a été jusqu'ici réalisée, que dans le cas des réactions acides–bases et en conséquence, on peut s'attendre à un développement considérable de l'oxydimétrie en milieu non-aqueux [1].

Un autre fait, venant à l'appui de cette constatation, c'est l'existence des domaines d'électroactivité très étendus de quelques solvants aprotiques (Acétonitrile, Nitrométhane, Diméthylformamide, etc.). Dans l'acétonitrile p.e., les réactions électrochimiques peuvent s'effectuer entre $+2{,}2$ et $-3{,}5$ volts (par rapport à l'électrode de référence Ag/Ag^+ $10^{-2}M$) sur l'électrode tournante de platine poli et les limitations par le milieu sont dues à l'oxydation et à la réduction de l'électrolyte de base ($LiClO_4$) et non pas au solvant lui-

même [2] (autrement dit, dans le solvant exempt de $LiClO_4$ on peut aller vers les milieux encore plus oxydants ou plus réducteurs).

Pour indiquer le point équivalent des titrages de ce genre, on utilise surtout des méthodes électrochimiques (telles que la potentiométrie, l'ampérométrie) et parfois seulement des indicateurs colorés d'oxydoréduction.

Cela s'explique par le fait, que les indicateurs de ce type, fonctionnant dans les solvants sont peu nombreux. Le quinalizarine [3] (1,2,5,8-tetrahydroxyanthraquinone) et la NN'-bis (*p,p'*-dimethoxy)-diphenylamine [4] ont été les premiers utilisés dans l'acide acétique. RAO et MURTHY [5] ont montré, que dans l'acétonitrile, le Ferroine et la Diphénylamine fonctionnent reversiblement; le virage du Vert de Janus et celui du Rouge de Méthyl, bien qu'ils s'utilisent dans certains cas, est irreversible; enfin la Phénosafranine et le Rouge Neutre ne peuvent être appliqués du tout.

KRAUSZ et ENDRŐI-HAVAS [6] ont récemment récommendé quelques nouveaux indicateurs dans la famille de base de l'aminoanthraquinone, fonctionnant dans l'acide acétique. Ils sont reversibles.

Signalons, que le mécanisme de virage de tous ces indicateurs n'est pas discuté dans ces travaux.

Dans un précédent mémoire [7], (Lettre à la Rédaction) en décrivant un nouvel indicateur d'oxydoréduction reversible (la Persantine), nous nous sommes proposé d'étudier systématiquement les mécanismes de virage des indicateurs colorés d'oxydoréduction. La présente étude se compose de la description détaillée de nos travaux relatifs à la Persantine et a pour but de tirer quelques conclusions générales, valables pour un groupe particulier des indicateurs d'oxydoréduction.

Cas de la Persantine

1. Oxydation chimique de la Persantine dans l'eau

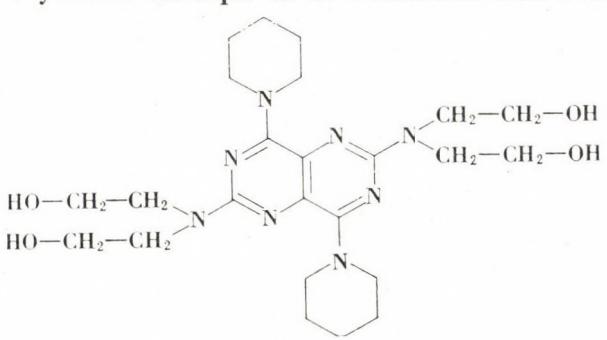

Persantine

(Dipiperidino-4,8-pyrimido-5,4 D-pyrimidine-diyl, -2,6-diimino- 2,2′2″2‴-tetraéthanol.)

La Persantine s'oxyde dans l'eau en milieu acide sous l'action d'oxydants chimiques tels que le bromate et le permanganate de potassium par perte de

deux électrons [8]. Au cours de cette oxydation un composé rouge se forme intermédiairement, dont la durée de vie n'est que de quelques secondes. A la base de cette réaction, la Persantine peut être utilisée comme indicateur d'oxydoréduction en Bromoatométrie et en Ferricioanométrie, bien que son virage ne soit par reversible [9].

Nous avons décidé d'étudier cette oxydation en milieu aprotique, afin de préciser la nature du produit intermédiaire et le mécanisme du virage.

2. L'oxydation électrochimique de la Persantine dans l'acétonitrile

L'oxydation électrochimique de la Persantine a été étudiée au sein de l'acétonitrile soigneusement déshydraté ($C_{H_2O} < 10^{-3} M$). Le solvant a été rendu conducteur par du perchlorate de Lithium $10^{-1} M$ et les potentiels sont répérés par rapport à l'électrode de comparaison Ag/Ag^+ 10^{-2} M fonctionnant dans l'acétonitrile [10]. L'électrode indicatrice est l'électrode tournante à disque de platine poli.

a) La courbe voltampérométrique de la Persantine

On constate, que dans le milieu précédemment défini, la Persantine présente deux vagues d'oxydation à une électrode de platine poli (fig. 1, courbe 1). Les potentiels de demi-vague $E_{1/2}$ I et $E_{1/2}$ II, se situent respectivement à

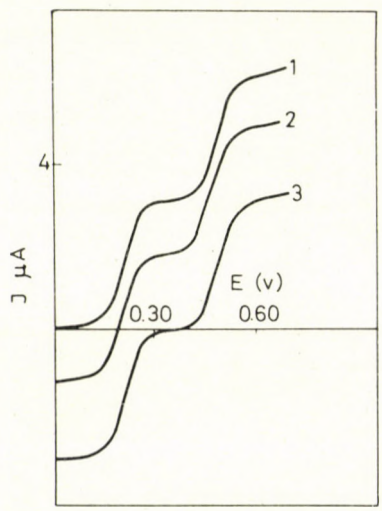

Fig. 1. Modification de la courbe intensité–potentiel au cours de l'oxydation à potentiel contrôlé sur la première vague. Concentration en Persantine: 4.10^{-4} M; Courbe 1: Persantine seule en solution; Courbe 2: 1/2 (env.) de la Persantine est oxydée en $R^{+\cdot}$; Courbe 3: Toute la Persantine est oxydée en $R^{+\cdot}$

+0,220 et +0,470 V par rapport à l'électrode de référence. La hauteur des paliers est reproductible à mieux que 1% et l'on constate, que les deux vagues ont sensiblement la même hauteur.

Le critère de LEVICH [11] nous a permis de vérifier, que les courants limits des vagues sont contrôlés par la seule diffusion.

Pour les deux vagues, les courbes représentant le potentiel en fonction du logarithme du rapport i/i_{max}-i sont des droites de pente 0,060 et 0,059 V/unité logarithmique respectivement; résultat, que laisse penser, que l'échange d'électron correspondant est une réaction rapide. Ces résultats indiquent, que la Persantine est oxydée à l'électrode en deux étapes qui correspondent chacune au départ d'un électron, ce que traduit le schéma suivant:

$$P \longrightarrow R^{+\cdot} + e \qquad R^{+\cdot} \longrightarrow Q^{++} + e$$

1ère étape 2ème étape

dans lequel P représente la Persantine, $R^{+\cdot}$ le produit oxydé intermédiaire et Q^{++} le produit le plus oxydé.

b) Oxydation à potentiel contrôlé sur la première vague

Il est possible de réaliser de façon sélective et quantitative la transformation par électrolyse de P en $R^{+\cdot}$. Il suffit pour cela d'appliquer à une électrode de platine de grande surface un potentiel compris entre $E_{1/2}$ I et $E_{1/2}$ II, par exemple +300 mV par rapport à l'électrode de réference (fig. 1).

On constate donc, que la courbe se déplace parallèlement à l'axe des intensités sans subir de déformation appréciable. Ceci signifie, que la transformation en radical cation résultant du départ d'un électron est pratiquement la seule réaction se produisant dans l'opération.

On observe en effet au dessous de l'axe des potentiels la courbe de réduction de ce radical cation en Persantine (courbe 3). La position relative de cette courbe et de celle qui correspond à l'oxydation du produit de départ non encore transformé montre, que ce radical se réduit au potentiel auquel, précisement s'oxydait le produit de départ. L'ensemble $P/R^{+\cdot}$ constitue donc un système oxydoréducteur rapide [8].

Dès la fermeture de circuit d'électrolyse, la solution de Persantine primitivement verte et fluorescente devient plus foncée et n'émet plus de lumière. Après quelques minutes, elle vire au violet et à mesure que l'oxydation s'effectue, la coloration violette de la solution s'intensifie.

Lorsque toute la Persantine est oxydée en $R^{+\cdot}$, le courant d'électrolyse tend vers zéro (fig. 1, courbe 3). La coulométrie à potentiel contrôlé indique en même temps, que le nombre d'électrons mis en jeu égale à 1. (Résultats de quelques expériences: $n = 0{,}94$, $n = 0{,}96$.)

c) Oxydation à potentiel contrôlé sur la deuxième vague

On peut poursuivre l'oxydation électrochimique au second stade, c'est à dire transformer $R^{+\cdot}$ en Q^{++} en imposant cette fois à l'électrode de platine de grande surface un potentiel supérieur à $E_{1/2}$ II (+600 mV par rapport à l'électrode de référence). La solution devient de plus en plus foncée et les courbes intensité-potentiels sont modifiées comme le montre le figure 2.

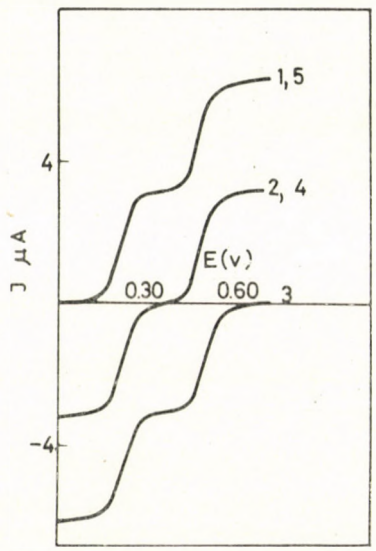

Fig. 2. Modification des courbes voltampérométriques au cours de l'oxydation à potentiel contrôlé sur la deuxième vague. Courbe 1: P seul en solution; Courbe 2: P est entièrement oxidée en $R^{+\cdot}$; Courbe 3: Q^{++} seul en solution; Courbe 4: Réduction complète de Q^{++} en $R^{+\cdot}$ (à + 0,300 Volt); Courbe 5: $R^{+\cdot}$ est réduit en P (à 0,00 Volt)

Ces résultats s'interprètent bien de la façon suivante: $R^{+\cdot}$ peut aussi bien être oxydé en perdant un second électron (courbe 3) pour donner Q^{++} ou réduit en captant un électron pour régénerer P. Q^{++} à son tour, est susceptible d'être réduit en $R^{+\cdot}$ (courbe 4) puis en P (courbe 5). Les deux systèmes $P/R^{+\cdot}$ et $R^{+\cdot}/Q^{++}$ sont rapides [12].

La coulométrie effectuée au cours de l'électrolyse sur la deuxième vague confirme l'échange d'un seul électron.

Si l'acétonitrile n'est pas assez déshydraté ($C_{H_2O} > 5 \cdot 10^{-3}$ M/L) $R^{+\cdot}$ peut se décomposer et dans ce cas-là, une nouvelle vague, relative à l'oxydation du produit de décomposition se présente vers +0,60 V, aux dépens des vagues précédemment décrites ($E_{1/2} = 0{,}65$ V).

Afin d'approfondir ce phénomène, nous avons laissé évoluer la solution du radical $R^{+\cdot}$, l'ayant obtenu de la Persantine par oxydation à potentiel contrôlé.

Après 48 heures, la solution primitivement rouge-violacée devient jaune, sans que sa fluorescence ait été rétablie. Le potentiel de demi vague du composé ainsi formé est voisin de 0,65 V. Il s'agit vraisemblablement d'une réaction d'oxydoréduction du radical $R^{+\cdot}$ sur l'eau résiduelle [13], dont le bilan global s'écrit

$$2R^{+\cdot} + H_2O \rightarrow 2PH^+ + 1/2\ O_2 \uparrow$$

Cette hypothèse est en accord avec le fait, que le produit de décomposition et la Persantine salifiée ($C_{H^+} = C_P$) s'oxydent au même potentiel ($E_{1/2} = 0{,}65$ Volt; voir encore plus loin).

d) Action d'un acide fort sur l'oxydation électrochimique de la Persantine

Lors de l'addition progressive de l'acide perchlorique à la solution de Persantine dans l'acétonitrile, on peut observer la modification des courbes intensité-potentiel comme l'indique la figure 3.

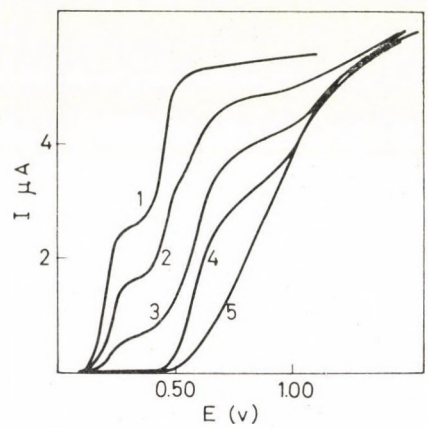

Fig. 3. Action de l'acidité de la solution sur les vagues d'oxydation de la Persantine. Concentration en Persantine: $7{,}5 \cdot 10^{-4}$ *M*. Courbe 1: Persantine seule en solution; Courbe 2: $C_{HClO_4} = 2{,}5 \cdot 10^{-4}$; Courbe 3: $C_{HClO_4} = 5 \cdot 10^{-4}$; Courbe 4: $C_{HClO_4} = 7{,}5 \cdot 10^{-4}$; Courbe 5: $C_{HClO_4} = 1{,}5 \cdot 10^{-3}$

Dans le cas des courbes 1, 2, et 3, la Persantine est en excés par rapport à l'acide ajouté et l'oxydation de la base non protonnée reste inchangée, tandis que la Persantine salifiée s'oxyde à un potentiel supérieur à celui qui, correspond à l'oxydation de P en $R^{+\cdot}$. Dans le cas de la courbe 4, il n'y a plus de base non protonnée et si on augmente encore l'acidité, l'oxydation s'effectuera directement à deux électrons (courbe 5).

e) Action d'une base forte sur l'oxydation électrochimique de la Persantine

En milieu basique (diphénylguanidine), la première vague voltampérométrique reste inchangée. La seconde vague n'apparaît, que lorsque la vitesse de balayage du potentiel est assez grande (20 mV/s). Dans le cas contraire (2 mV/s), l'intensité décroît brusquement, dès que la seconde vague commence à s'amorcer. Il paraît vraisemblable, qu'un produit d'oxydation insoluble provenant de la diphénylguanidine se dépose à la surface de l'électrode et empêche la réaction électrochimique de se poursuivre.

f) Oxydation à intensité imposée

Le potentiel normal apparent du système $R^{+\cdot}/Q^{++}$ étant très supérieur au potentiel normal du système $P/R^{+\cdot}$ (le potentiel de demi-vague d'un système oxydoréducteur rapide peut être assimilé au potentiel normal apparent de ce système [8]), la réaction chimique $P + Q^{++} = 2R^{+\cdot}$ doit avoir lieu chaque fois, que P et Q^{++} sont en présence. Si cette réaction chimique est instantanée, on pourra effectuer un titrage coulométrique à intensité constante comme BADOZ-LAMBLING et STOJKOVIČ l'ont décrit dans le cas de la Phénotiazine [14].

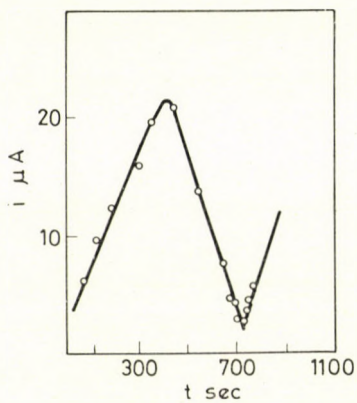

Fig. 4. Titrage coulométrique de la Persantine à intensité constante. Détermination du point équivalent par ampérométrie avec deux électrodes indicatrices. $E_a - E_c = 50$ mV. Concentration en P: $5{,}7 \cdot 10^{-4}$ M (11,40 mg P/40 ml CH_3CN). Intensité: 3,00 mA; Durée de l'électrolyse: temps calculé: 726,60 sec., temps mesuré: 720,12 sec

Au cours du titrage, on réalise l'oxydation d'une solution de Persantine avec une intensité i_0 inférieure à l'intensité limite de la première vagu et on obtient le radical $R^{+\cdot}$ avec 100% de rendement soit par la réaction directe

$$P - e \rightarrow R^{+\cdot} \tag{1}$$

soit par l'ensemble des réactions

$$R^{+\cdot} - e = Q^{++} \tag{2}$$

$$\frac{Q^{++} + P = 2R^{+\cdot}}{P - e = R^{+\cdot}} \tag{3}$$

Lorsque la dernière trace de Persantine a disparu, la réaction $R^{+\cdot} \rightarrow Q^{++} + e$ n'est plus accompagnée de la réaction chimique (3) et le produit le plus oxydé (Q^{++}) apparaît dans la solution. Le titrage est terminé; la quantité d'électricité $Q = i_0 t$ consommée pendant la durée t de l'électrolyse permet de

déterminer la quantité de Persantine de la solution. On peut indiquer le point équivalent par les méthodes électrochimiques indicatrices classiques (potentiométrie et ampérométrie).

Nous avons représenté sur la figure 4 la courbe de titrage ampérométrique de la Persantine.

Ce titrage lui-même a un intérêt pratique, mais du point de vue de l'utilisation de la Persantine comme indicateur d'oxydoréduction, c'est la réaction chimique $P + Q^{++} = 2R^{+\cdot}$, qui est très importante (voir encore plus loin).

3. Résonance paramagnétique électronique

L'obtention d'un spectre de résonance paramagnétique électronique au cours de l'oxydation de la Persantine sur la première vague de sa courbe intensité–potentiel (fig. 5) est chose facile à condition d'utiliser une cellule d'électroyse dans laquelle l'anolyte circule dans la cavité résonnante du spectromètre 15] sous l'action d'un courant d'azote pur, qui est également destiné à désoxy-[éner la solution.

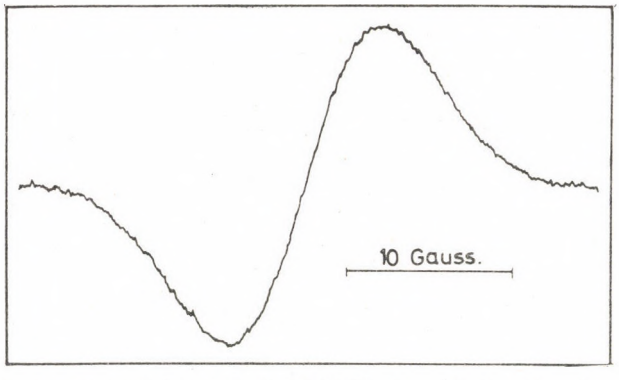

Fig. 5. Dérivée du spectre expérimentale de R. P. E. du radical cation obtenu par oxydation électrochimique de la Persantine au sein de l'acétonitrile

Le spectre obtenu confirme la nature radicalaire du produit $R^{+\cdot}$, bien qu'aucune structure hyperfine n'a pu être décélée en dépit de diverses modifications des conditions opératoires. Cela est sans doute la conséquence du couplage de l'électron non apparié avec un trés grand nombre de protons.

4. Spectroscopie d'absorption ultraviolette et visible

Les différences d'absorptions des produits d'oxydation permettent de suivre l'électrolyse par spectrophotométrie. Les courbes obtenus sont présentés à la figure 6.

Le faisceau de courbes présente deux points isobestiques bien définies (aux 42300 et 31000 cm^{-1}) en confirmant qu'il s'agit de deux transformations simples.

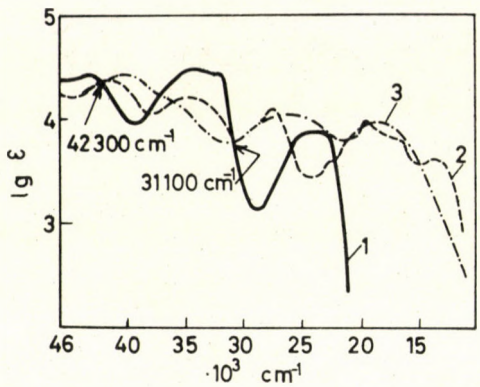

Fig. 6. Déformation du spectre d'absorption ultraviolette et visible d'une solution de la Persantine $3{,}1 \cdot 10^{-4}$ *M* dans l'acétonitrile 0.1 *M* en $LiClO_4$ au cours de l'oxydation à + 0,300, puis à + 0,600 V. Courbe 1: Persantine (*P*) seule en solution; Courbe 2: Radical ($R^{+\cdot}$) seul en solution; Courbe 3: Cation divalent (Q^{++}) seul en solution

5. Utilisation de la Persantine comme indicateur d'oxydoréduction reversible dans l'acétonitrile

Compte tenu des valeurs respectives des potentiels normaux de la Persantine et du couple Cu(I)/Cu(II), dans l'acétonitrile [11], il est possible d'utiliser la Persantine comme indicateur coloré pour les titrages rédox par le cuivre cuivrique. La méthode s'applique au dosage, décrit par ailleurs, de la thioürée par la perchlorate cuivrique dans l'acétonitrile [16], dont le bilan global s'écrit

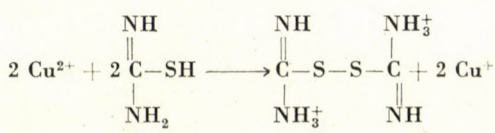

Nos expériences préliminaires ont montré, que 5 ml de la solution de Persantine de $4 \cdot 10^{-5}$ *M* (env.) dans l'acétonitrile, en y ajoutant 0,01 ml (env.) d'une solution de Cu(II) de 0,05 *M* dans l'acétonitrile vire au violet et la solution résultant de cette opération revire au jaune après avoir ajouté une goutte (0,01 ml env.) de la solution de thioürée de 0,05 *M* dans l'acétonitrile.

Ces virages peuvent être effectués plusieurs fois avec la même solution de Persantine.

Les résultats de quelques titrages sont rassemblés dans le tableau suivant:

Tableau I

Titrage volumétrique de la thioürée par le cuivre(II) dans l'acétonitrile
Indicateur: 0,05 ml solution de Persantine 4×10^{-3} *M* dans l'acétonitrile

Solution de thioürée 0,051 *M* à doser (ml)	Solution titrée de perchlorate cuivrique 0,089 *M*		Erreur (en %)
	Consommée (ml)	Théoriquement équivalente	
1,00	0,580		+1,2
	0,560	0.573	−2,3
	0,580		+1,2
3,00	1,700		−0,6
	1,720	1,719	±0,0
	1,730		+0,6
6,00	3,45		+0,3
	3,45	3,438	+0,3
	3,43		−0,3
10,00	5,75		+0,3
	5,72	5,730	−0,2
	5,74		+0,1

Discussion

Les propriétés chimiques et électrochimiques de la Persantine mettent en évidence le mécanisme et la réversibilité de son virage.

La Persantine possède en milieu neutre et basique deux potentiels de virage ($E_1^\circ = E_{1/2}$ I et $E_2^\circ = E_{1/2}$ II), correspondant respectivement aux potentiels normaux apparents des systèmes $P/R^{+\cdot}$ et $R^{+\cdot}/Q^{++}$.

La couleur de $R^{+\cdot}$ et celle de Q^{++} ne pouvant être differenciées à l'œil nu, pratiquement un seul virage est à considérer au potentiel E_1°. L'équilibre ci-dessous

$$P + Q^{++} \rightleftharpoons 2R^{+\cdot}$$

— selon le chapitre *f* — étant très déplacé à droite $\left(\log K = \dfrac{\Delta E^\circ}{0{,}060} = 4{,}0\right)$, les deux systèmes oxydoréducteur $P/R^{+\cdot}$ et $R^{+\cdot}/Q^{++}$ ne peuvent coexister. Autrement dit, le seul virage s'effectue en effet au voisinage de E_1°. Si la couleur de Q^{++} était visiblement différente de celle de $R^{+\cdot}$, un deuxième virage pourrait s'effectuer à E_2°.

Les titrages d'oxydoréduction réalisés dans les solvants n'exigent pas en général l'acidification du milieu [17], car les réducteurs à doser sont susceptibles d'être oxydés même en milieu neutre. C'est pourquoi nous n'avons pas tracé la fonction E_1°—pH et nous nous sommes contentés de la description qualitative du comportement de l'indicateur en milieu acide (voir le chapitre *e*).

Conclusions générales

A la base des expériences précédemment décrites, chaque système oxydoréducteur à deux électrons, s'oxydant (se réduisant) en deux étape monoélectronique et ayant:

1° des propriétés électrochimiques semblables à celles de la Persantine,

2° des couleurs visiblement différentes pour la forme réduite (ou oxydée) et le radical,

3° une stabilité suffisante pour l'espèce oxydée (ou réduite) à un électron peut être considéré comme indicateur d'oxydoréduction réversible en milieu organique.

S'il en est ainsi, connaissant les propriétés chimiques et électrochimiques d'un système oxydoréducteur quelconque, on peut prévoir la possibilité de son application éventuelle, ainsi que la réversibilité du virage, en l'utilisant comme indicateur d'oxydoréduction.

Des systèmes ayant de telles propriétés ont été déjà décrits. Parmi eux on peut citer la Phénothiazine et quelques-uns de ses dérivés [18], ainsi que ceux de la 5,10-dihydro-Phénazine [19] et la N,N,N',N'-tétraméthylbenzidine [20]. Ils peuvent être considérés comme indicateurs d'oxydoréduction réversible en milieu aprotique.

Partie expérimentale

1. Électrochimie

Le montage électrochimique et la purification du solvant ont été déjà décrit par ailleurs [21], ainsi que le dispositif [15] permettant de préparer au sein de la cavité résonnante d'un pectromètre un radical, dont on veut enregistrer le spectre de RPE.

2. Spectrophotométrie. Résonance paramagnétique électronique

Le spectrophotomètre enregistreur UNICAM SP 700 a été utilisé. Les spectres de RPE ont été obtenus à l'aide d'un spectromètre VARIAN V-4502.

3. Réactifs

Acétonitrile, Diphenylguanidine, Thioürée pro analysi (PROLABO) Perchlorate de Lithium anhydre (Frederick Smith Co.) ont été utilisés. L'échantillon de Persantine nous a été aimablement fourni par la "Société Boehringer und Sohn" (Ingelheim am Rhein, Allemagne Fédérale). Nous lui adressons nos très sincères remerciements. Nous remercions également MM. G. CAUQUIS et M. GENIÉS (Laboratoire de Chimie Organique Physique II du CEA de Grenoble) pour le tracer des spectres de R. P. E., ainsi que Mme J. BADOZ-LAMBLING, MM. GÉRARD FAUVELOT et Jean-Claude MARCHON (Laboratoire de Chimie Analytique de l'ESPCI de Paris) pour l'intérêt, qu'ils ont porté à ce travail.

REFERENCES

1. GYENES, I.: Titration in non aqueous solvents, Akadémiai Kiadó, Budapest, 1967
2. POPOV, A. I., GESKE, D. H.: J. Am. Chem. Soc. **79**, 2074 (1957)
3. TOMIČEK, O., WALCHA, J.: Coll. Czech. Chem. Commun. **16**, 113 (1951)
4. ERDEY, L., MEISEL, T., RÁDI, GY.: Acta Chim. Acad. Sci. Hung. **26**, 71 (1961)
5. PRABHAKER RAO, G., VASUDEVA MURTHY, A. R.: Z. Anal. Chem. **180**, 169 (1961)
6. KRAUSZ, I., ENDRŐI-HAVAS, Á.: SAC Congress, Nottingham, 1965
7. LADÁNYI, L., FAUVELOT, G., MARCHON, J. C., BADOZ-LAMBLING, J.: Bull. Soc. Chim. 1848 (1967)
8. BALKAY, A. M., TAKÁCSI-NAGY, G.: Acta Pharm. Hung. **19**, 14 (1964)
9. LADÁNYI, L.: Résultats non publiés
10. PLESKOV, V. A.: J. Phys. Chem. (USSR) **22**, 3351 (1948)
11. LEVICH, S.: Acta Physicochemica (USSR) **17**, 257 (1942)
12. CHARLOT, G., BADOZ-LAMBLING, J., TRÉMILLON, B.: Les Réactions Electrochimiques. Masson et Cie, Paris, 1959
13. CAUQUIS, G., GENIÉS, M.: Bull. Soc. Chim. 3220 (1967)
14. BADOZ-LAMBLING, J., STOJKOVIČ, D.: Bull. Soc. Chim. 2709 (1963)
15. BARRY, G., CAUQUIS, G., MAUREY, M.: Bull. Soc. Chim. 2510 (1966)
16. KRATOCHVIL, B., ZATKO, D. A., MARKUSZEWSKI, R.: Anal. Chem. **38**, 770 (1966)
17. PRABHAKAR, RAO, G., VASUDEVA MURTHY A. R.: J. Phys. Chem. **68**, 1573 (1964)
18. BILLON, J. P.: Ann. Chim. **7**, 183 (1962)
19. NELSON, R. F., LEDDY, D. W., SEO, E. T., ADAMS, R. N.: Z. anal. Chem. **224**, 184 (1967)
20. SAGET, J. P., PLICHON, V.: Bull. Soc. Chim. (1969) 1395
21. BILLON, J. P.: J. Electroanal. Chem. **1**, 486 (1960)

László LADÁNYI; Budapest VIII., Múzeum krt. 4/b.

Acta Chimica Academiae Scientiarum Hungaricae, Tomus 70 (4), pp. 355—368 (1971)

NEW NITROCHALCONES, XI

CONTRIBUTION TO THE STEREOCHEMISTRY OF SOME NITROHYDROXYCHALCONES

P. SOHÁR, T. SZÉLL* and T. DUDÁS*

*(Research Institute for Pharmaceutical Chemistry, Budapest and *Department of Applied Chemistry, A. József University, Szeged)*

Received October 20, 1970

It has been established by IR and NMR spectroscopic investigation of some nitrohydroxychalcones prepared under various reaction conditions that, regardless of the synthetic conditions, stereochemically homogeneous *trans* isomers are formed in all cases.

Introduction

The *cis-trans* isomerization of chalcones is dealt with extensively in the literature but relatively few statements can be generalized.

LUTZ *et al.* [1—5], IKEDA [6—8] and others [9—12] have reported that, upon irradiation with sunlight or a mercury vapour lamp, chalcones undergo isomerization leading to a photo-equilibrium. The *cis* isomer was in most cases predominant. The formation of the latter was also favoured by cooling with dry ice while on heating the *trans* isomer was formed. MIQUEL found that the *trans* isomer crystallized from dilute solutions while the *cis* isomer crystallized from concentrated solutions, and irradiation was without effect [13]. According to other authors [14], it was the *cis* isomer that crystallized from dilute solutions.

NOYCE *et al.* carried out *cis* to *trans* isomerization in aqueous dioxan with sulfuric acid and studied the mechanism of isomerization [15—18]. The authors have established that the rate of the reaction occurring *via* the oxonium salt varies with the acid concentration and depends on the substituents. Generally, the *cis* modifications melt at lower temperatures are weaker bases and less reactive.

Relatively little is known about the influence of synthetic conditions on the stereochemistry of the chalcones formed. The hydrolysis of 4,7-dihydroxyflavylium salts in acidic media yields *cis*-chalcones while in alkaline media [19] *cis–trans* mixtures are obtained. In the synthesis of 4-nitrochalcone carried out

Part IX: SZÉLL, T. and SOHÁR, I.: Canad., J. Chem. **47**, 1254 (1969)
Part X: SZÉLL, T. and SOHÁR, I.: Acta Chim. Acad. Sci. Hung. **62**, 429 (1969)
* Present address: United Nations International School, 418 East 54th Street, New York, N. Y. 100022, USA.

in the presence of potassium alkoxides, the *trans* isomer is formed [20]. TRAKROO and MUKHEDKAR [21—22] prepared several *cis* and *trans* nitrohydroxychalcones and found on the basis of their infrared spectra that an intramolecular hydrogen bond forms between the 2′-hydroxyl and the carbonyl group of the *trans* isomers, while in the *cis* isomers intramolecular association occurs between the 2′-hydroxyl and 3′-nitro groups.

In the present work several nitrohydroxychalcones were investigated which were prepared by various procedures to study the influence of the conditions of synthesis on the stereochemistry of the chalcones obtained. As condensing agents, aqueous ethanolic sodium hydroxide, dry hydrogen chloride and aluminium chloride were employed. The melting points of the chalcones obtained by any of these methods were practically identical. By spectroscopic examination of these compounds, it was established that *trans* isomers were obtained with all of the methods used regardless of whether or not the chalcones were recrystallized. Concerning the action of anhydrous aluminium chloride, our results are not in line with the observation of DIPPY *et al.* who have found that *trans*-chalcone and *trans*-2-chlorocinnamic acid can be converted into the *cis* isomers with aluminium chloride [23].

It is worth mentioning that from the studied chalcones, the isomeric flavanones [24, 25] can only be prepared with some difficulty.

Spectroscopic studies

The structure and ratio of *cis* and *trans* isomers in the product obtained via different reaction paths were determined by IR and NMR spectroscopy.

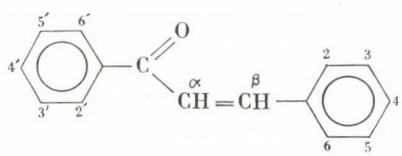

I

	4	2′	3′	4′	5′
Ia	**H**	**OH**	**H**	**H**	**NO_2**
Ib	H	H	NO_2	OH	H
Ic	**OMe**	**H**	**NO_2**	**OH**	**H**
Id	Cl	H	NO_2	OH	H

As the samples prepared in three different ways — in the cases of all the chalcones (**Ia—Id**) studied — gave identical IR and NMR spectra, the above problem was reduced to the question whether these stereochemically uniform products were *cis* or *trans* isomers.

IR spectra

The assumed structures have been confirmed by the IR spectra. The characteristic bands of the functional groups appear at the expected frequencies (Table I).

It is worth mentioning that the $\nu C{=}O$ and $\nu C{=}C$ bands have the lowest wavenumber in compound **Ia** since a continuously conjugated, intramolecular hydrogen bond system (six-membered chelate ring) is formed (**II**) with the par-

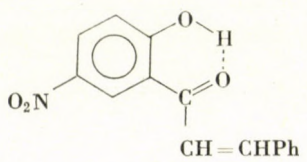

II

ticipation of the 2′-hydroxyl group. In the case of the other three compounds the $\nu C{=}O$ frequency changes depending on the electron withdrawal by the substituent in position 4 and increases in the order: **Ic**, **Id**, **Ib**.

The stretching frequency band of the 2′-hydroxyl group is extremely diffuse as a consequence of its chelation with the carbonyl group and, therefore, cannot be identified in the spectrum [26—29]. The 4′-hydroxyl group produced easily identified νOH and γOH bands [26—30] in the case of compounds **Ib**, **Ic** and **Id** as a result of the weak intramolecular hydrogen bond formed with the 3′-nitro group.

In the case of olefin, the *cis* and *trans* isomers can be distinguished by means of the out-of-plane CH deformation vibration — *i.e.* $\gamma(=CH)$ bands which appear in the range between 1000 and 675 cm^{-1} with variable intensity.

In the case of *trans* isomers, the appearance of a very intense $\gamma(=CH)$ band was expected in the IR spectrum between 980 and 960 cm^{-1}. The intensity of this band is medium with *cis* isomers; it appears generally in the interval of 730 to 675 cm^{-1} and is often split. The frequency, however, can increase up to 820 cm^{-1} [28, 31].

Since the scissoring deformation vibration ($\beta_s NO_2$) band of the nitro groups and the out-of-plane skeletal and CH deformation vibration ($\gamma C_{Ar}C_{Ar}$ and $\gamma C_{Ar}H$, respectively) bands of the aromatic rings are also in this region [28, 31, 32], this circumstance must be taken into consideration in the assignment of bands appearing between 1000 and 675 cm^{-1}.

After assignment of the $\beta_s NO_2$, $\gamma C_{Ar}H$, and $\gamma C_{Ar}C_{Ar}$ bands (Table I), more intense bands that were not yet assigned in the frequency region of 900 to 675 cm^{-1} remained only at the wavenumbers shown in the last column of

Table

Characteristic IR frequencies (cm^{-1})
Band intensities are indicated as follows: vs = very strong,

	νOH band	νC=O band	νC=C olefinic band	$\nu C_{Ar}C_{Ar}$ bands	$\nu_{as}NO_2$ band	$\nu_s NO_2$ band	Methoxy bands
Ia	unidentifiable	1650	1600	1580	1485	1350	—
Ib	3240	1675	1630	1605 1580	1540	1350	—
Ic	3270	1660	1630	1595	1520	1355	2840 1260
Id	3285	1670	1630	1605 1500	1540	1350	—

* Appears as a shoulder on the 820 cm^{-1} band.

Table I. Therefore it appeared obvious that these bands originated from CH vibrations of olefinic protons. On the basis of the experimental frequency values they may only be due to the *trans* structure. Since some weak bands are present in the spectra (Fig. 1) between 790 and 690 cm^{-1}, which lie in the wavenumber region expected for *cis* isomers, their alternative assignment (as *e.g.* $\gamma C_{Ar}H$ bands) is also possible.

Therefore, the homogeneous formation of the *trans* isomer is strongly indicated by the IR spectra.

NMR spectra

The analysis of the 60 MHz NMR spectra is complicated by the fact that the signals of olefinic and aromatic ring protons appear in the same frequency range and overlap with each other. Another problem arises from the low solubilities of the substances; the NMR spectra could be recorded only in deutero-dimethyl sulfoxide solutions.

In compounds **Ia**—**Id**, there are three different spin-systems.

1. The two olefinic protons give, as expected, an AB-type spectrum; the signal of the hydrogen in α-position to the carbonyl appears at the lower value [33, 34]. The identification of this part of the spectrum or at least of one of its band pairs is necessary for deciding between the *cis* and *trans* isomers. According to the literature, the $J^{cis}_{\alpha,\beta}$ coupling constants for *cis* 1,2-disubstituted

of the chalcones investigated
s = strong, m = medium, w = weak, vw = very weak

$\gamma C_{Ar}H$ band			$\gamma C_{Ar}C_{Ar}$ band	$\beta_s NO_2$ band	γOH band	γ(=CH) olefinic band
1,2,4-tri-	*p*-di-	mono-				
substitution						
880 m 840 m	—	740 s	715 s	860 m	750—650	980 m
870 w 825 w	—	765 s	695 s	840 m	750—650	1010 s
880 vw 810 m	825 vs	—	—	845 w	750—650	970 m
880 w 825*	820 vs	—	—	845 w	750—650	980 s

olefins are in the region of 5 to 14 Hz, while those of the *trans* isomers are usually between 11 and 19 Hz [35—37].

2. The protons of the 1,2,4-trisubstituted aromatic ring give an ABX type spectrum as the chemical shift (δX) of the 6′-proton in compound **Ia** and the 2′-proton in compounds **Ib—Id** is, owing to the presence of strongly electron-withdrawing substituents in adjacent positions, significantly greater than those of the other two ring protons. The expected value of the coupling constants for $J^{ortho} \equiv J_{AB}$; $J^{meta} \equiv J_{BX}$ and $J^{para} \equiv J_{AX}$ [36, 38, 39] are:

$$J^{ortho} = 7—10 \text{ Hz}; \; J^{meta} = 2—3 \text{ Hz and } J^{para} < 1 \text{ Hz}.$$

According to this symbol system, the relationship $\delta A < \delta B$ is valid for all four compounds as the 3′-proton in **Ia** and the 5′-proton in **Ib—Id** (marked with A) — being in *para* position to the X-protons (the 6′-proton in **Ia** and the 2′-proton in **Ib—Id**) — are adjacent to a hydroxyl group, which causes a smaller paramagnetic shift than the nitro (**Ia**) or the carbonyl substituents (**Ib—Id**) adjacent to the B hydrogens (the 4′-H in **Ia** and the 6′-H in **Ib—Id**).

The B part of the ABX spectrum can be easily distinguished from the AB spectrum of the olefinic protons, as both maxima of the B doublet should show a splitting of 2—3 Hz due to the $J_{BX} \equiv J^{meta}$ coupling. The small $J_{AX} = J^{para}$ splitting is often insignificant. This is worth mentioning, since by confusing the formally identic A part of the olefin AB spectrum with that of the

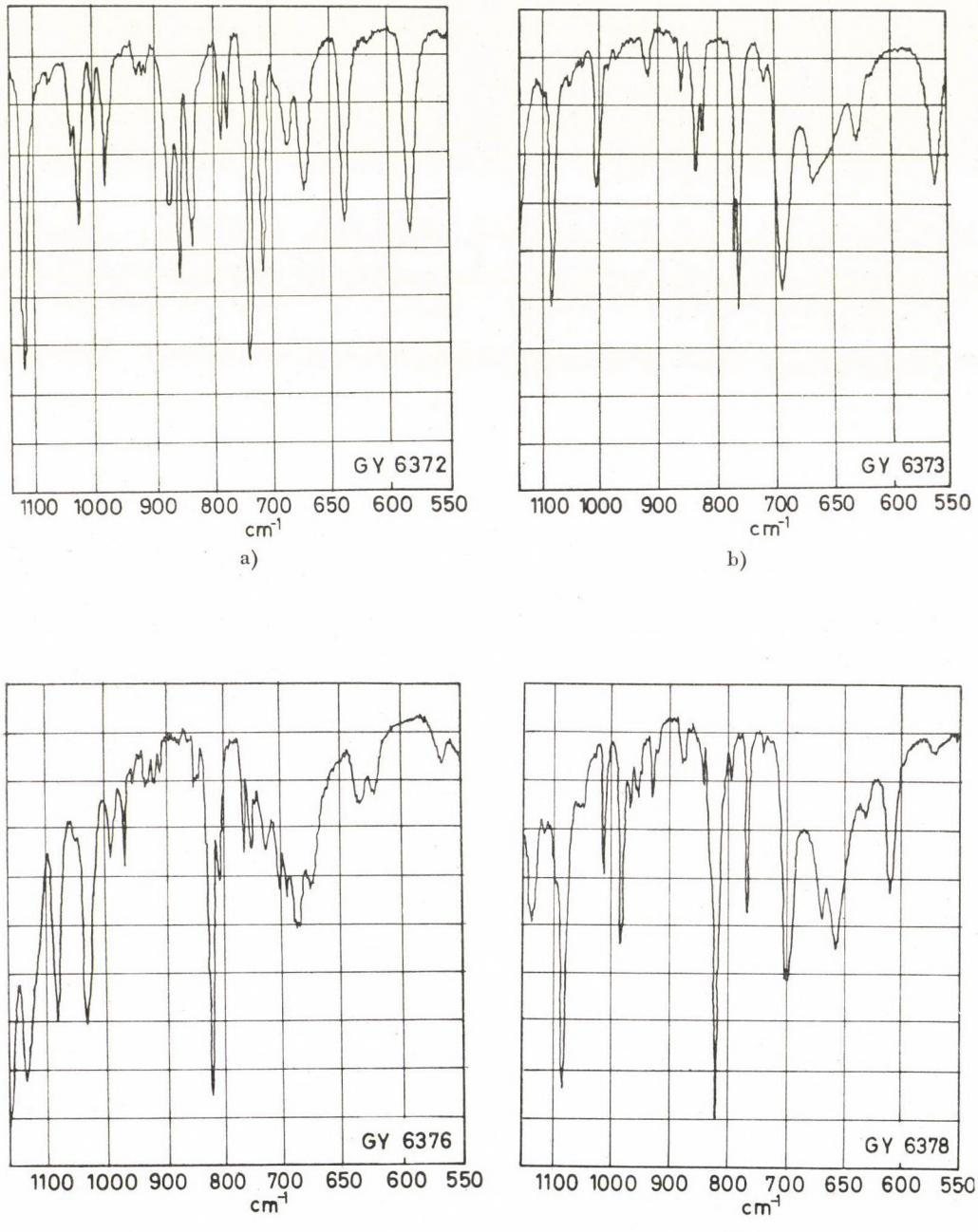

Fig. 1. IR spectra of compounds **Ia**—**Id** in the range of 1100—600 cm^{-1} in KBr pellets (2-fold scale expansion is twice below 700 cm^{-1}). a) 5′-Nitro-2′-hydroxy-chalcone (**Ia**); b) 3′-Nitro-4′-hydroxy-chalcone (**Ib**); c) 3′-Nitro-4′-hydroxy-4-methoxychalcone (**Ic**); d) 3′-Nitro-4′-hydroxy-4-chlorchalcone (**Id**)

ABX spectrum of the ring protons we may come to the erroneous conclusion that the olefinic protons are in *cis* relation. The *ortho* coupling constant remains naturally in the order of magnitude of the *cis* olefin protons (see the data above).

3. The aromatic ring attached to the β-carbon atom gives in the case of **Ia** and **Ib** an ABB'XX' type (monosubstituted ring) and in the case of **Ic** and **Id** an AA'BB' type multiplet. The former is very complicated and asymmetric. The latter may also be misleading because the four most intense signals of the AA'BB' spectrum give a pseudo AB spectrum. This signal system, however, can be easily recognized because of the attached weaker signals.

To illustrate this, two enlarged parts of the spectrum of compound **Ib** are shown in Fig. 2, containing the signals of the 2'- and 6'-protons of the ring adjacent to the carbonyl group and the signal of the β-olefinic proton, respectively (*i.e.* the BX part of the ABX spectrum and the B part of the AB spectrum, respectively), furthermore the enlarged BB' part of the AA'BB' spectrum of compound **Ic** showing the signals of the aromatic protons of the ring attached to the β-carbon atom (Fig. 2).

In the 60 MHz spectra (Fig. 3) the signals of the aromatic and olefinic protons overlap, forming a characterless absorption maximum from which only the signals of the B and X protons separate in the region of the higher δ values, since they are part of the ABX spectrum belonging to the protons of the aromatic ring attached to the carbonyl group. The signal of the B proton is half of an AB spectrum and consists of two lines of different intensities split into doublets; the signal of the X proton is a more intense doublet. Consequently, the 60 MHz spectra are not suitable for solving the structural problem of the *cis–trans* isomers as the signals of the olefinic protons cannot be identified.

For this reason we took the 90 MHz spectra of these compounds (Fig. 4). The higher frequency is advantageous not only because of the better resolution but because lower concentrations are sufficient for obtaining spectra of good quality. This fact enabled us to take the spectra in $CDCl_3$ solution instead of $(CD_3)_2SO$.

Under these recording conditions the resolution permitted the assignation of all lines (except in the case of **Ia** and **Ib** the signals of the monosubstituted aromatic ring protons). The frequency and the assignation of the spectral lines are shown in Table II, the corresponding chemical shifts and coupling constants are listed in Table III. The frequency values were determined from spectra recorded with an expanded time scale ($\times 5$) (see Fig. 2) for the sake of higher accuracy.

It can be seen from Table III that the value of J_{AB}^{olefin} is always between 15.0 and 15.3 Hz. According to the literature cited above, and to the parameters of some related compounds with known structures [33, 40], the value of 15 Hz for the coupling constant proves, in agreement with the IR data, that compounds **Ia**—**Id** are all stereochemically homogeneous *trans* isomers.

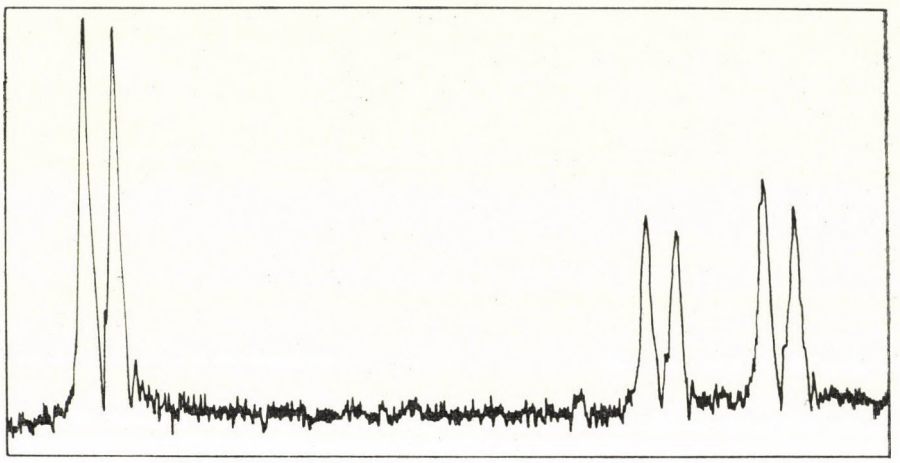

a)

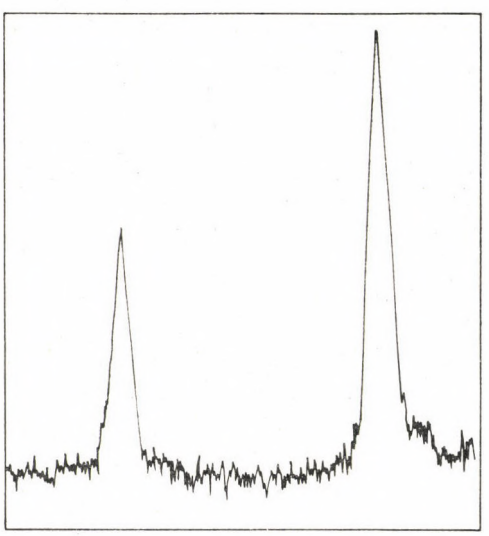

b)

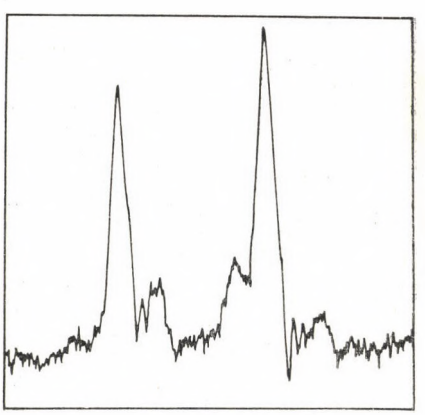

c)

Fig. 2. Parts of the 90 MHz proton resonance spectra expanded 5-fold. a) The BX fragment of the ABX spectrum of the aromatic ring protons adjacent to the carbonyl group in compound **Ib**: the doublet refers to the H-2′ protons (X) and the quartet to the H-6′ protons (B). b) The B part of the AB spectrum with the signal of the β proton, originating from the olefinic hydrogens of compound **Ib**. c) The BB′ part of the AA′BB′ spectrum of the aromatic protons attached to the β carbon atom in compound **Ic**

From Table III some other interesting conclusions can be drawn. The formation of the chelate ring in **Ia** causes an increase in the chemical shift of δH_α, δH_β, δH_4 and δH_6 by 0.35, 0.18, 0.09 and 0.08 ppm, respectively, as compared to the other model substances having rather constant parameters.

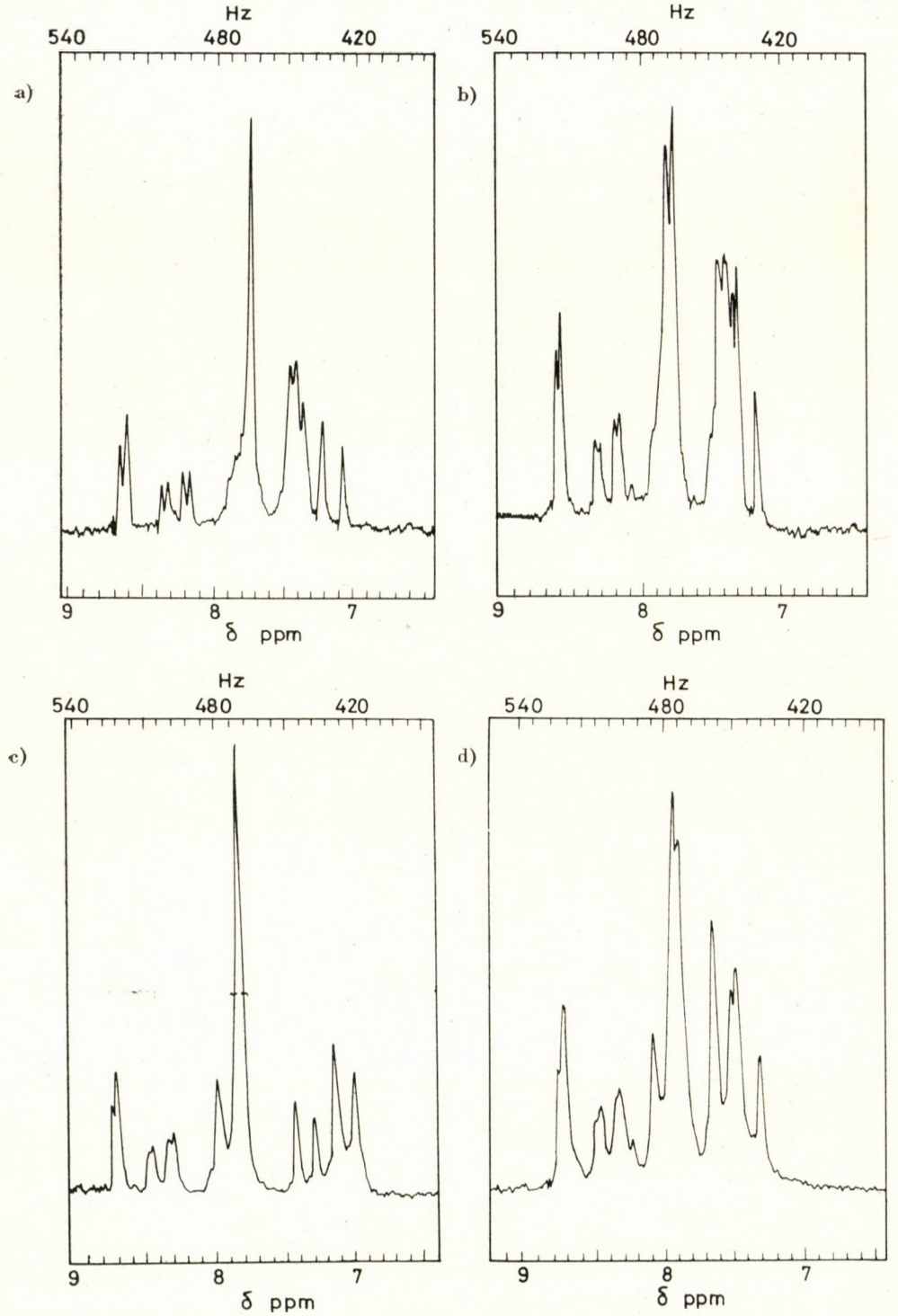

Fig. 3. The 60 MHz proton resonance spectra of compounds **Ia**—**Id** in deutero-dimethyl sulfoxide solution in the range of $\delta = 6.5-9.0$ ppm. a) 5′-Nitro-2′-hydroxy-chalcone (**Ia**); b) 3′-Nitro-4′-hydroxy-chalcone (**Ib**). c) 3′-Nitro-4′-hydroxy-4-methoxychalcone (**Ic**). d) 3′-Nitro-4′-hydroxy-4-chlorochalcone (**Id**)

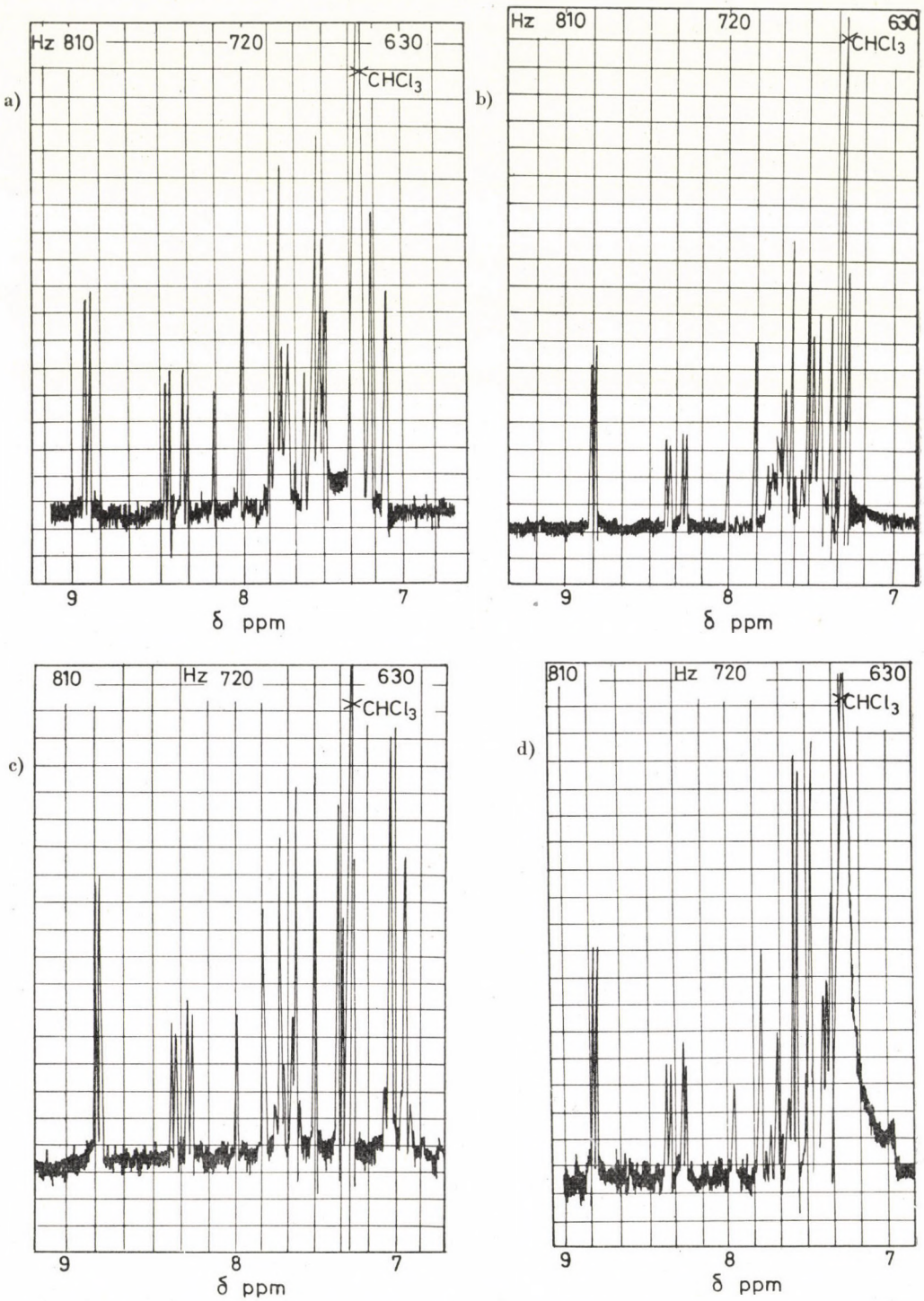

Fig. 4. 90 MHz proton resonance spectra of compounds **Ia**—**Id** in deuterochloroform solution in the range of $\delta = 6.5-9.0$ ppm. a) 5′-Nitro-2′-hydroxychalcone (**Ia**). b) 3′-Nitro-4′-hydroxychalcone (**Ib**). c) 3′-Nitro-4′-hydroxy-4-methoxychalcone (**Ic**). d) 3′-Nitro-4′-hydroxy-4-chlorochalcone (**Id**)

Table II

*Parameters of the 90 MHz proton resonance spectra of chalcone derivatives** **Ia—Id**

	Olefin			Aromatic ring adjacent to the carbonyl					Aromatic ring attached to the β-carbon atom		
	$J_{\alpha\beta}$	δH_α	δH_β	$J_{3'4'}$	$J_{4'6'}$	$\delta H_{3'}$	$\delta H_{4'}$	$\delta H_{6'}$			
Ia	15.3	7.71	8.04	9.1	2.7	7.16	8.40	8.93			
				$J_{5'6'}$	$J_{6'2'}$	$\delta H_{5'}$	$\delta H_{6'}$	$\delta H_{2'}$	J_{23}**	δH_3**	δH_2**
Ib	15.0	7,35—7.40	7.90	8.6	2.2	7.30	8.30	8.83	—	—	—
Ic	15.3	7.40	7.83	8.7	2.2	7.38	8.30	8.78	8.7	6.95	7.62
Id	15.3	7.31	7.84	8.7	2.2	7.34	8.34	8.90	8.7	7.41	7.61

* The coupling constants are given in Hz, the chemical shifts in ppm units.
** These values were obtained by approximating the AA'BB' spectrum as an AB spectrum. $J_{23} \equiv J_{56}$ $\delta H_3 \equiv \delta H_5$ and $\delta H_2 \equiv \delta H_6$

This can be explained by the paramagnetic shift caused by the aromatic ring currents in the chelate ring, the influence of which is compensated in the case of the 4′ and 6′ aromatic protons and even overcompensated at H-3′ (the δ value is decreased by 0.18 ppm) by the electron flood running from the carbonyl oxygen towards the hydroxyl group. At the same time this electron flood increases the paramagnetic shift of the α and to some extent even that of the β protons.

The relatively higher value of the $J_{3'4'}$ and $J_{4'6'}$ coupling constants can also be explained by the increased electron density in the aromatic ring. The change of the chemical shift of the H-3 and H-5 protons (depending on the substituent in position 4) towards higher values in the case of the methoxy group, and towards the lower values in the case of chloro substitution can be easily recognized.

Experimental*

1. Alkaline condensation

The appropriate nitrohydroxyacetophenone (2 mmoles) was mixed with one or two drops of ethanol, dissolved in 35 ml of 1 *N* NaOH at 78 °C, then a saturated warm ethanolic solution of benzaldehyde (9 mmoles) or benzaldehyde derivative (3 mmoles) was added to the mixture while shaken. After a few minutes, the sodium salt of the chalcone began to precipitate. The mixture was then shaken for another 15 min and set aside for one day. Next day the sodium salt was filtered, mixed with 15 ml of 2 *N* HCl and triturated for 20 min on a water

* Melting points are uncorrected.

Table III

Frequencies and assignation of the 90 MHz spectra of chalcone compounds **Ia—Id**
The frequency values are referred to the chloroform signal (654.3 Hz)

Assignation	Compound	Assignation	Compound			Type of the spectrum
	Ia		**Ib**	**Ic**	**Id**	
$H_{6'}$	807.6 804.9	$H_{2'}$	796.2 794.0	795.8 793.6	794.8 792.6	X-part of the ABX spectrum
$H_{4'}$	761.8 759.1 752.7 750.0	$H_{6'}$	754.6 752.4 745.8 743.6	754.8 752.6 746.1 743.9	753.7 751.5 745.0 742.8	B-part of the ABX spectrum
H_β	735.3 720.0		719.0 704.0	717.6 702.3	714.3 699.0	B-part of the AB spectrum
H_α	699.0 683.7		670.0 667.0 ?	672.3 657.0	679.5 664.2	A-part of the AB spectrum
$H_{3'}$	646.5 637.4	$H_{5'}$	660.0 (651.2)*	659.7 651.0	660.0 (651.3)*	A-part of the ABX spectrum
H_2 , H_6				692.7 684.0	690.0 681.3	B-part of the AA′BB′ spectrum**
H_3 , H_5				631.0 622.3	670.8 662.1	A-part of the AA′BB′ spectrum**

* Calculated value based on the splitting of $H_{2'}$ and $H_{6'}$ as this signal overlaps with the (light isotope) contamination of the chloroform solvent.
** AA′BB′ spectrum approximated as an AB spectrum

bath. After cooling, the chalcone was filtered, washed twice with 2 ml of ethanol and recrystallized* after drying if necessary. The melting points were as follows (literature data are given in parentheses):

5′-Nitro-2′-hydroxychalcone: 183—5 °C (183 °C) [25]
3′-Nitro-4′-hydroxychalcone: 161—2 °C (160—1 °C) [41]
3′-Nitro-4′-hydroxy-4-methoxychalcone: 151—2 °C (151 °C) [42]
3′-Nitro-4′-hydroxy-4-chlorochalcone: 185—6 °C (183—4 °C) [43]

2. Condensation by means of dry hydrogen chloride

An ethanolic solution saturated at 0 °C was prepared from the appropriate nitrohydroxyacetophenone (2 mmoles) and the benzaldehyde derivative (2 mmoles). Gaseous hydrogen chloride was bubbled into the solution maintained at 0 °C with ice, for half an hour. The mixture

* From ethyl acetate.

was set aside for one day at room temperature and then diluted to twice its volume with water. The precipitated chalcone was filtered, washed twice with 2 ml of ethanol and recrystallized after drying if necessary. Melting points were as follows:

5′-Nitro-2′-hydroxychalcone:	183 °C
3′-Nitro-4′-hydroxychalcone:	163—4.5 °C
3′-Nitro-4′-hydroxy-4-methoxychalcone:	151—2 °C*
3′-Nitro-4′-hydroxy-4-chlorochalcone:	186—7 °C

3. Condensation in the presence of aluminium chloride

The appropriate nitrohydroxyacetophenone (3 mmoles) benzaldehyde derivative (3 mmoles) and aluminium chloride (6 mmoles) were homogenized and held in a semi-molten state for half an hour at 120 °C on an oil bath. After cooling, the solidified product was decomposed with a mixture of 4 ml of iced water and 1 ml of concentrated hydrochloric acid. After being allowed to stand for several hours, the chalcone was filtered, washed three times with 5 ml of water, twice with 2 ml of ethanol and recrystallized after drying if necessary.

Melting points:

5′-Nitro-2′-hydroxychalcone:	183—4 °C*
3′-Nitro-4′-hydroxychalcone:	162—3 °C
3′-Nitro-4′-hydroxy-4-chlorochalcone:	184—7 °C

IR spectra were recorded on a Model ZEISS UR-10 (Jena) double beam spectrometer in KBr pellets. NMR spectra were taken on a Type JNM-C-60 (JEOL) instrument (60 MHz) in deutero-dimethyl sulfoxide solution using sodium-2,2-dimethyl-2-silopentanesulfonate (DSS) and tetramethylsilane (TMS) respectively, as internal standards. The measurements at 90 MHz have been carried out in deuterochloroform using the "SPEKTROSPIN" instrument of the Rheinische Friedrich Wilhelm University, Bonn.

*

The authors wish to express their thanks to the Ministry of Education (Budapest) for financial support of this work and one of them (P. SOHÁR) to the Heinrich Hertz Foundation for the fellowship granted and to Professor Dr. Günther SNATZKE (Institute of Organic Chemistry, Bonn University) as well as to Mrs. Miklós CSEJK and Mrs. Csaba MÉHESFALVI (Research Institute for Pharmaceutical Chemistry, Budapest) for the help given in recording the spectra.

REFERENCES

1a. LUTZ, R. E., JORDAN, R. H.: J. Am. Chem. Soc., **72,** 4090 (1950)
1b. KUHN, P., LUTZ, R. E., BAUER, C. R.: J. Am. Chem. Soc., **72,** 5058 (1950)
2. LUTZ, R. E., HINKLEY, D. F., JORDAN, R. H.: J. Am. Chem. Soc., **73,** 4647 (1951)
3. BLACK, W. B., LUTZ, R. E.: J. Am. Chem. Soc., **75,** 5990 (1953)
4a. LUTZ, R. E., WEISS, J. O.: J. Am. Chem. Soc., **77,** 1814 (1955)
4b. BLACK, W. B., LUTZ, R. E.: J. Am. Chem. Soc., **77,** 5134 (1955)
5. LUTZ, R. E., SLADE, L. T.: J. Org. Chem., **26,** 4888 (1961)
6. URUSHIBARA, Y., IIMURA, F., IKEDA, K.: J. Chem. Phys., **22,** 1943 (1954)
7. IKEDA, K.: J. Chem. Soc. Japan, Pure Chem. Sect., **76,** 899 (1955)
8. IKEDA, K.: Nippon Kagaku Zasshi, **78,** 1276, 1281, 1284 (1957)
9. TRYON, M., WALL, L. A.: J. Phys. Chem., **62,** 697 (1958)

* From ethyl acetate.

10. UNRUH, C. C.: J. Polymer. Sci., **45,** 325 (1960)
11. HAHN, L., MIQUEL, J. F.: Compt. Rend., **257,** 1948 (1963)
12. PADWA, A., HAMILTON, L.: J. Am. Chem. Soc., **87,** 1821 (1965)
13. MIQUEL, J. F.: Compt. Rend., **254,** 4479 (1962)
14. NAIK, V. G., MARATHEY, M. G.: J. Univ. Poona Sci. Technol., **18,** 55, 61 (1960)
15. NOYCE, D. S., PRIOR, W. A., KING, P. A.: J. Am. Chem. Soc., **81,** 5423 (1959)
16a. NOYCE, D. S., WOO, G. L., JORGENSON, M. J.: J. Am. Chem. Soc., **83,** 1160 (1961)
16b. NOYCE, D. S., JORGENSON, M. J.: J. Am. Chem. Soc., **83,** 2525 (1961)
17a. NOYCE, D. S., KING, P. A., KIRBY, F. B., REED, W. L.: J. Am. Chem. Soc., **84,** 1632 (1962)
17b. NOYCE, D. S., LANE, C. A.: J. Am. Chem. Soc., **84,** 1635 (1962)
17c. NOYCE, D. S., KING, P. A., LANE, C. A., REED, W. L.: J. Am. Chem. Soc., **84,** 1638 (1962)
17d. NOYCE, D. S., LANE, C. A.: J. Am. Chem. Soc., **84,** 1641 (1962)
17e. NOYCE, D. S., AVARBOCK, H. S.: J. Am. Chem. Soc., **84,** 1644 (1962)
17f. NOYCE, D. S., AVARBOCK, H. S., REED, W. L.: J. Am. Chem. Soc., **84,** 1647 (1962)
17g. NOYCE, D. S., JORGENSON, M. J.: J. Am. Chem. Soc., **84,** 4312 (1962)
18. NOYCE, D. S., JORGENSON, M. J.: J. Am. Chem. Soc., **85,** 2420, 2427 (1963)
19. JURD, L., GEISMAN, T. A.: J. Org. Chem., **28,** 2394 (1963)
20. WIELAND, H.: Chem. Ber., **37,** 1149 (1904)
21. TRAKROO, P. P., MUKHEDKAR, A. J.: J. Indian Chem. Soc., **41,** 959 (1964)
22. TRAKROO, P. P., MUKHEDKAR, A. J.: J. Univ. Poona Sci. Technol., **28,** 101 (1964)
23. DIPPY, J. F. J., MCGHIE, J. J., YOUNG, J. T.: Chem. and Ind., 195 (1952)
24. SZÉLL, T.: Monatsh. Chem., **94,** 992 (1963)
25. SZÉLL, T.: Chem. Ber., **91,** 2609 (1958)
26. SOHÁR, P.: Magy. Kém. Foly., **71,** 415 (1965)
27. SOHÁR, P., VARSÁNYI, GY.: Acta Chim. Acad. Sci. Hung., **55,** 189 (1968)
28. HOLLY, S., SOHÁR, P.: Infravörös Spektroszkópia, pp. 59, 67, 68. Műszaki Kiadó, Budapest, 1968
29. SOHÁR, P., VARSÁNYI, GY.: Spektrochim. Acta **23A,** 1947 (1967)
30. SOHÁR, P., SIPOS, GY.: Acta Chim. Acad. Sci. Hung., **46,** 63 (1965)
31. CROSS, A. D.: An Introduction to Practical Infra-Red Spectroscopy, p. 58. Butterworths Sci. Publ., London, 1960
32. NAKANISHI, K.: Infrared Absorption Spectroscopy — Practical. p. 27. Holden-Day. Inc., San Francisco and Nankodo Co. Ltd., Tokyo, 1962
33. SZÉLL, T.: Indian J. Chem., **6,** 470 (1968)
34. SIMON, W., CLERC, T.: Strukturaufklärung organischer Verbindungen mit spektroskopischen Methoden, p. 65. Akademische Verlagsgesellschaft, Frankfurt am Main, 1967
35. SUHR, H.: Anwendungen der kernmagnetischen Resonanz in der Organischen Chemie, pp. 146, 147, 153. Springer Verlag, Berlin, 1965
36. CHAPMAN, D., MAGNUS, P. D.: Introduction to Practical High Resolution NMR Spectroscopy, p. 105. Academic Press, London, New York, 1966
37. SIMON, W., CLERC, T.: Strukturaufklärung organischer Verbindungen mit spektroskopischen Methoden, p. 70. Akademische Verlagsgesellschaft, Frankfurt am Main, 1967
38. SUHR, H.: Anwendungen der kernmagnetischen Resonanz in der Organischen Chemie. p. 164. Springer Verlag, Berlin, 1965
39. SIMON, W., CLERC, T.: Strukturaufklärung organischer Verbindungen mit spektroskopischen Methoden, p. 71. Akademische Verlagsgesellschaft, Frankfurt am Main, 1967
40. NMR Spectra Catalog. Varian Associates, 1962
41. GERECS, Á., SZÉLL, T., WINDHOLZ, M.: Acta Chim. Acad. Sci. Hung., **3,** 559 (1953)
42. SIPOS, GY., SZÉLL, T.: Acta Phys. Chem., Szeged, **11,** 43 (1965)
43. SIPOS, GY., SZÉLL, T.: Acta Phys. Chem., Szeged, **5,** 70 (1959)

Pál SOHÁR; Budapest, IV., Szabadságharcosok útja 47—49.
Tamás SZÉLL; Szeged, Rerrich B. tér 1 (Present address: 95 West 95th Street, New York, N. Y., 10025 U.S.A.)
Tibor DUDÁS; Szombathely, Köztársaság tér 7.

Acta Chimica Academiae Scientiarum Hungaricae, Tomus 70 (4), pp. 369—372 (1971)

ON THE MECHANISM OF BENZENE HYDROGENATION ON METAL CATALYSTS

(PRELIMINARY COMMUNICATION)

YU. I. DERBENTSEV,* Z. PAÁL and P. TÉTÉNYI

(Institute of Isotopes of the Hungarian Academy of Sciences)

Received June 30, 1971

Catalytic hydrogenation of benzene belongs to those well-known heterogeneous processes the mechanisms of which have not yet been cleared up in every detail [1]. BALANDIN's multiplet theory [2] predicts a sextet hydrogenation in the presence of metal catalysts, without unsaturated intermediates. The recent observation of cycloolefins among the products of benzene hydrogenation on metals both in liquid [3—5] and gas phase [6, 7], however, led to the assumption of a stepwise hydrogenation mechanism *via* cycloolefins. The very small amount of cycloolefins found was explained in terms of cycloolefins being hydrogenated more rapidly than desorbed from the catalyst surface [3—5, 8]. The lack of unambiguous and convincing evidence concerning the mechanism of benzene hydrogenation prompted us to investigate this problem by means of radioactive tracers.

The experimental method involved reacting a mixture of the radioactive starting material and an inactive form of the supposed intermediate [9, 10, 11]. In order to avoid that the rapid hydrogenation and slow desorption of cyclohexene should cause errors in the specific radioactivity of cyclohexene in the gas phase, inactive cyclohexadiene was added to the radioactive benzene, cyclohexene being thus formed in the course of the reaction on the catalyst surface. The specific radioactivity of cyclohexene, therefore, must be identical in the gas phase and on the surface, regardless of the fact that part of it remains on the surface and reacts without desorption.

Measurements were carried out in a pulse-type microreactor described in Ref. [10]. Pure metal powders were used as catalysts. Fractions corresponding to individual peaks on the chromatogram were measured by a Tri-Carb scintillation spectrometer.

The effect of peak tailing was checked by a special experiment, in which narrow fractions were collected in such a way that more than one fraction

* Permanent address: Zelinsky Institute of Organic Chemistry, Academy of Sciences, USSR, Moscow.

should correspond to one component. The result of this experiment is shown in Fig. 1. It is obvious that both cyclohexene and cyclohexadiene contain some radioactivity, indicating that stepwise hydrogenation actually takes place. The correction due to the tailing of the cyclohexane peak was less

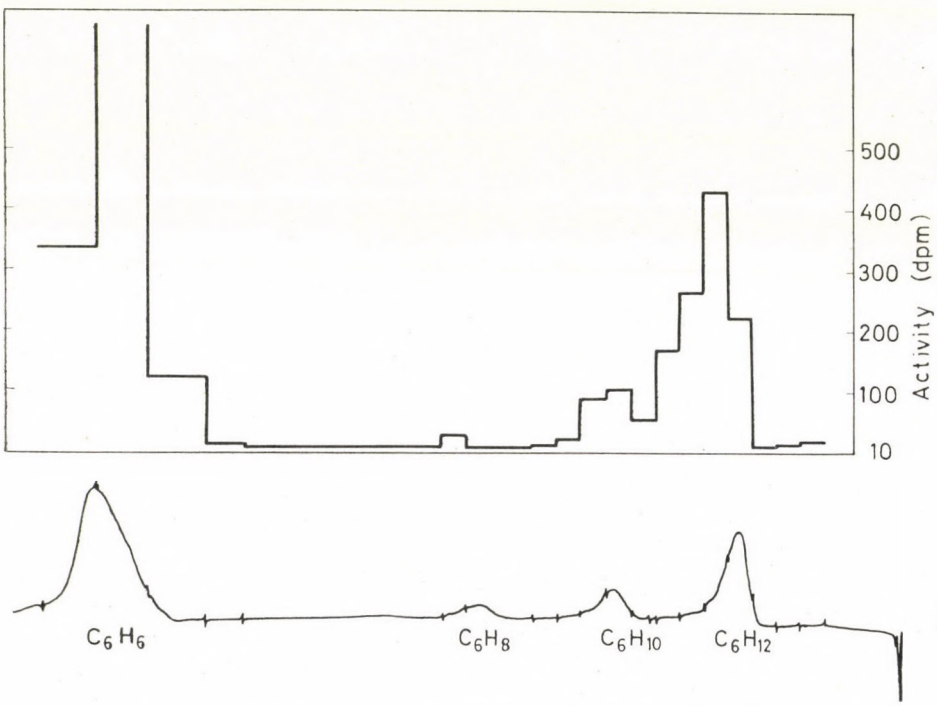

Fig. 1. Typical chromatogram of a hydrogenation run (mixture of benzene-^{14}C and cyclohexadiene) and the absolute radioactivities of narrow fractions. (The places of fraction changes are shown by small deflections on the chromatogram.) Catalyst: 1.7 mg of Pt; t = 190 °C; 3 μl of 1 : 1 mixture, $V(H_2)$ = 60 ml/min. Radioactivity peaks are corrected for the background

than 5% of the total radioactivity of the former which may, however, be not negligible compared with the total radioactivity of cyclohexene. Thus, the quantitative comparison of specific radioactivities must be performed with great care.

Data from typical runs obtained in the presence of a platinum catalyst are listed in Table I. Cyclohexadiene suffered almost total conversion, being partly hydrogenated, and partly dehydrogenated to benzene. This latter fraction caused the specific radioactivity of benzene to decrease. The degree of benzene conversion is shown by the amount of radioactivity transferred to other compounds (*cf.* the r% values). Clearly, both the cyclohexene and cyclo-

hexadiene were radioactive. On the other hand, even if not corrected for tailing, the specific radioactivities of the unsaturated species are definitely lower than that of cyclohexane which, in turn, indicates that both stepwise and "direct" hydrogenation of benzene do actually take place.

Table I

Hydrogenation of mixtures of benzene-^{14}C and inactive cyclohexadiene
Catalyst: 1.7 mg of Pt; Carrier gas: H_2 Pulses: 3 μl of each

No.	t °C	v(H_2) ml/min	Sample		Composition				Specific radioactivity* *(sp. r.)*			
					C_6H_{12}	C_6H_{10}	C_6H_8	C_6H_6	C_6H_{12}	C_6H_{10}	C_6H_8	C_6H_6
I			Starting mixture	w%	—	—	44.1	55.9				
				r%	—	—	0	100	—	—	0	1.79
I	192	85.5	Product	w%	26.2	5.6	3.8	64.4				
				r%	4.1	0.5	0.25	95.1	0.156	0.093	0.066	1.48
II			Starting mixture	w%	—	0.2	37.7	62.1				
				r%	—	0	0	100	—	0	0	1.61
II	190	73.2	Product	w%	26.4	5.3	2.0	64.4				
				r%	4.9	0.8	0.25	94.0	0.186	0.154	0.125	1.42
III			Starting mixture	w%	—	0.5	43.5	66.0				
				r%	—	—	0	100	—	0	—	1.52
III	197	87.2	Product	w%	17.0	8.1	2.8	72.1				
				r%	1.2	0.45	0.15	98.2	0.073	0.056	0.057	1.36

* Not corrected for tailing

w%: product composition in % (w/w):
r%: distribution of radioactivity over individual fractions in % of the total radioactivity of all fractions;
sp. r.: specific radioactivity of the fractions in arbitrary units (*sp. r.* = $r\%/w\%$)

In order to obtain a more general picture, several experiments have been carried out in the presence of various metals as catalysts, using a proportional gas-flow counter as the radioactivity detector. Table II shows some typical results obtained at different conversions. More detailed data and their possible explanation will be reported in a forthcoming paper.

Table II

Hydrogenation of mixtures of benzene-^{14}C and inactive cyclohexadiene on different metal catalysts

Carrier gas: 60 ml/min H_2; Pulse: 3 μl of hydrocarbon mixture (42—48% of C_6H_8 + 58—52% of C_6H_6); $t = 185 \pm 5$ °C

Catalyst		Composition				Specific radioactivity		
		C_6H_{12}	C_6H_{10}	C_6H_8	C_6H_6	C_6H_{12}	C_6H_{10}	C_6H_6
500 mg of Re	w%	86.1	0.7	—	13.2	—	—	—
	r%	81.7	1.0	—	17.3	0.95	1.43	1.31
7.7 mg of Ni	w%	42.6	4.0	—	53.4			
	r%	21.3	0.7	—	78.4	0.50	0.175	1.46
8.9 mg of Pd	w%	16.2	26.0	—	57.8			
	r%	1.5	0.1	—	98.4	0.093	0.004	1.70
66 mg of Ir	w%	21.8	18.2	5.1	54.9			
	r%	0.33	0.11	—	99.56	0.015	0.006	1.82

*

The authors are indebted to Dr. T. SZARVAS for kindly performing the radioactivity measurements.

REFERENCES

1. SMITH, H. A., in "Catalysis", Ed. P. H. Emmett, Vol. 5, p. 175. Reinhold Publ. Co., New York, 1957
2. BALANDIN, A.: Sovremennoye sostoyanie multipletnoi teorii geterogennogo kataliza. Izd. "Nauka", Moscow, 1968
3. SIEGEL, S., SMITH, G. V., DMUCHOVSKY, B., DUBBELL, D., HALPERN, W.: J. Am. Chem. Soc. **84**, 3136 (1962)
4. HARTOG, F., ZWIETERING, P.: Catalysis **2**, 79 (1963)
5. SIEGEL, S., KU, V., HALPERN, W.: J. Catalysis **2**, 348 (1963)
6. MADDEN, W. F., KEMBALL, C.: J. Chem. Soc. 302 (1961)
7. MISHCHENKO, A. P., DOBROSELSKAYA, N. P.: Neftekhimiya, **9**, 672 (1969)
8. GUDKOV, B. S., ZLOTINA, N. F., MAKHLIS, L. A., KIPERMAN, S. L.: Izv. Akad. Nauk SSSR, Ser. Khim. 2525 (1970)
9. TÉTÉNYI, P., BABERNICS, L., THOMSON, S. J.: Acta Chim. Acad. Sci. Hung. **34**, 335 (1962)
10. PAÁL, Z., TÉTÉNYI, P.: Acta Chim. Acad. Sci. Hung. **54**, 175 (1967)
11. DERBENTSEV, YU. I., BALANDIN, A. A. ISAGULYANTS, G. V.: Kinetika i kataliz, **2**, 741 (1961)

Yu. I. DERBENTSEV; Leninsky prospekt 47, Moscow, USSR.
Zoltán PAÁL, Pál TÉTÉNYI } Budapest, 114, P.O.B. 77.

Acta Chimica Academiae Scientiarum Hungaricae, Tomus 70 (4), pp. 373–378 (1971)

CONVERSION OF RETRO-DEHYDROCAROTENE INTO ISOZEAXANTHIN AND ISOZEAXANTHIN EPOXIDES WITH PERPHTHALIC ACID

J. SZABOLCS and GY. TÓTH

(Chemical Institute of the Medical University, Pécs)

Received January 16, 1970

The conversion of *retro*-dehydrocarotene into isozeaxanthin by perphthalic acid, and the formation of three hitherto unknown stereoisomers of isozeaxanthin monoepoxide are reported. This type of hydroxylation may provide a suitable method for preparing hydroxylated carotenoids from *retro*-dehydrocarotenoids.

Isozeaxanthin (4,4′-dihydroxy-β-carotene) was first synthetized by ISLER [1] *et al.* in 1956. Then several papers [2—7] were published about the preparation of isozeaxanthin and its derivatives, but only in 1966 was its occurrence in nature reported (marine isopod *Idothea granulosa*) by LEE [8].

During an investigation into the epoxidation of *retro*-carotenoids it was observed in our laboratory that *retro*-dehydrocarotene (**I**) gave isozeaxanthin (**III**) [m.p. 136 °C; λ_{max}(hexane) 478 and 450 mμ; $10^{-3}x\epsilon_{max}$ 121.6 and 135.6; ν_{max} ($CHCl_3$) 3618 cm^{-1}] when it was subjected to epoxidation with perphthalic acid, and the products were hydrolysed. At the same time 3 monoepoxide derivatives of isozeaxanthin (**V**) namely isozeaxanthin monoepoxide A, B and C were also isolated in crystalline form.

It is assumed that first an α, ω-addition takes place, that is 1 mol of perphthalic acid reacts with the chromophore of *retro*-dehydrocarotene (**I**) at carbon atoms 4 and 4′, yielding the monoester derivative of isozeaxanthin (**II**). This is followed by a normal epoxidation process which furnishes the isozeaxanthin monoepoxide derivatives (**IV**).

As is shown in Fig. 1 the light absorption properties of isozeaxanthin monoepoxides are very similar (the difference in ϵ_{max} values might be due to the omission of recrystallization), and none of them has a *cis*-peak. Although not characteristic, the IR-spectra are not at variance with structures **VI**, **VII** and **V**. By iodine-isomerization the compounds give *cis* isomers with absorption at lower wavelengths, but they cannot be isomerized into each other. All three isozeaxanthin monoepoxides react with acid resulting in their furanoid derivatives with the same absorption maxima [$\lambda_{max}(C_6H_6)$ 465 and 437 mμ].

Considering that isozeaxanthin (**III**) produced with perphthalic acid was certainly a mixture of the racemic and meso forms, which can all give *cis*- and *trans*-monoepoxides,the formation of more than one isozeaxanthin monoepoxide

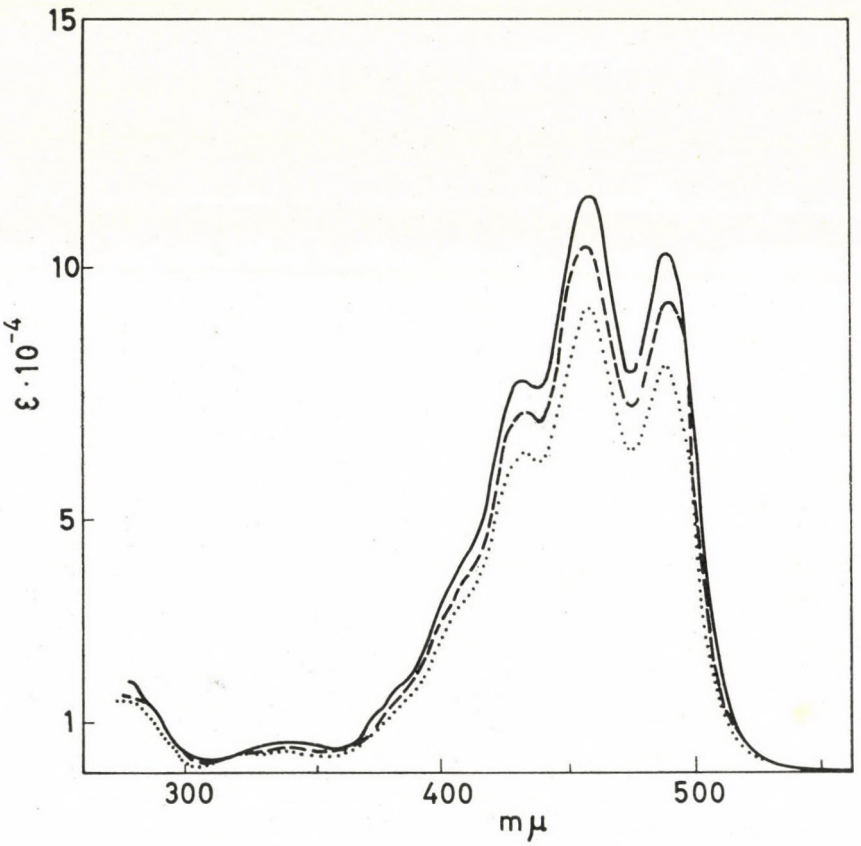

Fig. 1. Molar extinction curves of isozeaxanthin monoepoxides in benzene. Isozeaxanthin monoepoxide A —— (λ_{max} 488, 459, and 339 mμ): isozeaxanthin monoepoxide B ------- (λ_{max} 489, 459 and 339 mμ); isozeaxanthin monoepoxide C ... (λ_{max} 489, 458 and 339 mμ)

(**VI, VII**) is not surprising. This is in good agreement with, and lends support to, the results of an earlier experiment [9] in which we succeeded in separating the *cis* and *trans* monoepoxides of zeaxanthin and lutein, and which showed that the isomers only differed in the stereochemistry of the epoxide ring in relation to the C-3 hydroxyl group.

Similarly, when isozeaxanthin diacetate was subjected to epoxidation with perphthalic acid, the stereoisomers of isozeaxanthin monoepoxides were also obtained.

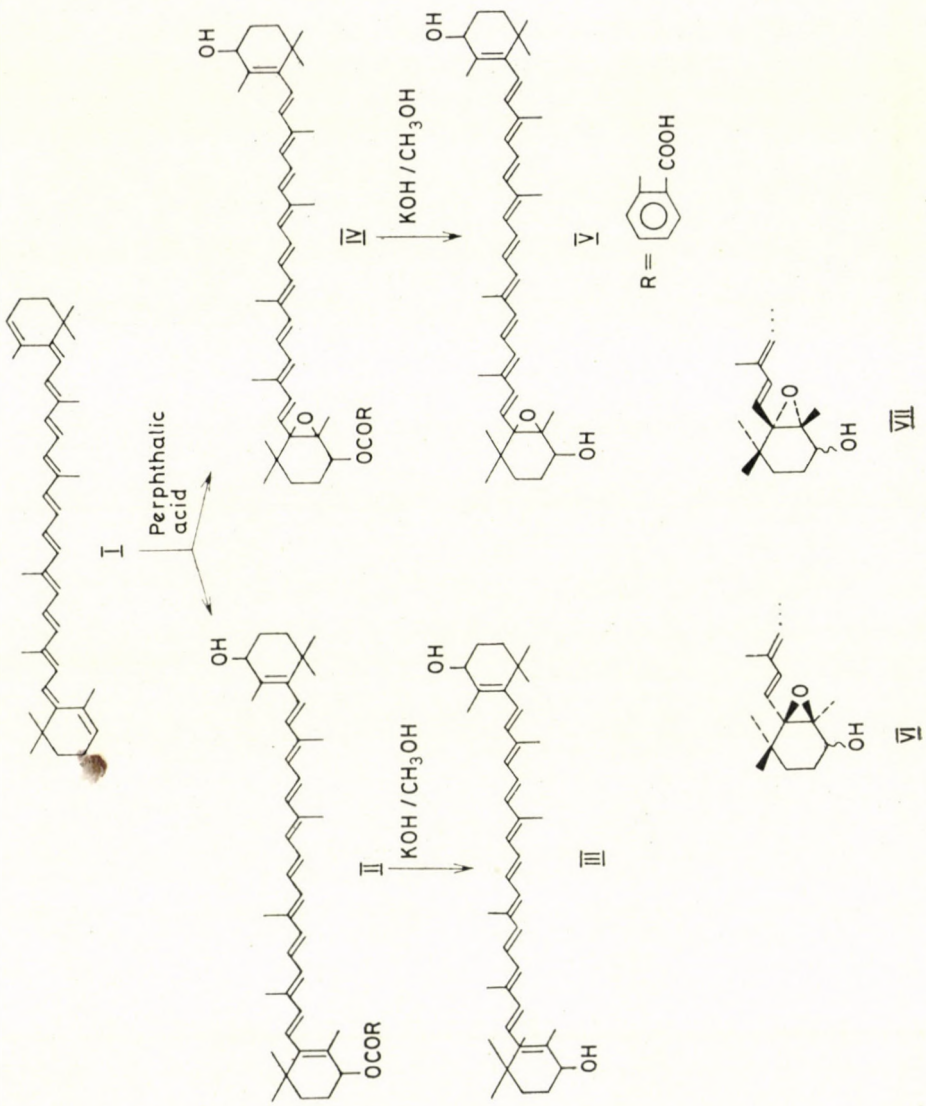
I
Perphthalic acid
II
KOH / CH3OH
III
IV
KOH / CH3OH
V
R =
COOH
VI
VII
OH
OCOR
O

Experimental

The procedures and methods used here have been summarized elsewhere [10]. *Retro*-dehydrocarotene was prepared from β-carotene according to KARRER et al. [11].

Epoxidation of retro-dehydrocarotene with perphthalic acid

270 mg of *retro*-dehydrocarotene (in portions of 90 mg) in 1 l of abs. ether was allowed to stand in the presence of perphthalic acid (140 mg) at room temperature in darkness for 13 hrs. It was then transferred to a separatory funnel, washed thoroughly with water and an aqueous sodium hydrogen carbonate solution, and dried over anhydrous Na_2SO_4. This ethereal solution was hydrolysed with 80 ml of 30% KOH methanol at room temperature for 5 hrs. On completion of the hydrolysis, the solution was transferred to a separatory funnel to remove the methanolic layer from which the pigments were extracted with ether. Then the two ethereal solutions were combined, washed with water until alkali free and dried over anhydrous Na_2SO_4; finally, the ether was evaporated. The residue was subjected to chromatography on calcium carbonate from benzene and petroleum ether (50—60 °C).

	Zone	Pigment	λ_{max} in benzene	
1	5 mm lemon	unidentified	485	454
	1 mm —			
	1 mm yellow	unidentified	—	—
	10 mm —			
2	20 mm ochre	isozeaxanthin monoepoxide A	490	457
3	10 mm ochre	isozeaxanthin monoepoxide B	489	458
	5 mm —			
4	15 mm ochre	isozeaxanthin monoepoxide C	489	458
	20 mm —			
5	15 mm yellow	isozeaxanthin	497	462
	5 mm —			
6	4 mm diffuse yellow	unidentified	488	457

The pigments were eluted with methanol, transferred to a separatory funnel, diluted with benzene, washed with water, dried over anhydrous Na_2SO_4, and evaporated under reduced pressure for crystallization.

Isozeaxanthin (Zone 5) was crystallized from a mixture (2 : 1) of ethyl acetate and petroleum ether (50—60 °C); the long, reddish needles (24 mg) melted at 136 °C. After recrystallization, 18 mg of isozeaxanthin was obtained; m. p. 137 °C.
$C_{40}H_{56}O_2$ (568.89). Calcd. C 84.45; H 9.93. Found C 84.10; H 10.39%.

Isozeaxanthin monoepoxide A (Zone 2)

Crystallization from warm methanol yielded 7.5 mg of yellow, tiny crystals; m. p. 168 °C. Relative polarity value 1.96. The visible and UV spectra are given in Fig. 1.
$C_{40}H_{56}O_3$ (584.89). Calcd. C 82.14; H 9.65. Found C 82.25; H 9.82%.

Isozeaxanthin monoepoxide B (Zone 3)

6.8 mg of yellow plates were obtained from methanol; m. p. 158 °C. The relative polarity value of isozeaxanthin monoepoxide B is 1.96. The visible and UV spectra are presented in Fig. 1.
$C_{40}H_{56}O_3$ (584.89). Calcd. C 82.14; H 9.65. Found C 82.18; H 9.85%.

Isozeaxanthin monoepoxide C (Zone 4)

Crystallized from warm methanol in long, yellow needles (1.2 mg); m.p. 160 °C. The relative polarity value of isozeaxanthin monoepoxide C is 1.97. Its visible and UV spectra are shown in Fig. 1.

It should be noted that isozeaxanthin epoxide A, B and C (R_F 0.42) separated readily from isozeaxanthin (R_F 0.55) but not from each other when subjected to thin-layer chromatography. (Aluminium oxide G; 15% acetone in benzene.)

Isomerization of isozeaxanthin monoepoxides by iodine

(a) Isozeaxanthin monoepoxide A. 2 mg of isozeaxanthin monoepoxide A was dissolved in 20 ml of benzene and allowed to stand in the presence of 0.02 mg of iodine at room temperature for 30 min. The solution was washed with aqueous sodium thiosulfate solution and water, and dried over anhydrous Na_2SO_4. It was then chromatographed on calcium carbonate from benzene–petroleum ether (1 : 1). After elution etc., the pigments were identified by their absorption maxima, and by mixed chromatography with authentic samples.

Zone	Pigment	λ_{max} in benzene	
10 mm ochre	*cis* isomer	485	453
5 mm light ochre	*cis* isomer	484	453
45 mm ochre	isozeaxanthin monoepoxide A	490	458

(b) Isozeaxanthin monoepoxide B. 2 mg of isozeaxanthin monoepoxide B was treated with iodine as described for isozeaxanthin monoepoxide A.

Zone	Pigment	λ_{max} in benzene	
10 mm ochre	*cis* isomer	484	453
8 mm light ochre	*cis* isomer	485	454
45 mm ochre	isozeaxanthin monoepoxide B	490	458

(c) Isozeaxanthin monoepoxide C. 1 mg of isozeaxanthin monoepoxide C was isomerized with iodine as described above.

Zone	Pigment	λ_{max} in benzene	
5 mm ochre	*cis* isomer	486	453
2 mm light ochre	*cis* isomer	486	454
10 mm ochre	isozeaxanthin monoepoxide C	491	458

Epoxidation of isozeaxanthin diacetate

10 mg of isozeaxanthin diacetate in 30 ml of abs. ether was epoxidized with 5 mg of perphthalic acid at room temperature in darkness for 15 hrs. On completion of the epoxidation (followed by t.l.c.) the ethereal solution was washed with 5% $NaHCO_3$ and water, dried over anhydrous Na_2SO_4, and hydrolyzed with 7 ml of 30% KOH methanol at room temperature for 6 hrs. After the usual procedures the products were separated on a calcium carbonate column from a mixture (3 : 2) of benzene and petroleum ether (50—60 °C).

	Zone	Pigment	λ_{max} in benzene	
1	6 mm lemon	isozeaxanthin difuranoide	436	(diffuse)
2	4 mm lemon	isozeaxanthin difuranoide	436	
3	15 mm ochre	isozeaxanthin monoepoxide A	489	457
4	10 mm ochre	isozeaxanthin monoepoxide B	489	457
5	12 mm ochre	isozeaxanthin monoepoxide C	488	456
6	3 mm pale yellow	unidentified	486	456

Zones 1, 2 and 3 were identified by their absorption spectra, partition between 90% methanol and petroleum ether, R_F values, and their furanoid tests.

*

The authors are indebted to the Ministry of Health for financial support. They also wish to thank Mrs. M. STEILER and Mr. L. TIMÁR for skilful technical assistance.

REFERENCES

1. ISLER, O., LINDLAR, H., MONTAVON, M., RÜEGG, R., ZELLER, P.: Helv. Chim. Acta **39,** 449 (1956)
2. ENTSCHEL, R., KARRER, P.: Helv. Chim. Acta **41,** 402 (1958)
3. ENTSCHEL, R., KARRER, P.: Helv. Chim. Acta **41,** 983 (1958)
4. BODEA, C., NICOARA, E., TAMAS, V.: Liebigs Ann. Chem. **627,** 237 (1959)
5. BODEA, C., FLORESKO, M.: Rev. Chim. (Bucureşti) **6,** 359 (1961)
6. BODEA, C., NICOARA, E., SALONTAI, T.: Studii Cercetari Chim. **12,** 153 (1961)
7. TSUKIDA, K.: Bitamin **33,** 185 (1966)
8. LEE, W. L.: Comp. Biochem. Physiol. **19,** 13 (1966)
9. BARTLETT, L., KLYNE, W., MOSE, W. P., SCOPES, P. M., GALASKO, G., MALLAMS, A. K., WEEDON, B. C. L., SZABOLCS, J., TÓTH, GY.: J. Chem. Soc. (C), 2527 (1967)
10. SZABOLCS, J., RÓNAI, A.: Acta Chim. Acad. Sci. Hung. **61,** 301 (1969)
11. KARRER, P., SCHÖPP, K., MORF, R.: Helv. Chim. Acta **15,** 1158 (1932)

József SZABOLCS
Gyula TÓTH
Pécs, Rákóczi út 80, Hungary.

Acta Chimica Academiae Scientiarum Hungaricae, Tomus 70 (4), pp. 379—389 (1971)

THE ACID HYDROLYSIS OF INULIN*

J. SZEJTLI,** R. D. HENRIQUES and M. CASTIÑEIRA

(Escuela de Bioquimica-Farmaceutica, Universidad de La Habana, La Habana, Cuba)

Received April 20, 1970; in revised form November 5, 1970

The acid hydrolysis of the β-1,2 glycosidic bonds between the D-fructofuranose units of inulin is extremely rapid, but cannot be characterized by a single rate constant, since in the initial phase the hydrolysis is slower than in the final phase. In the final phase, when the $\overline{DP}$ is less than 4, the rate of hydrolysis of inulin is higher, whereas in the initial phase it is lower than that of sucrose.

In all probability, the first step of the hydrolysis of the furanoside linkages is protonation of the oxygen in the furanoside ring, followed by heterolysis of the linkage by the formation of a tertiary cation. The value of the entropy of activation shows that the reaction is of type A-1. This mechanism is similar to the hydrolysis mechanism of sucrose and raffinose.

Introduction

Inulin is a polysaccharide, built of D-fructofuranose units connected by β-1,2 glycosidic bonds. The presence of 1.5—7% of D-glucose in its enzymatic hydrolyzate suggests that the molecule, which is a chain consisting of approximately 35 D-fructofuranoside residues, is completed at the reducing end of the chain by a D-glucose unit, bound by a linkage of the sucrose type [1—5]. A bibliography on fructanes and difructo-anhydrides prior to 1946 has been compiled by MCDONALD [17].

According to several authors [6—9], during the acid hydrolysis of inulin the first order rate constant determined at the outset (5—15% hydrolysis) increases to 2—6 times its original value until reaching a maximum; then it begins to decrease.

The half-life [7] of inulins of various origin, as determined by measurement of the reducing power in 1.0 *N* sulfuric acid at 20 °C, lies between 370 and 390 minutes [10], while under similar conditions 290 minutes were only necessary for a 50% hydrolysis of sucrose.

Data have been published in the literature for the hydrolysis of inulin by ion-exchange resins [11, 12], for the separation of the intermediary products of

* The present paper is a part of a series; the previous part has been published in Acta Chim. Acad. Sci. Hung., **66**, 213 (1970).

** Present address: Chinoin Pharmaceutical and Chemical Works Ltd., Budapest.

partial hydrolysis by paper chromatography [13], as well as for the secondary reactions [14].

On the other hand, systematic investigations of the hydrolysis of inulin have scarcely been reported. The published data are incongruent, *e.g.* the values of the activation energy (28.4 kcal/mole [9], 29.4 kcal/mole [15], and 25.4 kcal/mole; this latter can be calculated from the data published in Ref. [6]) are not adequate to draw conclusions for the mechanism of hydrolysis. Also the

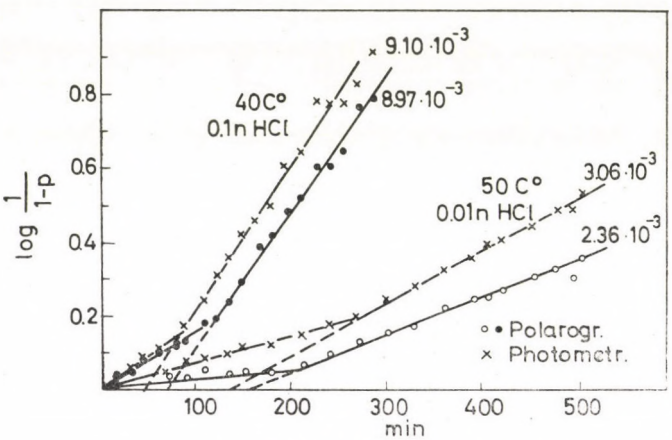

Fig. 1. Logarithmic hydrolysis curves

value of g ($= \Delta \log k / \Delta \mathrm{pH}$) shows an improbable variation, between 0.89 and 1.64 [6, 9]. Only a single value is known for the entropy of activation (+13.4 e.u.), but this is calculated from a value of E_a [15] which, if correct, allows the conclusion that the molecular mechanism of hydrolysis of inulin differs from the probable mechanism of the hydrolysis of sucrose.

The object of the present paper has been the determination of reliable values of k, E_a and ΔS^+, and to draw conclusions for the mechanism of hydrolysis of inulin, with special regard to the applicability of the hypothesis published in our previous paper [16] for the hydrolysis of sucrose and raffinose.

Experimental

250 mg of dry inulin (Merck; $[\alpha]_D^{20} = -40°$, $c = 2.5$, in water) was dissolved in 25 ml of distilled water and warmed at 60 °C for a few minutes to ensure complete dissolution. After adjustment to the temperature of hydrolysis, 25 ml of an acid of appropriate concentration and of the same temperature was added, mixed, and at regular intervals 2 ml samples were withdrawn from the solution kept in an ultrathermostat. The sample was added to 2 ml of a 1.2 or 0.12 N LiOH solution and 0.5 ml of the resulting solution was used for polarographic determination of the reducing power, in a similar way as published in our previous paper [16] dealing with the acid hydrolysis of raffinose and sucrose.

As it is seen in Fig. 1, the value of $\log \frac{1}{1-p}$ as a function of the reaction time shows two sections (p is the ratio of the actual value of reducing power to the experimentally attainable maximal value). Extrapolating the second section, the value of k can be determined, which is characteristic of the splitting of the terminal linkages. The constant which characterizes the splitting of non-terminal linkages is designated by k_r. The plotting of values of the constant calculated from various, experimentally determined points as a function of hydrolysis represents another method of extrapolation. This type of extrapolation is illustrated in Fig. 2. Evidently, after having reached 100% hydrolysis, only difructose can be hydrolyzed, therefore this extrapolation gives directly the value of k.

As it is seen in Fig. 1, there is a considerable discrepancy between the values determined by polarography and by the photometric method; however, these k values are within the limits of experimental errors. The polarographic method is more selective, it is supposed that only fructose is measured, while the photometric method determines all reducing groups. As a consequence, the polarographic curves reach the same values later than the photometric curves, but the difference is only in the duration of the first stage. Thus on the basis of Fig. 1, in the majority of the experiments, the same k value can be calculated by both methods, while there remains some discrepancy between the values extrapolated on the basis of Fig. 2. The rate constants in Table I represent averages of four data.

Table I

Rate constants and entropies of activation

t, °C	[HCl] N	pH*	$k \cdot 10^3$ min^{-1}	log k_r**	ΔS^+ e.u.	Determined by f = photometry, p = polarography
30.0	0.104	1.044	2.1	−1.578	8.30	p
			2.2	−1.558	8.39	f
40.0	1.044	−0.095	115	−1.040	7.99	p
			115	−1.040	7.99	f
	0.104	1.044	8.4	−0.976	8.29	p
			8.9	−0.950	8.40	f
	0.0104	2.018	0.72	−1.020	8.08	p
			0.74	−1.009	8.14	f
50.0	0.104	1.044	27.0	−0.469	8.46	p
			31.9	−0.396	8.79	f
	0.0104	2.018	2.5	−0.480	8.41	p
			3.0	−0.400	8.78	f
60.0	0.104	1.044	95.0	+0.078	8.06	p
			100.0	+0.100	8.16	f
	0.0104	2.018	7.5	−0.003	7.69	p
			8.1	+0.003	7.72	f
	0.00104	2.991	0.67	−0.016	7.63	p
			0.84	+0.082	8.08	f
			average:		8.13	

* = calculated pH (see Ref. [16])
** = $\log k_r = \log k + g \cdot pH$

The values of k_n were not calculated, because the applied experimental technique is not suitable for their determination with adequate precision. The values of k_n are, on the average, only 1/2—1/6th of k, depending on the experimental conditions and mainly on the origin of the inulin.

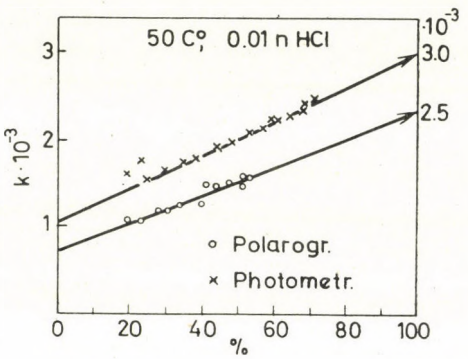

Fig. 2. Increase of the rate constant with the progress of hydrolysis

Influence of the acid concentration

Fig. 3 illustrates the dependence of log k on the pH. Table II contains the g values. In this sense the behaviour of inulin is similar to that of other neutral glycosides; the rate constant of its hydrolysis is a slightly exponential function of the acidity.

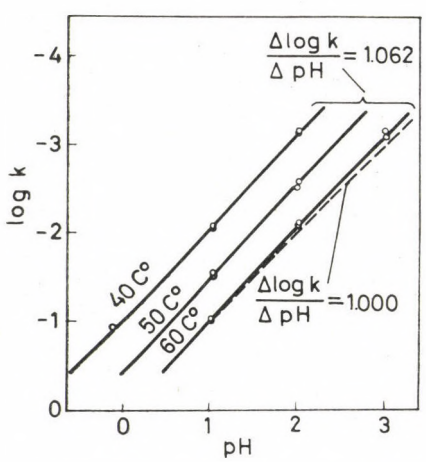

Fig. 3. Variation of log k with pH

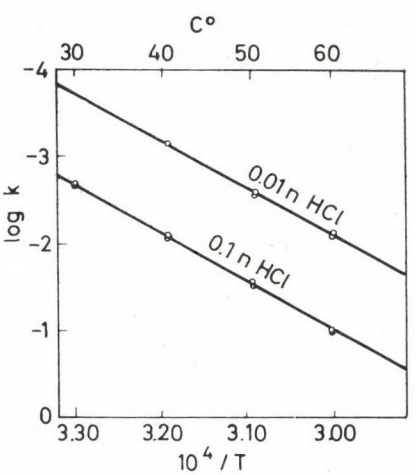

Fig. 4. Log k as a function of the reciprocal value of absolute temperature

Influence of temperature

The correlation of log k and $1/T$ is illustrated in Fig. 4. As it is shown, the points plotted at both acid concentrations result in straight lines, thus the value of E_a within the investigated temperature range does not show any remarkable variation. For the E_a and d values, see Table III.

Table II

Values of g

t, °C	HCl *N* range	*g*	Determined by p = polarography, f = photometry
40.0	0.104 —1.04	0.997	p
		0.966	f
	0.0104 —0.104	1.094	p
		1.110	f
50.0	0.0104 —0.104	1.061	p
		1.053	f
60.0	0.0104 —0.104	1.132	p
		1.121	f
	0.00104—0.0104	1.078	p
		1.011	f
	a v e r a g e:	1.062	

$g = \Delta \log k / \Delta \mathrm{pH}$

Table III

Determination of E_a and d

[HCl] *N*	t, °C	E_a kcal/mole	*d*	Determined by p = polarography, f = photometry
0.104	30—40	26.006	17.277	p
		26.366	17.485	f
	40—50	23.477	15.409	p
		26.653	16.952	f
	50—60	26.955	17.757	p
		24.441	16.131	f
0.0104	40—50	25.005	16.432	p
		28.200	18.671	f
	50—60	23.514	15.413	p
A v e r a g e:		25.513	16.725	

$$E_a = 2.303 \cdot R \frac{\Delta \log k}{\Delta\, 10^3/T}$$

$$d = \frac{\Delta \log k}{\Delta\, 10^3/T} \cdot \frac{1}{T_1} - \log k_{r1}$$

Results and discussion

The k value of inulin hydrolysis can be calculated from the following equation:

$$\log k = 1.062 \cdot \mathrm{pH} + 16.725 - 0.4343 \cdot 25513/1.987 \cdot T$$

The complete hydrolysis of inulin could be described as a result of two simultaneous reactions, but for that it would be necessary to know the value of k_{in} in each case.

From the experimental data it can be established that the first stage — in which k steadily increases — lasts until 20 or 25% of the hydrolysis has occurred. At higher than 25% hydrolysis, *i.e.* when $\overline{\mathrm{DP}} \approx 4$, k remains practically constant.

In the acid hydrolysis of inulin two problems will arise: the splitting mechanism of β-1,2 linkages, and the fact that with the progress of hydrolysis the rate constant keeps increasing. The splitting of ketofuranosides differs not only from the splitting of aldopyranosides, but also from that of aldofuranosides; the characteristic differences are shown in Table IV. On the other hand, the difference between the velocities of the acid hydrolysis of ketofuranosides and ketopyranosides is much smaller than in the case of aldosides. In the case of ketosides this is obviously explained by the formation of a tertiary carbonium cation as a result of the splitting of the glycosidic linkage. The values of the activation energy of furanosides and pyranosides are also similar [18] and substantially lower than in the case of aldopyranosides; also this fact suggests that the splitting mechanisms of ketopyranosides and ketofuranosides are similar.

The rapid hydrolysis of aldofuranosides appears to be explainable by A-2 mechanism. This conclusion is based on the fact that their entropies of activation are negative [19]. In this case it is conceivable that the furanoside ring, existing in an almost planar form, will have a transition state in which both groups are simultaneously present: the leaving group and the incoming group (Fig. 5) that is to say, the rate-determining step of the reaction will be the bimolecular attack of the entering group [20].

In the case of inulin, and in general, in ketoglycosides, the glycosidic carbon atom is so "crowded" that the above mechanism is not conceivable; the values of activation entropy do not indicate such a mechanism. Therefore the splitting mechanism of the β-1,2 linkages of inulin is, in all probability, identical with the splitting mechanism of sucrose and raffinose [16]. The characteristic features (see Table V) are very similar.

This mechanism consists of the following steps (see Fig. 6):

(a) the ring-oxygen (*a*) or the bridge-oxygen (*b*) is protonated;

(b) the furanosyl–oxygen linkage is split as a result of the formation of a tertiary carbonium cation (*c* —*e* or *g*);

(c) the tertiary cation causes the heterolysis of a water molecule (*h*).

Table IV

Characteristics of the acid hydrolysis of aldo- and keto-furanosides and -pyranosides

Ring	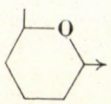 aldopyranoside	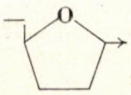 aldofuranoside	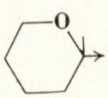 ketopyranoside	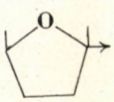 ketofuranoside
Change of ring conformation	yes	no	yes	no
Entropy of activation	positive	negative	positive	positive
The rate determining step	monomolecular	bimolecular	monomolecular	monomolecular
Order of magnitude of k_r, 100 °C min^{-1}	10^{-2}	10^{0}	10^{1}	10^{1}
The carbonium cation	secondary	secondary	tertiary	tertiary
Example	Me-β-D-glucopyranoside	Et-β-D-galactofuranoside	Me-β-D-fructopyranoside	sucrose
Ref.	[24]	[25]	[18]	[16]

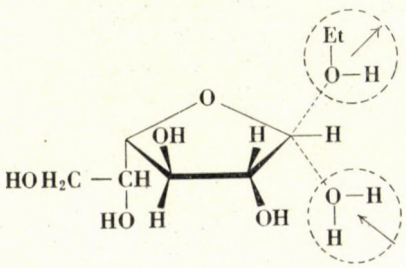

Fig. 5. Transition state

In the case of sucrose and raffinose, it has been proved by several arguments that fructose, and not glucose is the moiety which determines the stability of the bond and, in general, the characteristics of hydrolysis. The data obtained in the hydrolysis of inulin prove this hypothesis unambiguously: in this case glucose cannot play any role, while the characteristics of the hydrolysis are practically the same as in the case of sucrose and raffinose.

The available data do not allow to decide unambiguously whether the protonation of the ring-oxygen or the bridge-oxygen plays the decisive role (see Fig. 6). It seems probable that oxygen atoms can be protonated, but the protonated forms lead to the splitting of the bonds with different probabilities. The fact that the oxygen atoms of the ring and the bridge are competing for the

Table V

Characteristic data of the acid hydrolysis of sucrose, raffinose and inulin

	Sucrose	Raffinose	Inulin
k_r, 100 °C	56.36	48.75	71.40
E_a, kcal/mole	25.54	25.89	25.55
ΔS^+, e.u.	+8.07	+8.34	+8.13
g	1.038	1.033	1.062
d	16.82	16.95	16.72

proton, is proved by the hydrolysis of thiopyranosides. 1-Thiopyranosides are much more stable than O-pyranosides, because the S atom has less basic character than oxygen. Howewer, 5-thiopyranosides are hydrolyzed approximately 10 to 20 times more rapidly than pyranosides [22] as in this case there is no ring oxygen which would draw away one part of the protons available for the oxygen-bridge.

In the case of pyranosides the formation of a tertiary carbonium cation by diaxial elimination is not possible: hydrolysis can only occur by protonation of the bridge-oxygen. Howewer, in the case of ketosides the velocity of hydrolysis is greater by approximately three orders of magnitude than in the case of aldopyranosides, and from this diaxial elimination [21] and, indirectly a dominant role of the protonation of the ring-oxygen can be concluded. The acyclic *d—f* mechanism is improbable; there is no experimental proof for the existence of such a case.

The increase of the rate constant during hydrolysis, *i.e.* the dependence of k on $\overline{DP}$ may be caused by three factors:

(a) inductive effect

(b) conformational effect

(c) electrostatic shielding effect (impeding the protonation).

The existence of an inductive effect is possible, but its transfer along the chain seems to be improbable. In the case of an effect of this type, it should affect each oxygen-bridge equally causing identical changes in the electronic density.

The observation that at higher than 20—25% hydrolysis (approximately $\overline{DP} \approx 4$) the rate constant does not change any more, suggests that not only the reducing or non-reducing terminal groups are hydrolyzed more rapidly than the non-terminal bonds but, in general, the hydrolysis of the larger molecules is a slower process.

In the case of amylose and the homologues of maltose, as well as cellulose and homologues of cellobiose, the restriction of the conformation change of the

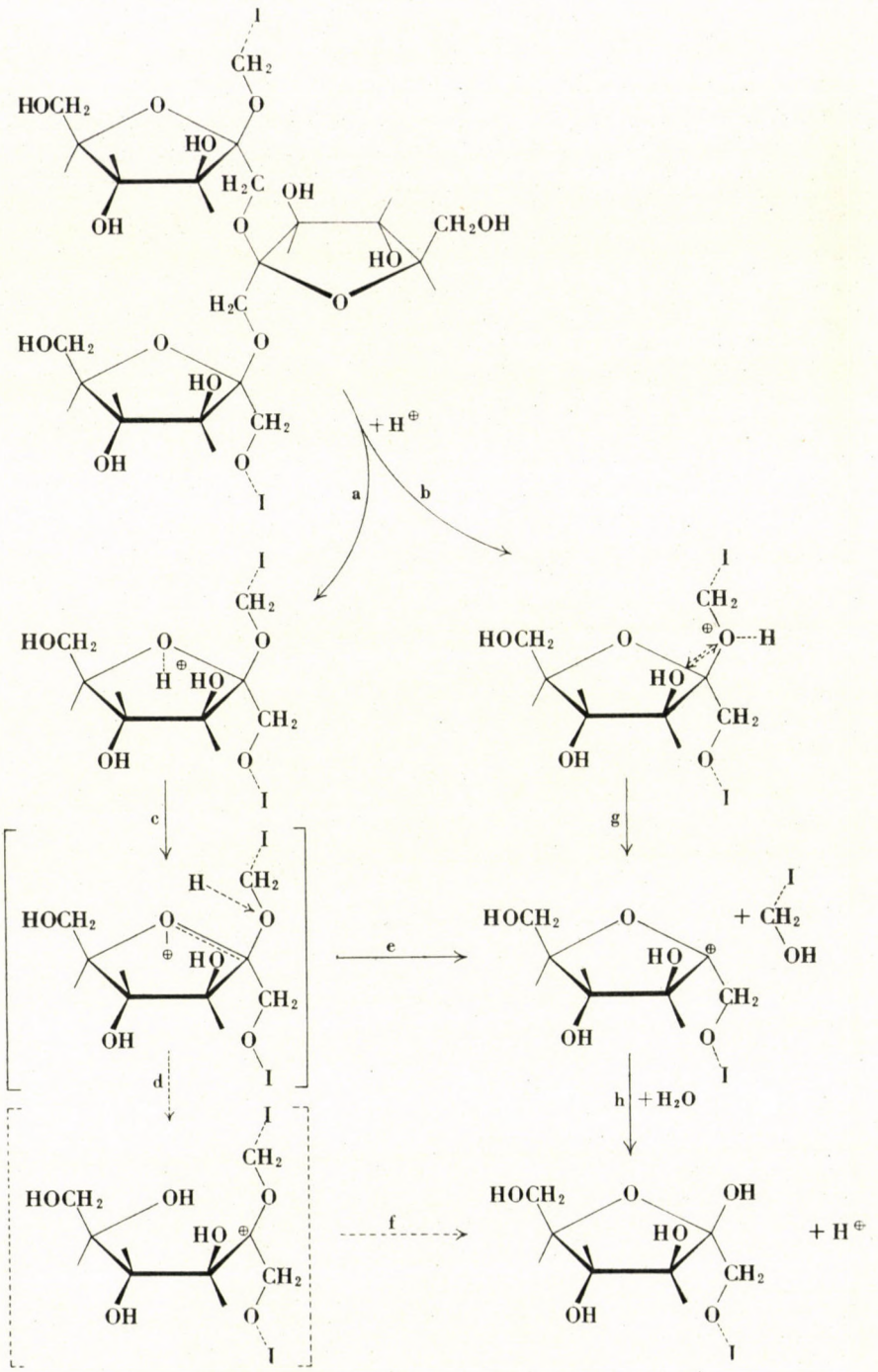

Fig. 6. Possible pathways of the hydrolysis

pyranose ring seems to explain the fact that the non-reducing terminal group is split more rapidly than the reducing one or, in general, non-terminal linkages [23].

The furanosid ring is almost planar; the formation of a tertiary carbonium cation requires neither a profound conformational change, nor a reorientation of the remaining parts of the chain molecule. Thus in this case the increase of k cannot be explained by a conformational effect. This propounds the question whether the increase of k is correctly attributed to a conformational effect in the case of amylose and the homologues of maltose, as well as in the case of cellulose and the homologues of cellobiose.

As we have published [16], in raffinose the splitting of the glucosyl–fructosyl bond is slower by about 19% than in sucrose. This may be accounted probably by the fact that a part of the bridge-oxygens between glucose and galactose are also protonated, depriving one part of the ring-oxygens from their protons, or electrostatically preventing their protonation. Presumably a similar mechanism causes the slower splitting of the non-terminal bonds in inulin.

Scrutinizing the properties of the aqueous solutions of inulin (viscosity and solubility) it can be ascertained that inulin does not form extended chains but rather random coils. Within the latter, the protonated parts electrostatically prevent the fixation of new protons, while this effect is much weaker in the vicinity of the terminal groups.

REFERENCES

1. Adams, M., Richguner, K., Hudson, C. S.: J. Am. Chem. Soc. **65**, 1969 (1943)
2. Micheel, F.: Chemie der Zucker und Polysaccharide. Akademie Verlag, Leipzig, 1956
3. Ohlmeyer, P., Pringsheim, P.: Chem. Ber. **66**, 1292 (1933)
4. Pigman, W., Goepp, R. M.: The Carbohydrates, p. 290. Academic Press, New York, 1957
5. Rominskij, I. R., Sushkova, A. S.: Biokhimija **19**, 261 (1954)
6. Holló, J., Szejtli, J., Tóth, M., Gantner, G. S., Kun, A.: Stärke **14**, 404 (1962)
7. Schlubach, H. H., Knoop, H.: Ann. **504**, 20 (1933)
8. Täufel, K., Steinbach, K. J.: Nahrung **2**, 631 (1958)
9. Thies, H., Souci, S. W., Kallinich, G.: Z. Lebensm. Unters.-Forsch. **96**, 41, 83 (1953)
10. Knoop, H.: Ann. **520**, 34 (1935)
11. Abdel-Akher, M.: Alexandria J. Agr. Res. **6**, 13 (1958)
12. Rominskij, I. R., Sushkova, A. S.: Ukrain. Khim. Zh. **26**, 753 (1960)
13. Dedonder, R., Bertrand, G.: Compt. rend. séances acad. sci. **230**, 548, 997 (1950); **232**, 1134 (1951)
14. Täufel, K., Steinbach, K. J.: Nahrung **3**, 832 (1959)
15. Senju, R., Shimizu, M.: Nippon Nogeikagaku Kaishi **25**, 298 (1951—52); C. A. **47**, 7872 (1953)
16. Szejtli, J., Henriques, R. D., Castiñeira, M.: Acta Chim. Acad. Sci. Hung. **66**, 219 (1970)
17. McDonald, E. J.: Adv. Carbohydrate Chem. **2**, 253 (1946)
18. Heidt, L. J., Purves, C. B.: J. Am. Chem. Soc. **60**, 1206 (1938)
19. Capon, B., Thacker, D.: J. Am. Chem. Soc. **87**, 4199 (1965)
20. Green, J. W.: Adv. Carbohydrate Chem. **21**, 95 (1966)
21. Ferguson, L. N.: The Modern Structural Theory of Organic Chemistry. Prentice-Hall, Englewood Cliffs, New Jersey, 1963

22. WHISTLER, R. L., VAN ES, T.: J. Org. Chem. **28,** 2303 (1963)
23. SZEJTLI, J.: Kémiai Közl. Budapest **31,** 59 (1969); Stärke **18,** 274 (1966)
24. SZEJTLI, J.: Acta Chim. Acad. Sci. Hung. **56,** 175 (1968)
25. OVEREND, W. G., REES, C. W., SEQUEIRA, J. S.: J. Chem. Soc. **1962,** 3429

József SZEJTLI; Chinoin Pharmaceutical and Chemical Works Ltd., Budapest

Ruth Daisy HENRIQUES, Mirtha CASTIÑEIRA } Escuela de Bioquimica-Farmaceutica, Universidad de La Habana, La Habana, Cuba.

Acta Chimica Academiae Scientiarum Hungaricae, Tomus 70 (4), pp. 391—394 (1971)

THE SYNTHESIS OF 1,2-DIISOBUTOXYBENZENE

(SHORT COMMUNICATION)

J. EGRI, J. HALMOS and J. RÁKÓCZI

(United Pharmaceutical Works, Budapest)

Received October 14, 1970

1,2-diisobutoxybenzene can be prepared in high yields by the alkylation of pyrocatechol with isobutyl arylsulfonates, *e.g.* isobutyl benzenesulfonate. The product is very pure and can be nitrated to 1,2-diisobutoxy-4-nitrobenzene in satisfactory yield.

The dialkyl ethers of pyrocatechol are intermediates in the preparation of 3,4-dialkoxyanilines, which latter are the starting materials of quinoline derivatives of great therapeutical importance.

In this paper, our experiences obtained in evolving an economical process suitable for the industrial production of 1,2-diisobutoxybenzene (pyrocatechol diisobutyl ether) are reported.

In the literature, several methods are given for the preparation of phenol ethers [1, 13, 14]. Alkyl halides are very often used for the alkylation of pyrocatechol. The use of straight-chain alkyl halides up to four carbon atoms gives the diethers [2] in high yields, while in alkylations with branched chain alkyl halides the yields are significantly lower. Etherification of pyrocatechol with isopropyl bromide and isobutyl bromide gives the product in yields of 47 and 33%, respectively [3, 4, 5, 6, 7]. In the present work, the possibilities of preparing 1,2-diisobutoxybenzene in high yield were investigated.

Results and discussion

Etherification with isobutyl bromide

The alkylation of pyrocatechol with isobutyl bromide was studied in different solvents. Unsatisfactory results were obtained in these experiments. This fact is demonstrated by some examples shown in Table I.

In alkaline medium, the etherification of pyrocatechol is accompanied by the simultaneous decomposition of isobutyl bromide:

$$\begin{array}{l} CH_3-CH-CH_2-Br \\ \quad\quad | \\ \quad\quad CH_3 \end{array} \longrightarrow \begin{array}{l} CH_3-C=CH_2 \\ \quad\quad | \\ \quad\quad CH_3 \end{array} \qquad (1)$$

Table I

Influence of the solvent, temperature and pressure on the alkylation of pyrocatechol with isobutyl bromide

Solvent	Reaction temperature, °C	Pressure, atm.	Yield of 1,2-diisobutoxybenzene %
Aqueous ethanol	90	—	32
Aqueous ethanol	90	—	34*
Abs. dioxan	100	—	12
Abs. isobutanol	120	2	22
Abs. ethanol	150	2—2.5	33

*In the presence of 2 g of sodium toluene-*p*-sulfonate

A similar phenomenon was observed by OLSON *et al.* [8] in the alkylation of phenol with isopropyl bromide.

In the reaction of pyrocatechol and isobutyl bromide, the first step is the formation of 2-isobutoxyphenol:

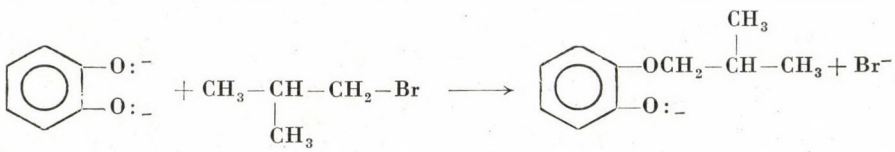

(2)

Reaction (2) is relatively rapid, taking place within 2—3 hours.

The next step is the formation of 1,2-diisobutoxybenzene:

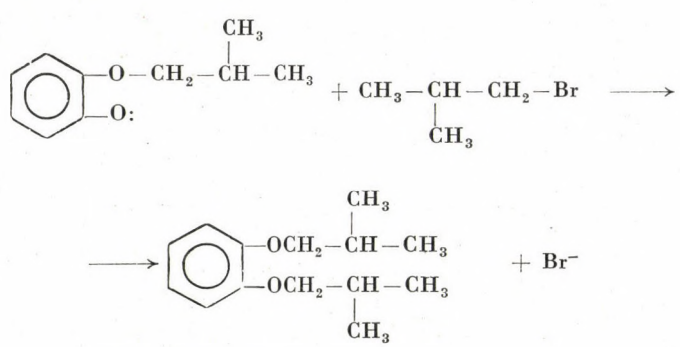

(3)

Reaction (3) proceeds considerably slower than reaction (2); this is probably due to steric hindrance.

Thus it can be seen that the reaction of pyrocatechol and isobutyl bromide involves two competitive reactions in the presence of alkali hydroxide. One of them — the formation of isobutene — is relatively rapid, while the formation of the diether, which is the desired compound, is slow. Therefore a better method of etherification was required.

Etherification with isobutyl arylsulfonate

When an isobutyl arylsulfonate, *e.g.* isobutyl *p*-toluenesulfonate or isobutyl benzenesulfonate is used as the alkylating agent instead of isobutyl bromide, the undesirable side-reactions are practically eliminated. Even with a small excess of arylsulfonic ester, if a sufficiently long reaction period is applied, 1,2-diisobutoxybenzene is obtained in satisfactory yields (80%, based on pyrocatechol). The yield can be increased to 85% by recovering 2-isobutoxyphenol from the mother liquor after the separation of 1,2-diisobutoxybenzene and by completing its alkylation, together with the pyrocatechol in the next experiment.

Arylsulfonic esters can be prepared from arylsulfonyl chlorides and isobutanol in the presence of a proper acid-binding agent (*e.g.* pyridine [9]), triethylamine or sodium carbonate [10], in high yields. In our case, the ether was synthesized according to the procedure given by PAGE and CLINTON [11], under somewhat modified reaction conditions. The 1,2-diisobutoxybenzene obtained was very pure and could be nitrated with conc. nitric acid in glacial acetic acid in high yield (87%).

When the mother liquor obtained after the separation of 1,2-diisobutoxybenzene is concentrated, potassium arylsulfonate can be recovered. This can be converted to the starting material, arylsulfonyl chloride, in a reaction with chlorosulfonic acid [12], in yields higher than 90%.

Experimental

Preparation of isobutyl benzenesulfonate

(A) 158 g (2.0 moles) of anhydrous pyridine was added dropwise during 3 hrs. to a mixture of 176.6 g (1.0 mole) of benzenesulfonyl chloride (containing 94% acid chloride) and 89 g (1.2 mole) of isobutanol (technical grade), under continuous stirring at 5 °C. The stirring was continued for another hour at 5 °C. Then the reaction mixture was mixed with 500 ml of 18% HCl, the ester was extracted with 3×100 ml of benzene, and the combined benzene phases were washed with water to neutral reaction. The benzene solution was dried over anhydrous magnesium sulfate, evaporated, and the product was fractionated at reduced pressure (1 mm Hg). The main fraction was collected between 110.5 and 112 °C. 182 g (91%) of isobutyl benzenesulfonate was obtained, $n_D^{20} = 1.4998$.

(B) A suspension of 85.0 g (0.8 mole) of anhydrous sodium carbonate in 111.2 g (1.5 mole) of isobutanol (technical grade) was heated to gentle reflux on an oil bath under continuous stirring, and 176.6 g (1.0 mole) of 94% benzenesulfonyl chloride was added dropwise to the mixture during 30 min. The mixture was stirred and further refluxed for 3 hrs., then cooled

to 20 °C. 300 ml of water was added, and the mixture was stirred until the inorganic salts dissolved. The ester produced was extracted with 3×100 ml of benzene, the combined benzene solutions were washed with water to neutral reaction, dried over magnesium sulfate and evaporated. 145 g (72.5%) of evaporation residue was obtained, which was suitable for the alkylation of pyrocatechol without fractionation.

Preparation of 1,2-diisobutoxybenzene with isobutyl benzenesulfonate

110 g (1.0 mole) of pyrocatechol (technical grade) was dissolved in 290 g ethanol. A solution of 84 g (1.5 mole) of potassium hydroxide in 140 ml of water was added under continuous stirring, the mixture was heated to reflux on an oil bath and 224.7 g (1.05 mole) of isobutyl benzenesulfonate was added by drops in 30 min. under gentle reflux. The mixture was refluxed for 3 hrs., and a solution of 84 g (1.5 mole) potassium hydroxide in 140 ml water and 224.7 g (1.05 mole) of isobutyl benzenesulfonate (in 30 min., under gentle reflux) were again added. The reaction mixture was further refluxed for 18 hrs., then cooled to 20—25 °C. The diether produced was extracted with 3×300 ml of benzene, the combined benzene solutions were dried over magnesium sulfate, evaporated and fractionated in vacuum (5 mm Hg). The main fraction was collected between 128 and 131 °C. 178 g (80%) of 1,2-diisobutoxybenzene was obtained, which solidified on standing for a few hours, m.p. 28—29 °C, $n_D^{30} = 1.4830$.

The aqueous mother liquor of the benzene extraction was acidified to pH 4—5 with conc. HCl, extracted with 3×50 ml of benzene, and the combined benzene solutions were dried over magnesium sulfate, evaporated and fractionated under reduced pressure (9 mm Hg). The main fraction was collected between 109 and 112 °C. 8.4 g of 2-isobutoxyphenol was obtained, m.p. 48—49 °C.

REFERENCES

1. Houben-Weyl: Chem. Meth. Org. Chemie, Bd. 6/3, p. 54
2. Collins, R. F., Davis, M.: J. Chem. Soc. Org. **1966,** 366
3. Belg. Pat. 640 906
4. Belg. Pat. 659 237
5. Belg. Pat. 670 520
6. DAS 1 238 476. West-German publication document
7. US Pat. 3 316 147
8. Olson, W. T., Hipsher. H. F., Buess, Ch. M., Goodman, I. A., Hart, I., Lamneck, J. H., Gibbons, L. C.: J. Am. Chem. Soc. **69,** 2451 (1947)
9. Braker, W., Pribyl, E. J., Lott, W. A.: J. Am. Chem. Soc. **69,** 866 (1947)
10. Slotta, K. H., Franke, W.: Ber. **63B,** 678 (1930)
11. Page, D. F., Clinton, R. O.: J. Org. Chem. **27,** 218 (1962)
12. Spriskov, A. A., Aparieva, N. V.: Zhurn. Obshej Khimii **20,** 1818 (1950); C. **1952,** 2656
13. Brown, W. G., Wilzbach, K. E., Urry, W. H.: Canad. J. Research (B) **27,** 398 (1949)
14. Irani, K. R., Phalnikar, N.L., Patel, N. Z., Chipalkati, H. R., Nargund, K. S.: J. Univ. Bombay **18,** Pt. 5, Sect. A. Sci. No. 27, 1 (1950)

János Egri
József Halmos
József Rákóczi
Budapest X., Keresztúri út 30—38.

Acta Chimica Academiae Scientiarum Hungaricae, Tomus 70 (4), pp. 395–412 (1971)

A STUDY OF DYNAMIC FOAMS

GY. SASVÁRI†, F. HITES and T. BLICKLE

(Research Institute for Technical Chemistry, Hungarian Academy of Sciences, Veszprém)

Received December 10, 1969; in revised form November 20, 1970

A study is first made of the elementary physical processes of bubble formation, and this is followed by an analysis of the foam state. The primary foam is formed by bubbles, the size and rate of ascent of which are determined by the physical properties of the liquid and the constants of the apparatus.

The term secondary foam is applied to that foam in which the continuous phase is no longer the liquid but the primary foam itself, and in which the much larger secondary bubbles ascend.

Based on this consideration, formulae are given for the calculation of the formal properties of dynamic foams.

The experimental method and results are reported, and the latter compared with the calculated results. As regards most parameters the agreement is surprisingly good; only in the case of the viscosity there was a considerable difference.

The method of dynamic foam formation is suitable for the intensification of processes between a liquid and a gas. By dynamic foam is understood a liquid–gas system of foam-like structure which is formed if gas is forced under pressure through the openings in the bottom plate into a liquid column. At first, depending on the amount of gas forced through per unit surface in unit time, only bubbles pass up, but then with the increase of the amount the structure is obtained which is called a dynamic foam. The name of this structure is derived from the fact that in contrast to stable foams the characteristic foam-like state is lost at once if the passage of gas is discontinued.

All types of transfer processes between the liquid and the gas in the dynamic foam state (including condensation and evaporation) are significantly accelerated because a very large internal surface is formed which is constantly renewed, while the relative rate difference between the gas and the liquid is also very great.

Processes with dynamic foam formation are spreading more and more in the chemical industry and recently in addition to transfer operations they have been used for liquid–liquid reactions, crystallization and other technologically important aims. The theoretical basis of the behaviour of dynamic foams has so far not been derived from an exact hydrodynamic model and the possibility of this is very slight. The authors who have dealt with the properties of dynamic foams until now have for the most part established empirical and

criterial equations to characterize the behaviour of dynamic foams. It is well known that such relations are capable of a good approximation of the true situation only in a narrow range of characteristics of the material and the apparatus. There have been authors who attempted to employ exact equations of theoretical hydrodynamics, but usable relations were not obtained.

In this paper an attempt is made to apply a transitional method of treatment in which, although the classical equations of hydrodynamics are not used, physically accurate relations are arrived at from some assumptions concerning the structure of the dynamic foam. It turns out from a comparison of many measurements and calculations, also given in this work, that with a few exceptions the agreement is good in the range of measurements between the theoretical values obtained from this working hypothesis and the actual experimental results.

The work comprises essentially two partially independent phenomena. As has already been mentioned, if gas is passed through a liquid column, then, depending on the gas rate, two significantly different structures arise. At low rates the gas passes through in the form of independent bubbles, and at high gas rates a dynamic foam is formed. The regularities of the two structures differ and the transitional state between the two is theoretically difficult to conceive. It is certain, however, that when the independently moving bubbles are present in such number that the liquid layer separating them is reduced to a film, then any further increase of the gas rate must involve the breaking of these films. Thus, if the proportion of bubbles approaches the structure of a spherical mass in a regular spatial arrangement, then the bubble state is terminated and the further increase of the rate leads to the dynamic foam state. Our working hypothesis does not give an adequate explanation of this transitional state.

An examination of the literature shows that the physics of dynamic foams has been dealt with primarily by Soviet research workers. Some of them used their measurements to establish empirical relations to describe the dynamic foam state, others described it in the form of criterial equations by the method of dimensional analysis or with the help of the Navier–Stokes equations [1—12]. USYUKIN and AXELROD [1] gave the pressure drop in the foam column by a suitable modification of the Bernoulli equation. Of the important parameters they considered the surface tension and the static pressure, but not the viscosity. Likewise setting out from the Bernoulli equation, MOLOKANOV [3] calculated the apparatus resistance in a foam column of the drip-through type. POZIN *et al.* [10] formulated the dependence of the foam column height and the resistance on the operational parameters in general functionalities. Correctly, the linear gas rate was found to be the determining parameter.

MUKHLENOV [11, 13] set out from the Navier–Stokes equations and have found that the characteristic parameters of the dynamic foam are in-

volved in the applied boundary conditions. A criterial equation in a stationary state was given for the foam height and the flow resistance.

Theoretical considerations

The principle of an apparatus containing the dynamic foam is shown in Fig. 1. The rapid gas stream introduced at the bottom of the column causes excellent mixing and a large internal surface, and hence the interaction between the gas and the liquid is very intense.

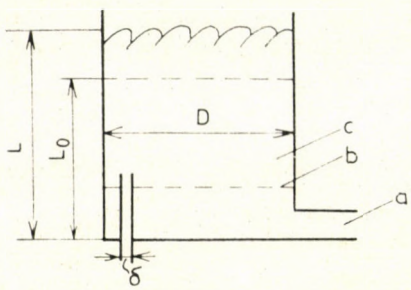

Fig. 1

The gas entering via the opening *a* passes into the liquid layer *c* through the perforated support *b* and forms a dynamic foam. The volume of the foam is substantially greater than that of the static liquid. Since the diameter D of the cylindrical vessel is constant, the ratio of the volumes is identical with the ratio of the foam column height L and the static liquid column height L_0.

The primary foam

Let us first consider the formation of the individual bubbles on the support. An opening in the support is selected with diameter δ. The gas forcing its way through this forms a blister above the support; this remains in contact with the gas space below the support through the opening until it breaks away from the support and rises in the form of a bubble. Directly after this the formation of the second bubble begins and the process is continuously repeated. The bubble diameter at which the upward force on the bubble is exactly equal to the adhesive force holding the bubble to the opening or to the support, which is proportional to the surface tension of the liquid, is called the critical diameter. The critical bubble diameter d_0 can be calculated by setting out from the formation mechanism shown in Fig. 2.

Fig. 2 depicts the environment of a support opening; the edge of the hole is rounded off and so the adhesive edge of the bubble can slide onto the surface of the support. The forming bubble assumes the form of a hemisphere because then the volume to surface ratio is a maximum. If the surface tension of the liquid is σ, then the adhesive force P can be expressed as:

$$P = \sigma d_0 \pi \tag{1}$$

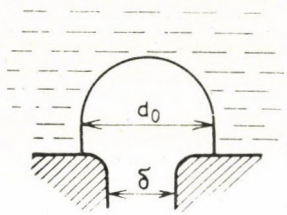

Fig. 2

If the density of the gas, which is about three orders of magnitude less than that of the liquid, is neglected, then the upward force F can be described by the following relation:

$$F = \frac{d_0^3 \pi}{12} \gamma \tag{2}$$

Since expressions (1) and (2) are identical, the critical bubble diameter d_0 is:

$$d_0 = \sqrt{\frac{12\sigma}{\gamma}} \tag{3}$$

It is necessary to deal separately with supports containing fewer but larger openings; here the bubbles forming simultaneously at two adjacent support openings attain a size corresponding to the critical diameter d_0 before their base circles reach one another and hence closely fill up the cross-section. In this case then, if the rate of passage of the gas is increased, the diameter of a primary bubble can increase to d_0' which is the distance between the centres of the adjacent holes. In such a support the critical diameter d_0 can be replaced by the distance d_0'.

Using other data for the support, the distance d_0 can be given as:

$$d_0' = \frac{\delta}{2} \sqrt{\frac{\pi}{\varepsilon_0}} \tag{4}$$

where δ is the diameter of an individual opening and ε_0 is the free cross-section of the support.

That material is called primary dynamic foam in which the ascending bubbles have average diameters d_0 and d_0' and completely fill the available volume.

We shall examine next the gas fraction $1 - x_0$ of the primary dynamic foam and the linear gas rate u_0 referring to the free cross-section at which this can be achieved.

The gas fraction of the foam is determined by the rate of ascent u of the primary bubbles and the gas rate u_0 according to the following equation:

$$u = \frac{u_0}{1 - x_0} \tag{5}$$

The rate of ascent of the primary bubble, however, can also be determined from the Bernoulli equation:

$$u = 2\sqrt{\frac{d_0 g}{3c_0}} \tag{6}$$

where c_0 is a flow resistance factor of the liquid towards the ascending bubble.

From Eqs (5) and (6) the gas proportion of the primary foam can be calculated:

$$1 - x_0 = \frac{u_0}{2}\sqrt{\frac{3c_0}{d_0 g}} \tag{7}$$

Let us consider the bubbles ascending in the primary foam as a mass of spheres of cubic spatial arrangement. Such a mass of spheres fills about half of the available volume. Such a packed arrangement of the bubbles, however, is not conceivable because this would mean the direct contact of the gas in the bubbles. For this reason the gas fraction of the primary foam, in agreement with the pertinent data, is always less than 0.4. If this value of the gas fraction is substituted into (7) with a suitable choice of the resistance factor c_0, then the value of u_0 is found to be less than 0.2 m/s.

In practice, 5—10 times higher linear gas rates are used in dynamic foam apparatuses and the gas fraction of the foam reaches 0.7—0.8.

The secondary foam

A foam is termed secondary if the linear rate v_0 of the forced-in gas is greater than the maximum linear gas rate u_0 relating to the primary foam. It follows from this that:

$$1 - x > 1 - x_0 \text{ and } v > u$$

Our working hypothesis for the further calculations is that the two phases in the secondary foam state are not the gas and the pure liquid as in the primary foam, but *the gas and the foam itself.*

As regards this assumption, Eqs (3) and (4) which express the critical bubble diameter must be suitably modified. Let us consider Eq. (3) valid in the form:

$$d = \sqrt{\frac{12\sigma'}{\gamma'}} \tag{8}$$

Here d is the critical bubble diameter of the secondary foam, σ' is the fictive 'surface tension' of the foam, and γ' is its density.

If it is assumed that the primary bubbles are arranged in a square planar configuration on the great circle of the secondary bubbles, then the number N of primary bubbles accommodated on the surface of the great circle is:

$$N = \frac{d^2\pi}{4d_0^2} \tag{9}$$

The adhesive force P in the secondary foam is calculated from the above equations and from (1):

$$P = d\,\sigma'\pi = \frac{d^2\pi}{4d_0^2}\,d_0\pi\sigma \tag{10}$$

From this equation the 'surface tension' of the secondary foam is:

$$\sigma' = \frac{d\pi}{4d_0}\,\sigma \tag{11}$$

If the liquid fraction of the foam is x, then its density γ' is trivially $\gamma \cdot x$.

Substituting the above γ' and (11) into expression (8) and rearranging for the critical bubble diameter of the secondary foam, the following expression is obtained:

$$d = \frac{3\pi\sigma}{d_0\gamma x} \tag{12}$$

If d_0 of (3) is substituted into expression (12), then:

$$d = \frac{\pi}{2x}\sqrt{\frac{3\sigma}{\gamma}} \tag{13}$$

If d_0 of (4) is used instead, then:

$$d = \frac{6\sigma}{\gamma\delta x}\sqrt{\pi\varepsilon_0} \tag{14}$$

We mention here what decides the alternative use of (13) and (14). If

$$\sqrt{\frac{12\sigma}{\gamma}} > \frac{\delta}{2}\sqrt{\frac{\pi}{\varepsilon_0}} \tag{15}$$

then (13) must be used, whereas if

$$\sqrt{\frac{12\sigma}{\gamma}} < \frac{\delta}{2}\sqrt{\frac{\pi}{\varepsilon_0}} \tag{16}$$

then (14) is the proper expression.

The diameter d of a bubble ascending in the secondary foam was also determined from the rate of ascent to be:

$$d = \frac{3}{4} c \frac{v_0^2}{g} \frac{1}{(1-x)^2} \tag{17}$$

Similarly to the considerations applied for the primary foam, the aim here is the expression of the gas fraction of the linear gas rate v_0. For this the right hand sides of (12) and (17) are made equal; after rearrangement we have:

$$\frac{x}{(1-x)^2} = 4\frac{g\sigma\pi}{cv_0^2 d_0\gamma} \tag{18}$$

Equation (18) is approximately valid because we have neglected that part of the gas flow which consists of the flow of primary bubbles always present. This neglect is justified because it is known from experience that the total volume of the primary bubbles in the dynamic foam state is a very small fraction of the total volume of the secondary bubbles.

In addition, Eq. (18) is only formal because if the resistance factor c depends on the Re number, then it also contains the diameter d and the rate of ascent v.

Derivation of equations suitable for practical calculations

Equation (18) was still unsuitable for actual calculation because the general resistance factor c which appears in it contains both the liquid fraction and the rate v_0.

We now turn to the use of a definite resistance factor, and set out from the following structure reminiscent of the Allen factor:

$$c = \alpha \sqrt{\frac{\nu'}{vd}} \tag{19}$$

The kinetic viscosity ν' of the secondary foam is defined by:

$$\nu' = x\nu + (1-x)\,\nu_g \tag{20}$$

For easier handling, however, we work with an integral average, and instead of (20) we use:

$$\nu' = \beta\nu \tag{21}$$

where

$$\beta = \frac{1}{x_2 - x_1} \int_{x_1}^{x_2} \left[x - \frac{\nu_g}{\nu}(1-x) \right] dx \tag{22}$$

Rewriting (19) according to this, we obtain:

$$c = \alpha \sqrt{\frac{\beta\nu(1-x)}{v_0 d}} \tag{23}$$

Let us substitute the resistance factor according to (23) into (17) expressing the bubble diameter:

$$d = \left(\frac{3\alpha}{4g}\right)^{2/3} \left(\beta\nu\right)^{1/3} \frac{v_0}{1-x} \tag{24}$$

By putting (14) and (24) equal we obtain the liquid fraction x and the gas fraction $1-x$:

$$x = \frac{k}{v_0 + k}\ (a); \qquad 1 - x = \frac{v_0}{v_0 + k}\ (b) \tag{25}$$

Here

$$k = \left(\frac{4g}{3\alpha}\right)^{2/3} \frac{1}{(\beta\nu)^{1/3}} \Delta \tag{26}$$

and in the latter

$$\Delta = \frac{\pi}{2} \sqrt{\frac{3\sigma}{\gamma}} \qquad \text{if (15) holds} \tag{27}$$

and

$$\Delta = \frac{6\sigma}{\delta\gamma} \sqrt{\varepsilon_0 \tau} \qquad \text{if (16) holds} \tag{28}$$

The expressions (25), however, still do not include the wall correction; neither do they take into account that in the lowest and uppermost layers of the real foam column the derived relations do not hold and because of this the gas fraction also depends on the height L_0 of the static liquid column.

Consideration of the effect of the foam column height

If gas is forced through a thin liquid layer, then the result can only be regarded as foam if its height is greater than 2 bubble diameters; according to the above this latter is determined by the gas rate, the material properties of the liquid, and the geometry of the support. If the height of the liquid layer is less than this, then it contains practically no enclosed and ascending bubbles on which the entire model is based. If the layer height is less than d, then only bubbles which are just forming or are already bursting can exist in it and the gas spaces below and above the foam are in direct contact. Such a degenerate foam is essentially no more than a thickened support, and so we must include the measured height of the foam layer, the anomalous lower layer amounting to about d, and also the foaming out at the top of the layer; because of this the actual expansion of the layer is larger than that given by (25). We proceed by multiplying expression (25a) for the liquid proportion by a factor f_1 (smaller than unity):

$$f_1 = \frac{L}{L+\zeta d} \tag{29}$$

According to (11), (26) and (27):

$$f_1 = \frac{L_0}{L_0+\zeta \Delta} \equiv w \tag{30}$$

That is, f_1 is independent of the expansion of the layer. Taking this correction into account, equation (25a) becomes:

$$x = \frac{wk}{v_0+k} \tag{31}$$

while (25b) becomes:

$$1 - x = \frac{v_0+(1-w)k}{v_0+k} = A \tag{32}$$

Consideration of the wall effect

With the decrease of the diameter of the apparatus and with the increase of the viscosity of the liquid, the relative thickness of the boundary layer adhering to the wall of the vessel increases; its free movement is impeded and

hence it keeps the ascending bubbles at a distance from itself. According to the pertinent theory, the ratio of the laminar boundary layer and the tube diameter is inversely proportional to the square root of the Re number:

$$\frac{\vartheta}{D} = \mu \sqrt{\frac{v'}{vD}} \tag{33}$$

Substituting according to (21) and (26), (33) becomes:

$$\frac{\vartheta}{D} = \mu \sqrt{\frac{\beta v x}{kD}} \tag{34}$$

The boundary layer of thickness ϑ is bubble-free pure liquid, and hence the gas fraction expressed by (32) must be multiplied by a factor

$$f_2 = 1 - \mu \sqrt{\frac{\beta v x}{kD}} \tag{35}$$

Let us denote the right hand side of (32) by A, when the modified gas proportion is:

$$1 - x = \left(1 - \mu \sqrt{\frac{\beta v x}{kD}}\right) A \tag{36}$$

The remodified and final gas proportion can be expressed explicitly from (36):

$$1 - x = 1 - \left(\frac{\varphi A}{2} + \sqrt{\left(\frac{\varphi A}{2}\right)^2 + (1 - A)}\right)^2 \tag{37}$$

where

$$\varphi = \mu \sqrt{\frac{\beta v}{kD}} \tag{38}$$

(37) is the final equation of the calculation. This contains every important parameter affecting the behaviour of the foam layer and also the layer height and wall corrections. It will be used for the description of our experimental results. With a knowledge of the gas fraction it is also possible to calculate the average bubble radius from (13) and (14), and from this in turn the specific internal surface of the foam can be determined.

3. Experimental method

The apparatuses shown in Fig. 3 were assembled for the hydrodynamic study of the foam column.

The apparatuses were set up from foam column units provided with three studs and supported by plastic clamps; the internal diameter D was 4.9 cm and the length 20 cm.

The volume flow rate of the gas V was measured with a rotameter.

The difference in the liquid column of an inclined tube micromanometer filled with alcohol was read off to determine the resistance of the dry plate.

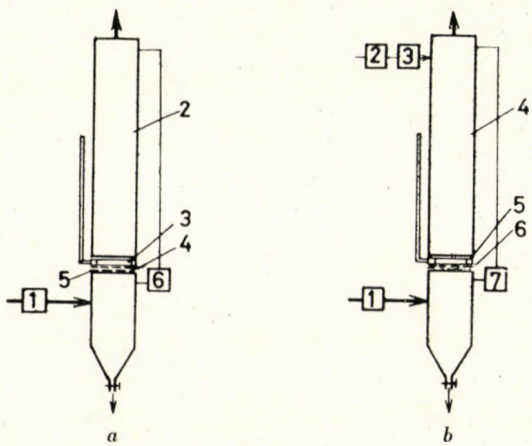

Fig. 3

a. Apparatus for the study of cross-flow foam column

1. Meter (air)
2. Foam column body with cm scale
3. Manometer for measurement of foam resistance
4. Perforated plate
5. Screening cloth
6. Manometer

b. Apparatus for the study of reverse-flow foam column

1. Meter (air)
2. Liquid feeder
3. Meter (liquid)
4. Foam column body with cm scale
5. Manometer for measurement of foam resistance
6. Perforated plate
7. Manometer

The amount of liquid in the foam state was determined by measurement with a graduated cylinder.

The foam height was determined visually in all cases using the cm scale on the apparatus.

Compressed air from the network was used as the flowing gas; the linear rate of this calculated for complete cross-section was varied between 0.2 and 1.6 m/s in 10 steps. In every case three parallel measurements were made.

The data for the perforated supports can be found in Table I.

The resistance of the foam layer and the gas volume proportion were studied in the following cases:

1. Experiments were carried out using $V = 100$ cm^3 water with plates 2/1—14—5/10—14 and 3/3—11—3/3—16.

2. With $V = 20$—200 cm^3 water, the amount of water was changed in 10 steps; plate 3/3—14 was used.

3. Experiments were carried out with plates 5/1—14, 5/10—14, 2/1—14 and 2/10—14 using 40, 60 and 200 cm^3 water.

Table I

Plate	y (cm)	d (cm)	n	m (cm)	ε_f (%)
2/1—14	0.10				
2/2—14	0.20				
2/3—14	0.32	0.20	88	0.40	14.71
2/6—14	0.66				
2/8—14	0.84				
2/10—14	1.09				
3/1—14	0.10				
3/2—14	0.20				
3/3—14	0.32	0.30	39	0.65	14.67
3/6—14	0.66				
3/8—14	0.84				
3/10—14	1.09				
4/1—14	0.10				
4/2—14	0.20				
4/3—14	0.32	0.40	22	0.80	14.71
4/6—14	0.66				
4/8—14	0.84				
4/10—14	1.09				
5/1—14	0.10				
5/2—14	0.20				
5/3—14	0.32	0.50	14	1.00	14.63
5/6—14	0.66				
5/8—14	0.84				
5/10—14	1.09				
3/3—1			1		0.37
3/3—2			2	0.30	
3/3—3			2	0.50	
3/3—4			2	0.80	
3/3—5	0.32	0.30	2	1.30	0.75
3/3—6			2	2.30	
3/3—7			2	3.30	
3/3—8			2	0.60	
3/3—9			2	0.70	
3/3—10			2	1.00	
3/3—11			12	1.20	4.51
3/3—12			20	1.00	7.51
3/3—13	0.32	0.30	30	0.75	11.22
3/3—15			50	0.55	18.70
3/3—16			60	0.45	22.44

4. With plate 3/3—14, the effects of the viscosity and density of the liquid were studied on the resistance of the foam layer and the gas volume fraction.

5. The effects exerted on the resistance of the foam layer and the gas volume fraction by the surface tension of the liquid were studied with plates 3/3—11, 3/3—12, 3/3—13, 3/3—14, 3/3—15 and 3/3—16.

6. The foam layer resistance and the gas volume fraction were studied with the plate 3/3—14 using 10 different concentrations of H_2SO_4.

The characteristic data of the solutions used are given in Table II.

Table II

Liquid	c (%)	γ (kp/m^3)	η (cP)	σ (dyn/cm)
Water		1000	1.10	73
Glycerine–water mixture	10	1022	1.31	
	20	1047	1.77	
	30	1073	2.50	
	40	1099	3.75	
	50	1126	6.05	
	60	1154	10.96	
Thelen solution		1200		
		1400		
		1600		
		1800		
		2000		
Ethanol–water mixture	2	994	1.2	63
	6	988	1.4	53
	14	977	1.8	43
	30	954	2.7	33
	96	801	1.3	23
Sulfuric acid–water mixture	10	1070	1.12	73.5
	20	1140	1.38	74.3
	30	1220	1.82	75.5
	40	1300	2.48	76.6
	50	1400	3.58	77.0
	60	1500	5.52	76.1
	70	1610	9.65	74.1
	80	1730	23.20	71.4
	90	1810	23.10	63.2
	96	1840	23.90	56.8

The average bubble diameter and the specific surface of the foam calculated from (37) using (13) and (14) are shown in Figs 4 and 5, respectively, as functions of the linear gas rate

Study of the agreement with the experimental data

The results obtained with the equations derived above which were suitable for practical calculations were compared with experimental data.

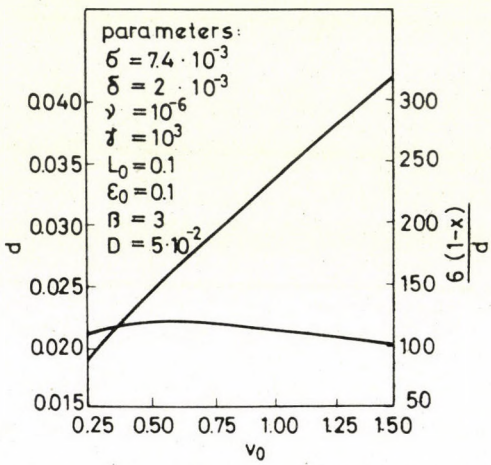

Fig. 4. Average bubble diameter and specific surface of foam calculated from Eqs (37) and (13) *vs.* linear gas rate

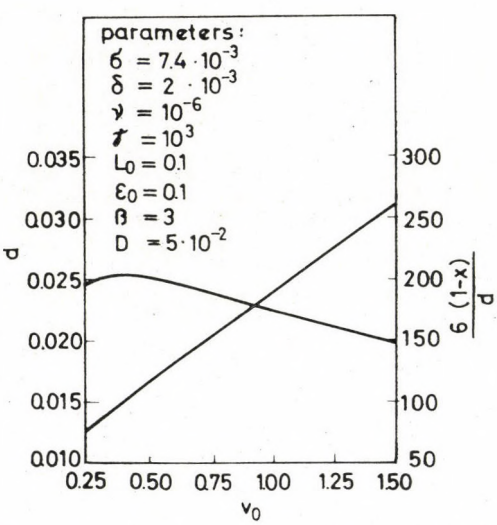

Fig. 5. Average bubble diameter and specific surface of foam calculated from Eqs (37) and (14) *vs.* linear gas rate. Variable v_0

The agreement of the measured (individual points) and calculated (continuous curve) gas fraction values as a function of the linear rate v_0 of the gas is shown

in Fig. 6, as a function of the opening diameter in Fig. 7, as a function of the opening fraction of the perforated support in Fig. 8, as a function of the

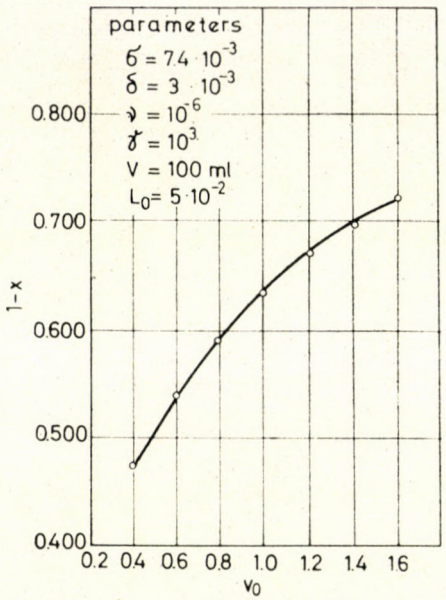

Fig. 6. Gas fraction of foam *vs.* linear rate of forced-in gas. Variable v_0

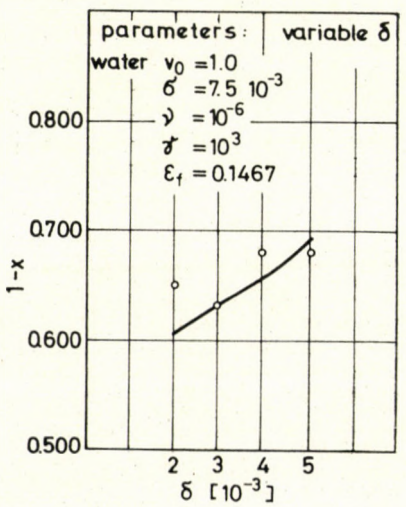

Fig. 7. Gas fraction of foam *vs.* opening diameter. Variable δ

surface tension of the liquid in Fig. 9, as a function of the liquid volume in Fig. 10, and as a function of the viscosity of the liquid in Fig. 11.

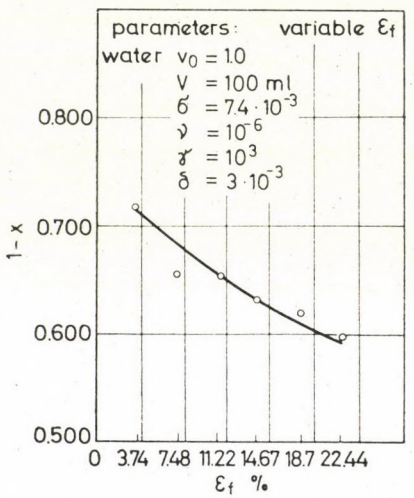

Fig. 8. Gas fraction of foam *vs.* fraction of openings. Variable ε_f

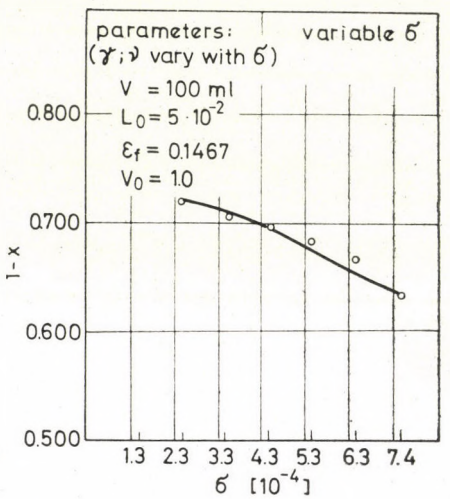

Fig. 9. Gas fraction of foam *vs.* surface tension. Variable σ

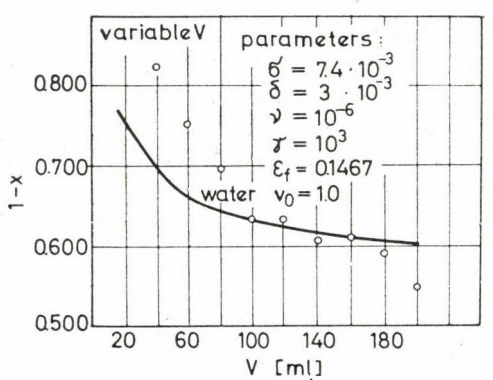

Fig. 10. Gas fraction of foam *vs.* volume of liquid. Variable V

Figs 10 and 11 show that corrections (29) and (33) should be improved. The existence of the maximum in Fig. 11 follows from (37) and here there is a need for further experiments.

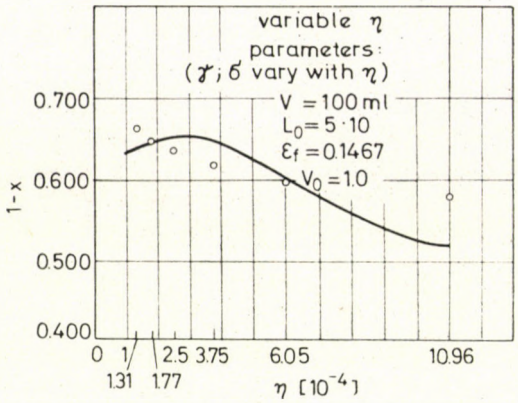

Fig. 11. Gas fraction of foam *vs.* dynamic viscosity. Variable η

LIST OF SYMBOLS

$\varDelta$	density of primary foam (kp/m³)
γ'	density of secondary foam (kp/m³)
γ_g	gas density (kp/m³)
$\varDelta p$	capillary depression (kp/m³)
δ	opening diameter (m)
ε	surface fraction remaining free
ε_0	support free cross-section fraction
ε_f	fraction of openings
ζ	formal resistance of support
ϑ	boundary layer thickness (m)
ν	kinematic viscosity (m²/s)
σ	liquid surface tension (kp/m)
σ'	fictive 'surface tension' of secondary foam (kp/m)
c	general resistance factor
c_0	liquid flow resistance factor (towards the ascending bubbles)
d	secondary foam critical bubble diameter (m)
d_0	bubble diameter (m)
d_0'	distance between centres of adjacent holes (m)
p	hydrostatic pressure (kp/m²)
p'	dynamic pressure of gas passing through opening
u	rate of ascent of primary bubble (m/s)
u_0	linear gas rate referring to free apparatus cross-section (m/s)
v	rate of ascent of bubble in secondary foam (m/s)
v_0	linear rate of forced-in gas (m/s)
v_f	linear rate of water flow (m/s)
x	liquid fraction of foam
D	apparatus diameter (m)
F	lifting force (kp)
L	foam column height (m)
L_0	static liquid column height (m)
P	adhesive force (kp)

REFERENCES

1. USYUKIN, I. P., AXELROD, L. S.: Kislorod No. 1, p. 1, and No. 2, p. 5 (1949)
2. POZIN, M. E., MUKHLENOV, I. P., TUMARKINA, E. S., TARAT, E. Y.: Penniy sposob obrabotki gazov i zhidkostyei. Goskhimizdat, Leningrad (1955)
3. MOLOKANOV, Y. K.: Khim. Prom., **38,** 291 (1962)
4. POZIN, M. E., MUKHLENOV, I. P., TUMARKINA, E. S., TARAT, E. Y.: Zhurn. Prikl. Khim., **27,** 13 (1954)
5. KOVALY, ZH. A.: Dissertation MHTI (1954)
6. KUZMINIH, I. N., AXELROD, L. S., KOVALY, ZH. A., RODIONOV, A. I.: Zhurn. Khim. Prom., No. **2,** 86 (1954)
7. KUZMINIH, I. N., RODIONOV, A. I.: Tr. MHTI No. **18,** 109 (1954)
8. POZIN, M. E., MUKHLENOV, I. P.: DAN SSSR, Novaya seriya, 92nd publication, No. 2, p. 393 (1953)
9. AXELROD, L. S., DILMAN, V. V.: Zhurn. Khim. Prom., No. **1,** 28; No. **9,** 29 (1940)
10. POZIN, M. E., MUKHLENOV, I. P., TARAT, E. Y.: Zhurn. Prikl. Khim., **30,** 45 (1957)
11. MUKHLENOV, I. P.: Zhurn. Prikl. Khim., **30,** 1750 (1957)
12. HITES, F., BLICKLE, T.: Conference of Veszprém Scientific Establishments. Veszprém, 1968, p. 221
13. MUKHLENOV, I. P.: Dissertation. L. T. I. im. Lensovyeta (1955)

György SASVÁRI†
Ferenc HITES
Tibor BLICKLE
Veszprém, Schönherz Z. u. 10, Hungary.

RECENSIONES

I. GYENES: *Titrationen in nichtwäßrigen Medien*

701 pp. Akadémiai Kiadó, Budapest, 1970

The idea that reactions occur not only in aqueous media, is for chemists nowadays not as strange as it was some decades ago. Nevertheless, the spreading of this new viewpoint and of the practical possibilities given by it has not been as quick as it would be desirable and reasonable. The effect of the inertia principle is reflected also in this field of development of chemistry. If we scrutinize the actual grounds of this effect, we can make some very important statements, which may also give help — as a diagnosis — to the setting of further tasks.

"The properties of electrically conducting systems" by KRAUS was published in 1922, "Elektrochemie nichtwäßriger Lösungen" by Walden in 1924, books which opened a new epoch in the chemistry of non-aqueous media; however, the time elapsed since then has not been enough to clarify the theoretical fundamentals of this new field. The book by I. GYENES published now on titrations in non-aqueous media still surveys this field so that some important parameters, such as solubility, are not quantitatively elaborated, which is a striking proof for the effectiveness of the inertia principle pointed out above.

The author regards his book as a fundamentally re-written and supplemented edition of his 10-year-old Hungarian and 3-year-old English publications. The book published in English was an enlargement of the Hungarian version to such an extent that the English edition can be considered a handbook as compared with the laboratory manual in Hungarian. The German issue expanded still further this character in its contents, up-to-dateness and treatment. To the four new chapters of the English edition ("Photometric endpoint", "Redox titration in non-aqueous media", "Titrations with complex formation in non-aqueous media" and "The determination of the alkoxyl group, carbamic acid esters, substituted phosphines and organosilicon compounds") still further chapters have been added in the German book enhancing its value to an extent which can hardly be overestimated. In the technical part the following chapters are new: "Konduktometrische Endpunktanzeige", "Oszillometrische Endpunktanzeige", "Differentielle polarographische Titration und dead-stop Methode", "Coulometrische Titrationen" and "Enthalpimetrische Endpunktanzeige". From among the new chapters of the practical part I should like to point out the following: "Bestimmung von Verbindungen, die alkoholische Hydroxylgruppen enthalten", where a new line is the catalytic acceleration of the processes applied in analysis.

Almost all chapters are somewhat extended. The theoretical principles are treated in greater detail, more exactly, and asserting broader viewpoints. The author illustrates the theoretical statements with a number of very useful examples. In the practical part a great many methods are given with full descriptions of the procedures and with detailed sketches of the equipment to be applied. The prescriptions are detailed and very accurate, also including hints which are usually missing in similar analytical handbooks.

The use of the book is greatly enhanced by a comprehensive discussion of the theoretical possibilities of the new field, enabling the chemist to take up a position also in cases which are not treated in the book. The tabulated compilations are demonstrative and instructive, because they contain the most important data. The reader has definitely the impression that the author has never forgotten his task that he must overcome a fairly great reluctance with his book. In doing this, he is especially successful in the introductory chapters, in discussing the competition between solvent and solute. The principle of competition is — in my opinion — a fundamental component of modern chemical thinking, but is perhaps nowhere so indispensable as in the case of reactions occurring in solutions. For the same reason the chapter "Zusammenhänge zwischen Acidität, Basizität und Molekülstruktur" is also very interesting.

The book lists 1330 literature references, which are by 432 more than those given in the English version, covering the literature up to 1967.

The book is complemented by a really interesting citation- and author index. First the literature references are listed in alphabetic sequence with increasing numbers. In the author index the corresponding page-numbers are given. This is completed with a subject index which gives a first class orientation and information about the abundant contents of the book.

The typographical presentation is still better than that of the English book, though a few reproductions are not perfectly clear.

The new book by I. GYENES represents a valuable further contribution to the chemistry of non-aqueous solvents, and will surely be of great help to those who are dealing with this field.

Z. G. SZABÓ

International Compendium of Numerical Data Projects. Produced by CODATA

295 pp. Springer-Verlag, Berlin—Heidelberg—New York, 1969

The studies in chemistry, physics and technology are in a process of immensely branching out. For being conversant at least with one's own field of research, one needs a lot of time to study a tremendous number of reviews and collect systematically the data coming from the most different sources. The effort against backwardness takes a considerable time originally devoted to research work. Research is aided to a great extent by the present Compendium, the material of which attempts to answer the following general questions:

What compilations containing critically evaluated data are now available; what centers or organizations produce or aid production of such data for publication on a continuing basis; what national programs exist for financial support and encouragement of data compilation; and what guidelines are available to compilers of all countries so that their products may be compatible.

The Compendium is divided into six chapters: In the first chapter the national data programs and the national committees for CODATA are enumerated. In the second one the centers covering a number of areas of science are discussed. The topics of the third chapter are: *Nuclear properties* (General nuclear properties, properties of neutrons, properties of nuclides, indexes), *Atomic properties and molecular properties* (Atomic properties including spectra, molecular properties including spectra, infrared and microwave spectra, Raman spectra, electronic spectra, mass spectra, NMR spectra, other atomic and molecular projects, indexes to compilations), *Solid state* (Crystallographic, mineralogical, electrical and magnetic, and related properties), *Thermodynamic and transport properties* (including thermophysical and solution properties, indexes to compilations), *Chemical kinetics*, *Gas Chromatographic Data*, *Optical properties* (Optical rotatory power: steroids, triterpenes, amino acids, alkaloids).

The entries in Chapter 3 of the Compendium, which is the most important part, are arranged under the following headings:

1. Organization, 2. Coverage, 3. Analysis and 4. Publications.

The first heading presents brief information about the organization under which the work is done, the second gives factual information as to the substances covered and their states, the properties covered and the range of variables if appropriate, and the period of time covered. Under the term "Analysis" an effort is made to present facts and observations that reflect the aims of the compiler in evaluating and distributing the results of his work. Under "Publications" information is given leading the user to the source of the publication and its cost.

In the fourth chapter the Compendium lists those new and secondary centers, which have had insufficient time to make their products available to the public. Some of these will in due course publish tables of data. Others are concerned, at least initially, with preparing complete bibliographies of pertinent papers for various fields. The main topics: Secondary nuclear data centers, colloid and surface properties, other specialized centers (high pressure, radiation chemistry, diffusion in metals and alloys, equilibrium constants in molten steel, molecular weights of polymers, electrolyte solutions).

In the fifth chapter handbooks are listed, giving only the necessary data without any evaluation. The sixth chapter (physical quantities, units and symbols, basic physical constants, nomenclature and related matters) gives a survey of national and international organizations which play a leading role in international scientific life related to the topics mentioned in the title. The most important issues are enumerated as well.

The volume is supplied by a detailed author and subject index. We welcome the Compendium of ICSU-CODATA with deep satisfaction and should like to call the attention of every library, research institute of natural sciences to this issue which is indispensable in scien-

tific and industrial lines alike, and can give valuable support to research work by its vast number of data.

We should like to quote the lines from the introduction written by Frederick D. Rossini, president of ICSU-CODATA, which makes the aim of the CODATA and the Compendium perfectly clear: "At the time of its establishment in 1966, by the International Council of Scientific Unions (ICSU), the Committee on Data for Sciences and Technology (CODATA) was given the basic mission of promoting and encouraging, on a worldwide basis, the production and distribution of compendia and other forms of collections of critically selected numerical data on substances of interest and importance to science and technology."

L. LÁNG

J. KORYTA, I. DVOŘÁK and V. BOHÁČKOVÁ: *Electrochemistry*

339 pp. + index. Methuen and Co. Ltd., London 1970

Persons active in the most varied branches of science, experts working in the most diverse fields of industry are confronted with electrochemical phenomena, and utilize the laws of electrochemistry in their everyday activity. Therefore, works dealing with this field of science are of great importance.

The book of KORYTA, DVOŘÁK and BOHÁČKOVÁ gives a short but almost complete survey of theoretical electrochemistry. Owing to its limited extent, some problems can be discussed only very briefly, but the list of references at the end of each chapter, comprising mainly general papers and monographs, partly fills this gap. The subdivision, the structure of the book is lucid, almost symmetrical. Of its four chapters the first two deal with electrolyte solutions (homogeneous electrochemical systems), while the third and fourth chapters discuss heterogeneous electrochemical systems. The first chapter treats the equilibria in electrolyte solutions, the second the transport processes occurring in electrolyte solutions, the third equilibria in heterogeneous electrochemical systems, and the fourth is concerned with processes in the latter systems (electrode processes).

Accordingly, the first chapter of the book deals with the structure of electrolyte solutions, the Debye—Hückel theory of strong electrolytes, the classical theory of electrolytic dissociation and equilibria, and with the acid–base theories.

In the second chapter ("Transport Phenomena in Electrolyte Solutions") phenomena produced by the passage of electric current through electrolyte solutions are discussed with a particular view to the diffusion of electrolytes, the methods for measuring the diffusion coefficient, and problems of convective diffusion. Within the scope of the latter, convective diffusion on the rotating disk and on an increasing sphere (dropping mercury electrode) are described.

The third chapter of the book treats equilibria established at the phase boundaries of electrochemical systems. In addition to metal-electrolyte equilibria, problems concerning membrane equilibria, glass electrodes and potentiometric methods are discussed. The structure of electrical double layers, important from the viewpoint of electrode processes is also treated.

The fourth chapter of the book is concerned with the kinetics of electrode processes. Among others, the authors succeeded in giving a short and lucid summary of transfer and concentration (diffusion) polarizations, and of the most important experimental methods in electrochemical kinetics. Finally, a few important electrode processes are described.

The book of KORYTA, DVOŘÁK and BOHÁČKOVÁ, written in a modern concept, is a valuable contribution to the literature on electrochemistry. It will facilitate for students and experts interested in and using electrochemistry to get acquainted with the fundamental theory of modern electrochemistry.

L. KISS

Carbohydrate Chemistry. Fortschritte der chemischen Forschung, Topics in Current Chemistry, Band 14, Heft 4

Springer Verlag, Berlin—Heidelberg—New York, 1970

Das 210 Seiten umfassende Heft enthält sechs Aufsätze über Kohlenhydratchemie, geschrieben von hervorragenden Wissenschaftlern auf diesem Gebiet. Diese berichten über neueste Ergebnisse in grundlegenden Themenkreisen, in denen auch gegenwärtig intensive Forschungsarbeit geleistet wird.

1. J. S. BRIMACOMBE: Some Recent Neighbouring-Group Participation and Rearrangement Reactions of Carbohydrates.

Die Wirkung der benachbarten Gruppen ist im Verlauf und in der Stereochemie der Substitutionsreaktionen von Kohlenhydraten von größter Bedeutung. Die Teilnahme von sauerstoff-, schwefel- und stickstoffhaltigen funktionellen Gruppen an den verschiedenen Reaktionen wird einzeln behandelt. Über die neuen Ringverengungsreaktionen der Zucker wird in einem besonderen Abschnitt berichtet.

In einem Umfang von nur 20 Seiten enthält der Aufsatz — kurz und gedrängt gefaßt — ein sehr reiches Material, mit verhältnismäßig viel (121) Formeln und 60 Literaturangaben.

Der Rezensent möchte sich eine einzige kritische Bemerkung erlauben: es fehlen die zusammenfassenden Auswertungen am Ende der einzelnen Absätze, so daß es dem Leser überlassen ist, Schlußfolgerungen zu ziehen.

2. R. J. FERRIER: Neuere Befunde über die Synthese von O-Glycosiden.

Der Aufsatz befaßt sich mit folgenden Fragen: Alkoholyse der Zucker, Glycosylierung mit Glycosylhaloiden sowie mit anderen Zuckerderivaten (Orthoester, 1,2-Oxazoline, Glycosylester, 1,2-Anhydride, ungesättigte Zuckerderivate), Probleme der Transglycosylierung und Anomerisation. Abschließend wird die Synthese der wichtigsten Glycosidentypen zusammenfassend behandelt. Die neuesten Methoden werden über 40 Seiten, mit 35 Formeln und 112 überwiegend neuen Literaturangaben an Hand interessanter Beispiele angeführt.

3. H. SIMON und A. KRAUS: Mechanistische Untersuchungen über Glycosylamine, Zuckerhydrazone, Amadori-Umlagerungsprodukte und Osazone.

Der Aufsatz liefert einen ausgezeichneten Überblick über das bezeichnete Thema. Die Bildung, die Struktur, die verschiedenen Umsetzungsreaktionen, die Mutarotation, die Hydrolyse, die Transglycosylierung und die Amadori- und Heyns-Umlagerung der Stickstoffglycoside sowie die Eliminierungsreaktionen der Zuckerhydrazone, die Zuckerformazane und die Bildung, Struktur und Reaktionen der Osazone werden ausführlich behandelt.

Der Aufsatz befaßt sich hauptsächlich mit der Frage der Reaktionsmechanismen; die früheren und neueren Ergebnisse werden kritisch behandelt und es werden viele offene Probleme auf Grund eigener Versuchsergebnisse gedeutet. Der 40 Seiten umfassende Aufsatz ist infolge des reichen und hervorragenden Formelmaterials und der hohen Zahl (141) der Literaturhinweise auf Originalarbeiten besonders wertvoll.

4. H. PAULSEN, H. BEHRE und C. P. HEROLD: Acyloxonium-Ionenumlagerungen in der Kohlenhydratchemie.

Diese sehr interessante und aktuelle Zusammenfassung gliedert sich auf folgende Weise: Es wird ein allgemeiner Überblick über die Acyloxoniumsalze der 1,2- und 1,3-Diole gegeben. Es werden die Umlagerungsreaktionen der Acyloxonium-Kationen bei Polyolen und Monosacchariden, die Umlagerung der Polyester und Monosaccharidester in flüssigem Fluorwasserstoff und die Umlagerung der Cyclite in Essigsäure-Schwefelsäure bzw. die Umlagerung der Saccharide in Lewis-Säuren behandelt.

Der 53 Seiten umfassende Aufsatz, einschließlich 251 Formeln und 72 Literaturangaben, ist klar und übersichtlich geschrieben.

5. M. CERNY und J. STANEK: 1,6-Anhydroaldohexopyranosen-Darstellung, Eigenschaften und Verwendung für Synthesen.

Der Aufsatz behandelt die Bildung und Herstellung von 1,6-Anhydroaldohexopyranosen und die allgemeinen Eigenschaften und Reaktionen dieser Verbindungen mit besonderer Rücksicht auf ihre Anwendung für Synthesen.

Die Epoxyderivate der 1,6-Anhydroaldohexopyranosen und die Glycosan-Analogen werden gesondert behandelt.

Die Literaturangaben (280 Hinweise auf Originalarbeiten) sind besonders reich und gut brauchbar. Der Aufsatz umfaßt 30 Seiten.

6. F. W. LICHTENTHALER: Branched-Chain Aminosugars and Aminocyclanols via Dialdehyde-Nitroalkane Cyclisation.

Auch dieser Aufsatz gibt einen guten Überblick des bezeichneten Gebietes.

Nach einer interessanten Einleitung wird die Chemie und Stereochemie der Cyclisierung mit Nitroäthan und Cyclisierung mit 2-Nitroäthanol, Äthylnitroacetat und zahlreichen Verbindungen vom Typ Nitromethylen behandelt.

Abschließend wird eine vorzügliche Zusammenfassung gegeben, worin der Verfasser auf die pharmakologische Bedeutung dieser leicht zugänglichen neuen Nitro- und Aminoderivate hinweist.

Der verhältnismäßig kurze Aufsatz (21 Seiten, mit 110 Formeln und 62 Literaturhinweisen) liefert einen interessanten und nützlichen Überblick über das behandelte Gebiet.

Das vorliegende Heft der Reihe schließt sich gleichrangig an die vorangegangenen wertvollen Veröffentlichungen der Reihe an und ist für Fachleute und Forscher auf dem Gebiet der Kohlenhydratchemie nicht nur äußerst nützlich, sondern geradezu unentbehrlich.

R. BOGNÁR

W. GUTMANN und E. HENGGE: *Allgemeine und anorganische Chemie*

362 Seiten. Verlag Chemie GmbH, Weinheim, 1971

Als Begründung ihrer Arbeit heben die Verfasser im Vorwort hervor, daß eine große Anzahl von deutschsprachigen Lehrbüchern der anorganischen Chemie für fortgeschrittene Studierende vorliegt, wogegen es an modernen und ihrem Umfang nach übersichtlichen Lehrbüchern für Grundstudien der allgemeinen und anorganischen Chemie mangelt. Dazu könnte noch hinzugefügt werden, daß der Mangel an derartigen Lehrbüchern eine Welterscheinung ist, und daß dies gerade für die ihr Studium beginnenden Studenten, für den Grundunterricht der Chemie an Hochschulen und Universitäten eine äußerst nachteilige Lage schafft.

Die beschleunigte Entwicklung der Kenntnisse, das Vordringen der physikalisch-chemischen Anschauungsweise in der anorganischen Chemie, die fortschreitende und äußerst wichtige industrielle Anwendung der besonderen mechanischen, elektrischen und magnetischen Eigenschaften der Festkörper sowie die Forschung neuer Werkstoffe benötigt eine theoretische Fundierung der anorganischen Chemie in breiterem Spektrum als früher, und zwar bereits auf der Studienstufe der Anfänger. Man könnte auch so formulieren, daß die stürmische Entwicklung der anorganischen Chemie notwendigerweise eine Umgestaltung der Thematik der allgemeinen Chemie zur Folge hat. Dies wird durch das vorliegende Buch gut illustriert. Es wird klar ersichtlich, daß eine Differenzierung zwischen der Thematik der allgemeinen Chemie und den anorganisch-chemischen Fundamentalkenntnissen immer weniger möglich ist.

Im ersten Abschnitt behandelt das Buch — neben den zur theoretischen Fundierung der anorganischen Chemie unbedingt benötigten minimalen physikalisch-chemischen Kenntnissen — größtenteils das Grundproblem der Strukturchemie, nämlich die Eigenschaften der chemischen Bindung. Die Anschauungsweise dieser Behandlung widerspiegelt treu die Ergebnisse der Quantenchemie und der modernen Strukturforschung. Die Verfasser betonen in diesem Abschnitt, wie aus den Kenntnissen über die Struktur der Stoffe auf die Stoffeigenschaften gefolgert wird und allgemeine Schlüsse und Zusammenhänge festgestellt werden. Diese werden dann in der ausführlichen Behandlung der anorganischen Chemie (im zweiten und dritten Abschnitt) reichlich illustriert. Ein besonders hervorzuhebender wertvoller Zug des Buches besteht in der sorgfältigen Selektion des Kenntnismaterials der anorganischen Chemie; demzufolge erhält der Leser ein umfassendes und modernes Bild über die Zusammenhänge der Elemente und Verbindungen.

Eine kurze Übersicht des Inhalts soll dem Leser dieser Rezension die Überprüfung des Werturteils erleichtern. Eine Einleitung von wenigen Seiten befaßt sich mit dem Zusammenhang zwischen der Chemie und den übrigen Zweigen der Naturwissenschaft, mit der historischen Entwicklung der Begriffe Stoff und Atom. Ein Unterkapitel von etwa 25 Seiten behandelt die Atomstruktur und das periodische System, und zwar in Form datenmäßiger Mitteilung, ohne die — meiner Meinung nach häufig störend wirkende — historische Entwicklung darzustellen. Der Leser erhält in diesem Abschnitt ein zwar nur qualitatives, jedoch modernes Bild über die Atomstruktur. Im Unterkapitel über die chemische Reaktion werden die Begriffe relative Atommasse, Molekularmasse, Formelgewicht, Stöchiometrie, Reaktionsenthalpie und Bindungsstärke, Reaktionsgeschwindigkeit und chemisches Gleichgewicht kurz (in insgesamt etwa 15 Seiten) behandelt. Im Unterkapitel über die chemische Bindung (30 Seiten) werden die Ionenbindung, der Ionenradius, die Ionisationsenergie, die Elektronenaffinität, die kovalente Bindung, die Molekülorbitale, das Wasserstoffmolekül, das hypothetische Heliummolekül, das Fluormolekül, das HF-Molekül, der kovalente Radius, die Hybridisation und die Stereochemie der Moleküle, die π-Bindung, die Molekülorbitale des N_2 und des O_2, die Elektronegativität, der Dipolcharakter des Moleküls, die Mehrzentrenbindung, die Theorie der metallischen Bindung, die Typen der Halbleiter behandelt. Das Thema des folgenden Unterkapitels (40 Seiten) ist der Stoffzustand. Hier werden die Phasenregel, der Gas- und Flüssigkeitszustand, die Zustandsgleichungen, die Gasgemische, Lösungen und Tensionsabnahme, die Gesetze der verdünnten Lösungen, die Destillation, sowie die Kennzeichen des Festzustandes: die Kristallstruktur, die Gitterenergie, die Madelungsche Konstante, das Zustandsdiagramm, Legierungen, reale Kristalle, der amorphe Zustand und der kolloide Zustand behandelt. Der Inhalt des Unterkapitels über Elektrolyte (23 Seiten) behandelt die elektrolytische Dissoziation

der Lösungsmittel, Ionenpaare, Löslichkeit und Löslichkeitsprodukt, Säure-Basen-Funktion, Pufferlösungen, Indikatoren, Säure–Basen-Titration, nichtwäßrige Lösungsmittel, Ionenaustauscher. Der nächste Teil (15 Seiten) befaßt sich mit der Oxydationszahl, den Redoxreaktionen, der Elektrolyse, dem Elektrodenpotential, dem Konzentrationselement, dem Redoxpotential, und den Disproportionierungsreaktionen. Dann werden (in 5 Seiten) die magnetischen Eigenschaften der Stoffe behandelt. Endlich wird der erste Abschnitt mit dem Unterkapitel über die Grundlagen der Koordinationschemie (13 Seiten) abgeschlossen: Donor–Akzeptor-Komplex, Chelat, Nomenklatur der Komplexe, Stereoisomerie, Koordinationschemie der Lösungen, Hybridisation in Komplexen, Ligandenfeldtheorie, oktaedrische und tetraedrische Komplexe.

Im zweiten Abschnitt (105 Seiten) werden die *s*- und *p*-Elemente und ihre Verbindungen, im dritten Abschnitt (85 Seiten) die *d*- und *f*-Elemente und ihre Verbindungen behandelt. Diese Abschnitte sind durch knappen, summarischen Stil, durch tabellarische Zusammenfassungen der physikalischen und chemischen Eigenschaften, durch Anwendung der Strukturkenntnisse und der Eigenschaftsfunktionen und durch die kritische Auswahl des Tatsachenmaterials gekennzeichnet; durch ihre Modernheit und Übersichtlichkeit bieten sie dem Leser mehr, als manche Lehrbücher der anorganischen Chemie mit mehrfachem Umfang.

Im Vorwort betonen die Verfasser, daß das Buch in erster Reihe nicht für die Selbstbildung gedacht ist, sondern ein Hilfsmittel zur Zusammenfassung ihrer Vorträge über allgemeine und anorganische Chemie darstellt. Der Rezensent ist der Meinung, daß dieses Lehrbuch nicht nur zu den einleitenden Studien der Chemiker, Chemielehrer und Chemieingenieure eine äußerst wertvolle Hilfe leistet, sondern auch in den Chemiestudien anderer Fachrichtungen: Physiker, Biologen, Geologen und verschiedenartigen Ingenieurstudenten erfolgreich verwendet werden könnte.

Wir begrüßen das Buch von V. GUTMANN und E. HENGGE weil seine Auffassung einen Ausweg aus dem Gewirr der infolge ihres Umfangs langsam unbrauchbar werdenden Lehr- und Fachbücher zeigt. Auch außerhalb des deutschen Sprachgebiets wird das Buch sicherlich hohes Interesse anregen und eine fruchtbare Wirkung ausüben.

B. CSÁKVÁRI

M. MOSER: *Grinding tools with ceramic bonding*

147 pp. Akadémiai Kiadó, Budapest, 1971

The selection of the theme of this work, which appeared as the 11th volume of the valuable series Silicate Chemistry Monographs, is fortunate and of current interest. Surface working by grinding finds increasing application in modern mechanical engineering technology, often replacing turning, cutting, planing, scraping. The theory of classical cutting has been developed during the past decades, whereas the the oryof grinding is still in the developmental stage, and even what is known is not readily available. It is characteristic that the bibliography of the book, comprising 100 references, does not cite any review, and could not have done so even if it wanted.

The historical survey and a brief general characterization of grinding tools are followed by a very detailed discussion of corundum grains (wear, microtexture, chemical and mineralogical structure, testing), and by a shorter description of carborundum and a few granular substances recently introduced.

Ceramic binding materials, their testing, bridges of binding materials, and the phase boundary properties of grinding grain-binder-air pore are treated extensively.

The chapter on the qualification of grinding tools is of practical importance.

The last chapter summarizes knowledge, yet in development, on the chemistry of grinding.

The principal merit of the monograph is its pioneering character. On the basis of the scattered subjects to be found in the literature, it forms a comprehensive entity of logical structure, which includes also the author's own testing results. The mode of discussion is lucid, the figures are of good quality and well selected. The description of results obtained with novel methods of testing (microprobe, acoustic methods) is noteworthy.

In summary, the monograph will be profitable to both producers and users of grinding tools, that is to say to ceramic experts and to mechanical engineers.

B. BEKE

INDEX

PHYSICAL CHEMISTRY – PHYSIKALISCHE CHEMIE – ФИЗИЧЕСКАЯ ХИМИЯ

ORGANIC CHEMISTRY – ORGANISCHE CHEMIE – ОРГАНИЧЕСКАЯ ХИМИЯ

CHEMICAL TECHNOLOGY – CHEMISCHE TECHNOLOGIE – ХИМИЧЕСКАЯ ТЕХНОЛОГИ

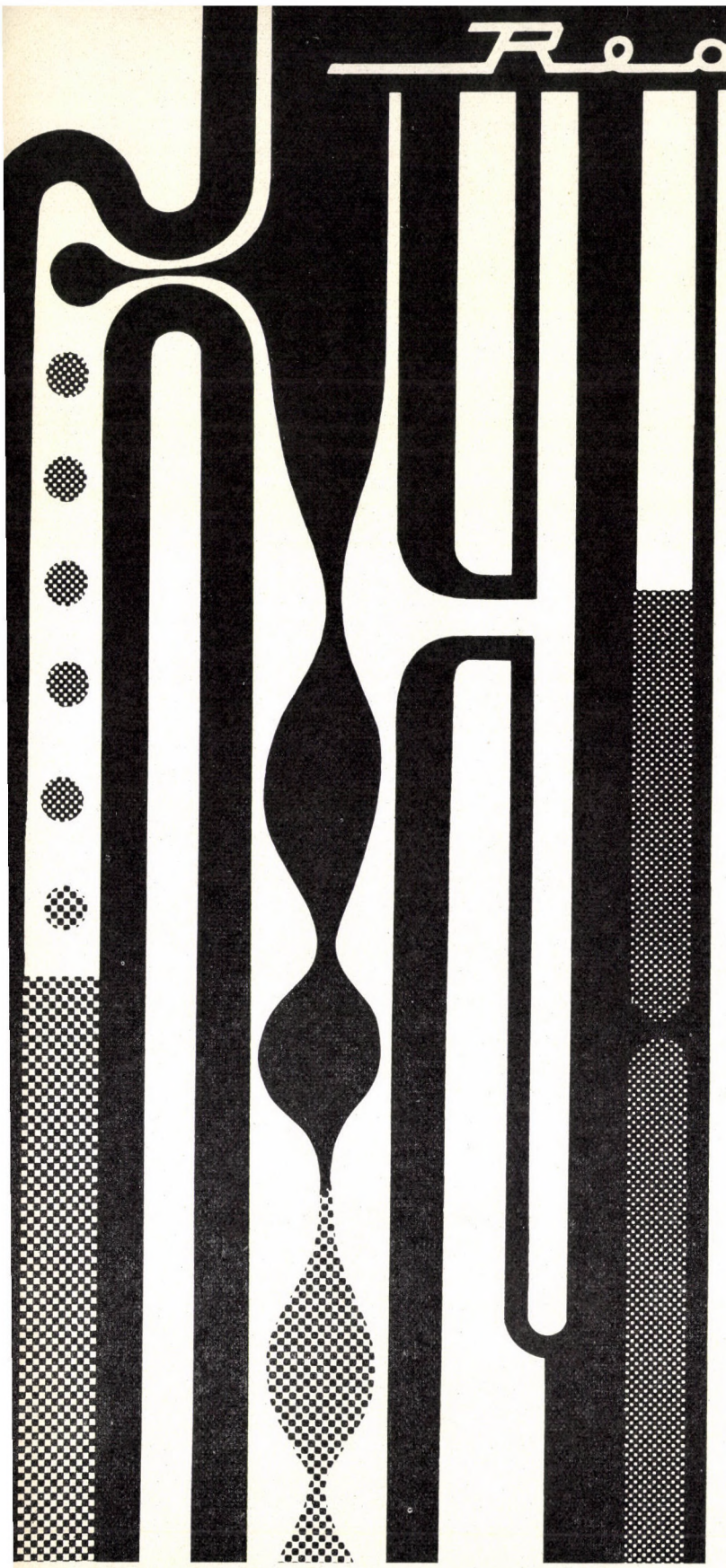

CHEMICALS FOR RESEARCH PURPOSES

Biochemicals

nucleosides, nucleotides
polynucleotides
enzymes
carbohydrates

Amino acids and derivatives

BOC-amino acids

Peptides and derivatives
Tetrazolium salts
Reagents for analytical use
Ion exchange celluloses and dextrans
ACRYLEX polyacrylamide gel for gelfiltration
CHROMEX resins for automatic analysis of amino acids and peptides

REANAL

Factory of Laboratory Chemicals Budapest

Exported by

MEDIMPEX

Hungarian Trading Company for Pharmaceutical Products

Budapest, 5 · P.O.B. 126
Telex 22—5477 · Hungary

ACTA CHIMICA

РЕЗЮМЕ

ТОМ 70 — ВЫП. 4

Изучение парциального каталитического окисления метана, I

Скорости превращений в однозернистом реакторе

К. ХУСАР, ДЬ. РАЦ и ДЬ. СЕКЕЙ

Были измерены скорости парциального окисления метана в 25%-ной метано—воздушной смеси в реакторе, содержащем единственное зерно катализатора никеля на керамическом носителе, при 760—900°С. Для характеризации реакции приводятся скорости превращения реагентов и образования продуктов в единицах $см^3$ (25°С)· $мин^{-1}$. Было установлено, что скорость превращения кислорода лишь весьма слабо зависит от температуры, но изменяется пропорционально концентрации кислорода в области стабильного действия катализатора. Основными продуктами реакции были водород, окись углерода и водяной пар, даже и в случае небольших степеней превращения подаваемой смеси. Такое парциальное окисление метана катализуется лишь никелем в восстановленном состоянии. На основе наблюдаемых явлений было сделано заключение о том, что вследствие торможения диффузией в газовой фазе, концентрация кислорода на поверхности катализатора практически равна нулю.

Изучение парциального каталитического окисления метана, II

Измерение и расчет скорости передачи компонента

ДЬ. РАЦ и ДЬ. СЕКЕЙ

На единственном шарообразном зерне катализатора была измерена скорость превращения кислорода в смеси 25%-ов метана с 75%-ами воздуха при различных скоростях подачи смеси. Скорость превращения кислорода во всех случаях превышает диффузионное предельное значение, рассчитанное на основе литературных данных. Это расхождение может быть объяснено, полагая, что превращение реагентов протекает не только на поверхности катализатора, но и в газовой оболочке вокруг катализатора. С помощью других исследований было доказано, что гомогенная реакция не распространяется на среду в потоке, а остается вблизи поверхности катализатора.

Изучение пассивирования железа в смеси уксусной кислоты с водой

Л. КИШ, ДО НГОК ЛИЕН и Л. М. ВАРШАНИ

С помощью потенциостатического метода было изучено анодное растворение железа в растворах ацетата натрия, хлорной кислоты и перхлората натрия, приготовленных в безводной уксусной кислоте и в смеси уксусной кислоты с водой. Определено, что в растворах ацетата натрия в присутствии воды возникает пассивирование железа, но в отсутствие воды в растворе — пассивирование не обнаруживается. В растворах хлорной

кислоты и перхлората натрия получается противоположная картина: в безводной среде возникает пассивирование, а в присутствии воды оно не имеет места. Это явление наверно объясняется различными свойствами ионных пар, образующихся в этих растворах.

Полимеризация акриламида в водных средах с восстановительно-окислительной системой $K_2S_2O_8$—аскорбиновая кислота при комнатной температуре

И. ГЕЦИ и М. И. НАСР

Акриламид полимеризовался в водных средах с помощью восстановительно-окислительной системы персульфат калия—аскорбиновая кислота при комнатной температуре. Кинетику полимеризации исследовали йодометрическим способом. Изучалось влияние концентраций инициатора и мономера на скорость реакции и определялось кинетическое уравнение для общей скорости полимеризации. Изучалось также влияние растворителей как передатчиков цепи.

Наконец, определялась зависимость среднечисленной степени полимеризации от начальной концентрации мономера, концентрации инициатора-активатора и от температуры.

Изучение замороженных растворов перхлората железа(III) при различных pH с помощью метода Мёссбауэра

И. ДЕЖИ, В. Д. ГОРОБЧЕНКО, М. КОМОР, И. И. ЛУКАШЕВИЧ, А. ВЕРТЕШ и К. Ф. ЦИЦКИШВИЛИ

Измерение эффекта Мёссбауэра в замороженных растворах перхлората железа(III) проводилось вплоть до 2,8°К. Наблюдалось присутствие различных ионов как функция pH. Было найдено, что гидролиз усиливается при предварительном нагревании перед замораживанием. Магнитные структуры полимерных ионов выводились из данных спектров Мёссбауэра и результаты сравнивались с заключениями, полученными другими авторами на основе спектрофотометрических измерений и измерений магнитной восприимчивости.

Изучение химических и электрохимических свойств редоксиндикаторов, применяемых в неводных средах

Л. ЛАДАНЬИ

Электрохимическое окисление Персантина (дипиперидино-4,8-пирамидо-5,4-D-пирамидиндиил-2,6-диимино-2,2′, 2″, 2‴-тетраэтанола) в ацетонитриле и нейтральной среде, в отсутствии буфера протекает в двух последующих обратимых одноэлектронных процессах ($P \rightleftarrows R^{+\cdot} + e$, $R^{+\cdot} \rightleftarrows Q^{++} + e$), где $R^{+\cdot}$ и Q^{++} — стабильные окисленные формы моно- и дикатиона, соответственно, а P — исходное вещество.

Разница в абсорбционных спектрах P и $R^{+\cdot}$ позволяет использование P в качестве редокси-индикатора в вышеупомянутых средах.

На основе модели Персантина, каждая редокси-система, которая окисляется (или восстанавливается) через последовательные одноэлектронные ступени и для которой

1. электрохимические свойства подобны модели Персантина;
2. восстановленная (или окисленная) форма, а также радикал наглядно различаются по цвету и

3. одноэлектронная окисленная (или восстановленная) форма сравнительно стабильна

может быть рассмотрена в качестве обратимого редоксиндикатора в соответствующих средах.

В литературе упоминается пелый ряд таких систем. Среди них следует отметить: фенотиазин, 5,10-дигидрофеназин, N,N,N′N′-тетраметилбензидин, 2,2′-дипиридил, 4,4′-дипиридил, бензоксазол, бензтиазол и бенздитиол, а также их некоторые производные.

Новые нитрохалконы, XI

К вопросу о стереохимии некоторых нитрогидрокси-халконов

П. ШОХАР, Т. СЕЛЛ и Т. ДУДАШ

С помощью ИК и ЯМР спектроскопии халконов, приготовленных различными путями, было установлено, что независимо от условий приготовления в случае всех моделей образуются стереоодначные *транс*-изомеры.

Превращение ретродегидрокаротина в изозеаксантин и эпоксиды изозеаксантина

Й. САБОЛЬЧ и ДЬ. ТОТ

Описывается превращение ретродегидрокаротина под влиянием перфталевой кислоты в изозеаксантин и три, неизвестных до настоящего времени эпоксида изозеаксантина. Исходя из ретродегидрокаротиноидов гидроксилирование такого типа может служить подходящим методом для получения каротиноидов, содержащих гидроксильную группу.

Кислый гидролиз инулина

Й. СЕЙТЛИ, Р. Д. ХЕНРИКЕЗ и М. КАСТИНЕИРА

Кислый гидролиз β-1,2-гликозидных связей между D-фруктофуранозидными звеньями инулина является необыкновенно быстрым. Его нельзя характеризовать единственной константой скорости, т. к. гидролиз в начальной стадии протекает медленнее, чем в конечной стадии. В конечной стадии, когда средняя степень полимеризации около 4, скорость гидролиза больше, а в начальной стадии меньше скоростей, наблюдаемых в случае сахарозы при тех же самых условиях.

Первой ступенью гидролиза фуранозидной связи, по всей вероятности, является протонирование кислорода фуранозидного кольца, а второй ступенью является гетеролиз связи с образованием четвертичного карбонийного катиона. Величина энтропии активации указывает на то, что реакция относится к типу A—1. Механизм гидролиза инулина подобен механизму гидролиза сахарозы и рафинозы.

Исследование получения 1,2-диизобутоксибензола

Й. ЭГРИ, Й. ХАЛМОШ и Й. РАКОЦИ

С помощью изобутиловых эфиров арилсульфоновых кислот, например, изобутилового эфира бензолсульфокислоты, может быть получен с хорошим выходом 1,2-диизобутоксибензол. Получаемый продукт является весьма чистым и нитрируется с хорошим выходом до 1,2-диизобутокси-4-нитробензола.

Исследование динамических пен

ДЬ. ШАШВАРИ, Ф. ХИТЕШ и Т. БЛИКЛЕ

Вначале изучается элементарный физический процесс образования пузырьков, а затем приводится анализ пенного состояния. Различаются два типа пен. Первоначальную пену образуют первичные пузырьки, размеры которых и вместе с этим скорость подъема определяются физическими свойствами жидкости и параметрами установки.

Вторичной пеной называется такая пена, в которой исходной фазой является уже не сама жидкость, а первоначальная пена, в которую поднимаются вторичные пузырьки с гораздо большими размерами.

На основе этих представлений приводятся уравнения для расчета формирующих свойств динамических пен.

Во второй части сообщения приводятся метод и результаты измерений, которые сравниваются с расчетными данными. Согласование в случае большинства параметров удивительно хорошее, лишь учет вязкости вызывает значительные расхождения.

ATLAS OF THERMOANALYTICAL CURVES

(TG-, DTG-, DDTA-Curves measured simultaneously)

Edited by G. Liptay

The present volume which is part of a series published continually contains a collection of exposures made by a derivatograph of inorganic, organic, synthetic organic materials, minerals, rocks, carbons, etc. of various origin. Two exposures were made in each case – because of certain analytical circumstances influencing the material under investigation – in order to provide a wide scale of informatory data.

In English · 13+50 pages · Loose-leaf cloth binders · 17×25 cm · Cloth

A co-edition — distributed in the socialist countries by KULTURA. Budapest, in all other countries by HEYDEN AND SON LTD., London

AKADÉMIAI KIADÓ

Publishing House of the Hungarian Academy of Sciences
Budapest

Printed in Hungary

A kiadásért felel az Akadémiai Kiadó igazgatója — Műszaki szerkesztő: Várhelyi Tamás

A kézirat nyomdába érkezett: 1971. VII. 20. — Terjedelem: 12 (A/5) ív, 76 ábra

71.72123 Akadémiai Nyomda, Budapest — Felelős vezető: Bernát György

The Acta Chimica publish papers on chemistry in English, German, French and Russian.

The Acta Chimica appear in volumes consisting of four parts of varying size, 4 volumes being published a year.

Manuscripts should be addressed to

Acta Chimica
Budapest 112/91 Műegyetem

Correspondence with the editors should be sent to the same address.

The rate of subscription is $ 16.00 a volume.

Orders may be placed with "*Kultúra*" Foreign Trade Company for Books and Newspapers (Budapest I., Fő utca 32. Account No. 43-790-057-181) or with representatives abroad.

Les Acta Chimica paraissent en français, allemand, anglais et russe et publient des mémoires du domaine des sciences chimiques.

Les Acta Chimica sont publiés sous forme de fascicules. Quatre fascicules seront réunis en un volume (4 volumes par an).

On est prié d'envoyer les manuscrits destinés à la rédaction à l'adresse suivante:

Acta Chimica
Budapest 112/91 Műegyetem

Toute correspondance doit être envoyée à cette même adresse.

Le prix de l'abonnement est de $ 16.00 par volume.

On peut s'abonner à l'Entreprise pour le Commerce Extérieur de Livres et Journaux «*Kultúra*» (Budapest I., Fő utca 32. Compte-courant No. 43-790-057-181) ou à l'étranger chez tous les représentants ou dépositaires.

«*Acta Chimica*» издают трактаты из области химической науки на русском, французском, английском и немецком языках.

«*Acta Chimica*» выходят отдельными выпусками разного объема. 4 выпуска составляют один том. 4 тома публикуются в год.

Предназначенные для публикации рукописи следует направлять по адресу:

Acta Chimica
Budapest 112/91 Műegyetem

По этому же адресу направлять всякую корреспонденцию для редакции.

Подписная цена – $ 16.00 за том.

Заказы принимает предприятие по внешней торговле книг и газет «*Kultúra*» (Budapest I., Fő utca 32. Текущий счет № 43-790-057-181) или его заграничные представительства и уполномоченные.

Reviews of the Hungarian Academy of Sciences are obtainable at the following addresses:

ALBANIA
Drejtorija Qändrone e Pärhapjes dhe Propagandimit të Librit
Kruga Konferenca e Päzes
Tirana

AUSTRALIA
A. Keesing
Box 4886, GPO
Sydney

USTRIA
GLOBUS
Höchstädtplatz 3
A-1200 Wien XX

BELGIUM
Office International de Librairie
30, Avenue Marnix
Bruxelles 5
Du Monde Entier
5, Place St. Jean
Bruxelles

BULGARIA
HEMUS
11 pl Slaveikov
Sofia

CANADA
Pannonia Books
2, Spadina Road
Toronto 4, Ont.

CHINA
Waiwen Shudian
Peking
P. O. B. 88

CZECHOSLOVAKIA
Artia
Ve Smečkách 30
Praha 2
Poštovní Novinová Služba
Dovoz tisku
Vinohradská 46
Praha 2
Mad'arská Kultura
Václavské nám. 2
Praha 1
SLOVART A. G.
Gorkého
Bratislava

DENMARK
Ejnar Munksgaard
Nörregade 6
Copenhagen

FINLAND
Akateeminen Kirjakauppa
Keskuskatu 2
Helsinki

FRANCE
Office Internationo de Documentation et Librairie
48, rue Gay-Lussac
Paris 5

GERMAN DEMOCRATIC REPUBLIC
Deutscher Buch-Export und Import
Leninstraße 16
Leipzig 701
Zeitungsvertriebsamt
Fruchtstraße 3—4
1004 Berlin

GERMAN FEDERAL REPUBLIC
Kunst und Wissen
Erich Bieber
Postfach 46
7 Stuttgart S.

GREAT BRITAIN
Blackwell's Periodicals
Oxenford House
Magdalen Street
Oxford
Collet's Subscription Import Department
Dennington Estate
Wellingsborough. Northants.
Robert Maxwell and Co. Ltd.
4—5 Fitzroy Square
London W. 1

HOLLAND
Swetz and Zeitlinger
Keizersgracht 471—487
Amsterdam C.
Martinus Nijhof
Lange Voorhout 9
The Hague

INDIA
Hind Book House
66 Babar Road
New Delhi 1

ITALY
Santo Vanasia
Via M. Macchi 71
Milano
Libreria Commissionaria Sansoni
Via La Marmora 45
Firenze
Techna
Via Cesi 16.
40135 Bologna

JAPAN
Kinokuniya Book-Store Co. Ltd.
826 Tsunohazu 1-chome
Shinjuku-ku
Tokyo
Maruzen and Co. Ltd.
P. O. Box 605
Tokyo-Central

KOREA
Chulpanmul
Phenjan

NORWAY
Tanum-Cammermeyer
Karl Johansgt 41—43
Oslo 1

POLAND
RUCH
ul. Wronia 23
Warszawa

ROUMANIA
Cartimex
Str. Aristide Briand 14—18
Bucureşti

SOVIET UNION
Mezhdunarodnaya Kniga
Moscow G—200

SWEDEN
Almquist and Wiksell
Gamla Brogatan 26
S—101 20 Stockholm

USA
F. W. Faxon Co. Inc.
15 Southwest Park
Westwood Mass. 02090
Stechert Hafner Inc.
31. East 10th Street
New York, N. Y. 10003

VIETNAM
Xunhasaba
19, Tran Quoc Toan
Hanoi

YUGOSLAVIA
Forum
Vojvode Mišića broj 1
Novi Sad
Jugoslovenska Knjiga
Terazije 27
Beograd

30. XII. 1971 Index: 26.007